ISSN 0021-9673

VOL. 660 NOS. 1 + 2 FEBRUARY 4, 1994

COMPLETE IN ONE ISSUE

17th International Symposium on Column Liquid Chromatography Hamburg, May 9–14, 1993 Part I

JOURNAL OF CHROMATOGRAPHY A

INCLUDING ELECTROPHORESIS AND OTHER SEPARATION METHODS

SYMPOSIUM VOLUMES

EDITORS
E. Heftmann (Orinda, CA)
Z. Deyl (Prague)

EDITORIAL BOARD
E. Bayer (Tübingen)
S.R. Binder (Hercules, CA)
S.C. Churms (Rondebosch)
J.C. Fetzer (Richmond, CA)
E. Gelpí (Barcelona)
K.M. Gooding (Lafayette, IN)
S. Hara (Tokyo)
P. Helboe (Brønshøj)
W. Lindner (Graz)
T.M. Phillips (Washington, DC)
S. Terabe (Hyogo)
H.F. Walton (Boulder, CO)
M. Wilchek (Rehovot)

ELSEVIER

JOURNAL OF CHROMATOGRAPHY A

INCLUDING ELECTROPHORESIS AND OTHER SEPARATION METHODS

Scope. The *Journal of Chromatography A* publishes papers on all aspects of **chromatography, electrophoresis** and related methods. Contributions consist mainly of research papers dealing with chromatographic theory, instrumental developments and their applications. In the *Symposium volumes*, which are under separate editorship, proceedings of symposia on chromatography, electrophoresis and related methods are published. *Journal of Chromatography B: Biomedical Applications* —This journal, which is under separate editorship, deals with the following aspects: developments in and applications of chromatographic and electrophoretic techniques related to clinical diagnosis or alterations during medical treatment; screening and profiling of body fluids or tissues related to the analysis of active substances and to metabolic disorders; drug level monitoring and pharmacokinetic studies; clinical toxicology; forensic medicine; veterinary medicine; occupational medicine; results from basic medical research with direct consequences in clinical practice.

Submission of Papers. The preferred medium of submission is on disk with accompanying manuscript (see *Electronic manuscripts* in the Instructions to Authors, which can be obtained from the publisher, Elsevier Science B.V., P.O. Box 330, 1000 AH Amsterdam, Netherlands). Manuscripts (in English; *four* copies are required) should be submitted to: Editorial Office of *Journal of Chromatography A*, P.O. Box 681, 1000 AR Amsterdam, Netherlands, Telefax (+31-20) 5862 304, or to: The Editor of *Journal of Chromatography B: Biomedical Applications*, P.O. Box 681, 1000 AR Amsterdam, Netherlands. Review articles are invited or proposed in writing to the Editors who welcome suggestions for subjects. An outline of the proposed review should first be forwarded to the Editors for preliminary discussion prior to preparation. Submission of an article is understood to imply that the article is original and unpublished and is not being considered for publication elsewhere. For copyright regulations, see below.

Publication information. *Journal of Chromatography A* (ISSN 0021-9673): for 1994 Vols. 652–682 are scheduled for publication. *Journal of Chromatography B: Biomedical Applications* (ISSN 0378-4347): for 1994 Vols. 652–662 are scheduled for publication. Subscription prices for *Journal of Chromatography A*, *Journal of Chromatography B: Biomedical Applications* or a combined subscription are available upon request from the publisher. Subscriptions are accepted on a prepaid basis only and are entered on a calendar year basis. Issues are sent by surface mail except to the following countries where air delivery via SAL is ensured: Argentina, Australia, Brazil, Canada, China, Hong Kong, India, Israel, Japan, Malaysia, Mexico, New Zealand, Pakistan, Singapore, South Africa, South Korea, Taiwan, Thailand, USA. For all other countries airmail rates are available upon request. Claims for missing issues must be made within six months of our publication (mailing) date. Please address all your requests regarding orders and subscription queries to: Elsevier Science B.V., Journal Department, P.O. Box 211, 1000 AE Amsterdam, Netherlands. Tel.: (+31-20) 5803 642; Fax: (+31-20) 5803 598. Customers in the USA and Canada wishing information on this and other Elsevier journals, please contact Journal Information Center, Elsevier Science Inc., 655 Avenue of the Americas, New York, NY 10010, USA, Tel. (+1-212) 633 3750, Telefax (+1-212) 633 3764.

Abstracts/Contents Lists published in Analytical Abstracts, Biochemical Abstracts, Biological Abstracts, Chemical Abstracts, Chemical Titles, Chromatography Abstracts, Current Awareness in Biological Sciences (CABS), Current Contents/Life Sciences, Current Contents/Physical, Chemical & Earth Sciences, Deep-Sea Research/Part B: Oceanographic Literature Review, Excerpta Medica, Index Medicus, Mass Spectrometry Bulletin, PASCAL-CNRS, Referativnyi Zhurnal, Research Alert and Science Citation Index.

US Mailing Notice. *Journal of Chromatography A* (ISSN 0021-9673) is published weekly (total 52 issues) by Elsevier Science B.V., (Sara Burgerhartstraat 25, P.O. Box 211, 1000 AE Amsterdam, Netherlands). Annual subscription price in the USA US$ 4994.00 (US$ price valid in North, Central and South America only) including air speed delivery. Second class postage paid at Jamaica, NY 11431. **USA POSTMASTERS**: Send address changes to *Journal of Chromatography A*, Publications Expediting, Inc., 200 Meacham Avenue, Elmont, NY 11003. Airfreight and mailing in the USA by Publications Expediting.

See inside back cover for Publication Schedule, Information for Authors and information on Advertisements.

© 1994 ELSEVIER SCIENCE B.V. All rights reserved.

0021-9673/94/$07.00

No part of this publication may be reproduced, stored in a retrieval system or transmitted in any form or by any means, electronic, mechanical, photocopying, recording or otherwise, without the prior written permission of the publisher, Elsevier Science B.V., Copyright and Permissions Department, P.O. Box 521, 1000 AM Amsterdam, Netherlands.

Upon acceptance of an article by the journal, the author(s) will be asked to transfer copyright of the article to the publisher. The transfer will ensure the widest possible dissemination of information.

Special regulations for readers in the USA. This journal has been registered with the Copyright Clearance Center, Inc. Consent is given for copying of articles for personal or internal use, or for the personal use of specific clients. This consent is given on the condition that the copier pays through the Center the per-copy fee stated in the code on the first page of each article for copying beyond that permitted by Sections 107 or 108 of the US Copyright Law. The appropriate fee should be forwarded with a copy of the first page of the article to the Copyright Clearance Center, Inc., 27 Congress Street, Salem, MA 01970, USA. If no code appears in an article, the author has not given broad consent to copy and permission to copy must be obtained directly from the author. All articles published prior to 1980 may be copied for a per-copy fee of US$ 2.25, also payable through the Center. This consent does not extend to other kinds of copying, such as for general distribution, resale, advertising and promotion purposes, or for creating new collective works. Special written permission must be obtained from the publisher for such copying.

No responsibility is assumed by the Publisher for any injury and/or damage to persons or property as a matter of products liability, negligence or otherwise, or from any use or operation of any methods, products, instructions or ideas contained in the materials herein. Because of rapid advances in the medical sciences, the Publisher recommends that independent verification of diagnoses and drug dosages should be made.

Although all advertising material is expected to conform to ethical (medical) standards, inclusion in this publication does not constitute a guarantee or endorsement of the quality or value of such product or of the claims made of it by its manufacturer.

This issue is printed on acid-free paper.

Printed in the Netherlands

For Contents see p. VII.

Reversed Phase CHIRAL HPLC Column

NEW CHIRALCEL® OD-R

Indapamide

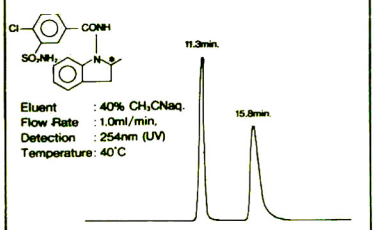

Eluent : 40% CH_3CNaq.
Flow Rate : 1.0ml/min.
Detection : 254nm (UV)
Temperature: 40°C

Verapamil

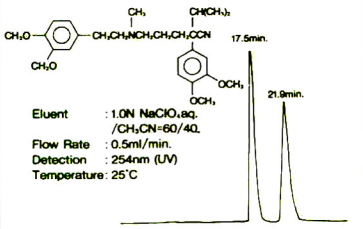

Eluent : 1.0N $NaClO_4$aq. /CH_3CN=60/40.
Flow Rate : 0.5ml/min.
Detection : 254nm (UV)
Temperature: 25°C

Hydroxyzine

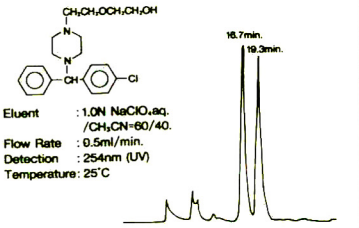

Eluent : 1.0N $NaClO_4$aq. /CH_3CN=60/40.
Flow Rate : 0.5ml/min.
Detection : 254nm (UV)
Temperature: 25°C

Propranolol

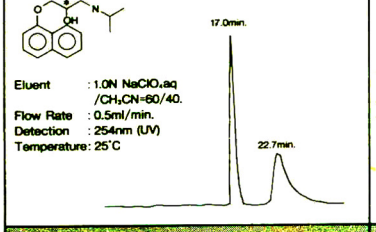

Eluent : 1.0N $NaClO_4$aq /CH_3CN=60/40.
Flow Rate : 0.5ml/min.
Detection : 254nm (UV)
Temperature: 25°C

Pindolol

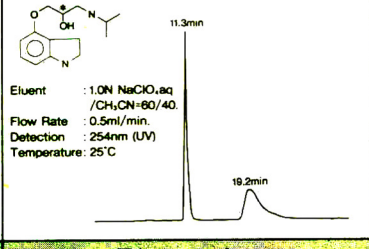

Eluent : 1.0N $NaClO_4$aq /CH_3CN=60/40.
Flow Rate : 0.5ml/min.
Detection : 254nm (UV)
Temperature: 25°C

1-Phenoxy-2-Propanol

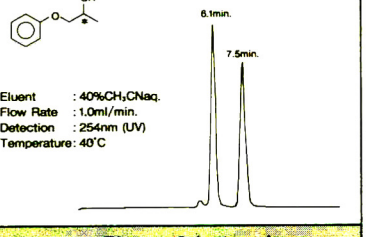

Eluent : 40%CH_3CNaq.
Flow Rate : 1.0ml/min.
Detection : 254nm (UV)
Temperature: 40°C

Alimemazine

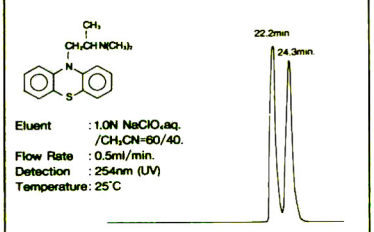

Eluent : 1.0N $NaClO_4$aq. /CH_3CN=60/40.
Flow Rate : 0.5ml/min.
Detection : 254nm (UV)
Temperature: 25°C

Trimepramine

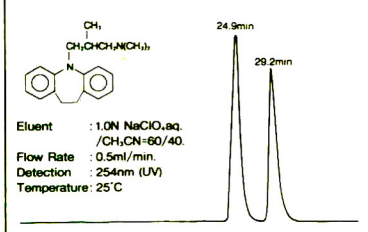

Eluent : 1.0N $NaClO_4$aq. /CH_3CN=60/40.
Flow Rate : 0.5ml/min.
Detection : 254nm (UV)
Temperature: 25°C

4-Pheny-2-butanol

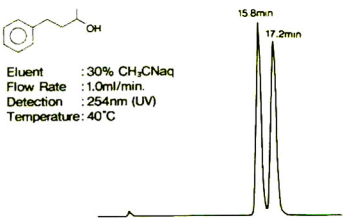

Eluent : 30% CH_3CNaq
Flow Rate : 1.0ml/min.
Detection : 254nm (UV)
Temperature: 40°C

CBZ-Val.

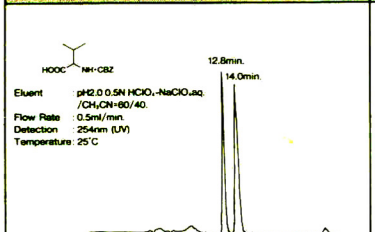

Eluent : pH2.0 0.5N $HClO_4$-$NaClO_4$aq. /CH_3CN=60/40.
Flow Rate : 0.5ml/min.
Detection : 254nm (UV)
Temperature: 25°C

3-Phenylbutyric acid

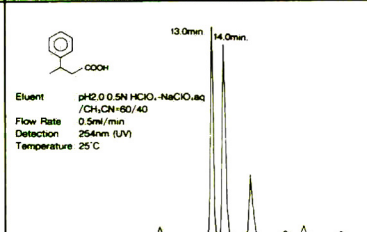

Eluent : pH2.0 0.5N $HClO_4$-$NaClO_4$aq. /CH_3CN=60/40
Flow Rate : 0.5ml/min
Detection : 254nm (UV)
Temperature : 25°C

2-Phenylbutyric acid

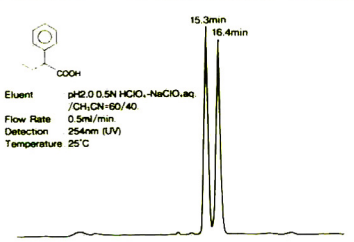

Eluent : pH2.0 0.5N $HClO_4$-$NaClO_4$aq. /CH_3CN=60/40
Flow Rate : 0.5ml/min.
Detection : 254nm (UV)
Temperature : 25°C

For more information about CHIRALCEL OD-R column, please give us a call.

DAICEL CHEMICAL INDUSTRIES, LTD.
CHIRAL CHEMICALS DIVISION 8-1, Kasumigaseki 3-chome, Chiyoda-ku, Tokyo 100, JAPAN
Phone: +81-3-3507-3151 Facsimile: +81-3-3507-3193

AMERICA
CHIRAL TECHNOLOGIES, INC.
730 SPRINGDALE DRIVE
DRAWER I EXTON, PA 19341
Phone: 215-594-2100
Facsimile: 215-594-2325

EUROPE
DAICEL (EUROPA) GmbH
Ost Street 22
4000 Düsseldorf 1, Germany
Phone: +49-211-369848
Facsimile: +49-211-364429

ASIA/OCEANIA
DAICEL CHEMICAL (ASIA) PTE. LTD.
65 Chulia Street #40-07
OCBC Centre, Singapore 0104.
Phone: +65-5332511
Facsimile: +65-5326454

Capillary Electrophoresis

Principles, Practice and Applications

by **S.F.Y. Li**, *National University of Singapore, Singapore*

Journal of Chromatography Library Volume 52

Capillary Electrophoresis (CE) has had a very significant impact on the field of analytical chemistry in recent years as the technique is capable of very high resolution separations, requiring only small amounts of samples and reagents. Furthermore, it can be readily adapted to automatic sample handling and real time data processing. Many new methodologies based on CE have been reported. Rapid, reproducible separations of extremely small amounts of chemicals and biochemicals, including peptides, proteins, nucleotides, DNA, enantiomers, carbohydrates, vitamins, inorganic ions, pharmaceuticals and environmental pollutants have been demonstrated. A wide range of applications have been developed in greatly diverse fields, such as chemical, biotechnological, environmental and pharmaceutical analysis.

This book covers all aspects of CE, from the principles and technical aspects to the most important applications. It is intended to meet the growing need for a thorough and balanced treatment of CE. The book will serve as a comprehensive reference work and can also be used as a textbook for advanced undergraduate and graduate courses. Both the experienced analyst and the newcomer will find the text useful.

Contents:

1. Introduction. Historical Background. Overview of High Performance CE. Principles of Separations. Comparison with Other Separation Techniques. **2. Sample Injection Methods.** Introduction. Electrokinetic Injection. Hydrodynamic Injection. Electric Sample Splitter. Split Flow Syringe Injection System. Rotary Type Injector. Freeze Plug Injection. Sampling Device with Feeder. Microinjectors. Optical Gating. **3. Detection Techniques.** Introduction. UV-Visible Absorbance Detectors. Photodiode Array Detectors. Fluorescence Detectors. Laser-based Thermooptical and Refractive Index Detectors. Indirect Detection. Conductivity Detection. Electrochemical Detection. Mass Spectrometric Detection. **4. Column Technology.** Uncoated Capillary Columns. Coated Columns. Gel-filled Columns. Packed Columns. Combining Packed and Open-Tubular Column. **5. Electrophoretic Media.** Electrophoretic Buffer Systems. Micellar Electrokinetic Capillary Chromatography. Inclusion Pseudophases. Metal-complexing Pseudophases. Other Types of Electrophoretic Media. **6. Special Systems and Methods.** Buffer Programming. Fraction Collection. Hyphenated Techniques. Field Effect Electroosmosis. Systematic Optimization of Separation. **7. Applications of CE.** Biomolecules. Pharmaceutical and Clinical Analysis. Inorganic Ions. Hydrocarbons. Foods and Drinks. Environmental Pollutants. Carbohydrates. Toxins. Polymers and Particles. Natural Products. Fuel. Metal Chelates. Industrial Waste Water. Explosives. Miscellaneous Applications. **8. Recent Advances and Prospect for Growth.** Recent Reviews in CE. Advances in Injection Techniques. Novel Detection Techniques. Advances in Column Technology. Progress on Electrolyte Systems. New Systems and Methods. Additional Applications Based on CE. Future Trends.

References. Index.

1992 608 pages Hardbound
US$ 225.75 / Dfl. 395.00
ISBN 0-444-89433-0
1993 608 pages Paperback
Price: US$ 114.25 / Dfl. 200.00
ISBN 0-444-81590-2

"Everything seems to be there, any detection system you have ever dreamed of, any capillary coating, enough electrolyte systems to saturate your wits, and more..."

"...by far the most thorough and comprehensive book in the field yet to appear."

P.G. Righetti, Milan

ELSEVIER SCIENCE B.V.

ORDER INFORMATION

For USA and Canada
ELSEVIER SCIENCE INC.
P.O. Box 945
Madison Square Station
New York, NY 10160-0757
Fax: (212) 633 3880

In all other countries
ELSEVIER SCIENCE B.V.
P.O. Box 330
1000 AH Amsterdam
The Netherlands
Fax: (+31-20) 5862 845

US$ prices are valid only for the USA & Canada and are subject to exchange rate fluctuations; in all other countries the Dutch guilder price (Dfl.) is definitive. Customers in the European Community should add the appropriate VAT rate applicable in their country to the price(s). Books are sent postfree if prepaid.

JOURNAL OF CHROMATOGRAPHY A

VOL. 660 (1994)

JOURNAL OF CHROMATOGRAPHY A

INCLUDING ELECTROPHORESIS AND OTHER SEPARATION METHODS

SYMPOSIUM VOLUMES

EDITORS

E. HEFTMANN (Orinda, CA), Z. DEYL (Prague)

EDITORIAL BOARD

E. Bayer (Tübingen), S.R. Binder (Hercules, CA), S.C. Churms (Rondebosch), J.C. Fetzer (Richmond, CA), E. Gelpí (Barcelona), K.M. Gooding (Lafayette, IN), S. Hara (Tokyo), P. Helboe (Brønshøj), W. Lindner (Graz), T.M. Phillips (Washington, DC), S. Terabe (Hyogo), H.F. Walton (Boulder, CO), M. Wilchek (Rehovot)

ELSEVIER
AMSTERDAM — LONDON — NEW YORK — TOKYO

The Hamburg exchange building

© 1994 ELSEVIER SCIENCE B.V. All rights reserved.

0021-9673/94/$07.00

No part of this publication may be reproduced, stored in a retrieval system or transmitted in any form or by any means, electronic, mechanical, photocopying, recording or otherwise, without the prior written permission of the publisher, Elsevier Science B.V., Copyright and Permissions Department, P.O. Box 521, 1000 AM Amsterdam, Netherlands.

Upon acceptance of an article by the journal, the author(s) will be asked to transfer copyright of the article to the publisher. The transfer will ensure the widest possible dissemination of information.

Special regulations for readers in the USA. This journal has been registered with the Copyright Clearance Center, Inc. Consent is given for copying of articles for personal or internal use, or for the personal use of specific clients. This consent is given on the condition that the copier pays through the Center the per-copy fee stated in the code on the first page of each article for copying beyond that permitted by Sections 107 or 108 of the US Copyright Law. The appropriate fee should be forwarded with a copy of the first page of the article to the Copyright Clearance Center, Inc., 27 Congress Street, Salem, MA 01970, USA. If no code appears in an article, the author has not given broad consent to copy and permission to copy must be obtained directly from the author. All articles published prior to 1980 may be copied for a per-copy fee of US$ 2.25, also payable through the Center. This consent does not extend to other kinds of copying, such as for general distribution, resale, advertising and promotion purposes, or for creating new collective works. Special written permission must be obtained from the publisher for such copying.

No responsibility is assumed by the Publisher for any injury and/or damage to persons or property as a matter of products liability, negligence or otherwise, or from any use or operation of any methods, products, instructions or ideas contained in the materials herein. Because of rapid advances in the medical sciences, the Publisher recommends that independent verification of diagnoses and drug dosages should be made.

Although all advertising material is expected to conform to ethical (medical) standards, inclusion in this publication does not constitute a guarantee or endorsement of the quality or value of such product or of the claims made of it by its manufacturer.

This issue is printed on acid-free paper.

Printed in the Netherlands

SYMPOSIUM VOLUME

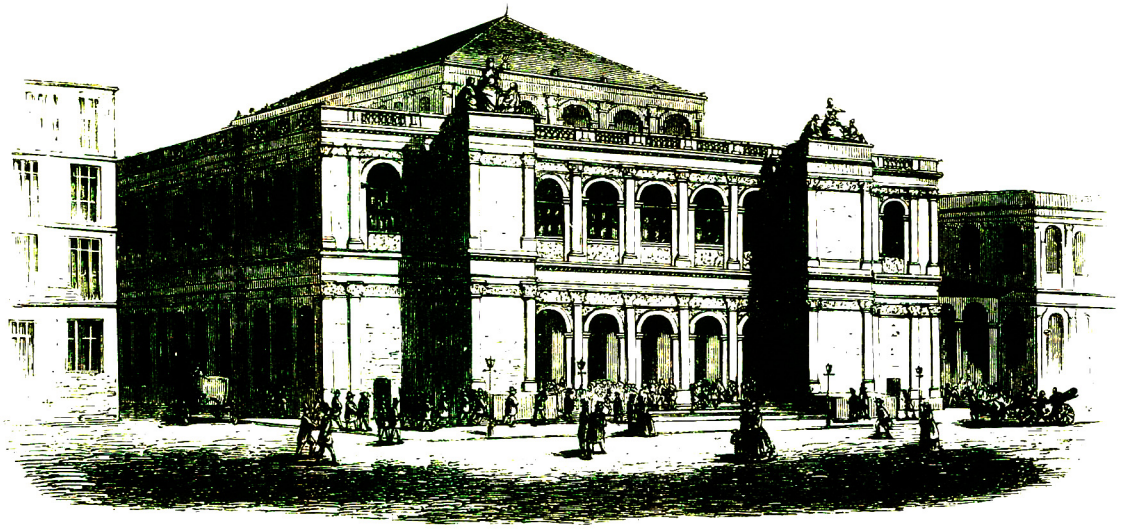

17TH INTERNATIONAL SYMPOSIUM ON COLUMN LIQUID CHROMATOGRAPHY

PART I

Hamburg (Germany), May 9–14, 1993

Guest Editor

K.K. Unger

(Mainz, Germany)

The proceedings of the *17th International Symposium on Column Liquid Chromatography, Hamburg, May 9–14, 1993*, are published in two consecutive volumes of the *Journal of Chromatography A*: Vols. 660 and 661 (1994). The Foreword to the proceedings only appears in Vol. 660. A combined Author Index to both Vols. 660 and 661 only appears in Vol. 661.

VOL. 660, NOS. 1 + 2 JOURNAL OF CHROMATOGRAPHY A FEBRUARY 4, 1994

CONTENTS

17TH INTERNATIONAL SYMPOSIUM ON COLUMN LIQUID CHROMATOGRAPHY, HAMBURG, MAY 9–14, 1993, PART I

Foreword
by K.K. Unger (Mainz, Germany) 1

THEORETICAL ASPECTS

Quantitative study of retention processes in reversed-phase liquid chromatography by means of reaction kinetics
by B.S. Ludolph, C.-Y. Jeng, A.H.T. Chu and S.H. Langer (Madison, WI, USA) 3

Explanation of the selectivity differences between reversed-phase ion-pair chromatographic systems containing trifluoroacetate or heptafluorobutyrate as pairing ion
by M. Patthy (Budapest, Hungary) 17

Determination of rate constants in a liquid chromatographic reactor by means of a fitting algorithm
by R. Thede, D. Haberland and E. Below (Greifswald, Germany) 25

Method development by an expert system. Advantages and limitations
by J. Fekete, G. Morovján, F. Csizmadia and F. Darvas (Budapest, Hungary) 33

Calculation of retention in reversed-phase liquid chromatography. IV. ChromDream software for the selection of initial conditions and for simulating chromatographic behaviour
by S.V. Galushko, A.A. Kamenchuk and G.L. Pit (Kiev, Ukraine) 47

Optimization of high-performance liquid chromatography and solvent parameters for the separation of polycyclic aromatic hydrocarbons compared with supercritical fluid chromatography with UV detection
by B.W. Wenclawiak and T. Hees (Siegen, Germany) 61

Mobile phase selection for high-performance liquid chromatographic analysis of novel zinc(II) carboxylates with N-donor ligands
by A. Oriňák and K. Gyoryová (Košice, Slovak Republic), E. Matisová (Bratislava, Slovak Republic) and L. Šlesárová, J. Skoršepa, I. Rosival and M. Ganajová (Košice, Slovak Republic) 67

PRACTICAL ASPECTS

High-performance liquid chromatography of amino acids, peptides and proteins. CXXV. Molecular dynamics simulation of *n*-butyl chains chemically bonded to silica-based reversed-phase high-performance liquid chromatography sorbents
by I. Yarovsky, M.-I. Aguilar and M.T.W. Hearn (Clayton, Australia) 75

Perfusion chromatography. Effect of micropore diffusion on column performance in systems utilizing perfusive adsorbent particles with a bidisperse porous structure
by A.I. Liapis and M.A. McCoy (Rolla, MO, USA) 85

Characterization of covalently bonded and adsorbed polymer coatings on silica, alumina and zirconia by means of physico-chemical and chromatographic methods
by A. Kurganov, V. Davankov and T. Isajeva (Moscow, Russian Federation), K. Unger (Mainz, Germany) and F. Eisenbeiss (Darmstadt, Germany) 97

Experimental study on the separation of silica gel supports by gravitational field-flow fractionation
by J. Pazourek, E. Urbánková and J. Chmelík (Brno, Czech Republic) 113

Determination of drugs by direct injection of plasma into a biocompatible extraction column based on a protein-entrapped hydrophobic phase
by J. Hermansson and A. Grahn (Hägersten, Sweden) 119

Polytrifluorostyrene-coated silica as a packing for column liquid chromatography
by A.D. Kataev, V.V. Saburov, O.A. Reznikova, D.V. Kapustin and V.P. Zubov (Moscow, Russian Federation) . 131

ห้องสมุดกลาง มหาวิทยาลัยศาสตร์บริการ
- 8 ส.ค. 2537

Perfusible and non-perfusible supports with monoclonal antibodies for bioaffinity chromatography of *Escherichia coli* penicillin amidase within its pH stability range
by V. Kasche, N. Gottschlich, A. Lindberg, C. Niebuhr-Redder and J. Schmieding (Hamburg, Germany) 137

Improvement of the performance of single-column ion chromatography by computerized detector signal processing and correlation chromatography
by M. Kaljurand, E. Urbas and U. Haldna (Tallinn, Estonia) 147

Enzyme-based biosensor as a selective detection unit in column liquid chromatography
by G. Marko-Varga, K. Johansson and L. Gorton (Lund, Sweden) 153

Synergies between micropreparative high-performance liquid chromatography and an instrumental optical biosensor
by E. Nice, M. Lackmann, F. Smyth, L. Fabri and A.W. Burgess (Melbourne, Australia) 169

Parallel-current open-tubular liquid chromatography with fluorimetric detection
by M. Horká, V. Kahle and K. Šlais (Brno, Czech Republic) 187

APPLICATIONS

Environmental

Application of high-performance gel-permeation chromatography clean-up in the determination of hexaflumuron residues in soil
by A. Khoshab and R. Teasdale (Wantage, UK) 195

Analysis of sulphonated polyphenols, synthetic tanning agents in heavily polluted tannery wastewaters
by T. Reemtsma and M. Jekel (Berlin, Germany) 199

Determination of traces of pyrethrins and piperonyl butoxide in biological material by high-performance liquid chromatography
by R. Wintersteiger, B. Ofner, H. Juan and M. Windisch (Graz, Austria) 205

Determination of aluminium and its fluoro complexes in natural waters by ion chromatography
by S. Motellier and H. Pitsch (Fontenay-aux-Roses, France) 211

Determination of triazines and dinitroanilines in waters by high-performance liquid chromatography after solid-phase extraction
by P. Vitali, E. Venturini, C. Bonora, R. Calori and R. Raffaelli (Bologna, Italy) 219

Clean-up by high-performance liquid chromatography of polychlorodibenzo-*p*-dioxins and polychlorodibenzofurans on a pyrenylethylsilica gel column
by U. Pyell (Marburg, Germany) and P. Garrigues (Talence, France) 223

Thermospray liquid chromatographic–mass spectrometric multi-residue determination of 128 polar pesticides in aqueous environmental samples
by D. Volmer, K. Levsen and G. Wünsch (Hannover, Germany) 231

Chiral

Influence of the structure of the alcoholic modifier on the enantioselective separation of nadolol
by A.M. Dyas and M.L. Robinson (Moreton, UK) and A.F. Fell (Bradford, UK) 249

Epimeric N-substituted L-proline derivatives as chiral selectors for ligand-exchange chromatography
by E. Veigl and W. Lindner (Graz, Austria) 255

Stereoselective effects in the separation of enantiomers of omeprazole and other substituted benzimidazoles on different chiral stationary phases
by K. Balmér, B.-A. Persson and P.-O. Lagerström (Mölndal, Sweden) 269

Retention and enantioselective properties of ovomucoid-bonded silica columns. Influence of physical properties of base materials and spacer length
by J. Haginaka, C. Seyama and T. Murashima (Nishinomiya, Japan) and H. Fujima and H. Wada (Kyoto, Japan) 275

Monitoring of optical isomers of β-methylphenylalanine in opioid peptides
by A. Péter, G. Tóth and E. Cserpán (Szeged, Hungary) and D. Tourwé (Brussels, Belgium) 283

Pharmacological

High-performance liquid chromatographic determination of FCE 24928, a new aromatase inhibitor, in human plasma
by E. Fontana, E. Pianezzola, G. Basileo and M. Strolin Benedetti (Milan, Italy) 293

Determination of paeoniflorin, ferulic acid and baicalin in the traditional Chinese medicinal preparation Dang-Guei-San by high-performance liquid chromatography
by Y.-C. Lee, C.-Y. Huang, K.-C. Wen and T.-T. Suen (Taipei, Taiwan) 299

Simultaneous determination of L-693,612, a topical carbonic anhydrase inhibitor, and two potential metabolites in human whole blood by ion-pair high-performance liquid chromatography
by E.J. Woolf, T. Au, M. Kasper, M. Constanzer and B. Matuszewski (West Point, PA, USA) 307

Retention of some monoamine oxidase inhibitory drugs on a β-cyclodextrin polymer-coated silica column
by T. Cserháti and E. Forgács (Budapest, Hungary) 313

Automated assay for GV104326, a novel tribactam antibiotic, in human plasma by high-performance liquid chromatography and solid-phase extraction
by R.J. Barnaby and L. Iavarone (Verona, Italy) 319

Rapid, high-resolution high-performance liquid chromatographic analysis of antibiotics
by K.M. Kirkland and D.A. McCombs (Wilmington, DE, USA) and J.J. Kirkland (Newport, DE, USA) 327

Liquid chromatographic retention behaviour and separation of promethazine and isopromethazine on a β-cyclodextrin bonded-phase column
by S. Piperaki, A. Perakis and M. Parissi-Poulou (Athens, Greece) 339

Sensitive procedure for the determination of reboxetine enantiomers in human plasma by reversed-phase high-performance liquid chromatography with fluorimetric detection after chiral derivatization with (+)-1-(9-fluorenyl)ethyl chloroformate
by E. Frigerio, E. Pianezzola and M. Strolin Benedetti (Milan, Italy) 351

Journal of Chromatography A, 660 (1994) 1
Elsevier Science B.V., Amsterdam

CHROM. 25 657

Foreword

The *17th International Symposium on Column Liquid Chromatography* (HPLC'93) took place in Hamburg from May 9th to 13th, 1993. It was attended by 810 delegates from about 40 countries. Twenty-two plenary lectures, 40 discussion lectures in two parallel sessions and 450 posters were presented. Seventy-two companies took part in the scientific exhibition of equipment and accessories. Professor H. Nöth, the President of the Gesellschaft Deutscher Chemiker (GDCh), welcomed the delegates and highlighted the role of HPLC in the life sciences.

The high quality of the scientific contributions, the fruitful discussions between delegates and the relaxing atmosphere of the Congress Centre made HPLC'93 a most rewarding and stimulating conference, at which the high scientific standards of the previous symposia were fully maintained. A number of companies and public bodies provided substantial support to the symposium. This support enabled the Organizing Committee to give financial help to about 40 students and young scientists and to about 30 delegates from East European countries to participate in the symposium. I gratefully acknowledge the generous support of the GDCh, the Deutsche Forschungsgemeinschaft and Elsevier Science B.V.

As Chairman of HPLC'93, I wish to express my personal appreciation to the members of the Organizing Committee: Professor H. Engelhardt, Professor K.P. Hupe, Dr. G. Synnatschke and Dr. J. Wendenburg, whose hard work and intellectual input made the preparation of the symposium very effective and enjoyable. It is with great sadness that I have to announce that Dr. J. Wendenburg passed away about 2 months after the symposium. We are indebted to Dr. Wendenburg for his outstanding contributions during the planning, preparation and conduct of the meeting and we will keep him in our memory as a warm friend.

The size of such a symposium requires experienced logistical organization. I would like to thank the staff of the GDCh, Frankfurt, Ms R. Maul, Ms K. Bruns and Ms Ch. Sztabelski, and also Ms E. Schramm and Mr. Rosenthal of the Congress Centre, Hamburg, for their excellent performance and cooperation in handling the registration, correspondence, printing of the programme and arranging of the social events.

I also express my thanks to the research students of Professor Engelhardt and my group, in particular to Ms Monika Hallmann and Mr. Jochen Meister for their help in the preparation of the book of abstracts and in arranging the poster session.

I am greatly indebted to the members of the Scientific Committee for their efforts in preparing an excellent scientific programme and for their encouragement and valuable advice throughout the preparations for the symposium. Finally, I want to thank all the delegates who attended HPLC'93 and made the symposium a great success.

This volume contains the papers which were submitted to the Symposium Editor and are representative of the high scientific standard of the symposium. We are indebted to Dr. Erich Heftmann and to the editorial staff of the *Journal of Chromatography* for their efforts in the rapid publication of this special issue.

Mainz (Germany) K.K. Unger
Symposium Chairman

SSDI 0021-9673(93)E1093-F

Journal of Chromatography A, 660 (1994) 3–15
Elsevier Science B.V., Amsterdam

CHROMSYMP. 2921

Quantitative study of retention processes in reversed-phase liquid chromatography by means of reaction kinetics

Brian S. Ludolph, Chawn-Ying Jeng, Alexander H.T. Chu[☆] and Stanley H. Langer*

Department of Chemical Engineering, University of Wisconsin–Madison, Madison, WI 53706 (USA)

ABSTRACT

Degrees of deviation from idealized partition and adsorption retention mechanisms are quantified for reversed-phase liquid chromatographic (RPLC) columns. Rate constants for an *in situ* chemical reaction were measured in octylsilyl and octadecylsilyl bonded stationary phases with a methanol mobile phase. The retention behavior of several types of relevant solute molecules was investigated as a function of chain length and column temperature. With a bonding density of 2.7–3.0 μmol/m^2 on the same support (Beckman Ultrasphere at 200 m^2/g), the chain length (C_8 *vs.* C_{18}) does not appear to impact the retention process, suggesting similar stationary phase characteristics and compositions. However, increased temperature tends to shift retention behavior toward adsorption. The degree of hydrocarbon ligand participation in retention and the phase ratio were also determined to provide a more complete description of the stationary phase composition in RPLC.

INTRODUCTION

Although many retention mechanisms have been proposed for reversed-phase chromatography [1–7], most fall within the two broad categories of partition and adsorption. Experimentally, retention mechanisms have generally been studied by observing retention behaviors of various compounds, often members of homologous series. Subsequently, important system parameters such as mobile phase composition and polarity, bonded-phase chain length and density, and temperature have been varied systematically to infer molecular information about the stationary phase environment [8–16]. Because conventional chromatographic retention studies often fail to provide the information needed to distinguish between theories, much recent experimental work has focused on alternative approaches for obtaining information about the stationary phase. These encompass the use of spectroscopic techniques such as NMR, IR and fluorescence spectroscopy [17–23] as well as *in situ* chemical reaction methods [24–26].

During an investigation of the base-catalyzed methanolysis of tetrachloroterephthaloyl chloride ($TCTPCl_2$) on a reversed-phase liquid chromatographic (RPLC) column with an octadecylsilane (C_{18}) bonded phase, it was observed by Bolme and Langer [24] that this reaction proceeded faster than might be explained by reaction occurring in the mobile phase volume alone. Since chemical reaction apparently was occurring in the stationary phase, it was suggested that such reaction might provide a probe for characterizing the stationary phase environment. In a subsequent study by Chu and Langer [25], information about the bonded C_{18} phase was inferred by evaluating stationary phase rate

* Corresponding author.
☆ Present address: Abbott Laboratories, N. Chicago, IL 60064, USA.

0021-9673/94/$07.00 © 1994 Elsevier Science B.V. All rights reserved
SSDI 0021-9673(93)E0884-W

ห้องสมุดกลางมหาวิทยาลัยศิลปากร

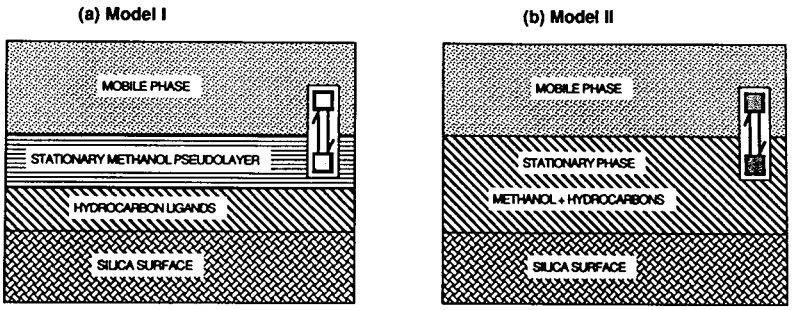

Fig. 1. Molecular retention in RPLC. (a) "Model I". Solute molecules interact with a methanol "pseudo-layer" without direct participation of bonded hydrocarbon ligands. (b) "Model II". Solute molecules interact through a dispersion type of mechanism with a composite stationary phase of methanol sheathing bonded hydrocarbon ligands.

constants, which were then compared with what might be expected from the extreme, generalized retention mechanisms of Knox and Pryde [2] (adsorption type, Fig. 1a) and Yonker *et al.* [3,4] (partition type, Fig. 1b). The observed rate constants fell between the two models, but much closer to the partition type model. It also appeared that temperature increase tended to shift the retention mechanism toward the adsorption model. Later, the phase ratio of the bonded-phase system was deduced through measuring reaction kinetic measurements for both mobile and stationary phases [27].

In this investigation, the bonded stationary phase of interest is octylsilane (C_8), and reaction kinetics in liquid chromatographic columns have been measured and analyzed in a fashion analogous to that with the earlier bonded phase. These experiments were performed to attempt to answer the following questions: (1) does the shorter chain length in C_8 relative to C_{18} significantly influence the retention mechanism in these systems? and (2) can the temperature effects observed in the C_{18} investigation also be observed with C_8 packings? In addition, the phase ratio and the degree of hydrocarbon ligand and associated methanol participating in retention were evaluated to determine phase compositions for these bonded-phase systems.

THEORY

In a chromatographic reactor for kinetic studies, a reactant is injected as a pulse onto a column where it proceeds to form product(s) while passing through the column [28,29]. If an inert reference material, I, is added to the reactant mixture it has been shown that for first-order reactions [28,29]

$$\ln\left(\frac{A_R}{A_I}\right) = \ln\left(\frac{A_R}{A_I}\right)_{t=0} - k_{app}t_R \quad (1)$$

where A_R and A_I are peak areas of reactant and inert standard, t_R is the reactant retention time, and k_{app} is the apparent rate constant for the column.

The apparent rate constant is related to rate constants in the mobile and stationary phases, k_M and k_S, by

$$k_{app} = k_M\left(\frac{t_M}{t_R}\right) + k_S\left(\frac{t_S}{t_R}\right) \quad (2)$$

A plot of ln (A_R/A_I) *vs.* t_R gives a straight line slope $-k_{app}$ from eqn.1. Since the residence time ratio between the mobile and stationary phases t_M/t_S is constant for a given chromatographic separation, k_M and k_S cannot be decoupled simply by flow-rate variation. Where k_M is known (*e.g.* from batch kinetic experiments in pure mobile phase), k_S can be determined using eqn. 2.

Once the stationary phase rate constant has been determined experimentally for a given set of conditions, it can be compared with values from proposed models. For this purpose, two generalized retention mechanism models compared and discussed by Chu and Langer [25] for characterization of the C_{18} phase are used here.

EXPERIMENTAL

Liquid chromatographic system

The basic liquid chromatographic array was similar to the one described earlier and operated in a similar manner [25] except that PTFE tubing [8 in. × 1/8 in. I.D. (1 in. = 2.54 cm), with 10 μm solvent filter] connected the pump inlet and the mobile phase reservoir. Approximately 4 ft. (1 ft. = 30.48 cm) of this tubing were submersed in a constant-temperature water bath as a pre-warming stage for the mobile phase. The HPLC pump outlet was connected to the injector with 10 ft. × 1/16 in. O.D. × 0.020 in. I.D. stainless-steel tubing. Approximately 6 ft. of this tubing were submerged in the constant-temperature water bath to bring the mobile phase to a temperature closer to that of the columns. A 0.5-μm pre-column filter was placed before the two analytical chromatography columns in series.

The liquid chromatographic columns of this study, 2 × (25 cm × 4.6 mm × 5 μm) Altex Ultrasphere Octyl (C_8) were connected as before [25]. Two columns in series gave good separation of reactants and products. Each column contained 3.2 g of 5-μm particles with surface area 200 m^2/g and average pore diameter of 80 Å. The C_8 columns used here are 6.4% (w/w) carbon and 2.7 μmol/m^2 bonded phase ligand [30]. Both types of packings were derivatized with monochlorodimethyl alkylsilanes to give monofunctional coverage. The columns were housed in glass water jackets (25 cm × 20 mm O.D. × 18 mm I.D.) insulated with approximately 3/4 in. layer of glass wool type insulation held in place by aluminum foil.

Reagents and kinetic measurements

Reagents and their preparation have been described earlier [25].

Kinetic studies of $TCTPCl_2$ methanolysis reaction with pyridine and 4-picoline catalysts were performed in the two C_8 column array at both 25 and 35°C. The columns were first equilibrated with the mobile phase for at least 1.5 h at approximately 0.9 ml/min flow-rate, corresponding to about 25 column volumes. The reactant mixture (*ca.* 0.24 m*M* $TCTPCl_2$, 26 m*M* 1-phenyloctane inert standard and 0.2 *M* tetrahydrofuran in methanol) was prepared immediately before injection to prevent experimental variations in the extent of uncatalyzed reaction. About ten experiments (flow-rates ranging from 0.1 to 0.9 ml/min) were performed at each temperature with several different catalyst concentrations. In addition to the columns, the other difference between C_8 and C_{18} experiments [25] was the use of a smaller sample loop size, 5 μl for C_8 and 20 μl for C_{18}.

Determination of associated methanol volume in the stationary phase

The amount of associated stationary phase methanol for the C_8 columns was determined in a manner similar to that for C_{18} columns [25] (see also refs. 3, 4, 32, 33). The total system volume between the pump drawoff valve and detector inlet was determined by equilibrating the system with methanol at 0.9 ml/min at the specified temperature for at least 1 h. The UV detector inlet fitting was then disconnected and the total system methanol volume flushed into a 100-ml volumetric flask, containing 10.0 ml of absolute ethanol internal standard. Flushing was performed with dioxane at 0.5 ml/min for GC analysis. No residual methanol was found in a second 100-ml aliquot. The volume of methanol associated with the stationary phase, V_{MeOH}, is given by

$$V_{MeOH} = V_{T,MeOH} - (V_M + V_{EC}) \quad (3)$$

where $V_{T,MeOH}$ is the total amount of methanol between the pump and detector inlet, V_M is the column mobile phase volume plus all dead volumes between the injector and detector inlet found from the unretained species method (Uracil) and V_{EC} is the extracolumn dead volume between the pump and injector. The injector inlet was disconnected and the extracolumn volume was measured after equilibrating it with methanol which was then flushed with dioxane into a 25.0-ml volumetric flask containing 2.5 ml ethanol internal standard.

A Hewlett-Packard (HP) 5890A gas chromatograph with a thermal conductivity detector was used for the "associated stationary phase methanol" determination. The column used was

297–177 μm diameter Poropak Q packed in 180 cm × 2 mm O.D. × 0.6 mm I.D. Pyrex coiled to fit the apparatus. The column wall was silylated to quench residual silanol groups which tend to cause peak tailing. Samples of 0.1 μl containing methanol and dioxane diluent were injected at 28.5 ml/min helium carrier flow and 160°C oven temperature. Starting at 2.5 min after injection, the oven temperature was programmed at a rate of 70°C/min until it reached 230°C to facilitate dioxane elution. An HP 3396A recording integrator was used for collecting and analyzing data.

RESULTS AND DISCUSSION

A typical series of liquid chromatographic reactor chromatograms for the first step in the base-catalyzed methanolysis of $TCTPCl_2$ for the C_8 system are illustrated for 4-picoline in Fig. 2.

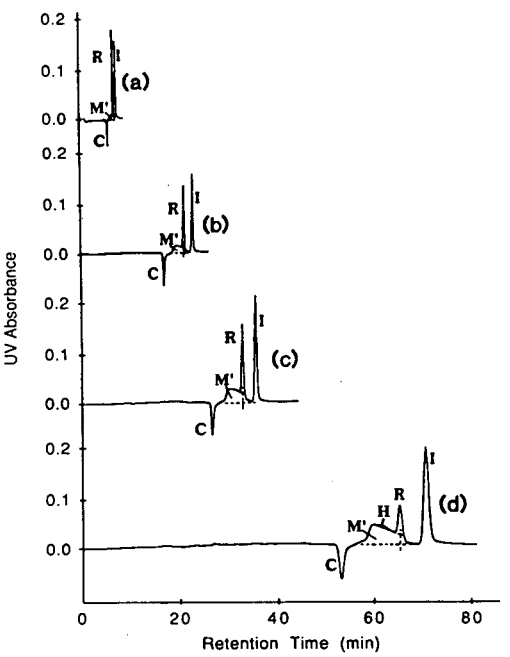

Fig. 2. Series of liquid chromatograms for first step in $TCTPCl_2$ (R) esterification catalyzed by 6.07 m*M* 4-picoline in methanol at 25°C (see eqn. 4b). The chromatographic system consists of two 25 cm × 4.6 mm Altex Ultrasphere Octyl (C_8) columns in series; mobile phase flow-rates (ml/min) were: (a) 0.995, (b) 0.33, (c) 0.228 and (d) 0.114. M′ = Quaternary salt; I = inert standard; C = catalyst vacancy peak from injection; H = methanolic half ester impurity.

These resemble those for the C_{18} system of Chu and Langer [25]. Mechanistic details for the complete methanolysis of $TCTPCl_2$ were studied previously [31]. In the present study, we are considering only the first steps in the organic base-catalyzed sequence:

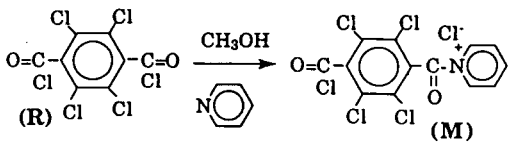

(4a)

and

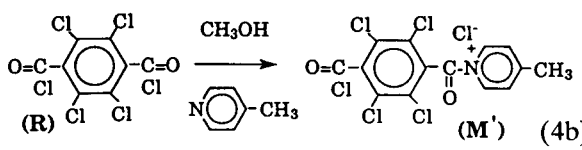

(4b)

Here $TCTPCl_2$(R) reacts with base (pyridine or 4-picoline) to form the quaternary ammonium salt (M or M′) intermediate which is stabilized by solvating methanol [31]. The reaction is second order, first order in reactant and first order in catalyst. As Illustrated in Fig. 2 for 4-picoline, quaternary ammonium salt product M′ forms as a continuous "wave" which grows with increasing retention time or decreasing flow-rate. The indicated methanolic half ester product H, Me,Cl-TCTP is original sample impurity conveniently manifested and separated from R as a "bump" on the product wave. The identity of this peak was confirmed in both C_8 and C_{18} experiments through comparison of retention times with those of isolated half ester prepared earlier in our laboratories. The small, albeit significant, product interference correction is indicated in Fig. 2.

Determination of amount of methanol associated with the stationary phase

For model predictions of the stationary phase rate constants, the amount of methanol associated with the stationary phase had to be determined. Procedural details for this adapted from Westerlund and Theodorsen [32], McCormick and Karger [33], and Yonker *et al.* [3,4] are discussed in the Experimental section. Table I

TABLE I

VOLUMES ASSOCIATED WITH ULTRASPHERE OCTYL AND OCTADECYL STATIONARY PHASES

Columns, 25 cm × 4.6 mm I.D.

Phase	Temperature (°C)	Methanol associated with stationary phase (see Experimental), V_{MeOH} (ml/column)	Hydrocarbon volumes in stationary phase based on %C, V_{HYD} (ml/column)	Calculated methanol molecules per bonded hydrocarbon chain
C_8	25	0.23 ± 0.06	0.225 [30]	3.3
	35	0.26 ± 0.07	0.225	3.7
C_{18}[a]	25	0.56 ± 0.07	0.50	7.2
	35	0.64 ± 0.06	0.50	8.1
$V_{MeOH}(C_{18})/V_{MeOH}(C_8) = 2.43 \pm 0.71$ (at 25°C), 2.46 ± 0.70 (at 35°C)				

[a] Adapted from ref. 25.

presents a summary of volumes of methanol associated with the stationary phases of interest in this work. Included are volumes of methanol associated with the stationary phase at two temperatures for the two systems determined by GC, as well as the hydrocarbon volumes of the stationary phases estimated from percentage carbon loading and density data. It can be noted that the ratios of $V_{MeOH}(C_{18})/V_{MeOH}$ (C_8) are approximately the same for 25 and 35°C and are about equal to 18/8 or 2.25, the ratio of bonded ligand chain lengths. This would indicate that the methanol volume extracted into the stationary phase is approximately proportional to the bonded phase ligand volume over the C_8 to C_{18} range. This result is not obvious. Several investigators [3,34,35] found that the eluent volume extracted into the stationary phase was *not* proportional to the carbon chain length for mixed aqueous–organic eluents. For pure organic eluent systems of the type used here, it would appear that hydrocarbon ligands are sufficiently solvated by methanol to establish a stable methanolic sheath around these chains. The methanol extracted into the stationary phase, then, indeed might vary in direct proportion to total bonded ligand volume (*i.e.* increasing with chain length for a constant degree of surface coverage).

Actually, the number of associated methanol molecules per bonded hydrocarbon chain (C_8 or C_{18}) can be calculated:

$$N_{MeOH} = \frac{V_{MeOH} d_{MeOH} / M_r\,(= 32\,\text{g/mol})}{3.2\,\text{g} \times 200\,\text{m}^2/\text{g} \times \text{surface coverage}\,(\text{mol/m}^2)} \quad (5)$$

where d_{MeOH} is the density of methanol at either 25 or 35°C. As shown in Table I, there are approximately 7.2–8.1 methanol molecules associated with each C_{18} ligand *versus* 3.3–3.7 molecules with the C_8 ligand. Considering the molecular volumes of both methanol (67.6 Å^3) and the straight chains of C_8 (*ca.* 220 Å^3) and C_{18} (*ca.* 430 Å^3), the bonded hydrocarbon moieties may be visualized as essentially covered by the intercalated methanol to provide a "liquid" layer or sheath. For the model system here, it is likely that this layer acts as the effective partition medium for solute retention as Dorsey and coworkers have indicated [6,14].

In the stationary phase formation scenario postulated by Yonker *et al.* [3,4], methanol binding to residual surface silanol groups is believed to be a driving force for stationary phase development in RPLC. Under completely non-aqueous conditions methanol access to the silanol surface is expected to be roughly the same for both C_{18} and C_8 systems. This has been described as "unzipping" of the C_{18} chains to form a brush-like structure, with hydrocarbon ligands more or less extended and perpendicular to the surface [3–5]. A consequence is an in-

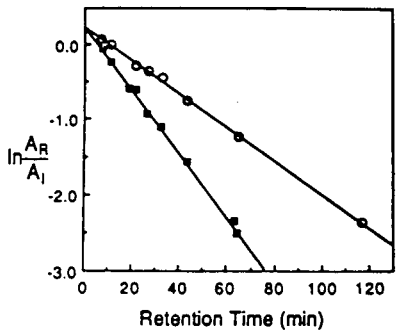

Fig. 3. First-order plot: area ratio A_R/A_I *vs.* reactant retention time on a semilogarithmic scale for $TCTPCl_2$ reaction in a C_8 system with 6.07 m*M* 4-picoline in mobile phase at 25°C (○) and 35°C (□).

crease in C_{18}–methanol Van der Waals dispersion interactions (compared to mixed aqueous systems) with a concomitant increase in total methanol brought into the stationary phase. Observing an associated methanol volume approximately proportional to ligand chain length suggests that the ligand–methanol dispersion interactions with C_{18} ligands resemble those of the more restricted C_8 chains.

Calculation of rate constant values in the stationary phase

The apparent rate constant k_{app} was determined from first-order plots of logarithm of A_R/A_I *vs.* reactant retention time as illustrated for 4-picoline in Fig. 3. Peak areas were measured by planimetry because of the need for correction from product overlap in the reactant area [25,36], as well as the lack of a software package for this specialized integration. Effects from internal diffusion and sorption kinetics have been shown to be negligible for this system [37].

The experimental rate constants for the stationary phase, k_S, as calculated from eqn. 2 are shown in Table II (25°C) and Table III (35°C). The stationary phase rate constants based on model I and model II calculated as explained earlier (eqns. 16 and 17 in ref. 25) are provided in these tables for comparison. Because values for the proposed model I and II rate constants vary with experimental conditions, a test statistic Y was used to quantitatively treat the effects of experimental variables on solute retention mechanism:

$$Y = \frac{[k_S - (I + II)/2]}{[(II - I)/2]} = 1 \quad \text{if} \quad k_S = k_S(II)$$
$$-1 \quad \text{if} \quad k_S = k_S(I) \qquad (6)$$

where I and II correspond to the stationary phase rate constants predicted by models I $[k_S(I)]$ and II $[k_S(II)]$, respectively. The test statistic Y is useful because it is dimensionless and independent of chemical kinetics; linear interpolation from model predictions is used to obtain the experimental Y value.

Comparison of experimental and model predicted stationary phase rate constants in Table II (25°C, C_8 system) supports a generalized retention mechanism involving the bonded C_8 ligands with associated methanol pseudo-layer. This is because although the experimental

TABLE II

STATIONARY PHASE RATE CONSTANTS AT 25°C IN THE C_8 SYSTEM, EXPERIMENTAL AND MODEL PREDICTIONS

Base catalyst	Base concentration (m*M*)	Batch k_M (10^{-4} s^{-1})	k_S (10^{-4} s^{-1})			Test statistic *Y*
			Experimental	Model I	Model II	
4-Picoline	6.07	4.02 ± 0.06	2.90 ± 0.07	6.52 ± 1.37	1.65 ± 0.58	0.49
	8.18	5.42 ± 0.09	3.55 ± 0.47	8.79 ± 1.85	2.23 ± 0.78	0.60
Pyridine	4.98	1.44 ± 0.05	0.64 ± 0.11	1.86 ± 0.39	0.47 ± 0.17	0.76
	5.10	1.47 ± 0.06	0.62 ± 0.07	1.91 ± 0.40	0.48 ± 0.17	0.81
	7.35	2.12 ± 0.08	0.89 ± 0.15	2.75 ± 0.58	0.70 ± 0.24	0.81
	7.55	2.18 ± 0.08	0.79 ± 0.06	2.82 ± 0.59	0.72 ± 0.25	0.93

TABLE III

STATIONARY PHASE RATE CONSTANTS AT 35°C IN THE C_8 SYSTEM, EXPERIMENTAL AND MODEL PREDICTIONS

Base catalyst	Base concentration (mM)	Batch k_M (10^{-4} s^{-1})	k_S (10^{-4} s^{-1})			Test statistic Y
			Experimental	Model I	Model II	
4-Picoline	2.93	3.46 ± 0.06	3.27 ± 0.16	5.00 ± 1.05	1.42 ± 0.50	−0.04
	4.12	4.86 ± 0.08	3.69 ± 0.24	7.03 ± 1.48	2.00 ± 0.70	0.33
	6.07	7.16 ± 0.11	6.36 ± 0.18	10.35 ± 2.17	2.94 ± 1.03	0.08
Pyridine	4.98	2.54 ± 0.10	2.34 ± 0.09	2.93 ± 0.62	0.83 ± 0.29	−0.44
	7.55	3.85 ± 0.15	3.15 ± 0.13	4.44 ± 0.93	1.26 ± 0.44	−0.19

stationary phase rate constants fall between the two model extremes, they are always closer to model II at 25°C. The data of Table III (35°C, C_8 system) further support a stationary phase operating with features between models I and II, but now shifting toward model I. These findings are consistent with the results of others [6,7,22,23]. Effects on retention models from variation of temperature, alkyl chain length, catalyst type and concentration are discussed below.

Effect of temperature

The retention mechanism for C_8 apparently shifts away from model II (partition type) toward model I (adsorption type) with a temperature increase from 25 to 35°C, consistent with a similar shift toward model I with increasing temperature observed for the earlier C_{18} stationary phase [25]. Fig. 4 shows a Y *vs.* temperature plot for all data in both studies. The C_8 and C_{18} data are plotted with different symbols and artificially spread apart on the temperature axis to allow comparison (all data were taken at either 25.0 or 35.0°C). Although the data scatters are admittedly large, the retention mechanism shift with temperature change is marked. The lower stationary phase volume for C_8 may well explain greater scatter than with C_{18}. In Table I, the amount of methanol associated with the C_8 stationary phase was found to increase slightly with temperature, similar to the trend found with C_{18}. An increase in thermal energy imparted to the bonded phase ligands at 35°C was postulated to induce chain stretching with accompanying increase in ligand–methanol dispersive interactions [25]. The experimentally determined rate constants might well be indicating that solute molecules preferentially interact with methanol molecules to shift retention toward model I behavior.

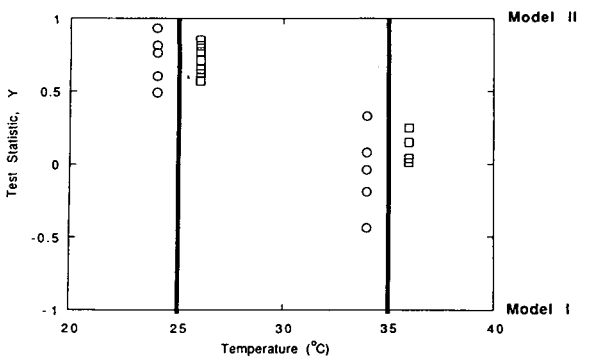

Fig. 4. Plot of test statistic Y values (see eqn. 6) *vs.* temperature. ○ = C_8; □ = C_{18}.

Although the temperature effect is difficult to interpret, there may well be one or more interacting factors worthy of consideration. The most plausible are discussed below:

(a) Heat-induced structural changes in the bonded phase layer were suggested by Hammer and Verschoor [16] and Yang and Gilpin [38] for aqueous conditions. For the octyl surface, a sigmoidal change was observed to occur at approximately 40°C (discontinuity temperature). For the octadecyl surface, this "transitional temperature" would probably increase to ≥70°C [15,17]. Since operational temperatures here are lower than 40°C, the structural change may not be significant enough to account for all retention behavior changes. Of course, the extent of

change also might be related to bonded chain density (surface coverage) and mobile phase composition differences. However, with the methanol environment here, the amounts incorporated into the bonded octyl and octadecyl layers are relatively constant from 25 to 35°C (see Table I), suggesting a structurally similar surface. Therefore, the magnitude of the retention change from 25 to 35°C indicated in Fig. 4 cannot be explained simply by conformational shift (or folding and unfolding of bonded ligands) resulting from temperature change.

(b) Adsorption interaction with residual silanol groups has been frequently invoked in RPLC literature to explain retention behavior observations [11,39–42]. For the octyl-modified silica surface, thermally induced reordering and/or resolvation has been shown by Gilpin and Wu [43] to be a function of microscopic silanol distribution. Retention contributions from silanophilic interactions have been postulated to be a function of the surface coverage (density) of bonded ligands [23,44]. For surface coverages between 2.7 and 3.0 μmol/m^2 studied here, about one third of maximum lateral packing density (8.1 μmol/m^2) in alkane crystals [6,7], steric constraints among neighboring bonded ligands would tend to force ordering or chain molecule alignment normal to the silica surface, thus facilitating solute access to the silanol functionalities. Therefore, it is possible that silanol groups act as "active sites" to bind both methanol and product base (M or M′, pyridinium chloride type of quaternary intermediate salt) molecules to provide a mixed or dual mechanism [45] manifested by the shifting between model I (adsorption) and model II (partition) with changing thermal conditions. With temperature increasing from 25 to 35°C and the increased thermal energy favoring straightening of the bonded ligands, the silanol interactions became more important through improved access of product molecules to silica surface functionalities.

Effect of alkyl chain length. Bonded alkyl chain length does not appear to be a major influence on retention mechanism over the range of experimental conditions here. This may be due to the relatively small solute probe size, so that the bonded ligand chains with their methanolic sheaths here would be sufficiently deep for solute immersion in the stationary phase environment. This observation is consistent with Tchapla *et al.* [46] who observed no marked change in selectivity when solute alkyl length was shorter than those of bonded hydrocarbon ligands. Although there is a difference in motional freedom with the alkyl chain distance from the silica surface for C_8 relative to C_{18} [47], the overall retention behavior based on kinetic analysis showed little impact of mobility on solute retention. Similar retention behavior for small solutes in a comparison between C_8 and C_{18} phases was observed by Melander *et al.* [11] in their study of retention energetics on alkyl bonded stationary phases using unmodified methanol eluent, but not with C_2 alkyl groups. In contrast to these short, highly restricted chains, C_8 chains are probably long enough to permit the same types and degrees of dispersion interactions with solute/solvent molecules observed in the C_{18} stationary phase.

Similarity of retention behavior for alkyl chain lengths greater than eight carbons has been discussed by others [6,7,48]. Comparable stability behavior for chain length greater than C_8 has also been reported [49]. Depending on size and polarity of solute and solvent composition, critical chain lengths can vary from seven to fourteen carbons [13,50,51] in terms of specific underlying retention mechanisms. However, it seems reasonable to conclude that reversed-phase chromatographic retention is generally a partition process [6,7], whereas adsorption is an extreme situation resulting from low surface hydrocarbon coverage [14] or short carbon chain length relative to solute molecular size [11].

Finally, neither catalyst type nor its concentration appear to have significant effects on the retention mechanism as indicated by the relatively constant Y values over the range of variables covered in this work (Tables II and III). Regression analysis of Y values in the 2^4 factorial design provided additional evidence that these effects are statistically insignificant (both t ratios less than 2). Furthermore, the observed negligible concentration effect provides some assurance that the UV detector response was linear

throughout the high catalyst concentration range.

Interpretation of stationary phase rate constants in terms of the fraction of operative stationary phase ligands and associated methanol. The hydrocarbon ligand volumes used in the model II predictions of stationary phase rate constants were made on the basis of 100% ligands participation in retention, and therefore represent upper limits. If some portion of the ligands did not contribute to the retention mechanism, as a result of steric hindrance or non-uniform sheathing with methanol for example, then the operative ligand fraction would be expected to be lower. However, there is probably an overcompensation for the amount of methanol employed in model predictions. Methanol concentration might well be expected to increase near the mobile phase boundary, and decrease close to the restricted access area of the stationary phase support surface [6,25]. Some methanol extracted into the stationary phase might be unavailable for interactions with solute molecules as a result of steric hindrance or other factors. It, therefore, becomes appropriate to consider any effects from overcompensating for hydrocarbon ligand amounts with associated methanol on model predictions for stationary phase rate constants.

In Fig. 5 a hypothetical plot is presented of model I and II stationary phase rate constants *vs.* associated methanol volume for several different volumes of active hydrocarbon ligands in the C_8 system, using 6.07 m*M* 4-picoline as a typical example. Model I is represented by the uppermost curve, where the volume of active hydrocarbon ligands, V_{HYD}, is essentially zero. Model II represents a situation where 100% of the hydrocarbon ligands (all 0.45 ml from the two Beckman columns) are assumed active and results in the lowest curve. Between these extremes are results from model II predictions where 0.35, 0.25 and 0.15 ml of the total 0.45 ml hydrocarbon ligands in the two columns participate in the retention mechanism. The experimentally determined stationary phase rate constant as determined with eqn. 2 is plotted as a single point at the measured amount of stationary phase methanol (0.46 ml) for comparison. In

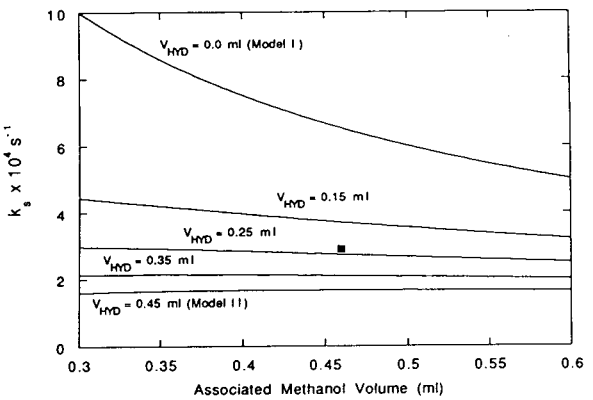

Fig. 5. Expected effects for operative stationary phase hydrocarbon ligands with associated methanol volume on model predictions for the stationary phase rate constant k_S. 6.07 m*M* 4-picoline in the mobile phase, 25°C for the C_8 system; k_S (experimental) = $2.90 \cdot 10^{-4}\ s^{-1}$, denoted by ■; V_{MeOH} = 0.46 ml; V_{HYD} (from %C loading) = 0.45 ml.

Fig. 5, the curve with 0.25 ml of the 0.45 ml hydrocarbon ligands active is seen to pass near the experimentally determined stationary phase rate constant. Therefore, if 100% of the methanol is operative in the retention mechanism, the data for this experiment could be explained by a generalized stationary phase in which about 0.25/0.45 or 0.55 fraction of the hydrocarbon ligands participate in solute retention.

With Fig. 5, it is also seen that the experimentally determined stationary phase rate constant cannot be rationalized on the basis of an overcompensated measure of associated methanol and model II with 100% of the hydrocarbon ligands active. While a smaller associated methanol volume might at first be thought to result in an increase in model stationary phase rate constant, the hydrocarbon ligand dilution effect counterbalances this yielding a model II rate constant which is relatively insensitive to the considered volume of associated methanol. Even using only 0.15 ml of the 0.45 ml stationary phase ligands, the model II predicted rate constant is still a weak function of associated methanol. It seems reasonable, therefore, to disregard non-participating methanol effects in the stationary phase, and to use the measured GC value without correction. The fraction of active hydrocarbon ligand and a fairly good estimate of the

column phase ratio can be calculated, therefore, as described below.

Phase ratio determination in C_8 and C_{18}. An alternative approach to rationalizing the results above is to calculate the phase ratio and "degree of bonded phase ligand participation". The data then would be interpreted using a degree of participation, δ, of bonded phase ligands defined by

$$\delta = (V_S - V_{MeOH})/V_{HYD} \quad (7)$$

where V_{MeOH} is the methanol volume associated with the stationary phase determined by GC and V_{HYD} is the ligand volume calculated from percentage carbon loading and ligand density. The effective bonded phase ligand volume participation in retention then becomes δV_{HYD}. Where $\delta = 1$, ligands participate fully in the retention mechanism and the system is equivalent to the partition type model II. With $\delta = 0$, ligands do not participate in the retention and adsorption type model I is fully operative. Values of δ reflect the fraction of ligands participating in partition.

The phase ratio, ϕ, is then

$$\phi = V_S/V_M = (V_{MeOH} + \delta V_{HYD})/V_M \quad (8)$$

where V_S is the stationary phase volume participating in retention, and V_M is the mobile phase volume determined by either the unretained species or homologous series method. The value of δV_{HYD} can be calculated as shown earlier (eqn. 17 in ref. 27) using V_{HYD}.

Table IV is a summary of δV_{HYD}, V_S and ϕ values from experiments here and earlier [25]. The phase ratio increase resulting from lengthening the bonded ligand chain from 8 to 18 is illustrated in the table. The phase ratio is approximately proportional to bonded phase chain length ($\phi_{C18}/\phi_{C8} = 2.2$ to 3.0) over the 8–18 range studied here. An approximate directly proportional increase can be explained by similar and significant methanol–ligand dispersive interactions in the C_{18} and C_8 stationary phase systems [3,4]. This could be a consequence of the well solvated chains developed in the non-aqueous stationary phase environment of this investigation. Thus, the proportionality between phase ratio and bonded phase chain length results from bonded hydrocarbon volume increase to the surface combined with methanol volume associated with the operative ligand surface area.

It is of further interest to compare the phase ratios here with the capacity factor ratios for the eluites from the C_{18} and C_8 systems as listed in Table V. Void volumes were obtained using Uracil as an unretained species. These retention volumes are essentially independent of temperature and mobile phase composition over the range of the study. The capacity factor ratio between the two columns for these eluites is of special interest. With the retention mechanism of

TABLE IV
PHASE RATIO CALCULATIONS; SUMMARY

Column	Temperature (°C)	Base	Total ligand volume V_{HYD} (ml)	Effective ligand volume δV_{HYD} (ml)	Effective stationary phase volume V_S (ml)	Phase ratio, ϕ
C_8	25	Pyridine	0.45	0.35	0.81	0.16
	25	4-Picoline	0.45	0.24	0.70	0.14
	35	Pyridine	0.45	0.08	0.59	0.12
	35	4-Picoline	0.45	0.15	0.66	0.13
C_{18}	25	Pyridine	1.00	0.49	1.61	0.35
	25	4-Picoline	1.00	0.63	1.75	0.38
	35	Pyridine	1.00	0.43	1.71	0.37
	35	4-Picoline	1.00	0.45	1.73	0.37

TABLE V

SOLUTE RETENTION VOLUMES FOR INDICATED PHASES

Compound	Retention volume (ml)		Capacity factor, k'		Ratio C_{18}/C_8
	C_8	C_{18}	C_8	C_{18}	
$TCTPCl_2$	7.1	9.1	0.38	0.98	2.58
1-Phenyloctane	7.6	10.7	0.47	1.33	2.83
Pyridine	5.8	5.2	0.11	0.13	1.18
4-Picoline	5.9	5.4	0.14	0.17	1.21
Product salts[a]					
Pyridinium salt (M)	6.3	6.6	0.22	0.43	1.95
4-Picolinium salt (M′)	6.5	7.1	0.26	0.54	2.08
Void volume (Uracil)	5.2	4.6	–	–	–

[a]See eqns. 6a and 6b.

any given solute molecule identical for both C_8 and C_{18} stationary phase systems, then we might expect that

$$k'_{C18}/k'_{C8} = \phi_{C18}/\phi_{C8} \quad (9)$$

for that molecule. As can be seen in Table V the capacity factor ratio for the two columns for reactant $TCTPCl_2$ (2.58) and 1-phenyloctane (2.83) inert standard are close to the ratio of the column phase ratios supporting the hypothesis of a similar retention mechanism for these two compounds on these columns.

The capacity factor ratios for catalyst bases pyridine (1.18) and 4-picoline (1.21), on the other hand, are considerably lower than the ratio of column phase ratios. This may well indicate that the retentions for these bases are influenced by residual silanol groups to shift retention mechanisms toward adsorption on the support. Bonded ligand chain length then may also play a role in terms of access. Strong interactions between nitrogeneous bases and residual silanol/siloxane groups on the support frequently are cited to explain irregular retention behavior of these compounds [40] (including significant peak tailing for the two bases used in this study). The capacity factor ratios for the quaternary ammonium salt products (1.95–2.08) fall between those for catalyst bases and reactant/inert standard. Quaternary ammonium compounds also might strongly interact with silanol groups to experience a dual retention mechanism [45]. Eluite interactions with silanol groups are expected to be greater under non-aqueous conditions where such interactions are not moderated by strongly adsorbed water [11,39]. On the other hand, for both C_8 and C_{18} columns, the resultant "relatively polar" quaternary ammonium type products (M or M′) are still retained less than the non-polar compounds ($TCTPCl_2$ and 1-phenyloctane), suggesting non-retention in the bulk bonded phase for the former and that non-specific dispersive interaction between eluite molecules and the bonded hydrocarbon ligand composite phase still dominates retention for the latter. However, the hydrocarbon volume increase from C_8 to C_{18} still resulted in longer retention for the quaternary ammonium salts than for the bases (pyridine and 4-picoline), the capacity factors of which increase little with the change from C_8 to C_{18}.

CONCLUSIONS

It is shown that a kinetic analysis allows a quantitative approach to retention mechanisms for octylsilyl and octadecylsilyl bonded chro-

matographic systems. A dynamic picture involving both stationary phase formation and particular solute interactions emerges. The participation of intercalated methanol with grafted hydrocarbon ligands and sometimes residual silanols gives a complex chromatographic scenario. Results here should assist in formulating a broad-based approach to put retention behavior on a quantitative basis. Although RPLC retention is a function of solvent composition, silica surface bonding chemistry, temperature, etc., it seems reasonable to conclude that it can be considered generally to be a partition process with adsorption becoming operative where possibilities for specific strong interactions become available.

ACKNOWLEDGEMENT

We thank the Army Research Office and the University of Wisconsin–Madison for support of this work. We also are grateful to Dr. Nelson Cooke of Altex (Beckman) for the C_8 columns used for this work. Helpful suggestions from the reviewers are gratefully acknowledged.

REFERENCES

1 H. Colin and G. Guiochon, *J. Chromatogr.*, 141 (1977) 289.
2 J.H. Knox and A. Pryde, *J. Chromatogr.*, 112 (1975) 171.
3 C.R. Yonker, T.A. Zwier and M.F. Burke, *J. Chromatogr.*, 241 (1982) 257.
4 C.R. Yonker, T.A. Zwier and M.F. Burke, *J. Chromatogr.*, 241 (1982) 269.
5 D.E. Martire and R.E. Boehm, *J. Phys. Chem.*, 87 (1983) 1045.
6 J.G. Dorsey and K.A. Dill, *Chem. Rev.*, 89 (1989) 331.
7 K.A. Dill, *J. Phys. Chem.*, 91 (1987) 1980.
8 E.J. Kikta and E. Grushka, *Anal. Chem.*, 48 (1976) 1098.
9 P. Jandera, H. Colin and G. Guiochon, *Anal. Chem.*, 54 (1982) 435.
10 P.J. Schoenmakers, H.A.H. Billiet and L. de Galan, *Chromatographia*, 15 (1982) 205.
11 W. Melander, J. Stoveken and Cs. Horváth, *J. Chromatogr.*, 199 (1980) 35.
12 H.J. Issaq, S.D. Fox, K. Lindsey, J.H. McConnell and D.E. Weiss, *J. Liq. Chromatogr.*, 10 (1987) 49.
13 K.D. Lork and K.K. Unger, *Chromatographia*, 26 (1988) 115.
14 K.B. Sentell and J.G. Dorsey, *J. Chromatogr.*, 461 (1989) 193.
15 R.K. Gilpin and J.A. Squires, *J. Chromatogr. Sci.*, 19 (1981) 195.
16 W.E. Hammers and P.B.A. Verschoor, *J. Chromatogr.*, 282 (1983) 41.
17 R.K. Gilpin, *J. Chromatogr. Sci.*, 22 (1984) 371.
18 R.K. Gilpin and M.E. Gangoda, *Anal. Chem.*, 56 (1984) 1470.
19 D.W. Sindorf and G.E. Maciel, *J. Am. Chem. Soc.*, 105 (1983) 1848.
20 L.C. Sander, J.B. Callis and L.R. Field, *Anal. Chem.*, 55 (1983) 1068.
21 C.H. Lochmuller, A.S. Colborn, M.L. Hunnicutt and J.M. Harris, *J. Am. Chem. Soc.*, 106 (1984) 4077.
22 J.W. Carr and J.M. Harris, *Anal. Chem.*, 59 (1987) 2546.
23 B. Buszewski, Z. Suprynowicz, P. Staszczuk, K. Albert, B. Pfleiderer and E. Bayer, *J. Chromatogr.*, 499 (1990) 305.
24 M.W. Bolme and S.H. Langer, *J. Phys. Chem.*, 87 (1983) 3363.
25 A.H.T. Chu and S.H. Langer, *Anal. Chem.*, 57 (1985) 2197.
26 C.Y. Jeng and S.H. Langer, *J. Chromatogr.*, 556 (1991) 383.
27 A.H.T. Chu and S.H. Langer, *J. Chromatogr.*, 389 (1987) 11.
28 S.H. Langer, J.Y. Yurchak and J.E. Patton, *Ind. Eng. Chem.*, 61 (1969) 10.
29 S.H. Langer and J.E. Patton, in J.H. Purnell (Editor), *New Developments in Gas Chromatography*, Wiley, New York, 1973, p. 293.
30 N.H.C. Cooke and T. Hill, Altex Instrument Co. (Beckman), Berkeley, CA, personal communication, 1986.
31 S.H. Langer, A.H.T. Chu, M.W. Bolme, M.S. Turner and G.R. Quinting, *J Chem. Res.(S).*, (1985) 342.
32 D. Westerlund and A. Theodorsen, *J. Chromatogr.*, 144 (1977) 27.
33 R.M. McCormick and B.L. Karger, *Anal. Chem.*, 52 (1980) 2249.
34 R.P.W. Scott and P. Kucera, *J. Chromatogr.*, 142 (1977) 213.
35 E.H. Slaats, J.C. Kraak, W.J.T. Brugman and H. Poppe, *J. Chromatogr.*, 149 (1978) 255.
36 S.H. Langer and J.E. Patton, *J. Phys. Chem.*, 76 (1972) 2159.
37 A.H.T. Chu and S.H. Langer, *Anal. Chem.*, 58 (1986) 1617.
38 S.S. Yang and R.K. Gilpin, *J. Chromatogr.*, 394 (1987) 295.
39 K.E. Bij, Cs. Horváth, W.R. Melander and A. Nahum, *J. Chromatogr.*, 203 (1981) 65.
40 G.B. Cox and R.W. Stout, *J. Chromatogr.*, 384 (1987) 315.
41 J. Nawrocki and B. Buszewski, *J. Chromatogr.*, 449 (1988) 1.
42 T. Welsch, H. Frank and Gy. Vigh, *J. Chromatogr.*, 506 (1990) 97.
43 R.K. Gilpin and L. Wu, *J. Chromatogr.*, 556 (1991) 415.
44 H. Engelhardt, H. Löw and W. Götzinger, *J. Chromatogr.*, 544 (1991) 371.

45 R.N. Nikolov, *J. Chromatogr.*, 286 (1984) 147.
46 A. Tchapla, H. Colin and G. Guiochon, *Anal. Chem.*, 56 (1984) 621.
47 K. Albert and E. Bayer, *J. Chromatogr.*, 544 (1991) 345.
48 S.J. Schmitz, H. Zwanziger and H. Engelhardt, *J. Chromatogr.*, 544 (1991) 381.
49 M.J.J. Hetem, J.W. de Haan, H.A. Claessens, L.J.M. van de Ven, C.A. Cramers, P.W.J.G. Wijnen and J.N. Kinkel, *Anal. Chem.*, 62 (1990) 2288, 2296.
50 G.E. Berendsen and L. de Galan, *J. Chromatogr.*, 196 (1980) 21.
51 C.H. Lochmüller and D.R. Wilder, *J. Chromatogr. Sci.*, 177 (1979) 574.

Journal of Chromatography A, 660 (1994) 17–23
Elsevier Science B.V., Amsterdam

CHROMSYMP. 2952

Explanation of the selectivity differences between reversed-phase ion-pair chromatographic systems containing trifluoroacetate or heptafluorobutyrate as pairing ion

Miklós Patthy

Institute for Drug Research, Berlini ut 47–49, 1045 Budapest (Hungary)

ABSTRACT

The well documented selectivity differences found between reversed-phase ion-pair chromatographic systems containing trifluoroacetate or heptafluorobutyrate as pairing ion were explained after determining sorption isotherms for trifluoroacetate and heptafluorobutyrate on Nucleosil 100-5 C_{18} from a solution similar to the eluents used for the separation of transmitteramines and peptides. Based on the isotherms and retention data obtained with reversed-phase, ion-exchange and reversed-phase ion-pair chromatographic systems, it is proposed that the selectivity differences between the systems studied are caused by the fact that trifluoroacetate and heptafluorobutyrate are not interchangeable in terms of their surface concentrations at the practical eluent concentrations of the pairing ions concerned.

INTRODUCTION

It was found in earlier studies that, in reversed-phase ion-pair chromatography (RP-IPC), C_4–C_{12}-alkanesulphonate pairing ions are interchangeable in terms of their surface concentrations [1], suggesting that no selectivity difference can be expected in such systems from changing the chain length of pairing ions belonging to the same homologous series.

In view of the well documented selectivity differences between RP-IPC systems with trifluoroacetate (TFA) and heptafluorobutyrate (HFBA) as pairing ion [2–5], the above finding needs some adjustment or addition to explain the observed differences. The need for an explanation is justified also by the fact that both TFA and HFBA have been widely used in the RP-IPC separation and isolation of peptides of natural or synthetic origin [6–10].

To elucidate the basis of the selectivity differences concerned, this work draws on the double-layer sorption (DLS) model of RP-IPC [11], after measuring sorption isotherms for TFA and HFBA on Nucleosil 100-5 C_{18} chromatographic packing material. Selectivity differences are exemplified by the separation of transmitteramines and some acidic metabolites and the separation of some synthetic peptides.

EXPERIMENTAL

The chromatographic system for the separation of monoamine transmitters and some prominent metabolites and also the chemicals used were described in an earlier paper [4]. Of the further compounds separated in this work, 3,4-dihydroxyphenylalanine (DOPA), 6-hydroxydopamine (HODA) hydrochloride and 3-methoxytyramine (MTA) hydrochloride were obtained from Sigma (St. Louis, MO, USA) and the peptides Ac–Ala–Tyr (II), Asp–Phe–Gly–amide (III), Ala–Pro–Val–Arg–Ser–amide (IV), Ala–Phe–Pro (V) and Ala–Phe–Ile–Gly

0021-9673/94/$07.00 © 1994 Elsevier Science B.V. All rights reserved
SSDI 0021-9673(93)E1046-3

(VI) were synthesized in this institute. The strong cation exchanger Mono S HR 5/5 was purchased from Pharmacia LKB Biotechnology (Uppsala, Sweden).

The stationary phase surface concentrations of TFA and HFBA formed from an acetonitrile–aqueous buffer (10:90, v/v) eluent were determined as previously described [12]. The aqueous part of the eluent consisted of TFA or HFBA at various concentrations and 15 m*M* phosphate (with the concentration of each component calculated for the whole of the eluent). The pH of the aqueous part was adjusted to 2.2 with a 2 *M* solution of sodium hydroxide. The eluent concentrations of TFA and HFBA chosen for the determination of the isotherms are given in Table I and Fig. 6. The chromatographic columns and the compositions of the mobile phases are specified in the figure captions.

RESULTS AND DISCUSSION

To demonstrate the selectivity differences between the RP-IPC systems with TFA or HFBA as pairing ion, we plotted the retentions (k' values determined in the usual way) of the transmitteramines, noradrenaline (NA), dopamine (DA) and serotonin (5-HT), the internal standard, α-methyldopamine (MDA), the acidic metabolites, 3,4-dihydroxyphenylacetic acid (DOPAC), 5-hydroxyindolacetic acid (5-HIAA) and homovanillic acid (HVA), and the peptides II, III, IV, V and VI as a function of the TFA and HFBA concentrations in the eluent (Figs. 1–3). The elution orders of the compounds examined, obtained at the most frequently used TFA or HFBA eluent concentrations (10–20 m*M*), were as follows:

in Fig. 1 (TFA system): NA, DA, MDA, DOPAC, 5-HT, 5-HIAA, HVA

in Fig. 2 (HFBA system): NA, DOPAC, DA, 5-HIAA, HVA, MDA, 5-HT

in Fig. 3 (TFA system): IV, III, II, V, VI

in Fig. 3 (HFBA system): II, III, IV, V, VI

The chromatograms of the amines and acidic metabolites in the TFA and HFBA systems are shown in Figs. 4 and 5, respectively.

To explain the selectivity differences demonstrated in Figs. 1–5, we first determined the

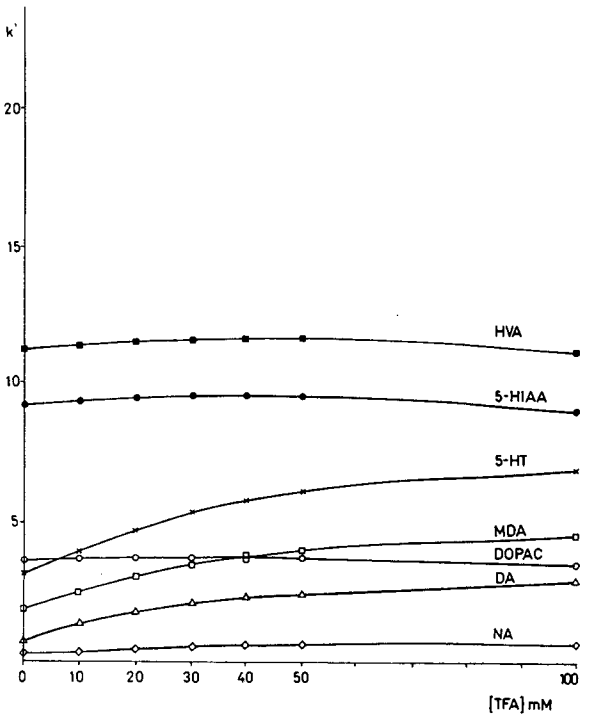

Fig. 1. Dependence of k' values of some amines and anionic metabolites on the concentration of TFA in the eluent. Column, Nucleosil C_{18} (5 μm), 100 × 4.0 mm I.D.; eluent, aqueous buffer (pH 4.15)–acetonitrile (94:6); the aqueous buffer consisted of 0.05 *M* K_2HPO_4, 0.1 m*M* EDTA and 0–100 m*M* TFA (TFA concentration 0, 10, 20, 30, 40, 50 or 100 m*M*). The pH of the aqueous buffer was adjusted with 42.5% (w/v) orthophosphoric acid or 5 *M* potassium hydroxide solution. Flow-rate, 0.83 ml/min. Detection, amperometric. From ref. 4.

surface concentrations of TFA and HFBA on the stationary phase (Nucleosil 100-5 C_{18}, 5 μm, with a BET surface area of 310 m^2/g and a carbon content of 14%) obtained after a 60-min equilibration with the respective eluent (see Experimental), using the elution method and gas chromatography, and also ion-pair extraction (for HFBA), as described in ref. 12. The surface concentrations of the pairing ions (in units of 10^{-8} mol/m^2) and the respective eluent concentrations are given in Table I. The isotherms drawn from the data in Table I are presented in Fig. 6.

As shown by the different elution orders found with the RP-IPC eluents containing TFA or HFBA (see Figs. 1–5), changing the chain length

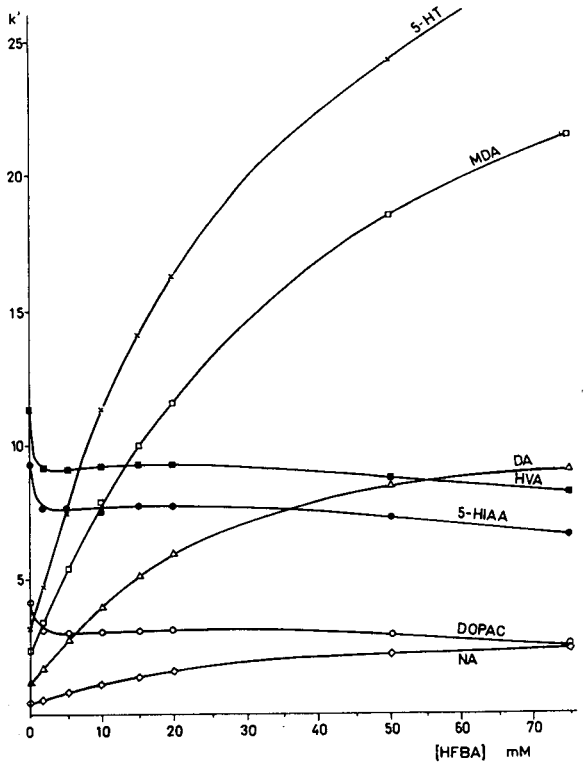

Fig. 2. Dependence of k' values of some amines and anionic metabolites on the concentration of HFBA in the eluent. HFBA concentration in the aqueous buffer: 0, 2, 5, 10, 15, 20, 50 or 75 mM. Other details, without TFA, were the same as in Fig. 1. From ref. 4.

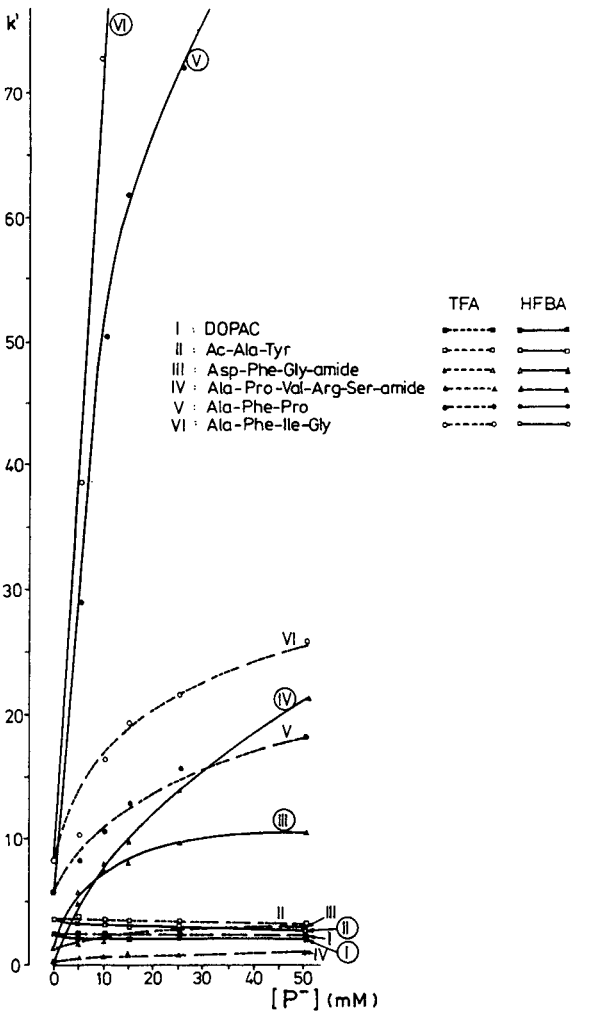

Fig. 3. Dependence of k' values of some synthetic peptides and DOPAC (for comparison) on the concentration of TFA (dotted lines) and HFBA (continuous lines) in the eluent. Column, Nucleosil C_{18} (5 μm), 170 × 4.0 mm I.D.; eluent, aqueous buffer (pH 2.20)–acetonitrile (90:10); the aqueous buffer consisted of 15 mM orthophosphoric acid and 0–50 mM TFA or HFBA (with the concentration of each component calculated for the whole of the eluent). TFA and HFBA concentrations: 0, 5, 10, 15, 25 and 50 mM. The pH of the aqueous buffer was adjusted with 2 M sodium hydroxide solution. Flow-rate, 1.0 ml/min. Detection, UV at 214 nm.

of the pairing ion resulted in a remarkable change in the system selectivity, which is in apparent contrast with the suggestion based on the results obtained for C_4–C_{12}-alkanesulphonate pairing ions [1]. The surface concentration data for the adsorbed pairing ions (which we denote as $[LP^-]$, with reference to the pairing ion, P^-, on the lipophilic adsorbent surface) and the isotherms drawn from them reveal that the $[LP^-]$ range within which TFA and HFBA are interchangeable and, therefore, can be regarded as identical from the point of view of their effect on system selectivity is very limited and too low for HFBA (see Fig. 6).

It should be pointed out that the results in ref. 1 were obtained with salt-controlled RP-IPC systems. However, as our primary aim was to explain the observed selectivity differences between TFA and HFBA systems under chromatographic conditions as close as possible to those applied in practice [typical elution conditions with TFA or HFBA systems used, *e.g.*, for the isolation of peptides include low ionic strength

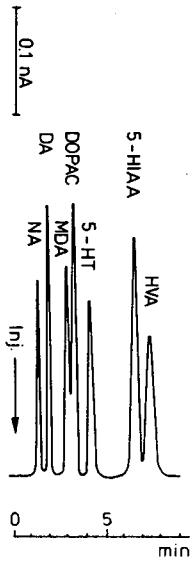

Fig. 4. Separation of some amines and acidic metabolites in a TFA system. Column, Nucleosil C_{18} (5 μm), 80 × 4.0 mm I.D. The TFA concentration in the eluent was 20 m*M*. Other conditions as in Fig. 1.

(<0.025), low pH (1.9–2.2) and an acetonitrile concentration of 0–40% (v/v)], the isotherms for TFA and HFBA were measured from eluents without salt control.

Salt control in the $[P^-]$ range studied would have required a counter ion concentration of at least 200 m*M* at each of the $[P^-]$ levels chosen for the isotherms, and although the results thus obtained might have been more tractable for a rigorous theoretical analysis, they might also have been less meaningful for the explanation of the elution orders found in practice. In addition, a comparison of isotherms for two different pairing ions should lead, in our case, to valid practical conclusions even when the ionic strength of the eluent is not controlled, because the difference between the isotherms measured under the same conditions is usually less affected (especially at lower $[P^-]$ levels) by the counter ion concentration level of the eluent than the position and shape of the individual isotherms themselves (compare the isotherms of two different pairing ions in Fig. 1 in ref. 1 at changing and constant counter ion concentrations).

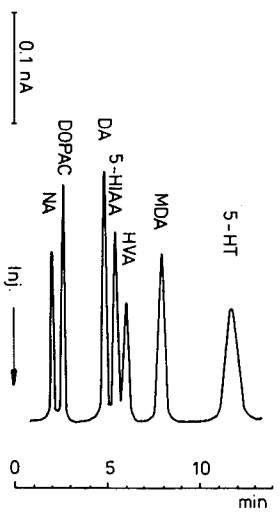

Fig. 5. Separation of some amines and acidic metabolites in an HFBA system. The HFBA concentration in the eluent was 20 m*M*. Column as in Fig. 4. Other conditions, without TFA, as in Fig. 1.

In eluents used for the separation of peptides, both pairing ions are mostly used at a 0.1% (v/v) concentration, which corresponds to an eluent concentration of 12.9 m*M* with TFA and 7.7 m*M* with HFBA. As shown by the isotherms, these eluent concentrations generate $[LP^-]$ levels of *ca.* $1.5 \cdot 10^{-8}$ mol/m^2 for TFA and *ca.* $10 \cdot 10^{-8}$ mol/m^2 for HFBA. It is fairly obvious from its isotherm that the latter $[LP^-]$ level is virtually unattainable with TFA.

The surface concentration of the pairing ion and the ionic strength in the eluent play a major role in determining the "character" of an RP-IPC system. As discussed by Liu and Cantwell [11], in RP-IPC an electrical double layer is formed on the hydrophobic surface of the stationary phase owing to the selective adsorption of the pairing ion used. It was pointed out that retention in such systems is governed both by dynamic ion exchange in the diffuse part of the double layer and adsorption on the electrically charged surface, and that it is the experimental conditions that determine which of the two is the dominant process.

It can be concluded from the discussion that at low ionic strength (<0.1) in the eluent, and at sufficiently high $[LP^+]$ or $[LP^-]$ levels (*e.g.*, at $[LP^+]$ levels between $35 \cdot 10^{-8}$ and $65 \cdot 10^{-8}$ mol/m^2, as tested by the authors), the dominant process governing the sorption of a sample ion is

TABLE I

ADSORPTION OF TFA AND HFBA ON THE STATIONARY PHASE[a] FROM AN ELUENT[b] CONTAINING THE RESPECTIVE PAIRING ION AT VARIOUS CONCENTRATIONS[c]

TFA			HFBA		
$[P^-]$ (mM)	$[LP^-]$		$[P^-]$ (mM)	$[LP^-]$	
	10^{-8} mol/m^2	R.S.D. (%)		10^{-8} mol/m^2	R.S.D. (%)
–	–	–	5	6.6	14.2
10	1.4	21.1	10	11.3	10.4
20	3.4	20.2	20	25.7	9.7
50	3.8	20.8	50	41.7	8.5
100	6.1	16.8	100	54.7	8.6
200	5.7	17.1	200	62.7	8.1

[a] Nucleosil 100-5 C_{18}, 100 Å, 5 μm.
[b] Acetonitrile–aqueous buffer (10:90, v/v); see Experimental.
[c] $[P^-]$ = eluent concentration of the pairing ion (mM); $[LP^-]$ = surface concentration of the adsorbed pairing ion (10^{-8} mol/m^2); R.S.D. = relative standard deviation; for the calculation of n for TFA and HFBA see ref. 12, p. 147.

dynamic ion exchange. The contribution of surface adsorption to the overall chromatographic distribution coefficient is well below 20% in such systems [11].

The ionic strength in both the TFA- and HFBA-containing eluents used for the separation of peptides or other compounds is low (usually less than 0.1). There is, however, a substantial difference of up to an order of magnitude between the $[LP^-]$ levels formed from the eluents, resulting in the consequence that, owing to the very low $[LP^-]$ levels, the conditions in a TFA system favour surface adsorption, whereas the higher $[LP^-]$ levels in HFBA systems increase the chances of dynamic ion exchange.

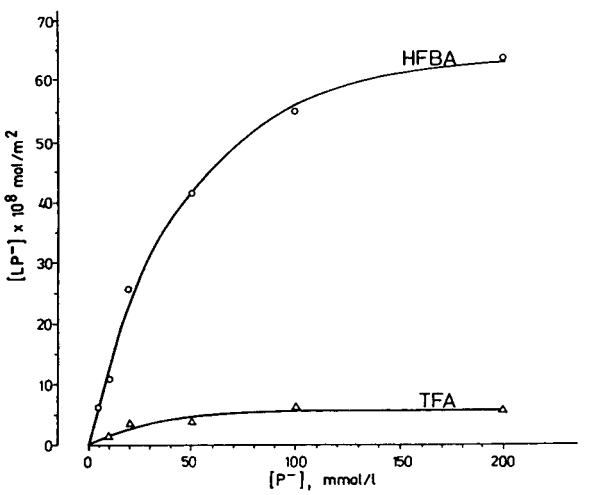

Fig. 6. Adsorption isotherms for TFA and HFBA on Nucleosil 100-5 C_{18}, 5 μm (170 × 4.0 mm I.D.), determined as described in Experimental, and constructed from the data in Table I.

Fig. 7 shows the chromatogram of some amines and acidic metabolites obtained with a simple reversed-phase system, without a pairing ion, but otherwise under the same conditions as those in Fig. 4. A comparison of the elution orders shown in Figs. 4 and 7 reveals essential similarities. Both systems are characterized by a relatively high retention for the acids and lower retention for the amines. It appears that TFA can effectively function as a pairing ion, *i.e.*, can satisfactorily increase the retention of cations, only if the cation concerned is sufficiently hydrophobic and exhibits a k' value of 2 or larger in the corresponding simple reversed-phase system (see the retention behaviour of MDA and 5-HT in Figs. 1 and 4 and the peptides III, V and VI in Fig. 3).

Fig. 8 shows the chromatogram of the same compounds as in Fig. 7 but obtained with a simple ion-exchange system, using the same eluent as in Fig. 7. When the elution orders in

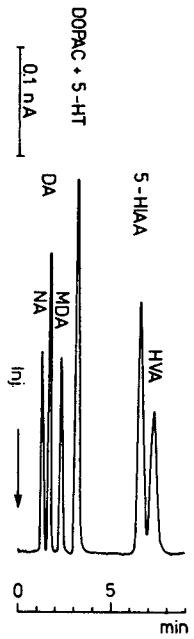

Fig. 7. Separation of some amines and acidic metabolites in a reversed-phase system. Column as in Fig. 4. The eluent contained 20 m*M* nitric acid to replace the pairing ion concentration. Other conditions, without TFA, as in Fig. 1.

Figs. 5 and 8 are compared, similar retention tendencies can be discovered, with an increased retention for most of the amines (NA is an exception) and a decreased retention for the acids, as compared with Figs. 4 and 7. These retention characteristics are stronger with the ion-exchange system because of the higher concentration of the negatively charged groups on the surface of the stationary phase.

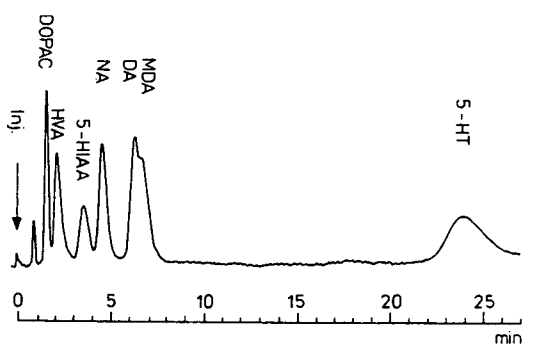

Fig. 8. Separation of some amines and acidic metabolites in an ion-exchange system. Column, Mono S HR 5/5 (10 μm), 50 × 5.0 mm I.D., with an ionic capacity of 0.14–0.18 m*M* per column. Eluent and flow-rate as in Fig. 7. Detection, UV at 274 nm.

The increased significance of dynamic ion exchange in HFBA systems is supported also by the fact that the retention of peptide IV, a compound with two positive charges, increased markedly with increase in the eluent concentration of HFBA, whereas the same compound was very poorly retained in the TFA systems studied (see Fig. 3). The poor retention of the

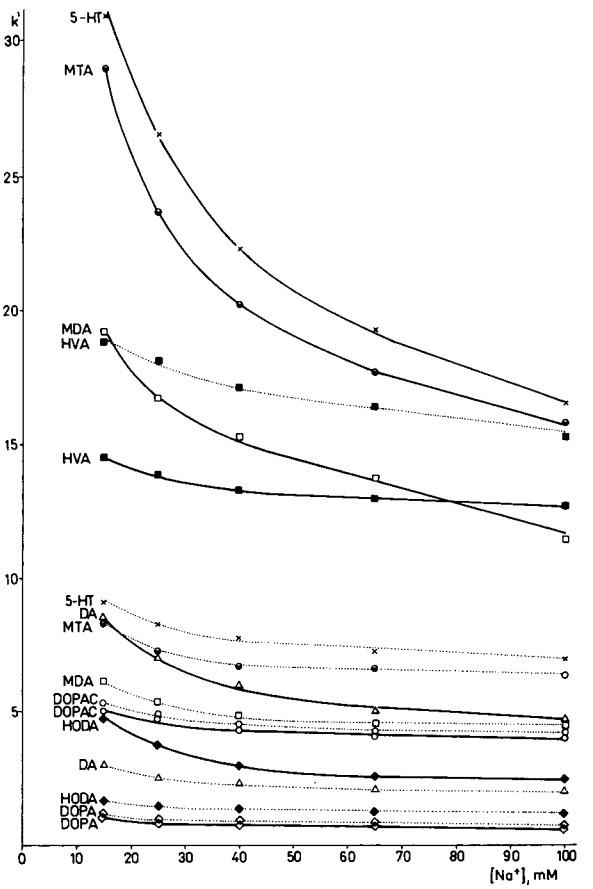

Fig. 9. Dependence of k' values of some amines, acidic metabolites and DOPA on the counter ion (Na^+) concentration in the eluent containing 10 m*M* TFA (dotted lines) or 10 m*M* HFBA (continuous lines). Column as in Fig. 1. The eluent consisted of 3% (v/v) acetonitrile and 97% aqueous component. Na^+ concentrations for the whole of the eluent were 15, 25, 40, 65 and 100 m*M*, adjusted with a calculated volume of 2 *M* sodium hydroxide solution. The pH of the aqueous component was adjusted to 4.25 using orthophosphoric acid (42.5%, w/v). Flow-rate and detection as in Fig. 1.

strongly hydrated, doubly charged cation in the TFA systems bears evidence of the dominance of non-specific surface adsorption with these systems.

Further support of the above distinction between TFA and HFBA systems is provided by Fig. 9. With HFBA systems (continuous lines), the retention of cations (HODA, DA, MDA, MTA and 5-HT) decreased "faster" with increase in the concentration of the eluent counter ion (Na^+) in the range 15–65 m*M* than the retention of the anions (DOPAC and HVA). With TFA systems (dotted lines), however, the difference between the retention behaviour of the cations and anions with increasing counter ion concentration of the eluent was negligible.

CONCLUSIONS

Selectivity differences between RP-IPC systems with TFA and HFBA as pairing ion can be explained by the fact that, as opposed to C_4–C_{12}-alkanesulphonates, the pairing ions concerned are not interchangeable in terms of their concentrations formed on the surface of the stationary phase at practical TFA and HFBA eluent concentrations. Most HFBA systems, depending on the [LP^-] level in the respective system, provide substantial evidence of an increased significance of dynamic ion exchange in governing the retention of a sample ion, whereas TFA systems, in general, are mainly characterized by non-specific surface adsorption.

In the light of the DLS theory, TFA and HFBA systems exhibit different selectivity effects, because the contributions of dynamic ion exchange and surface adsorption to the overall chromatographic distribution coefficient are very different with the two systems.

ACKNOWLEDGEMENTS

The author is grateful to Dr. É. Tomori for the GLC analyses, to Dr. A. Juhász for synthesizing the peptides, to Mrs. E. Blazsek for excellent technical assistance and to Mrs. J. Vámosi and Mrs. E. Tóth for their help in preparing the manuscript.

REFERENCES

1 Á. Bartha, Gy. Vigh, H.A.H. Billiet and L. de Galan, *J. Chromatogr.*, 303 (1984) 29–38.
2 G. Inchauspé, P. Delrieu, P. Dupin, M. Laurent and D. Samain, *J. Chromatogr.*, 404 (1987) 53–66.
3 C.A. Browne, H.P.J. Bennett and S. Solomon, *Anal. Biochem.*, 124 (1982) 201–208.
4 M. Patthy and R. Gyenge, *J. Chromatogr.*, 449 (1988) 191–205.
5 D. Guo, C.T. Mant and R.S. Hodges, *J. Chromatogr.*, 386 (1987) 205–222.
6 H.P.J. Bennett, C.A. Browne and S. Solomon, *J. Liq. Chromatogr.*, 3 (1980) 1353–1365.
7 H.P.J. Bennett, C.A. Browne and S. Solomon, *Biochemistry*, 20 (1981) 4530–4538.
8 H.P.J. Bennett, *J. Chromatogr.*, 266 (1983) 501–510.
9 T. Sasagawa, T. Okuyama and D.C. Teller, *J. Chromatogr.*, 240 (1982) 329–340.
10 M. Patthy, D.H. Schlesinger, J. Horváth, M. Mason-Garcia, B. Szőke and A.V. Schally, *Proc. Natl. Acad. Sci. U.S.A.*, 83 (1986) 2969–2973.
11 H.-J. Liu and F.F. Cantwell, *Anal. Chem.*, 63 (1991) 2032–2037.
12 M. Patthy, *J. Chromatogr.*, 592 (1992) 143–156.

Journal of Chromatography A, 660 (1994) 25–31
Elsevier Science B.V., Amsterdam

CHROMSYMP. 2911

Determination of rate constants in a liquid chromatographic reactor by means of a fitting algorithm

R. Thede* and D. Haberland

Department of Chemistry, University of Greifswald, Soldtmannstr. 23, D-17489 Greifswald (Germany)

E. Below

Institute of Forensic Medicine, University of Greifswald, Kuhstrasse 30, D-17489 Greifswald (Germany)

ABSTRACT

Based on the exponentially modified Gaussian profile, a new equation for the evaluation of product peaks of liquid chromatographic first-order reaction chromatograms is given. It is shown that this equation is able to fit reaction chromatograms corresponding to the linear model of chromatography.

INTRODUCTION

If chromatographic equipment is applied for the determination of rate constants, several methods can be used [1]. It seems that the so-called inert standard method is the most widespread, in which an inert standard is added to the reactant, and then the reactant is converted into one or more products, which are separated from the reactant. The conversion of the reaction can be evaluated from the ratio of the pulse area of the reactant and the inert standard. By variation of the flow-rate of the mobile phase, the duration of the reaction can be varied, and from the correlation between the retention time and the conversion an apparent rate constant can be found.

On the other hand, it may be time consuming to look for a suitable standard. Moreover, the method is suitable only for simple first-order reactions. For complex reactions only a composite rate constant can be determined. Even with a simple first-order reaction, the area of the reactant pulse must be corrected, as it is not possible to separate the reactant and the product completely from each other. Especially in liquid chromatography there may be the problem of comparable rate constants for the chemical reaction and the mass transfer, which makes the determination of statistical moments necessary [2,3].

For these reasons, we decided to develop an analytical function that represents the product curve for simple first-order reaction and for parallel reactions. Unfortunately, the situation becomes more complicated for consecutive reactions, and this aspect will be treated in a subsequent paper.

The derivations were based on the exponentially modified Gaussian (EMG) profile [4], because it is useful for many applications in chromatography [5] and Naish and Hartwell [6] showed its special advantage for liquid chromatography.

MATHEMATICAL MODELLING

The product peak formed by the simultaneous occurrence of chemical reaction and the chro-

* Corresponding author.

0021-9673/94/$07.00 © 1994 Elsevier Science B.V. All rights reserved
SSDI 0021-9673(93)E0877-W

matographic process (dynamic partitioning between the stationary and mobile phases) is the sum of differential product pulses, which are formed one after the other as the reactant pulse passes the column.

The product concentration, which appears at the end of the column at time t, is the sum of those concentration elements dc which are leaving the column together at time t. Every concentration element dc is related to an amount element dm, which is produced when the reactant passes the length coordinate x of the column. The concentration elements can be evaluated from the amount elements by a distribution or peak shape equation, the moments of which (first moment, second and third central moments) in linear chromatography are related to the moments of the pure substances by a linear equation (a list of symbols is given at the end of the paper):

$$dc_P(t,x) = dm_P(x)\Psi_P[\mu_i(x), t] = -\frac{dm_R(x)}{dx}\cdot\Psi_P[\mu_i(x), t]\,dx \quad (1)$$

$$\mu_i(x) = \frac{x}{l}\cdot\mu_{iR} + \frac{l-x}{l}\cdot\mu_{iP} \quad (2)$$

In a simple first-order reaction, we obtain for an amount element dm_P:

$$dm_p = k\,e^{-kt_0(x/l)}\,dx = k'\,e^{-k'(t-\mu_{1P})}\,e^{k'(\mu-t)} \quad (3)$$

In a parallel reaction we find a very similar term:

$$dm_p = k_1\,e^{-kt_0(x/l)}\,dx = k_1'\,e^{-k'(t-\mu_{1P})}\,e^{k'(\mu-t)}$$
$$k = k_1 + k_2 \quad (4)$$

Therefore, it will be possible to transfer the following results given for simple first-order reactions to product peaks from parallel reactions.

Introducing the EMG distribution:

$$\Psi_P(\mu,t) = \frac{1}{\tau}e^{-\frac{1}{2}\left(\frac{\sigma}{\tau}\right)^2}e^{-\frac{\sigma}{\tau}z}\int_{-\infty}^{z}\frac{e^{-\frac{y^2}{2}}}{\sqrt{2\pi}}dy$$
$$z = \frac{t-\mu}{\sigma} - \frac{\sigma}{\tau} + \frac{\tau}{\sigma} \quad (5)$$

for the peak shape equation in eqn. 1, we already have an EMG-based equation for the product curve of irreversible first-order reactions:

$$c_p = k'\,e^{-k'(t-\mu_{1p})}\frac{\sigma}{\tau}e^{-\frac{1}{2}\left(\frac{\sigma}{\tau}\right)^2}e^{k'\sigma\left(\frac{\sigma}{\tau}-\frac{\tau}{\sigma}\right)}I$$

$$I = \int_{z(\mu_{1R})}^{z(\mu_{1P})}e^{k_\sigma z}\int_{-\infty}^{z}\frac{e^{-\frac{y^2}{2}}}{\sqrt{2\pi}}dy\,dz \quad (6)$$

$$k_\sigma = k'\sigma - \left(\frac{\sigma}{\tau}\right)$$

There remains, two problems however: first, there is a contradiction between eq. 2 for the moments of the product peak and the moments of the EMG pulse [4]:

$$\mu_2 = \sigma^2 + \tau^2$$
$$\mu_3 = \frac{\tau^3}{2} \quad (7)$$

It is not possible to fulfil both eqs. 2 and 7 at the same time. The second problem is of a numerical nature: it is not possible to simplify eqn. 6 as long as it is assumed that both σ and τ depend on the length coordinate or, which means the same, as long as it is assumed that σ and τ of the product and the reactant differ markedly. On the other hand, it is not possible to assume simply that they are always equal, because then it will not be possible to fit real reaction chromatograms.

Investigating eqn. 6, it turned out that a larger part of the product curve between the μ_{1R} and the μ_{1P} values is nearly independent of σ and τ as long as the σ and τ values do not differ dramatically. Therefore, we suggest the following procedure. The concentration of the product is evaluated first with the pure σ and τ of the reactant and second with the pure σ and τ of the product. The final concentration will be found by a weighted average according to the equation

$$c_P = t_m c_P(\tau_R, \sigma_R) + (1-t_m)c_P(\tau_P, \sigma_P)$$
$$t_m = \frac{t-\mu_{1P}}{\mu_{1R}-\mu_{1P}} \quad (8)$$

Then the integral I in eqn. 6 can be simplified:

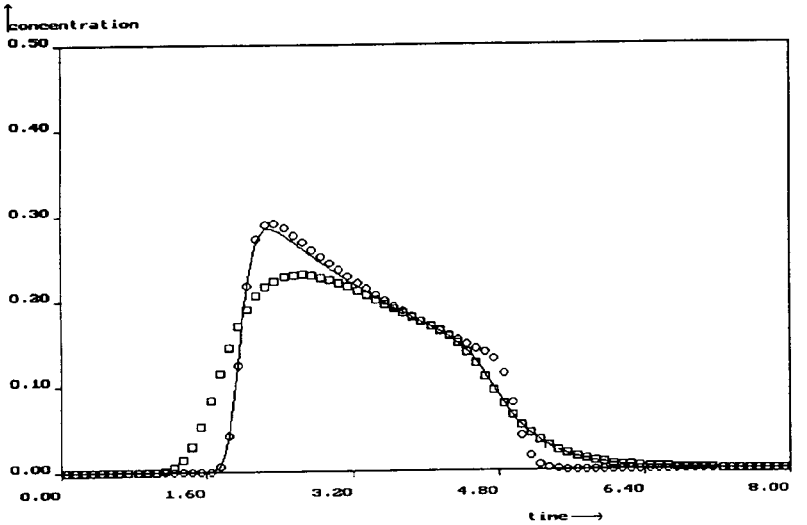

Fig. 1. Composition of the resulting product peak (line) from the product peak with the shape parameters of the reactant (squares) and the product peak with the shape parameters of the product (circles).

$$I = \frac{1}{k_\sigma}\left(e^{k_\sigma z(\mu_{1P})} F[z(\mu_{1P})] - e^{k_\sigma z(\mu_{1R})} F[z(\mu_{1R})] - e^{\frac{k_\sigma^2}{2}} \{F[z(\mu_{1P})] - F[z(\mu_{1R})]\}\right) \quad (9)$$

$$F[z] = \int_{-\infty}^{z} \frac{e^{-\frac{y^2}{2}}}{\sqrt{2\pi}} dy$$

The Gaussian integral function in these terms can easily be calculated by several polynomial approaches [7]. Fig. 1 displays the comparision of the final product peaks according to eqn. 8.

NUMERICAL EVALUATIONS

As there are nearly always reaction chromatograms obtained in which both the reactant and the product are present, the fitting equation has to be a sum of the shape equation for the reactant and the product peak taking into account that there can be different molar detector responses for both species. Therefore, we obtain the following fitting equation:

$$y = f_P(f_R c_R + c_P)$$
$$c_R = e^{-kt_0} \psi(\mu_R, \tau_R, \sigma_R, t) \quad (10)$$

It is obvious that it will not be very simple to fit this nine-parameter equation to the chromatograms. Fortunately, some initial values for the parameters can be taken from the chromatogram (*cf.*, Fig. 2).

The response factors f_P and f_R are calculated from the area ratio of the fitting equations and the chromatogram for selected parts of the chromatogram (in Fig. 2: $t_{22} - t_{23}$ for f_P and $t_{21} - t_{11}$ for f_R). The fitting itself starts then with the selection of the magnitude of the rate constant. Then the parameters are systematically varied using the sequence k, μ_{1P}, σ_P, τ_P, μ_{1R}, σ_R, τ_R.

We used a Turbo PASCAL program for the implementation of this algorithm on a personal computer.

In order to see if our approach meets the model of linear chromatography, we used the method of finite differences to solve the partial differential equations of the linear liquid chromatographic reactor and fitted our equation to the chromatogram numerically evaluated. Fig. 3 shows the very good agreement between the numerical chromatogram and our fitting equation. The results for the moments and the rate constant are given in Table I. There is only one greater deviation concerning the values for the

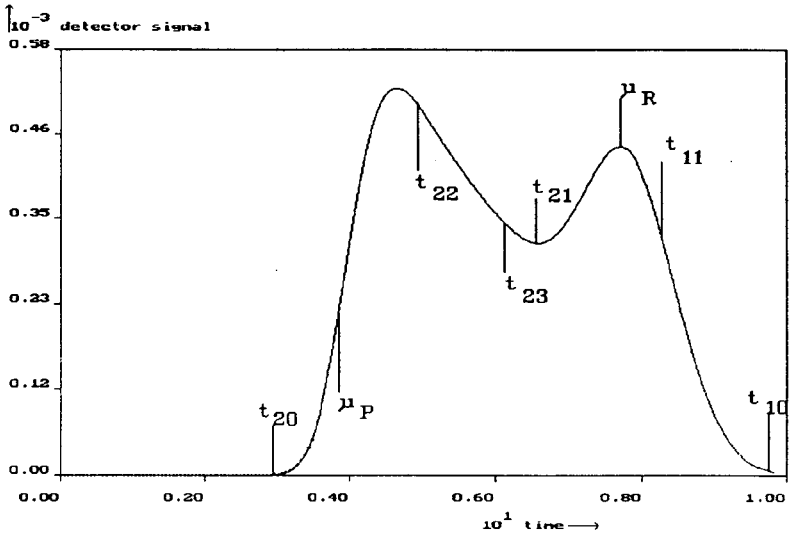

Fig. 2. Essential points in the reaction chromatogram for the estimation of initial values for several parameters t_{20} = Beginning of the fit; μ_P = initial value for μ_{1P}; initial value for σ_P, $\sigma_P = (\mu_P - t_{20})/2$; $t_{22} - t_{23}$ = region for the evaluation of f_P; $t_{21} - t_{10}$ = region for the evaluation of f_R; μ_R = initial value for μ_{1R}; t_{11}, $\sigma_R = t_{11} - \mu_R$.

third moment of the product, but this is due to the fairly symmetric shape of the product pulse.

We can conclude that our equation is well suited for the fitting of reaction chromatograms which are produced by linear chromatographic processes.

EXPERIMENTAL AND RESULTS

We used a modular liquid chromatographic system from GAT (Berlin, Germany), equipped with a 5μm RP-18 column and a GAT PHD 601 UV detector. The hydrolysis of acetic anhydride

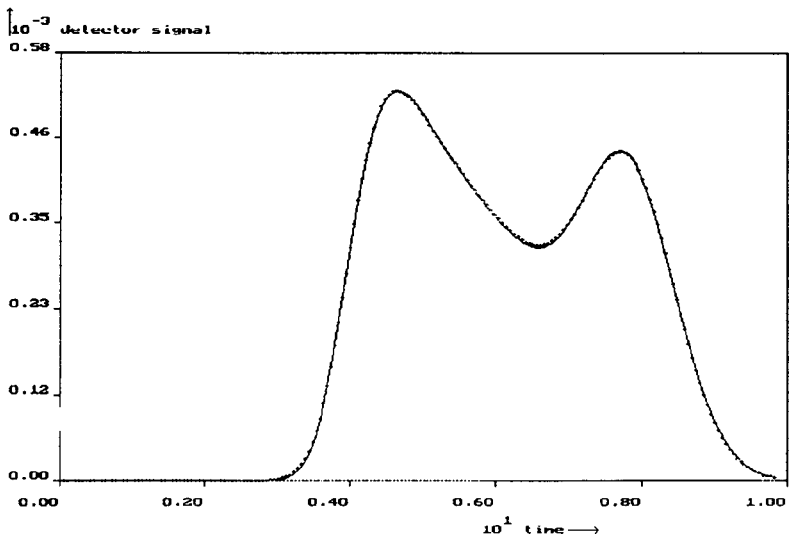

Fig. 3. Best fit (points) of eqn. 10 to a chromatogram numerically evaluated by a finite difference method.

TABLE I

RESULTS OF FITTING EQN. 10 TO A NUMERICAL CHROMATOGRAM

	μ_{1R}	$10\,\mu_{2R}$	$10\,\mu_{3R}$	μ_{1P}	$10\,\mu_{2P}$	$10\,\mu_{3P}$	k
Num.[a]	7.92	3.78	2.08	4.00	1.44	1.04	1.40
Fit.[a]	7.92	3.91	2.15	4.02	1.42	0.08	1.42

[a] Num. = from numerical chromatogram by integration; Fit. = from fitting eqn. 10 to the chromatogram.

was used for the investigation of a first-order reaction. With pure water as the eluent we obtained extremely skewed peaks, which obviously will not be in accordance with the assumptions of linear chromatography. Therefore, we added 20% of methanol to reduce the peak tailing. We used amounts of 0.3 μl of acetic anhydride and varied the flow-rates.

As can be seen from Figs. 4–6, the reactant is contaminated by impurities, which especially interfere with the product pulse. It is not surprising that one of them is obviously acetic acid, as the reaction with the eluent will begin within the sample loop. Because of this distortion of the product peak flank we could not fit the first moment and the EMG peak shape parameters of the product, but took the values from the chromatograms assuming that the acetic acid pulse is nearly a Gaussian.

The essential results of the fittings are summarized in Table II. It can be seen that the apparent rate constants are in agreement over a relatively wide range of conversion. In addition to the results of the numerical evulations, this shows that the application of an EMG-based product profile leads to reasonable results even in difficult cases.

SYMBOLS

c concentration
f_P molar detector response of the product
f_R ratio of molar dectector response of reactant and product
k apparent rate constant
k' $kt_0/(\mu_{1R} - \mu_{1P})$
l column length
m concentration–time area of the peak
P product
R reactant
t time
t_0 dead time
x length coordinate
ψ peak shape function

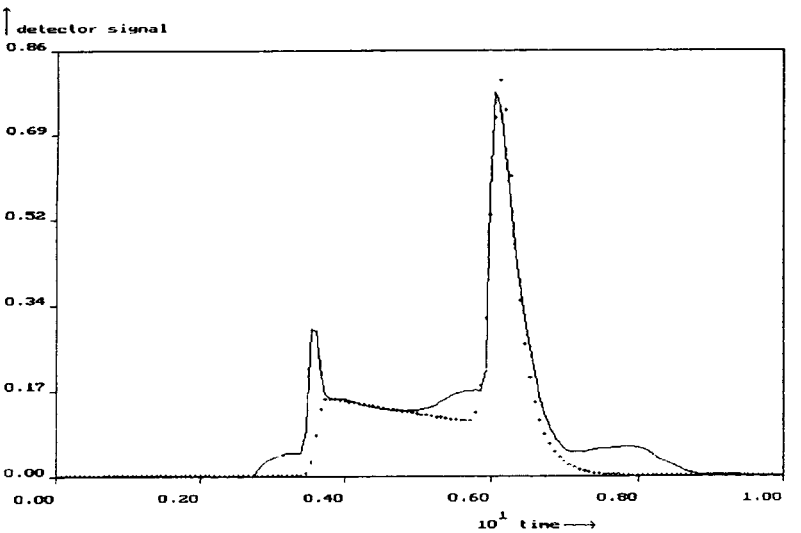

Fig. 4. Hydrolysis of acetic anhydride at a flow-rate of 0.3 ml/min. Points: best fit according to eqn. 10.

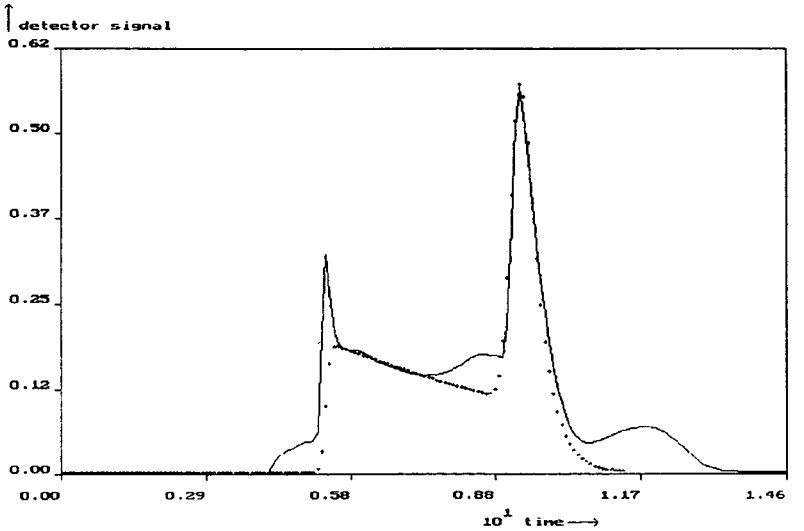

Fig. 5. Hydrolysis of acetic anhydride at a flow-rate of 0.2 ml/min. Points: best fit according to eqn. 10.

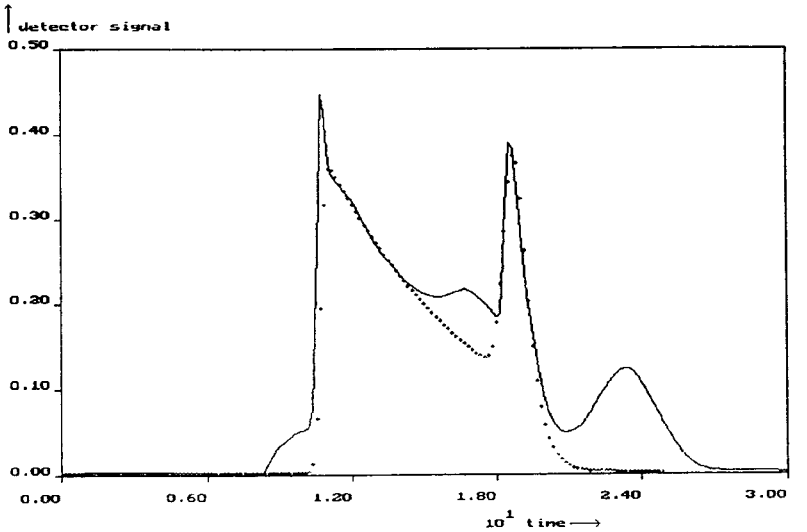

Fig. 6. Hydrolysis of acetic anhydride at a flow-rate of 0.1 ml/min. Points: best fit according to eqn. 10.

TABLE II

RESULTS OF FITTING EQN. 10 TO CHROMATOGRAMS FOR THE HYDROYLSIS OF ACETIC ANHYDRIDE

Flow-rate (ml/min)	Conversion (%)	k (fit)(min^{-1})
0.3	*ca.* 35	0.072
0.2	*ca.* 50	0.071
0.1	*ca.* 70	0.070

μ_i moment of the peak under normal chromatographic conditions:
- $i = 1$: first absolute moment
- $i = 2$: second central moment
- $i = 3$: third central moment

σ standard deviation parameter of the EMG function

τ skew parameter of the EMG function

REFERENCES

1 C.Y. Jeng and S.H. Langer, *J. Chromatogr.*, 589 (1992) 1.
2 R. Thede, H. Pscheidl and D. Haberland, *Z. Phys. Chem.*, 266 (1985) 1089.
3 C.Y. Jeng and S.H. Langer, *Ind. Eng. Chem. Res.*, 30 (1991) 1489.
4 J.A. Jönsson, *Chromatographic Theory and Basic Principles*, Marcel Dekker, New York, 1987.
5 M.S. Jeansonne and J.P. Foley, *J. Chromatogr. Sci.*, 29 (1991) 258.
6 P.J. Naish and S. Hartwell, *Chromatographia*, 26 (1988) 285.
7 M. Abramovitz and A. Stegun (Editors), *Handbook of Mathematical Functions*, US Government Printing Office, Washington, DC, 1966.

Journal of Chromatography A, 660 (1994) 33–46
Elsevier Science B.V., Amsterdam

CHROMSYMP. 2948

Method development by an expert system

Advantages and limitations

Jenő Fekete* and György Morovján

Institute of General and Analytical Chemistry, Technical University of Budapest, Gellért tér 4, H-1111 Budapest (Hungary)

Ferenc Csizmadia and Ferenc Darvas

CompuDrug Chemistry Ltd., P.O. Box 405, H-1395 Budapest 62 (Hungary)

ABSTRACT

Several approaches can be used for the prediction of the optimum eluent composition in RP-HPLC, but only a few are known that use the structure of the solute. The latest release of the computer program EluEx, version 3.0, was developed to help the chromatographer in practical work. The program is based on the prediction of the pK_a and log P (logarithm of 1-octanol–water partition coefficient) values of the solutes. The first eluent suggestion can be done without any preliminary practical work, based on the structural formulae of the solutes. In our experience, two or three experiments are usually sufficient to determine the optimized binary conditions. The surface heterogeneity and the diversity of RP columns, such as the effect of silanol interaction, can be handled by the program only to a limited extent. If the difference in hydrophobicity between two compounds is small, the elution order cannot be predicted properly in all instances. The same is true for some isomers, *e.g.*, diastereomers. In this paper, the results of applying the program to some neutral, acidic and basic solutes are summarized.

INTRODUCTION

In this paper, the results of applying the program EluEx [1], version 3.0, to some neutral, acidic and basic solutes are presented.

According to Mulholland *et al.* [2] and Tsuji *et al.* [3], an expert system embodies the knowledge-based component of an expert's skill in a computer, and the system can offer intelligent advice. Schoenmakers and Dunand [4] defined expert systems in liquid chromatography in a similar way and gave an outline of a complete expert system for method development in HPLC. Hindriks *et al.* [5] have presented an expert system for predicting the initial mobile phase composition., Hamoir *et al.* [6] used the term "first guess" for the selection of initial conditions.

The expert systems created by De Smet *et al.* [7] were based on retention indices introduced to HPLC by Smith [8]. Using retention indices in gas chromatography is a very practical way to predict the relative retentions of different solutes. In liquid chromatography, there are no homologous series such as *n*-alkanes in gas chromatography that are widely accepted for calculating retention indices. The idea of dividing the structure into structural elements and estimating the polarity of analytes has also been utilized in gas chromatography according to Takács *et al.* [9].

In the approach of De Smet *et al.* [7], all initially selected structural elements are related to a percentage of methanol and have a positive or negative value depending on the relative polarity of a structural element. In their earlier publications, a rough estimation was used for predicting the hydrophobicity of analytes, which

* Corresponding author.

0021-9673/94/$07.00 © 1994 Elsevier Science B.V. All rights reserved
SSDI 0021-9673(93)E0980-9

was obtained from the number of carbon atoms in the investigated molecule. If the carbon number is less than 10, the molecule is considered to be non-hydrophobic, if it is between 10 and 20, the molecule is of medium hydrophobicity, and otherwise it is hydrophobic [10].

De Smet *et al.* [10] used the presence of acidic and basic functional groups in the solutes for the prediction of their acidic and basic character. By applying the expert system for the determination of basic drugs, it was concluded that instead of using structural elements, it seems to be more practical to take the whole chemical structure into account for the prediction of selectivity [11]. To accomplish this, they tried to integrate the DARC system (a computer program for the storage and retrieval of chemicals developed by Télésysteme, Paris, France) with DASH (Drug Analysis System in HPLC), but the programs could only operate independently.

Smith and Burr [12–15] have developed a computer program for the calculation of retention indices and for the prediction of retention, based on molecular structure. They selected benzene as a parent compound and investigated the substituent effect [15]. They found particular problems when the ionized form of the compound was present. In the so-called Prisma model, the retention of compounds in HPLC separations can be predicted by using molecular connectivity indices [16], but no computer-aided method development was presented.

Reviews of expert systems and programs for chromatographic optimization are available elsewhere [17–25] and are outside the scope of this paper. The basics of quantitative structure–chromatographic behaviour can be found in a book by Kaliszan [26].

THEORETICAL BACKGROUND

Problems with the hydrophobicity of the solutes

The similarity of the process of partitioning in 1-octanol–water and RP-HPLC systems makes the prediction of eluent composition possible. A large database of experimental 1-octanol–water partition coefficients [27] and several methods for the prediction of this value can be found in the literature [27–29]. Valkó and co-workers [1,31–35] have described an approach which can be used for the prediction of the appropriate solvent composition from the log P value of the solutes. The basic rule used is the Collander-type rule [30]. The general Collander equation relates the partition coefficients determined in the given organic–water system:

$$\log P_a = m \log P_b + n \tag{1}$$

where P_a and P_b are partition coefficients in solvent systems a and b, respectively, and m and n are constants that are characteristic of the two solvent systems being used. Good agreement can be obtained if the polarity difference between the organic solvents in the two partition systems is small. This suggests that the Collander-type equations can be applied in RP-HPLC if the chromatographic system has similar properties to the 1-octanol–water system [31–35]. The theoretical relationship between reversed-phase retention for non-ionized compounds and the 1-octanol–water partition system has been published by Valkó [34]. Assuming that such a relationship exists, the following equation can be given [31,32]:

$$\log P = m \log K_{chr} + n \tag{2}$$

where K_{chr} is the chromatographic distribution coefficient, which can be related to the capacity factor, k', by

$$k' = \frac{V_s}{V_m} \cdot K_{chr} \tag{3}$$

where V_s/V_m is the phase ratio, which can be treated for practical purposes as a constant value. Substituting eqn. 3 into eqn. 1 and expressing log K_{chr} yields

$$\log P = m \log k' + m \log \left(\frac{V_s}{V_m}\right) + n \tag{4}$$

As $m \log (V_s/V_m) + n$ can be considered to be constant, we arrive at the following equation:

$$\log P = m \log k' + C \tag{5}$$

Eqn. 5 is almost the same as that used by Honai *et al.* [36,37]. It has been shown that retention in RP-HPLC can be approximated well by the

equation [38,39]

$$\log k' = \log k'_w - S\varphi \quad (6)$$

where $\log k'_w$ is the extrapolated value of k' for pure water (or buffer), φ is the volume fraction of the organic component of the solvent and S is a constant, the value of which depends mainly on the solute, but also to some extent on the experimental conditions. Substituting eqn. 6 into eqn. 5, we obtain

$$\log P = m \log k'_w - mS\varphi + m \log \left(\frac{V_m}{V_s}\right) + n \quad (7)$$

Although eqn. 7 is valid, the retention data cannot be predicted using it, because there are two unknown parameters (S and $\log k_w$). Valkó [35] found the following linear relationships:

$$\log P = a\varphi_1 + b \quad (8)$$

where φ_1 is the extrapolated volume fraction of the organic content, when $k' = 1$; φ_1 can be calculated by linear regression from eqn. 6; a and b are constants which can be calculated by linear regression. Rearranging eqn. 8 and applying it to other $\log k'$ values, we obtain

$$\varphi_x = c \log P + d \quad (9)$$

where φ_x is the extrapolated volume fraction when $k' = x$ and c and d are constants. The program EluEx [1] uses two equations with x values of 1 and 5, respectively. To obtain k' values between 1 and 5 we calculate the φ value of the first guess in the following way: φ_1 is calculated for the most hydrophilic (with the lowest $\log P$) and φ_5 for the most hydrophobic (highest $\log P$) compound (φ_1^*, φ_5^*). If $\varphi_5^* < \varphi_1^*$, and $\varphi_5^* < \varphi < \varphi_1^*$ then all k' values should fall in the range 1–5. Hence the following equation is used for the determination of the organic content of the starting eluent:

$$\varphi = \frac{\varphi_1^* + \varphi_5^*}{2} \quad (10)$$

The $\log P$ prediction method used by the program is based on the original work of Rekker and De Kort [40] and further developed by CompuDrug. The structural formula of the compound to be examined is fragmented into groups and interactions among these fragments are taken into account. The structure and the $\log P$ contribution values of the fragments are stored in a database. $\log P$ is calculated as the sum of the contributions of the fragments and the interactions, based on the supposition that substituents cause additive changes in free energy.

$$\log P = \sum_{i=1}^{n} a_i f_i + \sum_{j=1}^{m} b_j F_j \quad (11)$$

where n and m are the number of the type of fragments and interactions, respectively, that occur in the molecule, a_i and b_j are the incidences of fragment i and interaction j, respectively, and f_i and F_j are the $\log P$ contributions of fragment i and interaction j, respectively.

Only the $\log P$ of the non-ionized forms of the compounds are used for the calculation of the organic content, except in the case of ion-pair separations, where the $\log P$ values of the solutes are not directly applicable. The method by which EluEx calculates the eluent composition in ion-pair separations is still under development. This will be the subject of another paper.

Problems of pH determination in mixed aqueous–organic solvents

When secondary equilibrium occurs in a chromatographic system, the given solute may exist in several forms. This affects the distribution between the two phases (*i.e.*, the retention).

If $pH < pK_a - 2$, for an acidic compound, or $pH > pK_a + 2$ for a basic compound, then ionization is almost completely suppressed, which is the aim in most RP-HPLC separations. Because experimental pK_a values are difficult to access, a pK_a prediction module was developed for the current version of the program.

In EluEx the pK_a values are predicted using the Hammett equation for aromatic acids and bases and the Taft equation for aliphatic and alicyclic acids and bases [41]. The assumption of these theories is the same as for $\log P$ prediction, that free energy changes caused by substituents are additive. The form of these equations is

$$pK_a = pK_a^0 - \rho\Sigma\sigma \quad (12)$$

where pK_a^0 is the ionization constant for the parent compound (or protonation reaction cen-

tre), ρ is a constant for the particular equilibrium (characteristic of the centre) and σ is a constant characteristic of a given substituent on a given position for the reaction. EluEx contains a table which stores the pK_a^0 and ρ values of the centres and tables of substituents which store the σ values. The program uses different substituent tables according to the type of centre and the position of the substitution (*ortho*, *meta*, *para*). The centre types are the following:

centres connected to aliphatic parts of the molecule
centres connected to an aromatic system
  anilines
  benzoic acids
  phenols
  pyridines

In the case of condensed aromatic systems, the Dewar–Grisdale method is applied [41]. The distance of the substituent from the centre is also taken into account (*e.g.*, $\sigma_{CH_2Cl} = 0.4\sigma_{Cl}$). The calculation is detailed in a book by Perrin *et al.* [41].

To obtain acceptable k' values and plate numbers for weakly acidic or basic compounds, the dissociation of solutes should be suppressed, or they should be fully ionized. The program can predict the log P of the neutral form of ionizable compounds. Prediction for ionic forms is not yet possible in the current version of the program. As a consequence, the pK_a values must first be predicted, based on the structural formulae. Second, the ion-suppression pH must be derived from the pK_a values. If the program does not accurately estimate the pK_a value, the predicted pH value may be higher than that necessary to suppress the ionization. Because the solute polarity of the ionic species is higher than that of the neutral form, in these instances the retention of the solute investigated may be lower than predicted.

As can be seen, the critical step of the program in these predictions is the accurate estimation of the pK_a values and using these data to determine the pH of the eluent. In a mixed aqueous–organic medium, the pH and pK_a values differ from the values measured in water, and also depend on the ionic strength to some extent.

From the classical Born treatment, a qualitative estimation can be made for the dependence of pK_a on the solvent. In mixed water–organic solvents, the pK_a value can be calculated from

$$\Delta pK_a = \log {}_wK_a - \log {}_sK_a = 122 \cdot \frac{n}{r} \cdot \left(\frac{1}{\epsilon_s} - \frac{1}{\epsilon_w}\right) \quad (13)$$

where w and s refer to water and the given solvent, respectively, r is the ionic radius, ϵ is the dielectric constant and n is a constant which is characteristic of the ionization equilibrium.

For a given solute, $122n/r$ is nearly constant and the variation of the pK_a value with solvent depends on the dielectric constant of water–organic system. The dielectric constants of water, acetonitrile and methanol, frequently used solvents, are 78.5, 37.5, 32.6, respectively at 25°C. The values for acetonitrile and methanol are very close to each other. This means that the same correction can be used for both solvents, because the resulting error is less than that caused by the difference between two reversed phases.

In all instances the pK_a value will increase in water–organic mixtures with increasing organic content. It is known from the literature that a large deviation of pK_a in mixed aqueous solutions from the aqueous pK_a values begins above 80% organic content [42].

The ionic strength has the opposite effect on pK_a according to the Davis equation [43]:

$$\Delta pK_a = 0.512(n-1)I^{1/2} - 0.1(2n-1)I \quad (14)$$

where n = constant (0, 1, 2) and I = ionic strength.

An electrolyte (buffer) makes an acid stronger in the solvatation reaction. The ΔpK_a values depends on the ionization equilibria that occur in aqueous media. Some results were presented by Van de Venne *et al.* [44]. The published ΔpK_a values lie between 0.1 and 0.4. If we compare the solvent effect and the influence of the ionic strength on pK_a, we can conclude that usually there is a decrease in acidity and basicity in mixed water–organic solvents. For example, the pK_a values of benzoic acid is 4.2 in water and 5.0 in methanol–water (40:60, v/v).

To determine the pH of a mixed aqueous–organic solvent is difficult. Even the convention chosen for defining pH is controversial. Schoenmakers *et al.* [45] concluded that there is no generally accepted concept on how to measure the pH in mixed aqueous–organic solvents. If the so-called operational pH (pH*) is used, when the pH is measured by a glass electrode which has been calibrated with an aqueous buffer, then the pH value is usually uncertain [46]. From a thermodynamic point of view, the so-called thermodynamic pH_s should be used, which is based on $p(a_H\gamma_{Cl})$, an acidity function. pH_s will rise with increase in the content of the organic component [46]. The deviation of the pH in the pure aqueous system from pH_s at a 20% methanol content is at least 1 pH unit, at 40% methanol it is at least 2 pH units, and it increases with increasing methanol content [46]. Dissociation phenomena in water–methanol solvents have been widely studied by De Ligny *et al.* [47].

In the early period of liquid chromatography, the importance of pH was realized in the separation of ionogenic solutes [48]. The theoretical treatment of pH in the separation of ionogenic solutes is basically the same as that presented by Horváth *et al.* [48]. Optimization and computer simulation for the prediction of the eluent in the separation of ionogenic compounds has been attracting new interest recently [45,49–53]. Every approach uses the pK_a values of the compounds investigated. Schoenmakers *et al.* [45] measured the pH of the buffer and the retention times of solutes, but they concluded that a physically meaningful pK_a cannot be reliably derived from their model. A software package (Drylab I/mp) was developed for the determination of pK_a from three chromatographic runs, by varying the pH only [50]. For an acceptable determination of pK_a the pH values must be very carefully selected. An approximate value of pK_a is needed before the experiments.

When separating ionogenic compounds, the selectivity is the highest around the pK_a value, but Schoenmakers *et al.* [45] showed that the plate number and the asymmetry factor varied for nitrophenols. When the ionization was suppressed, higher plate numbers and better peak shapes were observed. In general, if two equilibria take place simultaneously, the peak will broaden and will be asymmetric. If the dissociation of the analyte is faster than its distribution process, then only one peak will appear on the chromatogram.

Rules for calculating the pH of the buffer

The sample may contain compounds with different acidic and basic characteristics. EluEx places every sample into one of the classes listed below. Because acidity and basicity are lower in a mixed aqueous–organic medium than in water, the following correction on the pK_a values was used:

$$pK_a^* = pK_a + a\varphi \quad (15)$$

where $a = 1$ for acids and -2 for bases. Eqn. 16 is supposed to consider both pK_a and pH changes in a mixed aqueous–organic eluent compared with pure water (or buffer). The replacement of this correction by a more theoretical approach, which is based on a pH and pK_a prediction in a mixed aqueous environment, is under development.

The following notations are used:

pK_a^{a*}	the lowest corrected acidic pK_a of the strongest acid in the sample
pK_a^{b*}	the highest corrected basic pK_a of the strongest base in the sample
NA	none of the solutes are acidic or $pK_a^{a*} > 11$ (that is, the acidities of all solutes are negligible)
NB	none of the solutes are basic or $pK_a^{b*} < 1$ (the basicities of all solutes are negligible)
min pH, max pH	set by the user, determined by the type of the column and the solutes
C	condition
A	action
E	explanation

(a)	C	NA and NB (neutral compounds or very weak acids or bases)
	A	buffer is not suggested
	E	the acidities and basicities of the solutes are so weak, if they exist, that they will not be ionized in a buffer-free eluent

(b) C min $pH + 2 < pK_a^{a*} \leq 11$ and NB (weakly acidic compounds)
A $pH = pK_a^{a*} - 2$
E ionization is suppressed if $pH \leq pK_a^{a*} - 2$, because $[A]/[B] \geq 100$ (see eqn. 21).

(c) C NA and $1 \leq pK_a^{b*} < \max pH - 2$ (weakly basic compounds)
A $pH = pK_a^{b*} + 2$, if $pK_a^{b*} > 4$ then a masking agent (*e.g.*, triethylamine) against the silanol effect is suggested
E ionization is suppressed if $pH \geq pK_a^{b*} + 2$, because $[B]/[A] \geq 100$.

(d) C $pK_a^{a*} \leq \min pH + 2$ and NB (acidic compounds, ionization cannot be suppressed in the given pH range)
A pH is set to be the furthest from all pK_a values of the acids in the pH range. Basic ion-pair reagent is suggested
E acids with $pK_a < pH$ will form ion pairs with the reagent, the dissociation of the other compounds will be suppressed

(e) C NA, $pK_a^{b*} \geq \max pH - 2$ (basic compounds, ionization cannot be suppressed in the given pH range)
A pH is set to be the furthest from all pK_a values of the bases in the pH range. Acidic ion-pair reagent is suggested.
E bases with $pK_a > pH$ will form ion pairs with the reagent, the dissociation of the other compounds will be suppressed

(f) C $pK_a^{a*} \leq 11$, $pK_a^{b*} \geq 1$, $pK_a^{a*} > pK_a^{b*} + 4$ (weak acids and weak bases)
A $pH = (pK_a^{a*} + pK_a^{b*})/2$, if $pK_a^{b*} > 4$ then a masking agent against the silanol effect is suggested
E if $pK_a^{b*} + 2 \leq pH \leq pK_a^{a*} - 2$ then the ionization of all compounds is suppressed

(g) C $pK_a^{a*} \leq 11$, $pK_a^{b*} \geq 1$, $pK_a^{a*} \leq pK_a^{b*} + 4$ and $pK_a^{a*} - \min pH < \max pH - pK_a^{b*}$ (acids and weak bases)
A pH is set to be the furthest from all pK_a values of the acids in the range $[\max(pK_a^{b*} + 2, pK_a^{a*} + 2), \max pH]$ if possible, otherwise max pH. Basic ion-pair reagent is suggested
E Acids and $pK_a < pH$ will form ion pairs with the reagent, the dissociation of the other compounds is assumed to be suppressed.

(h) C $pK_a^{a*} \leq 11$, $pK_a^{b*} \geq 1$, $pK_a^{a*} \leq pK_a^{b*} + 4$ and $pK_a^{a*} - \min pH \geq \max pH - pK_a^{b*}$ (weak acids and bases)
A pH is set to be the furthest from all pK_a values of the bases in the range $[\min pH, \min(pK_a^{a*} - 2, pK_a^{b*} - 2)]$ if possible, otherwise min pH. Basic ion-pair reagent is suggested
E bases with $pK_a > pH$ will form ion pairs with the reagent, the dissociation of the other compounds is assumed to be suppressed

There may be cases when there are both strong acids and strong bases in the sample. This version of the program cannot handle that situation, but it is under development.

Isocratic optimization

The optimization method of the program is based on the window diagram technique. The organic content is varied to obtain a model for the system. After two experiments, eqn. 7 is used for the k' prediction. The parameters log k_w and S are calculated from the data for the two chromatograms by linear regression. After three or more experiments a parabolic model is used for modelling the system's behaviour between the lowest and highest experimental φ values. Outside this range the curve's tangents for these two points are applied.

The goal of optimization is to obtain the fastest run with an $R_{s,min}$ value higher than or equal to the user defined value, with peaks in the k' range set by the user.

The optimization is completed when the difference between the last and the previous organic

content suggestion is less than 1%. Of course, users can stop at any time when they find the chromatogram to be acceptable.

Gradient optimization

In cases when isocratic elution could be completed but the resolution is poor or the elution time is long, it may be reasonable to run gradient elution. The simulation of LSS (linear solvent strength) gradient runs is possible using the data for two isocratic runs. The equations used for this prediction can be found in ref. 54.

The equation for the calculation of retention time in gradient elution is

$$t_g = \frac{t_0}{b} \cdot \log (2.3k_a b + 1) + t_0 \quad (16)$$

where k_a is the isocratic k' value with the starting eluent and b is the gradient steepness, which can be derived from the following equation:

$$b = \frac{t_0}{t_G} \cdot (\log k_a - \log k_b) \quad (17)$$

where k_b is the k' value using isocratic elution with the final eluent composition of the gradient; k_a and k_b can be calculated from eqn. 6.

The optimization criteria are the same as in isocratic elution. For LSS gradient elution the definition of R_s is the same as in the isocratic case, but we have to predict the band width of compound i, W_i, with the following equation:

$$W_i = \frac{G\left(1 + \frac{k_a}{2.3k_a b + 1}\right)t_0}{N^{1/2}} \quad (18)$$

where G is the band compression factor, which can be calculated from

$$G^2 = \frac{1 + p + p^2}{(1 + p)^2} \quad (19)$$

where p is given by

$$p = \frac{2.3k_a b}{k_a + 1} \quad (20)$$

Structure of the program

EluEx is written in C and C++ languages and runs on IBM AT-compatible computers. The program is built from several modules:

(1) The main module controls the activities of the other modules.

(2) In the structure maintenance module the structural formulae of the solutes can be entered into the compound database. The structures can be drawn easily using a mouse.

(3) The log P and pK_a prediction modules calculate these physico-chemical parameters from the structural formulae.

(4) The initial step module calculates the initial eluent composition, that is, the organic percentage, and if needed the pH of the buffer and the amount and type of the ion-pair agent or masking agent.

(5) The optimization module governs the optimization phase, which is made up of experiments and new suggestions which use the data obtained from the previous experiments.

(6) The simulation module can simulate the chromatogram graphically for varying organic percentages.

Working with the program

Fig. 1 shows the flowchart of the program. The following steps have to be made during a session:

(1) Entering the structures with a mouse, if they are not already in the compound database.

(2) Composing the list of solutes by selecting the compounds from the database.

(3) Defining:
- the plate number;
- the preffered k' range;
- the chosen organic modifier (six are available in the program);
- the chosen acidic or basic ion-pair reagent (six and five are available, respectively);
- the pH range; and
- $R_{s,min}$.

(4) As one enters the initial step module, it calculates the first-step eluent composition.

First the log P and pK_a values of the solutes are predicted using fragmentation methods.

The type of the sample is determined using the smallest acidic and the greatest basic pK_a values of the set of compounds.

If max log P − min log $P > 5$, gradient elution will be suggested.

The organic percentage will be calculated from the smallest and highest log P values.

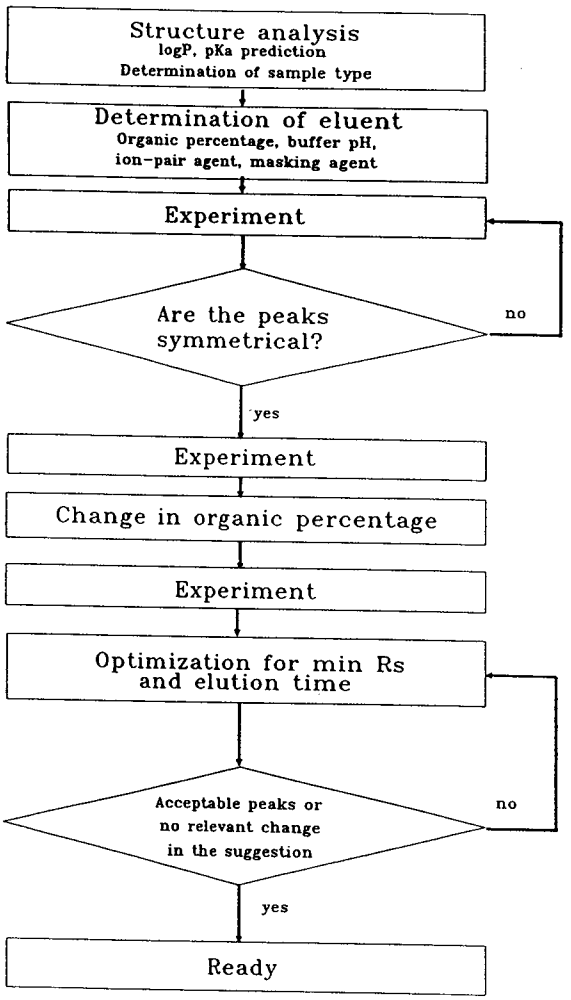

Fig. 1. Flow chart of the program.

(5) The user performs an experiment using the suggested eluent and enters the data into the program. If matrix components exist, their retention data should be entered, so that they too will be considered.

(6) As long as the peaks of interest are not symmetrical, modifications to the eluent composition will be suggested, such as changing pH to max pH in the case of bases or min pH in the case of acids, or increasing the amount of the ion-pair or the masking agent.

(7) If the peaks are symmetrical, the organic percent is changed to collect data for the modelling of the system. Again, following the experiment the data must be entered.

(8) At this point, as we have two φ–log k' data points for all solutes, the behaviour of the system can be modelled using eqn. 5. This equation is used for both the calculation of the optimized organic percentage and the chromatogram simulation.

(9) If the criteria for k' range and R_s can only be satisfied with gradient elution, an optimized gradient profile is suggested and the optimization process is halted.

(10) After each iosocratic run the model is refined (parabolic instead of linear) to obtain more exact k' predictions for the optimization and the simulation.

EXPERIMENTAL

Chromatographic apparatus

Two types of HPLC apparatus were used for the experiments: (1) Millipore (Milford, MA, USA) Model 510 isocratic pump and a Millipore DAD 911 diode-array detector and (2) an HP1090 system equipped with a Model 1040 UV–Vis detector and a Chemstat data station with HP7958B hardware and software (Hewlett-Packard, Rockville, MD, USA).

Chemicals and reagents

The solvents were of chromatographic grade. Methanol and acetonitrile were obtained from Merck (Darmstadt, Germany). Deionized water as purified by means of a Milli-Q system (Millipore). Other chemicals were of analytical-reagent grade from Merck. Some triazines were purchased from Supelco (Gland, Switzerland) and others were donated by the Hungarian National Plant Protection Institute. Fumagillin, mevinoline and mevinolinic acid were produced and purified at the Institute of General and Analytical Chemistry, Technical University of Budapest.

The column for chlorophenol, fumagillin and mevinolines was packed with LiChrosorb RP-18,10 μm (Merck) (250 × 4.6 mm I.D.) and for triazines with Supelcosil LC-18-DB (Supelco) (150 × 4.6 mm I.D.) and Spherisorb ODS-2,5 μm (Hewlett-Packard) (250 × 4.6 mm I.D.).

The pH was adjusted using a Horiba F-8 pH meter.

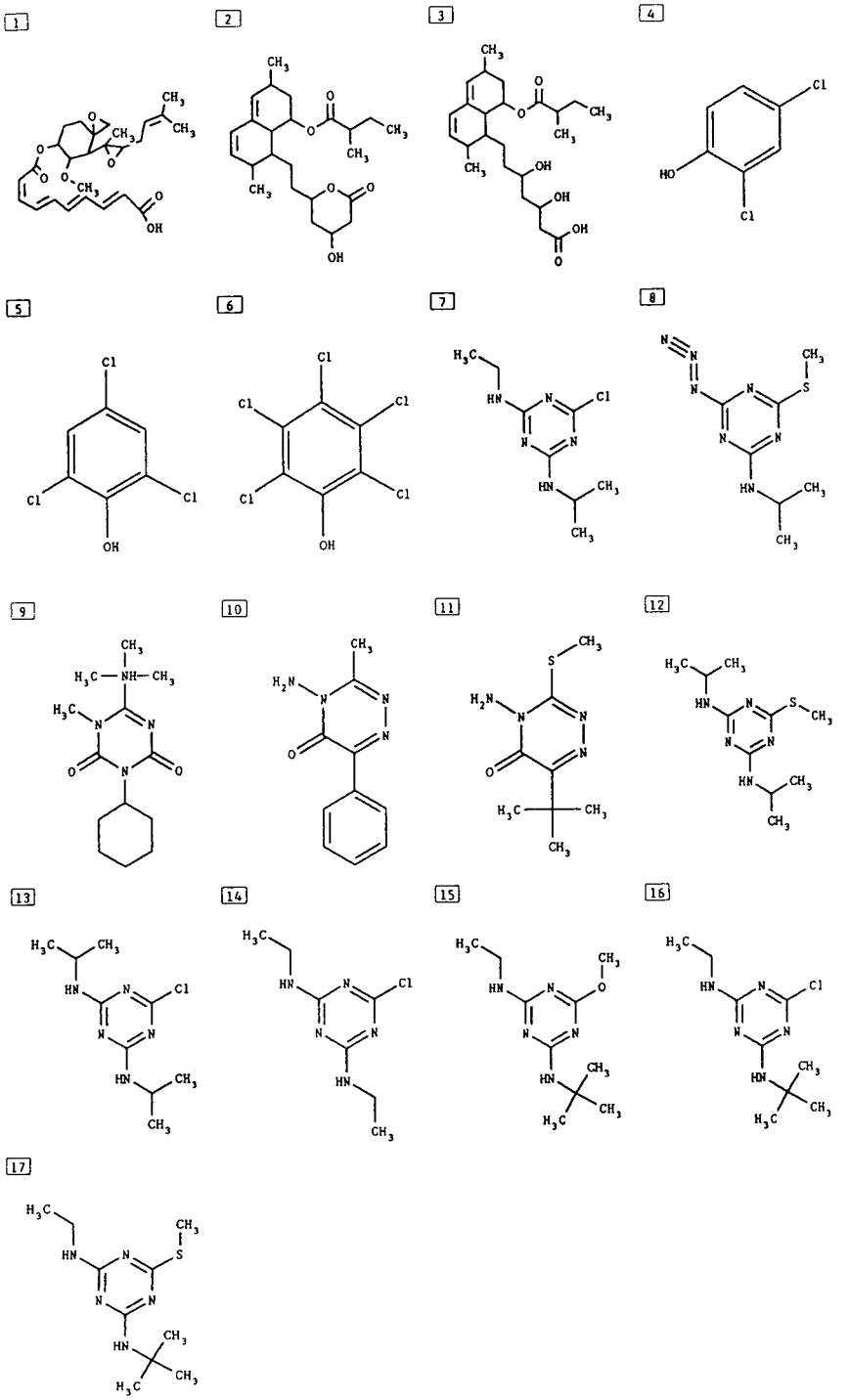

Fig. 2. Structures of solutes investigated. **1** = fumagillin; **2** = mevinoline; **3** = mevinolinic acid; **4** = 2,4-dichlorophenol; **5** = 2,4,6-trichlorophenol; **6** = pentachlorophenol; **7** = aziprotryne; **8** = metamitron; **9** = hexazinon; **10** = metribuzin; **11** = simazine; **12** = terbumeton; **13** = atrazine; **14** = terbutryn; **15** = prometryn; **16** = terbutilazine; **17** = propazine.

RESULTS

Determination of fumagillin in biological matrix

The separation of fumagillin (compound **1** in Fig. 2) from a fermentation liquid is considered. The predicted pK_a and log P values of fumagillin are 3.2 and 4.76, respectively. The suggested eluent composition in the first guess is 90.0% (v/v) acetonitrile–50 mM KH_2PO_4 buffer (pH 2.1). The measured value for k' is 0.66 (Fig. 3A). The matrix components were eluted near fumagillin. In the second guess, 75% (v/v) acetonitrile was suggested. The k' value of fumagillin became 1.29 and the separation was still not complete (Fig. 3B). In the third step, the program suggested 60% (v/v) acetonitrile. Using this composition, the separation became perfect and the k' of fumagillin was 3.45 (Fig. 3C).

Determination of mevinolines in biological matrix

The structures of mevinoline and mevinolinic acid are shown in Fig. 2 (compounds **2** and **3**). The program suggested 97.5% (v/v) methanol–

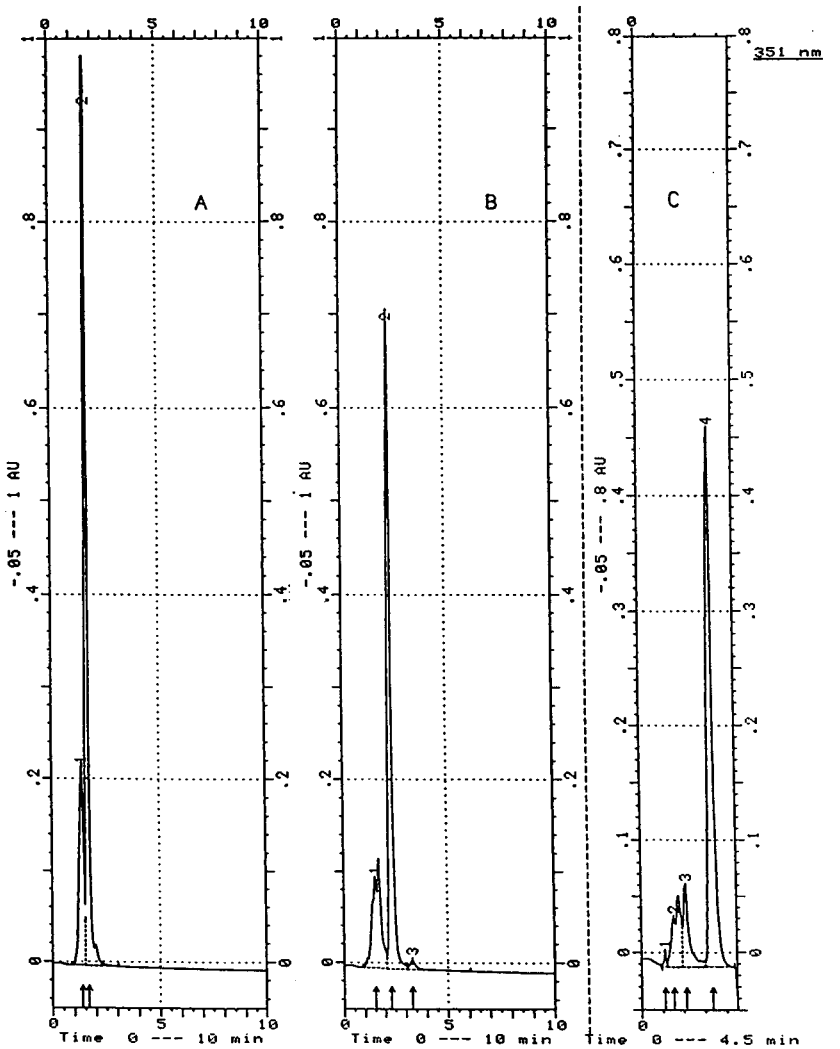

Fig. 3. Determination of fumagillin in fermentation liquid. Column, LiChrosorb RP-18, 10 μm (250 × 4.6 mm I.D.); buffer, 50 mM KH_2PO_4 (pH 2.1); eluent, (A) 90, (B) 75 and (C) 60% (v/v) acetonitrile–buffer; flow-rate, 1 ml/min.

m*M* KH_2PO_4 buffer (pH 3.3). There was no acceptable separation between the matrix components and the solutes investigated. In the second step, the program suggested 80% (v/v) methanol. Completing the experiment with this eluent, we obtained an acceptable separation (Fig. 4).

Determination of chlorophenols

The test compounds with pK_a values between 4 and 9 were 2,4-dichlorophenol,3,4,6-trichlorophenol and pentachlorophenol (compounds **4**, **5** and **6** in Fig. 2). The calculated pK_a values were 7.9, 6.3 and 4.7, respectively, and the log *P* values were 2.98, 3.72 and 5.20, respectively. The suggested eluent composition for the first trial was 79% (v/v) acetonitrile–50 m*M* KH_2PO_4 buffer (pH 3.5).

The capacity factors of the first compounds using these conditions [with 80% (v/v) acetonitrile] were 0.24, 0.40 and 0.80, respectively (Fig. 5A). As the peaks were symmetrical in the second guess, the suggested mobile phase composition differed only in the organic content. The new eluent suggestion was 50% (v/v) acetonitrile. On carrying out the measurement the capacity factors of the test solutes were 1.49, 2.59 and 6.21, respectively (Fig. 5B). The chromatogram was then acceptable, so the method development was completed.

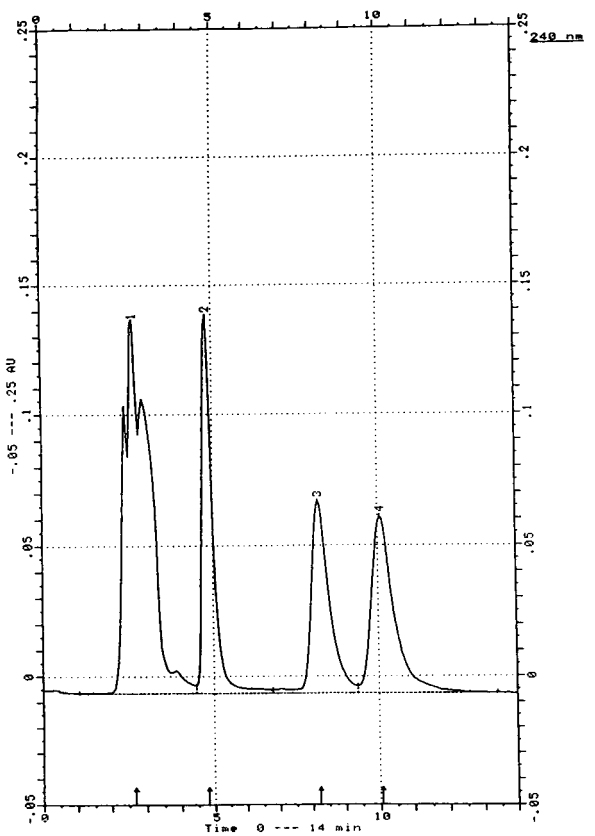

Fig. 4. Determination of mevinolines in fermentation liquid. Column, LiChrosorb RP-18, 10 μm (250 × 4.6 mm I.D.); buffer, 50 m*M* KH_2PO_4 (pH 3.3); eluent, 80% (v/v) methanol–buffer; flow-rate, 1 ml/min. Peaks: 1 and 2 = matrix components; 3 = mevinolinic acid; 4 = mevinoline.

Determination of some triazine herbicides

Triazine herbicides were used to test the program for weakly basic solutes. The pK_a values of triazine compounds are relatively small (pK_a < 4.5) [55]. Even at this small pK_a value, the silanophilic interaction can cause a large decrease in the efficiency of the separation and results in bad peak shapes. The structures of triazine compounds are given in Fig. 2 (compounds **7–17**).

The program suggested 39% (v/v) acetonitrile–50 m*M* KH_2PO_4 buffer (pH 5.5). First we used 40% (v/v) acetonitrile–buffer. In a conventional column (Spherisorb ODS-2) the separation was acceptable (Fig. 6A). The peak symmetry was fairly good except for azyprotryn. To diminish the effect of silanophilic interaction, a deactivated RP column was used (Supelcosil 8DB). The chromatographic separation is shown in Fig. 6B. All components are separated. In Table I the calculated log *P* and pK_a values are given. As can be seen from these values, the experimental retention order does not correspond to the predicted hydrophobicity order in some instances.

The eluent composition was predicted with methanol to check the selectivity. The program suggested 59% (v/v) methanol, so the solutes were separated at 60% (v/v) methanol. The chromatogram is shown in Fig. 6C. As can be seen, using methanol we did not obtain an acceptable separation.

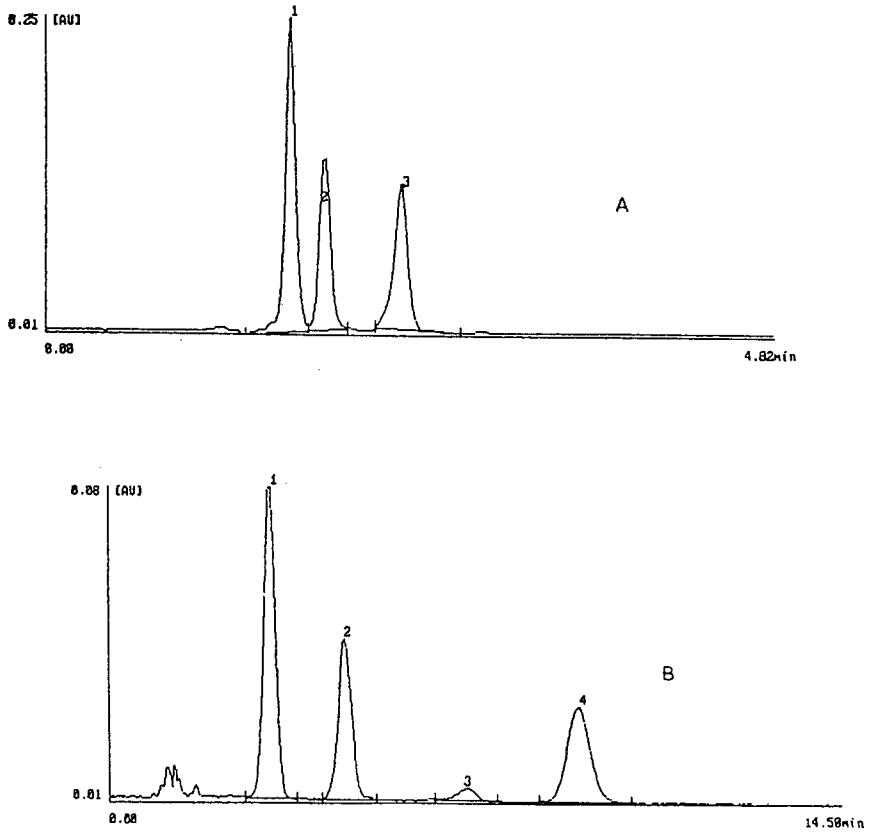

Fig. 5. Separation of chlorophenols. Column, LiChrosorb RP-18, 10 μm (250 × 4.6 mm I.D.); buffer, 50 mM KH_2PO_4 (pH 3.5); eluent, (A) 80 and (B) 50% (v/v) acetonitrile–buffer; flow-rate, 1 ml/min. Peaks: (A) 1 = 2,4-dichlorophenol; 2 = 2,4,6-trichlorophenol; 3 = pentachlorophenol; (B) 1 = 2,4-dichlorophenol; 2 = 2,4,6-trichlorophenol; 3 = impurity; 4 = pentachlorophenol.

TABLE I

HYDROPHOBICITY ORDER OF TRIAZINE HERBICIDES

Compound	Log P	pK_a
Aziprotryne	−0.41	1.4
Metamitron	0.88	<1
Hexazinon	1.21	<1
Metribuzin	1.65	<1
Simazine	2.24	1.4
Terbumeton	2.61	3.7
Atrazine	2.76	1.2
Terbutryn	3.14	4.1
Prometryn	3.14	4.3
Terbutilazine	3.28	1.2
Propazine	3.28	1.4

CONCLUSIONS

The program EluEx was tested for the prediction of eluent composition with neutral, weakly acidic and weakly basic compounds. The program predicts the distribution constant of the non-ionized form of the solutes from hydrophobic fragmental values. Assuming a linear relationship between log P and log k', the organic content can be predicted from the structural formulae. For acidic and basic solutes the program predicts pK_a values based on Hammett and Taft equations. For weak acids and bases the pK_a values are used for the prediction of buffer pH. It was shown that in most instances during the initial step the program can predict an eluent

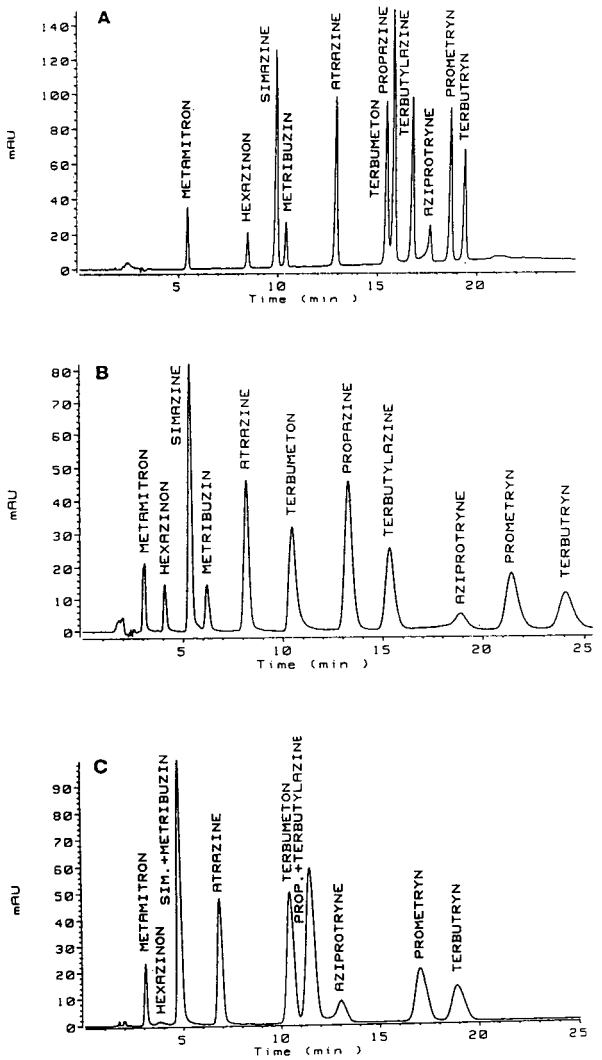

Fig. 6. Separation of triazine herbicides. Column, (A) Spherisorb ODS, 5 μm (250 × 4.6 mm I.D.) (B and C) Supelcosil LC-18-DB (150 × 4.6 mm I.D.); buffer, 50 m*M* KH_2PO_4 (pH 5.5) (adjusted with 1 *M* NaOH); eluent, (A and B) 40% (v/v) acetonitrile–buffer and (C) 60% (v/v) methanol–buffer; flow-rate, 0.8 ml/min.

composition that is a good starting point for the method development. By entering the experimental data as needed and following the suggestions of the program, the method development can be completed usually by the second or third experiment. In some instances the elution order differs from the predicted hydrophobicity order. The correction of the predicted pK_a value for mixed aqueous solvents has to be developed further.

SYMBOLS

pK_a negative logarithm of the acid dissociation constant:

$$pK_a = pH + \log \frac{[A]}{[B]} \quad (21)$$

where A is the acidic and B is the basic form of a compound (in the case of bases the pK_a value of the protonated compound as an acid is used as the pK_a).

Log *P* logarithm of the partition coefficient of a compound between 1-octanol and water.

t_0 column dead time (min).

t_R solute retention time (min).

k' capacity factor for a given band, equal to $(t_R - t_0)/t_0$.

R_s resolution, equal to $2(t_2 - t_1)/(W_1 + W_2)$, where t_1 and t are retention times $(t_2 > t_1)$ and W_1 and W_2 are their baseline band widths.

$R_{s,min}$ resolution of the most poorly resolved band pair.

φ volume fraction of organic solvent in a binary mobile phase.

ACKNOWLEDGEMENTS

This research was supported by the OTKA (contract number 117), SZTO and OMFB foundations. We acknowledge the assistance of Robert J. Longworth, Szilvia Kokai, Ildikó Szepesi and Csilla Sárközi.

REFERENCES

1 P. Csokán, K. Valkó, F. Darvas and F. Csizmadia, *LC·GC*, 6 (1993) 361.
2 M. Mulholland, N. Dunand, A. Cleland, J.A. van Leeuwen and B.G.M. Vandeginste, *J. Chromatogr.*, 485 (1989) 293.
3 K. Tsuji and K.M. Jenkins, *J. Chromatogr.*, 485 (1989) 297.
4 P.J. Schoenmakers and N. Dunand, *J. Chromatogr.*, 485 (1989) 219.

5 R. Hindriks, F. Maris, J. Vink, A. Peters and M. De Smet, D.L. Massart, *J. Chromatogr.*, 485 (1989) 255.
6 T. Hamoir, M. de Smet, H. Pyrins, P. Conti, N. Vandendriesche, D.L. Massart, F. Morris, H. Hindriks and P.J. Schoenmakers, *J. Chromatogr.*, 589 (1992) 31.
7 M. De Smet, G. Musch, A. Peeters, L. Buydens and D.L. Massart, *J. Chromatogr.*, 485 (1989) 237.
8 R.M. Smith, *Adv. Chromatogr.*, 26 (1987) 277.
9 J. Takács, C. Szita and G. Tarján, *J. Chromatogr.*, 56 (1971) 1.
10 M. De Smet, A. Peeters, L. Buydens and D.L. Massart, *J. Chromatogr.*, 457 (1988) 25.
11 F. Maris, R. Hindriks, J. Vink, A. Peeters, N.V. Priessche and L. Massart, *J. Chromatogr.*, 506 (1990) 211.
12 R.M. Smith and C.M. Burr, *J. Chromatogr.*, 465 (1989) 75.
13 R.M. Smith and C.M. Burr, *J. Chromatogr.*, 481 (1989) 71.
14 R.M. Smith and C.M. Burr, *J. Chromatogr.*, 485 (1989) 325.
15 R.M. Smith and C.M. Burr, *J. Chromatogr.*, 550 (1991) 335.
16 Sz. Nyiredi, *Application of the Prisma Model for the Selection of Eluent Systems in Overpressure Layer Chromatography (OPLC)*, Labor MIM, Budapest, 1987.
17 P.J. Schoenmakers, *Optimization of Chromatographic Sensitivity –Guide to Method Development*, Elsevier, Amsterdam, 1986.
18 J.C. Berridge, *Techniques for the Automated Optimization of HPLC Separations*, Wiley-Interscience, New York, 1989.
19 L.R. Snyder, J.L. Glajch and J.J. Kirkland, *Practical HPLC Development*, Wiley-Interscience, New York, 1989.
20 R.L. Glajch and L.R. Snyder (Editors), *Computer-Assisted Method Development for HPLC*, Elsevier, Amsterdam, 1990.
21 A. Peeters, L. Buydens, D.L. Massart and P.J. Schoenmakers, *Chromatographia*, 26 (1988) 101.
22 D. Goulder, T. Blaffert, A. Blokland, L. Buydens, A. Chhabra, A. Cleland, N. Dunand, H. Hindriks, G. Kateman, H. Van Leeuwen, D.L. Massart, M. Mulholland, G. Musch, P. Naish, A. Peeters, G. Postma, P. Schoenmakers, M. De Smet, B. Vandeginste and J. Vink, *Chromatographia*, 26 (1988) 237.
23 P.J. Schoenmakers, A. Peeters and R.J. Lynch, *J. Chromatogr.*, 506 (1990) 169.
24 J.W. Dolan, D.C. Lommen and L.R. Snyder, *J. Chromatogr.*, 535 (1990) 55.
25 L.R. Snyder, J.W. Dolan and D.C. Lommen, *J. Chromatogr.*, 535 (1990) 75.
26 R. Kaliszan, *Quantitative Structure–Chromatographic Retention Relationships*, Wiley, New York, 1987.
27 C. Hansch and A. Leo, *Substituent Constants for Correlation Analysis in Chemistry and Biology*, Wiley, New York, 1979.
28 Han van de Waterbeemd and F. Darvas (Editors), *Hydrophobicity of Organic Compounds*, CompuDrug, Vienna, 1986.
29 C. Hansch and A. Leo, *Log P and Parameter Database: a Tool for the Quantitative Prediction of Bioactivity*, Pomona College, Medicinal Chemistry Project, 1983, issue 22,23.
30 R. Collander, *Acta Chem. Scand.*, 5 (1951) 774.
31 G. Szepesi and K. Valkó, *J. Chromatogr.*, 550 (1991) 7.
32 K. Valkó and P. Segel, *J. Chromatogr.*, 631 (1993) 49.
33 K. Valkó, *J. Liq. Chromatogr.*, 10 (1987) 1663.
34 K. Valkó, *J. Liq. Chromatogr.*, 7 (1984) 1405.
35 K. Valkó, *Microcomputer Analysis of HPLC, the State of the Art*, Akadémiai Kiadó, Budapest, 1985, pp. 739–750.
36 T. Honai, *Chromatographia*, 12 (1979) 77.
37 T. Honai, K.C. Tran and J. Hubert, *J. High. Resolut. Chromatogr. Chromatogr. Commun.*, 4 (1981) 454.
38 W.R. Melander and Cs. Horváth, in Cs. Horváth (Editor), *High-Performance Liquid Chromatography –Advances and Perspectives*, Vol. 2, Academic Press, New York, 1980, p. 114.
39 P. Jandera and J. Churáček, *Gradient Elution in Column Liquid Chromatography*, Elsevier, Amsterdam, 1985, p. 19.
40 R.F. Rekker and H.M. de Kort, *Eur. J. Med. Chem.*, 14 (1979) 479.
41 D.D. Perrin, B. Dempsey and E.P. Serjeant, *pK_a Prediction for Organic Acids and Bases*, Chapman and Hall, London, 1981.
42 A.L. Bacarella, E. Gunwald, H.P. Marshall and E.L. Purlee, *J. Org. Chem.*, 20 (1955) 747.
43 C.W. Davies, *J. Chem. Soc.*, (1938) 2039.
44 L.L.M. van de Venne, I.L. Hendriks and R.S. Deelder, *J. Chromatogr.*, 167 (1978) 1.
45 P.J. Schoenmakers, S. van Molle, C.M.G. Hayes and L.G.M. Uunk, *Anal. Chim. Acta*, 250 (1991) 1.
46 R.G. Bates, *Determination of pH. Theory and Practice*, Wiley, New York, 1973, Ch. 8.
47 C.L. de Ligny, H. Loriaux and A. Ruitar, *Recl. Trav. Chim. Pays-Bas*, 80 (1961) 725.
48 Cs. Horváth, W. Melander and I. Molnár, *Anal. Chem.*, 49 (1977) 142.
49 R.M.L. Marques and P.J. Schoenmakers, *J. Chromatogr.*, 592 (1992) 157.
50 J.A. Lewis, D.C. Lommen, W.D. Raddatz, J.W. Dolan and L.R. Snyder, *J. Chromatogr.*, 592 (1992) 183.
51 L.J.W. Dolan and L.R. Snyder, *J. Chromatogr.*, 592 (1992) 183.
52 P.J. Schoenmakers, N. Mackie and R.M.L. Marques, *Chromatographia*, 35 (1993) 18.
53 R.M.L. Marques, P.J. Schoenmakers, C.B. Lucasius and L. Buyden, *Chromatographia*, 36 (1993) 83.
54 L.R. Snyder, in Cs. Horváth (Editor), *High-Performance Liquid Chromatography, Advances and Perspectives, Vol. 1*, Academic Press, New York, 1980, p. 207.
55 V. Packova, K. Stulik and M. Prihoda, *J. Chromatogr.*, 442 (1988) 147.

Journal of Chromatography A, 660 (1994) 47–59
Elsevier Science B.V., Amsterdam

CHROMSYMP. 2934

Calculation of retention in reversed-phase liquid chromatography

IV. ChromDream software for the selection of initial conditions and for simulating chromatographic behaviour

S.V. Galushko*, A.A. Kamenchuk and G.L. Pit

Institute of Bioorganic Chemistry and Oil Chemistry, Academy of Sciences of the Ukraine, 253660 Kiev 94 (Ukraine)

ABSTRACT

A computer-aided method to assist the chromatographer in the determination of initial conditions in reversed-phase HPLC has been developed. ChromDream software predicts the optimum methanol, acetonitrile or tetrahydrofuran concentration in a mobile phase on the basis of the structural formulae of the compounds. The effects of the concentration of an organic solvent in water on retention and chromatograms of compound mixtures are simulated. Reversed-phase column parameters responsible for selectivity and retention are calculated. Volume and energy increments for more than 100 volume fragments and more than 30 bond dipoles have been derived. An approach for the selection of reference compounds for column calibration is proposed.

INTRODUCTION

The selection of the initial conditions is the first step in HPLC method development and the possibility of using relationships between chemical structure and retention can save a lot of time and effort in this stage. Several software packages and expert systems for the calculation of retention in reversed-phase HPLC on the basis of chemical structure have been developed. An integrated expert system in HPLC contains LABEL and DASH expert systems for predictions of the initial conditions in reversed-phase HPLC [1]. LABEL suggests possible mobile phase conditions on a cyano-bonded column on entering the molecular size and polarity of the analyte [2]. DASH predicts the percentage of methanol in a mobile phase for capacity factors of basic drugs between 3 and 10 to be obtained [3,4]. The user is required to translate the structure of an analyte into fragments. Each fragment is linked to a percentage of methanol and the final concentration of methanol is calculated by summation of the fragment contributions.

The CRIPES expert system for calculating retention indices based on the alkyl aryl ketone scale has been described [5]. The retention index was calculated by summation of the retention index of a parent compound and different contributions. The user was required to enter analyte details such as the type and the numbers of aliphatic and aromatic substituents.

METABOLEXPERT and ELUEX software packages calculate the capacity factor (k') of an

* Corresponding author.

0021-9673/94/$07.00 © 1994 Elsevier Science B.V. All rights reserved
SSDI 0021-9673(93)E0943-O

analyte [6,7]. The programs are based on the assumption that log k' in reversed-phase (C_{18}) HPLC is linearly related to the calculated logarithm of the partition coefficient of an analyte in the octanol–water system (log P) and that only small differences exist between reversed-phase columns produced by different manufacturers. To calculate approximate log P values fragmental constants were used.

Empirical correlation approaches are normally not associated with model concepts of the retention mechanism, the surface layer structure and the character of interactions of retained substances with mobile and stationary phases. Previously we described a retention model and an approach for the calculation of the retention in reversed-phase HPLC (RP-HPLC) on the basis of the structural formula of a compound [8]. The possibility of predicting the retention of compounds on different octadecyl columns with water, water–methanol, water–acetonitrile and water–tetrahydrofuran mobile phases has been shown [8–12].

The aim of this work was to develop a flexible computer-aided method for selecting the initial conditions in reversed-phase HPLC and predicting the chromatographic behaviour of compounds on the basis of their structural formulae and calibrating reversed-phase columns.

MODEL

To calculate approximately the retention, a two-layer continuum model of a reversed-phase chromatographic system was employed [8]:

(1) The surface of a modifier sorbent in RP-HPLC has a surface layer (SL) that involves octadecyl radicals and some of the components of a mobile phase (MP).

(2) The SL is assumed to be a quasi-liquid that has its own characteristics, such as surface tension (γ_s) and dielectric constant (ε_s). The SL characteristics vary with varying MP composition and sorbent properties.

(3) The molecules of retained substances penetrate into the SL. The retention is determined by the difference in molecule solvation energies in the MP and SL.

To calculate the solvation energies, a molecule of a substance is considered to consist of volume fragments and bond dipoles, each of which interact separately with the surrounding continuum.

Hence the model takes into account several important points: (i) individuality of a packing; (ii) the surface and polarity of a solute; and (iii) the influence of mobile phase composition on the interaction of a solute with the stationary and mobile phases.

The model and approaches for calculating the energy of solvation and sorbent parameters have been described in detail and the equation derived for calculating the retention in reversed-phase HPLC and calibrating the column is [8,10]:

$$\ln k'_x = a\left(\sum_i V_i\right)^{2/3} + b\left(\sum_j \Delta G_{e.s.j,H_2O}\right) + c \qquad (1)$$

where V_i are the increments of the partial molar volumes of fragments in water, $G_{e.s.j,H_2O}$ are the increments of energy of interaction of bond dipoles with water, a, b and c are parameters of the reversed-phase chromatographic system and the column, including the phase ratio, and some characteristics of the SP and MP [8,10]. Each volume fragment i has its energy increment of the $G_{e.s.i,H_2O}$. Hence the energy of interaction of a molecule with water can be expressed in the form

$$\sum_j \Delta G_{e.s.j,H_2O} = \sum_i \Delta G_{e.s.i,H_2O} + \sum_f \Delta G_{e.s.f,H_2O} \qquad (2)$$

where $\Delta G_{e.s.f,H_2O}$ are increments of the contribution of $G_{e.s.H_2O}$ for dipoles that are not included in volume fragments.

EXPERIMENTAL

Chromatographic conditions

The experiments were performed on an LKB (Bromma, Sweden) liquid chromatographic system consisting of a Model 2140 rapid spectral detector set at 254 nm, a Model 2150 HPLC pumping system, a Model 2152 LC controller, a Model 2155 HPLC column oven, a Model 2154 injector and a Model 2220 recording integrator.

The columns used were (1) Polyol-SI 100, 5 μm (250 × 4.6 mm I.D.) (Serva, Heidelberg, Germany), (2) Nucleosil 120-5 C_{18} (100 × 4.0 mm I.D. and 30 × 4.0 mm I.D. cartridge) (Macherey–Nagel, Duren, Germany), (3) Eurospher 80-5 C_{18} (250 × 4.0 mm I.D.) (Eurochrom Knauer, Berlin, Germany), all stainless-steel columns, and (4) Separon SGX, 5 μm glass column (150 × 3.0 mm I.D.) (Tessek, Prague, Czech Republic). The mobile phase was phosphate buffer (pH 7.0; 0.01 *M* H_3PO_4 adjusted with 0.01 *M* sodium hydroxide) at a flow-rate of 0.5 ml/min. Separations were performed at 35°C for columns 1 and 4 and at 22°C for columns 2 and 3.

Software

Computer simulations were carried out using ChromDream software (Dr. Ing. H. Knauer GmbH, Berlin, Zehlendorf, Germany). The program was written in PASCAL language. The program was run on an IBM-compatible Piramida computer.

RESULTS AND DISCUSSIONS

Translating structure into fragments

To calculate the retention, a molecule must be translated into volume fragments and bond dipoles and subsequently increments V_i and also $\Delta G_{e.s.i,H_2O}$ and $\Delta G_{e.s.f,H_2O}$ must be used. One of the major difficulties is to provide a good user interface. It has been found earlier that when a user manually translates structures into fragments more than 50% of structures are incorrectly translated [4]. The conclusion was drawn that to avoid these mistakes a concise user manual is necessary in which it is explained how a structure can be translated into structure elements and additionally how the number of elements must be restricted [4]. Of course, the best alternative is to use a program to enter first the complete chemical structure and then to translate it automatically into fragments and to calculate the retention and simulate chromatographic behaviour and chromatograms. We have developed such a program and a structural formula drawn on the PC screen is translated automatically into fragments. This procedure enables us to employ many structural elements and to calculate the retention more precisely. Moreover, the program checks if a drawn structural formula fulfils the valency rules, indicates mistakes and determines some topological features of a compound: aromatic, cyclic, heterocyclic, saturated, etc. After drawing a structure on the screen, the software can analyse the structure immediately and display the list of fragments (see Table VIII) or save the structure in a current library file (Sample) for further simulating chromatograms or chromatographic behaviour. Up to 100 structures may be saved in each Sample and names of 100 Sample files may be displayed in the Sample Menu. A menu of alphanumeric and Boolean fields with topological features, different functional groups and heteroatoms allows a formula or a group of formulae to be found in a current library file.

Volume and energy parameters

Previously we derived volume and energy increments for some basic fragments and dipoles of organic compounds [8,10]. Possibilities of automatically translating a structural formula enabled us to expand the set of fragments and dipoles substantially. To obtain the values of V_i, experimental partial molar data for more than 300 compounds were used [14]. Experimental data have shown that the additivity of the action of separate molecule fragments is a good approximation for calculating partial molar volumes [8,14]. V_i values for the majority of the fragments were calculated from the experimental V values by the least-squares method and the rest were derived from Van der Waals volumes. The values of the increments obtained (Table I) enabled us to calculate the partial molar volumes of compounds belonging to the different classes with relative standard deviations of not more than 5% (Table II). It should be noted that the molecular volume of a compound is a popular parameter in liquid chromatography and we believe that it is useful to have the possibility for calculating it rapidly in the chromatographic software.

The energy of interaction of a molecule with water ($\Delta G_{e.s.,H_2O}$) is calculated as described previously [8]. As a first approximation, incre-

TABLE I

INCREMENTS OF PARTIAL MOLAR VOLUMES (V, IN $cm^3\ mol^{-1}$) AND ENERGY ($\Delta G_{e.s.i,H_2O}$, IN $kJ\ mol^{-1}$) FOR SOME FRAGMENTS

Fragment[a]	V	$-\Delta G_{e.s.i,H_2O}$	Fragment[a]	V	$-\Delta G_{e.s.i,H_2O}$
H	5.00	0.00	C=O	16.00	32.20
–C–	−7.01	0.00	C=O(ar)	11.00	33.20
cyC	−7.00	0.00	cyC=O	11.00	27.50
=C=	0.00	0.00	arC=O	13.00	20.00
=C–	−3.69	0.00	COOH	24.00	65.00
ar=C–	5.16	0.00	COOH(ar)	22.84	62.63
cy=C–	5.00	0.00	CHO	20.73	35.00
C_{sp}	7.00	0.00	CHO(ar)	22.23	32.00
CH	3.50	1.42	CN	17.74	31.25
cyCH	4.59	1.42	CN(ar)	17.74	18.25
ar=CH–	11.87	4.36	$CONH_2$	31.38	71.68
=CH–	15.00	4.36	$CONH_2$(ar)	27.90	60.00
cy=CH–	9.00	4.36	F	12.00	0.00
CH_{in}	12.00	9.84	F(ar)	14.00	0.00
CH_2	15.68	2.84	CF_3	36.00	5.00
CH_2(ar)	16.68	−2.00	CF_3(ar)	32.00	2.00
$cyCH_2$	15.17	2.84	Cl	24.00	0.00
$=CH_2$	22.00	2.84	Cl(ar)	24.00	0.00
CH_3	27.43	4.26	Br	29.00	0.00
CH_3(ar)	23.43	2.26	Br(ar)	29.00	0.00
CH_4	34.00	5.68	I	36.00	0.00
–N–	−5.08	−8.00	I(ar)	36.00	0.00
–N–(ar)	−5.08	−3.00	–P–	−3.00	2.00
=N–	−2.00	0.00	=P–	0.00	2.00
ar=N–	5.89	15.00	cy=P–	8.00	2.00
arN	−4.00	0.00	cyP	−3.00	2.00
cyN	−2.50	0.00	P=O	20.00	48.00
cy=N–	6.00	0.00	cyP=O	21.00	48.00
NH	6.15	19.20	=PO–	26.00	48.00
NH(ar)	6.15	15.20	cy=PO–	27.00	48.00
cyNH	6.66	12.00	POOH	37.00	70.00
arNH	11.74	17.20	OH(ar)	12.20	33.00
NHp	3.15	15.00	cyPOOH	38.00	70.00
NH(ar)p	3.15	14.50	$PO(OH)_2$	44.00	95.00
cyNHp	6.15	9.50	S	7.14	−1.00
arNHp	6.15	13.00	S(ar)	7.14	−1.00
NH_2	13.00	44.00	Sarar	7.14	−1.00
NH_2(ar)	15.00	36.00	S(co)	7.14	−1.00
=NO–	14.00	38.00	=S	9.00	0.00
N=O	10.00	38.00	cyS	11.00	−1.00
cy=NO–	15.00	38.00	SH	15.00	19.00
cyN=O	15.00	38.00	S=O	21.43	42.00
NO_2	20.33	24.00	cyS=O	22.00	42.00
NO_2(ar)	20.33	20.00	SO_2	28.00	60.00
O	4.40	−4.00	$cySO_2$	29.00	60.00
O(co)	1.40	0.00	SO_2–NH_2	40.00	100.00
O(COar)	1.40	−14.00	SO_2NH_2ar	40.00	96.00
O(ar)	3.40	5.50	SO_3H	41.00	100.00
Oarar	3.40	−2.00	SO_3Har	41.00	100.00
cyO	6.00	−3.00	SOOH	34.00	42.00
OH	12.20	38.80	cycl	10.01	0.00

[a] cy = fragment in a ring; ar = fragment in an aromatic ring; (ar) = fragment connected to an aromatic ring; C_{sp} = fragment C≡; CH_{in} = fragment HC≡; (co) = fragment connected to –CO– group; (COar) = fragment connected to CO(ar) group; arar = atom positioned between two aromatic rings; p = NH group in –NH–CO– fragment.

TABLE II

COMPARISON OF CALCULATED AND EXPERIMENTAL VALUES OF PARTIAL MOLAR VOLUME (V, IN $cm^3\ mol^{-1}$) IN WATER

Compound	V(calc.)	V(exp.) [13]
1-Pentanol	102.35	102.60
2-Pentanol	101.92	102.60
3-Pentanol	101.92	101.20
Benzyl alcohol	103.40	102.20
Sorbitol	118.56	119.20
Phenol	86.72	86.20
Cyanophenol	97.75	98.00
Anisole	105.35	105.60
Dimethyloxolane	110.39	111.00
Cyclohexanedione	100.69	92.80
Cyclohexanone	100.86	99.70
Benzimidazole	97.31	98.53
1,10-Phenanthroline	137.39	142.42
Quinazoline	104.19	104.20
Benzylamine	104.20	104.70
Hexanic acid	114.10	116.00
2-Phenylacetic acid	115.20	114.10
Glutaric acid	95.00	99.14
Acetanilide	121.30	121.30
Ribose	98.34	95.20
Glucose	115.60	111.70

ments $\Delta G_{e.s.j,H_2O}$ for bond dipoles have been used [8]. By analysing the deviations in calculating the retention of more than 400 compounds belonging to different classes we found the values of $\Delta G_{e.s.j,H_2O}$ and $\Delta G_{e.s.i,H_2O}$ increments that allow more exact results (Tables I and III). Of course, the values of $\Delta G_{e.s.j,H_2O}$ increments can be further refined.

The program searches for volume fragments and dipoles in the structural formula and calculates $\Sigma_i (V_i)^{2/3}$ and $\Sigma_j \Delta G_{e.s.j,H_2O}$ according to eqns. 1 and 2. Sometimes a fragment can be in several dipoles (*e.g.*, the fragment Cl can be involved in three dipoles: C_{sp^3}–Cl, C_{sp^2}–Cl and C_{sp}–Cl). In this case the program identifies the type of hybridization of a carbon atom bonded with a halogen atom and selects a corresponding value from the list of the parameters (Table III).

An opinion exists that "correct prediction ... cannot be expected for a wide range of ... compounds" [1]. On the other hand, experimental data show that fairly correct predictions can

TABLE III

INCREMENTS OF $\Delta G_{e.s.j,H_2O}$ (IN kJ mol^{-1}) FOR SOME DIPOLES

Dipole	$-\Delta G_{e.s.j,H_2O}$	Dipole	$-\Delta G_{e.s.j,H_2O}$
C_{sp}–H	9.84	S–N	2.00
C_{sp^2}–H	4.36	P–H	5.00
C_{sp^3}–H	1.42	C_{sp}–Cl	2.00
C_{sp^2}–C_{sp^3}	2.33	C_{sp^2}–Cl	3.00
C_{sp^2}–C_{sp}	6.68	C_{sp^3}–Cl	23.00
C_{sp^3}–C_{sp}	11.06	C_{sp}–F	4.00
C_{sp}–O	1.15	C_{sp^2}–F	9.00
C_{sp^2}–O	2.15	C_{sp^3}–F	18.00
C_{sp^3}–O	12.00	C_{sp}–Br	1.00
C_{sp}–N	1.00	C_{sp^2}–Br	3.50
C_{sp^2}–N	2.00	C_{sp^3}–Br	22.00
C_{sp^3}–N	12.00	C_{sp}–I	1.00
C_{sp^2}=N	1.24	C_{sp^2}–I	2.50
O–N	0.71	C_{sp^3}–I	20.00
O–P	0.70	C_{sp^2}–S	1.00
O–S	0.50	C_{sp^3}–S	4.00
C_{sp^3}–P	2.00	C_{sp^2}=S	2.00
C_{sp^2}–P	4.00		

be obtained for a certain family of substances, packing type and organic solvent in a mobile phase [4,5]. As will be shown further, a fairly large set of volume fragments and dipoles (Tables I and III) allows the satisfactory prediction of retention and acceptable mobile phase composition for various classes of substances [13]. However, it is possible that for a certain family of substances energy increments allowing more precise results can be obtained. To make the program more flexible, a special file PARAM.DAT is available. This file contains volume and energy parameters (Tables I and III) in a usual numerical format and these parameters may be changed by the user. Moreover, new dipoles can be added. For instance one can add an ar=C–Cl dipole to the list of the dipoles in the parameters file (Table III). In this case the program will differentiate a C_{sp^2}–Cl dipole from ar=C–Cl. Any fragment from Table I can be used to create new dipoles. Thus, in addition to the general system of the parameters derived (Tables I and III), one can develop several other more specific systems for certain classes or families of substances. The program allows the user to calculate the retention and to simulate a

chromatogram of a mixture of compounds using different systems of parameters simultaneously.

Column calibration

Eqn. 1 gives an opportunity to calibrate columns and to compare different reversed-phase columns and packings. By using several reference compounds, parameters *a*, *b* and *c* responsible for retention and selectivity can be calculated. In the framework of the approach used, the parameters *a* and *b* are determined by the differences in surface tension and dielectric permittivity of a sorbent surface layer and a mobile phase [8,10]. Hence these parameters enable us to evaluate column-to-column reproducibility and differences between columns quantitatively. The smaller the differences in parameters *a*, *b* and *c*, the smaller are the differences in the retention and selectivity of the separation. It has been shown that the parameters depend on bonded-phase structure, coverage density and concentration of silanol groups on the surface of a packing material [15]. The more silanol groups in the bonded layer, the higher are its surface tension and dielectric constant [15].

As each packing and column has a unique set of parameters [8,10,11,15], some procedure should be performed to determine the parameters. To calculate the column parameters (eqn. 1), capacity factor values for several reference compounds are entered and the software calculates the parameters *a*, *b* and *c* by the least-squares method. After determination of the column parameters, the capacity factors of the reference compounds are calculated to check the validity of the parameters and to evaluate deviations between experimental and calculated values of the capacity factors (Table IV). Of course, the proposed method, as with any semi-empirical method, is an approximation and some deviations should be expected in results of column calibrations and retention calculations when different sets of reference compounds are used. Hence to compare different columns more objectively, the same eluent and reference compounds should be used. One of the suitable sets of reference compounds for column calibration consists of phenol, benzene, *p*-hydroxybenzaldehyde and toluene (or chlorobenzene) (Table IV). Other sets may be chosen in order to obtain capacity factors of several compounds in either one or several runs.

One of the problems in HPLC is the limited stability of chromatographic columns. To evaluate reversed-phase HPLC columns, 50–60% methanol–water mobile phases and several test mixtures have been proposed [16,17]. We consider that the calculation of column parameters with the ChromDream software using retention data for these or other mixtures can be a rapid, sensitive and quantitative test procedure both for the evaluation of new reversed-phase columns and in daily routine work for column stability control.

Parameters for different columns (Hypersil ODS, Nucleosil 120-5 C_{18}, Spherisorb ODS-2, Eurospher 80-5 C_{18}, ODS Si-100 Polyol, Separon SGX C_{18}, etc.) have been calculated for a wide range of methanol, acetonitrile and tetrahydrofuran concentrations in the mobile phase. These

TABLE IV

RESULTS OF CALIBRATING A COLUMN (NUCLEOSIL 120-5 C_{18}, 10 cm × 4 mm I.D.)

Mobile phase: methanol–water (50:50). $a = 0.2756$; $b = 0.0562$; $c = -2.2020$. V in $cm^3\ mol^{-1}$; $-\Delta G_{e.s.H_2O}$ in $kJ\ mol^{-1}$; k'_e = experiment capacity factor values; k'_c = calculated capacity factor values.

Compound	V	$-\Delta G_{e.s.H_2O}$	Ln k'_e	Ln k'_c	k'_e	k'_c
Chlorobenzene	98.52	24.80	2.27	2.28	9.69	9.82
Benzene	81.23	26.16	1.47	1.50	4.37	4.50
Toluene	97.95	26.39	2.20	2.17	9.00	8.78
Phenol	86.22	56.95	0.03	0.00	1.03	1.00
p-Hydroxybenzaldehyde	101.74	85.59	−0.94	−0.93	0.39	0.40

parameters are employed by the program for simulating chromatograms and calculating retention under selected conditions (column, concentration of an organic solvent in water, etc.). In addition to these parameters, the user can determine parameters for other reversed-phase columns and eluents and save them in addition to a description of chromatographic conditions in a parameters library for further chromatogram simulation and retention calculation.

Selecting reference compounds

As has been described above, to calibrate a column the capacity factor values for several reference compounds must be entered. In many instances parameters that were determined using compounds belonging to one class of substances are acceptable for calculating the retentions of substances belonging to other classes (see Fig. 4) [14]. However, to obtain more correct predictions for a certain class or family of substances, several compounds belonging to the family can be used for column calibration. To determine column parameters more precisely, it is necessary to employ compounds that have substantial differences in $V^{2/3}$ and $\Delta G_{e.s.}$ (eqn. 1), *i.e.*, that differ in surface and polarity. As the number of reference compounds rises, the error in determining column parameters decreases. Hence the selection of an adequate set of reference compounds is an important point in a column calibration. To select reference compounds that represent a family of substances adequately, we propose to use a surface in $V^{2/3}$–$\Delta G_{e.s.}$ coordinates. In this case a polygon with points inside can be circumscribed (Fig. 1). We assume that the compounds located in corners of the polygon adequately represent a family of substances and may be selected as a reference. The software automatically analyses a family of substances and recommends a reference set. The results obtained have shown that this approach for selecting reference compounds allows fairly good predictions (Tables V and VI).

Simulation of chromatographic behaviour and chromatograms

When a column is calibrated under defined conditions, a chromatogram of a sample can be

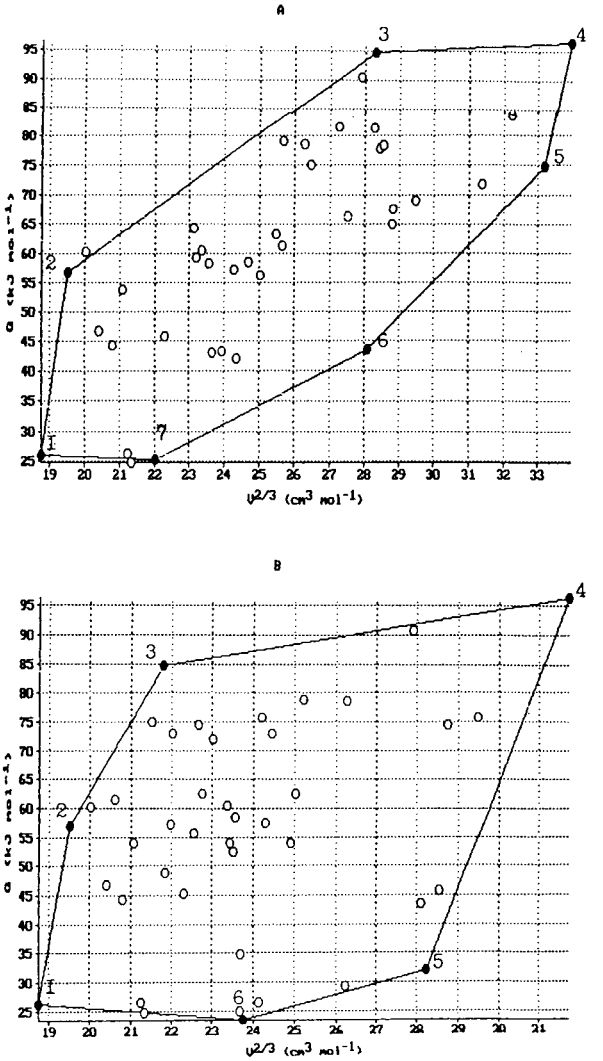

Fig. 1. (A) Selection of reference compounds from 43 compounds (Table VII). 1 = Benzene; 2 = phenol; 3 = *m*-propyl-*p*-hydroxybenzoate; 4 = α-bromo-*p*-phenylacetophenone; 5 = heptanophenone; 6 = biphenyl; 7 = bromobenzene. (B) Selection of reference compounds from 51 compounds (Table VI). 1 = Benzene; 2 = phenol; 3 = *p*-hydroxybenzaldehyde; 4 = diethyl phthalate; 5 = *o*-dichlorobenzene; 6 = butylbenzene.

simulated and a table of predicted k' and ln k' values can be displayed. A fairly large set of calibrated reversed-phase columns (Hypersil ODS, Nucleosil 120-5 C_{18}, Spherisorb ODS-2, Eurospher 80-5 C_{18}, ODS Si-100 Polyol, Separon SGX C_{18}, etc.) and a wide range of organic solvent concentrations (0–100% in steps of 10%)

TABLE V

COMPARISON OF COLUMN PARAMETERS CALCULATED USING DIFFERENT REFERENCE COMPOUNDS

Parameter	43[a]	7[b]	51[c]	6[d]
a	0.313 ± 0.009	0.321 ± 0.007	0.268 ± 0.01	0.279 ± 0.01
b	0.046 ± 0.001	0.046 ± 0.001	0.046 ± 0.001	0.048 ± 0.001
c	−3.775 ± 0.12	−3.783 ± 0.14	−2.569 ± 0.06	−2.698 ± 0.02
R[e]	3.17	3.43	4.47	4.65

[a] Reference compounds: 1–43 from Table VII. Column, Spherisorb ODS-2 [5,18]; mobile phase, acetonitrile–water (50:50).
[b] Reference compounds: 5, 12, 15, 17, 30, 36 and 40 from Table VII and Fig. 1A. Column and mobile phase as in footnote *a*.
[c] Reference compounds: 1–51 from Table VI. Column, Nucleosil C_{18} [19]; mobile phase, methanol–water (40:60).
[d] Reference compounds: 3, 7, 12, 26, 44 and 49 from Table VI and Fig. 1B. Column and mobile phase in footnote *c*.
[e] $R = \sum_i (\ln k'_{ei} - \ln k'_{ci})^2$.

enables suitable initial conditions to be predicted.

In addition to the possibility of simulating chromatograms and predicting the retention under calibration conditions, interpolation and extrapolation modes can be employed for predicting the retention with different concentrations of an organic solvents in water. When column parameters are determined over a wide range of organic solvent concentrations in a mobile phase, some polynomial can be used to describe the dependences of the column parameters on the concentration of the solvent. Parameters of polynomials have been fitted by the least-squares method from the dependences of column parameters on organic solvent concentration in water ($C_{solv.}$). The software contains a library of cubic polynomial parameters for different ODS columns with methanol–, acetonitrile– and tetrahydrofuran–water mobile phases. These parameters are employed to simulate the dependence of k' ($\ln k'$) on $C_{solv.}$, both for a single compound and for mixtures of compounds (up to 100). After drawing and saving several structural formulae in a current library of compounds (Sample), the software calculates partial molar volumes and energies of interaction of the compounds with water and using eqn. 1 and the library of column parameters calculates capacity factors and displays plots of k' ($\ln k'$) *vs.* $C_{solv.}$ for each compound of the Sample (Fig. 2). These dependences enable an acceptable concentration of organic solvent in a mobile phase to be selected. After selection of an organic solvent concentration, a chromatogram of the mixture on a column with 10 000 plates can be simulated and a table with predicted capacity factor values can be displayed.

Predicting optimum concentration of organic solvent

Some limits of capacity factor values can be considered as optimum depending on the chromatographer's requirements and the sample composition. The software takes two parameters into account: *ML*, minimum capacity factor value, and *MR*, maximum capacity factor value. Recommended values are $ML = 1$ and $MR = 10$; however, the limits may be changed by the user. If there is only one compound in a sample and $ML = MR$ the software predicts conditions for $k' = ML = MR$ to be obtained. It seems reasonable to have two modes of optimization, local and global. The local optimization mode considers only one column and one type of organic solvent in a mobile phase. In this case the program predicts the concentration of the organic solvent in water that can provide the maximum correspondence to present *ML* and *MR* values. In the global optimization mode the program calculates capacity factors of sample compounds for all columns and mobile phases in the parameters library and recommends conditions (column, type and concentration of organic solvent in water) for acceptable capacity factor values to be obtained. Experimental capacity factor values (range 1.5–5) for a number of compounds listed in refs. 5 and 16 were used to

TABLE VI

COMPARISON OF CALCULATED AND EXPERIMENTAL VALUES OF k'

Column, Nucleosil C_{18} [19]; mobile phase, methanol–water (60:40). V in $cm^3\ mol^{-1}$; $-\Delta G_{e.s.H_2O}$ in $kJ\ mol^{-1}$; k'_e = experimental capacity factor values [19]; $k'_{c,1}$ = calculated capacity factor values (column parameters were calculated using reference compounds: 3, 7, 12, 26, 44 and 49); $k'_{c,2}$ = calculated capacity factor values (column parameters were calculated using all 51 compounds as reference).

No.	Compound	V	$-\Delta G_{e.s.H_2O}$	k'_e [19]	$k'_{c,2}$	$k'_{c,1}$
1	Acetophenone	112.95	60.59	1.90	2.55	2.57
2	Benzaldehyde	96.75	53.80	1.62	1.83	1.88
3	Benzene	81.23	26.16	3.70	3.53	3.49
4	Benzonitrile	92.26	46.73	1.55	2.13	2.16
5	Benzophenone	160.04	75.80	8.04	7.05	6.72
6	Biphenyl	149.04	43.60	25.87	21.92	19.81
7	Butylbenzene	149.99	32.07	45.65	39.11	34.35
8	*p*-Chlorobenzaldehyde	114.04	52.44	1.48	3.79	3.85
9	Chlorobenzene	98.52	24.80	7.62	7.77	7.43
10	*p*-Chlorotoluene	115.24	25.03	14.56	14.99	13.85
11	*o*-Cresol	102.94	57.18	1.67	2.01	2.05
12	*o*-Dichlorobenzene	115.81	23.44	14.04	16.52	15.19
13	Dimethyl phthalate	147.47	90.66	1.78	2.24	2.26
14	*m*-Dinitrobenzene	108.47	62.44	2.38	1.96	1.99
15	*o*-Dinitrobenzene	108.47	62.44	2.03	1.96	1.99
16	*p*-Dinitrobenzene	108.47	62.44	2.38	1.96	1.99
17	2,4-Dinitrotoluene	125.19	62.67	4.02	3.70	3.66
18	2,6-Dinitrotoluene	125.19	62.67	3.53	3.70	3.66
19	3,4-Dinitrotoluene	125.19	62.67	3.09	3.70	3.66
20	Diphenyl ether	152.44	45.90	23.52	22.19	20.03
21	Ethylbenzene	118.63	26.39	12.23	16.02	14.75
22	*m*-Fluoronitrobenzene	102.14	48.94	3.53	2.88	2.88
23	*o*-Fluoronitrobenzene	102.14	48.94	2.49	2.88	2.88
24	*p*-Fluoronitrobenzene	102.14	48.94	2.48	2.88	2.88
25	*p*-Fluorophenol	93.51	61.59	1.10	1.11	1.17
26	*p*-Hydroxybenzaldehyde	101.74	84.59	0.58	0.52	0.57
27	*p*-Methoxybenzaldehyde	120.87	72.85	1.90	1.91	1.98
28	*p*-Methylbenzaldehyde	113.47	54.03	2.01	3.45	3.52
29	Naphthalene	115.29	34.88	13.31	9.43	8.91
30	*p*-Nitroacetophenone	126.57	78.73	1.98	1.83	1.86
31	*p*-Nitrobenzaldehyde	110.37	71.94	1.33	1.35	1.40
32	*p*-Nitrilobenzaldehyde	107.78	74.37	0.86	1.10	1.14
33	Nithrobenzene	94.85	44.30	2.72	2.66	2.68
34	*m*-Nitrophenol	100.34	75.09	1.48	0.76	0.81
35	*o*-Nitrophenol	100.34	75.09	2.38	0.76	0.81
36	*p*-Nitrophenol	100.34	75.09	1.34	0.76	0.81
37	*p*-Phenylphenol	154.03	74.39	5.57	6.10	5.86
38	3-Phenylpropanol	134.76	78.61	2.22	2.40	2.51
39	*n*-Propylbenzene	134.31	29.23	24.02	25.32	22.76
40	Toluene	97.95	26.39	7.30	7.04	6.76
41	2,4-Dimethylphenol	119.66	57.41	3.06	3.85	3.79
42	2-Phenylethanol	119.08	75.77	1.36	1.58	1.63
43	Benzyl alcohol	103.40	72.93	0.89	0.97	1.03
44	Phenol	86.72	56.95	0.94	1.08	1.07
45	N,N-Dimethylaniline	124.30	53.82	8.12	5.44	5.27
46	N-Methylaniline	108.10	55.26	2.84	2.54	2.56
47	Aniline	89.52	60.30	0.96	1.00	1.05
48	Anisole	105.35	45.21	3.66	3.91	3.86
49	Diethyl phthalate	178.83	96.34	4.74	5.08	4.91
50	Dimethyl phthalate	147.47	90.66	1.78	2.24	2.26
51	Methyl benzoate	114.35	58.41	3.58	2.99	2.98

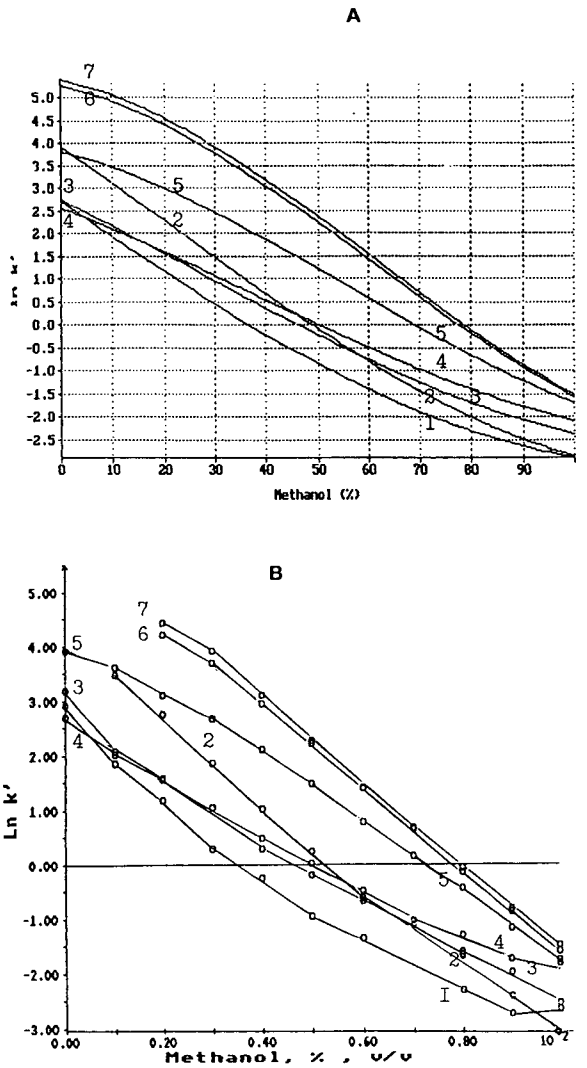

Fig. 2. (A) Simulated and (B) experimental plots of ln k' *versus* concentration of methanol in water. 1 = *p*-Hydroxybenzaldehyde; 2 = methylparaben; 3 = phenol; 4 = pyridine; 5 = benzene; 6 = toluene; 7 = chlorobenzene. Sorbent: Nucleosil 120-5 C_{18}; eluent: methanol–water.

check that the program was capable of predicting the concentration of an organic solvent in a mobile phase. The results obtained showed fairly good agreement between experimental and calculated concentrations of an organic solvent in a mobile phase for obtaining required capacity factor values (Table VII).

Isomeric and intramolecular interaction effects

The large set of volume and energies parameters enabled us to predict difference in retention for some isomers. For instance, the program correctly predicts the difference in retention of theobromine and theophylline (Fig. 3). We can request lists of fragments to obtain information on structures analysed (Table VIII).

The software does not take into account stereochemical and intramolecular interaction effects. Sometimes these and other effects can be predicted from a structural formula or from chromatographic experience. For example, capacity factors of *ortho* isomers of benzene derivatives that can form one intramolecular hydrogen bond are nearly twice as large as those for *para* isomers. This value holds fairly well (1.5–2.2) within a wide range of methanol and/or acetonitrile concentrations in a mobile phase [17]. To determine when intramolecular hydrogen bonds can be produced, some considerations should be used. In the simplest approach one can assume that this bond can be formed between H-donors (OH, NH, NH_2, COOH, SH, etc.) and H-acceptors (O- and N-containing groups: NO_2, OH, NH_2, COOH, etc.) if they are in an *ortho-* or α-position to one another, *e.g.*, in *o*-nitrophenol or ethylene glycol one intramolecular H-bond increases the capacity 1.5–2.0-fold. The software allows the user to enter a correction (H_{cor}) for the expected effects. In this case a corrected capacity factor value ($k'_{cor.}$) is calculated as $k'_{cor.} = H_{cor}k'_c$, where k'_c is a capacity factor value calculated without correction. The software takes into account a corrected value both for simulating plots and chromatograms and for predicting the optimum concentration of an organic solvent in a mobile phase. Each compound is saved in the library automatically with $H_{cor} = 1$ (ln $H_{cor} = 0$); however, it may be saved and/or copied with any factors in the range $0.01 < H_{cor} < 2000$.

CONCLUSIONS AND FUTURE DEVELOPMENTS

Software for the prediction of initial conditions in reversed-phase HPLC on the basis of the structural formula of compounds has been developed. The software translates a structural

TABLE VII

EXPERIMENTAL CONCENTRATIONS OF ACETONITRILE [ACN (%) (e)] AND CONCENTRATIONS PREDICTED BY CHROMDREAM [ACN (%) (p)] FOR EXPERIMENTAL CAPACITY FACTORS (k'_e) TO BE OBTAINED

Column, Spherisorb ODS-2 [5,18].

No.	Compound	k'_e	ACN (%) (e)	ACN (%) (p)	Difference (%)	k'_p [a]
1	Acetophenone	2.91	40	45	+5	
2	Aniline	2.21	30	30	0	
3	Anisole	3.43	50	49	−1	
4	Benzaldehyde	3.10	40	38	−2	
5	Benzene	3.42	50	47	−3	
6	Benzonitrile	3.27	40	40	0	
7	Benzyl acetate	2.87	50	50	0	
8	Benzyl alcohol	1.76	30	37	+7	2.42
9	Benzyl bromide	2.84	60	60	0	
10	Benzyl chloride	2.53	60	59	−1	
11	Benzyl cyanide	3.50	40	39	−1	
12	Biphenyl	3.10	70	70	0	
13	1-Bromo-2-nitrobenzene	3.30	50	56	+6	5.20
14	1-Bromo-4-methylphenol	2.38	50	58	+8	4.18
15	α-Bromo-*p*-phenylacetophenone	4.92	60	57	−3	
16	*m*-Bromoaniline	2.14	50	51	+1	
17	*m*-Bromobenzene	3.38	60	59	−1	
18	*p-tert.*-Butylhydroquinone	2.56	60	50	−10	1.35
19	*p-tert.*-Butylphenol	3.50	50	59	+9	7.13
20	Butyrophenone	2.49	60	60	0	
21	Chlorobenzene	3.01	60	59	−1	
22	α-Dibromo-*p*-phenylacetophenone	4.92	60	57	+3	
23	Dimethyl phthalate	1.73	50	54	+4	
24	2,4-Dimethylphenol	1.90	50	58	+8	3.30
25	2,5-Dimethylphenol	2.02	50	57	+7	3.30
26	Ethyl 3-phenylpropionate	3.12	60	63	+3	
27	Ethyl benzoate	2.70	60	56	−4	
28	Ethyl phenylacetate	3.30	50	53	+3	
29	N-Ethylaniline	3.03	50	52	+2	
30	Heptanophenone	2.21	80	79	−1	
31	Hexanophenone	2.90	70	67	−3	
32	Methyl benzoate	2.81	50	50	0	
33	Nitrobenzene	2.43	50	49	−1	
34	4-Nitrophenacyl bromide	2.61	40	40	0	
35	Phenacyl bromide	3.24	50	43	−7	2.00
36	Phenol	2.54	30	28	−2	
37	4-Phenyl-1-butanol	1.95	50	53	+3	
38	5-Phenyl-1-pentanol	2.38	50	56	+6	3.58
39	Propiophenone	2.89	50	52	+2	
40	*m*-Propyl-*p*-hydroxybenzoate	4.33	40	40	0	
41	Thymol	2.46	60	65	+5	
42	Toluene	3.02	60	58	−2	
43	Valerophenone	3.69	60	59	−1	

[a] When the deviation is >5% or <−5% then predicted values of k' (k'_p) are shown given.

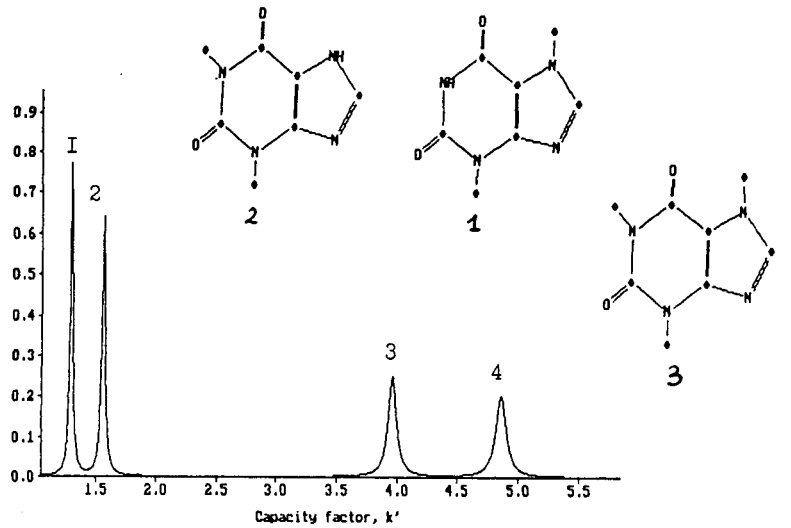

Fig. 3. Simulated chromatogram. 1 = Theobromine; 2 = theophylline; 3 = caffeine; 4 = phenol. Capacity factor range, 1.5–4 for compounds 1, 2 and 3 [20] and 1–10 for compounds 1, 2, 3 and 4 [21]. Sorbent: Nucleosil 120-5 C_{18}; eluent: methanol–water (20:80); column: 13 cm × 4 mm I.D.; flow-rate: 0.5 ml min^{-1}.

TABLE VIII

TRANSLATION OF STRUCTURAL FORMULAE INTO FRAGMENTS

Theobromine		Caffeine		Theophylline	
ar=C–	−2	ar=C–	−2	ar=C–	−2
ar=CH–	−1	ar=CH–	−1	ar=Ch–	−1
CH_3	−2	CH_3	−3	CH_3	−2
ar=N–	−1	ar=N–	−1	ar=N–	−1
arN	−2	arN	−3	arN	−2
arNHp	−1	arCO	−2	arNH	−1
arCO	−2			arCO	−2
V (cm^3 mol^{-1})	117.1		134.4		122.7
ΔG (kJ mol^{-1})	−123.6		−126.9		−127.8

formula of a compound into fragments and calculates the retention of the compound on different reversed-phase columns with methanol–, acetonitrile– or tetrahydrofuran–water mobile phases.

The software predicts the optimum concentration of methanol, acetonitrile or tetrahydrofuran in water to obtain acceptable values of capacity factors on different reversed-phase columns both for a single compound and for a mixture of compounds (up to 100).

The software simulates chromatograms and plots capacity factors or logarithms of capacity factors as a function of the concentration of an organic solvent in a mobile phase.

The software gives the opportunity to compare different reversed-phase columns, to calibrate columns and to determine parameters of a given column responsible for the retention and selectivity.

We are now working on extensions of the method in several directions: to develop a program for the prediction of the effect of mobile phase pH on retention and to develop a compu-

ter program for the prediction of retention on the basis of structural formulae in gradient reversed-phase HPLC.

ACKNOWLEDGEMENT

We are grateful to Dr. P.J. Schoenmakers for valuable discussions.

REFERENCES

1 T. Hamoir, M. De Smet, H. Phyrins, P. Conty, N.V. Driessche, D.L. Massart, F. Maris, H. Hindriks and P.J. Schoemmakers, *J. Chromatogr.*, 589 (1992) 31.
2 M. De Smet, A. Peeters, L. Buydens and D.L. Massart, *J. Chromatogr.*, 457 (1988) 25.
3 H. Hindriks, F. Maris, J. Vink, A Peeters, M. De Smet and D.L. Massart, *J. Chromatogr.*, 485 (1989) 255.
4 F. Maris, H. Hindriks, J. Vink, A. Peeters, N.V. Driessche and L. Massart, *J. Chromatogr.*, 506 (1990) 211.
5 R. Smith and C.M. Burr, *J. Chromatogr.*, 485 (1989) 325.
6 K. Valko, G. Szabo, J. Rohrich, K. Jemnitz and F. Darvas, *J. Chromatogr.*, 485 (1989) 349.
7 E. Janos, F. Csizmadia, K. Valko and F. Darvas, *19th International Symposium on Chromatography, Aix-en-Provence, 1992*, Abstract 1, p. 58.
8 S.V. Galushko, *J. Chromatogr.*, 552 (1991) 91.
9 S.V. Galushko, *19th International Symposium on Chromatography, Aix-en-Provence, 1992*, Abstract 4, p. 47.
10 S.V. Galushko, *Chromatographia*, 36 (1993) 39.
11 S.V. Galushko, *17th International Symposium on Column Liquid Chromatography, Hamburg, 1993*, Abstract 2-217.
12 S.V. Galushko, *Chromatographia*, in press.
13 S.V. Galushko, A.A. Kamenchuk and G.L. Pit, in preparation.
14 V.P. Belousov and M.Y. Penov, *Termodinamika Vodnyh Rastvorov Neelectrolitov*, Khimiya, Leningrad, 1983, p. 264.
15 B. Bushewski and S.V. Galushko, *Sep. Sci. Technol.*, in press.
16 R.J.M. Vervoort, S.A. Maris and H. Hindriks, *J. Chromatogr.*, 623 (1992) 207.
17 H. Engelhardt and M. Jungheim, *Chromatographia*, 29 (1990) 59.
18 Smith and C.M. Burr, *J. Chromatogr.*, 475 (1989) 57.
19 P.J. Schoemmakers, H.A. Billiet and L. de Galan, *J. Chromatogr.*, 218 (1981) 261.
20 *HPLC Liquid Chromatography 1991; Macherey–Nagel Applications Guide, Application No. 432*, Macherey–Nagel, Düren, 1991.
21 Y. Ohtsu, Y. Shiojima, T. Okumura, J. Koyama, K. Nakamura, O. Nakata, K. Kimata and N. Tanaka, *J. Chromatogr.*, 481 (1989) 147.

Journal of Chromatography A, 660 (1994) 61–65
Elsevier Science B.V., Amsterdam

CHROMSYMP. 2972

Optimization of high-performance liquid chromatography and solvent parameters for the separation of polycyclic aromatic hydrocarbons compared with supercritical fluid chromatography with UV detection

B.W. Wenclawiak* and T. Hees

Analytische Chemie I, Universität Siegen, Adolf-Reichwein-Strasse, 57068 Siegen (Germany)

ABSTRACT

Ten packed standard columns were evaluated for the separation of the sixteen US Environmental Protection Agency polycyclic aromatic hydrocarbons (PAHs) by gradient HPLC. This was done in a systematic way by the use of chemometric parameters such as window diagrams and chromatographic response factors and a computer program to calculate k', α, N and R_s. New approaches to a more economical and ecological use of HPLC solvents were evaluated. Good results were achieved by recycling acetonitrile–water waste by distillation as the azeotrope and using it again with methanol in an HPLC system. Supercritical fluid chromatography with carbon dioxide as supercritical fluid and acetonitrile as modifier was compared with HPLC, using the same column in both methods, for the determination of PAHs.

INTRODUCTION

Polycyclic aromatic hydrocarbons (PAHs) are environmental pollutants because of their carcinogenic, mutagenic and toxic potential [1] and they are ubiquitous in different concentrations in air, water and soils. Their identification and determination are a great challenge for the analytical chemist.

PAHs can be determined by various chromatographic techniques. High-performance liquid chromatography (HPLC) in combination with a fluorescence detector is the most powerful method [2]. It is a common procedure to use acetonitrile–water gradients in HPLC [3,4]. Supercritical fluid chromatography (SFC) is also possible, but at the moment only with UV detection.

The selection of a suitable stationary phase for PAH separation depends on the particle size, which should be small (<5 μm), and on the pore size. Commercially available RP-18 columns show great differences with respect to PAH separation, depending on the separation conditions and stationary phases used [5–7]. A comprehensive comparison of fused-silica capillary columns for GC–electron-capture detection for chlorinated hydrocarbons was published by Lopez-Avila *et al.* [8].

Nevertheless, often various PAHs cannot be separated from each other or only with poor quality. The reason for this is the very slight differences in their properties *e.g.*, polarity and polarizability. The quality of a column can be judged from the chromatographic resolution R_s

* Corresponding author.

0021-9673/94/$07.00 © 1994 Elsevier Science B.V. All rights reserved
SSDI 0021-9673(93)E1133-K

of pairs of compounds, which can be calculated as follows:

$$R_s = \frac{2\Delta t}{w_{b1} + w_{b2}} \quad (1)$$

where Δt is the difference of retention times of peaks 1 and 2 and w_b is the peak width at base. The peak separation function (f/g) (where f is the depth of valley below a straight line connecting the two adjacent peak maxima and g is the height of the straight line above the baseline at the valley) was developed by Kaiser [9] and generalized by Morgan and Deming [10], who developed the chromatographic response function (CRF):

$$CRF = \sum_{i=1}^{k} \ln (P_i), \quad P_i = \frac{f}{g} \quad (2)$$

where P_i is the peak separation for n peak pairs. This CRF value allows the separation of pairs of peaks to be judged in an easy manner.

The window diagram technique is a chemometric procedure for solvent optimization in HPLC [11]. The selectivity factor α is plotted against the solvent composition and the maxima of the curves show the most suitable separation conditions. This allows proper conditions to be selected and also permits other factors to be considered [12].

In this work we tested ten different reversed-phase columns for the determination of PAHs.

EXPERIMENTAL

An Applied Biosystems HPLC system was used. It consists of two pumps (Model 400 solvent-delivery system), an injector (Rheodyne Model 7125 with a 20-μl loop), a mixer (Model 491 dynamic mixer–injector), a fluorescence detector (ABI Model 980 programmable fluorescence detector) and a UV detector (ABI Model 783 A programmable absorbance detector). For data storage and evaluation, a PE Nelson interface (900 Series interface) with PE Nelson 2600 SI software and a Vector 80386 SX personal computer was employed. The column temperature was adjusted with a Colora column oven.

The Abimed–Gilson SFC system consists of two pumps (Model 308 Pump A Master 10 SC for carbon dioxide, Model 306 Pump B Slave 5 SC for acetonitrile as modifier), a mixer, an autosampler (Model 401 diluter with Model 231 ASI injection port), an oven (Model 831 temperature regulator), a UV detector (Model 117) and a back-pressure regulation valve as restrictor (regulation valve in Model 821 pressure regulator).

Acetonitrile (LiChrosolv; Merck, Darmstadt, Germany), doubly distilled water, methanol (b.p. 64°C) and acetonitrile–water azeotrope (b.p. 77°C) distilled through a 1.5-m column were used as solvents.

National Institute of Standards and Technology (NIST) (Gaithersburg, MD, USA) PAH standard containing sixteen US Environmental Protection Agency (EPA) priority PAHs was obtained from Promochem (Wesel, Germany).

The following columns were used: Eurosphere 80 C_{18} (250 × 2 mm I.D.; 5 μm) (column 1) and Eurosphere 80 C_{18} (250 × 4 mm I.D.; 5μm) from Knauer (Berlin, Germany); Nucleosil 5 C_{18} PAH, (150 × 4 mm I.D.; 5 μm) (column 2) from Macherey–Nagel (Düren, Germany); Aluspher 100 RP SelectB (250 × 4 mm I.D.; 5 μm) (column 4), Superspher 100 RP 18 (250 × 4 mm I.D.; 5 μm) (column 5) and special column KU 48 (250 × 4 mm I.D.; 5 μm) (column 10) from Merck; and Hypersil phenyl (250 × 4.6 mm I.D.; 5 μm) (column 6), Hypersil-MOS (250 × 4 mm I.D., 5 μm) (column 7), Hypersil-PAH C_{18} (100 × 4.6 mm I.D.; 5 μm) (column 8), Nucleosil C_{18} (120 × 4.6 mm I.D.; 3 μm) (column 9) and Nucleosil 120 C_{18} (250 × 4 mm I.D.; 5 μm) (column 3) from Muder & Wochele (Berlin, Germany).

A computer program was written to calculate the chromatographic parameters k', α, N and R_s from storage data files of a PE 2600 data system [13] using equations from the literature [14].

RESULTS AND DISCUSSION

In order to evaluate the differences between standard and special stationary phases, the chromatographic parameters (gradient, temperature, flow-rate) and the detector parameters (excita-

tion and emission wavelengths for fluorescence detection) were individually optimized for each column.

The resolution R_s for certain compounds was calculated. In Fig. 1, the resolution of all columns is plotted for four pairs of PAHs that are difficult to separate. Only three columns (2, 6 and 8) gave a sufficient separation ($R_s \geq 1$) for these pairs. The experiments showed that special materials as the stationary phase gave better results.

Another aim of this study was to find new ways for the more economical and ecological use of HPLC solvents. Acetonitrile–water solvent waste was distilled [azeotrope of acetonitrile–water (84:16), b.p. 77°C] and reused after adjusting it to acetonitrile–water (70:30) as solvent A with methanol as solvent B in an HPLC system.

With the help of the above-mentioned chemometric parameters, the time-consuming trial-and-error method should be replaced through systematic work. The following data were obtained from experiments with a Knauer Eurosphere 80 C_{18} column (250 × 4 mm I.S., 5 μm).

The window diagram can help to select the conditions for a good separation of mixtures, which are at the maxima of the curve. Here 0 or 40% methanol represented the best or second best conditions. For isocratic separation a ternary mixture with 40% methanol was chosen. Isocratic separation conditions offer many advantages, *e.g.*, no column equilibration is neces-

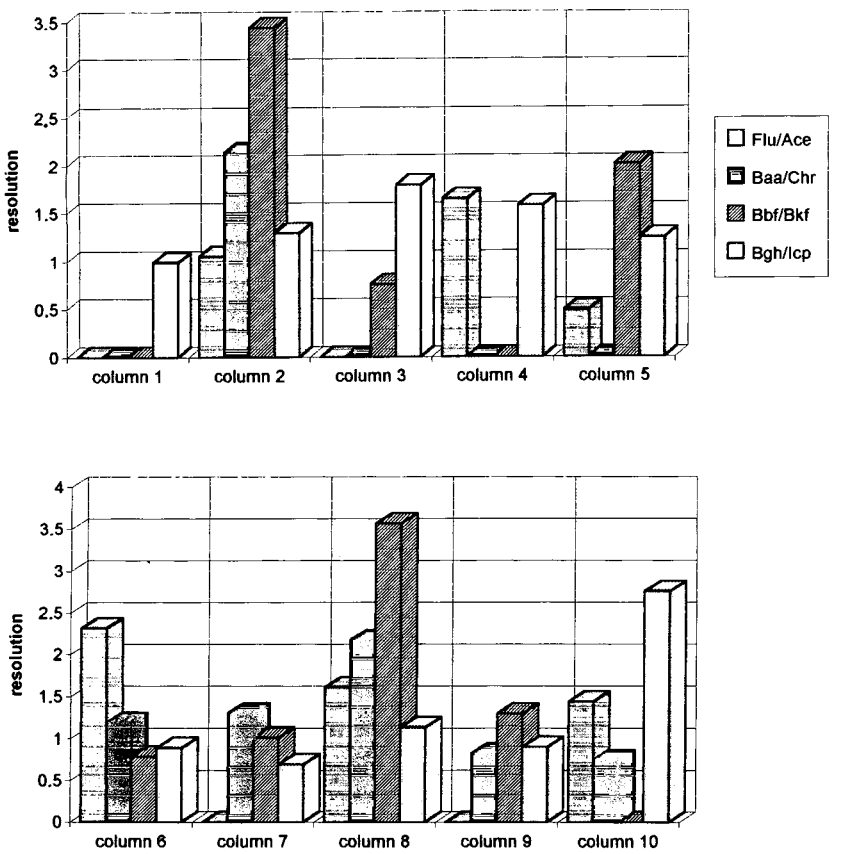

Fig. 1. Resolution of the four poorly resolved pairs acenaphthene–fluorene, benz[*a*]anthracene–chrysene, Benzo[*b*]fluoranthene–Benzo[*k*]fluoranthene and benzo[*ghi*]perylene–indeno[1,2,3-*cd*]pyrene with ten reversed-phase columns. For identification of columns see Experimental section.

sary, thus the analysis time can be decreased, or a straighter baseline, and/or less solvent noise under certain detection conditions.

A plot of the Van Deemter curve yielded an optimum flow-rate of 0.8 ml/min.

To judge the quality of the separation at different temperatures, the chromatographic response factor (CRF) was calculated. The CRF became less negative for all four pairs with increasing temperature (25°C, −2.600; 30°C, −2.125; 35°C, −1.954; 40°C, −1.598).

According to the retention times, the chromatographic parameters for the excitation and emission wavelengths of the fluorescence detector had to be adjusted so as to give optimum sensitivity.

Fig. 2 shows two chromatograms for an acetonitrile–water binary gradient and another binary gradient with a ternary mixture of methanol with acetonitrile–water (70:30) obtained with the Nucleosil 5 C_{18} PAH column.

The quality of the separation (α, k', N) is comparable for both methods. The α values are given in Table I.

A Hypersil-PAH C_{18} column was selected for a comparison of the HPLC and SFC methods. The SFC trace obtained with carbon dioxide as supercritical fluid and acetonitrile as modifier is shown in Fig. 3. The major advantage of SFC is the shorter analysis time, and further the

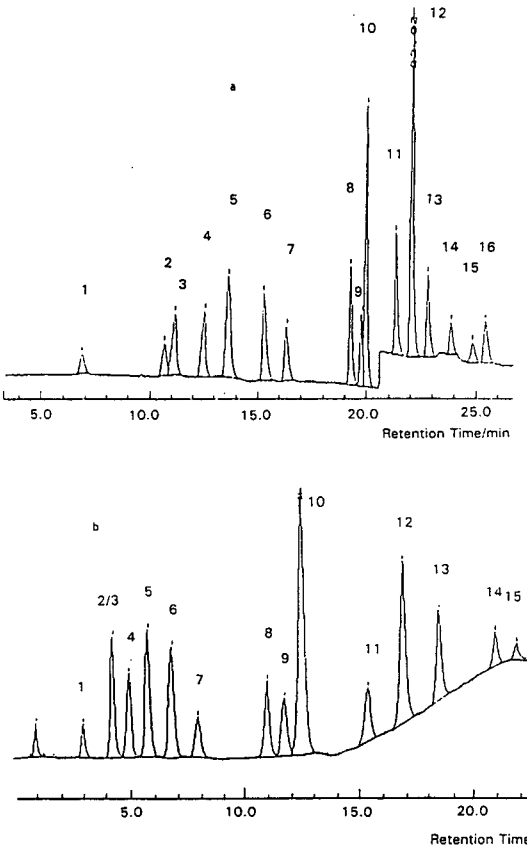

Fig. 2. HPLC of a PAH standard with (a) a binary acetonitrile (ACN)–water gradient at 30°C and a flow-rate of 1 ml/min and (b) a binary gradient of a ternary mixture of methanol with acetonitrile–water at 40°C and a flow gradient (0–8.5 min, 0.7 ml/min; 8.5–10.5 min, gradient to 1.1 ml/min; 10.5–26 min, 1.1 ml/min). Solvent gradient (a): $t = 0$, ACN–water (55:45); $t = 6$ min, gradient in 10 min to ACN–water (80:20); $t = 16$ min, gradient in 3 min to ACN; $t = 19$ min, ACN; $t = 32$ min, gradient in 2 min to ACN–water (55:45). Solvent gradient (b) [with B = MeOH and A = ACN–water (70:30)]: $t = 0$, 100% A; $t = 10$ min, gradient in 8 min to 100% B; $t = 18$ min, 10 min 100% B; $t = 28$ min, gradient in 2 min to 100% A. Wavelengths for excitation and emission were set to optimum sensitivity, similar to those explained in the literature [16]. For peaks 1–16, see Table I.

TABLE I

RESOLUTION α ACCORDING TO FIG. 2a AND b

No.	Compound	α	
		Gradient a	Gradient b[c]
1	Naphthalene		
	Acenaphthylene[a]	1.27	1.18
2	Acenapthene	1.37	1.38
3	Fluorene	1.04	1.00
4	Phenanthrene	1.14	1.22
5	Anthracene	1.12	1.20
6	Fluoranthene	1.11	1.21
7	Pyrene	1.07	1.20
8	Benz[*a*]anthracene	1.19	1.43
9	Chrysene	1.03	1.07
10	2,2'-Binaphthyl[b]	1.01	1.07
11	Benzo[*b*]fluoranthene	1.07	1.25
12	Benzo[*k*]fluoranthene	1.04	1.11
13	Benzo[*a*]pyrene	1.04	1.10
14	Dibenz[*a,h*]anthracene	1.05	1.14
15	Benzo[*ghi*]perylene	1.04	1.05
16	Indeno[1,2,3-*cd*]pyrene	1.03	1.04

[a] Acenaphthylene: UV detection in HPLC.
[b] As internal standard.
[c] According to Fig. 2.

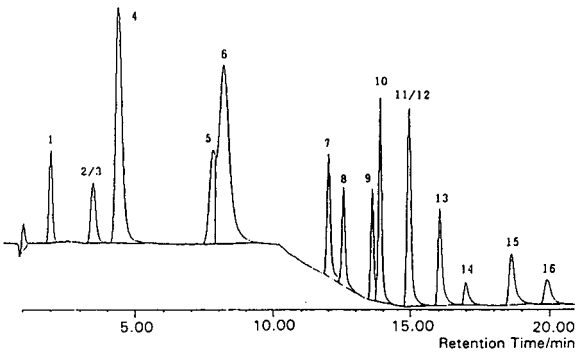

Fig. 3. SFC of a PAH standard obtained at 90°C with UV detection at 254 nm. Pressure gradient: $t = 0$, 150 bar; $t = 4$ min, gradient in 6 min to 160 bar; $t = 10$ min, gradient in 2 min to 400 bar. Flow gradient: $t = 0$, 1 ml/min; $t = 10$ min, gradient in 2 min to 2 ml/min. Modifier gradient: $t = 0$, 0% ACN; $t = 10$ min, gradient in 2 min to 2% ACN. For peaks 1 and 11–16 see Table I; peaks 2–10 correspond with acenaphthylene to chrysene, same order as in Table I.

equilibration time is lower. The separation of the sixteen EPA PAHs is comparable with both methods, but slightly better using HPLC. A different column material will improve the separation but is not yet commercially available [15].

CONCLUSIONS

The quality of the separation showed great differences for the ten columns tested. The special PAH columns gave better results than the standard columns, owing to the larger pore size is the former instance.

Each column requires an individual programme for the gradient, temperature, flow-rate and excitation and emission wavelengths for fluorescence detection. By using chemometric parameters such as the window diagram and CRF value and a computer program for the calculation of important chromatographic values, the solvent optimization and the judgement of peak separation can be achieved in an easy and systematic manner.

Recycling of the acetonitrile–water eluate and reusing it in a ternary mixture with methanol using a binary gradient showed new possibilities for the use of HPLC. The acetonitrile consumption can be reduced to 56% and the costs to nearly 23% when costs of solvents, disposal and additional costs for distillation, etc., are taken into account.

A comparison between HPLC and SFC with UV detection showed the great advantages of SFC, *i.e.*, shorter analysis time, lower operating costs and the use of carbon dioxide, which is non-toxic, non-flammable, inert and does not have to be discharged. The detection limits are similar with the HPLC and SFC methods, between 1.2 ng for phenanthrene and 17.7 ng for benzo[*ghi*]perylene. The importance of SFC will increase further in the future when it becomes possible to use fluorescence detection and columns specially made for SFC.

ACKNOWLEDGEMENTS

We thank Muder & Wochele (Berlin) and Merck (Darmstadt) for chemical support and Abimed (Langenfeld) for technical support.

REFERENCES

1 W.E. May and S.A. Wise, *Anal. Chem.*, 56 (1984) 225.
2 A. Obuchi, H. Aoyama, A. Ohi and H. Obuchi, *J. Chromatogr.*, 312 (1984) 247.
3 R.K. Sorell and R. Reding, *J. Chromatogr.*, 185 (1979) 655.
4 T. Gremm and F.H. Frimmel, *Wasser*, 75 (1990) 171.
5 H. Engelhardt and M. Jungheim, *Chromatographia*, 29 (1990) 59.
6 I. Stöber and R. Reupert, *Wasser*, 56 (1981) 115.
7 M. Lührmann, H.G. Kicinski and A. Kettrup, *Z. Wasser Abwasser Forsch.*, 20 (1987) 212.
8 V. Lopez-Avila, N. Dodhiwala and W.F. Beckert, *J. High. Resolut. Chromatogr. Chromatogr. Commun.*, 11 (1988) 234–41.
9 R.E. Kaiser, *Gas Chromatographie*, Geest and Portig, Leipzig, 1960.
10 S.L. Morgan and S.N. Deming, *J. Chromatogr.*, 112 (1975) 267.
11 R.J. Laub, *Int. Lab.*, (1981) 16.
12 J.C. Berridge, *Techniques for the Automated Optimization of HPLC Separations*, Wiley, Chichester, 1985.
13 T. Hees, *Diplomarbeit*, Universität-GH Siegen, Siegen, 1993.
14 V. Meyer, *Praxis der Hochleistungsflüssigchromatographie*, Moritz Diesterweg, Berlin, 1986.
15 W. Kleiböhmer, personal communication.
16 K. Ogan, E. Katz and W. Slavin, *Anal. Chem.*, 51 (1979) 1315.

Journal of Chromatography A, 660 (1994) 67–73
Elsevier Science B.V., Amsterdam

CHROMSYMP. 2945

Mobile phase selection for high-performance liquid chromatographic analysis of novel zinc(II) carboxylates with N-donor ligands

A. Oriňák* and K. Gyoryová

Department of Inorganic Chemistry, Faculty of Sciences, P.J. Safarik University, Moyzesova 11, 041 54 Košice (Slovak Republic)

E. Matisová

Department of Analytical Chemistry, Faculty of Chemical Technology, Slovak Technical University, Radlinského 9, 812 37 Bratislava (Slovak Republic)

L. Šlesárová

Department of Chemistry, Biochemistry and Biophysics, University of Veterinary Medicine, Komenského 73, 041 81 Košice (Slovak Republic)

J. Skoršepa

Department of Inorganic Chemistry, Faculty of Sciences, P.J. Safarik University, Moyzesova 11, 041 54 Košice (Slovak Republic)

I. Rosival

Department of Chemistry, Biochemistry and Biophysics, University of Veterinary Medicine, Komenského 73, 041 81 Košice (Slovak Republic)

M. Ganajová

Department of Inorganic Chemistry, Faculty of Sciences, P.J. Safarik University, Moyzesova 11, 041 54 Košice (Slovak Republic)

ABSTRACT

The PRISMA optimization project was used for mobile phase selection in the HPLC analysis of novel zinc(II) carboxylates of the type $Zn(RCOO)_2 \cdot L_n \cdot q(H_2O)$ with N-donor ligands. The composition of the mobile phase is characterized by the solvent strength (S_T) and the selection points (P_S). At a constant S_T the correlation between P_S and retention data can be described by a quadratic function. For constant P_S the solvent strength and retention data correlate with a logarithmic function. On the basis of the results obtained in the TLC separation of the single zinc(II) carboxylate, solvents were chosen (ethanol, acetonitrile, methanol, dioxane, 2-propanol) that are suitable for HPLC analyses of zinc(II) carboxylates on LiChrosorb RP-8 and RP-18 columns.

* Corresponding author.

0021-9673/94/$07.00 © 1994 Elsevier Science B.V. All rights reserved
SSDI 0021-9673(93)E0965-W

INTRODUCTION

Zinc(II) carboxylates of the type $Zn(RCOO)_2 \cdot L_n \cdot q(H_2O)$ (where R = H, CH_3, CH_3CH_2, $CH_3CH_2CH_2$, or $(CH_3)_2CH_2CH_2$, L = caffeine, thiourea, nicotinic acid or phenazone, $n = 1$ or 2 and $q = 0.5$, 1.5, 2.5, 3.5 and x is the variable content of water of crystallization) are an interesting group of substances. Nearest to them in pharmacological importance are zinc(II) compounds with pyrithione (1-hydroxypyridine-2-thione). Although the HPLC analysis of these substances is well known [1,2], there is very little information on the chromatographic analysis of novel zinc(II) carboxylates with N-donor ligands (their structure is unknown but is currently being investigated).

Successful tests of the biological activity of these newly synthesized compounds require analytical methods for the determination of zinc(II) cation, carboxylate anion, ligand metabolites and also non-metabolized forms of the original zinc(II) carboxylates. With regard to the nature of the compounds, HPLC [with comparative zinc(II) determination by atomic absorption spectrometry (AAS)] appears to be the most suitable method of analysis.

In the first phase of analysis, selection of the optimum mobile phase plays a most important role. Many studies have been based on the results of preliminary TLC or HPTLC analyses, the optimum composition of the mobile phase being chosen using the simplex method [3], statistical techniques [4] and multifactor analysis [5,6].

At present, optimization of mobile phase composition depends entirely on computer techniques and it is possible to select within a relatively short time the most suitable multicomponent mobile phase [7–13] or a buffer mixture [14], and it is also possible to identify individual peaks [15–17], in addition to the selection of both the mobile and stationary phases. More advanced computer techniques allow combined optimizations of the mobile phase, pH and the content of the organic modifying reagent in HPLC analyses [18].

For optimization of the mobile phase for the HPLC of zinc(II) carboxylates the PRISMA model [19,20], utilizing combinations of the elution strength of the solvents (based on the Snyder scale [21]), in RP-HPLC of the substances examined was used. By modifying the composition of the three solvents and water, in relation to the capacity factor of the substance analyzed, the optimum mobile phase composition for zinc(II) formate, acetate, propionate, butyrate and isobutyrate salts with bound N-donor ligands was selected by the PRISMA model.

EXPERIMENTAL

Chemicals

All solvents were of analytical-reagent grade. Dioxane, methanol (MeOH), 2-propanol (PrOH) and ethanol (EtOH) were purchased from Lachema (Brno, Czech Republic) and acetonitrile (ACN) from VEB Laborchemie (Apolda, Germany).

Redistilled water [prepared with an Ilmator system (Biplex, Jena, Germany)] had a conductivity of 0.4 μS.

All zinc(II) carboxylates tested were provided by the Department of Inorganic Chemistry, P.J. Safarik University (Košice, Slovak Republic).

Caffeine (1,3,7-trimethylxanthine), thiourea, phenazone (2,3-dimethyl-1-phenyl-3-pyrazolin-5-one) and nicotinic acid (3-pyridinecarboxylic acid) were purchased from Medika (Bratislava, Slovak Republic).

Instruments

An LCP 4000 high-pressure HPLC pump (ECOM, Prague, Czech Republic), a Model 2062.2 spectrophotometric detector (ECOM) and a GP 3 gradient programmer with a Model 7125 injection valve with a 20-μl sample loop (Rheodyne, Berkeley, CA, USA) were used.

Analyses were carried out on the following columns: (A) LiChrosorb RP-8 (stainless steel, 250 × 4.6 mm I.D., $d_p = 7$ μm) and (B) LiChrosorb RP-18 (stainless steel, 250 × 4.6 mm I.D., $d_p = 7.5$ μm), both purchased from Knauer (Berlin, Germany). Results of the analyses were evaluated by means of an APEX on-line computer integrator and the program SOLVENT (ECOM).

Preparation of stock solutions

Solutions of the analyte substances (Table I) were prepared by weighing 5 mg of each compound into a 10-ml volumetric flask and dissolving in and diluting to volume with redistilled water. Mixtures 1 (pure ligands), 2 (formates), 3 (acetates), 4 (propionates), 5 (butyrates) and 6 (isobutyrates) were prepared by dissolving 5 mg of each compound in and diluting to volume with redistilled water in a 10-ml glass volumetric flask.

Conditions of analysis

All HPLC analyses were run under the following conditions: flow-rate of mobile phase, 1 ml/min; detection wavelength, 253 nm; detector temperature, 25°C; sample amount injected, 20 μl; and elution mode, isocratic.

Analysis

A detailed description of the procedure by which a suitable composition of the mobile phase is selected by means of the PRISMA model can be found in the literature [19,20]. The method can be summarized as follows:

(1) Selection of the three solvents suitable for analysis according to the Snyder classification.

(2) The solvent strength is first adjusted at selectivity point $P_S = 333$. At the determined solvent strength (S_{T1}), the k' values of the selectivity points representing four solvent combinations along the edges of the triangle between the basic selectivity points (433–343–334) are measured.

(3) From each of the four measured selectivity points along a line, the mathematical function $k' = aP_s^2 + bP_s + c$ for each zinc(II) carboxylate was calculated.

(4) The strategy in points (1) and (3) is repeated at two other solvent strength levels. The difference between the three solvent strength levels should not exceed 10–15% [19,20].

(5) The optimum mobile phase composition was calculated by the SOLVENT program, which optimizes mobile phase composition on the principle of finding the isoeluotropic plane in the tetrahedron of the solvents in the corners of the triangle. It is the plane on which the composition of the mobile phase gives a similar solvent and elution strength. The position of the plain varies according to the nature of the mixtures that are to be separated.

To find the optimum means finding a plane inside the PRISMA on which the peaks of the single substances have a capacity factor in the range 1–10 and chromatographic resolution is suitable.

The program SOLVENT allows the optimum mobile phase composition to be found after seven chromatographic analyses.

RESULTS AND DISCUSSION

From the results of preliminary TLC analyses, it follows that formates start to separate in mobile phases containing acetonitrile ($S_T = 5.8$), methanol ($S_T = 5.1$), dioxane ($S_T = 4.8$) and water ($S_T = 10.2$). For acetate separations, a mixture of acetonitrile, methanol, 2-propanol ($S_T = 3.9$) and water appears to be suitable. Acceptable propionate, butyrate and isobutyrate separation takes place in methanol, dioxane and water mixtures as mobile phases. On the basis of these results, HPLC analysis of the zinc(II) carboxylates with N-donor ligands was started on the RP-8 and RP-18 columns. In the next step, gradient elution with ACN–water, MeOH–water, dioxane–water and PrOH–water was tested to predict the isocratic composition of the mobile phase. It can then be stated which plane inside the PRISMA can be used for optimization of the mobile phase composition. On a plane with $S_T = 0.5$ or lower, the capacity factors of the individual compounds tested were higher than 10. Increasing the S_T values to 1.95 and 2.4 led to more effective results. Subsequently, in zinc(II) carboxylate analyses on the LiChrosorb RP-8 and RP-18 columns the following mobile phases were used: (A) ACN–MeOH–dioxane–water ($S_T = 2.4$, $P_S = 333$, 181, 118, 811, 334, 343, 433, 136, 163, 316, 361, 613, 631) and (B) ACN–MeOH–PrOH–water [$S_T = 1.95$, P_S as for (A)].

Zinc(II) carboxylate analyses on the RP-8 column with mobile phase A revealed insufficient separation of the individual compounds and co-elution of nicotinic acid and thiourea salts. Using mobile phase B (on the same column), the

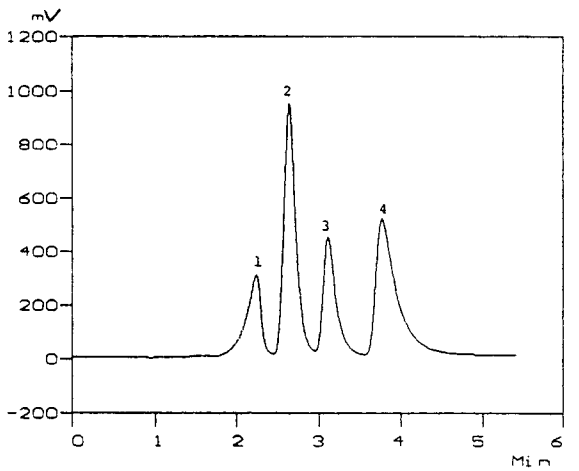

Fig. 1. HPLC of ligand mixture obtained on LiChrosorb RP-18 with mobile phase ACN–MeOH–PrOH–water (P_S = 343, S_T = 1.95), detection at 253 nm. Peaks: 1 = nicotinic acid; 2 = thiourea; 3 = caffeine; 4 = phenazone.

chromatographic resolution of the individual compounds in the mixtures was low with increasing capacity factors. In this system, partial separation of the mixture of compounds 1 and 10 [ligand and its zinc(II) carboxylate salt] was also observed.

Analyses on the RP-18 column with mobile phase A showed insufficient separation of thiourea- and caffeine-bound zinc(II) carboxylates, and the thiourea carboxylate peaks were non-symmetric.

Dioxane-containing mobile phases (the same selectivity points and elution strength) are not suitable for HPLC analysis of zinc(II) carboxylate mixtures. Probably decomposition of the original substances occurs or substitution of dioxane into the coordination sphere of the zinc(II) carboxylate salts takes place.

Mobile phase B appears to be more suitable

TABLE I

COMPOUNDS TESTED AND RETENTION TIMES (t_R) AND CAPACITY FACTORS (k') OF INDIVIDUAL COMPOUNDS ANALYSED ON LICHROSORB RP-18

Mobile phase: P_S = 333, ACN–MeOH–PrOH–water (10.09:11.47:15:63.44, v/v), S_T = 1.95.

No.	Compound	t_R (min)	k'
1	Caffeine (caff)	3.17	1.02
2	Thiourea (tu)	2.61	0.66
3	Phenazone (phen)	3.85	1.45
4	Nicotinic acid (nica)	2.21	0.41
5	$Zn(HCOO)_2(tu)$	2.55	0.62
6	$Zn(HCOO)_2(tu)_2(H_2O)_x$	2.55	0.62
7	$Zn(HCOO)_2(nica)(H_2O)_x$	2.23	0.42
8	$Zn(HCOO)_2(nica)_2(H_2O)_x$	2.49	0.59
9	$Zn(HCOO)_2(caff)(H_2O)_{0.5}$	3.16	1.01
10	$Zn(HCOO)_2(caff)_2(H_2O)$	3.19	1.03
11	$Zn(CH_3COO)_2(tu)$	2.59	0.65
12	$Zn(CH_3COO)_2(tu)_2(H_2O)_x$	2.59	0.65
13	$Zn(CH_3COO)_2(phen)_2(H_2O)_{1.5}$	4.00	1.55
14	$Zn(CH_3COO)_2(nica)_2(H_2O)_x$	2.56	0.63
15	$Zn(CH_3COO)_2(caff)(H_2O)_{2.5}$	3.28	1.09
16	$Zn(CH_3COO)_2(caff)_2(H_2O)_{3.5}$	3.35	1.13
17	$Zn(CH_3CH_2COO)_2(tu)_2$	2.68	0.71
18	$Zn(CH_3CH_2COO)_2(caff)_2$	3.56	1.27
19	$Zn[CH_3(CH_2)_2COO]_2(tu)$	2.69	0.71
20	$Zn[CH_3(CH_2)_2COO]_2(tu)_2$	2.89	0.84
21	$Zn[CH_3(CH_2)_2COO]_2(caff)_2$	3.68	1.34
22	$Zn[(CH_3)_2(CH_2)COO]_2(tu)$	2.73	0.74
23	$Zn[(CH_3)_2(CH_2)COO]_2(tu)_2$	2.94	0.87
24	$Zn[(CH_3)_2(CH_2)COO]_2(caff)$	3.29	1.10
25	$Zn[(CH_3)_2(CH_2)COO]_2(caff)_2$	3.60	1.29

for zinc carboxylate separations on the RP-18 column. All compounds chromatographed eluted within 5 min with acceptable chromatographic resolution (Fig. 1). At the selectivity point 118 splitting of the thiourea peak occurred and this effect was also observed with thiourea zinc(II) carboxylates.

The most advantegeous composition of the mobile phase for the separation of the compounds under examination is the composition found at the selectivity point $P_S = 334$ or $P_S = 343$.

The retention parameters (capacity factors of first and last peaks, volume of solvent, retention time of first and last peaks) obtained in zinc(II) carboxylate analyses (Table I) were used as input data for the SOLVENT program. By regression analysis a quadratic function was found that describes how the capacity factor k' depends on mobile phase composition (given by the P_S value) at constant S_T. From Fig. 2 it follows that an increasing content of ACN in the mobile phase causes anomalities in the retention behaviour of pure caffeine (as a ligand), zinc(II) formate with caffeine and also zinc(II) acetate with caffeine (the capacity factor and analysis time increase). The retention behaviour of zinc(II) propionate, butyrate and isobutyrate (with bound caffeine) is more similar to that of the compounds with other ligands. Increasing the ACN content and a parallel PrOH decrease (Fig. 3) result in higher capacity factors for phenazone and its zinc(II) acetate salt. The k' values for all salts with nicotinic acid show a slight decrease. The same anomaly was observed in the retention behaviour of zinc(II) caffeine salts. Analysis of caffeine and phenazone is also more time consuming in the mobile phase at selectivity point 181. The optimum mobile phase compositions for individual zinc(II) carboxylate HPLC analyses are given in Table II.

The hydrophobicity of the compounds examined increases with the increase in the aliphatic chain length of the anion, being evident

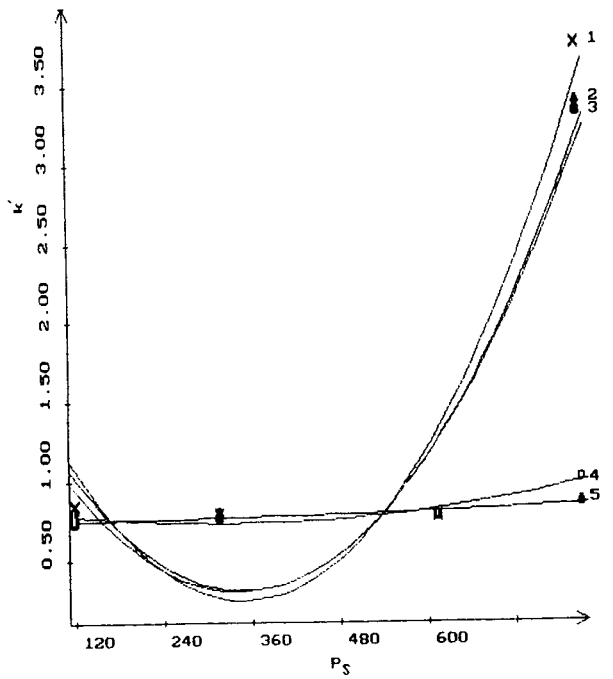

Fig. 2. Effect of P_S changes on the k' of the zinc(II) carboxylates. 1 = Pure caffeine; 2 = $Zn(HCOO)_2(caff)_2$; 3 = $Zn(CH_3COO)_2(caff)_2$; 4 = $Zn[CH_3(CH_2)_2COO]_2(caff)_2$; 5 = $Zn[(CH_3)_2CH_2COO]_2(caff)_2$.

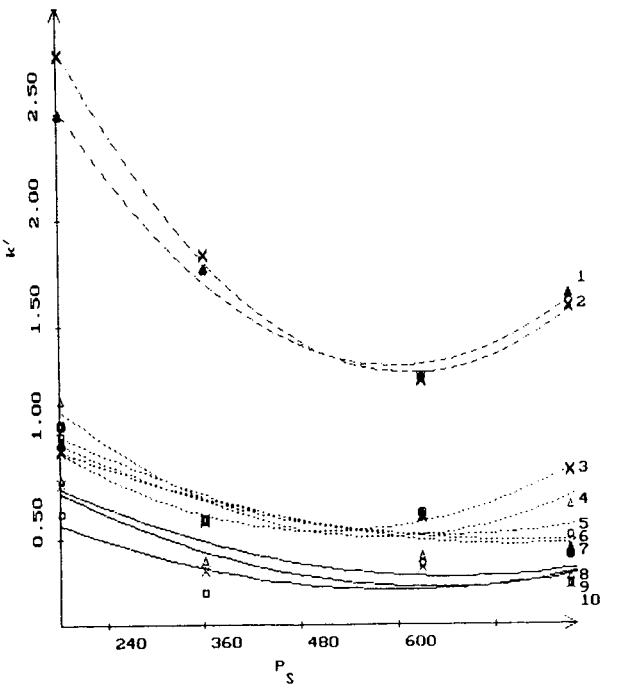

Fig. 3. Effect of mobile phase composition on the k' of zinc(II) carboxylates (P_S = 118, 163, 181, 316, 361, 613, 631, 811). 1 = Phenazone; 2 = $Zn(CH_3COO)_2(phen)_2$; 3 = thiourea; 4 = $Zn[CH_3(CH_2)_2COO]_2(tu)_2$; 5 = $Zn[(CH_3)_2CH_2COO]_2(tu)_2$; 6 = $Zn(HCOO)_2(tu)_2$; 7 = $Zn(CH_3COO)_2(tu)_2$; 8 = nicotinic acid; 9 = $Zn(CH_3COO)_2(nica)_2$; 10 = $Zn(HCOO)_2(nica)_2$.

TABLE II

OPTIMUM MOBILE PHASE COMPOSITION FOR SEPARATION OF ZINC(II) CARBOXYLATES ON RP-18 COLUMN, $S_T = 1.95$

Compound[a]	Mobile phase composition	P_S
4, 8, 14, 7	ACN–MeOH–PrOH–H_2O (26.9:3.83:5.0:64.27, v/v)	811
2, 5, 6, 11, 12, 17 19, 20, 22, 23	ACN–MeOH–PrOH–H_2O (20.2:3.8:15.0:61.0, v/v)	613
1, 9, 10, 15, 16, 18, 21, 24, 25	ACN–MeOH–PrOH–H_2O (20.2:3.8:15.0:61.0, v/v)	613
3, 13	ACN–MeOH–PrOH–H_2O (3.4:3.8:40.0:52.8, v/v)	118

[a] See Table I.

already in the analysis of propionates, in contrast to the formates and acetates, whose hydrophobicity is the same as for the pure ligand (Fig. 4).

The problem of the good chromatographic resolution of zinc(II) carboxylates (with an N-donor ligands) and its pure ligand or zinc(II) carboxylate–zinc(II) carboxylate mixtures (differing in their ligand numbers) is reminiscent of the problem in positional isomer separations [22]. For the identification and isolation of co-eluting components, the deconvolution process, based on the principal component analysis (PCA) technique [23], is frequently used. If the fact is taken into consideration that in mixtures consisting of a dissolved pure ligand and a corresponding zinc(II) carboxylate salt, a change in its ligand numbers or mutual ligand exchange may occur in the aqueous solution (complexation equilibria), the analysis of mixtures containing a zinc(II) carboxylate salt and the same ligand presents a problem which must be solved before starting tests on biological activity.

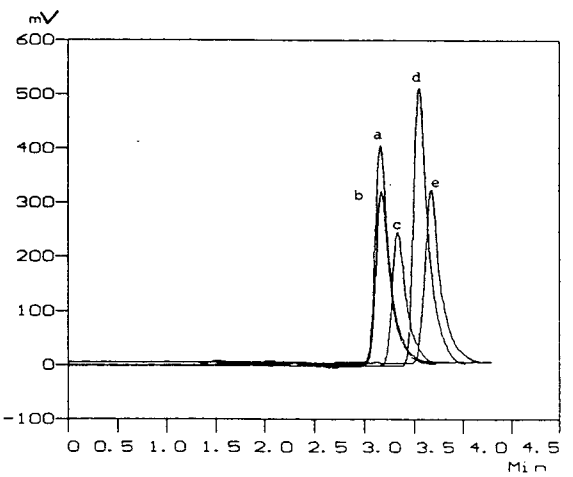

Fig. 4. Overlay of caffeine zinc(II) carboxylates showing aliphatic chain effect on the separation of individual compounds. Peaks: a = caffeine; b = zinc(II) formate with caffeine; c = zinc(II) propionate with caffeine; d = zinc(II) buthyrate with caffeine; e = zinc(II) isobutyrate with caffeine.

The mobile phase composition for the separation of zinc(II) carboxylates containing the same ligand in the molecule but with a different ligand number from a mixture (which mutually co-elute) has not yet been elucidated.

CONCLUSIONS

Novel $Zn(RCOO)_2 \cdot L_n \cdot q(H_2O)$ compounds were analysed on RP-8 and RP-18 columns. The optimum mobile phase composition for HPLC analysis of novel $Zn(RCOO)_2 \cdot L_n \cdot q(H_2O)$ compounds was chosen by using the PRISMA mathematical model and the program SOLVENT.

Good separations of the compounds observed were obtained with mobile phases containing acetonitrile, methanol, 2-propanol and water, at different P_S and constant S_T. Dioxane-containing mobile phases caused co-elution of zinc(II) carboxylates with nicotinic acid and thiourea. Separation on the RP-18 column is more effective than on the RP-8 column.

Some deviations in the retention behaviour of zinc(II) caffeine carboxylates were found and

analyses of caffeine and phenazone are more time consuming in mobile phase with $P_S = 181$. Gradient elution is also time consuming and does not give the required results.

A high 2-propanol content present in the mobile phase causes splitting of the thiourea and its zinc(II) carboxylate peaks.

The optimum mobile phase composition lies near to the acetonitrile corner of the solvent triangle and the area of optimal P_S is specified by the selectivity points 811, 613, 433, 344 and 631.

The results obtained (together with mobile phase flow optimization and confirmation of identity of each analyte separated) provide some of the information required before it will be possible to start analyses of zinc(II) carboxylates in the biological samples.

ACKNOWLEDGEMENT

This work is supported by the Slovak Ministry of Education Grant No. 1/990917/93 and it is gratefully acknowledged. The authors wish to thank Mr. Formanek from ECOM for the devices he provided. The authors also thank Miss Marta Stročeková for technical assistance.

REFERENCES

1 K. Nakajima, T. Yasuda and H. Nakazawa, *J. Chromatogr.*, 502 (1990) 379.
2 R.J. Fenn and M.T. Alexander, *J. Liq. Chromatogr.*, 11 (1988) 3403.
3 L.G. Sabaté and X. Tomás, *J. High Resolut. Chromatogr. Chromatogr. Commun.*, 7 (1984) 104.
4 Q.-S. Wang and B.-W. Yan, *Chromatographia*, 28 (1989) 473.
5 P.M.J. Coenegracht, M. Dijkman, C.A.A. Duineveld, H.J. Metling, E.T. Elema and M.Th., Malingré, *J. Liq. Chromatogr.*, 14 (1991) 3213.
6 J.I. Haleem and K.L. McNitt, *J. Liq. Chromatogr.*, 5 (1982) 1771.
7 S. Ahuja, *Selectivity and Detectability Optimizations in HPLC*, Wiley, Chichester, 1989, pp. 461–505.
8 S. Heinisch, P. Riviere and J.L. Rocca, *Chromatographia*, 32 (1991) 559.
9 T.P. Bridge, *Chromatogr. Anal.*, 11 (1990) 13.
10 H.A. Billiet and L. de Galan, *J. Chromatogr.*, 485 (1989) 27.
11 M. de Smet, A. Peeters, L. Buydens and D.L. Massart, *J. Chromatogr.*, 457 (1988) 25.
12 M. Gazdag, G. Szepesi and K. Fabian-Varga, *J. Chromatogr.*, 454 (1988) 95.
13 C.F. Poole and S.K. Poole, *Chromatography Today*, Elsevier, Amsterdam, 1991, pp. 469–485.
14 M. Gazdag, G. Szepesi and E. Szelecki, *J. Chromatogr.*, 454 (1988) 83.
15 B. Law and P.F. Chan, *J. Pharm. Biomed. Anal.*, 9 (1991) 271.
16 Y. Zhang, H. Zou and P. Lu, *Sepu*, 8 (1990) 285.
17 J.H. Wahl, C.G. Enke and V.Z. McGuffin, *J. High Resolut. Chromatogr. Chromatogr. Commun.*, 11 (1988) 858.
18 V. Satcs and O.V. Sakhartova, V.A. Belikov, L. Brivkalus and V.D. Grigoreva, *Zh. Anal. Khim.*, 39 (1984) 331.
19 S. Nyiredy, K. Dallenbach-Toelke and O. Sticher, *J. Liq. Chromatogr.*, 12 (1989) 95.
20 S. Nyiredy, W. Wosniok, H. Thiele and O. Sticher, *J. Liq. Chromatogr.*, 14 (1991) 3077.
21 L.R. Snyder, *J. Chromatogr. Sci.*, 16 (1978) 223.
22 J.R. Lynch, S.D. Patterson and R.E.A. Escott, *LC · GC*, 3, No. 9 (1990) 54.
23 P.J. Schoenmakers, *Optimization of Chromatographic Selectivity*, Elsevier, Amsterdam, 1986.

Journal of Chromatography A, 660 (1994) 75–84
Elsevier Science B.V., Amsterdam

CHROMSYMP. 2949

High-performance liquid chromatography of amino acids, peptides and proteins

CXXV☆. Molecular dynamics simulation of *n*-butyl chains chemically bonded to silica-based reversed-phase high-performance liquid chromatography sorbents

Irene Yarovsky, Marie-Isabel Aguilar and Milton T.W. Hearn*

Department of Biochemistry and Centre for Bioprocess Technology, Monash University, Wellington Road, Clayton, Victoria 3168 (Australia)

ABSTRACT

The molecular dynamics method has been applied to investigate the conformations of *n*-butyl ligands immobilised onto an amorphous silica surface analogous to those utilised with silica-based RP-HPLC sorbents. Three systems were constructed which corresponded to ligand densities of 1.64, 2.67 and 3.69 μmol/m^2. A number of parameters related to the structure of the sorbent materials were derived in order to characterise the molecular properties of each system. These parameters included the hydrocarbon layer thickness, the frequency of gauche conformations, the distance distribution for carbon atoms and the diffusion coefficients of individual atoms in the *n*-butyl ligands. From these properties, the positions of chains with respect to the surface as well as their mobility were estimated. It was found that at higher densities, the *n*-butyl chains are predominantly perpendicular to the surface while at low density they are highly tilted or lying almost parallel to the surface. The degree of ligand flexibility decreased with increasing surface density. Mobility of individual carbon atoms as well as chain disorder increased with distance from the surface for all ligand densities. The simulated properties of *n*-butyl chains immobilised to a silica surface correlated well with results obtained by Fourier transform IR and ^{13}C-cross polarisation magic angle spinning NMR experimental methods and statistical predictions of the behaviour of immobilised chains.

INTRODUCTION

High-performance liquid chromatography (HPLC) with microparticulate silica-based sorbents is now the central technique for the analysis and purification of many chemical and biological molecules. This popularity is due to a large number of factors, including the high reproducibility, selectivity and sensitivity of HPLC techniques. While significant advances continue to be made in chromatographic applications with high-performance adsorbents, there has been much less progress in the development of mechanistic models which describe, in detailed molecular terms, the interactive processes which occur between the immobilised stationary phase ligands, the mobile phase and the solute. This can be attributed, in part, to the lack of knowledge about the precise interactive structure and conformational properties of the immobilised ligands. The development of such knowledge would not only aid interpretation of re-

* Corresponding author.
☆ For Part CXXIV, see ref. 35.

0021-9673/94/$07.00 © 1994 Elsevier Science B.V. All rights reserved
SSDI 0021-9673(93)E0998-A

tention mechanisms *per se* but also provide the basis for significant improvements in the design of new adsorbents.

Current understanding of the structure and relative dynamics of ligands immobilised to silica stationary phases has been largely derived from spectroscopic techniques [1–8]. For example, it has been demonstrated [1–6] by solid state NMR studies on *n*-alkylsilica reversed-phase sorbents that the mobility of the immobilised *n*-alkyl chains is dependent on the degree of functionalisation of the silanol groups, the composition of the *n*-alkyl groups, the extent of endcapping and the composition of the mobile phase. Fourier transform infrared (FT-IR) spectroscopy has also been used [9,10] with *n*-alkyl silicas to study the conformational disorder of immobilised *n*-alkyldimethyl ligands and has revealed a significant increase in the molecular ordering of the hydrocarbon ligands when immobilised compared to the corresponding non-immobilised but chemisorbed silanes. Additional information about the flexibility of *n*-alkyl ligands with silica-based stationary phases has also been indirectly obtained from chromatographic measurements. For example, the transitions which occur in the retention behaviour of solutes, when chromatographed on *n*-alkylsilicas under experimental conditions involving increases in temperature, have been related to the structural reordering of the ligand [11,12]. Furthermore, the extent of self assembly and association between two immobilised groups has been found to be dependent on the distance between their points of attachment [11]. Other studies have suggested that longer *n*-alkyl chains may exist as aggregates or clusters of chains under conditions of maximum ligand density [13]. In addition to revealing the effect of ligand density on ligand conformation, (which clearly affects chromatographic retention, resolution and peak shape), NMR studies have shown [3] that for dense ligand coverages, there is a steric masking of unreacted silanol groups present on the stationary phase surface.

Current theories of reversed-phase chromatography are based on very incomplete data on the distribution and conformation of the *n*-alkyl ligands bonded to the silica surface. A statistical theory has been developed to describe the mechanism of retention of small molecules in terms of partition or adsorption with *n*-alkyl ligands used in RP-HPLC [14–16]. The partition model involves the formation of a solute-sized cavity in the stationary phase which is followed by transfer of the solute from the aqueous cavity in the mobile phase to the stationary phase and closure of the cavity in the mobile phase. As a consequence, the partition model, in contrast to the adsorption model [17], predicts a critical role of the *n*-alkyl ligand density. These studies have also led to the prediction that the segments of the chain nearest to the silica surface are the most highly ordered and are thus aligned normal to the surface, and that increasing the surface density of the chains leads to increased ordering of the entire chain. As far as the effects of chain ordering on solute retention is concerned, there are two principal predictions by this statistical theory. Firstly, it is anticipated from entropic considerations that a solute will prefer to interact with the ends of the chain rather than with the immobilised section of the chain. Secondly, as the surface density approaches its maximum value, the solute is predicted to become increasingly expelled from the stationary phase due to the entropic effects of chain ordering. At low ligand densities, solute partitioning should increase linearly with the surface coverage of the ligand chains. The partition coefficient should reach a maximum at the point at which neighbouring interactions between chains become significant and at a maximum surface density, no solute will partition into the stationary phase. Although this partitioning dependence on chain density is not directly observable in chromatographic retention, experimental data of Sentell and Dorsey [18] support these theoretical predictions. A major conclusion from these experiments is that the chain organisation of the stationary phase plays a major role in the retention. These results can be contrasted with predictions of the solvophobic or adsorption theory [17] which does not incorporate the entropic role of the stationary phase ligand structure. The evolution of a comprehensive mechanistic description of the chromatographic process at the molecular level requires significantly more detailed information on the microscopic characteristics of the *n*-alkyl ligand struc-

ture in terms of the molecular dynamics of individual backbone atoms as they interact with the surrounding solvent or the specific solutes. Advances in molecular modelling techniques provide a powerful approach to study the conformational properties of *n*-alkyl chain molecules in solution [19–22] as well as immobilised onto surfaces [23–29]. Availability of sophisticated computer graphics systems which allow the construction of complex molecular models, together with advanced forcefields for the calculation of potential energy surfaces, has made it possible to create and investigate the models of chromatographic support materials.

The aim of this work involved simulation of the reversed-phase chromatographic environment for further modelling of the retention process for various biological molecules. In the present study, a molecular dynamics method has been applied to the study of the conformational and dynamical properties of *n*-butyl ligands immobilised onto silica.

MATERIALS AND METHODS

Molecular model

n-Butyldimethyl ligands were covalently bonded to a model amorphous silica surface [23,24] with three different surface densities. The structure of a single attached ligand is shown in Fig. 1. The silica lattice contained 285 silicon and 570 oxygen atoms with the total hydroxyl groups surface density equal to 6.57 μmol/m^2. Atomic coordinates for the silica matrix determined previously [23,24] were fixed during the simulation.

Three molecular systems were designated A, B and C, corresponding to the surface ligand density 3.69, 2.67 and 1.64 μmol/m^2, respectively. Periodic boundary conditions with unit cell dimensions [28.5 × 28.5 × 25.0 Å] were applied to mimic an infinite *n*-alkyl modified chromatographic surface. The initial conformation of the chains was all-*trans* and the chains were oriented normal to the surface. Table I summarises the main parameters of the simulated systems. Computational results were obtained using software programs from Biosym Technologies (San Diego, CA, USA): dynamics calculations were performed with *Discover* and graphic displays were created using *InsightII*. All calculations were performed on a CONVEX C210 supercomputer.

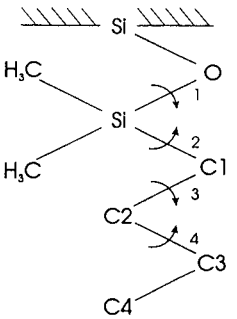

Fig. 1. Schematic structure of an *n*-butyldimethylsilyl ligand attached to a silica surface indicating the torsion angles.

Computational method

The molecular dynamics (MD) simulation method was applied to the molecular systems described above. The potential energy of the system was calculated as a sum of the terms reflecting energy needed to stretch bonds, bend

TABLE I

MOLECULAR DETAILS OF SIMULATED SYSTEMS

System name	Ligand surface density (μmol/m^2)	Hydroxyl surface density (μmol/m^2)	Surface area per ligand (Å^2)	Near neighbour spacing (Å)	Number of atoms	Hydrocarbon layer thickness (Å)
A	3.69	2.88	45.12	6.71	1420	5.63
B	2.67	3.90	62.48	7.90	1315	5.45
C	1.64	4.93	101.53	10.08	1210	3.43

bond angles, rotate torsion angles as well as the terms representing the non-bond Van der Waals and electrostatic interactions. The Consistent Valence Forcefield [30] from the Biosym Library, which is parameterised for the silicon atom, was used to approximate the potential energy of the simulated systems. The non-bonded interactions for pairs of atoms separated by distances greater than a cutoff value of 12 Å were neglected. The neighbour list was updated every 20 steps. A distance-dependent dielectric constant was used to model the effect of solvent. Although such a model cannot account for the structural contribution of solvent, it still provides a screening effect of solvent on electrostatic interactions [30, and references therein]. The aim of this study was to create a molecular model of a reversed-phase sorbent which is physically consistent with available experimental data on ligand structure which are obtained in various solvent environments (including dry). As the end point of these investigations is the molecular modelling of the peptide–sorbent–solvent interactions, it was considered appropriate at the initial stage to use the approximation of a distance-dependent dielectric constant rather than the use of explicit solvent which would significantly increase the computational time of the experiments.

To avoid bad contacts arising from the initial model building, the energy of each system was first minimised by steepest descents followed by conjugate gradients method until the derivatives decreased to 1 kcal mol^{-1} $Å^{-1}$. Systems were then subjected to the constant volume molecular dynamics with periodic boundary conditions. Temperature of simulation was set to 300 K. Initial velocities were randomly assigned according to a Maxwell–Boltzmann distribution for the given temperature. The equations of motion were solved using the Verlet algorithm [31] with the integration time step of 1 fs. The initial equilibration stage, in which the temperature was adjusted by scaling the velocities, was continued until such properties as total energy, temperature, and *trans* fraction of chain torsion angles had stabilised. The duration of equilibration runs was 20–40 ps (20 000–40 000 time steps) depending on the size of the system. An equilibration period was followed by a data collection stage of 100 ps (100 000 time steps) in which Berendsen's method of a weak coupling of the system to a temperature bath at 300 K was applied [32]. The atomic coordinates were stored on disk every 100 time steps for analysis.

RESULTS AND DISCUSSION

Hydrocarbon layer thickness and surface accessibility

The aim of this study was to create a molecular model of an RP-HPLC system to allow the simulation of the reversed-phase chromatographic process. Following molecular dynamics, a number of physical parameters were derived to characterise the molecular properties of each system. The thickness of the hydrocarbon layer is an important quantity which can be used for the estimation of the position of the ligands with respect to the surface as well as accessibility of the unreacted surface silanols to solvent and solute under chromatographic conditions. To assess the average thickness of the hydrocarbon layer in the systems under investigation, the average distances between the terminal methyl group (C4 atom) and the mean Si-plane were calculated. The mean Si-plane was constructed as an average plane containing Si atoms from the upper layer of the surface of the molecular models displayed in Figs. 2–4. The Si–O–$Si(CH_3)_2$– atoms (Fig. 1) were considered as part of the chains thus contributing to the thickness value.

It was found that the average thickness of the most dense hydrocarbon layer (system A) amounts to 5.63 Å (Table I). For the intermediate density (system B) it is equal to 5.45 Å while for the lowest density (system C), the thickness is equal to 3.43 Å. The value for the more dense systems (A, B) is similar to the thickness of the starting structure which was about 6 Å and corresponds to fully extended (*i.e.* all-*trans*) chain conformation (the value of the thickness of the extended configuration is an estimate as any relaxation of the starting structure which was built up manually results in changes in the chain conformation). The small decrease in the thickness of systems A and B

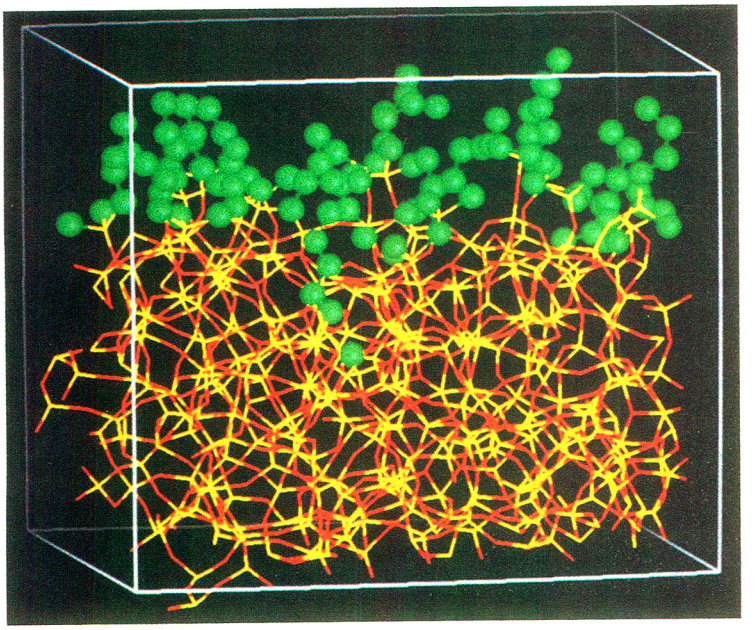

Fig. 2. Instantaneous conformation of *n*-butyl ligands immobilised onto amorphous silica with ligand density = 3.69 μmol/m^2, taken from the later stages of the dynamics run. Atoms are colour-coded as follows: silicon, yellow; oxygen, red; carbon, green. Carbon atoms are presented in a space filling mode. Hydrogens are not displayed.

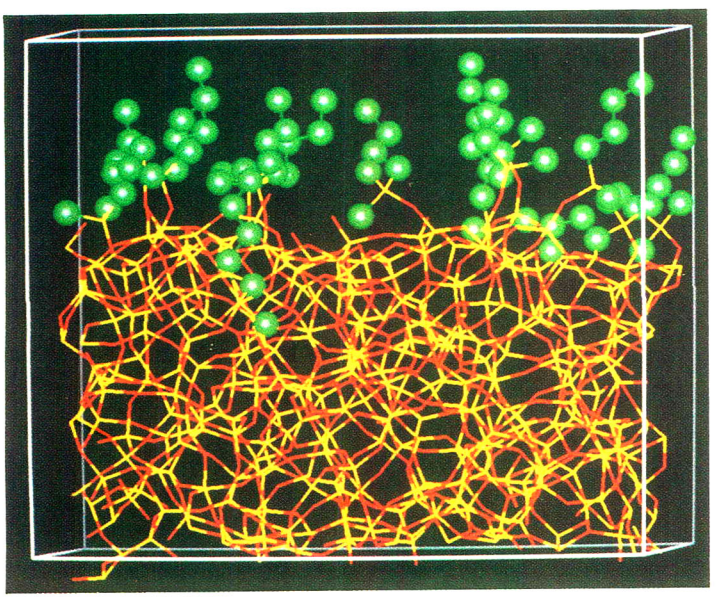

Fig. 3. Instantaneous conformation of *n*-butyl ligands immobilised onto amorphous silica with ligand density = 2.67 μmol/m^2, taken from the later stages of the dynamics run. See Fig. 2 for colour codes.

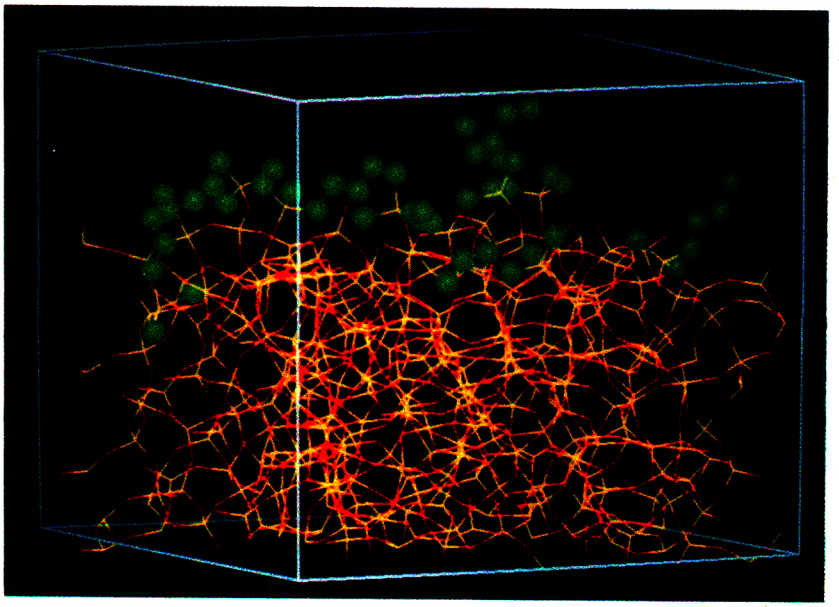

Fig. 4. Instantaneous conformation of *n*-butyl ligands immobilised onto amorphous silica with ligand density = 1.64 μmol/m^2, taken from the later stages of the dynamics run. See Fig. 2 for colour codes.

indicates that the equilibrium positions of the chains are normal to the surface or slightly tilted (Figs. 2 and 3) which is a consequence of the steric restrictions imposed on each chain by the neighbouring ligands. These results also show that the *trans* conformation is predominant for higher ligand densities. For the lowest ligand density system C, the hydrocarbon layer thickness is much lower which demonstrates that the *n*-alkyl chains are bent, highly tilted or are lying almost parallel to the surface (Fig. 4). The near neighbour spacing (Table I) for system C is 2.18 Å larger than for system B, while there is a much smaller difference between systems A and B, *i.e.* 1.19 Å. Thus for the lowest ligand density system, the *n*-alkyl chains possess much more space for movement which results in their ability to cover the surface.

The average thickness of the hydrocarbon layer can also be used to estimate the solute approach distance taking into account allowed van der Waals interaction distances. Thus in the higher ligand density systems a solute molecule cannot approach the surface closer than about 6–7 Å (because of the high ligand density and thick hydrocarbon layer) while for the lowest density the solute can approach the surface to 4–5 Å which could significantly increase the solute interaction with any unreacted silanols and influence the retention. At the same time it should be noticed that the ability of chains at low density to form a bent structure and to cover the surface may create an additional protection for unreacted silanols.

In addition, the total solvent-accessible surface area of each system was calculated using the Connolly algorithm [33] with a water probe radius of 1.4 Å. The accessible area with chains in the starting conformations (*i.e.* all-*trans* and perpendicular to the silica surface) was compared with the average surface accessibility of equilibrium conformations stored during the dynamics run. The percentage decrease in surface accessibility was 11.20, 6.63 and 1.38% for systems A, B and C, respectively, indicating that the percentage decrease in surface accessibility was highest for the high density system A. This result demonstrates that for *n*-butyl ligands, the surface silanols are more highly protected with higher ligand densities. In spite of the ability of the low density ligands to approach very close to the silica surface, this extra surface protection is still

low compared to the higher ligand density systems.

Trans–gauche statistics

The codes used for assignment of the hydrocarbon chain dihedral angles were the customary g^+, t, and g^-, corresponding to the three intervals: (0° to 120°), (120° to −120°), and (−120° to 0°) respectively. The state of the internal dihedral angles of a molecule (g^+, t, g^-) is the factor determining the overall orientation of the molecule with respect to the surface. The overall proportion of *gauche* conformation in the chains is 14, 15, and 25% for the systems A, B and C, correspondingly. This result reflects the fact that the number of *gauche* defects increases as the spacing between the ligands increases which is also in agreement with the theoretical predictions [16].

The fractions of the *gauche* conformation for each dihedral angle along the C4 chain are shown in Fig. 5 for the different ligand densities. The numbers of torsion angles are assigned as shown in Fig. 1. Torsion angles 1 and 2 describe the geometry of ligand attachment to the silica surface. It can be seen from Fig. 5 that a relatively high proportion of *gauche* conformation for torsion 1 is established for all systems. This results in the perpendicular orientation of the O–Si bond to the surface. The frequency of *gauche* conformations at this position increases with ligand density. This result indicates that the probability of chain orientation which is perpendicular to the surface at this position is higher for high density systems which would be anticipated from steric considerations. Torsion number 2 is predominantly in a *trans* conformation, thus maintaining the chain orientation to the surface created by the conformation of torsion number 1.

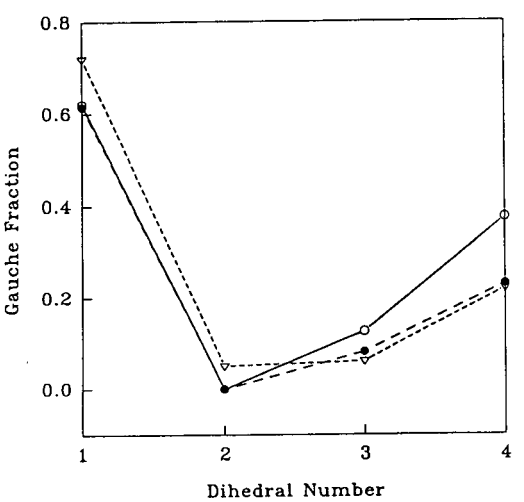

Fig. 5. Fraction of gauche dihedral angles in *n*-butyl ligands as a function of dihedral number. ○ = 1.64 μmol/m²; ● = 2.67 μmol/m²; ▽ = 3.69 μmol/m².

The relative statistics of the next two torsion angles number 3 and 4 is determined by an energetically inexpensive internal rotation about single C–C bonds. Theoretically, the structure with a higher chain density will prefer a *trans* conformation which sterically allows more dense packings. This steric effect is reflected by an increase in the *gauche* population for dihedral angle 4 for the low density system. In terms of the overall *n*-alkyl chain geometry, most of the *gauche* conformations are concentrated around the C2–C3 bond demonstrating that the end-*gauche* defect is the most probable for the *n*-butyl ligands and that the degree of order of the carbon chains increases near the silica surface. This observation is also in agreement with Fourier transform infrared spectroscopy studies of RP-HPLC ligands [9] and is consistent with the theoretical treatment of Dorsey and Dill [16].

End-to-end distance distribution functions

To characterise the average length of the hydrocarbon chains, the distribution function of the end-to-end distance, *i.e.* the distance between C1 and C4 atoms of the ligands, was constructed and is shown in Fig. 6. It can be seen that there are 2 peaks which correspond to distances of 3.25 Å and 3.95 Å between C1 and C4. The first peak of the distribution function ($r = 3.25$ Å) corresponds to the *gauche* conformation for the C1–C2–C3–C4 torsion angle. It can be seen in Fig. 6 that the probability of the *gauche* conformation is highest for the low density system C. In contrast, the probability of the end-to-end distance of 3.95 Å which corresponds to the all-*trans* conformation is higher for systems A and B.

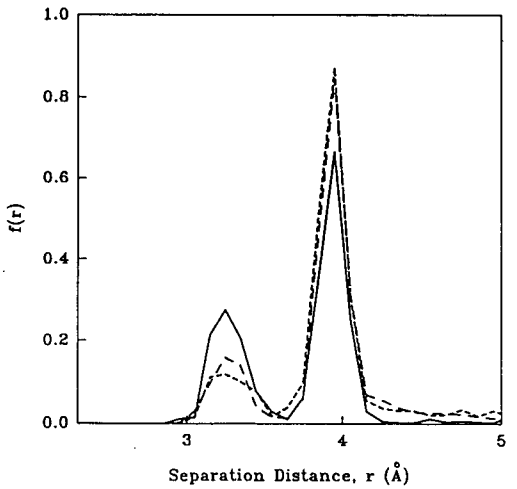

Fig. 6. End-to-end distance distribution of *n*-butyl ligands at different densities. ——— = 1.64 μmol/m^2; – – – – = 2.67 μmol/m^2; ---- = 3.69 μmol/m^2.

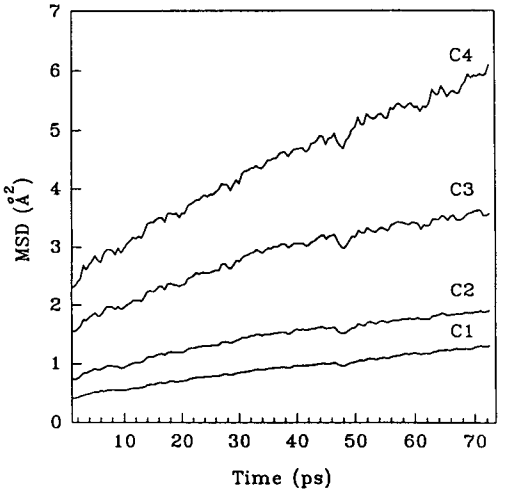

Fig. 7. Mean squared displacements (*MSD*) of carbon atoms in *n*-butyl ligands as a function of time for ligand density = 2.67 μmol/m^2.

Mobility

Differences in the mobility of the *n*-butyl ligands can also be revealed by studying the dynamic behaviour of the carbon atoms. The time dependence of the average mean squared displacements (MSD) of individual carbon atoms over the all chains in the simulation and multiple time origins t_0 were calculated according to the following relationship:

$$MSD = [\Delta R(t)]^2 = \sum \langle |r_i(t + t_0) - r_i(t_0)|^2 \rangle \quad (1)$$

where R is the average distance travelled and r_i represents the coordinates of atom i. Fig. 7 shows the dependence of the *MSD* over time for the individual carbon atoms in System B. The overall appearance of these plots is similar for all the systems under investigation. To estimate the relative mobilities of individual carbon atoms diffusion coefficients (D) for these atoms were calculated. Diffusion constants were obtained using the Einstein relation [34] as follows:

$$2tD = 1/3 \lim_{t \to \infty} \langle [\Delta R(t)]^2 \rangle \quad (2)$$

A plot of the calculated diffusion constants for individual carbon atoms in different systems is given in Fig. 8. It can be seen from Fig. 7 and Fig. 8 that for all ligand densities, the mobility increases from the C1 atom to the C4 atom, *i.e.* atoms closer to the surface are more restricted by immobilisation than the remote atoms. This result is in agreement with ^{13}C cross polarization magic angle spinning NMR spectroscopy measurements of the proton relaxation times in the rotating coordinate system which have been

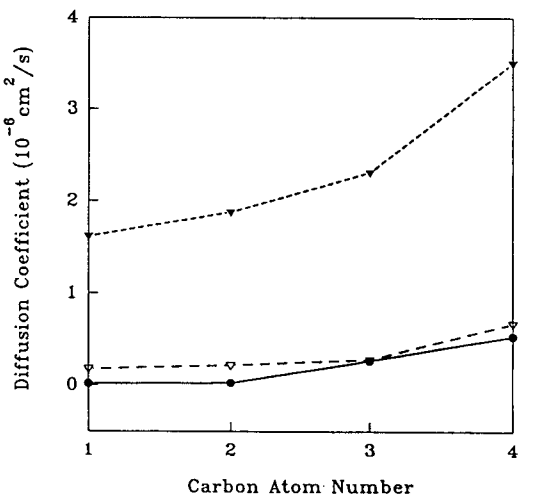

Fig. 8. Diffusion coefficients of individual carbon atoms of *n*-butyl ligands at different ligand densities. ▼ = 1.64 μmol/m^2; ▽ = 2.67 μmol/m^2; ❂ = 3.69 μmol/m^2.

described as a measure of mobility of the alkyl chains [2]. It is interesting to notice that the increased mobility of the atoms remote from the surface also correlates with the increased number of *gauche* defects around the C1–C2–C3–C4 dihedral angle (Fig. 5).

The results obtained for the mobility of *n*-butyl ligands are also consistent with the results of previous NMR studies [2] in which a ligand density of 3.5 ± 0.2 μmol/m^2 was employed which corresponds to our highest density system A. These workers found that the overall mobility of *n*-butyl ligands was relatively low, indicating a low motional freedom for all the carbon atoms of this phase, and increases slightly for the terminal methyl group which is in agreement with our simulation (Fig. 7).

It is evident from Fig. 8 that the mobility of carbon atoms is highest in the lowest density system C. This observation also can be explained by steric restrictions resulting from the different near neighbour ligand spacing at different densities. The mobility of ligands in systems A and B is very low and increases dramatically in the lowest density system C where chains possess much more space for movement which results in a higher diffusion coefficient for individual carbon atoms. This result also correlates with the general conclusion of previous NMR studies [4] which showed that *n*-alkyl chain mobility is a function of surface coverage, since the available space of a single chain decreases with increasing coverage.

CONCLUSIONS

In the present study, a molecular model of an *n*-butylsilica sorbent has been constructed. The molecular properties of the model have been characterised by a number of physical parameters. The results of the conformational analysis indicate that the simulation reproduces the behaviour of the *n*-alkyl ligands which is qualitatively consistent with published spectroscopic data. These studies are currently being extended to the simulation of *n*-octyl and *n*-octadecyl sorbents, with the model presented here used to further study the molecular basis of the chromatographic process in RP-HPLC.

ACKNOWLEDGEMENTS

The support of the Australian Research Council is gratefully acknowledged. The simulations were carried out on the CONVEX C210 computer of the Biomolecular Research Institute (Parkville, Australia). The comments and suggestions of the reviewers are also appreciated.

REFERENCES

1 K.D. Lork, K.K. Unger, H. Bruckner and M.T.W. Hearn, *J. Chromatogr.*, 476 (1989) 135.
2 B. Pfleiderer, K. Albert, K.D. Lork, K.K. Unger, H. Bruckner and E. Bayer, *Angew. Chem., Int. Ed. Engl.*, 28 (1989) 327.
3 B. Buszewski, Z. Suprynowicz, P. Staszczuk, K. Albert, B. Pfleiderer and E. Bayer, *J. Chromatogr.*, 499 (1990) 305.
4 E. Bayer, A. Paulus, B. Peters, G. Laupp, J. Reiners and K. Albert, *J. Chromatogr.*, 364 (1986) 25.
5 G. Lindgren, B. Lundstrom, I. Kallman and K.-A. Hansson, *J. Chromatogr.*, 296 (1984) 83.
6 H.A. Claessens, J.W. De Haan, L.J.M. Van de Ven, P.C. De Bruyn and C.A. Cramers, *J. Chromatogr.*, 436 (1988) 345.
7 P.B. Wright, E. Lamb, J.G. Dorsey and R.G. Kooser, *Anal. Chem.*, 64 (1992) 785.
8 M.E. Montgomery Jr., M.A. Green and M.J. Wirth, *Anal. Chem.*, 64 (1992) 1170.
9 L.C. Sander, J.B. Callis and L.R. Field, *Anal. Chem.*, 55 (1983) 1068.
10 D.E. Leyden, D.S. Kendall, L.W. Burggraf, F.J. Pern and M. DeBello, *Anal. Chem.*, 54 (1982) 101.
11 S.S. Yang and R.K. Gilpin, *J. Chromatogr.*, 449 (1988) 115.
12 D. Morel, K. Tabar, J. Serpinet, P. Claudy and J.M. Letoffe, *J. Chromatogr.*, 395 (1987) 73.
13 C.H. Lochmuller, A.S. Colbarn, M.L. Hunnicutt and J.M. Harris, *Anal. Chem.*, 55 (1983) 1344.
14 K.A. Dill and P.J. Flory, *Proc. Natl. Acad. Sci. USA*, 77 (1980) 3115.
15 K.A. Dill, *J. Phys. Chem.*, 91 (1987) 1980.
16 J.G. Dorsey and K.A. Dill, *Chem. Rev.*, 89 (1989) 331.
17 Cs. Horváth, W. Melander and I. Molnar, *J. Chromatogr.*, 125 (1976) 125.
18 K.B. Sentell and J.G. Dorsey, *Anal. Chem.*, 61 (1989) 930.
19 E. Egberts and H.J.C. Berendsen, *J. Chem. Phys.*, 89 (1988) 3718.
20 J.P. Ryckaert, I.R. McDonald and M.L. Klein, *Mol. Phys.*, 67 (1989) 957.
21 I.L. Shamovsky and I.Yu. Yarovskaya, *J. Molec. Struct. (Theochem.)*, 236 (1991) 333.
22 S. Karaborny and S. Toxvaerd, *J. Chem. Phys.*, 97 (1992) 5876.

23 S.M. Levine and S.H. Garofalini, *Surf. Sci.*, 163 (1985) 59.
24 S.M. Levine and S.H. Garofalini, in F.L. Galeener, D.L. Griscom and M.J. Weber (Editors), *Defects in Glasses, Proc. Material Research Society Symposia, Boston, MA, December 2–4, 1985*, Vol. 61, Materials Research Society Press, 1986, p. 29–37.
25 J. Hautman and M.L. Klein, *J. Chem. Phys.*, 91 (1989) 4994.
26 J. Hautman and M.L. Klein, *J. Chem. Phys.*, 93 (1990) 7483.
27 A. Biswas and B.L. Schurmann, *J. Chem. Phys.*, 95 (1991) 5377.
28 N.G. Almazza, E. Enciso and F.J. Bermejo, *J. Chem. Phys.*, 96 (1992) 4625.
29 T.K. Xia, J. Ouyang, M.W. Ribarsky and U. Landman, *Phys. Rev. Lett.*, 69 (1992) 1967.
30 *Discover User Guide*, Version 2.9.0., Biosym Technology, San Diego, CA, 1993.
31 L. Verlet, *Phys. Rev.*, 159 (1967) 98.
32 H.J.C. Berendsen, J.P.M. Postma, W.F. van Gunsteren, A. DiNola and J.R. Haak, *J. Chem. Phys.*, 81 (1984) 3684.
33 M.L. Connolly, *Science*, 221 (1983) 709.
34 M.P. Allen and D.J. Tildesley, *Computer Simulation of Liquids*, Clarendon Press, Oxford Science Publications, Oxford, 1987.
35 G. Dasari, I. Prince and M.T.W. Hearn, *J. Chromatogr.*, 631 (1993) 115.

Journal of Chromatography A, 660 (1994) 85–96
Elsevier Science B.V., Amsterdam

CHROMSYMP. 2941

Perfusion chromatography

Effect of micropore diffusion on column performance in systems utilizing perfusive adsorbent particles with a bidisperse porous structure

A.I. Liapis* and M.A. McCoy☆

Department of Chemical Engineering and Biochemical Processing Institute, University of Missouri–Rolla, Rolla, MO 65401-0249 (USA)

ABSTRACT

A mathematical model describing single-component and multi-component adsorption in columns with bidisperse perfusive or bidisperse purely diffusive adsorbent particles is constructed and presented. The model is used to study the adsorption of lysozyme onto monoclonal anti-lysozyme in columns with bidisperse porous adsorbent particles. The influence of the effective pore diffusion coefficient of the adsorbate in the microparticles (microspheres) and the effects of particle size and intraparticle convective flow on column performance are examined. The results for the systems studied indicate that the systems with bidisperse perfusive particles provide a higher dynamic utilization of the adsorptive capacity of the column than the systems having bidisperse purely diffusive particles.

INTRODUCTION

The separation process that involves the flow of a mobile phase (*i.e.*, liquid phase) through the pores of porous chromatographic particles [1–6] has been called by Afeyan *et al.* [1] perfusion chromatography. In perfusive adsorbent particles the intraparticle convective fluid velocity, v_p, is non-zero [4], whereas in purely diffusive adsorbent particles the value of v_p is considered to be equal to zero.

Liapis and McCoy [4] constructed a theory of perfusion chromatography, and their mathematical models could describe the dynamic behavior of single- and multi-component adsorption in columns having perfusive ($v_p > 0$) adsorbent particles and also in columns having purely diffusive ($v_p = 0$) adsorbent particles. The results obtained by Liapis and McCoy [4], McCoy *et al.* [5] and McCoy [6] suggest that the dynamic behavior of columns with perfusive adsorbent particles could be more effective than that of columns with purely diffusive particles when both the intraparticle Peclet number [4–6] and the Porath parameter [4–11] are large. The intraparticle Peclet number is a general measure of the importance of intraparticle convection, as a means of mass transfer, compared with pore diffusion. The Porath parameter may be considered [4–11] to provide a measure of the speed of the adsorbate–active site (adsorbate–ligand) association step relative to the pore diffusion of the adsorbate in the pores of the adsorbent particle. It is important to note that the intraparticle Peclet number alone is inadequate to describe fully intraparticle mass transfer when adsorption

* Corresponding author.
☆ Present address: PerSeptive Biosystems, University Park at MIT, 38 Sidney Street, Cambridge, MA 02139, USA.

0021-9673/94/$07.00 © 1994 Elsevier Science B.V. All rights reserved
SSDI 0021-9673(93)E0970-6

occurs [4–6]. In adsorption systems, a second quantity, the Porath parameter [4–11], also comes into play. Also, the results obtained from the binary adsorption (competitive adsorption involving two components) system studied in the work of McCoy *et al.* [5] suggest that the times at which breakthrough begins for components 1 and 2, and the dynamic (unsteady state) relative separation between components 1 and 2 obtained from the column with perfusive particles, are higher than those obtained from the column having purely diffusive particles, especially as the particle size, z_0, and the column fluid superficial velocity, V_f, increase. The improved separation efficiency obtained from the chromatographic columns with perfusive adsorbent particles is mainly due [4–6] to the intraparticle fluid flow which enhances intraparticle mass transport.

In porous adsorbent particles with a bidisperse [1,2,4,5,12,13] porous adsorbent structure, the microporous region of the particles has a large surface area, and hence a large proportion of the adsorptive capacity of such particles is within their micropores. In Eqns. 6–8 in ref. 4, the intraparticle fluid velocity and the effective pore diffusion coefficients characterize the overall intraparticle convective and pore diffusion mass transfer mechanisms, respectively, for a perfusive particle; of course, the value of the intraparticle fluid velocity and the values of the effective pore diffusion coefficients in perfusive particles with a monodisperse porous structure could be different than those obtained in perfusive particles with a bidisperse porous structure. In perfusive particles with a bidisperse porous structure, one could expect that intraparticle fluid flow occurs mainly within the macroporous [14] region (the region of the through-pores [1]) of the particle. Hence the degree of utilization of the adsorptive capacity of a perfusive particle with a bidisperse porous structure could depend on the relative magnitude of the time constants for pore diffusion and adsorption (the interaction mechanism between the adsorbate molecules and the active sites) in the microporous region, and for intraparticle fluid flow (convection), pore diffusion and adsorption in the macroporous region.

In this work, a mathematical model that could describe single- and multi-component adsorption in columns having perfusive particles with a bidisperse porous structure is presented. The model is then solved and used to study the dynamic behavior of a column system involving the adsorption of lysozyme onto monoclonal anti-lysozyme immobilized in perfusive particles having a bidisperse porous structure.

MATHEMATICAL MODEL

Adsorption is considered to take place from a flowing liquid stream in a fixed bed of perfusive adsorbent particles of bidisperse porous structure under isothermal conditions. The differential mass balance for each adsorbate i ($i = 1, 2, \ldots, n$) in the flowing fluid stream is given by eqn. 1 in ref. [4], and eqns. 2–4 in ref. 4 are considered to provide the initial and boundary conditions for the differential mass balance equation of each adsorbate; if the contribution of axial dispersion in the column can be neglected then eqn. 3 in ref. 4 is replaced with eqn. 5 in ref. 4.

The perfusive particles with a bidisperse porous structure are considered to have a microporous region made by spherical microparticles (microspheres [1]) [1,4] that are taken to be purely diffusive, and a macroporous region made by the through-pores [1,4] in which intraparticle convection and pore diffusion occur. Most of the adsorptive capacity of the perfusive particles is in the microporous region. The transport of the species in the macroporous region is considered to involve the following mass transfer mechanisms: (a) intraparticle convection, (b) diffusion in the pore fluid and (c) the mass transfer step involving the interaction of the adsorbates with the active sites on the surface of the pores (this step represents the adsorption mechanism). The transport of the species in the purely diffusive spherical microparticles of which the microporous region is composed involves the following mass transfer mechanisms: (i) diffusion in the pore fluid of the spherical microparticle and (ii) the mass transfer step involving the interaction (adsorption) of the adsorbates with the active sites on the surface of the pores of the spherical microparticle. In Fig. 1a a diagram of a perfusive

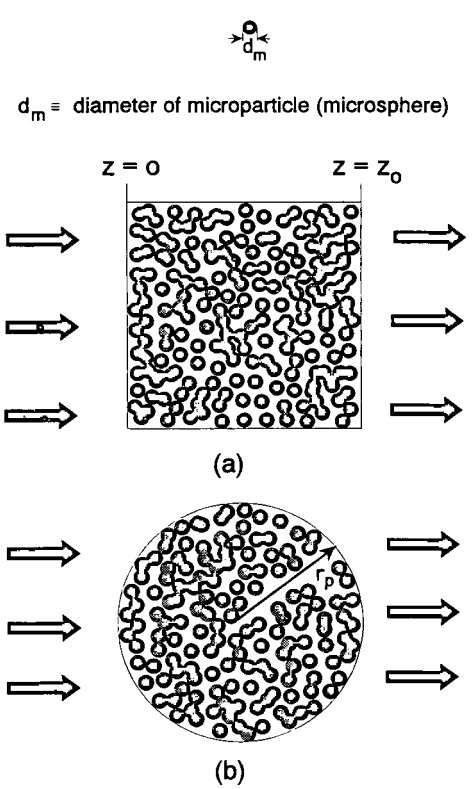

Fig. 1. Perfusive adsorbent particles with a bidisperse porous structure (the arrows indicate the direction of fluid flow): (a) perfusive particle of slab geometry; (b) perfusive particle of spherical geometry.

particle of slab geometry is shown and in Fig. 1b a diagram of a perfusive particle of spherical geometry is presented.

The differential mass balance for each adsorbate i in the macroporous region of a perfusive adsorbent particle of slab geometry is given by

$$\varepsilon_p\left(\frac{\partial C_{pi}}{\partial t}\right)+\varepsilon_p v_p\left(\frac{\partial C_{pi}}{\partial z}\right)+(1-\varepsilon_p)\frac{\partial \bar{C}_{si}}{\partial t}$$
$$=\varepsilon_p D_{pi}\left(\frac{\partial^2 C_{pi}}{\partial z^2}\right),\ i=1,2,\ldots,n \qquad (1)$$

The mixtures of components to be separated by chromatographic systems are usually dilute and the form of eqn. 1 is appropriate for dilute mixtures [4]; for non-dilute mixtures, ref. 4 should be consulted. The value of the intraparticle velocity v_p in eqn. 1 could be estimated from eqn. 20 in ref. 4. The initial and boundary conditions of eqn. 1 are as follows:

$$\text{at } t=0\ C_{pi}=0,\ 0\leq z\leq z_0,\quad i=1,2,\ldots,n \qquad (2)$$

$$\text{at } t=0\ \bar{C}_{si}=0,\ 0\leq z\leq z_0,\ i=1,2,\ldots,n \qquad (3)$$

$$\text{at } z=0\ C_{pi}=C_{di},\ t>0,\ i=1,2,\ldots,n \qquad (4)$$

$$\text{at } z=z_0\ C_{pi}=C_{di},\ t>0,\ i=1,2,\ldots,n \qquad (5)$$

The expressions in eqns. 4 and 5 were obtained by neglecting the external film mass transfer resistance. The external film mass transfer resistance is neglected because its contribution to the overall mass transfer resistance of porous particles has been found, for most systems of practical importance, to be negligible [4,6,11, 15,16].

The differential mass balance for each adsorbate i in a purely diffusive spherical microparticle is given by

$$\varepsilon_{pm}\left(\frac{\partial C_{pmi}}{\partial t}\right)+\left(\frac{1}{1-\varepsilon_p}\right)\frac{\partial C_{smi}}{\partial t}$$
$$=\varepsilon_{pm}D_{pmi}\left(\frac{\partial^2 C_{pmi}}{\partial r^2}+\frac{2}{r}\cdot\frac{\partial C_{pmi}}{\partial r}\right),$$
$$i=1,2,\ldots,n \qquad (6)$$

Eqn. 6 is appropriate for dilute mixtures [4–11]; for non-dilute mixtures, ref. 11 should be consulted. The accumulation term, $\partial C_{smi}/\partial t$, of the adsorbed species i can be quantified if a thermodynamically consistent mathematical model could be constructed that could describe the mechanism of adsorption for component i. For isothermal adsorption systems, the term $\partial C_{smi}/\partial t$ could be of the form

$$\frac{\partial C_{smi}}{\partial t}=f_i(\boldsymbol{C}_{pm},\boldsymbol{C}_{sm},\boldsymbol{k}),\ i=1,2,\ldots,n \qquad (7)$$

where f_i represents the functional form of the dynamic adsorption mechanism for component i; $\boldsymbol{C}_{pm}$ represents the concentration vector of the adsorbates in the pore fluid of the purely diffusive spherical microparticle, $\boldsymbol{C}_{pm}=(C_{pm1}, C_{pm2},\ldots,C_{pmn})$; $\boldsymbol{C}_{sm}$ denotes the concentration

vector of the adsorbates in the adsorbed phase of the purely diffusive spherical microparticle, $\boldsymbol{C}_{sm} = (C_{sm1}, C_{sm2}, \ldots, C_{smn})$; and $\boldsymbol{k}$ represents the vector of the rate constants that characterize the interaction kinetics between the adsorbates and the active sites. For certain single- and multi-component adsorption systems, dynamic adsorption models of the form given in eqn. 7 have been constructed and presented in the literature. One well known form of eqn. 7 for single-component adsorption ($A + S \underset{k_2}{\overset{k_1}{\rightleftharpoons}} AS$) is as follows (the subscript i is dropped as only one component is adsorbed) [4,7]:

$$\frac{\partial C_{sm}}{\partial t} = k_1 C_{pm}(C_T - C_{sm}) - k_2 C_{sm} \tag{8}$$

In some adsorption systems, the rates of interaction between the adsorbates and the active sites may be much higher than the intraparticle convection and diffusional rates, and in such systems it may be possible to assume that equilibrium exists between the adsorbates in the pore fluid and in the adsorbed phase at each point in the pores. The term $\partial C_{smi}/\partial t$ in eqn. 6 is then given by

$$\frac{\partial C_{smi}}{\partial t} = \sum_{j=1}^{n} \left(\frac{\partial g_i}{\partial C_{pmj}}\right)\left(\frac{\partial C_{pmj}}{\partial t}\right), \quad i = 1, 2, \ldots, n \tag{9}$$

where

$$C_{smi} = g_i(\boldsymbol{C}_{pm}, \boldsymbol{K}), \quad i = 1, 2, \ldots, n \tag{10}$$

The functions g_i represent the equilibrium adsorption isotherms for the adsorbates, and $\boldsymbol{K}$ represents the vector of the equilibrium constants that characterize the equilibrium interactions between the adsorbates and the active sites. One well-known form of eqn. 10 for single-component adsorption [4,7] is as follows (the subscript i is dropped as only one component is adsorbed):

$$C_{sm} = \frac{C_T K C_{pm}}{1 + K C_{pm}} \tag{11}$$

Eqn. 11 represents the equilibrium Langmuir adsorption isotherm and is obtained from eqn. 8 by setting $\partial C_{sm}/\partial t$ equal to zero; the parameter K in eqn. 11 is the equilibrium adsorption constant ($K = k_1/k_2$). When eqn. 11 is employed in the right-hand side of eqn. 9, the following expression is obtained for $\partial C_{sm}/\partial t$:

$$\frac{\partial C_{sm}}{\partial t} = \left(\frac{\partial C_{sm}}{\partial C_{pm}}\right)\left(\frac{\partial C_{pm}}{\partial t}\right) = \left[\frac{C_T K}{(1 + K C_{pm})^2}\right]\left(\frac{\partial C_{pm}}{\partial t}\right) \tag{12}$$

The initial and boundary conditions of eqns. 6 and 7 are considered to be as follows:

$$\text{at } t = 0 \quad C_{pmi} = 0, \quad 0 \leq r \leq r_m, \quad i = 1, 2, \ldots, n \tag{13}$$

$$\text{at } t = 0 \quad C_{smi} = 0, \quad 0 \leq r \leq r_m, \quad i = 1, 2, \ldots, n \tag{14}$$

$$\text{at } r = 0 \quad \frac{\partial C_{pmi}}{\partial r} = 0, \quad t > 0, \quad i = 1, 2, \ldots, n \tag{15}$$

$$\text{at } r = r_m \quad C_{pmi} = C_{pi}(z, t), \quad t > 0, \quad i = 1, 2, \ldots, n \tag{16}$$

The variable $\bar{C}_{si}$ in eqn. 1 could be calculated from the following expression:

$$\bar{C}_{si} = \frac{3}{r_m^3}\left[\int_0^{r_m}\left(\frac{1}{1 - \varepsilon_p}\right) C_{smi} r^2 \, dr + \int_0^{r_m} \varepsilon_{pm} C_{pmi} r^2 \, dr\right], \quad i = 1, 2, \ldots, n \tag{17}$$

The accumulation term $\partial \bar{C}_{si}/\partial t$ in eqn. 1 is obtained by differentiating eqn. 17 with respect to time, and hence

$$\frac{\partial \bar{C}_{si}}{\partial t} = \frac{3}{r_m^3}\left\{\frac{\partial}{\partial t}\left[\int_0^{r_m}\left(\frac{1}{1 - \varepsilon_p}\right) C_{smi} r^2 \, dr\right] + \frac{\partial}{\partial t}\left(\int_0^{r_m} \varepsilon_{pm} C_{pmi} r^2 \, dr\right)\right\}, \quad i = 1, 2, \ldots, n \tag{18}$$

Finally, the term $\partial \bar{C}_{psi}/\partial t$ in eqn. 1 in ref. 4 is given by

$$\frac{\partial \bar{C}_{psi}}{\partial t} = \frac{1}{z_0}\left\{\frac{\partial}{\partial t}\left[\int_0^{z_0}(1-\varepsilon_p)\bar{C}_{si}\,dz\right] + \frac{\partial}{\partial t}\left(\int_0^{z_0}\varepsilon_p C_{pi}\,dz\right)\right\}, \quad i = 1, 2, \ldots, n \quad (19)$$

since

$$\bar{C}_{psi} = \frac{1}{z_0}\left[\int_0^{z_0}(1-\varepsilon_p)\bar{C}_{si}\,dz + \int_0^{z_0}\varepsilon_p C_{pi}\,dz\right] \quad (20)$$

If the geometry of the perfusive adsorbent particle is spherical, then eqn. 1 should be replaced by eqn. 21 in ref. 4; in this case, the variable r in eqn. 21 in ref. 4 represents the radial distance in the perfusive particle and its physical meaning is different than that of the variable r in eqns. 6 and 13–18 in this work. In eqns. 6 and 13–18 in this work, the variable r represents the radial distance in the purely diffusive spherical microparticle. The values of the intraparticle velocity components v_{pr} and $v_{p\theta}$ in eqn. 21 in ref. 4 could be estimated from the expressions presented in ref. 14. Further, for spherical perfusive particles the term $\partial \bar{C}_{psi}/\partial t$ in eqn. 1 in ref. 4 is given by

$$\frac{\partial \bar{C}_{psi}}{\partial t} = \frac{1}{V_{pv}}\left\{\frac{\partial}{\partial t}\left[\int_0^{V_{pv}}(1-\varepsilon_p)\bar{C}_{si}\,dV\right] + \frac{\partial}{\partial t}\left(\int_0^{V_{pv}}\varepsilon_p C_{pi}\,dV\right)\right\}, \quad i = 1, 2, \ldots, n \quad (21)$$

The dynamic behavior of a column adsorption system involving perfusive adsorbent particles with a bidisperse porous structure could be obtained by solving eqns. 1–4 in ref. 4 simultaneously with eqns. 1–7, 13–16, 18 and 19 in this work, when the perfusive adsorbent particles have slab geometry. If the geometry of the perfusive adsorbent particles with a bidisperse porous structure is spherical, then eqns. 1–4 and 21 in ref. 4 should be solved simultaneously with eqns. 6, 7, 13–16, 18 and 21 in this work. The solution of the equations of the mathematical model presented in this work was obtained by employing the method of orthogonal collocation [6,17,18] on the space variables of the continuity equations of the adsorbates in the macroporous and microporous regions of the perfusive particle, and the method of orthogonal collocation on finite elements [6] on the space variable along the axis of the column. The resulting ordinary non-linear differential equations were integrated by using Gear's method [18], which is employed in the LSODES component of the ODEPACK [19] software package. It should be mentioned that if the intraparticle velocity, v_p, is set equal to zero in eqn. 1, then the solution of the above-mentioned equations would provide the dynamic behavior of an adsorption system in a column having purely diffusive adsorbent particles with a bidisperse porous structure in which there is no intraparticle fluid flow [13,20–24].

RESULTS AND DISCUSSION

Frontal analysis results are presented for the system involving the adsorption of lysozyme onto monoclonal anti-lysozyme immobilized on the surface of adsorbent particles with a bidisperse porous structure. Purely diffusive ($v_p = 0$) and also perfusive ($v_p > 0$) adsorbent particles with a bidisperse porous structure are considered. The dynamics of the adsorption step are described by eqn. 8, and two different values for the particle size, z_0, were considered: (i) $z_0 = 10^{-5}$ m and (ii) $z_0 = 2 \cdot 10^{-5}$ m. The diameter of the microparticle (microsphere), d_m, was taken to be equal to 10^{-6} m [1,12]. In Table I, the values of the parameters used in the model for the simulation of the adsorption system studied in this work are presented. The values of other parameters of the model are reported in the captions of the figures. The values of the parameters in Table I are from adsorption systems reported in the literature [4–6,11] and, for the purposes of the simulations of this work, are considered to have appropriate magnitudes; it should be mentioned that the value of C_T in Table I represents the largest (maximum) amount of adsorbate that could be adsorbed per unit volume of the particle.

The effect of micropore diffusion on column

TABLE I

VALUES OF THE PARAMETERS OF THE MODEL (ADSORPTION OF LYSOZYME ONTO MONOCLONAL ANTI-LYSOZYME)

$C_{d,in} = 0.1\ kg/m^3$	$C_T = 2.2\ kg/m^3$	$D_L = 0$
$d_m = 2r_m = 10^{-6}\ m$	$D_p = 17.885 \cdot 10^{-12}\ m^2/s$	$k_1 = 4.108\ m^3/kg \cdot s$
$k_2 = 0.2222\ s^{-1}$	$K = k_1/k_2 = 18.488\ m^3/kg$	$L = 0.1\ m$
$r_m = d_m/2 = 0.5 \cdot 10^{-6}\ m$	$V_f = 2.778 \cdot 10^{-3}\ m/s$	$T = 282.5\ K$
$\varepsilon = 0.35$	$\varepsilon_p = 0.50$	$\varepsilon_{pm} = 0.50$

performance may be examined by varying the value of the ratio of the diffusional time constants for the microparticle and the adsorbent particle, Φ. The expression for Φ is as follows:

$$\Phi = \frac{D_{pm}/r_m^2}{D_p/(z_0/2)^2} \tag{22}$$

From eqn. 22 the following expression is obtained for the ratio D_{pm}/D_p:

$$\frac{D_{pm}}{D_p} = \Phi\left[\frac{r_m^2}{(z_0/2)^2}\right] \tag{23}$$

For given values of r_m and z_0, eqn. (23) indicates that the ratio D_{pm}/D_p increases as Φ increases. In adsorbent particles with a bidisperse porous structure, one could practically consider that the value of D_{pm} would be less than or equal to the value of D_p ($D_{pm} \leq D_p$), and hence the ratio D_{pm}/D_p would be less or equal to unity ($D_{pm}/D_p \leq 1$); this condition could then imply that the value of Φ could be less than or equal to $(z_0/2)^2/r_m^2$ [$\Phi \leq (z_0/2)^2/r_m^2$]. Hence, for the system with $z_0 = 10^{-5}$ m and $r_m = 0.5 \cdot 10^{-6}$ m, the parameter Φ could be ≤ 100; for the system with $z_0 = 2 \cdot 10^{-5}$ m and $r_m = 0.5 \cdot 10^{-6}$ m, the parameter Φ cold be ≤ 400. In this work, the values of D_p and r_m are kept fixed (see Table I) while the values of z_0 and Φ are varied; therefore, for a given value of z_0, an increase in Φ would imply an increase in the effective pore diffusion coefficient of the lysozyme, D_{pm}, in the micropores (microparticle).

In Figs. 2 and 3, the breakthrough curves of lysozyme are presented for different values of v_p, z_0 and Φ. The results clearly indicate that, for a given value of Φ, the performance of the systems

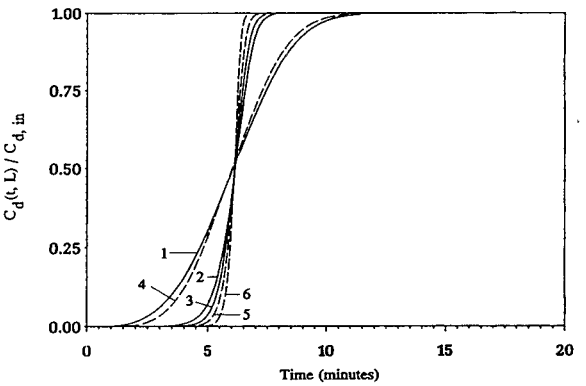

Fig. 2. Breakthrough curves of lysozyme for different values of v_p and Φ (the solid curves are for $v_p = 0.00$ and the broken curves are for $v_p = 0.01V_f$); the particle size is $z_0 = 10^{-5}$ m. (1) $v_p = 0.00$, $\Phi = 0.10$; (2) $v_p = 0.00$, $\Phi = 1.00$; (3) $v_p = 0.00$, $\Phi = 10.00$; (4) $v_p = 0.01V_f$, $\Phi = 0.10$; (5) $v_p = 0.01V_f$, $\Phi = 1.00$; (6) $v_p = 0.01V_f$, $\Phi = 10.00$.

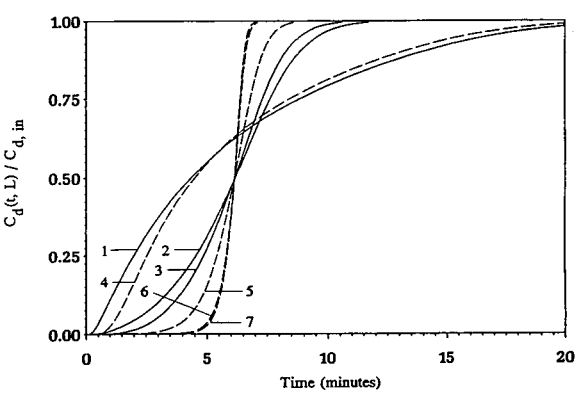

Fig. 3. Breakthrough curves of lysozyme for different values of v_p and Φ (the solid curves are for $v_p = 0.00$ and the broken curves are for $v_p = 0.01V_f$); the particle size is $z_0 = 2 \cdot 10^{-5}$ m. (1) $v_p = 0.00$, $\Phi = 0.10$; (2) $v_p = 0.00$, $\Phi = 1.00$; (3) $v_p = 0.00$, $\Phi = 10.00$; (4) $v_p = 0.01V_f$, $\Phi = 0.10$; (5) $v_p = 0.01V_f$, $\Phi = 1.00$; (6) $v_p = 0.01V_f$, $\Phi = 10.00$; (7) $v_p = 0.01V_f$, $\Phi = 50.00$.

employing perfusive particles is higher than the performance obtained from the systems having purely diffusive particles, and the difference in the performance increases as the particle size, z_0, increases. In Figs. 2 and 3, the results also indicate that, for a given value of z_0, the performance of the column improves as Φ increases. Further, for a given value of Φ, the performance of the column with smaller size, z_0, adsorbent particles is higher than that obtained from the column having larger size, z_0, adsorbent particles (compare the results in Figs. 2 and 3); this behavior is clearly shown, for the column systems with perfusive ($v_p = 0.01V_f$) adsorbent particles, by the results presented in Fig. 4.

In Fig. 2, results are presented for $\Phi = 0.10$, 1.00 and 10.00. For $\Phi > 10.00$ and $\Phi \leq 100.00$, the breakthrough curves obtained from the columns with purely diffusive ($v_p = 0$) or perfusive ($v_p = 0.01V_f$) adsorbent particles almost coincide [for the scales selected for the variables $C_d(t, L)/C_{d,in}$ and t in Fig. 2] with their corresponding breakthrough curves obtained when $\Phi = 10.00$; this result suggests that for the systems examined and presented in Fig. 2, an increase in the value of D_{pm} above $0.1D_p$ ($D_{pm} > 0.1D_p$) might not provide a significant improvement in the breakthrough behavior of the column.

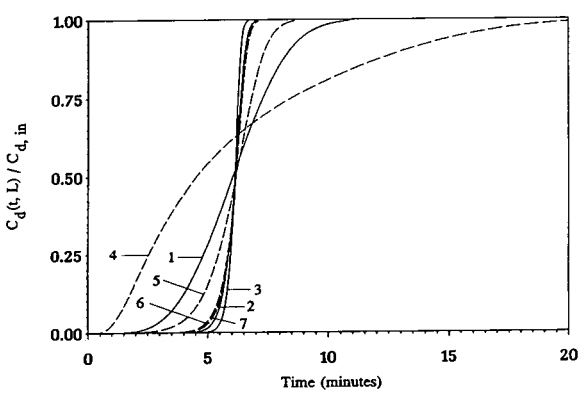

Fig. 4. Breakthrough curves of lysozyme for different values of z_0 and Φ (the solid curves are for $z_0 = 10^{-5}$ m and the broken curves are for $z_0 = 2 \cdot 10^{-5}$ m); the intraparticle convective velocity is $v_p = 0.01V_f$. (1) $z_0 = 10^{-5}$ m, $\Phi = 0.10$; (2) $z_0 = 10^{-5}$ m, $\Phi = 1.00$; (3) $z_0 = 10^{-5}$ m, $\Phi = 10.00$; (4) $z_0 = 2 \cdot 10^{-5}$ m, $\Phi = 0.10$; (5) $z_0 = 2 \cdot 10^{-5}$ m, $\Phi = 1.00$; (6) $z_0 = 2 \cdot 10^{-5}$ m, $\Phi = 10.00$; (7) $z_0 = 2 \cdot 10^{-5}$ m, $\Phi = 50.00$.

For the systems presented in Fig. 3, the breakthrough curves obtained from the columns with purely diffusive or perfusive adsorbent particles for $\Phi > 50.00$ and $\Phi \leq 400.00$ almost coincide [for the scales selected for the variables $C_d(t, L)/C_{d,in}$ and t in Fig. 3] with their corresponding breakthrough curves obtained when $\Phi = 50.00$; this result suggests that for the systems examined and presented in Fig. 3, an increase in D_{pm} above $0.125D_p$ ($D_{pm} > 0.125D_p$) might not provide a significant improvement in the breakthrough behavior of the column.

In Tables II and III, the percentage utilization of the adsorptive capacity of the column at 1% and 10% breakthrough, respectively, are presented. The total adsorptive capacity of the column is defined as the total amount of adsorbate in the adsorbed phase (in the column) at equilibrium (evaluated with respect to the value of $C_{d,in}$). The dynamic utilization of the adsorptive capacity of the column is defined as the ratio of the total amount of the adsorbate in the adsorbed phase of the column when the desired breakthrough occurs to the total adsorptive capacity of the column. The percentage utilization of the adsorptive capacity of the column is obtained by multiplying the dynamic utilization of the adsorptive capacity of the column (defined above) by 100. The results in Tables II and III clearly show that the dynamic adsorptive capacity of the systems with perfusive particles is higher than that of the systems with purely diffusive particles, and the difference becomes significantly larger as the particle size, z_0, increases; also, the difference is larger, for given values of z_0 and Φ, at 1% breakthrough when compared with the difference obtained at 10% breakthrough. Further, it can be observed that the increase in the percentage utilization of the adsorptive capacity at 10% breakthrough compared with that obtained at 1% breakthrough is larger for the column systems with purely diffusive particles; this result also indicates that the columns with perfusive particles are more effective than the columns with purely diffusive particles in the dynamic utilization of the adsorptive capacity of the column. Hence the use of perfusive particles could allow one to make a column switch at a percentage breakthrough

TABLE II

PERCENTAGE UTILIZATION OF THE ADSORPTIVE CAPACITY OF THE COLUMN AT 1% BREAKTHROUGH $\{[C_d(t, L)/C_{d,in}] \cdot 100 = 1\%\}$

z_0 (m)	Φ	$\frac{D_{pm}}{D_p}$	Utilization of the adsorptive capacity of the column (%)		
			$v_p = 0.00$	$v_p = 0.01V_f$	$v_p = 0.02V_f$
10^{-5}	0.10	10^{-3}	29.1	38.3	41.0
10^{-5}	1.00	10^{-2}	66.9	80.5	84.5
10^{-5}	10.00	10^{-1}	75.0	87.3	91.3
10^{-5}	50.00	0.50	75.8	88.0	92.0
10^{-5}	100.00	1.00	75.9	88.1	92.0
$2 \cdot 10^{-5}$	0.10	$0.25 \cdot 10^{-3}$	3.7	11.3	13.3
$2 \cdot 10^{-5}$	1.00	$0.25 \cdot 10^{-2}$	15.7	51.8	60.2
$2 \cdot 10^{-5}$	10.00	$0.25 \cdot 10^{-1}$	30.6	73.9	83.4
$2 \cdot 10^{-5}$	50.00	0.125	33.0	76.2	85.8
$2 \cdot 10^{-5}$	100.00	0.25	33.3	76.5	86.2
$2 \cdot 10^{-5}$	200.00	0.50	33.5	76.7	86.3
$2 \cdot 10^{-5}$	400.00	1.00	33.5	76.8	86.4

lower than that which would be desirable if the column were using purely diffusive particles, as the system with the perfusive particles has a higher dynamic utilization of the adsorptive capacity of the column for a given percentage breakthrough; this result suggests that for a given overall time of operation more adsorption cycles could be obtained when columns with perfusive adsorbent particles are used, and less amount of adsorbate could have left the column by the time that column switching occurs.

The results in Tables II and III also show that, for given values of z_0 and Φ, the highest percentage utilization of the adsorptive capacity of the column is obtained from the systems having perfusive particles with intraparticle velocity $v_p = 0.02V_f$, which corresponds to the largest intraparticle velocity studied in this work. Fur-

TABLE III

PERCENTAGE UTILIZATION OF THE ADSORPTIVE CAPACITY OF THE COLUMN AT 10% BREAKTHROUGH $\{[C_d(t, L)/C_{d,in}] \cdot 100 = 10\%\}$

z_0 (m)	Φ	$\frac{D_{pm}}{D_p}$	Utilization of the adsorptive capacity of the column (%)		
			$v_p = 0.00$	$v_p = 0.01V_f$	$v_p = 0.02V_f$
10^{-5}	0.10	10^{-3}	55.9	61.7	63.2
10^{-5}	1.00	10^{-2}	84.5	91.0	92.8
10^{-5}	10.00	10^{-1}	88.0	94.3	96.1
10^{-5}	50.00	0.50	88.3	94.6	96.4
10^{-5}	100.00	1.00	88.4	94.7	96.4
$2 \cdot 10^{-5}$	0.10	$0.25 \cdot 10^{-3}$	13.5	24.4	26.0
$2 \cdot 10^{-5}$	1.00	$0.25 \cdot 10^{-2}$	48.3	76.1	79.9
$2 \cdot 10^{-5}$	10.00	$0.25 \cdot 10^{-1}$	59.5	88.7	92.7
$2 \cdot 10^{-5}$	50.00	0.125	60.4	89.8	93.9
$2 \cdot 10^{-5}$	100.00	0.25	60.6	89.9	94.0
$2 \cdot 10^{-5}$	200.00	0.50	60.6	90.0	94.1
$2 \cdot 10^{-5}$	400.00	1.00	60.7	90.0	94.1

ther, the results indicate that, for given values of z_0 and Φ, the largest increase in the percentage utilization of the adsorptive capacity of the column is obtained when the value of the intraparticle velocity, v_p, is changed from 0.00 to $0.01V_f$ (this increase is significantly larger than that obtained when v_p is changed from $0.01V_f$ to $0.02V_f$). These results suggest that a high dynamic utilization of the adsorptive capacity of a column with perfusive particles could be obtained by employing intraparticle fluid velocities of moderate magnitude. Perfusive particles with high permeabilities (see eqn. 20 in ref. 4) could permit high intraparticle fluid velocities that could lead to a high dynamic utilization of the adsorptive capacity of the column having these perfusive particles; however, perfusive particles with high permeabilities might not have the appropriate structural strength for a particular use of practical interest. Again, the results in Tables II and III suggest that a high dynamic utilization of the adsorptive capacity may be obtained by employing perfusive particles with permeabilities that could provide appropriate structural strength and permit intraparticle fluid velocities of moderate magnitude.

For the results presented in Tables II and III, it can be observed that as the value of D_{pm} increases from $10^{-3}D_p$ (highly restricted pore diffusion in the microparticle) to $10^{-1}D_p$ for the particles with $z_0 = 10^{-5}$ m, or as the value of D_{pm} increases from $0.25 \cdot 10^{-3}D_p$ (highly restricted pore diffusion in the microparticle) to $0.125D_p$ for the particles with $z_0 = 2 \cdot 10^{-5}$ m, the dynamic utilization of the adsorptive capacity of the column increases; further, as the value of D_{pm} increases, the relative increases in the dynamic utilization of the adsorptive capacity of the column become smaller as the value of v_p increases from 0.00 to $0.02V_f$. Also, a careful examination of the data presented in Tables II and III indicates that for values of D_{pm} between $10^{-2}D_p$ and $1.0D_p$ for the particles with $z_0 = 10^{-5}$ m, or for values of D_{pm} between $0.25 \cdot 10^{-2}D_p$ and $1.0D_p$ for the particles with $z_0 = 2 \cdot 10^{-5}$ m, the dynamic utilization of the adsorptive capacity of the column obtained from the systems with perfusive particles is higher than that obtained from the systems with purely diffusive particles, even when the value of D_{pm} in the microparticles of the perfusive particles is lower than the value of D_{pm} in the microparticles of the purely diffusive particles. The results in Tables II and III suggest that while the value of D_{pm} plays an important role in determining the dynamic performance of the systems with perfusive particles, the effect of the value of D_{pm} on the dynamic performance of systems using purely diffusive particles is higher than the effect of the value of D_{pm} on the dynamic performance of systems using perfusive particles. Also, the results in Tables II and III indicate that for values of D_{pm} greater than $0.1D_p$ for particles with $z_0 = 10^{-5}$ m, or for values of D_{pm} greater than $0.125D_p$ for the particles with $z_0 = 2 \cdot 10^{-5}$ m, the effect of the value of D_{pm} on the dynamic performance of the columns with perfusive or purely diffusive adsorbent particles, is rather small.

CONCLUSIONS AND REMARKS

A mathematical model that could be used to describe single- and multi-component adsorption in columns with bidisperse perfusive or bidisperse purely diffusive adsorbent particles was constructed and presented.

The model was used to study the adsorption of lysozyme on to monoclonal anti-lysozyme in columns with bidisperse perfusive or bidisperse purely diffusive adsorbent particles, for (i) different values of the effective pore diffusion coefficient of the adsorbate in the micropores (microparticles), D_{pm}, (ii) different values of the intraparticle convective velocity, v_p, in the macroporous region of the perfusive particles, and (iii) different values of the adsorbent particle size, z_0. The results indicate that the systems with bidisperse perfusive particles provide a higher dynamic utilization of the adsorptive capacity of the column than that obtained from the systems with bidisperse purely diffusive particles. The dynamic utilization of the adsorptive capacity of the column was found to increase when the particle size, z_0, decreases, or when the intraparticle convective velocity, v_p, increases. The results also indicate that a high dynamic utilization of the adsorptive capacity of a column with perfusive particles could be ob-

tained by employing intraparticle fluid velocities of moderate magnitude. Further, the results show that the dynamic utilization of the adsorptive capacity of the column increases as the effective pore diffusion coefficient of the adsorbate in the microparticles, D_{pm}, increases. However, while the value of D_{pm} is important in determining the dynamic performance of the systems with perfusive particles, the results for the systems studied in this work suggest that the effect of the value of D_{pm} on the dynamic performance of systems using purely diffusive particles is greater than that of the value of D_{pm} on the dynamic performance of systems using perfusive particles.

Further studies could be directed at determining the bounds of perfusive behavior. This includes, but is not limited to, studying the bounds of the effects of model parameters on the dynamic performance of columns with bidisperse perfusive adsorbent particles.

SYMBOLS

A	molecule of adsorbate
A_0	external surface area of adsorbent particle, m^2
AS	adsorbate–active site complex
C_d	concentration of adsorbate (single-component system) in the flowing fluid stream of the column, kg/m^3 of bulk fluid
C_{di}	concentration of component i (multi-component system; see eqn. 1 in ref. 4) in the flowing fluid stream of the column, kg/m^3 of bulk fluid
$C_{d,in}$	concentration of adsorbate (single-component system) at $x<0$ when $D_L \neq 0$, or at $x=0$ when $D_L = 0$, kg/m^3 of bulk fluid
$C_{di,in}$	concentration of component i (multi-component system; see eqn. 3 in ref. 4) at $x<0$ when $D_{Li} \neq 0$, or at $x=0$ when $D_{Li} = 0$, kg/m^3 of bulk fluid
C_p	concentration of adsorbate (single-component system) in the fluid of the macropores (throughpores), kg/m^3 of macropore volume
C_{pi}	concentration of component i (multi-component system) in the fluid of the macropores (throughpores), kg/m^3 of macropore volume
C_{pm}	concentration of adsorbate (single-component system) in the fluid of the micropores, kg/m^3 of micropore volume
$\boldsymbol{C}_{pm}$	vector of concentration variables defined after eqn. 7
C_{pmi}	concentration of component i (multi-component system) in the fluid of the micropores, kg/m^3 of micropore volume
$\bar{C}_{psi}$	average concentration of component i defined in eqn. 20, kg/m^3 of perfusive particle
$\bar{C}_s$	average concentration of adsorbate (single-component system) defined in eqn. 17 (the subscript i is dropped for a single-component system), kg/m^3 of microparticle
$\bar{C}_{si}$	average concentration of component i (multi-component system) defined in eqn. 17, kg/m^3 of microparticle
C_{sm}	concentration of adsorbate (single-component system) in the adsorbed phase of the microparticle, kg/m^3 of perfusive particle
$\boldsymbol{C}_{sm}$	vector of concentration variables defined after eqn. 7
C_{smi}	concentration of component i (multi-component system) in the adsorbed phase of the microparticle, kg/m^3 of perfusive particle
C_T	maximum equilibrium concentration of adsorbate (single-component system) in the adsorbed phase of the microparticle, kg/m^3 of perfusive particle
D_L	axial dispersion coefficient of adsorbate (single-component system), m^2/s

D_{Li} axial dispersion coefficient of component i (multi-component system), m^2/s

d_m diameter of microparticle (microsphere), m

D_p effective pore diffusion coefficient of adsorbate (single-component system) in the macropores (through-pores), m^2/s

D_{pi} effective pore diffusion coefficient of component i (multi-component system) in the macropores (through-pores), m^2/s

D_{pm} effective pore diffusion coefficient of adsorbate (single-component system) in the micropores, m^2/s

D_{pmi} effective pore diffusion coefficient of component i (multi-component system) in the micropores, m^2/s

dV volume differential in eqn. 21

$f_i(\boldsymbol{C}_{pm}, \boldsymbol{C}_{sm}, \boldsymbol{k})$ functional form defined after eqn. 7

$g_i(\boldsymbol{C}_{pm}, \boldsymbol{K})$ functional form defined after eqn. 10

K equilibrium adsorption constant of adsorbate (single-component system), $K = k_1/k_2$, m^3/kg

$\boldsymbol{K}$ vector of equilibrium adsorption constants defined after eqn. 10

$\boldsymbol{k}$ vector of adsorption rate constants defined after eqn. 7

k_1 adsorption rate constant in $A + S \underset{k_2}{\overset{k_1}{\rightleftharpoons}} AS$, m^3 of micropore volume/kg · s

k_2 adsorption rate constant in $A + S \underset{k_2}{\overset{k_1}{\rightleftharpoons}} AS$, s^{-1}

L column length, m

n total number of components

Pe_{in} intraparticle Peclet number $[Pe_{in} = (v_p z_0)/D_p]$, dimensionless

Po Porath parameter in macropores $[Po = (k_1 A_0)/(\varepsilon_p D_p)]$, m^3/kg

Po_m Porath parameter in micropores $[Po_m = (k_1 A_0)/(\varepsilon_{pm} D_{pm})]$, m^3/kg

r radial distance in microparticle, m

r_m radius of microparticle (microsphere), m

r_p radius of spherical perfusive particle, m

S active site

T temperature, K

t time, s

V_f column fluid superficial velocity, m/s

v_p intraparticle (interstitial) fluid velocity (intraparticle convective velocity), m/s

V_{pv} volume of perfusive particle, m^3

x axial distance in column, m

z space coordinate of perfusive particle of slab geometry, m

z_0 length (size) of perfusive particle of slab geometry, m

Greek letters

ε void fraction in column

ε_p macropore (throughpore) void fraction

ε_{pm} micropore void fraction

Φ ratio of diffusional time constants for the microparticle and the adsorbent particle $\{\Phi = (D_{pm}/r_m^2)/[D_p/(z_0/2)^2]\}$, dimensionless

ACKNOWLEDGEMENTS

The authors gratefully acknowledge support of this work by Monsanto and the NATO Scientific Affairs Division under Grant No. 880770.

REFERENCES

1 N.B. Afeyan, N.F. Gordon, I. Mazsaroff, L. Varady, S.P. Fulton, Y.B. Yang and F.E. Regnier, *J. Chromatogr.*, 519 (1990) 1.
2 N.B. Afeyan, S.P. Fulton and F.E. Regnier, *J. Chromatogr.*, 544 (1991) 267.
3 L. Lloyd and F. Warner, *J. Chromatogr.*, 512 (1990) 365.
4 A.I. Liapis and M.A. McCoy, *J. Chromatogr.*, 599 (1992) 87.
5 M.A. McCoy, A.I. Liapis and K.K. Unger, *J. Chromatogr.*, 644 (1993) 1.

6 M.A. McCoy, *Ph.D. Dissertation*, Department of Chemical Engineering, University of Missouri–Rolla, Rolla, MO, 1992.
7 B.H. Arve and A.I. Liapis, *AIChE J.*, 33 (1987) 179.
8 B.H. Arve and A.I. Liapis, *Biotechnol. Bioeng.*, 30 (1987) 638.
9 B.H. Arve and A.I. Liapis, *Biotechnol. Bioeng.*, 31 (1988) 240.
10 B.H. Arve and A.I. Liapis, *Biotechnol. Bioeng.*, 32 (1988) 616.
11 A.I. Liapis, *Sep. Purif. Methods*, 19 (1990) 133.
12 J. Ugelstad, A. Berge, T. Ellingsen, R. Schmid, T.-N. Nilsen, P.C. Mork, P. Stenstad, E. Hornes and O. Olsvik, *Prog. Polym. Sci.*, 17 (1992) 87.
13 J.H. Petropoulos, J.K. Petrou and A.I. Liapis, *Ind. Eng. Chem. Res.*, 30 (1991) 1281.
14 G. Neale, N. Epstein and W. Nader, *Chem. Eng. Sci.*, 28 (1973) 1865.
15 G. Stephanopoulos and K. Tsiveriotis, *Chem. Eng. Sci.*, 44 (1989) 2031.
16 M.A. McCoy and A.I. Liapis, *J. Chromatogr.*, 548 (1991) 25.
17 J. Villadsen and M.L. Michelsen, *Solution of Differential Equation Models by Polynomial Approximation*, Prentice-Hall, Englewood Cliffs, NJ, 1978.
18 C.D. Holland and A.I. Liapis, *Computer Methods for Solving Dynamic Separation Problems*, McGraw-Hill, New York, 1983.
19 T. Wicks, *Scientific Computing and Analysis Library Report, SCA-LR-52*, Boeing Computer Services, Seattle, WA, 1988.
20 E. Ruckenstein, A.S. Vaidyanathan and C.R. Youngquist, *Chem. Eng. Sci.*, 26 (1971) 1305.
21 M. Sahimi, G.R. Gavalas and T.T. Tsotsis, *Chem. Eng. Sci.*, 45 (1990) 1443.
22 S. Reyes and K.F. Jensen, *Chem. Eng. Sci.*, 40 (1985) 1723.
23 G.R. Gavalas and S. Kim, *Chem. Eng. Sci.*, 36 (1981) 1111.
24 J. Benzoni and H.-C. Chang, *Chem. Eng. Sci.*, 39 (1984) 161.

Journal of Chromatography A, 660 (1994) 97–111
Elsevier Science B.V., Amsterdam

CHROMSYMP. 2962

Characterization of covalently bonded and adsorbed polymer coatings on silica, alumina and zirconia by means of physico-chemical and chromatographic methods

A. Kurganov*, V. Davankov and T. Isajeva

Institute of Organo-Element Compounds, Russian Academy of Sciences, Moscow (Russian Federation)

K. Unger

Institut für Anorganische Chemie und Analytische Chemie, Johannes Gutenberg-Universität, Mainz (Germany)

F. Eisenbeiss

R & D Chromatography, E. Merck, Darmstadt (Germany)

ABSTRACT

Polymer coatings on porous silica, alumina and zirconia were prepared by covalent bonding of a copolymer of styrene and vinylsilane on the oxidic surface with or without subsequent cross-linking of the immobilized polymeric layer. Polybutadiene and polychloromethylstyrene were adsorbed on the surface of porous alumina without covalent bonding and were cross-linked after deposition. Analysis of the pore structure of coated oxides by means of nitrogen adsorption, mercury porosimetry and inverse size-exclusion chromatography revealed different polymer distributions across the modified surface and different changes of the porosity of the initial oxides depending on the method of polymer immobilization. By covalent bonding of the copolymer of styrene and vinylsilane to alumina and zirconia with subsequent cross-linking the modifying polymeric layer, highly hydrolytic stable packings were synthesized and their applications in separations with aggressive eluents were demonstrated.

INTRODUCTION

Modified silica packings are the most commonly used stationary phases in HPLC [1]. Depending on the HPLC mode being applied, they differ in the chemical nature of the modifying layer. Among these, polymer-coated packings have attracted considerable interest over the last decade. Their synthesis [2,3], chromatographic properties [4] and application to the separation of biologically active compounds [5] have been reviewed.

One of the essential features in the coating process is the spreading of the modifying polymer across the modified surface and the change in the porosity of the initial packing after modification. Figge *et al.* [6] investigated the porosity of silicas coated with poly(*n*-octadecylmethylsiloxane) and polybutadiene by means of nitrogen adsorption and inverse size-exclusion chromatography and reported retaining the pore size distribution of the initial matrix even at high polymer loadings. The pore structural and chromatographic properties of silicas modified with copolymers of styrene and vinylsilane have been examined [7] and marked changes in the pore

* Corresponding author.

0021-9673/94/$07.00 © 1994 Elsevier Science B.V. All rights reserved
SSDI 0021-9673(93)E1105-9

structure of the materials with pore sizes smaller than 10 nm were observed. Later Hanson and co-workers investigated the distribution of adsorbed polybutadiene on the surface of non-porous [8] and porous silicas [9,10] and detected a non-homogeneous distribution of the polymer across the modified surface.

In this work, the primary focus was on the comparison of the porosities of polymer-coated packings obtained by covalent bonding or by adsorption of the polymers. The second aspect of interest was to elucidate the effect of cross-linking of the polymeric layer on the porosity of the final packing. From polymer chemistry it is well known that cross-linking can generate non-porous (gel-like) or porous products depending on the method used. The third aspect was to examine the influence of the chemical nature of the surface to be modified on the polymer distribution and on the structure of the cross-linked polymer layer. As supports silica, alumina and zirconia were used.

EXPERIMENTAL

Chemicals and materials

LiChrospher Si 100, LiChrospher Si 300, Alox T and Aluspher 100, all of particle diameter $d_p = 5$ or 10 μm, were obtained from Merck (Darmstadt, Germany). Experimental silica was a gift from MZ Analysentechnik (Mainz, Germany). Alusorb N 200 was obtained from Lachema (Prague, Czech Republic). Alumina A5Y was obtained from Phase Separations (Deeside, UK). Zirconia was a gift from Thermoxide (Jekaterinburg, Russian Federation).

Polystyrene standards with molecular mass ranging from 182 to 3 340 000 were purchased from Polymer Laboratories (Church Stretton, UK), Polymer Standards Service (Mainz, Germany) and Merck.

All solvents employed for the synthesis were of analytical-reagent grade and were used without additional purification. HPLC-grade solvents for chromatographic measurements were obtained from Merck.

3-Chloromethylstyrene and polybutadiene of average molecular mass 5000 containing 20% vinyl fragments and 80% *cis*- and *trans*-1,4-fragments were purchased from Aldrich-Chemie (Steinheim, Germany).

Synthesis of polymers

A copolymer of styrene and vinylmethyldiethoxysilane (copolymer I) was synthesized by radical copolymerization. Both monomers were subjected to reaction at a ratio 1:1. Dicumyl peroxide was added to the reaction mixture as an initiator at a concentration of 1% (w/w) of monomers. Polymerization was carried out at 120°C under a nitrogen atmosphere for 6 h. The reaction mixture was then diluted with toluene and the copolymer formed was precipitated in dry methanol. The precipitation was repeated twice after dissolving the polymer in toluene and dropping the solution into methanol under agitation. The polymer was then filtered off through a glass frit and dried under vacuum at 40°C. The ratio of styrene to silane units was found to be 8:1 from elemental analysis. The mean molecular mass of the copolymer was determined to be 5500 using size-exclusion chromatography (SEC) with polystyrene standards.

The radical polymerization of 3-chloromethylstyrene was performed in toluene solution at 110°C for 6 h. Dicumyl peroxide was used as an initiator at a concentration of 2.5% (w/w) of monomers. After the polymerization, polychloromethylstyrene was precipitated in methanol and purified as described above. The mean molecular mass was 4500 as determined by SEC.

Preparation of coated oxides by covalent bonding and by adsorption of polymers

Deposition of copolymer 1 on the oxidic surface was carried out by the following procedure. A weighed amount of the oxide was placed in a three-necked flask equipped with a stirrer and Dean–Stark separator and 100 ml of toluene per 10 g of oxide were added. The suspension was heated under reflux until no further water was liberated, then a solution of copolymer in toluene was added (*ca.* 0.2 mg of the copolymer 1 per square metre of specific surface area of silica). The suspension was heated under reflux for 5 h and the hot suspension was filtered off, washed twice with hot

toluene and dried under vacuum at 60°C. The amount of bonded copolymer was assessed by means of elemental analysis and from thermogravimetric measurements (Tables I and III).

The chloromethylation of the immobilized polystyrene was performed according to the conventional procedure by reaction of the coated packing with a mixture of thionyl chloride, dimethoxymethane and zinc chloride in dichloroethane at room temperature. Cross-linking of the chloromethylated polymer was then carried out by boiling the suspension of the corresponding material in dichloroethane or toluene in the presence of zinc chloride as a catalyst. With dichloroethane as a solvent cross-linking occurred, whereas in toluene the cross-linking was additionally accompanied by arylation of the polymeric layer. In the latter instance the degree of cross-linking was lower, but the resulting carbon content was higher compared with the procedure using dichloroethane.

Adsorption of polybutadiene was performed according to Schomburg *et al.* [11]. A 10-g amount of oxide was weighed into a chamfered flask. A solution of 0.8 g of polybutadiene and 40 mg of dicumyl peroxide in 50 ml of *n*-pentane was added to the oxide and the solvent was evaporated by means of a Rotavapor. The subsequent cross-linking was performed at 120°C. The modified oxide was suspended in hot toluene by means of ultrasonic treatment and then filtered off. This procedure was repeated three times. The filtered oxide was then dried under vacuum at 60°C. The same procedure was used for immobilization of polychloromethylstyrene. No cross-linking initiator was used in this instance because cross-linking of polychloromethylstyrene took place due to the self-condenzation of chloromethyl phenyl groups by heating the material up to 150°C.

Thermal analysis

Thermogravimetric analysis (TGA) and differential thermal analysis (DTA) were conducted with a Model 2100 TGA-Analyser (DuPont, Wilmington, DE, USA). The temperature was increased to 1000°C at a rate of 20°C/min under a dry nitrogen or air atmosphere.

Electron spectroscopy for chemical analysis (ESCA)

ESCA measurements were performed with a Contron (Munich, Germany) ESCA analyser at the Institute of Organo-Element Compounds, Moscow, according to the standard procedure.

Mercury porosimetry

Mercury porosimetry was conducted on a Carlo Erba (Milan, Italy) porosimeter with a maximum pressure of about 2500 bar. The pore size distribution was calculated on the basis of the Washburn equation using the standard software supplied by Carlo Erba.

Low-temperature nitrogen adsorption

The nitrogen adsorption isotherms of native and polymer-coated oxides were measured at 77 K with an ASAP 2400 system from Micromeritics (Norcross, GA, USA). The BET specific surface area, the specific pore volume and pore size distribution were calculated by means of the standard software implemented in the ASAP 2400 system.

Chromatographic experiments

The coated oxides were packed into columns of 250 × 4 mm I.D. or 125 × 4 mm I.D. (Merck) using a 5% (w/w) suspension of cyclohexanol–toluene (1:1, v/v). Methanol was used as a displacing solvent. Chromatographic experiments were performed using an HPLC system consisting of an L-6200 pump, an L-4250 variable-wavelength detector and a D-2500 integrator (all from Merck).

RESULTS

Modified silica packings

The coating of porous silicas by covalent bonding of the copolymer of styrene and vinylmethyldiethoxysilane led to packings with coating densities ranging from 2.8 to 12 μmol of monomer units per square metre of specific surface area (Table I). The coating density increased with increase in the pore diameter of the parent silica. The observed changes in the coating density reflect the better accessibility of large pores for the polymer coils bonded to the

TABLE I

CHARACTERISTIC PARAMETERS: SPECIFIC SURFACE AREA (a_s), SPECIFIC PORE VOLUME (V_p) AND MEAN PORE DIAMETER (d_p) FOR NATIVE AND COATED SILICA PACKINGS[a]

No.	Silica	Type of modification	Polymer content (mg/g)	Coating density (μmol/m^2)	Coating thickness (Å)	Low-temperature nitrogen adsorption			Mercury porosimetry			Inverse size-exclusion chromatography		
						a_s (m^2/g)	V_p (ml/g)	d_p (Å)	d_p (Å)	V_p (ml/g)	a_s[b] (m^2/g)	V_p (ml/g)	d_p (Å)	a_s (m^2/g)
1	LiChrospher Si 100	Native	–	–	–	352	1.23	140[b] 140[c]	–	–	–	1.31	150	349
2		Coated with PS[d]	96	2.8	3.0	282	0.95	135	–	–	–	1.20	86	558
3		Cross-linked[e]	137	2.8	4.5	470	1.01	110[b] 130[c]	–	–	–	1.06	44	963
4	LiChrospher Si 300	Native	–	–	–	59	0.56	383[b] 300[c]	350	0.75	86	1.05	474	162
5		Coated with PS	70[g] 83[h]	12.1	12.7	65	0.51	319[b] 250[c]	300	0.62	83	0.79	134	313
6		Cross-linked[f]	77[g] 84[h]	12.1	14.3	123	0.58	189[b] 200[c]	300	0.61	81	0.96	268	143
7	LiChrospher Si 300	Native	–	–	–	80	0.68	341[b] 320[c]	330	0.80	97	1.25	434	115
8		Coated with PS	85[g] 84[h]	11.1	11.6	79	0.61	309[b] 316[c]	300	0.55	73	1.25	126	396
9		Cross-linked[f]	100[g] 99[h]	11.8	14.0	173	0.59	137[b] 290[c]	300	0.54	72	0.86	252	136
10		Cross-linked[e]	134[g]	–	19.4	159	0.56	141[b] 300[c]	300	0.55	73	0.80	260	123
11	Experimental silica	Native	–	–	–	58	0.67	462[b] 400[c]	350	0.82	94	1.15	480	94
12		Coated with PS	47	8.9	8.5	59	0.61	413[b] 370[c]	300	0.63	84	0.87	174	200
13		Cross-linked[f]	52	8.1	9.4	97	0.62	258[b] 350[c]	300	0.61	81	0.88	282	125

[a] All values are normalized for 1 g of modified silica.
[b] Calculated according to Wheeler, $d_p = 4V_p/a_s$.
[c] Maximum of d_p from pore size distribution curve.
[d] PS = polystyrene.
[e] Cross-linked in toluene (see Experimental).
[f] Cross-linked in dichlorethane (see Experimental).
[g] Calculated from elemental analysis.
[h] Derived from TGA experiments.

surface. These observations agreed with our previous results [7] and those of other workers [12,13] who also used the same method for polymer immobilization.

The distribution of elements at the surface of LiChrospher Si 300 determined by means of ESCA shows that the content of silicon atoms at the surface layer decreased from 35% for native silica to 20% for the cross-linked packing after the modification (see Table II). Complete shielding of the silica surface was not reported for either a conventional "brush-type" RP packing (26.9%) or a highly polymer-loaded non-porous packing, Monospher (7.9%) [8]. Taking the amount of silicon in the polymer chain into account, one can assume the same degree of shielding of the surface by the copolymer as found by ESCA for common RP packings.

The polymer content of composites calculated from elemental analysis agreed fairly well with the polymer content assessed from thermal analysis (TGA) (Table I). The thermal decomposition of the immobilized and cross-linked polymer layer occurred to equal extents (Fig. 1A), but the thermal decomposition curve for the packing with non-cross-linked layer (curve 1 in Fig. 1A)

TABLE II

DISTRIBUTION OF CARBON, OXYGEN AND SILICON ATOMS IN THE SURFACE LAYER OF LICHROSPHER SI 300 COATED WITH COPOLYMER OF STYRENE AND VINYLMETHYLDIETHOXYSILANE

LiChrospher Si 300	Amount of copolymer (mg/g)	C (atom%)	O (atom%)	Si (atom%)
Native	–	14.6	50.4	35.1
Coated with copolymer	92	32.3	37.5	30.2
Coated with chloromethylated copolymer	109	47.5	28.4	22.4
Coated with cross-linked copolymer	109	50.5	27.7	21.0

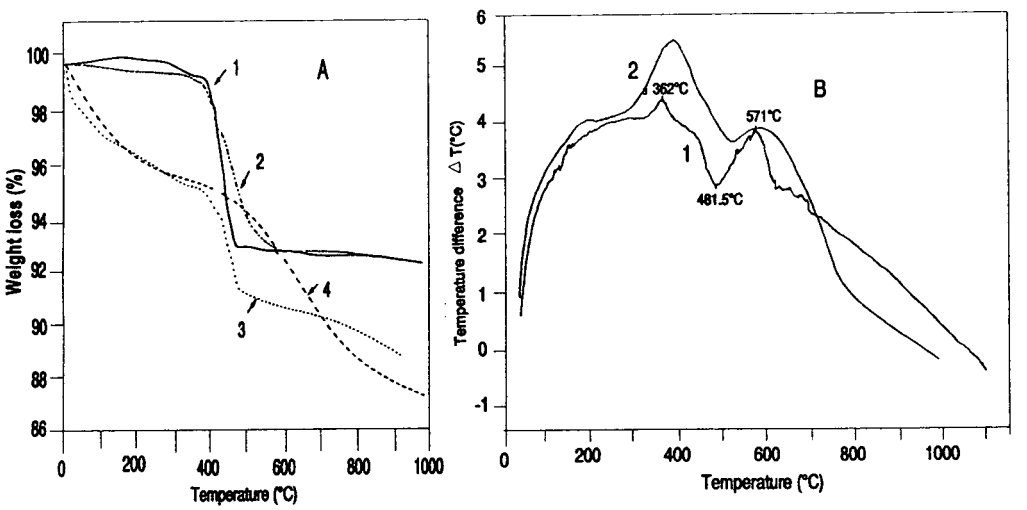

Fig. 1. (A) Thermogravimetric and (B) differential thermogravimetric analysis of silica LiChrospher Si 300 (1, 2) and alumina Aluspher 100 (3, 4) coated with covalent bonded copolymer of styrene and vinylsilane (1, 3) and subjected to additional cross-linking (2, 4).

was steeper than that for the packing with the cross-linked layer (curve 2 in Fig. 1A). The mass loss was in all instances independent of the probe type and the atmosphere in which the decomposition was carried out.

DTA indicated a difference between the packings bearing the non-cross-linked and the cross-linked polymeric film (Fig. 1B). The DTA curve under a nitrogen atmosphere for the non-cross-linked packing showed a less pronounced endothermic peak at 362°C and two other exo- and endothermic peaks at 481 and 571°C, respectively. For the cross-linked packing the same was observed, but the first peak at 362°C was much more pronounced. It is highly probable that the first endothermic effect is connected with the destruction of the polymeric network and bonds at the oxidic surface, which is in agreement with the small mass loss of 1% (w/w) up to 400°C (Fig. 1A).

The specific surface area of the 100 Å pore size silica decreased by about 20% after coating with the copolymer I (see Table I). The decrease for the wide-pore supports was only 5%. In all instances the cross-linking of the polymeric layer caused an increase in the specific surface area by a factor of about two. This increase was probably due to the formation of small pores in the polymer layer, as described earlier by Davankov and Tsyurupa [14] for bulk polystyrene which was intensively cross-linked in the dissolved state.

The specific pore volume of the native 100 Å pore size silica decreased by about 26% after the modification. The changes in V_p for wide-pore silicas were within the accuracy of the measurement. Cross-linking of the polymer layer did not cause any significant changes in the specific pore volume of the packings.

The mean pore diameter of silicas determined by the nitrogen adsorption technique diminished only slightly after the coating with the copolymer, but dropped sharply after the cross-linking (Table I). The mean pore diameter according to Wheeler and the maximum of the pore size distribution coincided well for native and coated non-cross-linked packings. For the cross-linked packings the deviation of these values was up to 50%.

As a representative example, the pore size distributions of LiChrospher Si 300 (sample No. 7 in Table I) and its polymer-coated derivatives are shown in Fig. 2. The position of the peak maximum of the pore size distribution curve did

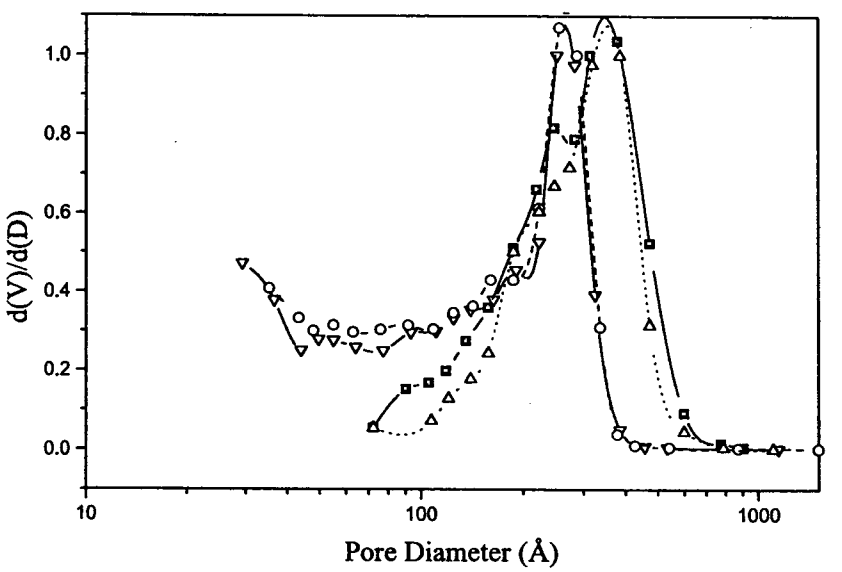

Fig. 2. Pore size distribution of silica LiChrospher Si 300, (□) native, (△) modified with covalent bonded copolymer I and (○, ▽) modified with cross-linked covalently bonded copolymer I determined from nitrogen adsorption isotherm.

not change after the coating with the copolymer and moved slightly to lower values after the cross-linking, independently of the method used (compare curves 3 and 4 in Fig. 2).

The parameters determined by means of mercury porosimetry coincided fairly well with those obtained from nitrogen adsorption measurements for native silicas or packings coated with non-cross-linked polymer (Table I). However, the mean pore diameter and the specific surface area of the cross-linked packings derived from mercury porosimetry differed significantly from the corresponding values obtained from nitrogen adsorption measurements.

The third method used for the evaluation of the pore structure parameters was inverse size-exclusion chromatography (ISEC). The specific pore volume assessed by this method is related to the volume of packing in the column. To recalculate this value per gram of packing in the column, it was assumed that the specific density of the pore walls of all silicas is equal to the true density of quartz (2.2 g/ml). This assumption seems to be reasonable. Stegeman *et al.* [15] determined the specific density of walls for one sample of silica and found an identical value. The density of polymer-coated packings was assumed to be a linear function of their composition. The calculated values are given in Table I. The specific pore volume of the 100 Å pore size silica determined by ISEC coincided reasonably well with those determined by nitrogen adsorption. The specific pore volume of wide-pore packings markedly exceeded the values calculated from nitrogen adsorption. This difference is probably caused by uncertainties in the determination of V_p for wide-pore packings, as pointed by Stegeman *et al.* [15]. In this case one cannot clearly discriminate between the size-exclusion and hydrodynamic mechanism of separation. Within a series of silicas and their coated derivatives a decrease in the specific pore volume is observed (Table I). The subsequent cross-linking slightly increased the specific pore volume or did not change it at all.

The pore size distribution from ISEC data was calculated according to the Knox method [16]. For non-modified silicas the calculated pore diameter was in good agreement with the value determined from nitrogen adsorption. In all instances coating with the polymer caused a marked decrease in the mean pore diameter (Table I). The pore diameter of coated silica packings determined by ISEC did not coincide with those calculated from nitrogen adsorption and from mercury porosimetry. Inspection of the SEC calibration graph reveals that the plot for the packing with a cross-linked polymeric layer lies between those for the native and coated non-cross-linked silica (Fig. 3A). Another interesting feature of Fig. 3A is that the calibration graphs are of almost the same shape. Similar changes were observed for the silica with 100 Å pore diameter, with the only difference that the calibration graphs for the packings coated with a non-cross-linked and with a cross-linked polymeric layer were very close to each other (Fig. 3B). This seems to be an indication that native and modified packings have approximately the same width of the pore size distribution, which is shifted for coated packings to smaller mean pore diameters. The latter is evidenced by the diminution of the size exclusion limit.

Modified alumina and zirconia packings

The coating procedure for aluminas and zirconia was essentially the same as that applied to the silicas. The results are given in Table III. The coating density of the packings based on Aluspher 100, Alumina A5Y and Alox T was comparable to the value obtained for LiChrospher Si 100. Alusorb N 200 gave a lower coating density, probably owing to its broader pore size distribution (not shown). The latter extended to the lower pore size and the main part of these small pores remained unmodified in the coating procedure.

The modification of alumina by means of covalent bonding of copolymer I caused the same changes in the pore structure as discussed for silicas. The cross-linking of the adsorbed polymer layer generated a bimodal pore size distribution (Fig. 4). The nitrogen adsorption isotherm exhibited two distinct steps in the desorption branch in the range of the capillary condensation ($0.4 < p/p_0 < 0.9$). Correspondingly, the pore size distribution curve showed two maxima (Fig. 4). One was identical with the

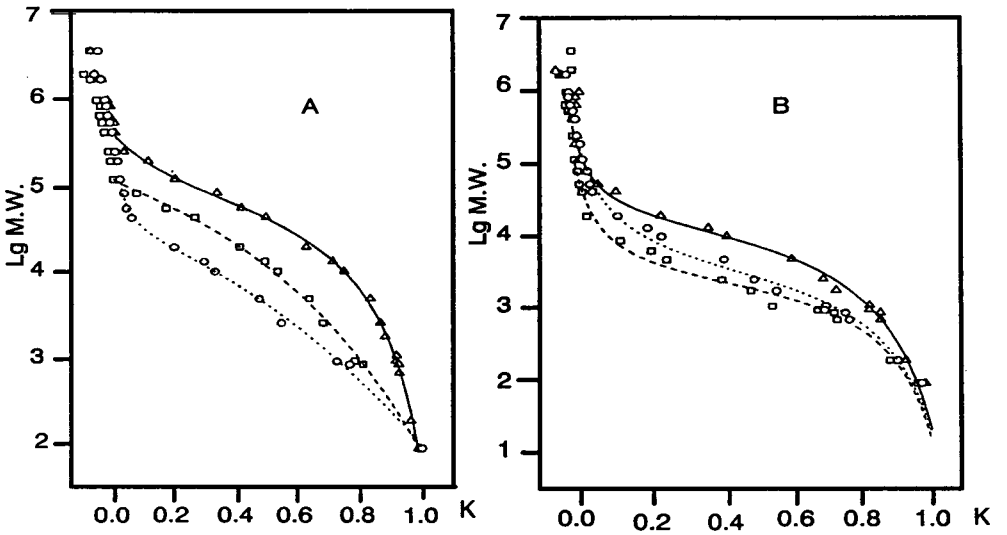

Fig. 3. SEC calibration graphs for (A) silica LiChrospher Si 300 and (B) silica LiChrospher Si 100: □ = coated with cross-linked covalently bonded copolymer I; ○ = coated with covalently bonded copolymer I; △ = native. M.W. = Molecular mass.

maximum of the pore size distribution curve of the unmodified alumina. The second maximum occurred at slightly lower values of about 40–60 Å.

The SEC calibration graphs for polymer-modified aluminas are shown in Fig. 5A. In accordance with the decrease in d_p, the exclusion limit of the polymer-modified aluminas also decreased as compared with the native oxide. However, in the low-molecular-mass range there was a slight difference in fractionation ability as compared with the parent material. The calibration graphs for native alumina and for the polymer-coated packing are very close to each other in this molecular mass range (Fig. 5).

Cross-linking of the polymeric layer decreased the exclusion limit much further and the calibration graph exhibited an extremely small slope in the range of the size-exclusion distribution coefficient, K, between 0 and 0.6. However, the pore size distribution from such a type of calibration graph cannot be calculated by ISEC owing to the lack of an appropriate fitting function.

The TGA experiments revealed that there is no significant difference in the thermal stability of the polymer layer deposited on the alumina surface compared with silicas. Unexpectedly, an enhanced thermal stability was observed for aluminas with a cross-linked polymer layer in a nitrogen atmosphere (Fig. 1A, curve 4). As is seen from the slightly sloping curve, the mass loss was minor up to 800°C for this packing (Fig. 1A, curve 3).

Contrary to the method of covalent bonding, the polymer load for Aluspher 100 modified by the adsorption of polybutadiene and polychloromethylstyrene is not limited. It is simply adjusted by the amount of the polymer employed for modification (Table III). The progressive increase in the polymer content was accompanied by a strong decrease in the specific surface area and the specific pore volume determined by nitrogen adsorption (Table III). The mean pore diameter and the pore size distribution of the modified packings were exactly the same as for the starting alumina (Fig. 6).

The ISEC method demonstrated distinct changes in the pore size distribution after modification. The SEC calibration graph for the polybutadiene-coated packing was different to that for the native alumina and major alterations were observed in the low-molecular mass range (Fig. 5). The exclusion limit of alumina was only slightly changed after the modification. Hence SEC clearly proved the appearance of small pores in the structure of coated packing.

The available sample of zirconia exhibited an

TABLE III

CHARACTERISTIC PARAMETERS: SPECIFIC SURFACE AREA (a_s), SPECIFIC PORE VOLUME (V_p) AND PORE DIAMETER (d_p) FOR DIFFERENT OXIDES COATED WITH POLYMERS[a]

No.	Oxide	Type of coating procedure	Polymer content (mg/g)	Coating density (μmol/m^2)	Low-temperature nitrogen adsorption			Inverse size-exclusion chromatography		
					a_s (m^2/g)	V_p (ml/g)	d_p[b] (Å)	V_p ml/g	d_p (Å)	a_s[b] m^2/g
1	Alumina	Native	–	–	155	0.50	130	0.55	146	151
2	Aluspher 100	PS[c]	43[g] 98[h]	2.8	140	0.43	122	0.37	64	231
3		Cross-linked PS[d]	61[g] 93[h]	3.0	175	0.43	99	0.31	–	–
4		Cross-linked PS[e]	54[g]	3.1	184	0.46	100	0.40	–	–
5		Polybutadiene[f]	80[g]	12.3	108	0.35	128	0.37	48	308
6		Chloromethyl-PS	70[g]	3.0	135	0.41	122	–	–	–
7		Chloromethyl-PS	162[g]	8.3	86	0.27	124	–	–	–
8	Alumina	Native	–	–	75	0.24	131	–	–	–
9	Alox T	Coated with PS	52[g]	7.0	102	0.29	114	–	–	–
10	Alumina	Native	–	–	226	0.29	52	–	–	–
11	Alusorb N 200	Coated with PS	40[g]	1.7	214	0.26	47	–	–	–
12	Alumina A5Y	Coated with PS[d]	66[g]	4.0	172	0.28	65	–	–	–
13	Zirconia	Native	–	–	17	0.07	157			
14		Coated with PS	7.7	4.1	9	0.02	89			

[a] All values are normalized for 1 g of modified oxide.
[b] Calculated according to Wheeler, $d_p = 4V_p/a_s$.
[c] PS = polystyrene.
[d] Cross-linked in dichloroethane (see Experimental).
[e] Cross-linked in toluene (see Experimental).
[f] Coated according to Figge *et al.* [6].
[g] Calculated from elemental analysis.
[h] Derived from TGA experiments.

extremely low specific pore volume. The specific surface area of zirconia of 17 m^2/g clearly indicated that the sample was porous. Coating of zirconia with the polymer affected only slightly the shape of its pore size distribution. However, the values of a_s, V_p and d_p of the modified packing were reduced to half the initial values.

Chromatographic characterization

SEC was performed to evaluate the changes in pore structure parameters after the coating of the oxides with polymers. The results of these investigations are presented in Tables I and III and have already been discussed in context with the results of low-temperature nitrogen adsorption and mercury porosimetry. From the chromatographic point of view, the modification by means of covalent bonding diminished the exclusion limit and did not significantly change the molecular mass of the solutes enabling them to penetrate the pores of the packing. The selectivity [*i.e.*, the derivative d(log M_r)/dV] of the packing remained nearly unaffected, while the calibration graphs of the modified and the native silicas are almost parallel to each other (Fig. 3). The cross-linking of the polymeric layer moved the calibration graph of the packing closer to those of native silica, thus increasing the exclusion limit.

The modification of oxides by means of adsorption of polybutadiene decreased only slightly the exclusion limit, but diminished strongly the

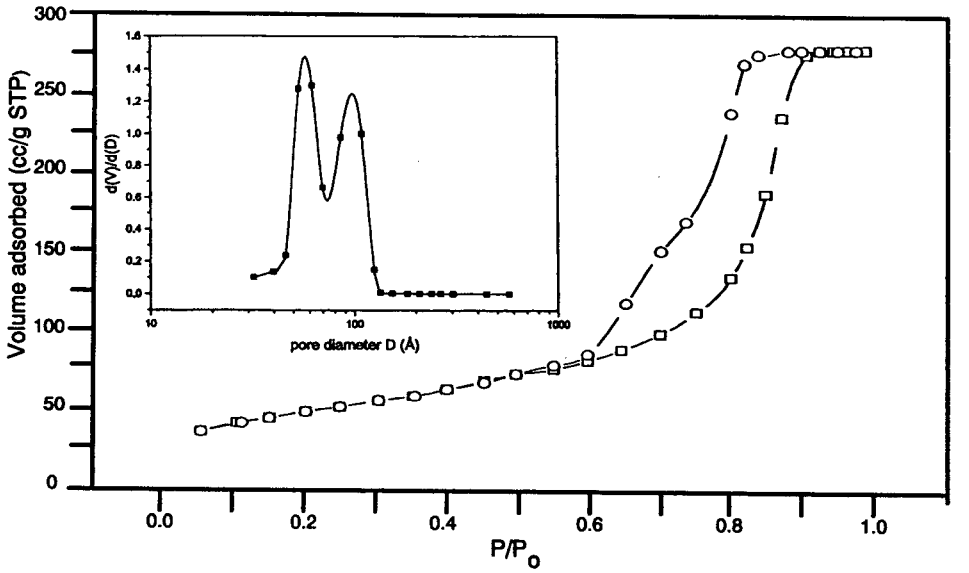

Fig. 4. Low-temperature nitrogen adsorption isotherm and calculated pore size distribution of alumina Aluspher 100 coated with cross-linked covalent bonded copolymer I: □ = adsorption; ○ = desorption. cc = ml.

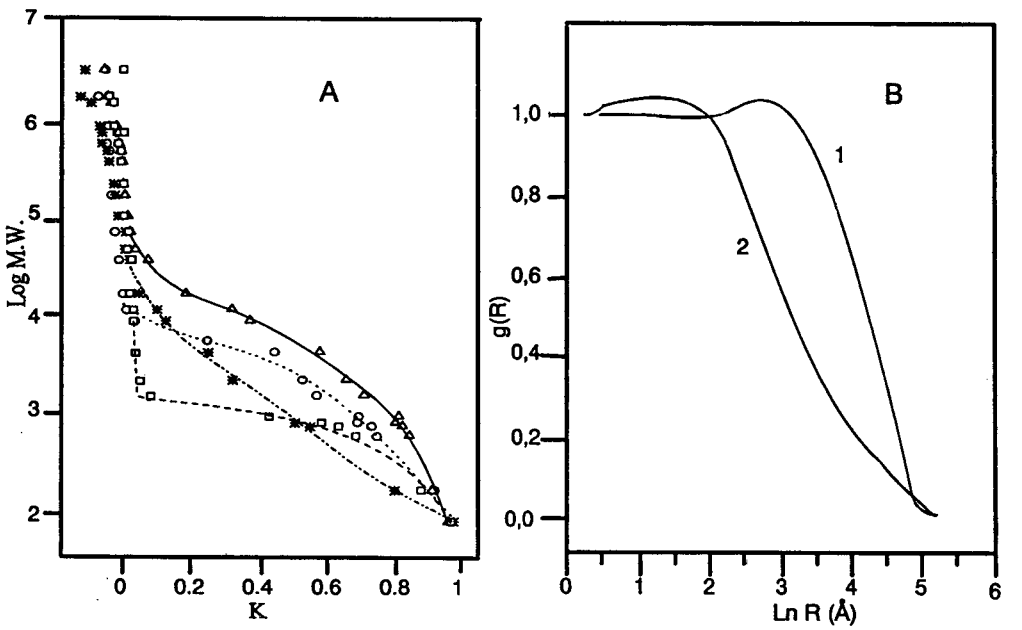

Fig. 5. (A) SEC calibration graphs and (B) calculated pore size distribution for alumina Aluspher 100 and its derivatives. (A) △ = native; □ = coated with covalently bonded cross-linked copolymer I; ○ = coated with covalently bonded copolymer I; * = coated with adsorbed polybutadiene. (B) 1 = Native; 2 = coated with adsorbed polybutadiene. M.W. = Molecular mass.

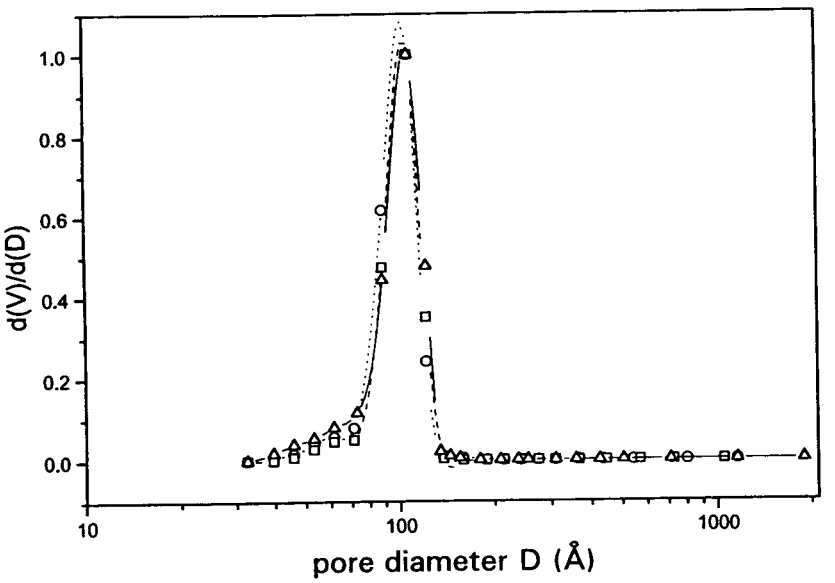

Fig. 6. Pore size distribution of alumina Aluspher 100 modified with adsorbed polychloromethylstyrene determined from low-temperature nitrogen adsorption: ○ = native; □ = 7% loading; △ = 16.2% loading.

molecular mass, enabling molecules to penetrate all pores of the packing. The calibration graph for the coated packing was therefore much steeper than that for the native material (Fig. 5). As a consequence, the selectivity of the modified packing was markedly decreased because its fractionation range became wider.

The impact of cross-linking of the polymeric layer of the packings on the selectivity of separation in the RP mode of chromatography is demonstrated in Fig. 7. There is actually no large difference between the two sorbents in the separation of basic compounds. Good efficiency and peak symmetry were observed for amines on both cross-linked and non-cross-linked coated silicas, reflecting the good shielding of the silica surface by the polymeric layer. It should be emphasized that no end-capping of the polystyrene-modified silica was carried out and no addition of any other basic or salt compounds to the eluent was required. The separation were performed with a simple water–acetonitrile eluent.

Basic compounds were also eluted with symmetrical peaks on alumina and zirconia modified by covalent bonding of copolymer I, indicating no specific surface–solute interaction (Fig. 8). As the chemical stability of alumina or zirconia towards strong alkali or strong acid eluents is much higher than that of silica, separations can be carried out with acidic and alkaline eluents which are not compatible with modified silicas (Fig. 9).

DISCUSSION

The modification of porous silicas and aluminas by means of adsorption of different types of cross-linkable polymers has been intensively investigated by Schomburg [3,4]. Coatings with covalently bonded pre-synthesized reactive copolymers have been studied in the chiral ligand-exchange chromatography of enantiomers [17] and in the reversed-phase [18] and ion-exchange chromatography [19] of proteins and peptides. Whereas the main focus of the previous investigations was on the assessment of the chromatographic performance, in this work we addressed the problem of the distribution of polymers in the pores of modified oxides.

The pore size distribution of alumina Aluspher 100 determined by means of low-temperature nitrogen adsorption was not changed after the coating with polychloromethylstyrene (Fig. 6) or

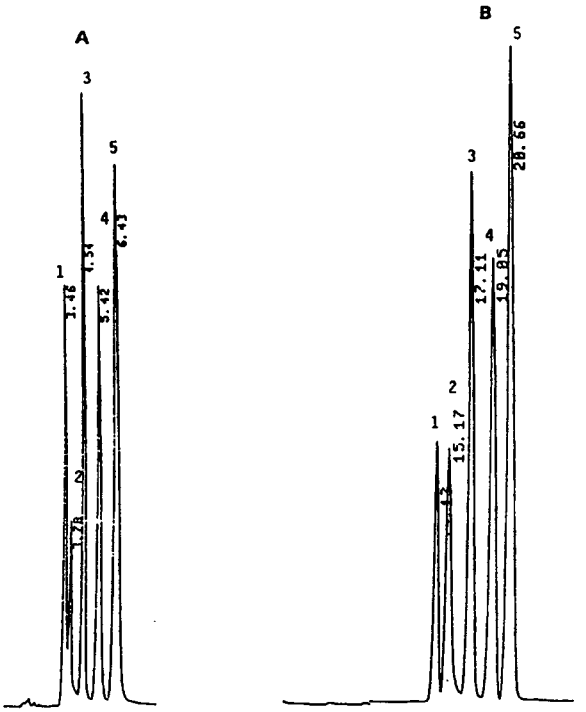

Fig. 7. Separation of a mixture of basic compounds on (A) silica LiChrospher Si 300 coated with covalently bonded copolymer and (B) silica LiChrospher Si 100 coated with cross-linked covalent bonded copolymer. (A) $d_p = 10$ μm; column, 125 × 4 mm I.D.; flow-rate, 0.5 ml/min; eluent, acetonitrile–water (1:1). (B) $d_p = 10$ μm; column, 125 × 4 mm I.D.; flow-rate, 0.25 ml/min; eluent, acetonitrile–water (6:4). Analytes; 1 = pyridine; 2 = *o*-toluidine; 3 = N-methylaniline; 4 = N,N-dimethylaniline; 5 = 2-ethylaniline. Retention times (min) indicated at the peaks.

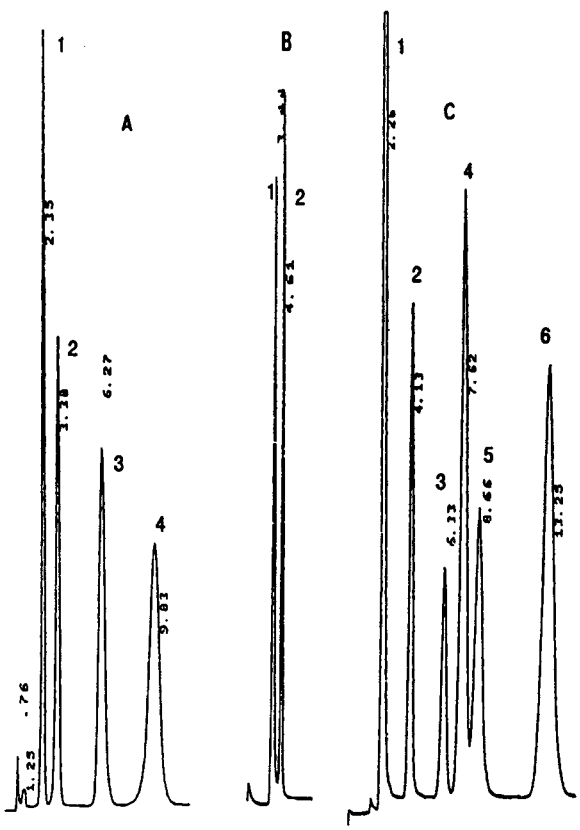

Fig. 8. Chromatographic separations on alumina Aluspher 100 coated with covalent bonded cross-linked copolymer I. Column, 125 × 4 mm I.D.; $d_p = 10$ μm; flow-rate, 0.5 ml/min; eluent, acetonitrile–water (1:3). (A) Separation of a mixture of barbiturates: 1 = barbitole; 2 = allo-barbitole; 3 = luminale; 4 = prominale. (B) Separation of a mixture of (1) 2,6-dimethypyridine and (2) pyridine. (C) Separation of a mixture of basic compounds: 1 = N-methylaniline; 2 = pyridine; 3 = aniline; 4 = N,N-dimethylaniline; 5 = *o*-toluidine; 6 = 2-ethylaniline. Retention times (min) indicated at the peaks.

polybutadiene (not shown), in spite of a strong decrease in the specific pore volume and specific surface area (Table III). Since the same results have been observed earlier for other oxides coated with other polymers [6,9,10], it seems that the preservation of the pore size distribution of the native material after modification by the adsorption method is a fairly general phenomenon.

The preservation of the pore size distribution of the parent oxide after modification with a polymer cannot be expected assuming the common model of modification where the polymer is deposited on the surface of pores. Another model has been suggested [10] in which the pores are not coated, but simply filled with the polymer. However, this model is not yet able to explain the preservation of pore size distribution. This phenomenon can be explained by the model of Lecourtier *et al.* [20], in which the polymer is deposited mainly on the outer surface of the particles. This model is strongly supported by scanning electron micrographs of Aluspher 100 coated with polybutadiene, where the presence of polymer agglomerates on the other surface of particles was detected. The micrographs demonstrate the same picture as was reported earlier for polybutadiene-coated LiChrospher Si 300 [9].

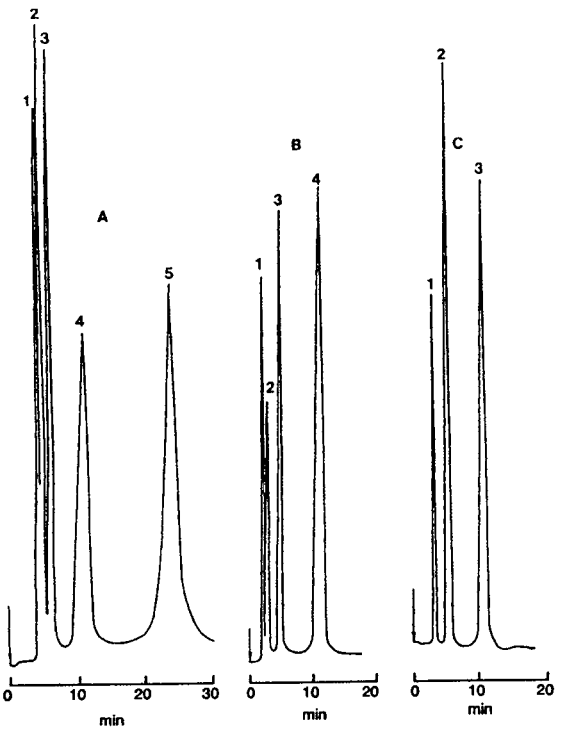

Fig. 9. Chromatographic separations on zirconia coated with cross-linked covalent bonded copolymer I. Column, 150 × 6 mm I.D.; d_p = 10–20 μm. (A) Eluent, acetonitrile–0.1 *M* HNO_3 (1:9); flow-rate, 0.5 ml/min. Analytes: 1 = pyridine; 2 = dipyridyl; 3 = 2,6-dimethylpyridine; 4 = phenanthroline; 5 = acridine. (B) Eluent, acetonitrile–water (1:5); flow-rate, 1.0 ml/min. Analytes: 1 = 2-aminopyridine; 2 = pyridine; 3 = aniline; 4 = *p*-nitroaniline. (C) Eluent, methanol–0.13 *M* NaOH (1:1); flow-rate, 1.0 ml/min. Analytes: 1 = 2-aminopyridine; 2 = aniline; 3 = *p*-nitroaniline.

The pore size characteristics of packings modified by the adsorption method obtained by ISEC were in contradiction with the results from nitrogen adsorption measurements and provide evidence for the formation of small pores in the polymer layer. As a result, the pore size distribution of polybutadiene-coated Aluspher 100 calculated from SEC data shifted to smaller pore diameters (Fig. 5B). According to the method of synthesis applied, the polybutadiene layer should have a gel-like structure, which normally demonstrates no porosity when in the dry state [21]. The polymeric layer swells under SEC conditions and generates small pores, which shift the pore size distribution of composite packings to lower diameters compared with the native oxide.

The properties of the packings modified by means of covalent bonding of copolymer I supported the common model of modification assuming the deposition of modifier on the surface of pores. For silicas and aluminas with a mean pore diameter of 100 Å, an addition to the normal decrease in the specific pore volume and the specific surface area was observed owing to the blocking of small pores by the bounded polymer (Tables I and III). Wide-pore oxides of pore diameter ≥300 Å modified by this method show little change in their porosity after the modification, and small pores were absent in the structure of these materials (Fig. 2). The decrease in the mean pore diameter for modified packings from SEC data was found to be more pronounced than was determined from nitrogen adsorption measurements (Tables I and III). This is strong evidence for the swelling of the polymeric layer under SEC conditions.

The cross-linking of the immobilized copolymer causes a strong increase in the specific surface area determined by nitrogen adsorption (Table I) whereas the specific pore volume was found to be changed only slightly. The pore size distribution determined from the nitrogen adsorption isotherm reveals the formation of small pores in the polymer film after the cross-linking and in the case of Aluspher 100 even a bimodal mesopore structure was found (Fig. 4).

The SEC measurements provided clear evidence that the cross-linking of the bonded copolymer I decreased the swelling ability of the polymeric layer because the exclusion limit of the modified wide-pore packings was increased after the cross-linking (Fig. 3A). For LiChrospher Si 100 the changes (Fig. 3B) were small and for Aluspher 100 even a progressive decrease in the molecular mass exclusion limit after cross-linking was detected (Fig. 5). The molecular mass fractionation range of Aluspher 100 coated with a cross-linked polymer layer was between 1000 and 300 only. Nevertheless, it was not decreased to the level of low-molecular mass compounds (*e.g.*, benzene, toluene) as took place for Aluspher 100 modified with adsorbed polybutadiene (Fig. 5). The shape of the SEC curve observed for Aluspher 100 modified with a cross-linked polystyrene layer is a challenge for

theoretical considerations in SEC because according to model used even for the packing having pores of a single size only the fractionation range should be at least 1.5 log M_r [22]. Nevertheless, SEC calibration graphs with a very narrow fractionation range have been reported for different types of packings [23,24] and elucidation of their pore structures needs additional investigations.

The modification of oxides other than silica by covalent bonding of copolymer I containing reactive silane groups leads to the formation of surface Si–O–E bonds, the hydrolytic stability of which decreases in the order E = Si > AI > Ti > Zr [25]. Because the hydrolytic stability even of Si–O–Si bonds is not sufficient in many applications, it is essential to cross-link the polymeric film as the ultimate step in the synthesis of coated oxides. The chromatographic separations with coated aluminas or zirconia clearly demonstrate that not only the oxide was stable against aggressive eluents, but also the polymer layer. The separation of basic compounds on these packings can be easily performed with neutral, basic or acid eluents, as the packings are stable towards hydrolysis (Fig. 9). It is interesting that alumina coated with polystyrene demonstrates a different selectivity towards amines compared with polystyrene-coated silica (Figs. 7 and 8), but there was no evidence for any decrease in column performance due to the kinetic hindrance in spite of the different pore structures of composites synthesized from silica or alumina.

CONCLUSIONS

Two different methods of polymer coating of oxides have been discussed, namely modification by adsorption of cross-linkable polymers and by covalent bonding of pre-synthesized reactive copolymers. Examination of the pore structure characteristics of the packings by means of low-temperature nitrogen adsorption, mercury porosimetry and inverse size-exclusion chromatography revealed two different modes of polymer distribution on the surface of the oxides. Cross-linking of the immobilized polymeric layer produced additional porosity which can be detected by means of SEC or nitrogen adsorption measurements, but has little impact on the separations by means of adsorption chromatography. Good chromatographic analytical-scale separations can be achieved with both types of coated packings. Examples of separations on packings with covalent bonded polymeric layer have been presented.

Coating by means of covalent bonding with subsequent cross-linking of the immobilized polymeric layer can be applied to oxides other than silica. The changes in the porosity of the parent oxide after deposition of the polymer was found to be the same as observed for silica packings. The chemical nature of the surface to be modified strongly influenced the changes in the composite porosity in the cross-linking step and different pore structures were detected for alumina and silica modified with cross-linked polystyrene. The chromatographic separations on the coated aluminas and zirconia demonstrate excellent chemical stability of these packings towards aggressive eluents.

REFERENCES

1 K. Unger (Editor), *Packings and Stationary Phases in Chromatographic Techniques*, Marcel Decker, New York, 1990.
2 M. Hanson and K. Unger, *Trends Anal. Chem.*, 11 (1992) 368.
3 G. Schomburg, *Trends Anal. Chem.*, 10 (1991) 163.
4 G. Schomburg, *LC · GC Mag.*, 6 (1988) 37.
5 A.E. Ivanov, V.V. Saburov and V.P. Zubov, *Adv. Polym. Sci.*, 104 (1992) 136.
6 H. Figge, A. Deege, J. Köhler and G. Schomburg, *J. Chromatogr.*, 351 (1986) 393.
7 A. Kurganov, O. Kuzmenko, V. Davankov, B. Eray, K. Unger and U. Trüdinger, *J. Chromatogr.*, 506 (1990) 391.
8 M. Hanson, K. Unger and G. Schomburg, *J. Chromatogr.*, 517 (1990) 269.
9 M. Hanson, *Ph.D. Thesis*, Johanes Gutenberg-Universität, Mainz, 1992.
10 M. Hanson, B. Eray, K. Unger, A. Neimark, J. Schmidt, K. Albert and E. Bayer, *Chromatographia*, 35 (1993) 403.
11 G. Schomburg, J. Köhler, H. Figge, A. Digge and U. Bien-Vogelsang, *Chromatographia*, 18 (1984) 265.
12 A. Alpert and F. Regnier, *J. Chromatogr.*, 185 (1979) 340.
13 A. Ivanov, L. Zhigis, E. Chekhovskykh, P. Reshetov and V. Zubov, *Bioorg. Khim.*, 11 (1985) 1527.
14 V.A. Davankov and M.P. Tsyurupa, *React. Polym.*, 13 (1990) 27.

15 G. Stegeman, J. Kraak and H. Poppe, *J. Chromatogr.*, 550 (1991) 721.
16 J.H. Knox and H.P. Scott, *J. Chromatogr.*, 316 (1984) 333.
17 A. Kurganov, A. Tevlin and V. Davankov, *J. Chromatogr.*, 261 (1983) 479.
18 V. Davankov, A. Kurganov and K. Unger, *J. Chromatogr.*, 500 (1990) 519.
19 A. Kurganov, V. Davankov and K. Unger, *J Chromatogr.*, 548 (1991) 207.
20 J. Lecourtier, R. Audebert and C. Quivoron, *J. Liq. Chromatogr.*, 1 (1978) 479.
21 D.H. Freeman and S.B. Schram, *Anal. Chem.*, 53 (1981) 1235.
22 L. Hagen, in P.L. Dubin (Editor), *Aqueous Size-Exclusion Chromatography*, Elsevier, Amsterdam, 1988, p. 147.
23 K. Unger, N. Becker and E. Krämer, *Chromatographia*, 8 (1975) 283.
24 A. Maruska, A. Sérys, J. Liesiené, J. Urbonavicienė and A. Zygas, *J. Chromatogr.*, 596 (1992) 157.
25 U. Trüdinger, G. Müller and K. Unger, *J. Chromatogr.*, 535 (1990) 111.

Journal of Chromatography A, 660 (1994) 113–118
Elsevier Science B.V., Amsterdam

CHROMSYMP. 2903

Experimental study on the separation of silica gel supports by gravitational field-flow fractionation

Jiří Pazourek*, Eva Urbánková and Josef Chmelík

Academy of Sciences of the Czech Republic, Veveří 97, 611 42 Brno (Czech Republic)

ABSTRACT

The separation and characterization of silica gel particles were investigated by gravitational (1 *g*) field-flow fractionation. The experiments were performed in a ribbon-like glass-walled channel with a photometric (turbidimetric) detector. Solutions of several surfactants were tested as carrier liquids. Factors affecting the separation process are discussed and the deductions are compared with experimental results. Some aspects concerning the activity of lift forces were confirmed.

INTRODUCTION

The separation and characterization of particles are of great importance for particular products, *e.g.*, silica gel supports for chromatographic columns, where the size distribution, density, porosity, etc., are basic parameters of the support. In order to determine the parameters, chemical methods (chemical affinity) cannot be used, and therefore other methods based on physical principles have to be employed. The determination of support characteristics is commonly performed by expensive and/or slow procedures (*e.g.*, evaluation of photomicrographs, laser optical methods, adsorption analysis). A solution may lie in methods based on hydrodynamic forces which appear intrinsically in shear flows with solid particles. An advantage of this approach is the simple experimental arrangement because the flow works simultaneously as a carrier medium.

Employing the Earth's gravity as the external field, gravitational field-flow fractionation (GFFF) is such a technique, suitable for the separation and/or characterization of particles because the peak dispersion of the fractograms corresponds to the size distribution of the particles. The technique is effective only for micrometre-sized particles owing to the relatively weak field strength (1 *g*). GFFF has been used for the separation and characterization of various particulate materials, *e.g.*, glass and latex beads [1–4]. Giddings *et al.* [5] made an attempt to characterize silica gel supports by GFFF but their results were not very satisfactory even after using calibration beads because their calculations were based on a simple steric model without the activity of lift forces that evidently acted there. On the other hand, these forces were utilized by Ratanathanawongs and Giddings [6], who reported a rapid method to characterize silica gel particles by flow/hyperlayer FFF. Giddings and co-workers [7,8] worked out a complete methodology to determine the size distribution, density and porosity of silica gel supports by combining sedimentation FFF (SdFFF) with electron microscopy.

Some effects that play an important role in the separation process have been studied by FFF. Beckett *et al.* [9] were able to detect the adsorption of proteins on polystyrene latex beads with a coverage of less than a monolayer by SdFFF and Li and Caldwell [10] studied the adsorption of polymeric surfactants on cores of

* Corresponding author.

0021-9673/94/$07.00 © 1994 Elsevier Science B.V. All rights reserved
SSDI 0021-9673(93)E0818-F

polystyrene latex particles also by SdFFF. Jones *et al.* [11] used SdFFF to separate aggregates from doublets to sextuplets in suspensions of poly(methyl methacrylate) latex particles and Barman and Giddings [12] studied the aggregation of polystyrene and poly(methyl methacrylate) latex particles caused by addition of a cationic surfactant to the suspension of an anionic surfactant by SdFFF. Karaiskakis and Koliadima [13,14] investigated changes in the retention of suspensions of submicrometre metal oxide particles caused by reversible adsorption in a centrifugal steel-walled channel, which were in accordance with their calculations involving Hamaker constants and surface potentials; they suggested a new technique called potential barrier FFF (PBFFF). Pazourek and Chmelík [4] studied the elution of polystyrene latex bead mixtures in different carrier liquids containing surfactants by GFFF.

The aim of this work was to investigate the possibility of the separation and characterization of silica gel supports by GFFF. Although a methodology for silica gel support characterization (by SdFFF) has already been reported [7,8], and silica gel supports have been characterized by flow/hyperlayer FFF [6], we carried out this study with a much simpler experimental arrangement: the apparatus for SdFFF consists of a channel built in a centrifuge rotor and the channel for flow FFF must have a rigid frit (frits) with an ultrafiltration membrane (membranes) which are sensitive to pressure changes and fouling, whereas we used a channel made of two glass plates sandwiching a foil (see Experimental). This paper is the first part of a study leading to the size and density characterization of solid particles by GFFF.

EXPERIMENTAL

The experimental arrangement has been described elsewhere [3,4]. We tested five separation channels; all were made by sandwiching a 40-, 80- or 150-μm foil with a channel-shaped cut (spacer) between two 8-mm thick pieces of glass and clamping the latter together between two Lucite bars. The width of all the channel spacer cuts was 2 cm and the lengths were as follows: channel I, 36 cm; channel IIb, 80 cm; channel III, 108 cm. The dead volumes were 0.52, 1.20 and 1.57 ml (80-μm spacer), respectively, channel IIa 0.60 ml (40-μm spacer) and channel IIc 2.25 ml (150-μm spacer), respectively. Inlet and outlet steel tubes (0.5 mm I.D.) were glued into holes drilled in the glass plates.

The analysis was performed with an HPP 4001 high-pressure pump (Laboratory Instruments, Prague, Czech Republic) coupled with a UVM 4 spectrophotometric detector (Development Workshops ČSAV, Prague, Czech Republic) operated at 254 nm, or with a Spectra 100 capillary spectrophotometric detector (Spectra-Physics, San Jose, CA, USA) at 200 or 210 nm (Triton X-100). The former detector had a Z-shaped cell with an optical path of 5 mm and the latter had a quartz capillary detection cell of 300 μm I.D. All experiments were performed at 25°C.

The carrier liquids were solutions of Tween 60 (polyoxyethylene sorbitan monostearate) (Fluka, Buchs, Switzerland), Triton X-100 (*tert.*-octyl phenyl polyoxyethylene ether) (Fluka), solutions of sodium dodecyl sulphate (SDS) (Lachema, Brno, Czech Republic) and benzyldimethylhexadecylammonium chloride (BDHAC) (Fluka), all in distilled water.

The samples were of two types: (i) porous spherical particles (diameters 3, 5 and 10 μm) (Tessek, Prague, Czech Republic) and (ii) non-porous spherical particles 1.43 μm in diameter (a kind gift from Professor E. sz. Kováts). In most of the experiments we used a model mixture of two porous spherical silicas with nominal diameters of 10 and 5 μm (Tessek) with non-porous silica gel particles with the diameter 1.43 μm. The concentration of each type of particle in the mixture was 10 mg/ml.

The experiment consisted of several steps. Initially, after 3 min of ultrasound stirring, 2–6 μl of sample were injected, with a syringe, through a septum into the channel inlet. After the relaxation time, the flow was switched on and the sample was eluted through the channel to the detector. The relaxation time was calculated (for porous and non-porous particles $\Delta\rho$ = 0.5 and 1.2 g/cm^3), respectively, as

$$t_R = 18\frac{\mu w}{d^2 \Delta\rho g} \quad (1)$$

where μ is viscosity of the carrier liquid, w is the channel width, d is the particle diameter, $\Delta\rho$ is the density difference between the particle and the liquid and g is the gravitational acceleration constant (9.8 m/s^2).

RESULTS AND DISCUSSION

One factor affecting the separation process in the channel is the smoothness and inertness of the channel walls. An uneven wall surface can mechanically disturb the flow which, together with adsorption on the channel bottom, can cause retardation of the particles and artificial dispersion of the peaks. The adsorption was a more important factor because of the relaxation process performed: in order to force the particles to start from the channel bottom, after injection of a sample the flow was stopped for a sufficient time to allow the particles to sediment through the channel width w. We tested unmodified glass plates which are almost perfectly smooth but particles in the vicinity of the glass could be adsorbed on the surface. According to conclusions of Bories *et al.* [15], we deduced that the surfactant in the carrier medium covers the channel wall faster and more stably when the glass is modified. We observed that the unmodified glass plates needed about 1 day to condition whereas silicone oil-modified glass plates gave reproducible results earlier. As deduced from the higher retention ratios and sharper peaks, the best results were obtained using glass plates modified with MS200 silicone oil (Midland Silicones, Barry, UK). This was similar to our observations on the separation of polystyrene latex particles by GFFF [4].

Surfactants are added to the carrier medium to reduce the surface tension that exists between the solid surface of the particles and the carrier liquid, between the particles and the channel walls and between the channel walls and the carrier liquid. We tested solutions of surfactants in the concentration range 0.0005–0.5% because at lower concentrations we did not detect retained peaks and at higher concentrations the solutions were too opaque. The surfactants used were cationic (BDHAC), anionic [SDS, critical micellar concentration (CMC) = 0.24%] and two non-ionic (Tween 60, CMC = 0.005%; Triton X-100, CMC = 0.013%), so in some instances we used surfactants above the CMC. The separation channel then represented a complicated multiphase system [16]. We observed that an increase in surfactant concentration resulted in a slight increase in the retention ratios but in a significant decrease in peak dispersion. We explained this by a decrease in adsorption on the channel walls. Fig. 1 shows the dependence of retention times and peak dispersions on surfactant concentration. It is obvious that the smallest particles (1.43 μm) are mostly affected in this way, probably as they move closer to the channel bottom. The simultaneous increase in density of the surfactant solutions which led to an increase in the buoyant force on the particles was negligible (less than 0.1% for a 0.5% solution of Tween 60).

On the other hand, the retention ratio can be increased by adsorption of a surfactant on the particle surface (a decrease in apparent density and an increase in hydrodynamic size [10]) or by aggregation of the particles. This would explain our observation that small particles (about 3 μm)

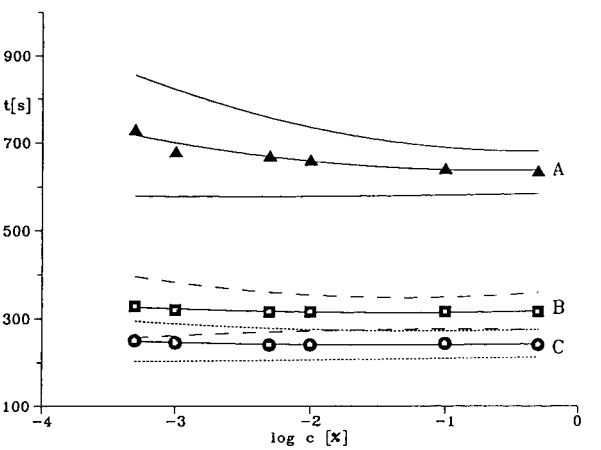

Fig. 1. Dependence of retention times on concentration of Tween 60 in the carrier liquid. In each instance the central curve with symbols shows the retention time of the peak mass centre, and the two lines above and below define the time width of the peak base. The top three curves A (▲) are for 1.43-μm particles, the middle three curves B (□) for 5-μm particles and the bottom three curves C (○) for 10-μm particles. Data were obtained with the model mixture in channel III at a flow-rate of 0.96 ml/min; 2 μl of suspension were injected.

exhibited at low flow-rates the same retention ratio as 10-μm particles. We tried to confirm the presumed aggregation by optical microscopy, trapping a drop of the eluted liquid on a microscope slide, but unfortunately we were not able to distinguish between the primary aggregation in the channel and the secondary aggregation at the liquid drop/air interface.

Pores of the particles influence the apparent density. The porosity of silica gel supports can decrease the apparent density down to 1.5 g/cm^3 [8]. Moreover, the particles can contain gas bubbles not released even after a 6-h sonication [8]. Another consequence of the particle porosity relating to interfacial effects could be higher sensitivity of the porous particles to changes in experimental conditions with respect to the type and concentration of surfactants used. We observed different retention ratios of the same sample in different surfactants, which can be explained by different physico-chemical interactions between the particle surface and the carrier liquid. The surfactant influences the particle–wall interaction (adsorption) and particle–particle interaction (aggregation). We deduced that the former effect results in a shift of the retention ratio (the lower the retention ratio the more intensive is the adsorption) and the latter affects resolution (the poorer the resolution the more intensive is the particle–particle interaction). This is illustrated in Fig. 2, which compares four fractograms obtained in different carrier liquids. The first sharp peak (its left-hand edge retention ratio is 1.5) corresponds to light fragments or microbubbles, the second (clear in D, overlapped with the first in A–C) is the dead volume peak [3]. Based on these observations, we chose 0.1% Tween 60 solution as the best carrier liquid, (Fig. 2A).

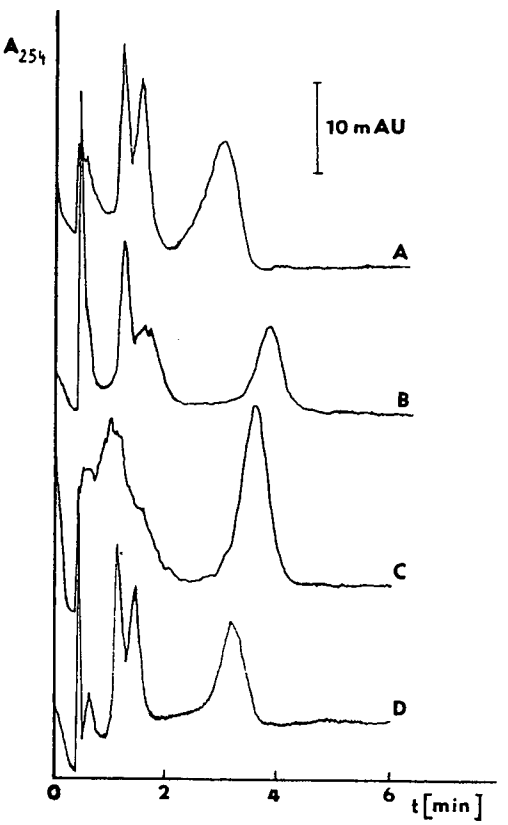

Fig. 2. Comparison of fractogram of the model mixture of silica gel particles (10, 5 and 1.43 μm) in different surfactants (0.1% solutions): (A) Tween 60; (B) SDS; (C) BDHAC; (D) Triton X100. The flow-rate was 0.95 ml/min and 1 μl of the model mixture suspension was injected into channel I.

Fig. 3 compares fractograms obtained under optimized conditions (the carrier liquid is a 0.1% solution of Tween 60 and the channel bottom is modified with MS200 silicone oil) at different flow-rates in channel III. There is an increase in the retention ratio with increasing flow-rate for all three sizes of particles in the mixture. This is

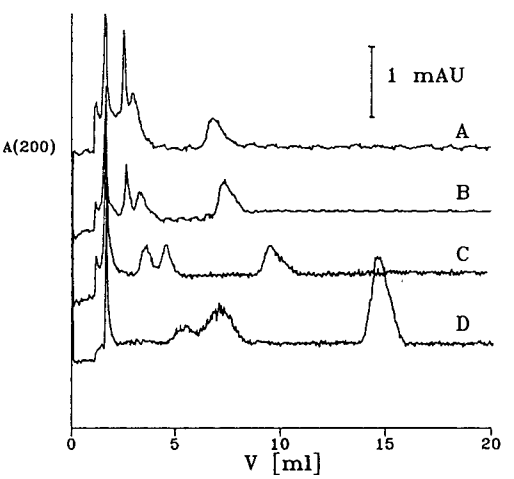

Fig. 3. Fractograms of the model silica mixture at different flow-rates: (A) 2.87; (B) 1.94; (C) 0.96; (D) 0.212 ml/min. A 4-μl volume of the suspension was injected into channel III.

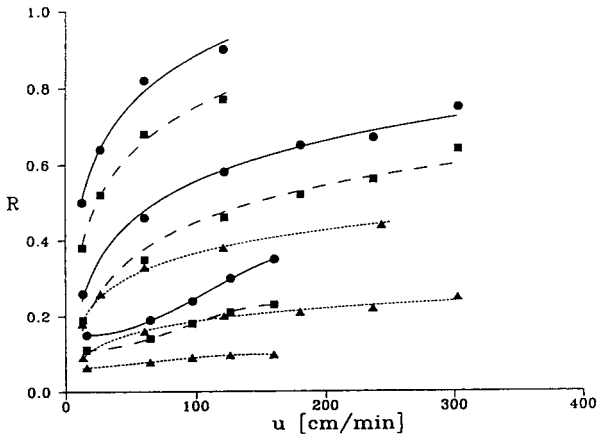

Fig. 4. Dependence of retention ratio R on linear flow velocity u in channels with different heights w (length $l = 80$ cm). Solid lines are for channel IIa ($w = 40$ μm, 0.5 μl injected), dashed lines for channel IIb ($w = 80$ μm, 1 μl injected) and dotted lines for channel IIc ($w = 150$ μm, 2 μl injected). Particle size in the model mixture: ○ = 10 μm; □ = 5 μm; ▲ = 1.43 μm. The carrier liquid was a 0.1% solution of Tween 60.

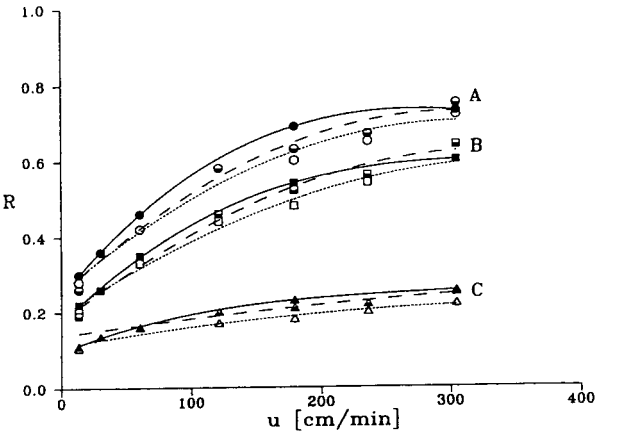

Fig. 5. Dependence of retention ratio R on linear flow velocity u in channels with different lengths l (height $w = 80$ μm). Solid lines (with closed symbols) are for channel I ($l = 36$ cm, 0.5 μl of suspension injected), dotted lines (with open symbols) for channel II ($l = 80$ cm, 1 μl injected) and dashed lines (with half-closed symbols) for channel III ($l = 108$ cm, 2 μL injected). The three curves A (circles) represent silica gel particles of nominal diameter 10 μm in the model mixture, B (squares) those of nominal diameter 5 μm and C (triangles) those of diameter 1.43 μm.

in accordance with the activity of lift forces and a similar increase was observed with all kinds of supports tested. Moreover, the retention ratios increased with a decrease in the channel width w.

Fig. 4 shows the dependences of the retention ratio on the linear velocity for three different channel widths w. One can see that the smallest retention ratios were obtained in the channel with the highest w (150 μm).

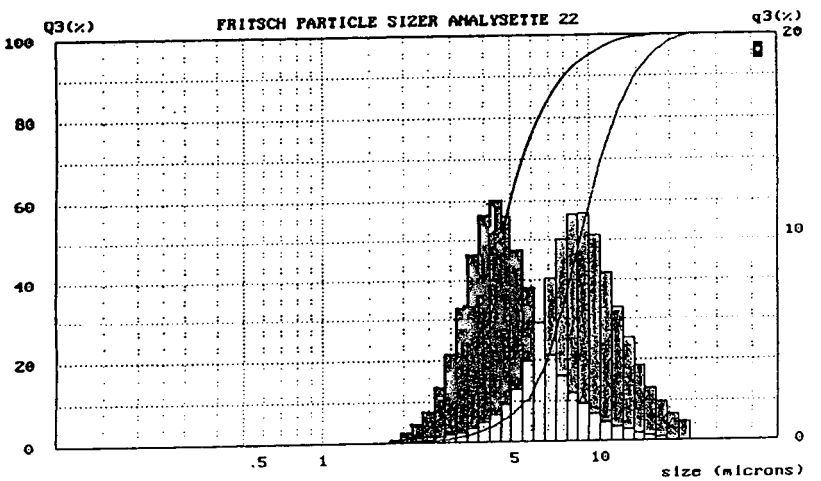

Fig. 6. Size distribution curves of silica gel particles of nominal diameters 5 and 10 μm (in the model mixture) measured on a Fritsch Analysette 22 particle sizer. The black histogram holds for the 5-μm silica and the grey histogram for the 10-μm particles in the model mixture. To distinguish the two histograms, their common part is shown in white. The histograms were obtained separately (not from a mixture) and were overlapped graphically.

Fig. 5 demonstrates that the lift forces acted very rapidly as the retention ratios were almost identical in channels I–III with lengths of 36, 80 and 108 cm, respectively. The plateau on the curves is in qualitative agreement with the lift force function [4].

The peaks in all the fractograms are relatively broad because their dispersions correspond to the size distributions which are relatively broad for silica gel particles (20–50%) compared with, *e.g.*, standard latex particles (usually <2%). This is illustrated in Fig. 6 by two overlapped size distribution histograms of samples that we tested. The histograms were obtained separately by light-scattering measurements on a Fritsch (Idar-Oberstein, Germany) Analysette 22 particle sizer. There is a broad distribution of the two silica gel particles used, which prevent complete separation and also the total resolution of GFFF peaks in fractograms.

CONCLUSIONS

The separation process is influenced by the quality of the channel wall surface and by the quality and concentration of the surfactant used. Under particular experimental conditions, GFFF enables a mixture of silica gel particles to be separated. The GFFF technique is performed with an extremely simple experimental arrangement, in contrast to other FFF techniques (flow FFF, SdFFF). The channel height w is a natural parameter of the separation defining the particle sizes that can be effectively separated.

With respect to the separation mechanism we can conclude that the lift forces drive particles in the vertical equilibrium position δ_F very quickly.

ACKNOWLEDGEMENTS

We thank Professor E. sz. Kováts (Lausanne, Switzerland) for his kind gift of the non-porous monodispersed spherical silica gel. Also we thank Fritsch for kindly measuring the two samples in Fig. 6. The work was supported by the Grant Agency of the Czech Republic grant No. 203/93/0351.

REFERENCES

1 J.C. Giddings and M.N. Myers, *Sep. Sci. Technol.*, 13 (1978) 637.
2 K.D. Caldwell, T.T. Nguyen, M.N. Myers and J.C. Giddings, *Sep. Sci. Technol.*, 14 (1979) 935.
3 J. Pazourek, P. Filip, F. Matulík and J. Chmelík, *Sep. Sci. Technol.*, 28 (1993) 1859.
4 J. Pazourek and J. Chmelík, *Chromatographia*, 35 (1993) 591.
5 J.C. Giddings, M.N. Myers, K.D. Caldwell and J.W. Pav, *J. Chromatogr.*, 185 (1979) 261.
6 S.K. Ratanathanawongs and J.C. Giddings, *J. Chromatogr.*, 467 (1989) 341.
7 J.C. Giddings, M.H. Moon, P.S. Williams and M.N. Myers, *Anal. Chem.*, 63 (1991) 1366.
8 J.C. Giddings and M.H. Moon, *Anal. Chem.*, 63 (1991) 2869.
9 R. Beckett, J. Ho, Y. Jiang and J.C. Giddings, *Langmuir*, 7 (1991) 2040.
10 J. Li and K.D. Caldwell, *Langmuir*, 7 (1991) 2034.
11 H.K. Jones, B.N. Barman and J.C. Giddings, *J. Chromatogr.*, 455 (1988) 1.
12 B.N. Barman and J.C. Giddings, *Langmuir*, 8 (1992) 51.
13 G. Karaiskakis and A. Koliadima, *Chromatographia*, 28 (1989) 31.
14 A. Koliadima and G. Karaiskakis, *J. Chromatogr.*, 517 (1990) 345.
15 C. Bories, P.J.P. Cardot, V. Abramowski, C. Poüs, A. Merino-Dugay and B. Baron, *J. Chromatogr.*, 579 (1992) 143.
16 G.J. Fleer and J. Lyklema, *Macromol. Chem., Macromol. Symp.*, 17 (1988) 39.

Journal of Chromatography A, 660 (1994) 119–129
Elsevier Science B.V., Amsterdam

CHROMSYMP. 2922

Determination of drugs by direct injection of plasma into a biocompatible extraction column based on a protein-entrapped hydrophobic phase

Jörgen Hermansson* and Anders Grahn

ChromTech AB, Box 6056, 129 06 Hägersten (Sweden)

ABSTRACT

Drugs were determined by direct injection of plasma samples into a biocompatible extraction column. The column is based on particles with a biocompatible external surface and a hydrophobic internal surface. The pores of the particles are small enough to exclude the protein molecules; the drug molecules can penetrate the porous particle and are retained on the hydrophobic internal surface. Biocompatibility of the particles was obtained by reaction of the external surface with the human plasma protein α_1-acid glycoprotein. The surface within the pores of the particles contains hydrophobic C_8 or C_{18} groups. The biocompatible extraction column was used in a fully automated system for the determination of ibuprofen, naproxen, propranolol, carbamazepine and phenytoin in plasma. No pressure increase was observed during the analysis of several hundred plasma samples. Plasma concentrations of propranolol in the range 4.5–125 ng/ml were determined with a precision (R.S.D.) of 0.75–1.8%. Linear calibration graphs were observed for the five drugs, and correlation coefficients of 1.0000 were obtained for four of the five model compounds.

INTRODUCTION

The determination of drugs, metabolites and endogenous compounds in biological fluids usually involves an isolation procedure prior to the chromatographic step. The most frequently used procedures are liquid–liquid extraction, protein precipitation and off-line solid-phase extraction with disposable extraction columns. All isolation methods are time consuming and introduce errors in the assay. The more manipulations the sample undergo prior to the quantification step, the lower are the accuracy and precision obtained. Therefore, it is advantageous to inject the sample directly into a liquid chromatographic system without off-line isolation procedures.

Different approaches have been used for direct injection of biological fluids [1,2]. The sample can be injected directly on to the analytical column [3–5], or by using a precolumn in the foreflush mode according to Arvidsson and co-workers [6,7] or in the backflush mode [8,9]. An early method describing the direct injection approach was published in 1978 [3]; Standard columns were utilized and very small sample volumes were injected, *i.e.*, 1–3 μl. A special type of column for the direct injection of biological fluids was developed by Hagestam and Pinkerton [4]; the surface chemistry within the pores is different to that on the external surface of silica particles.

One limitation with these types of columns is that the content of organic solvent that can be used in the mobile phase is limited. Concentrations higher than 15–20% precipitate plasma proteins, especially albumin, which also is present at a high concentration. Other similar phases have also been used [10]. By using the approach with a precolumn in the backflush mode, the compound of interest is extracted from the protein-containing biological sample and the

* Corresponding author.

0021-9673/94/$07.00 © 1994 Elsevier Science B.V. All rights reserved
SSDI 0021-9673(93)E0888-2

precolumn is washed with a buffer. After washing, the solute is eluted from the extraction column on to the analytical column by pumping a mobile phase containing an organic solvent. As the plasma proteins do not come into contact with the organic modifier, there are no limitations concerning the concentration of organic modifier that can be used in this approach.

This paper describes a biocompatible trapping column that can be used as an extraction column for the direct injection of protein-containing biological fluids. The column is packed with silica particles having a biocompatible external surface and a hydrophobic surface within the pores. The external surface of the particles is covered with the human plasma protein α_1-acid glycoprotein (AGP), which makes the external surface of the particles compatible with the plasma proteins. The pores of the silica are small enough to exclude the plasma proteins.

EXPERIMENTAL

Chemicals and reagents

Methanol and acetonitrile of, HPLC grade were obtained from Lab-Scan (Dublin, Ireland). The drug compounds were gifts from drug companies. All other chemicals were of analytical-reagent grade.

Apparatus

The liquid chromatograph consisted of an LKB 2151 pump (Pharmacia–LKB Biotechnology, Uppsala, Sweden) and a Kontron Model 420 pump (Tegimenta, Rotkreutz, Swizerland), a Kontron Model 360 autosampler, equipped with 10- or 50-μl loops, or a manual Valco injector (Vici AG Valco, Schenkon, Swizerland), a C6W six-port switching valve with an electric acuator (Vici AG Valco), a Shimadzu (Kyoto, Japan) RF 535 fluorimeter and a Spectra 100 variable-wavelength UV detector (Spectra-Physics, San Jose, CA, USA). All experimental data were collected and analysed on a Kontron (Eching/Munich, Germany) 450 MT2 data system. This system also controlled the switching valve and the autosampler. The LKB 2151 pump (Pharmacia–LKB Biotechnology) was used for continuous pressure registration on both the analytical and the extraction column. The pressure was recorded with an LKB 2210 two channel recorder.

The following CT-sil columns (ChromTech, Norsborg, Sweden) were used in the study: CT-sil C_{18}, 100 × 4.6 mm I.D., 5 μm; CT-sil C_{18}, 150 × 4.6 mm I.D., 5 μm; and CT-sil C_8, 100 × 4.6 mm I.D., 5 μm. CT-sil C_8 or C_{18} guard columns (10 × 3.0 mm I.D., 5 μm) were used. The extraction columns were BioTrap Amine (for extraction of amines) and BioTrap Acid (for extraction of acids and non-protolytes), 10 × 3.0 mm I.D., from ChromTech. The filter holder in PEEK and the filter, used in front of the extraction column, were obtained from ChromTech.

Chromatographic system

On-line filter. Fig. 1A and B show schematic diagrams of the chromatographic systems used. The filter is used in the fully automated system (Fig. 1B) when the samples are injected with an autosampler. The filter is coupled between the injection valve and the extraction column in order to remove particles from the biological samples. The on-line filter is inserted in a special PEEK holder (ChromTech).

Extraction column. In the manual method the extraction column is a BioTrap Amine (for extraction of amines) or a BioTrap Acid (for extraction of acids or non-protolytes) column (10 × 3.0 mm I.D.). The column is coupled as a loop to a conventional loop injector as demonstrated in Fig. 1A. A volume of 1.5–2 ml of a buffer is injected on to the extraction column followed by an exact volume of a plasma sample. The buffer used to equilibrate the extraction column prior to injection differs for the different drugs. The methods for the different compounds are given in detail in the captions to the figures. After injection of the sample, the extraction column is washed with *ca.* 1.5 ml of the same buffer as was used for equilibration of the column prior to sample injection.

In the automated method, the extraction column can be coupled to a six-port switching valve with an electric actuator and an autosampler as demonstrated in Fig. 1B. The equilibration and the washing volumes are the same as for manual

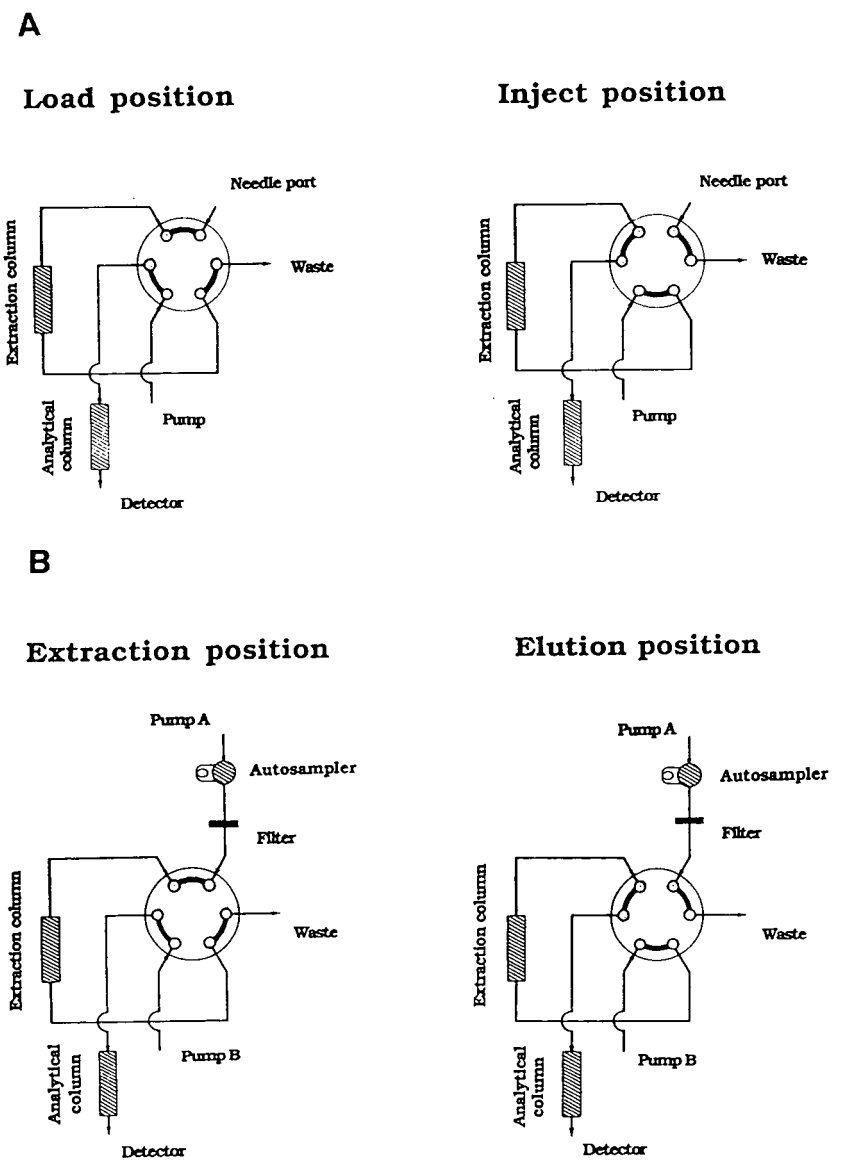

Fig. 1. (A) Schematic illustration of the chromatographic system used for manual injection with the BioTrap column coupled as a loop in a conventional injector. The plasma sample is injected in the load position. The plasma proteins are eluted by injection of buffer whereas the drug compound is enriched within the pores of the particles. After switching the valve to the inject position the sample is eluted (backflushing of the extraction column) on to the analytical column. (B) Schematic illustration of the fully automated system. The plasma sample is injected by an autosampler.

operation (see also the captions to the figures for the methods for the different drugs).

Guard column. The guard column is used to protect the analytical column from particles and endogenous compounds which are bound to the analytical column with high affinity. The guard column must be exchanged before it is overloaded with endogenous compounds otherwise these compounds are transported to the analytical column.

Calibration graphs, recovery and reproducibility studies

Calibration graphs were prepared by adding known amounts of the drug compounds to an exact volume of blank plasma. These samples were also used for the reproducibility studies. To evaluate the absolute recovery, known amounts of the different drug compounds were added to either blank plasma or to the mobile phase for the analytical column. The plasma samples were injected on to the extraction column and the peak areas were calculated. The samples dissolved in the mobile phase were injected directly on to the analytical column and the peak areas were determined. The absolute recovery was calculated by dividing the peak area obtained for the plasma samples with that obtained for the samples dissolved in the mobile phase and injected directly on to the analytical column. Plasma samples from patients and blank plasma were stored at −20°C.

Detailed descriptions of the conditions used for the determination of ibuprofen, naproxen, propranolol, phenytoin and carbamazepine in human plasma are given in the captions to the figures.

RESULTS AND DISCUSSION

The chromatographic systems described under Experimental and in Fig. 1A and B have been used for the determination of drugs in human plasma samples. The determination of drugs, metabolites and endogenous compounds in protein-containing biological fluids by direct injection of the sample into the liquid chromatographic system is very complicated owing to the high concentration of proteins and the large number of endogenous compounds present in this kind of sample. A hydrophobic silica such as a C_8 or a C_{18} matrix is not wetted at all when mixed with plasma, nor are the plasma proteins compatible with such a silica [6,11]. Particles with a biocompatible external surface that is wetted by the highly aqueous plasma sample have been obtained by covering the external surface of silica particles with AGP, which is a hydrophilic human plasma protein with a molecular mass of about 40 000. This protein was introduced in chromatography by Hermansson, who developed a chiral column based on the use of AGP as a chiral selector [12,13]. The protein is a glycoprotein containing five carbohydrate units constituting *ca.* 45% of the molecular mass. This protein is extremely stable in both native and immobilized forms. Immobilized AGP tolerates pure organic solvents such as alcohols and nitriles and can be used at extreme temperatures without being denatured [13]. The extraction column can be used with the mobile phases normally used for standard reversed-phase columns without affecting the performance of the extraction column.

Extraction column

Five different model compounds of different character were used, two carboxylic acids, the non-steroidal antiinflammatory drugs (NSAIDs) ibuprofen and naproxen, the β-blocker propranolol, an amine, and the weak acids phenytoin and carbamazepine, two antiepileptic drugs. The extraction column can be used in two different ways. The simplest way is to couple the column as a loop in a conventional loop injector according to Fig. 1A. It is also possible to fully automate the system using an autosampler and a switching valve as demonstrated in Fig. 1B. The sample is injected on to the extraction column, normally in volumes between 10 and 50 μl and sometimes larger, *e.g.*, 100 μl. Carboxylic acids and also weaker acids are extracted at a pH 2.1–6. Basic drugs are extracted at pH ≤7.5, normally between pH 6 and 7.5. Higher pH cannot be used because the column is silica based. The pH to be used during extraction of a drug compound depends on the pK_a value of the drug and how the recoveries of the endogenous compounds are affected by the pH.

After injection of the serum or plasma sample on to the extraction column, the plasma proteins are washed out by pumping 1.1–2 ml of extraction mobile phase. After washing, the sample is eluted from the extraction column with the mobile phase for the analytical column in the backflush mode, by switching the manual injector to the inject position or by switching the six-port valve (see Fig. 1A and B). The complete methods for the different drug compounds are

given in detail under Experimental and in the captions to the figures.

Two different extraction columns were used, BioTrap Acid C_{18} (for extraction of acidic and non-protolytic drugs) and BioTrap Amine C_{18} (for extraction of basic compounds). The external surfaces of the two extraction columns are identical, but the internal surface of the BioTrap Amine column is end-capped in order to minimize the band broadening in the extraction column. The extraction column has the dimensions 10×3.0 mm I.D., which means that the amount of packing material in the column is small. The reasons for using a short extraction column are to shorten the washing time and to shorten the time for re-equilibration with the extraction buffer, after the backflushing of the extraction column with the mobile phase containing an organic modifier. This means that the total time of analysis, including extraction and analysis, can be short.

Plasma and serum contain a very large number of endogenous compounds of different kinds, both low-molecular-mass compounds of different hydrophobicity and macromolecules. The endogenous compounds, drugs and metabolites are retained on the extraction column and the amount extracted is affected by the affinity to the plasma proteins and the affinity to the internal surface of the extraction column. Backflushing the extraction column with a mobile phase containing an organic modifier elutes the compound of interest together with endogenous compounds. Some endogenous compounds in plasma are highly retained on the extraction column even when the column is eluted with a mobile phase containing a high concentration of organic modifier. This means that after injection of a certain amount of samples the extraction column must be replaced. The extraction column will be deactivated by adsorption of endogenous compounds with high affinity and they are not completely washed out on backflushing the column. This gives a broadening of the peaks on the analytical column because the sample is spread out in the extraction column, giving a broad starting zone on the analytical column. The number of samples that can be injected before replacement of the extraction cartridge is necessary depends on the mobile phases used in the extraction and analytical columns, and also the volume of serum or plasma that has been injected. By injection of <20 μl of plasma samples it is possible to inject several hundred samples before replacement of the small extraction cartridge. This means a low cost per sample compared with other isolation procedures such as the use of disposable off-line extraction cartridges and liquid–liquid extraction, both of which are very time consuming procedures.

The described method can also be fully automated. One of the major problems with direct injection of protein-rich samples is that the proteins precipitate in the column, either in the filter or when they come into contact with the hydrophobic packing material [6,11]. It is well known that sintered stainless-steel frits precipitate plasma proteins [6]. This results in increased pressure on repeated injections of this kind of sample.

Another problem is the decrease in the separation efficiency of the analytical column because endogenous compounds are transferred to and adsorbed on the analytical column. This can be avoided by changing the guard column coupled in front of the analytical column before it is overloaded with endogenous compounds.

Table I demonstrates how the pressure over the extraction column and the analytical column is affected by the injection of 465 plasma samples (10 μl) containing ibuprofen. The effects on the number of theoretical plates, the retention time and the peak symmetry are also included in

TABLE I

STABILITY OF THE SYSTEM

Analyte: ibuprofen (4.99 μg/ml) injection volume: 10 μl.

Parameter	Sample No.	
	1	465
Pressure, analytical column (bar)	74	73
Pressure, extraction column (bar)	0	0
t_r (min)	3.63	3.50
N	4004	3804
Asymmetry factor	1.27	1.12

Table I. As can be seen, no pressure increase was obtained on the extraction column and the analytical column after injection of 465 plasma samples, nor were the other parameters significantly affected. It can also be mentioned that no guard column was used in front of the analytical column during this experiment.

It was observed that the ibuprofen peak shape was affected to some extent after 200–300 plasma samples. Therefore, the analytical column was backflushed once for about 2–5 min during the analysis of the 465 plasma samples. However, during routine use it is recommended to use a guard column which is exchanged before it is overloaded with endogenous compounds.

During this study the samples were analysed with the fully automated system as shown in Fig. 1B. After injection of the 465 plasma samples, six standard samples, in the therapeutic concentration range, between 0.52 and 40.4 μg/ml, were injected to test whether the calibration graph was linear. The linear regression equation was $y = 0.2016 + 3.6411\ x$ (y = peak area; x = concentration in μg/ml) and the correlation coefficient was 1.000, which clearly demonstrates that the extraction column had not deteriorated and gave a constant recovery over the whole concentration range.

Recovery

The retention of a solute on a reversed-phase extraction column can be expressed by

$$k'_{(s)} = qD_{(s)} \quad (1)$$

where q is the phase ratio and $D_{(s)}$ is the distribution ratio of the solute between the solid and the mobile phase. However, injection of plasma samples containing large amounts of proteins, such as albumin and AGP, involved in the binding of drugs and endogenous compounds affects the chromatographic properties of the low-molecular-mass solutes. Albumin is the drug-binding protein that is present in plasma at the highest concentration and it is involved in the binding of many different types of drugs. Albumin has a molecular mass of about 66 000 with the dimensions 150 × 38 Å [14]. The Stokes radius has been determined to be 33.4 Å [14], which means that a pore with a diameter of about 60 Å will exclude the albumin molecules from the internal surface of the particles. AGP has a larger Stokes radius than albumin. If a certain solute (S) is bound to only one binding site on albumin (P), and if the protein is excluded from the pores and the binding of the protein to the external surface of the particles in the extraction column can be neglected, the distribution ratio, D_s, of the solute (S) can be expressed by

$$D_S = [SA_S]/([S] + [PS]) \quad (2)$$

where [S] and [PS] are the concentrations of the free drug and the drug–protein complex, respectively, and $[SA_S]$ is the concentration of the drug bound to the binding site, A_S, on the internal surface of the particles in the extraction column.

An expression for the retention of a solute in a sample containing proteins can be derived from eqns. 1 and 2:

$$k'_{(S,P)} = k'_{(S)}/(1 + [PS]/[S]) \quad (3)$$

where [PS]/[S] is the drug–protein binding ratio and $k'_{(S)}$ is the retention of the solute (S) in the absence of proteins. From eqn. 3, it can be seen that the retention of the solute in the sample zone decreases on increasing the drug–protein binding ratio, [PS]/[S]. This means that the sample migrates a longer distance in the extraction column if the sample contains proteins. If a short extraction column is used, a high recovery will be obtained if the drug–protein binding ratio is not too high and/or if an extraction column with high hydrophobicity is used.

In the chiral analysis of enantiomers in plasma, it is very important to have a high recovery in the isolation step independently of whether liquid–liquid extraction, precipitation of plasma proteins or an off-line or on-line extraction column are used. As enantiomers are bound stereoselectively to the plasma proteins, *i.e.*, the [PS]/[S] ratio differs for enantiomers, the retention, $k'_{(S,P)}$, according to eqn. 3 for the enantiomers is different. From this it follows that the concentration ratio between enantiomers, determined by the chromatographic method, can

be affected by the isolation step if an isolation procedure giving low recovery is used. The enantiomer with the highest affinity to the plasma proteins gives the lowest recovery.

The absolute recoveries of the drug compounds were determined by comparing the peak areas of three spiked plasma samples and three reference samples at different concentrations. The reference samples were injected directly on to the analytical column and the spiked plasma samples were injected on to the extraction column coupled to the analytical column through the switching valve. The results are summarized in Table II. The absolute recoveries vary between 78 and 96% for the five different drug compounds. The lowest recovery was obtained for propranolol because it is extracted at pH 7, which means that it is fully ionized. Using a higher pH for extraction increases the recovery. However, a silica-based column cannot be used at such a high pH that reduces the charge on the propranolol molecules ($pK_a = 9.5$).

The reproducibility of the recovery for three different extraction columns, produced from three different batches of packing material, was also tested using ibuprofen as a model compound, and a mean recovery of 96.2% was obtained with a relative standard deviation (R.S.D.) of 2.0%. When determining the absolute recovery it is very important to be sure that the reference sample is not adsorbed on the walls of the glassware, plastic tubes or containers used for the reference samples. The adsorption of a compound on the walls of a vial or other container depends on the nature of the material in the container, the nature of the compound and the solvent used to dissolve the compound. For example, when the propranolol reference sample was dissolved in phosphate buffer (pH 7.4), recoveries between 110 and 130% were obtained. This was the result of adsorption of the relatively hydrophobic propranolol on the polypropylene vials. Using such a reference sample and such vials gives a too small peak area of the reference sample and a too high a recovery. By dissolving propranolol in the mobile phase containing 33% acetonitrile this problem with adsorption on the vials was avoided. No indications of adsorption of propranolol on the polypropylene vials from the plasma samples were observed. This is most likely the result of the protein binding and the presence of endogenous compounds in the plasma sample which compete with the drug for binding to the walls of the vials.

Precision

The intra- and inter-day variations were determined for the various compounds and the results of the former studies are summarized in Table III. The studies were performed in a concentration range normally obtained after administration of a single dose of the different drugs, *i.e.*, the therapeutic concentrations are higher. It can be seen that a very good precision can be obtained even at the lowest concentration levels studied. Table IV summarizes the inter-day variations. This study was performed in the same concentration interval as in the intra-day study. The inter-day variation was determined at

TABLE II

ABSOLUTE RECOVERIES FROM PLASMA

Compound	Injection volume (μl)	Concentration (μg/ml)	Recovery (%)	R.S.D. (%)[a]
Carbamazepine[b]	50	8.1	89.7	1.2
Phenytoin[b]	50	13.3	84.1	2.1
Propranolol[c]	50	$11.6 \cdot 10^{-3}$	77.8	4.5
Ibuprofen[b]	10	12.5	96.0	1.5

[a] $n = 3$.
[b] BioTrap Acid extraction column (see Experimental).
[c] BioTrap Amine extraction column (see Experimental).

TABLE III

INTRA-DAY VARIATIONS

Compound	Concentration (μg/ml)	R.S.D. (%)[a]
Ibuprofen	0.52	6.7
	3.11	2.0
	40.4	0.96
Naproxen	1.05	2.80
	5.27	0.44
	10.5	1.18
	21.1	0.52
	42.1	0.62
Propranolol	$4.45 \cdot 10^{-3}$	1.8
	$8.92 \cdot 10^{-3}$	1.0
	$22.3 \cdot 10^{-3}$	0.75
	$53.5 \cdot 10^{-3}$	1.54
	$89.2 \cdot 10^{-3}$	1.40
	$124.8 \cdot 10^{-3}$	1.54
Phenytoin	1.76	2.92
	13.5	1.03
	30.0	0.92
Carbamazepine	2.05	0.73
	5.13	1.00
	10.3	0.31
	15.2	0.54
	20.5	0.49

[a] $n = 6$.

two different concentrations of each drug. As can be seen from Table IV, a high inter-day reproducibility was obtained for the different drugs.

TABLE IV

INTER-DAY VARIATIONS

Compound	Concentration (μg/ml)	R.S.D. (%)	n
Ibuprofen	3.24	3.00	6
	14.9	1.92	6
Propranolol	$4.11 \cdot 10^{-3}$	4.58	6
	$36.6 \cdot 10^{-3}$	2.36	6
Phenytoin	7.63	2.49	5
	23.8	1.21	5
Carbamazepine	5.27	1.28	5
	15.8	1.42	5

Determinations

Manual isolation procedures such as liquid–liquid extraction, the use of off-line extraction cartridges or precipitation of plasma proteins followed by centrifugation are very time consuming. This type of isolation procedure also introduces errors in the determination that decrease both the accuracy and precision. Therefore, a method that requires a minimum of manipulations of the sample prior to the quantification step is to be preferred. This is of special importance, of course, in large clinical projects where several thousand plasma samples must be analysed with high precision and accuracy.

Ibuprofen. Ibuprofen was determined using the method described under Experimental and in Fig. 1. A representative chromatogram of a plasma sample from a patient who had received a single oral dose of 200 mg of ibuprofen is demonstrated in Fig. 2. No disturbing endogenous peaks were detected, owing to the high detection selectivity obtained with fluorimetric detection. The maximum sensitivity was obtained using an excitation wavelength of 227 nm and an emission wavelength of 555 nm. However, at high drug concentrations these wavelengths gave too high a response and therefore wavelengths of 225 and 535 nm, respectively, were used. Plasma concentration *versus* time curves for two patients are presented in Fig. 3. Ibuprofen was also determined using the manual method, by coupling the extraction column to a conventional loop injector according to Fig. 1A, which works well when the number of samples is so small that automation is unnecessary.

Naproxen. Naproxen is a well known NSAID and can easily be determined using the described method with either UV or fluorimetric detection. Fig. 4 shows a chromatogram of naproxen using UV detection at 328 nm. No disturbing endogenous compounds are detected, because a high detection selectivity is obtained using this wavelength. Using fluorimetric detection with an exitation wavelength of the 230 nm and an emission wavelength of 350 nm a very high detection selectivity and a very high sensitivity can be obtained. Using UV detection at 328 nm it is necessary to inject about 50 μl of sample. By using fluorimetric detection and if the fluorime-

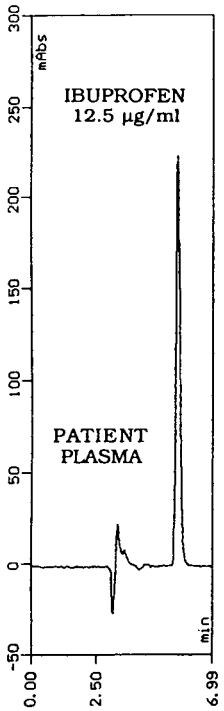

Fig. 2. Isolation of ibuprofen from human plasma after administration of a single oral dose of 200 mg. Chromatographic conditions: injection volume, 10 μl; extraction column, BioTrap Acid C_{18} (10 × 3.0 mm I.D.); extraction buffer, 0.20 *M* phosphate buffer (pH 2.1); flow-rate, 0.55 ml/min; extraction position, 2 min; analytical column, CT-sil C_{18} (100 × 4.6 mm I.D., 5 μm) equipped with a CT-sil C_{18} guard column (10 × 3.0 mm I.D., 5 μm); mobile phase, methanol–82 m*M* phosphate buffer (pH 6.0) (65:35); flow-rate, 1.0 ml/min; elution position, 2 min; fluorimetric detection (exitation wavelength 225 nm, emission wavelength 535 nm).

ter is operated in the low-sensitivity mode, 1 μl can be injected. Such small volumes are difficult to handle with conventional autosamplers. In order to obtain an optimum method for naproxen using fluorimetric detection, the excitation and/or the emission wavelengths must be adjusted to decrease the sensitivity so that 10-μl plasma samples can be injected.

Propranolol. Propranolol was extracted from plasma samples using a BioTrap Amine C_{18} column and a pH of the extraction mobile phase of 7. This is not the optimum pH for extraction as propranolol has a pK_a value of >9, which means that it is fully protonated at pH 7.

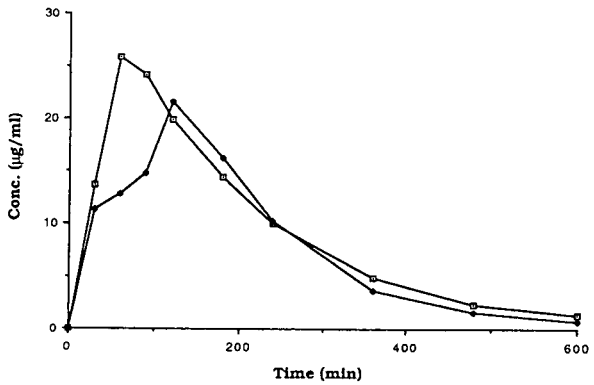

Fig. 3. Plasma concentration *versus* time curves for ibuprofen in samples from two patients after administration of a 200-mg single oral dose.

However, a recovery of about 80% was obtained despite the low extraction pH. Propranolol was detected using fluorescence detection with an excitation wavelength of 200 nm and an emission wavelength of 340 nm. This gives a high detection selectivity and a high sensitivity, making possible the determination of propranolol in

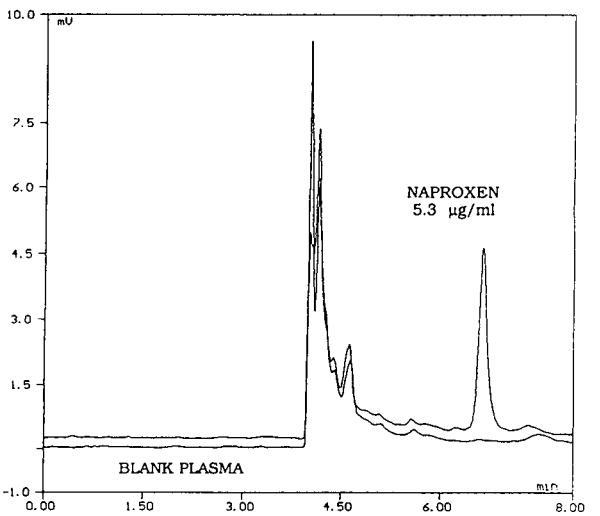

Fig. 4. Isolation of naproxen from spiked human plasma. Chromatographic conditions: injection volume, 50 μl; extraction column, BioTrap Acid C_{18} (10 × 3.0 mm I.D.); extraction buffer, 0.20 *M* phosphate buffer (pH 2.1); flow-rate, 0.55 ml/min; extraction position 3 min; analytical column, CT-sil C_{18} (100 × 4.6 mm I.D., 5 μm); mobile phase, methanol–0.12 *M* phosphate buffer (pH 3.0) (65:35); flow-rate, 1.0 ml/min; elution position, 4 min; UV detection at 328 nm.

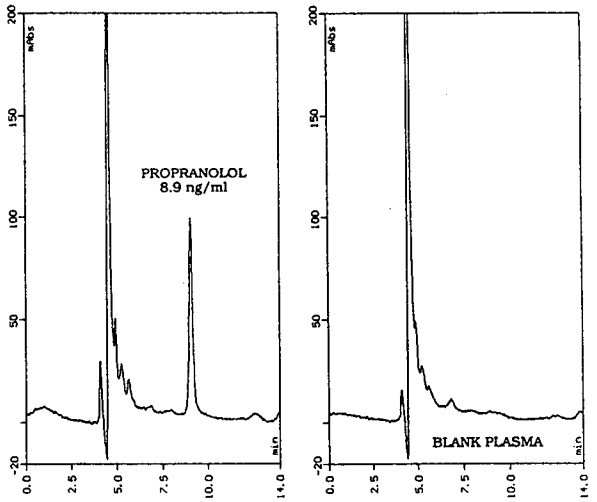

Fig. 5. Isolation of propranolol from spiked human plasma. Chromatographic conditions: injection volume, 50 μl; extraction column, BioTrap Amine C_{18} (10 × 3.0 mm I.D.); extraction buffer, 48 m*M* phosphate buffer (pH 7.0); flow-rate, 0.55 ml/min; extraction position, 3 min; analytical column, CT-sil C_8 (100 × 4.6 mm I.D., 5 μm); mobile phase, acetonitrile–0.12 *M* phosphate buffer (pH 3.0) (28:72); flow-rate, 1.0 ml/min; elution position, 6 min; fluorimetric detection (excitation wavelength 220 nm, emission wavelength 340 nm).

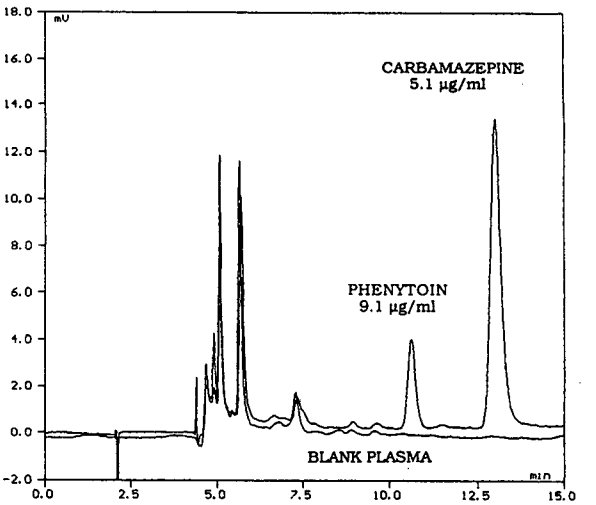

Fig. 6. Isolation of phenytoin and carbamazepine from spiked human plasma. Chromatographic conditions: injection volume, 50 μl; extraction column, BioTrap Acid C_{18} (10 × 3.0 mm I.D.); extraction buffer, 82 m*M* phosphate buffer (pH 6.0); flow-rate, 0.55 ml/min; extraction position, 3 min; analytical column, CT-sil C_{18})150 × 4.6 mm I.D., 5 μm) equipped with a CT-sil C_{18} guard column (10 × 3.0 mm I.D., 5 μm); mobile phase, methanol–82 m*M* phosphate buffer (pH 6.0) (50:50); flow-rate, 1.0 ml/min; elution position, 6 min; UV detection at 254 nm.

plasma samples after administration of a single oral dose of about 40 mg of propranolol hydrochloride. Fig. 5 shows representative chromatograms of blank plasma and propranolol in a spiked human plasma sample using the described method.

Phenytoin and carbamazepine. The antiepileptic drugs phenytoin and carbamazepine, at therapeutic concentrations, can be determined simultaneously by the described method using UV detection at 254 nm, a BioTrap Acid C_{18} column for extraction and injection of 50 μl of plasma. A chromatogram is presented in Fig. 6 together with that for a blank plasma sample. The sensitivity obtained at 254 nm is good enough to detect carbamazepine in the therapeutic concentration range. Detection of carbamazepine at 285 nm gives about a 90–100% higher sensitivity than at 254 nm, which means that it is sufficient to inject only 10 μl of plasma. By using this method the carbamazepine concentrations in several hundred of plasma samples have been determined without disturbances. This method is also rapid, with a retention time of 5.7 min for carbamazepine. It has been observed that by using an extraction mobile phase with a pH of 2.1 the system was more stable compared with a pH of 6. However, more endogenous compounds were detected using pH 2.1.

Calibration graphs

Calibration graphs in the therapeutic concentration range were obtained for all the drug compounds studied. The slopes and the intercepts, with the confidence limits at $P = 0.05$, of the linear regression equations are presented in Table V together with the correlation coefficients. Correlation coefficients of 1.0000 were obtained for four of the five model compounds. The calibration graphs cover both sub-therapeutic and therapeutic concentration ranges.

CONCLUSIONS

A biocompatible extraction column has been developed. The internal surface of the particles

TABLE V

CALIBRATION GRAPHS: LINEAR REGRESSION ANALYSIS

Compound	Concentration interval (μg/ml)	n^a	Slope and confidence limits ($P = 0.05$)	Intercept	Correlation coefficient
Ibuprofen	0.52–40.4	6	3.6411 ± 0.0458	0.2016 ± 1.2305	1.0000
Naproxen[b]	1.05–42.1	5	0.1216 ± 0.0010	0.0026 ± 1.5342	1.0000
Phenytoin	4.56–30.0	5	0.0907 ± 0.0019	0.0047 ± 1.8504	0.9999
Carbamazepine[c]	2.05–20.5	5	0.6671 ± 0.0079	−0.0204 ± 1.7896	1.0000
Propranolol	$(4.5–125) \times 10^{-3}$	6	2.4981 ± 0.0165	−0.0885 ± 1.3555	1.0000

[a] Number of calibration points.
[b] UV detection at 328 nm, 50 μl injected.
[c] UV detection at 254 nm, 50 μl injected.

is hydrophobic as it is covered by alkyl chains of different length, whereas the external surface is covered with the human plasma protein AGP in order to make the surface compatible with the plasma proteins. Acidic and non-protolytic samples are extracted using a BioTrap Acid C_{18} column, whereas basic drugs are extracted using a BioTrap Amine C_{18} column. Several hundred plasma samples can be injected without a pressure increase or affecting the chromatographic properties of the column. The intra- and interday precisions are high and calibration graphs with excellent linearity were obtained. A correlation coefficient of 1.0000 was obtained for four of the five model compounds.

REFERENCES

1 D. Westerlund, *Chromatograhia*, 24 (1987) 155.
2 T.C. Pinkerton, *J. Chromatogr.*, 544 (1991) 12.
3 D.J. Popowitch, E.T. Batts and C.J. Lancaster, *J. Liq. Chromatogr.*, 1 (1978) 469.
4 I.H. Hagestam and T.C. Pinkerton, *Anal. Chem.*, 57 (1985) 1757.
5 H. Yoshida, I. Morita, G. Tamai, T. Masujima, T. Tsuru, N. Takai and H. Imai, *Chromatographia*, 19 (1984) 466.
6 T. Arvidsson, K.-G. Wahlund and N. Daoud, *J. Chromatogr.*, 317 (1984) 213.
7 N. Daoud, T. Avidsson and K.-G. Wahlund, *J. Pharm. Biomed. Ana.*, 4 (1986) 253.
8 W. Roth, K. Beschke, R. Jauch, A. Zimmer and F.W. Koss, *J. Chromatogr.*, 222 (1981) 13.
9 P.O. Edlund and D. Westerlund, *J. Pharm. Biomed. Anal.*, 2 (1984) 315.
10 J. Haginaka and J. Wakai, *Chromatographia*, 29 (1990) 223.
11 M.T.W. Hearn, *Adv. Chromatogr.*, 20 (1982) 4.
12 J. Hermansson and G. Schill, in P.A. Brown and R.A. Hartwick (Editors), *High Performance Liquid Chromatography (Monographs on Analytical Chemistry Series)*, Wiley-Interscience, New York, 1988, pp. 337–374.
13 J. Hermansson, *Trends Anal. chem.*, 8 (1989) 251; and references cited therein.
14 T. Peters, Jr., in F. Putnam, (Editor), *The Plasma Proteins*, Academic Press, New York, 1975, p. 146.

Journal of Chromatography A, 660 (1994) 131–136
Elsevier Science B.V., Amsterdam

CHROMSYMP. 2961

Polytrifluorostyrene-coated silica as a packing for column liquid chromatography

A.D. Kataev*, V.V. Saburov, O.A. Reznikova, D.V. Kapustin and V.P. Zubov

Laboratory of Polymers for Biology, Shemyakin and Ovchinnikov Institute of Bioorganic Chemistry, Russian Academy of Sciences, Miklukho-Maklaya 16/10, 117871 Moscow (Russian Federation)

ABSTRACT

A reversed-phase hydrolytically stable packing material prepared by chemisorption of a trifluorostyrene-containing copolymer on to the surface of porous silica was tested by high-performance liquid chromatography of various aromatic compounds. It was found that the polytrifluorostyrene (PTFS) phase has an intermediate adsorption activity between those of polytetrafluoroethylene and polystyrene phases. A high selectivity of PTFS-coated silica in the separation of haloaryl compounds was observed. Wide-pore silica coated with PTFS was found to give an efficient resolution of peptides and proteins.

INTRODUCTION

The great expansion of reversed-phase high-performance liquid chromatography (RP-HPLC) has been largely the result of the development of new stationary phases and recently some aspects of support materials and their bonded stationary phases have been reviewed in a special issue of this journal [1]. At present there are three general approaches to the synthesis of adsorbents for reversed-phase chromatography: polymerization of monomers (such as styrene and tetrafluoroethylene) and the use of polymer particles with appropriate pore size and diameter as adsorbents; surface modification of silica by low-molecular-mass substances (such as alkyl- and fluoroalkylsilanes); and modification of packing materials by coating with thin layers of polymers. Polymeric sorbents are compressible under pressure and frequently change their bead volumes on replacement of eluents, so that their application in HPLC is restricted. Silica-based stationary phases are still the most widely used sorbents in HPLC owing to their mechanical stability and availability in a wide range of pore sizes and particle diameters. Polymer-coated silicas are promising materials having improved pH stability over bonded silica packings [2–4]. This is assumed to be caused by multi-point attachment of the polymer to the silica surface [2].

Adsorbents for RP-HPLC based on fluorine-containing substances are attractive owing to their high chemical stability and their useful chromatographic properties, and they have been used for the separation of low-molecular-mass solvents and biopolymers [5]. Recently, it was shown that silicas coated with PTFE are very useful for the separation of biomolecules such as proteins, peptides and nucleic acids [6,7]. These sorbents, however, do not allow the attachment of some specific ligands and groups that could be useful for certain separation tasks. To overcome these disadvantages of PTFE-silica sorbents, efforts have been made to modify the silica by incorporating trifluorostyrene chains [8] using the approach of chemical binding of copolymers with active functional groups on to the silica surface [2].

This paper describes the preparation of polytrifluorostyrene-coated silica by binding a copolymer of α,β,β-trifluorostyrene and vinyl-

* Corresponding author.

0021-9673/94/$07.00 © 1994 Elsevier Science B.V. All rights reserved
SSDI 0021-9673(93)E1106-A

methyldiethoxysilane on to the silica surface, some aspects of this procedure and the chromatographic properties of the column packing obtained in comparison with PTFE- and polystyrene (PST)-coated silicas.

EXPERIMENTAL

Chemicals and materials

Controlled-pore glass (CPG-2000) with a pore diameter of 200 nm ($d_p = 0.25–0.5$ mm) (GOZ VNII NP, N. Novgorod, Russian Federation), Silasorb 300 ($d_p = 5$ μm) (Lachema, Brno, Czech Republic) and Nucleosil 1000 ($d_p = 7$ μm) (Machery–Nagel, Düren Germany) were used as packing materials.

α,β,β-Trifluorostyrene (TFS) was of laboratory grade and vinylmethyldiethoxysilane (VMDES) was of research grade and both were purified by distillation under vacuum and stored at low temperature in sealed glass tubes.

All solvents used for the syntheses were of research grade. Mobile phases were prepared from HPLC-grade methanol and acetonitrile (Merck, Darmstadt, Germany) and deionized water purified with a Milli-Q system (Millipore).

A copolymer of VMDES and TFS (TFS–VMDES) was synthesized by the radical polymerization method [8] with dicyclohexyl peroxydicarbonate as initiator. The copolymer was precipitated by hexane from a solution in benzene. The ratio of TFS to VMDES units in the copolymer was calculated using results of elemental analysis.

The molecular mass of the copolymers was determined by size-exclusion chromatography on a column of Zorbax PSM 60S (DuPont) using tetrahydrofuran (Fluka, Buchs, Switzerland) as the mobile phase.

Kinetic data for the polymer binding were obtained by incubation of 2% (w/w) copolymer solution in dry toluene with CPG or silica at 110°C. The amount of chemisorbed copolymer was determined by elemental analysis of the coated packings and UV spectrometry of non-bonded copolymer in solution. The extraction of coated packings with toluene in a Soxhlet apparatus was performed for testing for the presence of physically sorbed copolymer.

Preparation of coated silica supports

Silasorb 300 (3 g) was weighed into a three-necked flask equipped with a stirrer and a Dean–Stark separator, then 30 ml of dried toluene were added. The suspension was heated under reflux for 1 h until no further water was liberated from the silica, then a solution of 0.5 g of copolymer in 10 ml of toluene was added and the suspension was agitated and heated under reflux for 3 h. The hot suspension was filtered through a porous PTFE membrane and remaining silica was washed twice with 30 ml of hot, dried toluene. End-capping of the product was performed by heating the coated silica with 1 ml of hexamethydisilazane dissolved in 15 ml of dried toluene under reflux for 2 h. The silica was then filtered through a porous PTFE membrane, washed with hot toluene, ethanol and water and dried overnight at 100°C.

All other silicas and porous glass were coated using the procedure described for Silasorb 300. The amount of copolymer used depended on the specific surface area of the silica or glass packings.

Chromatographic experiments

The coated silicas were slurry packed into columns (250 × 4.6 mm I.D.) using a 5% (w/w) suspension of cyclohexanol–toluene (50:50, v/v). Ethanol was employed as a displacing solvent. The column packing pump (Shandon) was used in this step. The pressure used to pack the columns was 310 bar. Chromatographic experiments were performed on a system consisting of a Model 114M pump, a Model 160 UV detector with a fixed wavelength of 214 or 254 nm and a Model 421A controller (all from Beckman). The column temperature was ambient and the injection volumes were 1–5 μl.

RESULTS AND DISCUSSION

Polymer coating

The synthesized TFS–VMDES copolymer was analysed by size-exclusion chromatography and it was found that the profile of elution contained two peaks with molecular masses (M_r) of 12 700 ($M_w/M_n = 2.9$) and 400 ($M_w/M_n = 1.1$). The substance with $M_r = 400$ was the dimer of TFS.

This mixture was fractionated by precipitation of the copolymer from the solution in benzene by adding *n*-hexane. Four fractions of the polymer had $M_r = 11\,700$, 6000, 6000 and 4000 with M_w/M_n from 1.12 to 1.3.

The ratio of TFS to VMDES units in the polymer found from element analysis was 10:1, so the copolymer had the following structure:

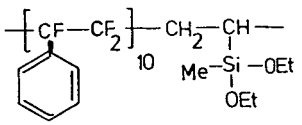

CPG-2000 was used for the investigation of the kinetics of the chemisorption of copolymers of TFS or styrene (ST) with VMDES ($M_r = 11\,700$ and 10 000, respectively) on a glass surface to avoid size-exclusion effects. Two conclusions could be drawn by comparing the data found for PST and PTFS copolymers. First, a reaction time of only 10–15 min was sufficient for completion of these procedures owing to the large amount of reacting ethoxysilyl groups in each of the macromolecules. Second, the rates of chemisorption were very similar for ST- and TFS-containing copolymers, so the type of polymer backbone had no influence on the reaction ability of the polymer.

No polymer was liberated from the coated samples after extraction with hot toluene, which is evidence that all the copolymer was chemisorbed rather then physisorbed on the glass surface.

The ligand density values were calculated from the data on carbon content and the specific surface area of the native silica. For Silasorb 300–PTFS it was found to be *ca.* 7.5 μmol/m^2 (carbon content 9%, w/w; specific surface area 240 m^2/g [2]).

Chromatographic properties

The completeness of coverage of the silica by the copolymer can be checked by monitoring the retention and peak width of basic compounds under the reversed-phase chromatographic conditions at neutral pH. The separation profiles for pyridine, 4,4′-diaminodibenzyl and 3,4-dimethylpyridine on the column with Silasorb 300

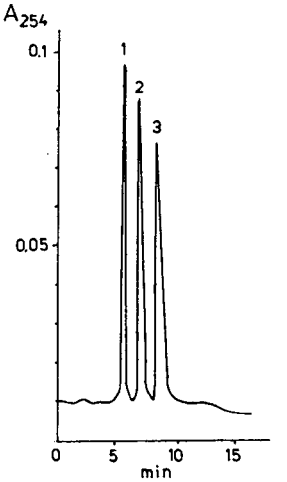

Fig. 1. Separation of a mixture of basic compounds on a column of Silasorb 300–PTFS (250 × 4.6 mm I.D.). Eluent, water–acetonitrile (50:50, v/v); flow-rate, 1 ml/min. Peaks: 1 = pyridine; 2 = 4,4′-diaminodibenzyl; 3 = 3,4-dimethylpyridine.

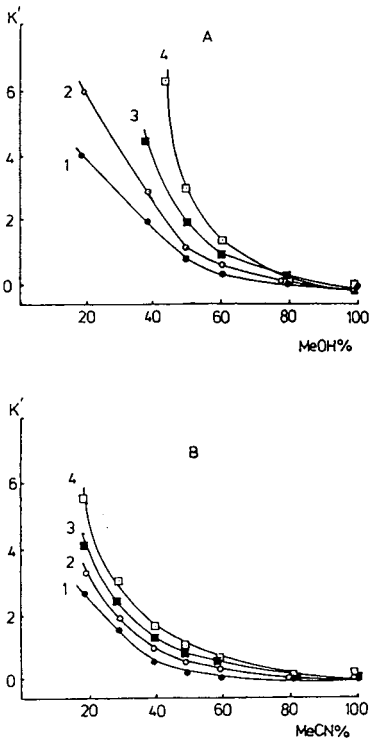

Fig. 2. Dependence of capacity factors (k') of halobenzenes on the contents of (A) methanol and (B) acetonitrile in the eluent using a column of Silasorb 300–PTFS. 1 = Benzene; 2 = fluorobenzene; 3 = bromobenzene; 4 = iodobenzene.

coated with copolymer (Fig. 1) showed symmetrical peaks, indicating the absence of a significant effect of the residual silanols on retention.

Further characterization of the chromatographic properties of PTFS-coated silica was carried out with a variety of functionalized benzenes. The dependences of the retention of haloaryl compounds on the type and composition of the mobile phase are shown in Fig. 2. The rapid decrease of k' with increase in acetonitrile content in the mobile phase can be attributed to the greater enrichment of the stationary phase by acetonitrile compared with methanol. The same situation was pointed out by Siergiej and Danielson [9] for the chromatographic properties of polychlorotrifluoroethylene powder (KEL-F) modified with phenyllithium. The shapes of the dependences of k' on organic content in the mobile phase were the same as for the usual *n*-alkyl-bonded reversed phases, hence the retention mechanism on polytrifluorostyrene-coated silica was the same.

Capacity factors (k') and hydrophobic selectivies ($\alpha^* = k'_{\text{substituted benzene}}/k'_{\text{benzene}}$) for functionalized benzenes are given in Table I. Previously, it has been reported [10,11] that fluorocarbon-bonded phases exhibited specific selectivity toward halogen-containing compounds. Confirmation of this effect could be made by comparing the retentions of the compounds in Table I. The retention times of halogen-containing benzenes are higher than those for their analogues without halogen groups.

The k' and α^* values for Silasorb 300–PTFS were compared with those for the PTFE- and PST-coated silicas. These sorbents were synthesized as described [2,4,6] using Silasorb 300 as the support. The results indicated that the retentions of all the compounds tested increase in the order PTFE < PTFS < PST phases. This is evidence that the polymer backbone and the

TABLE I

CAPACITY FACTORS (k') AND HYDROPHOBIC SELECTIVIES (α^*) FOR VARIOUS FUNCTIONALIZED BENZENES

Mobile phase: methanol–water (45:55, v/v) (pH 4.5).

Functional group	PTFE		PTFS		PST	
	k'	α^*	k'	α^*	k'	α^*
H	2.17	1.0	2.5	1.0	5.6	1.0
NO_2	2.32	1.07	2.5	1.0	5.5	0.98
F	2.7	1.3	2.9	1.16	6.1	1.09
Cl	3.13	1.44	3.17	1.3	10.07	1.9
Br	3.1	1.43	5.1	2.0	14.0	2.5
I	3.16	1.46	6.7	2.68	19.0	3.4
CH_3	2.53	1.17	3.8	1.52	8.3	1.48
o-F; CH_3	3.27	1.51	5.13	2.12	12.8	2.29
CH_2CH_3	3.37	1.56	5.0	2.0	>9.0	>1.61
OH	1.54	0.7	1.2	0.48	2.0	0.36
p-Cl; OH	1.56	0.72	1.6	0.64	4.1	0.73
CH_2NH_2	1.97	0.92	2.0	0.8	3.0	0.54
COH	2.09	0.96	2.13	0.8	3.6	0.64
o-Cl; COH	2.05	0.94	2.15	1.16	4.0	0.71
COOH	1.5	0.7	0.34	0.14	2.6	0.46
p-F; COOH	1.6	0.71	0.57	0.23	4.6	0.82
o-F; COOH	1.97	0.92	0.13	0.05	5.13	0.90
o-Br; COOH	1.00	0.5	0.43	0.17	2.2	0.39

phenyl ligand contributed to the adsorption activity of the sorbents and to the retention of the adsorbates.

The intermediate adsorption activity of the PTFS phase helped to provide a good resolution for the four halobenzenes, as shown in Fig. 3. With PTFE-coated silica the differences in retention times were too small to separate these molecules. However, the PST phase turned out to be much more active under the same conditions and provided acceptable retention times.

A Nucleosil 1000-7–PTFS HPLC column was tested for the reversed-phase chromatography of peptides and proteins. The dependences of k' on the content of acetonitrile in 0.1% TFA for several peptides and proteins are shown in Fig. 4. There was a sharp decrease in the retention of all peptides tested with increase in acetonitrile concentration in the eluent. The retention curves on PTFS-coated silica have essentially the same shape as on the usual C_8–C_{18} reversed-phase packings. This column was able to separate both relatively small peptides and proteins. Some enhancement of the retention of proteins due to silanophilic interactions could be observed on the PTFS-coated packing at concentrations of acetonitrile higher than 70%.

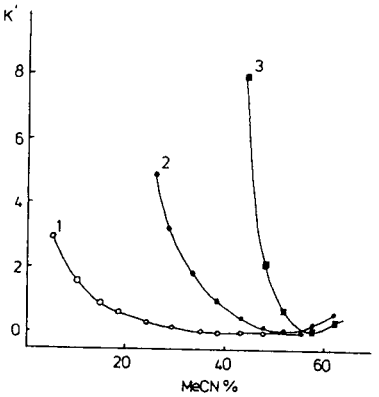

Fig. 4. Dependence of capacity factors (k') of proteins and peptides on the content of acetonitrile in the eluent using a column of Nucleosil 1000–PTFS (250 × 4.6 mm I.D.). Eluent, acetonitrile–water containing 0.1% TFA. 1 = Met-Cys-bradikinin; 2 = cytochrome *c*; 3 = bovine serum albumin.

The PTFS-coated sorbents easily separated peptide and protein mixtures under gradient elution conditions. The separation of bee venom components (natural sample) using a gradient of acetonitrile in 0.1% TFA is shown in Fig. 5.

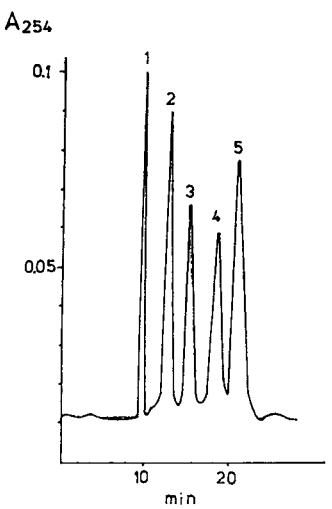

Fig. 3. Separation of a mixture of halobenzenes on a column of Silasorb 300–PTFS (250 × 4.6 mm I.D.). Eluent, acetonitrile–water (50:50, v/v); flow-rate, 1 ml/min. Peaks: 1 = benzene; 2 = fluorobenzene; 3 = chlorobenzene; 4 = bromobenzene; 5 = iodobenzene.

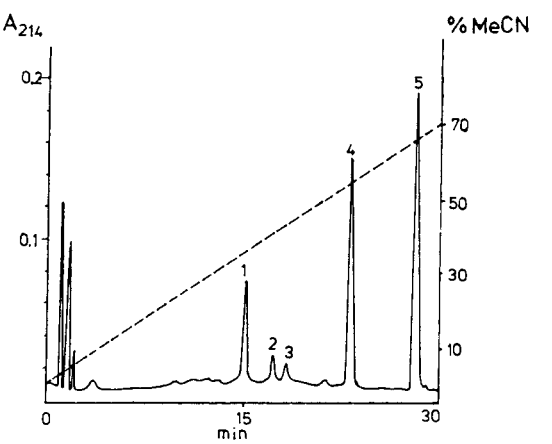

Fig. 5. Separtion of bee venom components on a column of Silasorb 300–PTFS (250 × 4.6 mm I.D.). Eluent, gradient from 5 to 70% acetonitrile in 0.1% TFA in 30 min; flow-rate, 1 ml/min. Peaks: 1 = apamin; 2 = MCD peptide; 3 = secapin; 4 = phospholipase A^2; 5 = melittin.

The higher hydrolytic stability of silicas with a covalently bonded PTFS phase was typical for materials obtained by such a procedure [2,6]. An HPLC column containing Silasorb 300–PTFS was used for 1 year at pH 2–8.5 without considerable changes in peak resolution. The unusual adsorption properties and the possibility of introducing several functional groups make PTFS-coated silicas attractive for future studies.

REFERENCES

1 F.E. Regnier, K.K. Unger and R.E. Majors (Guest Editors), *Liquid Chromatography Packings; J. Chromatogr.*, 544 (1991).
2 A.A. Kurganov, O. Kuzmenko, V.A. Davankov, B. Eray, K.K. Unger and U. Trudinger, *J. Chromatogr.*, 506 (1990) 391.
3 V.A. Davankov, A.A. Kurganov and K.K. Unger, *J. Chromatogr.*, 500 (1990) 519.
4 A.E. Ivanov, V.V. Saburov and V.P. Zubov, *Adv. Polym. Sci.*, 104 (1992) 136.
5 N.D. Danielson, L.G. Beaver and J. Wangsa, *J. Chromatogr.*, 544 (1991) 187.
6 V.V. Saburov, M.R. Muydinov, A.D. Kataev, S.A. Guryanov, S.I. Turkin and V.P. Zubov. *Zh. Fiz. Khim.*, 65 (1991) 2692.
7 A.D. Kataev, V.V. Saburov, L.A. Fonina, S.A. Guryanov, in A. Kalnins (Editor), *Proceedings of the 8th Conference on Organic and Bioorganic Chemistry, Riga, November 1991*, Latvian Academy of Sciences, 1991, p. 292.
8 A.D. Kataev, *Ph.D. Thesis*, Lomonosov University of Fine Organic Chemistry, Moscow, 1993.
9 R.W. Siergiej and N.D. Danielson, *Anal. Chem.*, 55 (1983) 17.
10 G. Berendsen, K.A. Pikaart, L. de Galan and C. Olieman, *Anal. Chem.*, 52 (1980) 1990.
11 H.A. Billiet, P.J. Schoenmakers and L. de Galan, *J. Chromatogr.*, 218 (1981) 455.

Journal of Chromatography A, 660 (1994) 137–145
Elsevier Science B.V., Amsterdam

CHROMSYMP. 2956

Perfusible and non-perfusible supports with monoclonal antibodies for bioaffinity chromatography of *Escherichia coli* penicillin amidase within its pH stability range

V. Kasche*, N. Gottschlich, Å. Lindberg, C. Niebuhr-Redder and J. Schmieding

AB Biotechnologie II, TU Hamburg-Harburg, D-21071 Hamburg (Germany)

ABSTRACT

Several monoclonal antibodies (mABs) have been prepared and immobilized for the biospecific isolation of penicillin amidase (PA) from *Escherichia coli* (EC 3.5.1.11), an enzyme without S–S bridges and a pH stability range of 4–9. During the immobilization the fluorescence emission maxima of the mABs were found to change from 336 nm to *ca.* 350 nm. Only one of these mABs was found to be suitable for preparative bioaffinity chromatography of PA within the pH stability range. This mAB was immobilized on different spherical supports (Eupergit C 250 L and Sepharose) and one perfusible support (Knauer Quick Disc) and used for analytical and preparative bioaffinity chromatography. Under isocratic conditions the plate height for the perfusible biospecific adsorbent was found to be an order of magnitude lower than for the other supports. The different forms of this proteolytically processed bacterial enzyme could not be separated, however, by the biospecific adsorbents. At the mAB density used in the adsorbents (10–30 μM), less than 30% of the theoretical binding capacity of the immobilized mABs could be used to adsorb the enzyme.

INTRODUCTION

Immobilized monoclonal antibodies (mABs) and inhibitors against enzymes, antigens and other antibody-binding proteins are suitable adsorbents for bioaffinity chromatography [1]. With these the enzyme or mAB can be quantitatively isolated from homogenates. The adsorbed proteins can generally be desorbed using H^+ as acid–base equilibria control its interaction with the immobilized ligate [2]. For enzymes without S–S bridges and oligomeric enzymes the pH range within which they retain their biological function is limited. Outside this range such enzymes rapidly denature owing to partial unfolding of dissociation caused by charge–charge repulsions. The denatured proteins can be renatured in a time-consuming procedure. For the isolation of these enzymes only those mABs or inhibitors that allow the desorption within the pH range where the enzyme is stable can be used for biospecific affinity chromatography. This was investigated to select mABs against *Escherichia coli* penicillin amidase (PA) that are suitable for the biospecific isolation of this enzyme from homogenates. This bacterial enzyme consists of two polypeptide chains ($M_r \approx 88\,000$) formed by proteolytic processing of a single polypeptide pro-enzyme ($M_r \approx 90\,000$). It has no S–S bridges and denatures rapidly (half-life <1 h) at pH <4 and pH >9. Several active enzyme forms that differ in the composition of the smaller peptide chain have been observed [3]. When their dissociation constant for the interaction with the biospecific support differs, they have different capacity factors. Then these and the plate height determine the possible resolution of these different enzyme forms by bioaffinity chromatography. The plate height for different biospecific supports varying in particle and pore size, includ-

* Corresponding author.

0021-9673/94/$07.00 © 1994 Elsevier Science B.V. All rights reserved
SSDI 0021-9673(93)E1062-5

ing one perfusible support, was therefore determined.

For preparative purposes, the binding capacity of the immobilized mABs should be large. It is frequently observed, however, that at high mAB densities only a fraction of the immobilized molecules retain their function to interact biospecifically with soluble ligands. This may be due to steric hindrance when the ligand is so large that its binding to one ligate molecule sterically hinders the simultaneous binding of ligands by the nearest neighbour ligates [4–6]. This indicates the existence of an optimum ligate concentration for biospecific affinity chromatography that depends on the size of ligand. Another possibility is that some mABs lose their binding function owing to partial unfolding on immobilization. This was studied by direct determination of the fluorescence spectra of the immobilized mABs using a specially designed cuvette with a fibre-optic light guide [7–9].

EXPERIMENTAL

Materials and methods

The following supports were used for immobilization: cyanogen bromide-activated Sepharose 4B (average particle radius 40 μm) was obtained from Pharmacia (Uppsala, Sweden) and Eupergit C 250 L (average particle radius 100 μm) and Knauer Quick-Disc [10] were kindly provided by Röhm (Darmstadt, Germany) and Knauer Säulentechnik (Berlin, Germany), respectively. Crude PA (EC 3.5.1.11) preparations were a gift from Röhm. The PA forms with isoelectric points (p*I*) of 7.0 ($PA_{7.0}$) and 6.7 ($PA_{6.7}$) were prepared as described previously [3]. All other chemicals were of analytical-reagent grade.

Monoclonal antibody production and purification

Hybridoma cell lines that produced mABs against $PA_{7.0}$ were isolated from mouse (Balb/c) spleen cells and myeloma (PAI/0) cells using a standard immunization and fusion protocol. Different hybridoma cell lines, which secrete mABs (IgG1) against *E. coli* PA, were used throughout this study. Cell line IV F 19 was grown in continuous culture in a membrane dialysis bioreactor as described previously [11]. The media for all cell lines was a 1:1 mixture of Iscove's MDM and Ham's F12 (Gibco, Paisley, UK) supplemented with 3% foetal calf serum (FCS), 2 mmol/l L-glutamine from Gibco and 2 g/l $NaHCO_3$. The other cell lines were grown in a roller bottle unit (Tecnomara, Fernwald, Germany). Cells and debris were removed from the supernatant by centrifugation with a Contifuge (Heraeus, Osterode, Germany) and the spent medium was concentrated [Heraeus cross-flow or Amicon (Beverly, MA, USA); M_r cut-off 10 000] and filtered with a 0.2-μm filter. If necessary, the pH was adjusted to 6–7 and this medium was directly applied to a protein G column [protein G Sepharose Fast Flow (Pharmacia), 70 mm × 10 mm]. The column was washed with 50 m*M* phosphate buffer (pH 6.5) and the bound antibodies were eluted with 0.2 *M* glycine–HCl (pH 2.7). The pH of the eluted antibodies was immediately adjusted to 7. For comparison of fluorescence spectra, one part of the antibodies was purified by 50% $(NH_4)_2SO_4$ precipitation according to ref. 12. The precipitate was dissolved in phosphate-buffered saline (PBS), dialysed against PBS and the antibody-containing solution was concentrated to 2–5 mg/ml with Centricon or Centriprep concentrators (Amicon). Further purification was achieved by size-exclusion chromatography on Superdex 200 in a HiLoad 16/60 column (Pharmacia). The purity of antibodies was determined by sodium dodecyl sulphate–polyacrylamide gel electrophoresis (SDS-PAGE) and isoelectric focusing (IEF).

Determination of monoclonal antibodies

Mouse IgG contents in the media were determined with a Mouse-IgG-ELISA kit (Boehringer, Mannheim, Germany) or with an antigen-specific enzyme-linked immunosorbent assay (ELISA). For pure antibodies the antibody content was determined at 280 nm using a molar absorptivity of 13.5 for a 1% solution with a UV spectrophotometer [13].

Electrophoretic methods

IEF was carried out with Ampholine-PAG plates (pH 3.5–9.5) on a Pharmacia Multiphor II apparatus according to the instructions of the manufacturer.

SDS-PAGE was performed on SDS gels according to the method of Laemmli [14] in a MINI-Gel system from Bio-Rad (Richmond, CA, USA).

Immobilization

The immobilization of the antibodies on the solid supports was carried out according to the instructions of the manufacturer with the following change. For the coupling reaction, 0.2 *M* phosphate buffer (pH 7.0) was used, as this has been found to decrease the heterogeneity in the dissociation constants and to increase the resolving power of biospecific supports when the ligate is bound via the ε-amino group of lysine side-chains [2]. Remaining binding sites were blocked overnight with 1 *M* ethanolamine (pH 8.0).

Determination of enzyme activity

Penicillin amidase activity was determined with 2-nitro-5-phenylacetaminobenzoic acid (NIPAB) as substrate as described previously [3].

Determination of dissociation constants and static capacity

For the determination of dissociation constants, equal amounts of antibodies coupled to the solid supports were incubated with various amounts of purified $PA_{7.0}$ at different pH values using phosphate buffers (ionic strength, $I = 0.2$ *M*). The time course of the binding of the enzyme to the immobilized mABs was determined from the enzyme activity outside the particles as a function of time. The adsorption was virtually completed within 1 h as the amount adsorbed between 1 and 24 h of equilibration was found to be negligible. The equilibrium K_{diss} value and the static capacity could therefore be determined after 1 h of equilibration. The suspensions were then filtered and the concentration of unbound PA was determined from the enzyme activity in the filtrate. The amount of bound PA was determined from the mass balance.

Analytical and preparative bioaffinity chromatography

An LKB–Pharmacia (Pharmacia, Uppsala, Sweden) HPLC solvent delivery system (Model 2150 pump, Model 2152 controller) and a Knauer (Berlin, Germany) Typ 87.00 UV–Vis detector were used for these experiments. Analytical affinity chromatography was performed under isocratic conditions with buffers (phosphate, $I = 0.2$ *M*) in the pH range 4–5 in small columns (radius 5 mm) packed with *ca.* 2 ml of biospecific support, except for the cylindrical Knauer Quick Disc (radius 25 mm, height 4 mm), which was used in a specially designed holder [10]. Samples (50 μl) of purified $PA_{7.0}$ and $PA_{6.7}$ (*ca.* 1 mg/ml) were applied to the columns and eluted under isocratic conditions at various flow-rates. When the active enzyme was eluted the plate height was determined from its peak in the elution curve.

For the preparative isolation of PA from homogenates and crude enzyme preparations, a 20 mm × 14 mm column packed with IV F 19 mAB (4.9 mg/ml wet support) was used. For the adsorption of the enzyme from a 0.5-ml sample of crude enzyme (20 mg/ml, total protein content *ca.* 80 mg/ml) the column was equilibrated and eluted (flow-rate 0.5 ml/min) with buffer of pH 7.0 (phosphate, $I = 0.2$ *M*). When the first peak had been eluted the pH of the elution buffer was changed to 4.0 to desorb the active enzyme. When the enzyme had been eluted, the column was regenerated with the buffer of pH 7.0.

Determination of fluorescence spectra of free and immobilized proteins

The fluorescence spectra of free and immobilized enzymes were measured with a Shimadzu (Kyoto, Japan) RF-540 spectrofluorimeter. For the determination of the fluorescence spectra of immobilized proteins a specially designed cuvette and fibre-optic device as described previously [9,15] were used (excitation slit width 10 nm, emission slit width 5 nm, excitation at 280 nm). A small flow-through cuvette (15 μl) was packed with unreacted supports in phosphate buffer and the fluorescence spectrum was determined. In a second step, ligate-coupled support was packed

into the same cuvette and the fluorescence was measured as the difference spectrum between the coupled and uncoupled support.

RESULTS AND DISCUSSION

Isolation and characterization of mABs against penicillin amidase

Hybridoma cells from different stable clones that produced mABs against PA were cultivated in a specially designed bioreactor or in roller flasks [11]. The medium from these cultures was concentrated by ultrafiltration. The mABs in these solutions were purified either by Protein G affinity chromatography or a combination of salt precipitation and gel exclusion chromatography. The yield of mABs isolated was >95%. The purities of the mABs derived from IEF patterns are shown in Fig. 1A. The IEF patterns for the same mAB purified by different methods were identical, as shown in Fig. 1B. The mAB from hybridoma clones that produced most antibody and a mAB with a high and a low isoelectric point were selected for further experiments.

All mABs were heterogeneous with respect to IEF patterns. For the IV F 19 mAB this pattern was not changed during long-term fermentation or using cells that after frequent recultivations had changed their mean chromosome number from 66 to 61.

Immobilization of mABs: determination of fluorescence spectra and dissociation constants

The immobilization yields and the wavelengths of the fluorescence emission maxima for free and bound mABs using different supports are given in Table I. Fluorescence spectra of free and immobilized antibody are shown in Fig. 2. During immobilization, the wavelength of maximum fluorescence emission (λ_{max}) was found to increase more than has been observed previously for the globular enzymes α-chymotrypsin, β-trypsin and PA, where λ_{max} remained virtually unchanged on immobilization [7,15]. The fluorescence emission of proteins at 330–340 nm is due to the tryptophan residues. Their fluorescence emission maximum increases when they

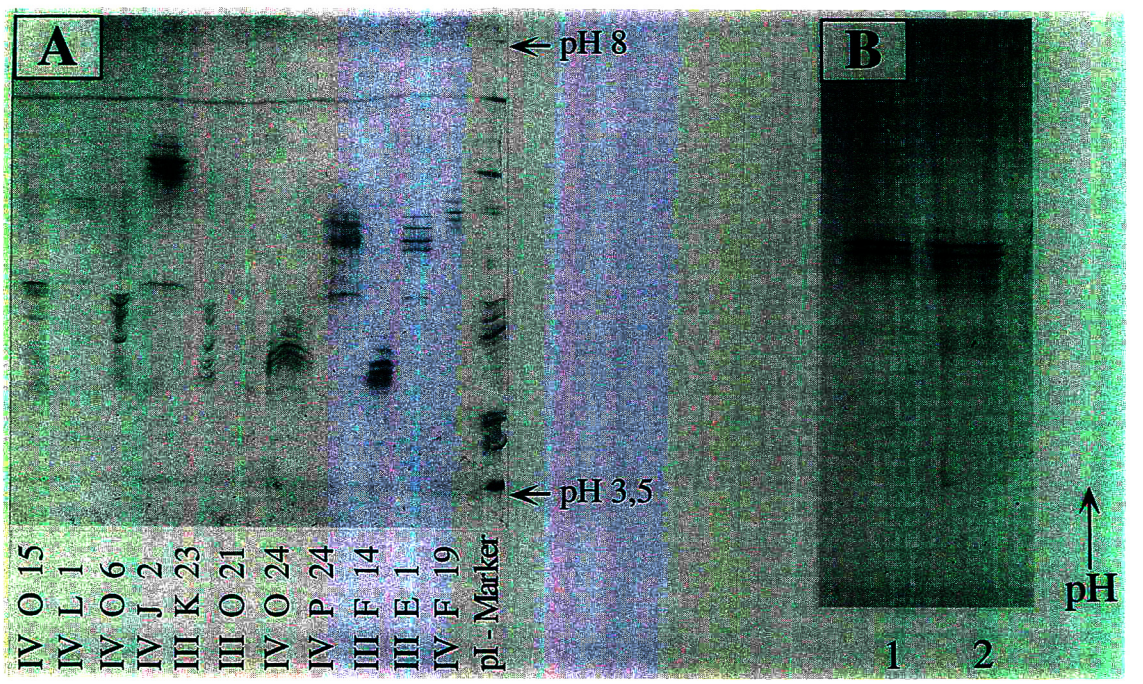

Fig. 1. Isoelectric focusing patterns of different mABs against *E. coli* penicillin amidase. (A) Monoclonal antibodies from different clones isolated by protein G chromatography. (B) mAB IV F 19 isolated by protein G chromatography (lane 1) and by a combination of salt precipitation and gel exclusion chromatography (lane 2).

TABLE I

WAVELENGTH OF MAXIMUM FLUORESCENCE EMISSION, λ_{max} (UNCORRECTED AT pH 7.0, 25°C), BINDING YIELD (IN % OF mABs ADDED TO THE ACTIVATED SUPPORT) AND mAB CONTENT IN THE SUPPORTS DETERMINED FROM THE MASS BALANCE

Support	Property	Monoclonal antibody			
		III E 1	III F 14	IV F 19	IV J 2
Sepharose	λ_{max} (nm)	336	335	336	n.d.[a]
	Binding yield (%)	47	68	>90	>90
	[mAB] (mg/ml)	2.9	3.9	4.9	4.7
Eupergit C 250 L	λ_{max} (nm)	355	350	352	n.d.[a]
	Binding yield (%)	84	76	60	–
	[mAB] (mg/ml)	4.2	4.5	3.0	–
Knauer Quick-Disc	λ_{max} (nm)	348	n.d.[a]	350	n.d.[a]
	Binding yield (%)	–	–	90	–
	[mAB] (mg/ml)	–	–	1.5	–

[a] Not determined.

are transferred from non-polar (alcohol) to a more polar (water) surrounding. When proteins unfold, some tryptophan residues become more exposed to water and λ_{max} increases. This has been used to study the stabilization of β-trypsin against thermal unfolding on immobilization [7]. The data for the mABs indicate a partial unfolding due to the immobilization procedure. The function to bind PA was, however, retained, as follows from the determination of K_{diss} as a function of pH (Fig. 3). From Scatchard plots the fraction of the immobilized antibodies that can bind the enzyme could be determined and the results are given in Table II. The experimental error in K_{diss} (±30%) depends on the error in the activity determinations (±5%) and can be calculated as described previously [16,17]. From these data and Fig. 3, it follows that K_{diss} differs significantly for the different antibodies with high

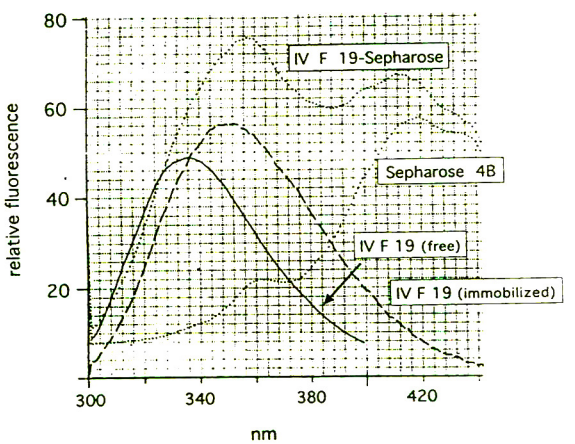

Fig. 2. Fluorescence spectra of free and immobilized mAB IV F 19 (excitation at 280 nm, excitation slit width 10 nm and emission slit width 5 nm) in phosphate buffer of pH 7.0 ($I = 0.2$ M) at 25°C. No change in the fluorescence emission maximum of the immobilized mABs was observed after 20 adsorption–desorption cycles.

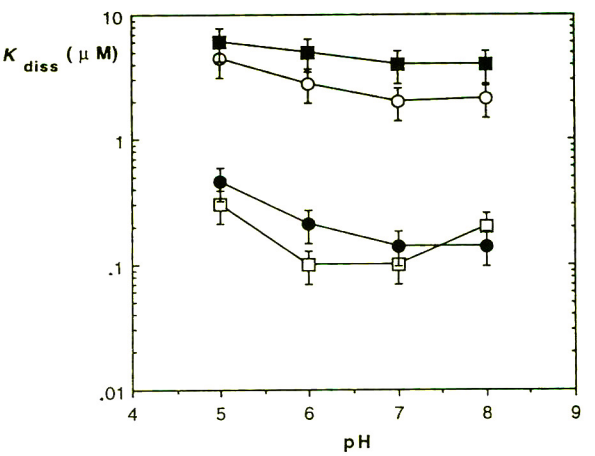

Fig. 3. pH dependence of the dissociation constant for the interaction of different mABs with penicillin amidase $(PA)_{7.0}$ at 25°C. The ionic strength in the buffers was 0.2 M. ■ = IV J 2; ○ = III E 1; ● = IV F 19; □ = III F 14.

TABLE II

FRACTION OF mABs USED FOR ADSORPTION FROM CAPACITY DETERMINATIONS USING EQUILIBRIUM BINDING AND CHROMATOGRAPHIC DATA WITH DIFFERENT SUPPORTS AND ANTIBODY DENSITIES

Antibody	Support	mAB immobilized (μM/l wet support)	Fraction of mABs used for adsorption in % of theoretical value (2 mol antigen/mol mAB)	
			From equilibrium data	From chromatography
IV F 19	Sepharose	10	> 90	
		32	20	17 (0.006)[b]
	Knauer Quick-Disc	10	n.d.[a]	5 (0.01)[b]
III E 1	Sepharose	15	60	
III F 14	Sepharose	11	80	
IV J 2	Sepharose	30	30	

[a] Not determined.
[b] Interstitial flow-rate (cm/s) in parentheses.

and low isoelectric points, whereas the fraction of immobilized antibodies at similar mAB densities in the support that can bind the enzyme is equal, within experimental error.

Only the mABs whose K_{diss} have a marked pH dependence can be used for the desorption of adsorbed enzyme by changing the pH within the pH stability range of the enzyme (4–9). For quantitative adsorption, the distribution coefficient that to a first approximation equals n/K_{diss} should exceed 10. From Table II and Fig. 3, it follows that this applies only for the two mAB with the lowest K_{diss} value.

Analytical bioaffinity chromatography and plate height determinations

Samples of pure $PA_{7.0}$ or $PA_{6.7}$ were separated with the different biospecific supports under isocratic conditions. Of the four mABs tested, only IV F 19 was found to be suitable for the preparative isolation of PA within its pH stability range (4–9). The enzyme adsorbed to III F 14 could not be desorbed within this range. The other mABs had too large K_{diss} values to allow a good separation from the impurities under isocratic conditions. The elution volumes for $PA_{7.0}$ and $PA_{6.7}$ for the supports with the same mAB were equal, within experimental error, indicating a small difference in their K_{diss} values. For all supports where the active enzyme could be desorbed, more than 90% of the applied protein and enzyme activity was recovered in the eluates. From the elution curves of the separations of $PA_{7.0}$ the plate heights of the different biospecific adsorbents were determined under isocratic conditions in the pH range 4–5. Their dependences on the interstitial flow-rate are shown in Fig. 4, where they are compared with published data for other biospecific adsorbents [2,17,18]. The new data for the low-pressure, wide-pore supports Sepharose and Eupergit C 250 L are within the experimental error. They are approximately an order of magnitude better than older data obtained with Sepharose [17]. This may be due to improved methods of preparing this support. The lowest plate heights were observed for the perfusible support Knauer Quick-Disc. They are similar to the data published for other perfusible supports [19,20]. The plate heights lie on the part of the Van Deemter curve that is mainly influenced by the diffusion (coefficient and/or distance) from the mobile phase to the binding sites of these supports. The data in Fig. 4 can be explained by the larger pore

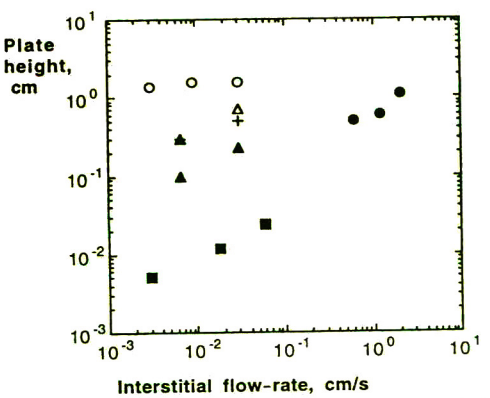

Fig. 4. Plate height as a function of interstitial flow-rate in isocratic analytical biospecific affinity chromatograph of PA using different supports and monoclonal antibodies. ○ = STI–Sepharose; ● = STI–Lichrospher. Supports with monoclonal antibodies IV F 19 and III E 1: △ = IV F19–Sepharose; + = IV F 19–Eupergit 250; ■ = IV F 19–Knauer Quick-Disc; ▲ = III E 1–Eupergit 250. The Knauer support is a macroporous perfusible disc (radius 50 mm, height 4 mm) [10]. They are compared with published data for other ligate (STI soybean trypsin inhibitor)–ligand (α-chymotrypsin, M_r = 25 000) systems immobilized on Sepharose and Lichrosphere (radius 10 μm) [17,18].

sizes or smaller diffusion distances compared with the non-perfusible supports of similar particle size.

Preparative isolation of PA

In Fig. 5 the isolation of PA from a crude enzyme preparation with IV F 19–Sepharose is shown. There was virtually no change in the amount isolated between the first and tenth isolations, indicating that the biospecific adsorbent has a high stability. The same was also observed for the mABs immobilized on the perfusible support Knauer Quick-Disc. The isolated PA is a mixture of different PA forms formed by proteolytic processing, as shown by the IEF immunoblot and zymogram in Fig. 5. They could not be separated by the biospecific adsorbents used here. That different enzyme forms along a processing chain or modified enzymes with similar K_{diss} values can be separated by bioaffinity chromatography has been shown previously for α-chymotrypsin and α- and β-trypsin [2,21]. The resolution in these separations depends on the plate height and differences in K_{diss}. These and the data from the analytical chromatography indicate that for the PA forms the difference in K_{diss} and the plate height do not allow their separation with the biospecific adsorbent used. The dissociation rate constant k_{diss} and the resolution are expected to increase when a less specific interaction, such as in ion-exchange chromatography, is used to separate the enzyme forms with different p*I*. This applies also for PA. The different forms, especially the dominating forms with p*I* 7.0 and 6.7 ($PA_{7.0}$ and $PA_{6.7}$) can be separated by ion-exchange chromatography [3]. $PA_{7.0}$ form can also be processed to $PA_{6.7}$, either autocatalytically or by immobilized α-chymotrypsin [3].

The operational capacities of the supports were determined from breakthrough curves at enzyme concentrations $>K_{diss}$. The results are shown in Table II. The fraction of immobilized mABs that can bind PA was found to depend on their concentration (Table II). In the equilibrium binding experiments this is expected to decrease when the binding of one ligand sterically hinders the binding to adjacent immobilized mABs. The supports used here have a surface area of *ca.* 10 m^2/ml. At ligate densities of 6 μ*M* (ca. 1 mg/ml) and 30 μ*M* (*ca.* 5 mg/ml) the average distance between adjacent ligate molecules is about 50 and 20 nm, respectively. For molecules of the size studied here (radius *ca.* 5 nm), a decrease in the fraction of immobilized ligates that can bind ligand molecules is expected to occur in this concentration range. Similar conclusions have been derived in other studies [4–6]. This also gives an upper limit for the static capacity for preparative supports with biospecific supports with a surface area of 10 m^2/ml for molecules of the size studied here; it is of the order of 1 mg/ml. In the dynamic adsorption step in preparative chromatography, this may be decreased owing to steric hindrance for diffusion in the pores that reduces the rate of adsorption. This can be also be studied directly with the fluorescence measuring device for adsorbents used here for the determination of the fluorescence spectra of immobilized mABs [9,15]. For the perfusible support Knauer Quick-Disc a much smaller fraction of the immobilized mAB could be used to adsorb PA than for Sepharose. This may be

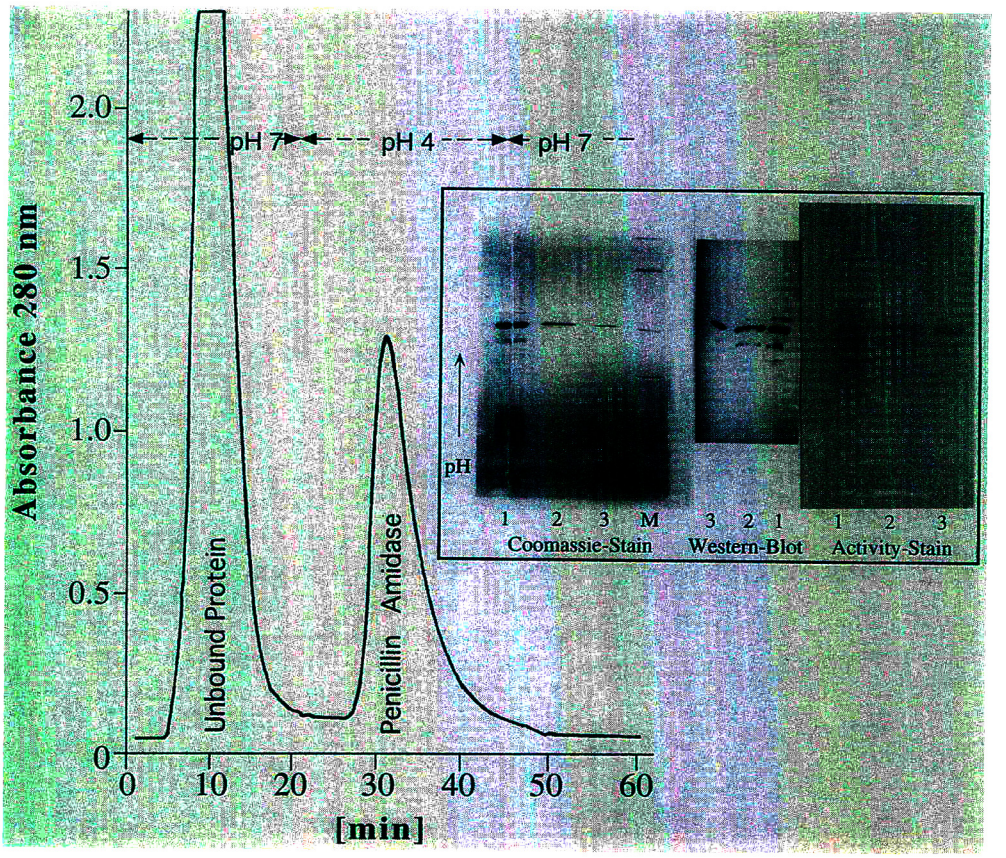

Fig. 5. Preparative PA isolation with the mAB IV F 19 immobilized on Sepharose. Elution curve for a 0.5-ml sample of crude enzyme (*ca.* 20 mg PA/ml; total protein content *ca.* 80 mg/ml). When the impurities had been eluted the pH of the buffer was changed to 4.0 to desorb the adsorbed enzyme. No enzyme activity was observed in the first peak of these diagrams. Inset: isoelectric focusing pattern as protein stain (Coomassie Brilliant Blue), activity stain (M = marker proteins) and Western blot using IV F 19 mAB for (1) crude enzyme, (2) the adsorbed peak in the above elution diagram and (3) $PA_{7.0}$ purified by ion-exchange chromatography.

partly because the liquid flow is not distributed over the whole support [10].

CONCLUSIONS

Of four mABs against PA from *E. coli*, an enzyme without S–S bridges and a pH stability range of 4–9, only one (IV F 19) could be used for the preparative biospecific isolation of the enzyme from homogenates. Owing to steric hindrance, the maximum capacity of the biospecific adsorbents was found to be *ca.* 1 mg/ml support for PA (M_r 88 000).

In contrast to globular enzymes, the fluorescence emission maximum was found to change from 336 to ≥350 nm when the mABs were immobilized in different supports. This indicates partial unfolding of the protein. In contrast to the enzymes, this does not lead to a loss of the biological function, *i.e.*, to binding of the antigen.

The plate heights for the biospecific adsorbents with immobilized mABs were an order of magnitude lower for the perfusible support Knauer Quick-Disc than for the non-perfusible spherical porous supports (Eupergit C 250 L and Sepharose).

ACKNOWLEDGEMENTS

This work was supported by the Bundesministerium für Forschung und Technologie (0319348A) and partly performed within the Graduiertenkolleg Biotechnologie funded by DFG (Ka 505/5-1).

REFERENCES

1 I.M. Chaiken, M. Wilchek and I. Parikh, *Affinity Chromatography and Biological Recognition*, Academic Press, New York, 1983.
2 V. Kasche and B. Galunsky, in T. Gribneau and J. Visser (Editors), *Affinity Chromatography IV*, Elsevier, Amsterdam, 1982, pp. 93–110.
3 V. Kasche, U. Haufler, D. Markowsky, S. Melnyk and A. Zeich, *Ann. N.Y. Acad. Sci.*, 501 (1987) 97–102.
4 G. Fleminger, E. Hadas, T. Wolf and B. Solomon, *Appl. Biochem. Biophys.*, 23 (1990) 123–137.
5 M. Nachmann, *J. Chromatogr.*, 597 (1992) 167–172.
6 W. Schramm and S.H. Paek, *Anal. Biochem.*, 205 (1992) 47–56.
7 D. Gabel and V. Kasche, *Acta Chem. Scand.*, 27 (1973) 1971–1981.
8 P. Oroszlan, R. Blanco, X.-M. Lu, D. Yarmush and B.L. Karger, *J. Chromatogr.*, 500 (1990) 481–493.
9 V. Kasche, E. Renken, G. Schietke, R. Ulrich, R. Bücke, H. Gnewuch and K. Jansen, in S. Scheller and R. Schmid (Editors), *Biosensors, Fundamentals, Technologies and Applications*, VCH, Weinheim, 1992, pp. 262–274.
10 H. Abouh-Rebyeh, F. Körber, K. Schubert-Rehberg, J. Reusch and D.J. Josic, *J. Chromatogr.*, 566 (1991) 341–350.
11 A. Bohmann, R. Pörtner, J. Schmieding, V. Kasche and H. Märkl, *Cytotechnology*, 9 (1992) 51–57.
12 E. Harlow, E. and D. Lane, *Antibodies—A Laboratory Manual*, Cold Spring Harbor Laboratory, Cold Spring Harbor, NY, 1988.
13 J.R. Little and H. Donahue, in C.A. Williams and M.A. Chase (Editors), *Methods in Immunology and Immunochemistry*, Vol. 2, Academic Press, New York, 1967, p. 343.
14 U.K. Laemmli, *Nature*, 227 (1970) 680.
15 E. Renken, *Thesis*, Technische Universität Hamburg-Harburg, Hamburg, 1993.
16 D.A. Deranleau, *J. Am. Chem. Soc.*, 91 (1969) 4044–4049.
17 V. Kasche, *Acta Univ. Ups.*, 2 (1971) 1–135.
18 V. Kasche, K. Buchholz and B. Galunsky, *J. Chromatogr.*, 216 (1981) 169–174.
19 N.B. Afeyan, S.P. Fulton and F.E. Regnier, *LC·GC Int.*, 4, No. 12 (1991) 14–19.
20 K. Mosbach, personal communication, 1992.
21 V. Kasche and I. Büchtmann, *Hoppe Seyler's Z. Physiol. Chem.*, 362 (1981) 1007–1012.

Journal of Chromatography A, 660 (1994) 147–152
Elsevier Science B.V., Amsterdam

CHROMSYMP. 2893

Improvement of the performance of single-column ion chromatography by computerized detector signal processing and correlation chromatography

M. Kaljurand*, E. Urbas and U. Haldna

Institute of Chemistry, Estonian Academy of Sciences, Tallinn EE0026 (Estonia)

ABSTRACT

The performance of medium-quality ion chromatographic equipment was improved by using pseudo-random sample introduction correlation chromatography (CC). The importance of the digital preprocessing of the detector signal prior to decorrelation was demonstrated for realization of the multiplex advantage of the CC method. The detection limits obtained for single-column ion chromatography using conductivity detection were 0.1, 0.12 and 0.17 ppm for Cl^-, NO_3^- and SO_4^{2-} ions, respectively. Using the same apparatus without CC the detection limits are in the range 1–3 ppm.

INTRODUCTION

Although various high-performance ion chromatographic (IC) products (columns, sampling valves and detectors), are commercially available, they may sometimes be too expensive, *e.g.*, in Eastern European laboratories. However, environmental monitoring in the regions concerned is even more necessary than in better developed countries because of their high levels of industrial waste pollution. To meet the demands of environmental monitoring, local manufacturers provide analytical instruments but these may provide much poorer performance than modern Western instruments.

The performance of less sophisticated local instrumentation can be improved by computerized measurement control and data processing. Mars and Smit [1] have demonstrated that the detection limit in HPLC can easily be improved by an order of magnitude. The same applies to single-column IC with UV detection [2]. Instead of a common approach to trace enrichment and single injections, in both of these studies a sample was introduced into the column directly according to a pseudo-random binary sequence (PRBS), followed by computation of the chromatogram from a random function-like detector output by correlating the input signal pattern with the detector output. This technique is known as correlation chromatography (CC) [3].

Generally in single-column ion chromatography (SCIC), injection and system peaks are present. For anion determinations the injection peak is due to the passage of non-retained cations, water and eluent anions to the detector [4]. Their peak usually appears first on a single-injection chromatogram. The second system peak is due to the transport of the deficiency of the eluent cations and its position on the chromatogram depends on the eluent composition. The areas of the injection and system peaks are related to the total areas of the remainder of the peaks and are therefore the highest on the chromatogram [5]. Using UV detection, a suitable working wavelength can be selected to avoid detecting the injection peak. Using con-

* Corresponding author.

0021-9673/94/$07.00 © 1994 Elsevier Science B.V. All rights reserved
SSDI 0021-9673(93)E0820-K

ductivity detection the injection and system peaks are usually neglected by being off the scale of the recorder. If the injection and system peaks are well separated from the other peaks, they have little effect on the determination of the analytes of interest.

In correlation IC, the injection and system peaks represent a serious problem. As in CC about 1000 injections are made during one measurement, variations in the sample amounts injected can disturb the resulting chromatogram (correlogram) obtained after transformation of the detector signal. This happens because the decorrelation operation converts all variations in the sample amounts introduced into a special type of noise that appears on the chromatogram, *i.e.*, correlation noise [3]. This noise frequently appears in the form of a "ghost" peak. It follows that the correlation noise due to variations in the cationic components of the injected sample (resulting in variations in the amplitudes of the injection peaks in anion IC) can mask small-amplitude peaks on the chromatogram On the other hand, the injection quality depends directly on the quality of the sampling device. In HPLC the only choice is the mechanical valve, whose performance depends strongly on the material of the valve rotor.

In addition to the injection reproducibility, there are other distortions of the detector signal that prevent the effective use of CC, such as baseline drift. This is a very frequent phenomenon in SCIC that cannot be neglected when working on detection limits. Also, power-line spikes and pump oscillations appear on the output signal. As the main aim of CC is to reduce the high-frequency noise power, the other detector signal distortions should be removed before applying the decorrelation procedure to ensure the ability of CC to establish detection limits.

In this work, effective means for decreasing the influence of baseline drift and pump oscillations on the decorrelation procedure were sought. The importance of preprocessing the detector signal by digital filtering prior to decorrelation is demonstrated. A special modification to the sample solution is provided to decrease the injection and system peak amplitudes in order to lessen the influence of the irreproducibility of the injection device.

EXPERIMENTAL

The experimental set-up was the same as that described in a previous paper [2], except that the UV detector was replaced with a conductivity detector. The heart of the system is a six-port, two-position valve. The loop of the valve is continuously flushed with the sample solution by a peristaltic pump to waste. The other flow path of the sample valve is flushed with the eluent to the column. The sampling control and data recording are performed by an Apple IIe personal computer via laboratory-made interface electronics.

The equipment used in the measurements is as follows: sample pump, Zalimp peristaltic pump (Warsaw, Poland); eluent pump, Knauer Type 64.00 HPLC pump; sample valve, six-way mechanical rotary valve with an air actuator, a 140-μl loop and a PTFE rotor surface (Design Office, Estonian Academy of Sciences); column, anion-exchange column with sorbent RM, particle diameter 25–40 μm, phase ratio 1.1 (w/w), dimensions 150 × 4 mm I.D., with a capacity of 0.004 ± 0.002 mgeq/cm^3 (Institute of Chemistry, Estonian Academy of Sciences); detector, Knauer conductivity detector and a conductivity detector from the Design Office, Estonian Academy of Sciences (with the latter it is difficult to match the detector output voltage with the ADC input); analogue to digital converter (ADC), AKM-2, floating point (Design Office, Estonian Academy of Sciences); computer, Apple IIe; and valve actuator, a laboratory-made interface for converting the computer code into the corresponding air pulses.

The eluent was 1.3 m*M* phthalic acid (pH 4.36) at a flow-rate of 1.2 ml/min. Several sample solutions with concentrations of 0.1–10 ppm (w/w) were prepared in 1.3 m*M* phthalic acid.

Procedure

A continuous flow of sample through the valve loop was established by means of a peristaltic

pump. The flow-rate was about 7 ml/min, which ensured complete filling of the loop during a 1.95-s filling cycle. A pseudo-random injection sequence was generated by an Apple IIe computer using a 511-element pseudo-random binary sequence (PRBS) with a 1.95-s interval for each pulse. The detector signal was digitized with the same interval. During each experiment two sequences were generated, *i.e.*, 512 injections were performed during each experiment. During each injection a 1.95-s time interval was left for valve loop filling. As the flow-rate through the column was lower than that set by the peristaltic pump, the sample volume introduced in each injection was 1.95 s · 1.2 ml/min = 39 μl (not all of the 140-μl loop volume was used).

Experiment control and data processing software

The experiment control program was written in BASIC. This program generates PRBS and controls the sampling procedure via a laboratory-made digital valve interface and a pneumatic actuator. The program also records the digitized detector voltage. The detector signal after experiment was transported to an Olivetti M26 computer via cables using PROCOM software.

Detector signal preprocessing and decorrelation were performed by the Olivetti M26 computer. All this software was written in C language. Prior to decorrelation, the baseline drift was estimated by a piece-wise linear function on the monitor using the computer mouse and an interactive procedure, and subtracted from the detector signal. The occasional spikes were removed similarly. Ready-made computer programs also exist for this purpose. Decorrelation was done by a fast Hadamard transform [3]. The power spectrum of the correlogram was estimated using MATLAB software (Mathworks) to determine the cut-off frequency, applying digital filtering of the chromatograms. The cut-off frequency was determined at a point at which the standard deviation of the power spectrum amplitudes computed from higher to lower noise components remains constant. MATLAB provides several low-pass digital filters, of which we used the fifth-order Butterworth filter. After filtering the amplitudes peak areas were measured.

Injection and peak amplitude reduction

The eluent was 1.3 m*M* phthalic acid with the pH adjusted to 4.36 by adding sodium carbonate. The sample solution was prepared in phthalic acid (1.3 m*M*) without adding sodium carbonate. For such a sample the injection peak intensity is determined using two factors: the eluent anions displaced by sample anions on the ion-exchanger surface and the difference in cation concentrations between the sample and eluent solution. This gave rise to a negative system peak, as there is a deficiency of cations in the sample, unlike in the eluent. Then the sodium concentration in the sample solution was adjusted to be equal to that of the eluent solution by adding small portions of sodium carbonate to the sample vessel and registering the system peak area at the same time. This procedure was repeated until the system peak intensity was reduced to an acceptable level.

RESULTS AND DISCUSSION

Signal filtering

A typical detector output is shown in Fig. 1. Strong baseline drift is evident. Decorrelation of the detector output correlogram with and without baseline drift is shown in Fig. 2. The effect of the baseline subtraction before decorrelation is evident.

The power spectrum of the ion correlogram illustrated in Fig. 2b is shown in Fig. 3a. The

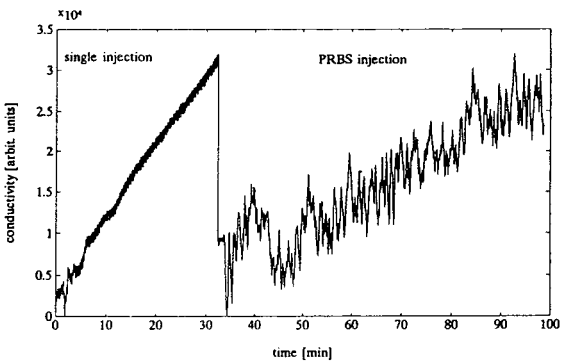

Fig. 1. Conductivity detector output obtained by single injection and PRBS injection of sample. Concentrations: Cl^- 1 ppm, NO_3^- 1.1 ppm and SO_4^{2-} 1.6 ppm. The recorder signal has been attenuated four times for PRBS injection.

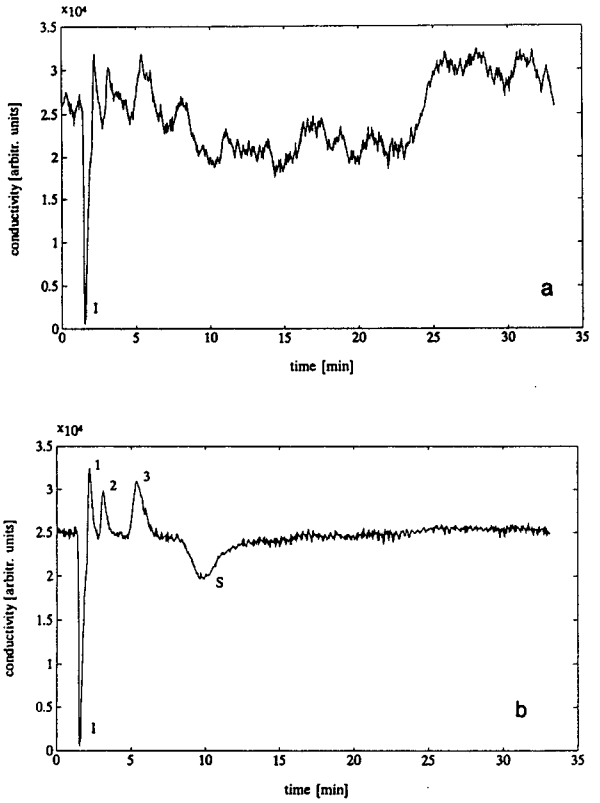

Fig. 2. Decorrelated detector outputs: (a) without and (b) with baseline subtraction before decorrelation. Peaks: I = injection; 1 = Cl^-; 2 = NO_3^-; 3 = SO_4^{2-}; S = system. Concentrations as in Fig. 1.

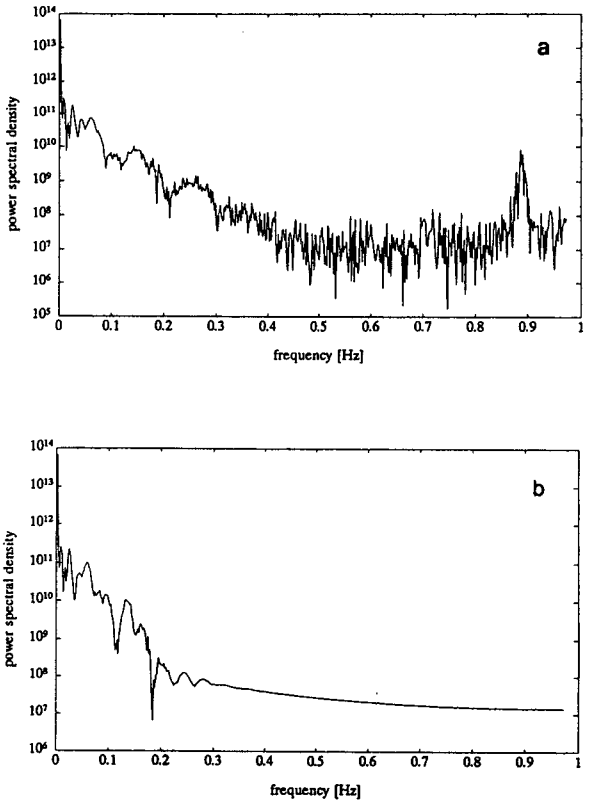

Fig. 3. Power spectrum of the chromatogram from Fig. 2b: (a) before and (b) after digital filtering with fifth-order Buttworth filter.

peak frequency components (peak information) are located at lower frequencies (from 0 to 0.3 Hz), whereas the noise components spread at higher frequencies. The cut-off point is around 0.3 Hz, as is clearly distinguishable. Also, the sharp-noise components present at 0.9 Hz are apparently related to the pumping system of the chromatograph used. They were present all of the power spectra. The presence of the peak that corresponded to the pump pulsations demonstrated that the efficiency of the laboratory-made damper is inadequate. The power spectrum of the same correlogram after applying the fifth-order Buttworth low-pass filter with a cut-off frequency of 0.25 Hz is shown in Fig. 3b.

The PRBS injection chromatogram after applying a low-pass filter is presented in Fig. 4. A comparison of Figs. 4 and 2b demonstrates that

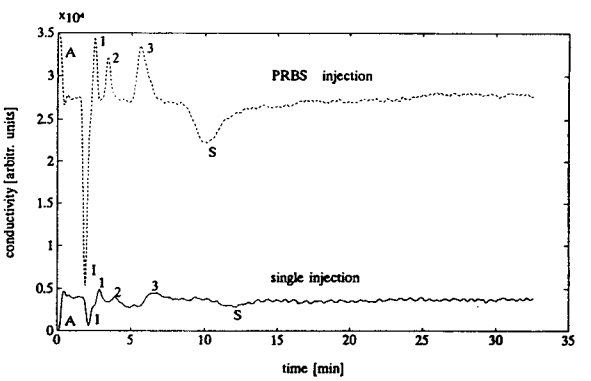

Fig. 4. Decorrelated chromatogram from Fig. 2b after filtering, and baseline-subtracted and filtered single-injection chromatogram from Fig. 1. A = artifact due to filtering procedure; other peaks and concentrations as in Fig. 2.

the digital filtering was an efficient means of removing high-frequency components from the ion correlograms. This proved to be especially true of the removal of narrow-band deterministic signal components such as disturbances from pump oscillations. The same filtering procedure and baseline subtraction were also performed for the single-injection chromatogram shown in Fig. 1. The result shown in Fig. 4 demonstrates that CC can improve the signal-to-noise ratio of a chromatogram under the present experimental conditions. The improvement in the signal-to-noise ratio was *ca.* 10-fold, compared with the theoretical improvement of 11.3-fold.

Valve and column performance

Careful inspection of the correlogram in Fig. 4 reveals that the intensities of the ghost peaks are too low compared with those of real peaks to appear in the chromatogram as deviations distinguishable from the baseline. The low intensity of the ghost peaks demonstrates that the sampling valve performance is acceptable within one correlation experiment. However, after 8–10 correlation experiments the valve performance decreased significantly, being manifested by an increase in the ghost peak amplitude on the correlogram (Fig. 5). This was indicative of the need for valve rotor treatment. The position of a ghost peak should indicate the nature of the sampling system imperfection [6]. Inspection of the rotor flow paths used demonstrated that they are filled with PTFE rotor material. Evidently the PTFE particles in the flow paths are scrubbed from the rotor surface by a stator.

An increase in the number of PTFE particles in rotor flow paths and their possible penetration into the sampling loop will apparently reduce the sampling loop and path volumes and one could therefore expect an increase in the restriction of the sample flow and a decrease in the sample flow-rate within the valve, which in turn would result in incomplete loop filling, leading to a specific ghost peak at the end of the correlogram [6]. Hence the behaviour of the sampling valve in our experiments seems to be in accordance with the predictions of CC theory. However, this explanation is a preliminary one and further studies are required in order to establish this fact exactly. After cleaning PTFE particles from the flow paths the ghost peak problems were eliminated.

In most specifications of IC columns, the column lifetime is given as the number of injections that the column is able to accept, which is in the range 5000–10 000. In ion CC this number is exhausted during only one or two experiments. No deterioration in column performance was observed during our experiments. This discrepancy with previous observations means that the column lifetime in IC probably depends on the volume and cleanliness of the eluent and samples that have passed through the column, which on the other hand can be related to the number of injections (as a measure of number of recorded chromatograms) in single-injection chromatography.

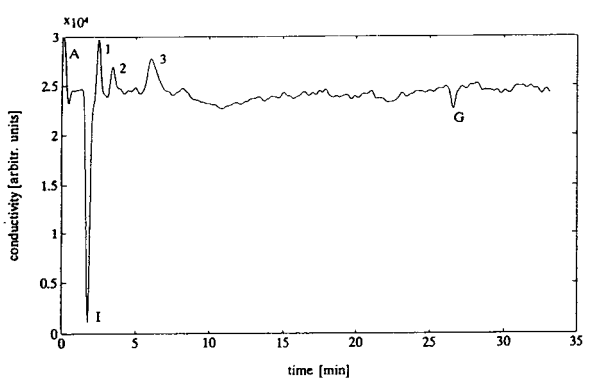

Fig. 5. A correlogram obtained with an imperfect input valve. G = ghost peak.

Measurement of sample concentrations near the detection limit

The calibration graph for common anions measured over a concentration range of about 1.5 decades is shown in Fig. 6. the limits of detection calculated for a signal-to-noise ratio for Cl^-, NO_3^- and SO_4^{2-} were 0.1, 0.12 and 0.17 ppm, respectively. The example chromatograms given in the Knauer detector manual for the Vydac column demonstrate that the detection limit for common anions for this detector is about 1–3 ppm in single-injection non-suppressed ion chromatography [7]. Thus, CC enables the detection limit to be decreased by

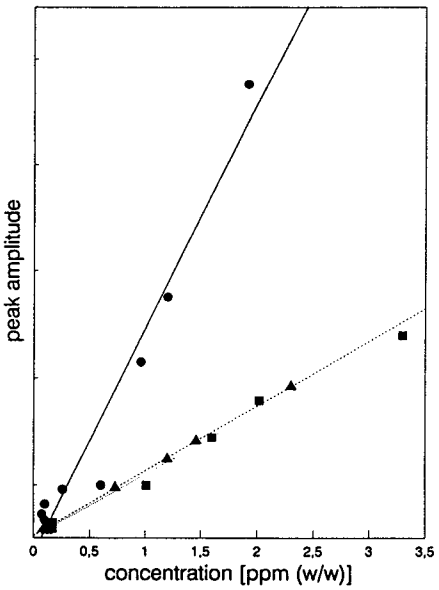

Fig. 6. Calibration graph. ● = Cl^-; ▲ = NO_2^-; ■ = SO_4^{2-}.

about one order of magnitude. The calibration points lie on the regression lines with correlation coefficients of 0.95, 0.996 and 0.993 for Cl^-, NO_3^- and SO_4^{2-}, respectively. The relatively low correlation coefficient for the Cl^- ion is due to the errors in Cl^- peak-area measurements because its peak badly interferes with the negative injection peak.

The detection limits obtained in this work reflect the possibilities achievable with the available equipment. By combining CC with eluent conductivity suppression the detection limit can be lowered by a further order of magnitude. Also, modern conductivity detectors allow work in the ppb region. Using the trace enrichment technique detection limits in the sub-ppb region have been obtained [8]. Hence CC provides an alternative to trace enrichment methods, the drawbacks of which are well known.

REFERENCES

1 C. Mars and H.C. Smit, *Anal. Chim. Acta*, 228 (1990) 193.
2 M. Kaljurand, E. Urbas and U. Haldna, *Chromatographia*, 34 (1992) 417.
3 M. Kaljurand and E. Kullik, *Computerized Multiple Input Chromatography*, Ellis Horwood, Chichester, 1989.
4 P.R. Haddad and P.E. Jackson, *Ion-Chromatography—Principles and Application*, Elsevier, Amsterdam, 1990.
5 R. Strassburg and J.S. Fritz, *J. Chromatogr.*, 482 (1989) 343.
6 R. Mulder, P.J. Hoogerbrugge and H.C. Smit, *Chemometr. Intell. Lab. Syst.*, 1 (1987) 243.
7 *Knauer Conductivity Detector Operating Manual*, No. 206.1106600, Knauer, Berlin, 1983.
8 G. Blo, M. Remelli, F. Pedrielli, L. Balconi and F. Sigon, *J. Chromatogr.*, 556 (1991) 249.

Journal of Chromatography A, 660 (1994) 153–167
Elsevier Science B.V., Amsterdam

CHROMSYMP. 2931

Enzyme-based biosensor as a selective detection unit in column liquid chromatography

György Marko-Varga*, Kristina Johansson☆ and Lo Gorton

Department of Analytical Chemistry, University of Lund, P.O. Box 124, S-221 00 Lund (Sweden)

ABSTRACT

A reagentless enzyme electrode based on co-immobilized alcohol oxidase and horseradish peroxidase was used as the working electrode in an amperometric flow-through cell connected to a column liquid chromatographic (CLC) system for the selective detection of methanol and ethanol. The enzymes were covalently immobilized in carbon paste (graphite–phenylmethylsilicone oil) in the presence of polyethylenimine. Electrodes prepared from the enzyme-modified carbon paste were optimized with respect to their sensitivity and selectivity. Different membranes were cast or electropolymerized directly on the surface of the electrode to increase the long-term stability of the biosensor. The compatibility with the reversed-phase chromatographic system was established. A PLRP-S polymer-based separation column was used with phosphate buffer as the mobile phase. The selectivity of the enzyme electrode was also determined by injecting some easily oxidizable and possibly interfering species normally present in biological samples. The enzyme electrode was also used in an on-line system, consisting of a microdialysis probe as the sampling unit, the CLC system and the biosensor detection device, for the selective following of the ethanol produced when a paper pulp industrial waste water was fermented with *Saccharomyces cerevisiae*.

INTRODUCTION

Derivatization techniques are widely used in column liquid chromatography (CLC) in both the pre- and postcolumn modes in order to enhance detectability and/or increase sensitivity [1–4]. Most commonly the reagents taking part in the reaction detection are solid-phase reagents immobilized on a liquid support. Both silica and polymeric supports are used and the coupling of the reactive modifier to the support is commonly achieved by physical adsorption, covalent binding or coating through precipitation. Solid-phase reagents offer advantages such as more efficient derivatization yield due to an improved chemical stability of the immobilized reagents, increased reaction capacities due to the high local concentration of the derivatization reagent, and in many cases the derivatization reactions are subject to fewer side-reactions [5]. Biological recognition is used to improve selectivity further by the use of enzymes or antibodies mainly immobilized in solid-phase reactors. Enzymes are by far the most commonly used catalytic derivatization reagents in CLC. They are easily made compatible in various flow systems and are therefore nowadays common and acknowledged as bioselective detection units in CLC and flow injection (FI), determining solutes in a selective and sensitive way [6–9]. It is predicted that highly selective immunological interactions between antibodies and antigens will have a great impetus in future selective detection systems in both CLC and FI [10–12]. The increased commercial availability of various enzymes and antibodies will be of great importance in this field. Immobilized enzymes on solid supports are already commercially available from several manufacturers, also supplying chromatographic col-

* Corresponding author.
☆ Present address: Astra Draco, P.O. Box 34, S-221 00 Lund, Sweden.

0021-9673/94/$07.00 © 1994 Elsevier Science B.V. All rights reserved
SSDI 0021-9673(93)E0940-V

umns and optimized integrated systems for applications in various fields.

The most commonly studied field of biosensors is the enzyme electrode. Clark and Lyons [14] predicted the construction of an enzyme electrode in 1962 [13] and in 1967 Updike and Hicks [14] were the first to report on the construction and use of a glucose electrode by physically entrapping glucose oxidase by a dialysis membrane close to a Clark-type oxygen electrode. Since then, there has been rapid progress in the development of enzyme electrodes and more than 1200 original papers have appeared on glucose determinations alone. The enzyme electrode is based on the immobilization of the enzyme in close proximity to, *e.g.*, in a membrane, or directly on or in the electrochemical transducer, most commonly consisting of noble metals or various carbonaceous-type electrodes including carbon paste. Enzyme electrodes have most often been developed for batch analysis or in combination with non-chromatographic flow systems. Enzyme-based detection in CLC has, however, most often been effected by the use of immobilized enzyme reactors (IMERs), where the enzyme is bound on an inert solid support [8,9]. Only a few papers have reported on the use of such materials in detectors in conjunction with CLC [15], mainly because the sensors studied were developed for the specific analysis of one analyte only. However, Yao and Wasa [16] illustrated in a very elegant way the possible use of enzyme electrodes in conjunction with CLC by using a double electrochemical flow cell approach in which L- and D-amino acid oxidase were immobilized on two different electrodes for the stereoselective analysis of L- and D-amino acids. Both of these enzymes are group- rather than one substrate-specific enzymes [16–20]. This makes it possible to use common liquid chromatographic supports and separations in comparison with highly specific chiral stationary phases.

Ethanol and other alcohols are important compounds to be determined in a number of different fields, such as in medicine, the food industry and biotechnology. A variety of methods for their determination already exist. However, the simultaneous determination of, *e.g.*, the sugar and alcohol contents in biotechnical processes would benefit greatly if the same (on-line) system could be used for their sampling and separation but using selective detection devices reflecting their individual concentrations. With respect to alcohol measurements, the selective and sensitive detection of methanol, ethanol and other short-chain aliphatic alcohols in FI and CLC can be achieved by the use of either alcohol oxidase (AOD) or alcohol dehydrogenase (ADH) [21–33], both enzymes being group- rather than absolute substrate-specific. As with all redox enzymes, AOD and ADH depend on a co-factor for activity. In the case of AOD, the redox cofactor is flavin adenine dinucleotide (FAD) strongly bound within the enzyme structure, whereas ADH depends on nicotinamide adenine dinucleotide (NAD^+) acting as a soluble co-substrate. Both of these enzymes have been studied in amperometric biosensor configurations and in immobilized enzyme reactors with both silica- and polymer-based supports [34]. There are pros and cons with both of these enzymes. AOD needs molecular oxygen as the natural reoxidation agent (electron–proton acceptor) resulting in the production of hydrogen peroxide:

$$\text{alcohol} + O_2 \xrightarrow{\text{AOD}} \text{aldehyde} + H_2O_2 \qquad (1)$$

The equilibrium of the reaction strongly favours the product side, owing to the strong oxidizing power of oxygen. The low solubility of molecular oxygen and the difficulties encountered with following electrochemically either the decrease in oxygen or the production of hydrogen peroxide are the main obstacles to be overcome. Additionally, AOD has been reported to suffer from a restricted long-term stability [35,36].

Some problems with restricted long-term stability of enzymes can be solved with their immobilization. Of particular interest is the reported increase in operational stability when the enzyme is immobilized into an organic phase [37]. Organic phase electrochemical transducers are found within the group of carbon paste and composite electrodes [38]. These electrodes are easily bulk modified compared with solid electrodes only allowing surface modification. Enzymes, stabilizers, activators, necessary cofac-

tors, mediators, etc., can be introduced and homogeneously distributed in the electrode material [19,20,27–30,32,33,37,38]. The coupling of charge-transfer reactions between redox enzymes and electrochemical transducers can be greatly facilitated by the use of redox mediators shuttling the electrons between the conducting material and the cofactor of the redox enzymes at substantially decreased overvoltages.

Recent reports on the further stabilization of a series of redox enzymes including AOD by adding polyelectrolytes and sugar derivatives suggest AOD rather than ADH to be a good candidate for further studies for the construction of reliable amperometric biosensors for alcohol measurements [27,35,36]. As a step in that direction, we report here on the use of a reagentless amperometric alcohol biosensor based on co-immobilized alcohol oxidase (AOD) and horseradish peroxidase (HRP) in carbon paste. Increased stabilization of the enzymes in the paste and improved response characteristics of the sensor are obtained by a proper choice of immobilization reagents and other additives to the paste. The biosensor was used as a selective detector in CLC for the analysis of short-chain aliphatic alcohols. Further optimizations were made in order to improve the stability of the sensor by covering the electrode surface with different membranes. The biosensor detection unit–CLC system was implemented in an on-line system using a microdialysis sampling unit to follow the ethanol production in a fermentation based on a technical lignocellulose hydrolysate as substrate.

EXPERIMENTAL

Chemicals

Ethanol of the highest quality (99.5%, spectrographic grade; Kemetyl, Stockholm, Sweden) was used as received. All solutions, the mobile phase of the chromatographic system and the perfusion medium in the microdialysis unit were prepared by using a Milli-Q water purification system (Millipore, Milford, MA, USA). The mobile phase used in the chromatographic system consisted of either 50 m*M* phosphate buffer (pH 7.5) or 4 m*M* sulphuric acid prepared by dilution of concentrated sulphuric acid (Merck, Darmstadt, Germany), depending on the chromatographic column used (see below). The mobile phase and the perfusion medium used in the microdialysis probes were first filtered through 0.22-μm sterile filters (Millex HA, Millipore) and then degassed with helium. *o*-Phenylenediamine (*o*-PDA), phenol, aniline, pyrrole, *m*-phenylenediamine (*m*-PDA) and resorcinol were of analytical-reagent grade and used as received. Eastman AQ-29D was a gift from Dr. W. Waeny, Eastman Chemical International, Zug, Switzerland. All other chemicals were of analytical-reagent grade and used as received.

Preparation of the enzyme electrode

Alcohol oxidase (AOD) (EC 1.1.3.13, from *Candida boidinii*, Serva, 30.3 U mg^{-1}) and horseradish peroxidase (HRP) (EC 1.11.1.7, Sigma, 270 U mg^{-1}) were used as received. Chemically modified carbon paste (CMCP) electrodes were prepared according to a previous investigation [27]. Graphite powder (Fluka) was heated at 700°C for 15 s in a muffle furnace and cooled to ambient temperature in a desiccator. Next, the graphite powder was activated with 1-cyclohexyl-3-(2-morpholinoethyl)carbodiimide metho-*p*-toluenesulphonate ("carbodiimide") (Janssen Chimica). A 4.2-mg amount of carbodiimide was dissolved in 300 μl of 0.05 *M* acetate buffer at pH 4.8 per 100 mg of graphite and allowed to react for 2 h at ambient temperature. The activated graphite was then rinsed with pure water seven times and dried under vacuum for 4.5 h before addition of 1.5 mg (*ca.* 400 U) of HRP and 4.5 mg (*ca.* 140 U) of AOD dissolved in 200 μl of 0.1 *M* phosphate buffer (pH 7.0). The immobilization reaction mixture also contained 0.12% of glutaraldehyde (Sigma, 25% aqueous solution) added to the enzyme solution just prior to mixing with the graphite powder. The glutaraldehyde was purified from polymers by centrifugation with active carbon. Finally, 200 μl of a 0.32% solution of polyethyleneimine (PEI) (Sigma, 50% aqueous solution) were also added before allowing the mixture react for 16 h at 4°C. Subsequently, the reaction mixture was dried under vacuum before addition of the pasting liquid, 40 μl of phenylmethylsilicone oil

(silicone DC 710; Alltech Associates, Arlington Heights, IL, USA) to produce the final CMCP.

Plain graphite–paraffin oil paste (40 μl of paraffin oil were mixed with 100 mg of graphite powder) was filled into plastic syringe holders (1.0-ml syringe, Brunswick 81/79J03, with a tip of 7.0 mm O.D. and 1.8 mm I.D.), leaving about 3–4 mm empty at the top to be filled with the CMCP to produce the final electrode. Electrical contact was made by inserting a gold wire in the CP. After the tip of the syringe had been filled with enzyme-modified carbon paste, the end was gently rubbed on glass to produce a flat, shiny electrode surface with an area of about 0.024 cm^2. A schematic diagram of the electrode is shown in Fig. 1.

The surface of some electrodes was covered with an electropolymerized layer of poly-*o*-phenylenediamine, polyaniline, polyphenol, polypyrrole or a copolymer obtained through the combination of *m*-phenylenediamine and resorcinol. The poly-*o*-phenylenediamine film was made by dipping the electrode into a 0.5 *M* acetate buffer solution (pH 5.2) containing 5 m*M* *o*-PDA [39] and running a series of cyclic voltammograms (scan rate 50 mV s^{-1}) between 0 and +650 mV *vs.* a saturated calomel electrode (SCE) [27]. The electropolymerized layers of the other monomers were similarly obtained with some alterations to the experimental conditions. Polypyrrole was formed in 5 m*M* pyrrole dissolved in 1 *M* KCl [40]. Polyaniline or polyphenol was formed in solutions containing 5 m*M* of the monomer dissolved in 0.1 *M* phosphate buffer (pH 7.0) [41,42]. The electropolymerized layer of the combination *m*-PDA and resorcinol was formed in 0.1 *M* phosphate buffer (pH 6.5) also containing 1.5 m*M* of each monomer [43]. Cyclic voltammetry was employed using a platinum gauze as the counter electrode and an SCE, as the reference electrode in these experiments. Additionally, some electrodes were further surface modified through the following procedure. After rinsing the electrode carefully with distilled water, the electrode was covered with an Eastman AQ 29D cation-exchange membrane by dipping the electrode into a solution containing 0.5% of the cation exchanger dissolved in water and letting the electrode dry for at least 20 min between dippings [21,27,44,45]. This procedure was repeated five times. After the last dipping the electrode was dried for 1 h before use. In all instances, when not in use the electrodes were kept in a dry state at 4°C.

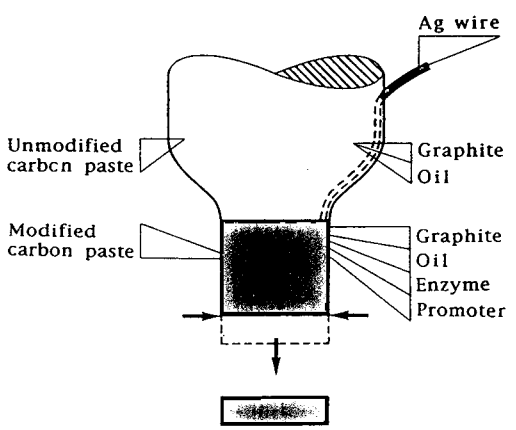

Fig. 1. Schematic diagram of the enzyme-modified carbon paste electrode.

Apparatus

The final electrodes were mounted in a flow-through amperometric cell of the confined wall-jet type [46] under three-electrode potentiostatic control using a Princeton Applied Research Model 174A instrument. A platinum wire and Ag/AgCl (0.1 *M* KCl) served as the counter and reference electrodes in the cell. The detector was connected to either a single-line flow-injection (FI) system or a column liquid chromatographic (CLC) system. The FI system consisted of a peristaltic pump (Gilson Minipuls 2) and a pneumatically operated valve (Cheminert, Type SVA) with an injection volume of 50 μl. Connections between the different parts of the FI system were made of Teflon tubing of 0.5 mm I.D. and with Altex screw couplings. The flow buffer, consisting of 0.1 *M* phosphate buffer (pH 7.5), was pumped at a flow-rate of 0.8 ml min^{-1}. The chromatographic system is depicted in Fig. 2 and consisted of a Model 2150 HPLC pump (LKB, Bromma, Sweden), a CMA/160 on-line injector (CMA/Microdialysis, Stockholm, Sweden) fitted with a 20-μl injection loop (Valco CGW-K; Vici, Zug, Switzerland), and one

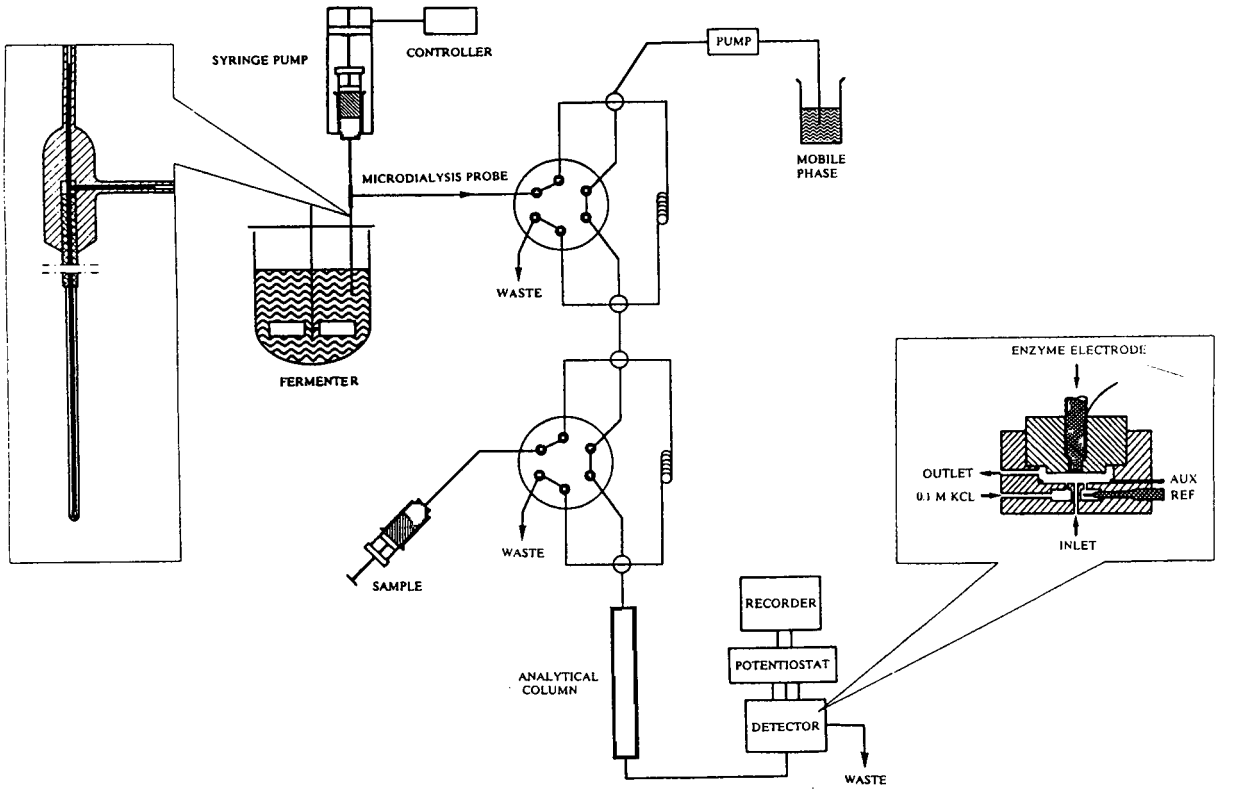

Fig. 2. Set-up for on-line analysis of fermentation broth including microdialysis sampling probe, CLC system and the electrochemical flow-through cell incorporating the biosensor.

Model 7045 six-port switching valve (Rheodyne, Cotati, CA, USA) equipped with a 19.6-μl injection loop, a polymer-based analytical column (50 × 4.0 mm I.D.) (PLRP-S, Polymer Labs., Church Stretton, Shropshire, UK), the same amperometric flow cell as described above, a potentiostat (Zäta Elektronik, Lund, Sweden) and a Model 2077 chart recorder (LKB). With the chromatographic system 50 m*M* phosphate buffer (pH 7.5) was used.

Another CLC system was also used (not shown) consisting of the pump, one injector and the recorder as above but with a polymeric cation-exchange analytical column in the hydrogen form (Model HPX-87H; Bio-Rad Labs., Richmond, CA, USA) operated at an elevated temperature of 40°C in a column oven (Model 2055, LKB) with sulphuric acid (4 m*M*) used as the mobile phase, and a refractive index detector (model 2142, LKB).

The fermentation substrate, spent sulphite liquor (SSL), used for ethanol production was a waste water from the pulp industry. It originally had a pH of 3.2, which was adjusted by addition of sodium hydroxide (5 *M*) to a final pH of 6.0. SSL was obtained from a paper pulp plant (MoDo, Örnsköldsvik, Sweden). Baker's yeast, *Saccharomyces cereviseae* (Jästbolaget, Stockholm, Sweden), was first dissolved in 5.0 ml of water and then added to the substrate to give a final concentration of 80 g l^{-1}. A beaker (10 ml) was used, sealed with a rubber screw fitting, for the ethanol fermentation broths. Microdialysis probes (CMA/10, CMA/Microdialysis) containing a polycarbonate membrane (0.5 mm O.D., length 10 mm, M_r cut-off 20 000) were used in conjunction with a syringe pump incorporating a control unit (CMA/100 microinjection pump, CMA/Microdialysis) and coupled on-line with the CLC system as indicated in Fig. 2.

RESULTS AND DISCUSSION

The direct electrochemical conversion of hydrogen peroxide suffers from too high an applied potential at the working electrode, which may open up the detection system for other possibly present compounds that are easily oxidizable and would thus contribute to the response signal and counteract the use of a selective enzyme in the detection system. Much work has been focused on trying to make it possible to operate oxidase-based electrodes at less extreme potentials, either by the use of chemically modified electrodes incorporating catalysts for electrochemical conversion of hydrogen peroxide or by the use of artificial mediators exchanging molecular oxygen as the electron acceptor in the enzymatic process and also facilitating the charge transfer to the electrode at substantially lower applied voltages. Recently, several papers have described the use of electrodes on which peroxidase has been immobilized, acting as a very efficient catalyst for electrochemical reduction of hydrogen peroxide [27,32,33,47–50]:

$$H_2O_2 + 2H^+ + 2e^- \xrightarrow{\text{peroxidase}} 2H_2O \qquad (2)$$

Reaction 2 starts at about +600 mV *vs.* Ag/AgCl and its rate increases as the applied potential is made more negative. Maximum response currents are obtained within the optimum working potential range for an amperometric biosensor, between about −150 and 0 mV *vs.* Ag/AgCl, where the background current switches signs, resulting in low noise and background current levels and where molecular oxygen and easily oxidizable compounds contribute not at all or very little to the response signal. In most cases, a direct electron transfer exchange between a redox enzyme and an electrode is obscured by steric or kinetic limitations, and the use of artificial mediators has often been used to facilitate electric communication between the enzyme and the electrode [51]. In the case of immobilized peroxidases on preferentially carbonaceous electrodes, it seems as though a direct charge-transfer process can be accomplished. HRP in its native form reduces hydrogen peroxide in a single two-electron step whereby water and an oxidized form of the enzyme denoted compound I are formed. Compound I is re-reduced to the native form in two separate one-electron steps with the intermediate formation of compound II as described previously [25].

A series of different reducing agents are able to donate these necessary electrons [52]. Here, the carbon material in the electrode can obviously function as a source of electrons without the deliberate addition of any other reducing agent, thus making it possible to produce a reagentless sensor for hydrogen peroxide. The mechanism, however, has been much debated [27,47,50].

The alcohol oxidase sensor consists of two enzymes, alcohol oxidase (AOD) and HRP, co-immobilized in a carbon paste electrode material. AOD, a non-substrate-specific enzyme, oxidizes its substrates to form H_2O_2 according to reaction 1 using molecular oxygen as the electron acceptor. In a following step, H_2O_2 is electrochemically reduced through the action of HRP. The entire reaction sequence utilizing the coupled enzyme reactions in the amperometric biosensor is illustrated in Fig. 3.

Membrane deposition and its impact on the selectivity of the biosensor performance

Membranes cast directly on or formed through electropolymerization of electroactive monomers on electrode surfaces have been used for different purposes in conjunction with enzyme-based amperometric biosensors [25,27,34,39–45,53]. Enzymes can be immobilized within the membranes, an increased stability has been observed of enzymes immobilized on/in the membrane-covered electrodes, and membranes can act as size- or charge-exclusion barriers to prevent possible interfering compounds in the sample

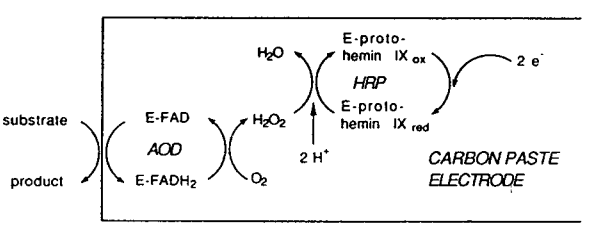

Fig. 3. Reaction sequence of the biosensor incorporating co-immobilized AOD and HRP.

matrix from reaching the true electrode surface and also prevent enzymes from leaking out from bulk modified electrode material. A membrane can also act as an additional diffusion resistance for the substrates of the enzymes to reach the electrode surface. The noticeable effect will be that the linear part of the calibration graph will be shifted towards higher concentrations of the substrate as an effect of an increase in the apparent Michaelis–Menten constant, K_M^{app}. This may be advantageous in biosensor systems when using enzymes with low K_M values, as the linear part of the calibration graph will be extended even though the sensitivity will decrease.

A series of different membranes were therefore investigated for this alcohol sensor in order to increase the operational stability and extend the linear calibration characteristics. In order to determine the substrate specificity of the biosensor, some possible substrates were investigated on a naked uncoated electrode surface (see Table I). Five different types of electropolymerized membranes were thereafter investigated, poly-*o*-PDA, polyphenol, polypyrrole, polyaniline and a copolymer obtained from *m*-PDA and resorcinol. Additionally, covering with a cation-exchange membrane formed through evaporation of the aqueous solvent directly on the electrode surface was also investigated. The procedures for making electropolymerized membranes have been described previously [39–43]. Essentially the same procedures were used in this work with the exception that the concentration of the monomers when forming the polyaniline, polypyrrole and polyphenole membranes was decreased from the molar to the millimolar level. Fig. 4 shows some cyclic voltammograms obtained when forming these electropolymerized membranes. Included are background voltammograms obtained in the absence of the electroactive monomers (the lower flat-looking voltammograms) and also the voltammograms registered after five voltammetric cycles. For all monomers (A, *o*-PDA; B, phenol;

TABLE I

RELATIVE RESPONSE FOR SOME POSSIBLE SUBSTRATES FOR THE ALCOHOL BIOSENSOR IN A FI SYSTEM

Compound	Relative response (%)
Ethanol	100
Methanol	240
Formaldehyde	170
Acetaldehyde	<0.2
Propionaldehyde	<0.2
Butyraldehyde	<0.2
Formic acid	<0.2
Acetic acid	<0.2
Propionic acid	<0.2
Butyric acid	<0.2
Monochloroacetic acid	<0.2
Citric acid	1.8
Lactic acid	11
Malic acid	0.4
Pyruvic acid	8.4
Inositol triphosphates	0.9
Dihydroxyacetone	2.6

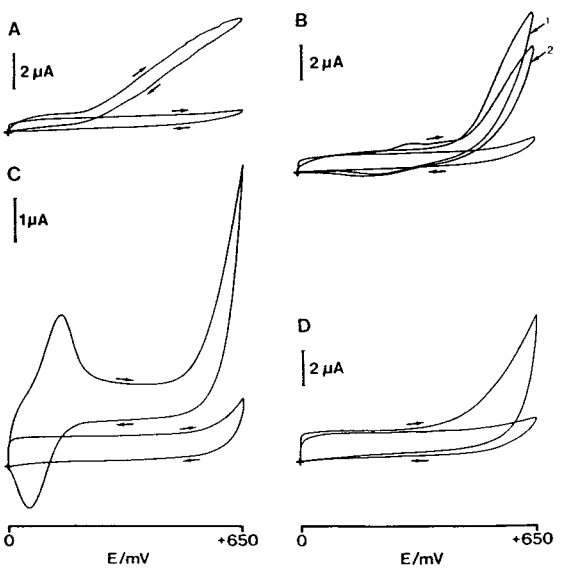

Fig. 4. Cyclic voltammograms obtained when electropolymerizing (A) poly-*o*-PDA, (B) polyphenol, (C) polyaniline and (D) polypyrrole on the biosensor surface. The cyclic voltammograms shown were obtained after running five cycles, except in (B) where both the first (1) and the fifth (2) cyclic voltammograms are shown as indicated. The lower cyclic voltammograms also included in all figures are those obtained in the absence of monomers in the contacting solution. The arrows indicate sweep direction and + the starting potential. For further details, see Experimental.

C, aniline; and D, pyrrole) a drastic increase in the anodic current is seen, at potentials determined by the monomer, reflecting the oxidation of the monomers to form reactive radicals which in turn will react with unoxidized monomers forming the membrane on the electrode surface. In Fig. 4B is also the first voltammograms in the presence of phenol, included to illustrate the difference in wave form compared with the fifth scan. What can be noticed is that the anodic wave will successively decrease as a result of partial blocking of the electrode surface by membrane formation preventing phenol from reaching the electroactive surface. What is also noticed on comparing the different voltammograms is that a second electroactive species is formed when electropolymerizing phenol (B) and aniline (C), but not for *o*-PDA (A) and pyrrole (D), reflected by the reversible voltammetric waves appearing at around +150 V for polyaniline and +300 mV for polyphenol. The structures in these films will incorporate redox functionalities in their respective reduced states basically of *p*-quinone (polyphenol) or *p*-phenylenediamine structures known to acts as electron donors for compounds I and II (discussed above). Even though an increased diffusional barrier has been created at the electrode surface, the FI response to hydrogen peroxide will increase after forming the initial polyaniline and polyphenol membranes, reflecting the electroactivities of these membranes (see Table II). This is not observed for the other electropolymerized membranes lacking electroactivity. In Table II are shown the effect on the response to both ethanol and hydrogen peroxide for two equivalently prepared electrodes obtained in the FI mode as a result of various thicknesses of the electropolymerized layers.

Recently, a series of papers have appeared describing electrodes covered with a new anion-exchange polymer, which, contrary to another very popular electrode anion-exchange modifier, Nafion [54], can be obtained in an aqueous soluble form [27,44,45]. A series of premade polymers, denoted AQ, containing negatively charged groups covalently bound within the polymeric backbone are available from Eastman Chemical. This special kind of polymer suits the purpose of casting an ion-exchange membrane directly on an enzyme-covered electrode surface very well [27,44,45]. Because of the charged

TABLE II

SIGNAL RESPONSE FOR VARIOUS ELECTROPOLYMERIZED MEMBRANES ON THE ALCOHOL BIOSENSOR IN A FI SYSTEM

Membrane	Number of CVs	Response, *i* (nA)		Relative response (%)	
		EtOH	H_2O_2	EtOH	H_2O_2
Polypyrrole	0	571	806	100	100
	2	374	716	65	89
	5	338	660	59	82
	20	208	586	36	73
	0	510	722	100	100
	2	392	630	77	87
	5	364	618	71	86
	20	344	548	67	76
Aniline	0	436	605	100	100
	2	511	761	117	126
	5	430	721	99	119
	20	233	597	53	99
	0	577	676	100	100
	2	584	844	101	125
	5	502	824	87	122
	20	260	666	45	99
Phenol	0	588	584	100	100
	2	504	592	86	100
	5	446	462	76	79
	20	213	182	36	35
	0	645	613	100	100
	2	639	611	99	89
	5	548	484	85	82
	20	305	214	47	73
o-Phenylenediamine	0	632	633	100	100
	2	519	477	82	75
	5	503	494	80	78
	20	420	317	66	50
	0	525	503	100	100
	2	447	371	85	74
	5	444	390	85	78
	20	376	288	72	57
	0	647	737	100	100
m-Phenylenediamine and resorcinol	2	486	326	75	44
	5	407	249	63	34
	20	228	53	35	7
	0	698	652	100	100
	2	511	379	73	58
	5	391	211	56	32
	20	178	41	35	6

groups, the polymer can be dissolved in water at an elevated temperature (95°C). This polymer–water solution will stay in a homogeneous state at room temperature, but once dried it is no longer water soluble. The pH of the polymer–water solution is between 5 and 6, causing no serious effects when applied to an electrode surface containing biochemical ingredients. There are obvious advantages of casting the membrane directly on the electrode surface compared with covering an electrode with a premade membrane. Thinner membranes can be made and direct adhesion of the membrane to the electrode surface is possible, etc. The AQ membrane was shown to have excellent properties with both oxidases [27,44] and dehydrogenases [21,45] and also with HRP with respect to stability (see below). Membranes of this type will certainly be of continuous use in further studies of enzyme electrodes. The possibility of using the negative charges within the membrane as possible immobilization sites for enzymes has already been investigated [55]. The effect on the use of the AQ membrane on this AOD/HRP electrode was therefore also investigated. As expected, after membrane formation the response to ethanol and hydrogen peroxide decreased by about 10–20% depending on the membrane thickness (data not shown).

The selectivity of the alcohol sensor is shown in Table III and IV for a number of possible electroactive interfering compounds and well known solutes in biological fluids and biotechnological samples, respectively. The values given are the mean values obtained after at least five injections of each compound. The relative responses for ethanol of the different electrodes after exposure to these compounds are also included for comparison. For the uncovered electrode, some decrease in the response to ethanol is obtained, whereas the stability-enhancing effect on the response to ethanol is shown for the covered electrodes. A drastic decrease in the relative response to ascorbate is registered for the polypyrrole- and Eastman AQ-covered electrodes, as expected by the negatively charged AQ membrane.

Table IV shows some additional results obtained for some other possibly interfering compounds not necessarily electroactive within the applied potential range but known to foul the electrode surface. For all electrodes, including the uncovered type, virtually the initial response remains after exposure to these compounds.

TABLE III

MEMBRANE CHARACTERISTICS OF ALCOHOL BIOSENSOR WHEN EXPOSED TO WELL KNOWN BIOMEDICAL INTERFERENTS (EXPERIMENTS PERFORMED IN THE FI SYSTEM)

Analyte	Relative response (%)						
	Without membrane	Eastman AQ-29D	Polypyrrole	Polyaniline	Polyphenol	Poly-*o*-PDA	Copolymer of *m*-PDA and resorcinol
Ethanol	100	100	100	100	100	100	100
Adenosine	0.4	0.7	1.4	1.8	0.8	1.4	1.3
Ascorbate	−806	−134	−70	−552	−249	−995	−453
Glucose	0.6	0.4	<0.2	1.7	0.4	1.9	0.9
Lactate	15	15	17	13	14	16	13
Paracetamol	0.8	0.7	1.0	2.5	0.4	1.9	1.3
L-Phenylalanine	0.4	<0.4	0.2	2.1	0.6	1.6	0.9
Terbutaline sulphate	1.7	<0.4	1.4	1.4	0.9	2.2	1.3
Ethanol		82	115	95	97	100	112

TABLE IV

MEMBRANE CHARACTERISTICS OF THE ALCOHOL BIOSENSOR WHEN EXPOSED TO POSSIBLE ELECTROACTIVE BIOTECHNICAL INTERFERENTS IN THE FI SYSTEM

Analyte	Relative response (%)				
	Without membrane	Eastman AQ-29D	Poly-*o*-PDA	Polyphenol	Polyaniline
Ethanol	100	100	100	100	100
Phenol	<0.1	<0.3	<0.1	<0.2	<0.1
m-Cresol	<0.1	<0.3	<0.1	0.2	<0.1
Benzaldehyde	<0.1	<0.3	<0.1	<0.2	<0.1
Furfuralaldehyde	<0.1	<0.3	<0.1	<0.2	<0.1
5-Hydroxymethyfurfural	1.7	2.8	1.8	0.8	0.3
Saccharomyces cerevisiae	0.2	<0.3	0.8	<0.2	<0.1
Bovine serum albumin	130	96	115	117	142
Ethanol	104	95	101	83	94

What is clear is that the AQ membrane has the most strongly excluding effect for BSA and yeast cells.

The results in Tables III and IV suggest that a combination of first forming one electropolymerized membrane on the electrode surface followed by an additional covering with a layer of the Eastman AQ would give the most suitable and versatile protection of the electrode surface. A series of electrodes were therefore made with the combination of poly-*o*-PDA (five cyclic voltammograms) and Eastman AQ 29D (dipping three times). These electrodes were used in conjunction with the on-line measurement of ethanol production in the fermentation experiments described below.

Optimization of CLC system for optimum performance of the biosensor

Optimization of different parameters of the CLC systems has to be taken into consideration when an enzyme-based detection system is utilized. Enzymes are inherently made to work in an aqueous-based medium as they are most often found not to be very stable in organic–aqueous mobile phase mixtures. However, the stability of the enzyme might vary depending on the enzyme and the conditions under which the enzyme-based detection system is operated. It was found, *e.g.*, when using this alcohol sensor as a detector, that it has a very high operational stability using acetonitrile–50 m*M* phosphate buffer (pH 7.0) (20:80) as the mobile phase in a CLC system over one day [56].

The flow dependence of the alcohol sensor incorporated in a reversed-phase separation system was investigated with respect to retention times, signal response and band-broadening effects ($w^{1/2}$). Ethanol and methanol were chosen as the test analytes in this investigation. As can be seen from Table V, the flow-rate has a great influence on all the parameters investigated. A short analytical column was chosen in order to perform fast separations preferentially within 5 min. This was done in order to be able to follow

TABLE V

VARIATION OF SOME RESPONSE CHARACTERISTICS OF THE BIOSENSOR FOR METHANOL AND ETHANOL WITH THE FLOW-RATE OF THE MOBILE PHASE

Flow-rate (ml min^{-1})	Methanol			Ethanol		
	t_R (min)	$w^{1/2}$	i (nA)	t_R (min)	$w^{1/2}$	i (nA)
0.1	31.7	7.5	735	47.7	6.8	620
0.2	16.7	3.6	775	24.0	3.4	635
0.4	8.3	1.7	820	12.3	1.7	620
0.6	5.7	1.3	775	8.3	1.3	575
0.8	4.7	1.0	750	6.5	1.0	590
1.0	3.5	0.9	735	5.3	0.9	570
1.2	2.8	0.8	725	4.8	0.8	550

continuously the change in biotechnical fermentation processes (see below). The PLRP-S stationary phase was found to fulfil these chromatographic requirements. The column was also found to have a better operational stability than different types of silanized C_{18} phases such as LiChrosper 100 RP-18 (Merck, Darmstadt, Germany) and Nucleosil C-18 (5 SY-308; Bioseparation Technology, Budapest, Hungary). The instability of these silica columns with time was probably due to hydrolysis of the silica support. On opening these columns it was found that the front of the column with the packing had partly gone. The various capacity factors at the different flow-rates were mostly acceptable with respect to times of analysis. This was made possible by choosing a small reversed-phase separation column, but with a sufficient length to give the separation needed. The amperometric signal peak response generated by the catalytic activity of the enzymes was found to change only slightly with the flow-rate. The amperometric signal reflects both the enzyme kinetics and the mass transport of solutes to/from the electrode surface. Generally, the higher transport of solutes to the electrode surface at higher flow-rates results in an increase in the current registered. This is also the case for hydrogen peroxide, the substrate for HRP, the second enzyme in the reaction sequence of the sensor, when the response for this substrate was investigated in the FI mode. However, as argued above, the combined effect of hydrogen peroxide being produced by AOD at the electrode surface from injected samples containing alcohol and the turnover kinetics of AOD being low results in higher currents being registered at lower flow-rates than at increased flow-rates.

The band-broadening effect determined as the peak width at half-height ($w^{1/2}$) is more than doubled on comparing peaks obtained for flow-rates of 1.2 and 0.4 ml min^{-1}, and becomes much broader at very low flow-rates (see Table V). In order to see any possible additional band broadening effect given by the biosensor reflecting any kinetic limitations in the reaction sequence outlined in Fig. 3, a separate investigation was made with the same set-up, exchanging the biosensor for a refractive index detector. Similar $w^{1/2}$ values were found at these flow-rates, indicating that the additional band-broadening effect from the sensor itself was not a critical factor.

The dependence of the injection volume on the peak height was investigated, choosing a flow rate of 0.8 ml min^{-1}. The results are shown in Table VI, where the effect for ethanol was found to be much more pronounced than for methanol. The current is almost three times higher for ethanol on increasing the injection volume from 15 to 200 μl but only about twice for methanol. The effect seen is due to two different reasons. The K_M of AOD for methanol is lower than that for ethanol [57] and, as stated above, formaldehyde produced in the enzymatic oxidation of methanol is also a substrate for AOD. At the flow-rate chosen it will partly disappear from the electrode surface before it is trapped by AOD in a second reaction cycle. A typical separation of methanol and ethanol using a 20-μl injection volume with a flow-rate of 0.8 ml min^{-1} is shown in Fig. 5. It can be clearly seen that the biosensor performance is well adapted for use as a detection device in conjunction with CLC.

Determination of alcohols in fermentation broths and substrates

The development of new sample handling techniques that can offer higher selectivity with larger capacity has grown over the last 10 years. This rapid development is due to an increasing demand for the characterization and quantification of progressively smaller amounts of compounds in complex biological matrices. There is

TABLE VI

VARIATION OF THE RESOLUTION (R_s) BETWEEN THE PEAKS OBTAINED FOR METHANOL AND ETHANOL AND THEIR MAXIMUM RESPONSE VALUES WITH THE INJECTION VOLUME

Injection volume (μl)	i (nA)		R_s
	Methanol	Ethanol	
5	430	160	3.3
15	440	215	2.0
20	450	240	2.4
50	740	575	0.8
200	775	650	0.6

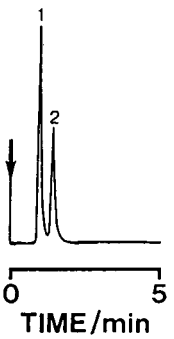

Fig. 5. Chromatographic recording of the separation of methanol (peak 1) and ethanol (peak 2) using the set-up shown in Fig. 2, omitting the microdialysis unit and the switching valves. Conditions: mobile phase, 50 m*M* phosphate buffer (pH 7.5); flow-rate, 0.8 ml/min; injection volume, 20 μl; operational potential, 50 mV *vs.* SCE.

also a need for the development of automated systems for the screening of large numbers of samples and a trend towards increasing the selectivity in the sample clean-up procedure and/or in the detection step in order to reduce the chromatographic requirements. This will result in the need for shorter analytical columns with simpler and faster separations. The use of biological recognition in detection systems for the analysis of highly complex samples is easily rationalized by the need for selectivity when analysing such samples. The number of papers on utilizing biosensors for on-line monitoring of fermentation processes has increased lately and thus reflects this general trend in the development of highly sophisticated and selective detection methods.

Microdialysis can be used as an online sampling unit in continuous *ex vivo* and *in vivo* monitoring in combination with CLC. This method has been used, *e.g.*, in rat brain for choline and acetylcholine monitoring with a detection limit of *ca.* 2–5 fmol [58] and for the determination of glucose in serum [59].

In a previous report study we investigated the potential use of a microdialysis probe as a sampling unit for the analysis of industrial waste waters from the pulp industry, which have been investigated as possible fermentation substrates for ethanol production [31,60].

The stability and reproducibility of the microdialysis unit in the industrial waste water (a lignocellulose hydrolysate, spent sulphite liquor, SSL) were investigated in an earlier study for 24- and 36-h continuous sampling in stirred shake-flask experiments with excellent results showing no drastic decrease (<5%) of the dialysis factor of the sampling device for ethanol [60]. The recovery value will differ depending on the type of dialysis membrane and on the structure of the actual analytes. The naturally occurring carbohydrates in the waste water were used as analytes in these experiments and recoveries above 90% were obtained, reflecting no serious clogging effects or other interactions taking place on or close to the polycarbonate membrane surface interacting in the diffusion process. Although these fermentation substrates and broths have been shown to contain a wide range of lignin poly-, oligo- and monomers [61,62]. The recovery for ethanol was *ca.* 92%, and was stable over a period of typically 10 h. One should consider these data bearing in mind that the ethanol present in the broth makes the solubility of less polar compounds increase, *i.e.*, the complexity of the broth for hydrophobic compounds has increased.

On the basis of these earlier studies, an on-line system was used as shown in Fig. 2, consisting of the microdialysis probe, the CLC system and the AOD/HRP electrode. The microdialysis unit is positioned in the fermenter with the membrane-covered probe immersed in the fermentation solution. The perfusion solution is pumped through the capillary in the probe down to the tip of the probe. From there it is transported upwards through a laser-drilled hole in the capillary wall. The perfusion liquid that is transported upwards on the inner side of the dialysis tubing now also contains representative amounts of each diffusable compound present in the fermentation solution. The flow reaches the T-connection (on the top of the probe) and is then pumped and trapped in the switching valve (see Fig. 2). Next, the valve is positioned in the inject position, whereby the dialysed sample is introduced into the analytical column, separated and then detected at the enzyme electrode that is mounted in the flow cell. Continuous monitoring of ethanol production was made when adding *Saccharomyces cerevisiae* to a sample of SSL

contained in an aseptic and continuously stirred flask. The process was followed for 10 h with injections of the microdialysate into the CLC system every 5th min the first 2 h, and thereafter every 30th min. The set-up in Fig. 2 also gives the possibility of intermittently injecting standard samples of ethanol into the chromatographic system through the second injector, permitting the control of possible variations in the separation and in the detection performance.

The pH of the waste water was adjusted to 6.0 prior to the start of each fermentation in order to minimise contamination from bacteria.

The difference in selectivity using one of the most commonly used monosaccharide CLC separation systems utilizing a polymer-based cation-exchange column and refractive index detection and the on-line system described is demonstrated in Fig. 6. The difference in analysis time for ethanol measurements is also clearly demonstrated in Fig. 6. The retention times for other possible analytes that are detectable with this system were investigated (data not shown). These retention data did not cause any co-elution problems with the ethanol fermentation process.

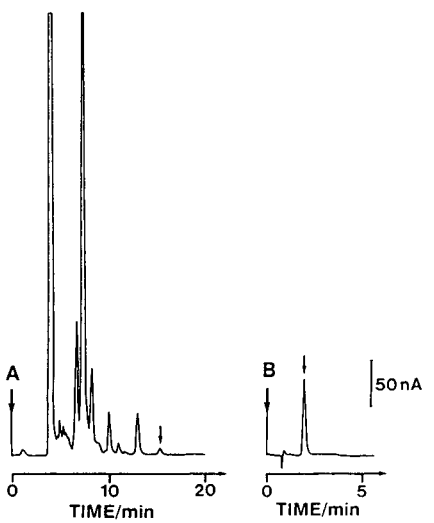

Fig. 6. Chromatograms obtained when injecting the microdialysate into two different chromatographic systems. (A) Cation-exchange column (mobile phase, 4 m*M* sulphuric acid) with refractive index detection; (B) PLRP-S column [mobile phase, 50 m*M* phosphate buffer (pH 7.5)] using the biosensor for enzymatic–electrochemical detection. For further details, see Experimental.

The current system differs from an earlier on-line monitoring system [31] in that the current system does not involve further sample handling other than the sampling itself (dialysis). In earlier work with a cross-flow filtration sampling unit, solid-phase extraction was essential and it was made by a coupled column clean-up system [63]. Increased selectivity in sample handling makes the system less complex with respect to instrumentation, *i.e.*, the need for additional switching valves and columns. One drawback in future might be some adsorption on the analytical column with time, which might influence the stability and the reproducibility of the system. However, during the 10-h fermentations made in this study, this was not a problem, although minor colouring in the front of the separation column was noticed.

The decline in the catalytic performance of the biosensor with time in these complex biotechnological substrates can easily be adjusted for by renewal of the electrode surface. Discarding the outer layer of the electrode is achieved by cutting, exposing a fresh and fully active surface. This is also illustrated in Fig. 1.

CONCLUSIONS

An on-line fermentation monitoring system has been developed for the analysis of alcohols present in fermentation broths. The system utilizes membrane-covered enzyme-based biosensors as a postcolumn detection system in combination with a microdialysis sampling unit and a polymer-based chromatographic separation system. The improved selectivity of the biosensor with different membranes deposited on the electrode surface can easily be applied not only in this process but in others as well. Analytical information on alcohols and also aldehydes and carboxylic acids can be obtained very rapidly by using the set-up. On-line separations of ethanol can be analysed every 5th minute.

The whole system is totally automated and is therefore simple to operate, providing highly reproducible process data. Although only short fermentations were run with the described system, the same performance has been observed for more extended fermentations. In current

work, new types of microdialysis probes are being investigated in terms of operational stability over 24-h fermentations. Applications with similar waste waters for the analysis of phenolic compounds are under study and show similar high recoveries as for the carbohydrates [64].

New types of alcohol sensors with broader selectivity have been developed and are also being studied in combination with these fermentations, and carbohydrate sensors are being developed for the simultaneous monitoring of sugars in these processes.

ACKNOWLEDGEMENTS

The authors thank Mr. Christer Grönstervall, CMA/Microdialysis, Lund, Sweden, for the loan of the microdialysis unit and Mr. A. Rappenberger for drawing the figures. Financial support from the Swedish Natural Science Research Council (NFR), the Swedish Board for Technical and Industrial Development (NUTEK), Stiftelsen Futura and Magnus Bergwalls Stiftelse is gratefully acknowledged.

REFERENCES

1 R.W. Frei and K. Zech (Editors), *Selective Sample Handling and Detection in High-Performance Liquid Chromatography*, Part A, Elsevier, Amsterdam, 1988; K. Zech and R.W. Frei (Editors), *Selective Sample Handling in High-Performance Liquid Chromatography*, Part B, Elsevier, Amsterdam, 1989.
2 H. Lingeman and J.M. Underberg (Editors), *Detection Oriented Derivatization Techniques in Liquid Chromatography*, Marcel Dekker, New York, 1990.
3 I.S. Krull (Editor), *Reaction Detection in Liquid Chromatography*, Marcel Dekker, New York, 1988.
4 U.A.Th. Brinkman, *Chromatographia*, 24 (1987) 190.
5 F.-X. Zhou, J.M. Thorne and I.S. Krull, *Trends. Anal. Chem.*, 11 (1992) 80.
6 P. Vadgama and P.W. Crump, *Analyst*, 117 (1992) 1657.
7 R. Schmid and W. Kunecke, *J. Biotechnol.*, 14 (1990) 3.
8 G. Marko-Varga and L. Gorton, *Anal. Chim. Acta*, 234 (1990) 13.
9 G.A. Marko-Varga, *Electroanalysis*, 4 (1992) 403.
10 A. Farjam, H. Lingeman and U.A.Th. Brinkman, *J. Chromatogr.*, 589 (1992) 141.
11 H. Irth, A.J. Oosterkamp, W. van der Welle, U.R. Tjaden and J. van der Greef, *J. Chromatogr.*, 633 (1993) 65.
12 P. Chandrani and G. Wilson, *Anal. Chem.*, 6 (1993) 1152.
13 L. Clark and C. Lyons, *Ann. N. Y. Acad. Sci.*, 102 (1962) 29.
14 S.J. Updike and G.P. Hicks, *Nature*, 214 (1967) 986.
15 R.P. Baldwin and K.N. Thomsen, *Talanta*, 38 (1991) 1.
16 T. Yao and T. Wasa, *Anal. Chim. Acta*, 209 (1988) 259.
17 E. Domínguez, G. Marko-Varga, M. Carlsson and L. Gorton, *J. Pharm. Biomed. Anal.*, 8 (1990) 825.
18 G. Marko-Varga, L. Gorton, E. Domínguez and D. Barceló, *Chromatographia*, 36 (1993) 381.
19 V. Kacaniklic, K. Johansson, G. Marko-Varga, L. Gorton, G. Jönsson-Pettersson and E. Csöregi, *Electroanalysis*, in press.
20 E. Johansson, G. Marko-Varga and L. Gorton, *J. Biomater. Appl.*, in press.
21 L. Gorton, G. Bremle, E. Csöregi, G. Jönsson-Pettersson and B. Persson, *Anal. Chim. Acta*, 249 (1991) 43.
22 S. Yabuki, H. Shinohara, Y. Ikariyama and M. Aizawa, *J. Electroanal. Chem.*, 277 (1990) 179.
23 M. Aizawa, *Anal. Chim. Acta*, 250 (1991) 249.
24 I. Karube, E. Tamaiya, K. Sode, K. Yokohama, Y. Kitagawa, H. Suzuki and Y. Asano, *Anal. Chim. Acta*, 213 (1988) 69.
25 L. Gorton, E. Csöregi, E. Domínguez, J. Emnéus, G. Jönsson-Pettersson, G. Marko-Varga and B. Persson, *Anal. Chim. Acta*, 250 (1991) 203.
26 E. Domínguez, H.L. Lan, Y. Okamoto, P.D. Hale, T.A. Skotheim, B. Hahn-Hägerdal and L. Gorton, *Biosensors Bioelectron.*, 8 (1993) 229.
27 L. Gorton, G. Jönsson-Pettersson, E. Csöregi, K. Johansson, E. Domínguez and G. Marko-Varga, *Analyst*, 117 (1992) 1235.
28 E. Domínguez, G. Marko-Varga, H.L. Lan, Y. Okamoto, P.D. Hale, T.A. Skotheim, B. Hahn-Hägerdal and L. Gorton, *Ann. NY Acad. Sci.*, 672 (1992) 230.
29 K. Johansson, G. Jönsson-Pettersson, L. Gorton, G. Marko-Varga and E. Csöregi, *J. Biotechnol.*, in press.
30 G. Marko-Varga, K. Johansson and L. Gorton, *Quim. Anal.*, 12 (1993) 24.
31 T. Buttler, K. Johansson, L. Gorton and G. Marko-Varga, *Anal. Chem.*, 65 (1993) 2628.
32 L. Gorton, E. Domínguez, G. Marko-Varga, B. Persson, G. Jönsson-Pettersson, E. Csöregi, K. Johansson, D. Narasaiah, S. Ghobadi, V. Kacaniklic, T. Skotheim, P. Hale, Y. Okamoto and H.-L. Lan, in E. Pungor (Editor), *Bioelectroanalysis, 2, 2nd Symposium, held at Mátrafüred, Hungary, October 11–15, 1992*, Akadémia Kiadó, Budapest, 1993, pp. 33–52.
33 L. Gorton, G. Marko-Varga, B. Persson, Z. Huan, H. Jarskog, E. Johansson, S. Ghobadi, M. Smolander, S. Sahni and T. Skotheim, in L. Bülow and B. Danielsson (Editors), *Proceedings of Mosbach Symposium on Biochemical Technology, Lund, Sweden, December 2–5, 1992*, JAI Press, in press.
34 F. Scheller and F. Schubert (Editors), *Biosensors (Techniques and Instrumentation in Analytical Chemistry*, Vol. 11), Elevier, Amsterdam, 1992.
35 T.D. Gibson, I.J. Higgins and J.R. Woodward, *Analyst*, 117 (1992) 1293.
36 T.D. Gibson and J.R. Woodward, in P.G. Edelman and J. Wang (Editors), *Biosensors and Chemical Sensors (ACS Symposium Series*, No. 487), American Chemical Society, Washington, DC, 1992, pp. 40–55.

37 S. Saini, G.F. Hall, M.E.A. Downs and A.P.F. Turner, *Anal. Chim. Acta*, 249 (1991) 1.
38 K. Kalcher, *Electroanalysis*, 2 (1990) 419.
39 S.V. Sasso, R.J. Pierce, R. Walla and A.M. Yacynych, *Anal. Chem.*, 62 (1990) 1111.
40 H. Shinohara, T. Chiba and M. Aizawa, *Sensors Actuators B*, 13 (1987) 79.
41 P.N. Bartlett and R.G. Whitaker, *Biosensors*, 3 (1987/88) 359.
42 C. Malitesta, F. Palmisano, L. Torsi and P.G. Zambonin, *Anal. Chem.*, 62 (1990) 2735.
43 E.R. Reynolds, R.J. Geise and A.M. Yacynych, in P.G. Edelman and J. Wang (Editors), *Biosensors and Chemical Sensors* (*ACS Symposium Series*, No. 487), American Chemical Society, Washington, DC, 1992, pp. 186–200.
44 L. Gorton, H.I. Karan, P.D. Hale, T. Inagaki, Y. Okamoto and T. Skotheim, *Anal. Chim. Acta*, 228 (1990) 23.
45 G. Bremle, B. Persson and L. Gorton, *Electroanalysis*, 3 (1991) 77.
46 R. Applelqvist, G. Marko-Varga, I. Gorton, A. Torstensson and G. Johansson, *Anal. Chim. Acta*, 169 (1985) 237.
47 J. Kulys and R.D. Schmid, *Bioelectrochem. Bioenerg.*, 24 (1990) 305.
48 G. Jönsson and L. Gorton, *Electroanalysis*, 1 (1989) 465.
49 E. Csöregi, L. Gorton and G. Marko-Varga, *Anal. Chim. Acta*, 273 (1993) 59.
50 E. Csöregi, G. Jönsson-Pettersson and L. Gorton, *J. Biotechnol.*, 30 (1993) 315.
51 P.N. Bartlett, P. Tebbutt and R.G. Whitaker, *Prog. React. Kinet.*, 16 (1991) 55.
52 B. Olsson, *Mikrochim. Acta*, 2 (1985) 211.
53 G.G. Guilbault (Editor), *Analytical Uses of Immobilized Enzymes*, Marcel Dekker, New York, 1984.
54 R.W. Murray, A.G. Ewing and R.A. Durst, *Anal. Chem.*, 59 (1987) 379A.
55 J. Wang, in P.G. Edelman and J. Wang (Editors), *Biosensors and Chemical Sensors* (*ACS Symposium Series*, No. 487), American Chemical Society, Washington, DC, 1992, pp. 125–132.
56 H. Jarskog, L. Gorton and G. Marko-Varga, unpublished results, 1993.
57 T.E. Barman (Editor), *Enzyme Handbook, Supplement I*, Springer, Berlin, 1969, p. 70.
58 B.H.C. Westerink, *Trends Anal. Chem.*, 11 (1992) 176.
59 M.C. Linhares and P. Kissinger, *Anal. Chem.*, 11 (1992) 171.
60 G. Marko-Varga, T. Buttler, L. Gorton and C. Grönsterwall, *Chromatographia*, 35 (1993) 285.
61 G. Marko-Varga and D. Barceló, *Anal. Chim. Acta*, 270 (1992) 63.
62 E.E.E. van der Hage, W.M.G.M. van Loon, J.J. Boon, H. Lingeman and U.A.Th. Brinkman, *J. Chromatogr.*, 634 (1993) 263.
63 G. Marko-Varga, unpublished results, 1993.
64 T. Buttler, L. Gorton and G. Marko-Varga, *Anal. Chim. Acta*, 279 (1993) 27.

Journal of Chromatography A, 660 (1994) 169–185
Elsevier Science B.V., Amsterdam

CHROMSYMP. 2902

Synergies between micropreparative high-performance liquid chromatography and an instrumental optical biosensor

Edouard Nice*, Martin Lackmann, Fiona Smyth, Louis Fabri and Antony W. Burgess

Ludwig Institute for Cancer Research, Melbourne Tumour Biology Branch and The Cooperative Research Centre for Cellular Growth Factors, PO Royal Melbourne Hospital, Melbourne, Victoria 3050 (Australia)

ABSTRACT

The recent development of an automated surface plasmon resonance technology for the measurement of biomolecular interactions (Pharmacia BIAcore) has provided new opportunities for the detection and analysis of protein–protein interactions. In the BIAcore, detection is based on changes in surface plasmon resonance which are monitored optically. Changes in surface plasmon resonance correspond to changes in surface concentration of macromolecules and can be monitored in real time.

We have found that the detection sensitivity obtainable with this technology (ng/ml concentrations of specific ligands are readily detectable for many applications) is complementary "in a bidirectional manner" to micropreparative HPLC. Thus micropreparative HPLC may be used to purify and characterise reagents for the biosensor, whilst the biosensor may be used to define chromatographic parameters such as elution conditions for affinity chromatography or serve as an affinity detector for fractions obtained during chromatographic purification.

Examples of such applications, including the potential of the biosensor to search for and monitor the purification of unknown ligands for which the target molecule has been identified, are shown. In particular, the use of the biosensor to monitor the purification of soluble epidermal growth factor receptor from A431 cell conditioned media is demonstrated.

INTRODUCTION

The development of an instrumental optical biosensor (Pharmacia BIAcore) [1,2] to measure biomolecular interactions in real time has opened new perspectives for the detection of protein–protein interactions, including receptor ligand [3,4] and antibody–antigen [5–14] interactions and interactions between components of signal transduction pathways [15,16]. One of the interacting components is immobilised onto the carboxymethylated gold surface of the sensor [17] using conventional protein chemistry techniques {*e.g.* N-hydroxysuccinimide–N-ethyl-N'-(3-diethylaminopropyl)carbodiimide coupling [18]}. This coupling can be performed *in situ* using the integrated microfluidics of the instrument. Monoclonal antibodies, purified receptors, protein or peptide ligands can be readily coupled onto the surface, and real time binding studies performed by sequentially flowing reagents of interest over the derivatised sensor surface to which the target protein has been attached [1,2]. The automated injection system and sample loops are designed for injection volumes of 1–50 μl to be introduced at constant flow-rates typically between 1–5 μl/min. Detection is based on the phenomenon of surface plasmon resonance (SPR) [19,20], a technique which measures small changes in refractive index at, or near to, a metal surface. Such changes are directly proportional to the change in adsorbed mass [2], and have a potential lower limit of detection of 10 pg/mm^2

* Corresponding author.

0021-9673/94/$07.00 © 1994 Elsevier Science B.V. All rights reserved
SSDI 0021-9673(93)E0831-E

[1]. This corresponds to the injection of samples at ng/ml concentration [1].

Fundamental to the success of the biosensor technology is the ability to produce, in a homogeneous form, the specific component for immobilisation onto the surface. We have previously shown [21–28] the potential of short (less than 10 cm) micropreparative (1–2 mm I.D.) columns for the purification, concentration and buffer exchange of samples prior to microsequence analysis. Such systems have been used for the purification of a number of growth factors [29–36] and related compounds [27,37], using not only reversed-phase, but also hydrophobic interaction [27,37], anion- and cation-exchange [27,37] and micro size-exclusion HPLC [37] to render the methods compatible with a wide range of proteins. With this methodology proteins and peptides are recovered in small eluent volumes (typically 50–100 μl). The resultant concentrations achieved permit detection (at 215 nm) of nanogram quantities [21,24, 27,28]. The sensitivity and sample/recovery volumes of micropreparative HPLC would therefore appear to be complementary with the biosensor. We describe the use of micropreparative HPLC to monitor sample purity, quantitation and heterogeneity, and to purify reagents suitable for application to the biosensor. We also demonstrate the use of micropreparative HPLC to desalt and buffer exchange proteins into solvent systems compatible with the BIAcore immobilisation chemistry.

Whilst material for immobilisation onto the sensor surface needs to be homogeneous, subsequent analyses can be performed on crude extracts, tissue culture media or bacterial broth without the need for prior purification [2], allowing the biosensor to be used for the rapid screening of potential sources of interacting ligands. This approach should be particularly useful in the search for "unknown ligands" of, for example, monoclonal antibodies raised against complex mixtures of proteins and carbohydrate, or for new members of receptor gene families (*e.g.* tyrosine kinases [38,39]) which have been elucidated from sequence homologies and polymerase chain reaction (PCR) based molecular biology techniques. In such cases the biosensor can then be used as a specific detector for monitoring fractions obtained during chromatographic purification of the ligand of interest. To demonstrate the feasibility of such an approach we describe the use of the biosensor, using immobilised recombinant human epidermal growth factor (hEGF), to monitor the purification of the soluble form of the epidermal growth factor receptor (sEGF-R) from A431 cells [40]. Purified sEGF-R, in a form suitable for immobilisation onto the sensor surface, is obtained by the sequential use of wheat germ lectin affinity chromatography, anion-exchange, size-exclusion and micropreparative anion-exchange HPLC.

Since, in the case of the search for new ligands, one of the interacting species (*e.g.* the receptor or antibody) will have already been purified, the use of affinity chromatography as part of the purification protocol would appear obvious. However, in many cases the specificity and/or the affinity of the interaction makes affinity chromatography quite difficult. Both binding and elution conditions must be defined if a reasonable yield of the active ligand is to be obtained. We illustrate how the biosensor can be used to define and optimise elution conditions for affinity chromatography, with the ability to check quantitatively the surface, or the purified ligand, for denaturation.

MATERIALS AND METHODS

Micropreparative HPLC

Separations were performed on a Pharmacia SMART system [26] equipped with a variable wavelength μPeak monitor, a built-in on-line conductivity meter and a microfraction collector (Pharmacia LKB Biotechnology, Uppsala, Sweden). Columns used were (a) Pharmacia Mono Q PC 1.6/5 anion-exchange, (b) Pharmacia Superose 12 PC 3.2/30 micro size-exclusion, (c) Pharmacia PC 3.2/10 Fast Desalting and (d) Pharmacia μRPC C2/C18 PC 3.2/3 reversed-phase. Samples were loaded by means of a 1-ml or 100-μl external loop. Chromatographic conditions used for particular separations are given in the appropriate figure legends.

Matrix assisted laser desorption mass spectrometry (MALD-MS)

Mass spectra were obtained using a Lasermat mass spectrometer (Finnigan-MAT, San Jose, CA, USA) as described previously [41]. α-Cyano-4-hydroxy cinnamic acid [42] (10 mg/ml in 30% (v/v) acetonitrile, Aldrich, Milwaukee, WI, USA) was used as the matrix.

Biosensor measurements

All measurements were performed on the BIAcore biosensor (Pharmacia Biosensor, Uppsala, Sweden) [1,2]. Sensor chip CM5, surfactant P20 (a 10% solution of a non-ionic detergent), N-hydroxysuccinimide (NHS) and N-ethyl-N′-(3-diethylaminopropyl)carbodiimide (EDC) were also obtained from Pharmacia Biosensor. Tern neuraminidase, NC10 and NC41 Fab antibody fragments [43] were a kind gift from Dr. L.C. Gruen, CSIRO Division of Biomolecular Engineering, Melbourne, Australia. Peptide P20, corresponding to residues 306–328 of the C-terminus of the HA1 chain of influenza virus hemagglutinin subtype H3 [44] and the corresponding monoclonal antibody, 2/1 IgG, and 1/1 Fab′ fragment were a kind gift from Dr. D. Jackson, Department of Microbiology, University of Melbourne, Australia. Recombinant hEGF was purchased from PeproTech (Rocky Hill, NJ, USA).

Immobilisation of proteins and peptides to the sensor surface

Proteins and peptides were immobilised onto the sensor surface essentially as described previously [8]. Briefly, immobilisation was performed at a constant flow-rate of 4 μl/min using HBS buffer [10 m*M* Hepes, pH 7.4 containing 0.15 *M* NaCl, 3.4 m*M* ethylenediaminetetraacetic acid (EDTA), 0.05% (v/v) surfactant P20]. The carboxymethylated surface of the sensor chip was first activated with 35 μl of a NHS–EDC mixture (0.05 *M* NHS, 0.2 *M* EDC in distilled water). Peptides or proteins (peptide P20, 50 μg/ml in 10 m*M* sodium acetate buffer, pH 6.0; recombinant hEGF, 100 μg/ml in 10 m*M* sodium acetate pH 4.5; NC10 and NC41 Fab fragments, 50 μg/ml in 10 m*M* sodium acetate pH 4.5) were then injected (50-μl aliquots) over the activated surface for covalent attachment. Following the coupling to the sensor surface, residual activated ester groups were blocked by the injection of 35 μl of 1 *M* ethanolamine hydrochloride, pH 8.5, followed by washing with 10 μl of 10 m*M* HCl in the case of peptide P20 and recombinant hEGF, or 10 m*M* sodium acetate pH 4.5 in the case of NC10 and NC41 Fab, to remove non-covalently bound material.

Preparation of membrane extracts containing EGF receptor (M_r 170 000 form) from A431 cells

A431 cells were grown in 600-ml Nunclon flasks (Nunc, Kamstrup, Denmark) in Dulbecco's modified Eagle's medium (DME) containing 10% foetal calf serum. Confluent cell monolayers (approximately 10^7 cells) were washed and then scraped from the flask in 10 ml PBS, and the cells collected by centrifugation at 5000 rpm (1700 *g*) for 5 min at 4°C in an Hereaus minifuge (Heraeus Sepatech, Osterode, Germany). The cells were then lysed in 1 ml PBS containing 1% (v/v) Triton X-100, 10 m*M* EDTA, 1 m*M* phenylmethylsulfonyl fluoride (PMSF) (Sigma, St Louis, MO, USA) and 100 units/ml Trasylol (Bayer, Leverkusen, Germany). After leaving on ice for 30 min the sample was centrifuged at 5000 rpm (1125 *g*) for 5 min at 4°C in an Eppendorf microfuge (Eppendorf, Hamburg, Germany) and the supernatant, containing the membrane extract, retained for further studies.

Preparation of soluble secreted EGF receptor (sEGF-R, M_r 105 000 form) from A431 cells

sEGF-R was obtained from conditioned media from A431 cells using a modification of the method of Basu *et al.* [45]. Briefly, A431 cells were grown to confluence as described above and then changed into serum free DME for a further 24 h. The medium was collected and centrifuged at 2000 rpm (270 *g*) for 5 min at 4°C in an Hereaus Minifuge to remove cell debris. EDTA, PMSF, Trasylol, Leupeptin (Sigma) and Pepstatin (Sigma) were added to the clarified supernatant at final concentrations of 10 m*M*, 1 m*M*, 100 units/ml, 10 μ*M* and 1 μ*M*, respectively.

Chromatographic purification of sEGF-R

Lectin affinity chromatography. The combined conditioned supernatants of $3–4 \cdot 10^8$ A431 cells (320–360 ml) were concentrated 8-fold by ultrafiltration on YM-30 membranes (45 mm diameter, Amicon, Beverly, MA, USA). The concentrated medium was then incubated, at 4°C for 10 h on an end-over-end rotator, with 1 ml of wheat germ lectin (WGL)–Sepharose (Pharmacia). Unabsorbed material was removed by centrifugation [1200 rpm (65 *g*) for 5 min at 4°C in an Heraeus Minifuge] and the gel washed sequentially, for 2 h at 4°C, with 50-ml volumes of HG buffer (20 m*M* Hepes, pH 7.5, 10% glycerol, 10 μg/ml leupeptin, 2 m*M* PMSF), HG buffer containing 500 m*M* NaCl and finally by a further wash with HG buffer. Bound protein was eluted by incubation, for 2 h at 4°C, with 2 × 2 ml HG buffer containing 600 m*M* N-acetyl-D-glucosamine (Sigma-Aldrich, Castle Hill, NSW, Australia). Eluted material was recovered after "pelleting" the WGL–Sepharose by centrifugation. At each stage of the purification protocol aliquots (40 μl) were tested for EGF-binding activity using the biosensor.

Anion-exchange HPLC on Mono Q HR 5/5. The combined eluates from the WGL–Sepharose were adjusted to pH 8.5, using 20 m*M* Tris-base (pH 9.2) containing 0.02% Tween 20 to promote trace enrichment, before loading onto a Mono Q HR 5/5 anion-exchange column (Pharmacia), which had previously been equilibrated with 20 m*M* Tris–HCl, pH 8.5 containing 0.02% Tween 20. Proteins were eluted from the column, at a flow-rate of 1 ml/min, with a linear 40-min gradient of 0–600 m*M* NaCl in the equilibration buffer. Fractions were collected at 1-min intervals. Aliquots of each fraction (40 μl) were tested for EGF-binding activity using the biosensor.

Size-exclusion HPLC on Superose 12 HR 10/30. Fractions from the Mono Q column with maximum EGF binding activity were pooled and the volume reduced to 800–900 μl by concentration in a SpeedVac centrifuge (Savant Instruments, Hicksville, NY, USA). The concentrate was loaded onto a Superose 12 HR 10/30 column (Pharmacia) and proteins eluted at a flow-rate of 0.5 ml/min with HBS buffer. Fractions were collected at 1-min intervals. Aliquots (75 μl) from each fraction were diluted to 125 μl with HBS buffer for assay on the biosensor.

Micropreparative HPLC on Mono Q PC 1.6/5. Fractions from the Superose 12 size-exclusion column with EGF binding activity were pooled (1.5 ml total) and diluted 4-fold with 20 m*M* Tris-base (pH 9.2) containing 0.02% Tween 20 for trace enrichment by multiple injection onto a micropreparative anion-exchange HPLC column (Mono Q PC 1.6/5) as described previously [27,37]. Retained proteins were eluted, at a flow-rate of 100 μl/min and a column temperature of 25°C, with a linear 40-min aqueous sodium chloride gradient between 0 and 600 m*M* NaCl. The gradient solutions were adjusted to pH 8.5 with 10 m*M* sodium phosphate buffer (final concentration less than 1 m*M*, *i.e.* they were essentially buffer free [27,37]) immediately before use. Fractions were collected at 1-min intervals using the microfraction collector of the SMART system. Aliquots from each fraction (16 μl) were assayed for EGF binding activity following dilution (1:2.5) with the HBS biosensor buffer. Proteins were analysed by sodium dodecyl sulphate–polyacrylamide gel electrophoresis (SDS-PAGE) on 4–15% gradient Phastgels using a PhastSystem (Pharmacia LKB Biotechnology, Uppsala, Sweden), and visualised by silver staining using a semi-automated protocol for the PhastSystem described previously [41].

Biosensor assay of EGF binding activity in chromatographic fractions

Aliquots of fractions obtained during the purification were assayed directly, or following dilution in HBS, as indicated above. Samples were loaded into the autosampler of the BIAcore and analysed automatically at a constant HBS flow-rate of 5 μl/min using a sensor chip which had previously been derivatised with recombinant hEGF (as described above). Injection volumes were 40 μl. The operating temperature was 25°C. Between measurements, material non-covalently bound to the sensor surface during sample assay was desorbed by injection of 15 μl of a buffer containing 6 *M* guanidine hydrochloride, 0.1 *M* Tris–HCl (pH 8.0), 5 m*M* EDTA and 5 m*M* ethyleneglycol-bis(β-aminoethyl ether)-N,N,N′,N′-tetraacetic acid (EGTA). Following desorption, the surface was re-equili-

brated with HBS buffer (25 μl) prior to injection of the next sample. The ability of immobilised EGF to bind sEGF-R was not affected by the regeneration procedure as shown by equivalent binding if duplicate samples were injected sequentially.

RESULTS AND DISCUSSION

Sample compatibility between micropreparative HPLC and the biosensor

We have shown previously the ability of micropreparative HPLC to generate samples in small eluent volumes (at concomitant high concentrations) suitable for microsequence analysis [21,23–28], or subsequent structure–function studies [33,35]. Using short (less than 10 cm) small diameter (1–3 mm I.D.) columns it is routinely possible to elute samples with high recovery in peak volumes of 100 μl or less [21,24,27]. Limits of sensitivity are in the low nanogram range using UV-detection at 214 nm (Fig. 1A). Thus samples can be readily separated, detected and recovered at concentrations of 100 ng/ml or greater. The signal response is linear at least over the range 12–500 ng (Fig. 1B) indicating that no band broadening (and hence eluent sample dilution) occurred over this range. Indeed, in previous studies on reversed-phase micropreparative columns [24,28] we had noted no apparent band broadening even with loads of 5 μg.

For the micropreparative HPLC to be compatible with the biosensor then, ideally, it should be possible to load samples from one instrument to the other without further manipulation. The autoinjection system of the biosensor is capable of injecting accurately samples of between 1 and 50 μl volume. In the case of the SMART system samples can be directly transferred from the microfraction collector of the HPLC to the autosampler racks of the biosensor.

It has been shown [1] that the potential lower limit of SPR detection of the BIAcore is 10 pg/mm^2, which corresponds to a signal of 10 refractance units (RU). Since the detection is based on changes in refractive index at, or close to, the surface, and since the refractive index increment for proteins is constant up to high

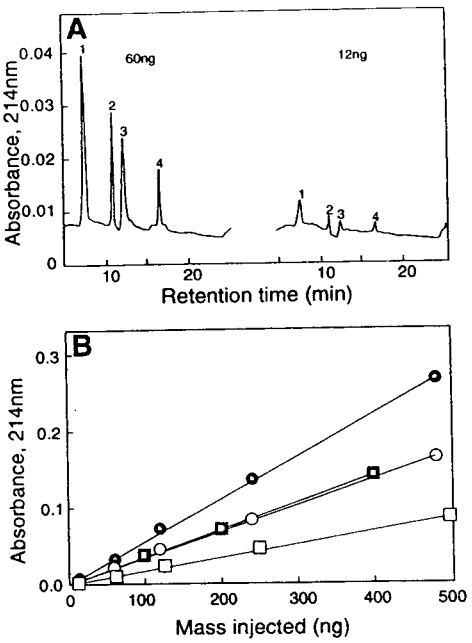

Fig. 1. (A) Sensitivity of detection with micropreparative anion exchange HPLC. Protein standards were separated, at a flow-rate of 100 μl/min, on a Mono Q PC 1.6/5 column (50 × 1.6 mm I.D.) using a linear 50-min gradient between 0 and 1 *M* NaCl in 20 m*M* Tris buffer (pH 7.5). The column temperature was 25°C. Protein standards used were (1) mouse EGF, (2) α-lactalbumin, (3) hEGF and (4) trypsin inhibitor. Chromatograms obtained with loadings of 60 and 12 ng/protein are shown. The absorbance is expressed in absorbance units (AU). (B) Linearity of detector response. The observed peak height (AU, 214 nm) for protein standards, separated on a Mono Q PC 1.6/5 column using the chromatographic conditions described in Fig. 1A, is plotted against the mass of protein standard injected (data from Fig. 1A is included). ● = mEGF, ○ = α-lactalbumin, ■ = rhEGF and □ = trypsin inhibitor.

bulk concentrations [46], the detection limit should be independent of the sample injected, although glycoproteins and lipoproteins have a slightly lower refractive index increment and hence give a slightly lower (approximately 8%) SPR signal [1]. To estimate the sensitivity of detection in terms of bulk analyte concentration these authors [1] calculated, assuming that 40% of the total analyte in the sample could bind to the surface uniformly in a univalent manner, that concentrations of 1 ng/ml would be required for a measurable response.

That such sample concentrations do indeed result in a measurable signal is shown in Fig. 2A.

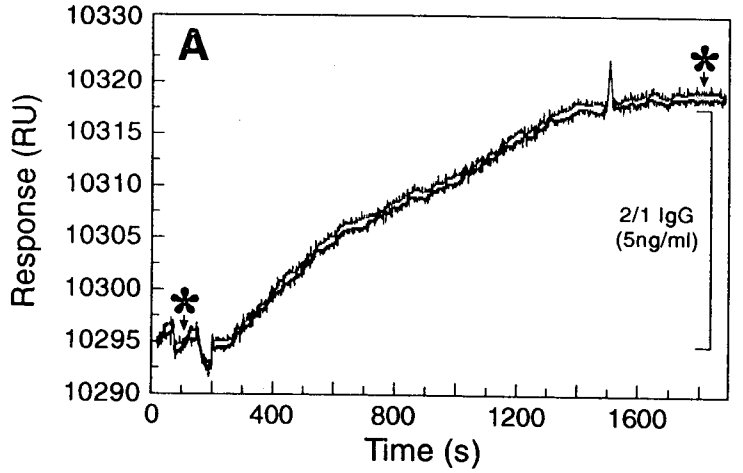

Time	AbsResp	Baseline	RelResp	Id
103.50	10295	YES	0	INJ_2/1IgG_(0.005µg/ml)
1791.00	10319	NO	24	2/1IgG_(0.005µg/ml)

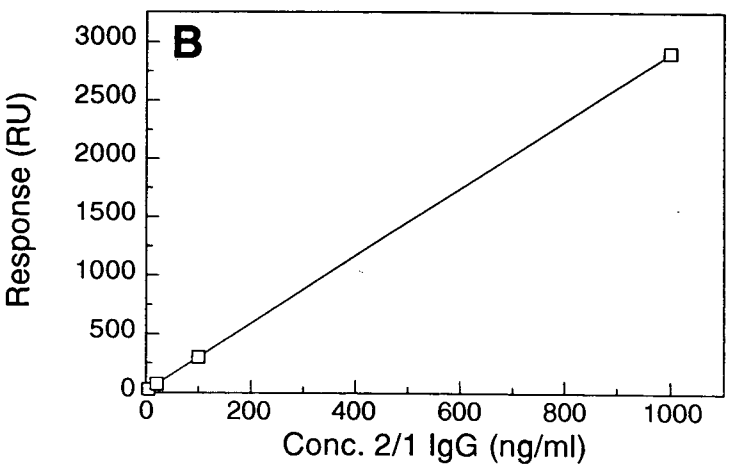

Fig. 2. Low level detection with the BIAcore biosensor. Aliquots (50 µl) of a monoclonal antibody (2/1 IgG) were injected at a flow-rate of 2 µl/min over a sensor surface which had been immobilised with the corresponding peptide antigen (P20). Immobilisation conditions are given in Materials and Methods. The change in detector response (resonance units, RU) with time was recorded as a sensorgram. (A) The sensorgram obtained with 2/1 IgG at a concentration of 5 ng/ml. The corresponding report table is shown below. (B) Linearity of detector response. 2/1 IgG was injected (50-µl aliquots) over the P20 sensor surface at concentrations of 5, 20, 100 and 1000 ng/ml as described above. The relative response (RU) between the initial baseline and the signal at the end of the injection pulse is plotted as a function of the concentration injected.

In this example 50 µl of a high-affinity monoclonal antibody (2/1 IgG, 5 ng/ml), raised against a synthetic peptide (P20) representing the C-terminal 24 residues of the HA1 chain of influenza virus hemmagglutinin [44], were injected, at a flow-rate of 2 µl/min, over the sensor surface onto which had been immobilised the corresponding peptide antigen (P20). A steady increase in the SPR signal with time resulted, with a final relative response of 25 RU being obtained. A linear response was observed for injections of the 2/1 IgG antibody over the concentration range 5–1000 ng/ml (Fig. 2B).

The use of micropreparative HPLC to generate reagents for the biosensor

The specificity of the sensor surface necessarily depends critically on the homogeneity of the

material used for immobilisation, particularly if kinetic studies are to be undertaken. Heterogeneity of the immobilised material frequently gives rise to non-linear plots when analysing data for association or dissociation rate constants [47]. Additionally the presence of any amine containing buffers in the sample "poisons" the N-hydroxysuccinimide coupling via primary amino groups. Amine containing buffers therefore need to be removed before immobilisation. In the example shown (Fig. 3) a Fab fragment of a monoclonal antibody to influenza N9 neuraminidase (NC10 Fab), of which the three-dimensional structure of the antibody/ligand

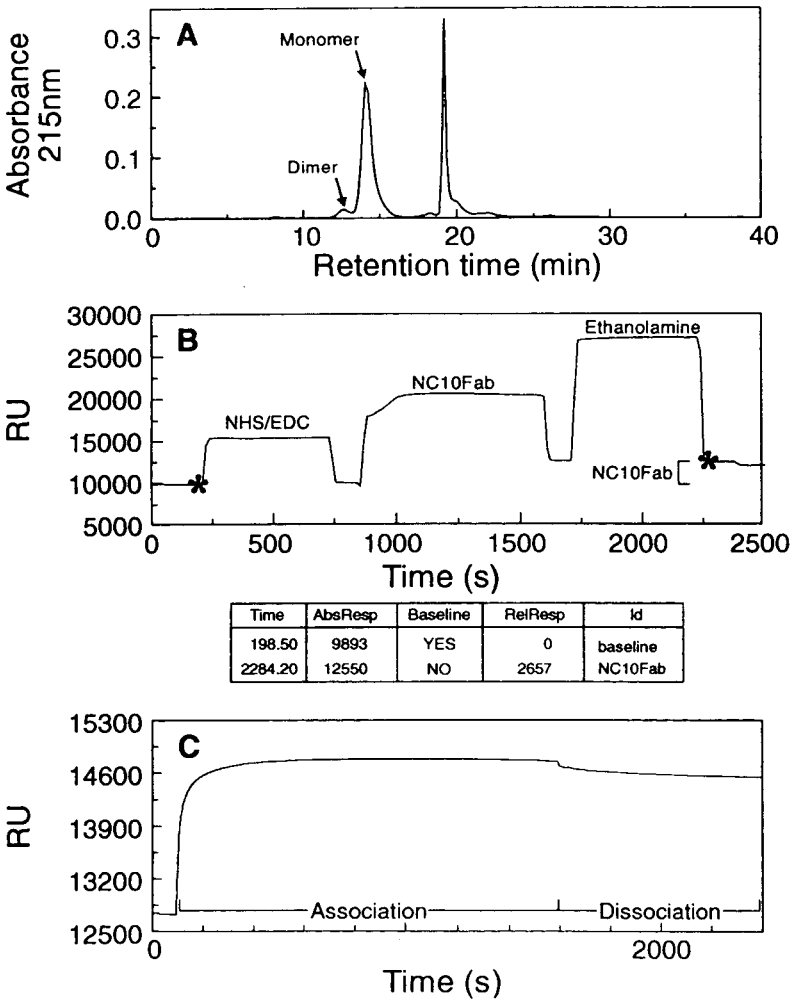

Time	AbsResp	Baseline	RelResp	Id
198.50	9893	YES	0	baseline
2284.20	12550	NO	2657	NC10Fab

Fig. 3. The use of micropreparative size-exclusion HPLC to purify and buffer exchange a Fab fragment for immobilisation onto the BIAcore. (A) NC1O Fab (100 μg/ml, 100 μl injection volume) in 50 m*M* Tris buffer (pH 8.0) was purified and buffer exchanged into a buffer compatible with NHS–EDC immobilisation using a Superose 12 PC 3.2/30 column. The mobile phase was 20 m*M* sodium acetate (pH 4.5) and the flow-rate 100 μl/min. Column temperature was 25°C. Note the presence of a small impurity with the apparent molecular mass of the dimer. (B) The HPLC-purified NC10 Fab was adjusted to a concentration of 50 μg/ml with 20 m*M* sodium acetate buffer (pH 4.5) and immobilised onto the sensor surface as described in Materials and Methods. The resulting sensorgram and associated report table are shown. The regions of the sensorgram corresponding to the surface activation with NHS–EDC, the covalent binding of the NC10 Fab fragment and subsequent blocking of residual activated ester groups with ethanolamine are indicated. The net relative response (2657 RU) corresponds to a surface concentration of approximately 2.6 ng/mm^2 [1]. (C) Binding of tern neuraminidase to the immobilised NC10 Fab. To confirm the viability of the sensor surface, tern neuraminidase (100 μg/ml, 50-μl injection) was passed, at a flow-rate of 2 μl/min, over the sensor surface. The association and dissociation phases of the resultant sensorgram are indicated.

complex has been determined by X-ray crystallography [48], was required for immobilisation onto the sensor surface. An aliquot of the NC10 Fab (100 μl, 100 μg/ml in 50 m*M* Tris buffer, pH 8.0) was purified and buffer exchanged into a buffer compatible with NHS/EDC immobilisation (10 m*M* sodium acetate, pH 4.5) using a Superose 12 PC 3.2/30 micro size-exclusion column (Fig. 3A). The NC10 Fab fragment was effectively buffer exchanged and at the same time separated from a small impurity with an apparent molecular mass of the dimer. The purified NC10 Fab fragment, which was recovered in a volume of 150 μl, was made up to 200 μl (final concentration 50 μg/ml) with the 10 m*M* sodium acetate buffer, and used for immobilisation onto the sensor chip (Fig. 3B). The net increase in signal following the immobilisation (2657 RU) corresponds to a NC10 Fab surface concentration of approximately 2.6 ng/mm^2 [1,49]. The ability of the immobilised antibody to bind neuraminidase is shown in Fig. 3C. A sample (50-μl injection) of tern neuraminidase (100 μg/ml) was passed over the immobilised NC10 Fab (see Fig. 3B) at a flow-rate of 2 μl/min. A positive response of 2187 RU was observed, demonstrating the integrity of the immobilised HPLC purified NC10 Fab.

A further example of the use of micropreparative HPLC to generate suitable reagents for immobilisation is given in Fig. 4. In this case a synthetic peptide, P20, corresponding to residues 306–328 of the C-terminus of the HA1 chain of the influenza virus hemmagglutinin subtype H3 [44] was purified by RP-HPLC on a Pharmacia μRPC C2/C18 3.2/3 column prior to immobilisation. A major species was resolved from an earlier eluting contaminant, as well as a later eluting shoulder (Fig. 4A). MALD-MS of the RP-HPLC purified P20, using 1 μl of the eluent

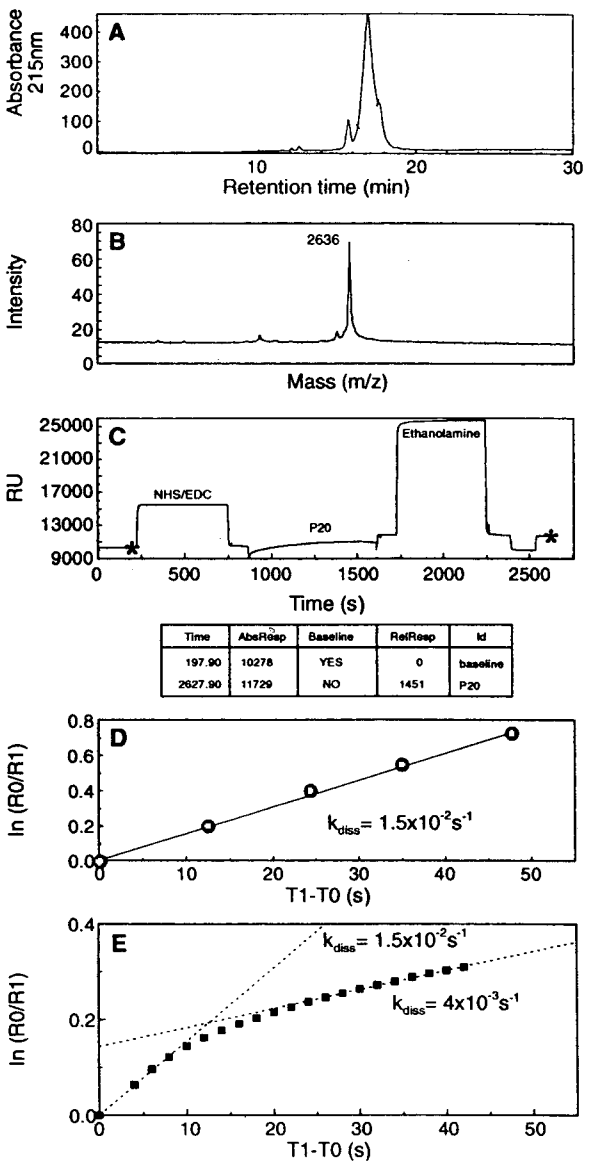

Fig. 4. The use of micropreparative RP-HPLC to purify a synthetic hemagglutinin peptide prior to immobilisation on the BIAcore. (A) A sample (7 μg) of a synthetic peptide (P20) corresponding to residues 306–328 of the C-terminus of the HA1 chain of influenza virus hemagglutinin subtype H3 [44] was purified by RP-HPLC on a Pharmacia μRPC PC 3.2/3 column (30 × 3.2 mm I.D.). Proteins were eluted with a linear 60-min gradient between 0.15% (v/v) trifluoroacetic acid (TFA) and 60% aqueous acetonitrile containing 0.125% (v/v) TFA. The flow-rate was 240 μl/min and the column temperature 45°C. The sample was recovered manually as indicated by the dashes. Absorbance is expressed in mAU. (B) An aliquot (1 μl) of the RP-HPLC purified P20 was analysed by MALD-MS as described in Materials and Methods. (C) The remainder of the RP-HPLC purified P20 was dried using a Speed Vac concentrator, and redissolved in 10 m*M* sodium acetate buffer (pH 6.0) for immobilisation onto the sensor surface using NHS–EDC chemistry as described in Materials and Methods. (D) Following binding of a Fab' fraction of a monoclonal antibody raised against peptide P20 (1/1 Fab') to the sensor surface, dissociation was monitored under conditions of constant HBS buffer flow. R_0 and R_1 refer to the resonance values at times T_0 and T_1 respectively. A linear first order dissociation plot was obtained. (E) If peptide P20 was immobilised without prior RP-HPLC purification a markedly biphasic dissociation plot was obtained.

fraction, yielded the anticipated mass of the synthetic peptide. As we have noted previously [41] the concentration of proteins or peptides recovered from micropreparative columns is ideally suited to direct analysis by MALD-MS. The recovered peptide was dried using a SpeedVac concentrator and redissolved in 10 m*M* sodium acetate buffer, pH 6.0, (final concentration 50 μg/ml) for immobilisation onto the sensor surface using the NHS–EDC chemistry (Fig. 4C). A surface concentration of approximately 1.5 ng/mm^2 was achieved. When the surface was exposed to a Fab′ fragment of a monoclonal antibody raised against this peptide (1/1 Fab′) and, following association, the dissociation monitored at constant buffer flow, linear first order kinetics were observed (Fig. 4D) with an apparent k_{diss} of $1.5 \cdot 10^{-2}$ s^{-1}. When the peptide was immobilised without prior RP-HPLC purification a markedly biphasic dissociation plot was observed (Fig. 4E).

Since the SPR detector is sensitive to refractive index changes at, or near to, the surface, the system is sensitive to differences in sample or buffer components (note the rapid changes in signal at the beginning and end of the injection cycles during immobilisation, Figs. 3B and 4C). Whilst measurements can be made at "steady state" conditions when buffer alone is flowing between injections, buffer-related refractive index changes confuse interpretation of the data when analysing equilibrium binding, with rapid dissociation kinetics, or when studying weak or low level interactions. In order to minimise such refractive index effects, we have used microdesalting columns (Pharmacia Fast Desalting PC 3.2/10) to buffer-exchange samples into the BIAcore running buffer. In the example shown (Fig. 5A) an aliquot (50 μl) of the Triton X-100 membrane extract of A431 cells, containing the M_r 170 000 form of the EGF-R [50], was injected at a flow-rate of 5 μl/min over a sensor chip onto which recombinant hEGF had been immobilised. Because of refractive index differences between the Triton X-100 membrane extract and the HBS buffer, a buffer-related decrease of 2450 RU was observed at the end of the injection cycle. The overall relative response due to the specific interaction between the EGF-R and the hEGF on the sensor surface was 1479 RU. An aliquot of the membrane extract (100 μl) was then desalted in the HBS running buffer used on the BIAcore (Fig. 5B). The protein fraction was recovered, as indicated, in an eluent volume of 140 μl. Injection of this fraction (50 μl, flow-rate 5 μl/min) over the hEGF sensor surface (Fig. 5C) gave rise to a final relative response of 1064 RU, with a refractive index change of only 94 RU at the end on the injection cycle (*cf.* Fig. 5A). It should be noted that the Triton X-100 membrane extract contains proteins which will not bind to hEGF which account for the small negative refractive index change observed at the end of the injection cycle. Since the desalted sample has been diluted during the chromatographic procedure (100–140 μl), the relative EGF-R related binding responses observed (1479 and 1064 RU, Fig. 5A and C, respectively) suggest that recovery from the micro-desalting column was essentially quantitative (a dose–response curve of the A431 Triton X-100 membrane extract in HBS was linear over the range 50–1500 RU (correlation coefficient 0.999), data not shown).

The use of the biosensor to monitor fractions during chromatographic purification

Having immobilised a specific reagent onto the sensor surface, the BIAcore can be used to screen rapidly a wide range of biological extracts for possible sources of interacting proteins. Once a source has been identified, then the biosensor can be used to monitor the purification of the protein of interest. To demonstrate the potential of such co-operativity we have used the biosensor, with recombinant hEGF immobilised onto the surface, to develop and monitor a purification protocol for sEGF-R (M_r 105 000 form) secreted into tissue culture medium by A431 cells [40].

Highly purified sEGF-R, in a form suitable for immobilisation onto the sensor surface, was obtained from concentrated A431 cell conditioned supernatants by sequential use of WGL affinity chromatography, anion-exchange, size-exclusion and micropreparative HPLC.

BIAcore-measurements of crude supernatant, wash buffers (see Materials and Methods) and eluates from the WGL–Sepharose indicated that approximately 65% of the EGF binding activity

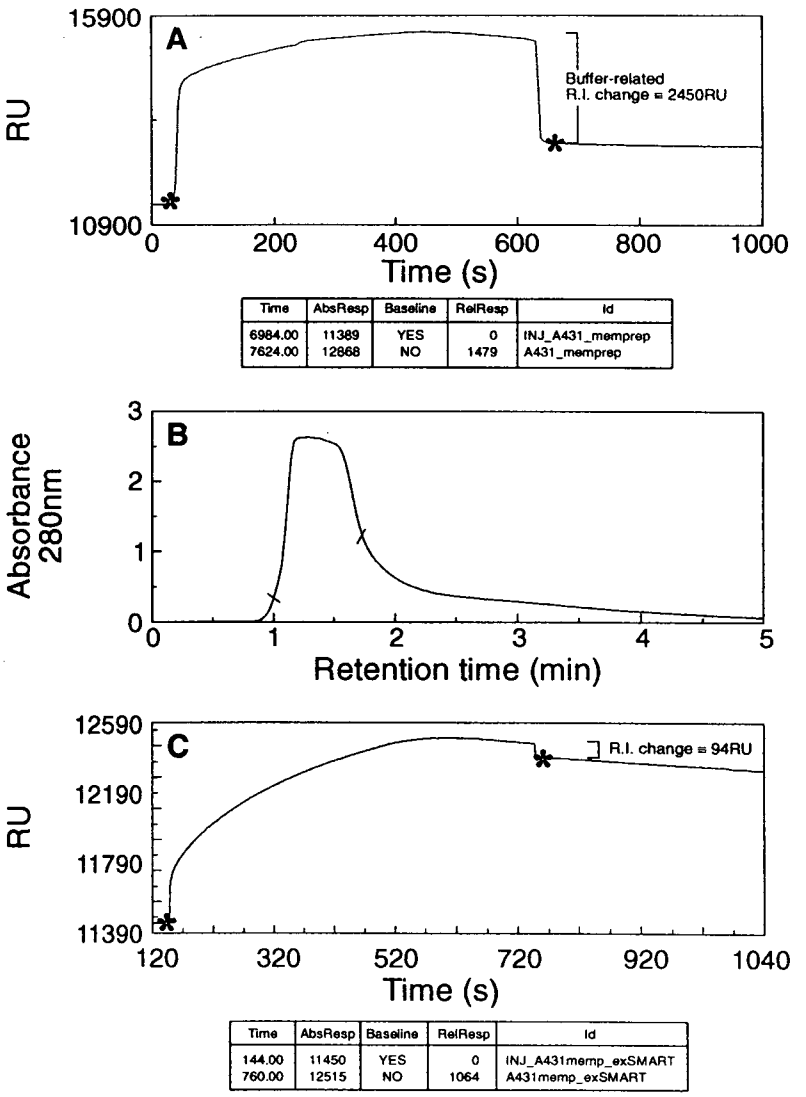

Time	AbsResp	Baseline	RelResp	Id
6984.00	11389	YES	0	INJ_A431_memprep
7624.00	12868	NO	1479	A431_memprep

Time	AbsResp	Baseline	RelResp	Id
144.00	11450	YES	0	INJ_A431memp_exSMART
760.00	12515	NO	1064	A431memp_exSMART

Fig. 5. The use of a micropreparative Fast Desalting column to buffer exchange samples into BIAcore buffer. (A) An aliquot (50 μl) of a Triton X-100 extract of A431 membranes containing hEGF receptor [50] was injected, at a flow-rate of 5 μl/min, over the sensor surface onto which hEGF had been immobilised. Note the rapid buffer related decrease in response (−2450 RU) at the end of the injection pulse. (B) An aliquot (50 μl) of the Triton X-100 extract was desalted into the BIAcore buffer (see Materials and Methods) using a Pharmacia Fast Desalting PC 3.2/10 column. The flow-rate was 180 μl/min and the column temperature 25°C. The desalted sample was recovered, as indicated by the dashes, in a volume of 140 μl. (C) The buffer exchanged sample from the Fast Desalting column (panel B) was injected over the hEGF sensor surface as described in (A). Note the greatly reduced buffer related signal decrease (−94 RU) at the end of the injection pulse compared with that observed with the same extract before buffer exchange (see panel A).

of the starting material was found in the unbound fraction, although the amount of lectin used in our protocol was in 10-fold excess compared to a previously reported method of Basu *et al.* [45]. Further incubation of the unbound fraction with an additional 2 ml of fresh WGL–Sepharose only reduced this value by a further 15% (data not shown), suggesting carbohydrate heterogeneity of the EGF-binding components of the starting material. Indeed, Hurwitz *et al.* [51] have shown that sEGF-R from A431 cells could be resolved into at least 24 discrete bands

TABLE I

RECOVERY DATA FOR THE PURIFICATION OF sEGF-R OBTAINED USING THE BIOSENSOR

Stage	RU loaded[a]	RU recovered[a]	Stage recovery (%)	Overall recovery (%)
WGL-MonoQ	63 938	45 100	71	71
Mono Q-Sup 12	30 450	14 196	49	22.5[b]
Sup12-μMono Q	9146	7525	82	12[b]
μMono Q No. 7	N/A[c]	1436	N/A	2.2
μMono Q No. 8	N/A	406	N/A	0.6
μMono Q No. 9	N/A	1244	N/A	1.9
μMono Q No. 10	N/A	1923	N/A	3.0
μMono Q No. 11	N/A	1931	N/A	3.0
μMono Q No. 12	N/A	581	N/A	0.9

[a] The total signal was obtained by extrapolating the signal observed with a given injection volume to the total sample volume.
[b] The difference between the overall recovery and the cumulative stage recovery is due to the fact that only the major active fractions from the Mono Q HR 5/5 (Nos. 9–12) and Superose 12 columns (Nos. 21–23) were used at the next stage of the purification.
[c] N/A = Calculation not applicable to these fractions.

by isoelectric focusing. Only the sEGF-R which binds to WGL–Sepharose [45] was taken for further purification, and EGF-binding activity in the eluate was given a relative value of 100% for subsequent recovery calculations (Table I). Anion-exchange HPLC of this preparation (Fig. 6A) yielded a complex elution profile, demonstrating further the heterogeneity of the preparation. SDS-PAGE of the WGL eluate demonstrated the presence of at least 10 protein components, ranging in M_r from 20 000–200 000 (Fig. 6A, inset). This finding is in marked contrast to the data of Basu *et al.* [45], who claimed to obtain homogeneous sEGF-R from A431 cell conditioned medium by the sole use of WGL chromatography.

Biosensor measurements revealed that fractions with EGF-binding activity eluted from the Mono Q column as a distinct peak between 8 and 13 min, corresponding to a salt concentration of 100–200 m*M*. This is in good agreement with the data of Lax *et al.* [52] who found that recombinant sEGF-R expressed in Chinese hampster ovary (CHO) cells also eluted from a Mono Q column between 150 and 200 m*M* NaCl. By contrast, sEGF-R produced using a baculovirus expression system eluted from a Mono Q column between 75 and 100 m*M* NaCl [53], presumably due to alternative patterns of glycosylation. SDS-PAGE of the peak fractions of EGF binding activity from the Mono Q HR 5/5 column (Fractions 9, 10, and 11, Lanes 4–6 in Fig. 6A) showed the presence of a major protein band with an apparent M_r of 110 000. The total activity recovered (expressed in response units, RU) for the peak fractions was 71% relative to the WGL-eluate (Table I).

Further separation of the sEGF-R from contaminating proteins was achieved by size-exclusion HPLC on Superose 12 HR 10/30 of concentrated active Mono Q fractions (Fig. 6B). A major peak of binding activity (fractions 21–24) corresponding to a protein with an apparent M_r of 100 000 was observed. SDS-PAGE of these fractions (inset) showed that fractions 21, 22 and 23 were highly enriched for the M_r 110 000 component. Fraction 24 also contained proteins of M_r 80 000, 65 000 and 55 000 (data not shown), and was therefore not taken for further purification. A total of 49% of the applied activity was recovered from the size-exclusion column (Table I).

Final micropreparative anion-exchange chromatography [27,37] performed on a Pharmacia SMART system (Fig. 6C) concentrated the sEGF-R preparation into a buffer suitable for immobilisation onto the sensor chip of the biosensor. The total recovery of activity from this column was 82% (Table I). This activity was associated with an early eluting sharp peak, and

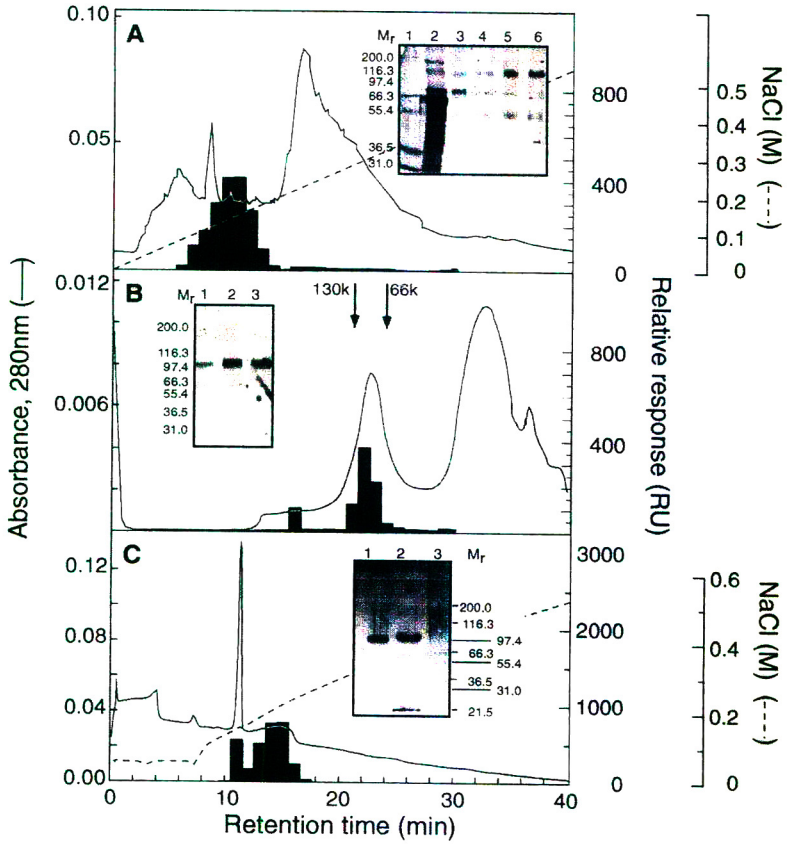

Fig. 6. The use of the biosensor to monitor the purification of sEGF-R. Conditioned medium from A431 cells, containing sEGF-R [40,45], was concentrated and purified on WGL–Sepharose as described in Materials and Methods. (A) The WGL eluates were adjusted to pH 8.5 and purified on a Mono Q HR 5/5 column. Chromatographic conditions are given in Materials and Methods. 1-min fractions were collected and aliquots (40 μl) tested for EGF-binding activity using the biosensor (■). Inset: SDS-PAGE analysis of (Lane 1) molecular mass standards, (Lane 2) A431 conditioned medium concentrate, (Lane 3) WGL–Sepharose eluent, (Lanes 4–6) fractions 9, 10, and 11 respectively from the Mono Q HR 5/5 column. (B) Size-exclusion HPLC of active sEGF-R fractions from Mono Q HR 5/5. Fractions 9–12 from the Mono Q 5/5 column (see panel A) were concentrated and loaded onto a Superose 12 HR 10/30 size-exclusion column. Experimental conditions are given in Materials and Methods. Fractions were collected at 1-min intervals. Aliquots (20 μl) from each fraction were taken for biosensor assay (■). Inset: SDS-PAGE analysis of (Lane 1) fraction 21, (Lane 2) fraction 22, (Lane 3) fraction 23. (C) Micropreparative HPLC on Mono Q PC 1.6/5. Fractions 21–23 from the Superose 12 column (see Panel B) were concentrated and buffer exchanged using a Mono Q PC 1.6/5 micropreparative anion-exchange column. Experimental details are given in Materials and Methods. Fractions were collected at 1-min intervals and aliquots (16 μl) were assayed for EGF binding activity (■) following dilution (1:2.5) with HBS biosensor buffer. Inset: SDS-PAGE analysis of (Lane 1) fraction 12, (Lane 2) fraction 15, (Lane 3) molecular mass standards.

a later eluting, more diffuse, component (Fig. 6C). SDS-PAGE analysis of these peak fractions (Fig. 6C, inset) demonstrated essentially homogeneous proteins of M_r 100 000–105 000, in agreement with the previously reported size of sEGF-R [40,45]. Careful investigation of the gel showed that the early eluting species had a slightly lower M_r than the later eluting form(s), suggesting that glycosylated variants had been resolved.

Biosensor analysis of EGF-binding ability provided a reliable and rapid means of monitoring the recovery from the various column matrices used during the purification. Since BIAcore measurements are compatible with the buffer systems used in the purification protocol, no sample preparation was necessary prior to the assay, therefore minimising both sample consumption and manipulation between purification

steps. In addition to the quantitative data obtained from the relative response observed at the completion of the biosensor injection cycle, we also noted that analysis of the dissociation phase of the sensorgram provided a very sensitive and specific distinction between "specific" and "non-specific" responses (Fig. 7). When crude A431 supernatant was applied to the BIAcore (Fig. 7A), at the end of the injection cycle, and following the buffer related refractive index change, a dissociation curve was obtained (Fig. 7B) which showed that, whilst a minor component of the preparation showed a rapid initial dissociation ($k_{diss1} = 1.4 \cdot 10^{-2}\ s^{-1}$), the majority of the bound activity exhibited a much slower dissociation ($k_{diss2} = 7.6 \cdot 10^{-4}\ s^{-1}$). Indeed, after

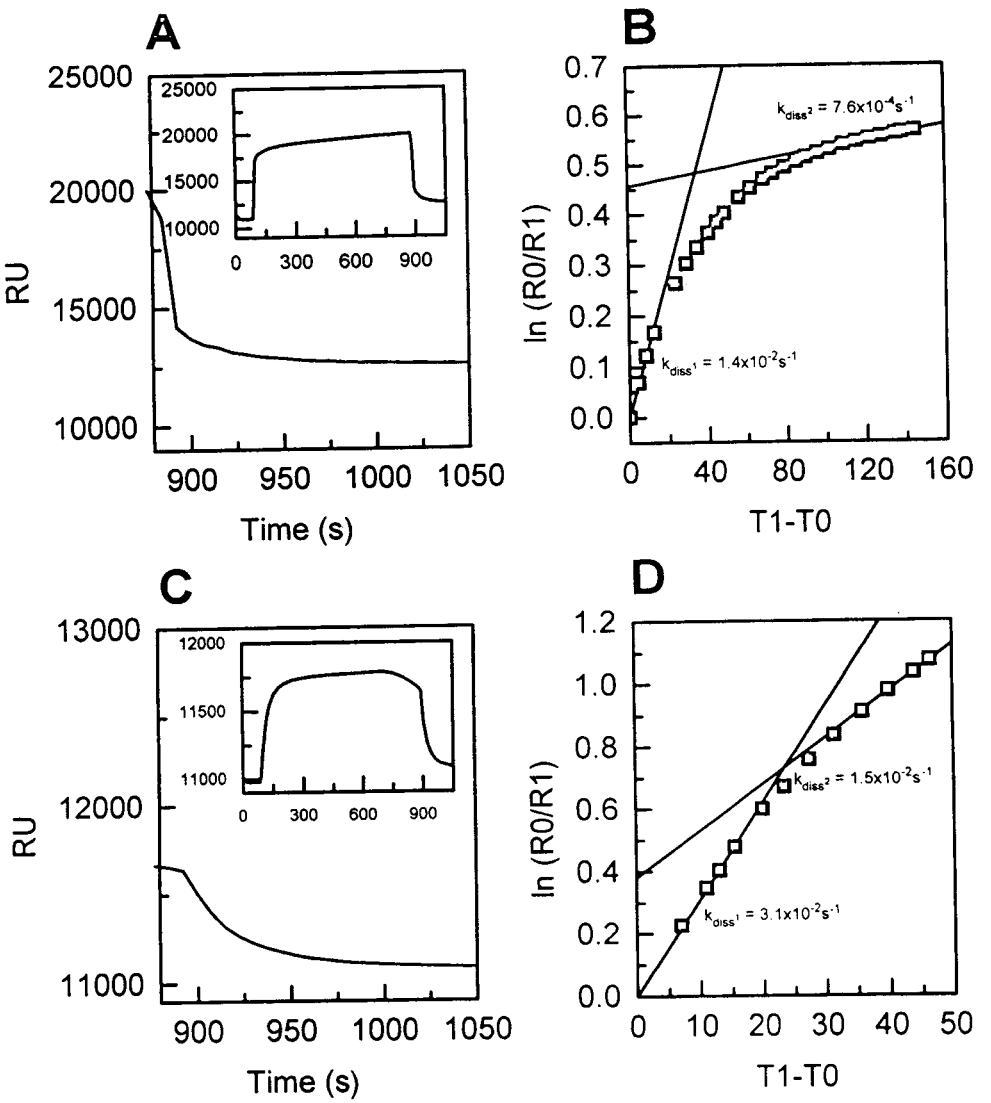

Fig. 7. Kinetic analysis of sEGF-R chromatographic fractions. (A) Sensorgram showing the dissociation of bound material in the A431 supernatant from hEGF under constant buffer flow (3 μl/min). Inset: sensorgram showing the total interaction curve for the injection of A431 supernatant (40 μl). (B) Dissociation plot obtained from the data in Panel A. (C) Sensorgram showing the dissociation of purified sEGF-R from hEGF under constant buffer flow (3 μl/min). Inset: sensorgram showing the total interaction curve for the injection of purified sEGF-R (40 μl). (D) Dissociation plot obtained from the data in panel C.

160 s only 55% of the bound material had dissociated. Fractionation of the crude A431 supernatant on WGL–Sepharose resulted in the separation of EGF binding activity into a lectin-bound component characterised by a fast off-rate and a non-bound component with negligible dissociation from the immobilised EGF. Biosensor assays of fractions from size-exclusion HPLC of the non-bound component indicated no activity in the expected molecular mass range of sEGF-R, the activity eluting predominantly in the void volume of the column (data not shown). The biosensor analysis of the purified fraction obtained from the micropreparative anion-exchange column (Fig. 6C) also displayed an initial fast off rate ($k_{diss1} = 3.1 \cdot 10^{-2}$ s^{-1}, Fig. 6D). Although this dissociation plot also indicated a biphasic dissociation, the later dissociation was still rapid ($k_{diss2} = 1.5 \cdot 10^{-2}$ s^{-1}) In this case 70% of the bound material had dissociated after 50 s. It has been suggested [16] that biphasic dissociation plots may be due, in part, to rebinding of dissociated material before it can diffuse out of the matrix. However, similar dissociation rates (k_{diss} $6.2 \cdot 10^{-2}$ s^{-1} [54]) have been observed for biosensor measurements of the dissociation of sEGF-R, purified from CHO cell expression systems [52], from hEGF. By providing qualitative data on the interaction between purified protein and known (*i.e.*, immobilised) ligand during final purification stages the kinetic information derived from the biosensor detection system can deliver complimentary and very specific information on the characteristics of the purified molecule.

The use of the biosensor as a detector as described above would appear to be particularly valuable in the search for "unknown ligands" for, as an example, antibodies raised against complex mixtures of proteins and carbohydrate, or for new members of gene families (*e.g.* tyrosine kinases [38,39]) which have been elucidated from sequence homologies and PCR-based molecular biology techniques. In such cases the biosensor can firstly be used to screen for possible sources of the ligand (*e.g.* tissue extracts, conditioned media) and then subsequently be used as a specific detector for monitoring fractions obtained during chromatographic purification of the ligand of interest, provided that sufficient quantities of the purified recombinantly derived target protein (1–10 μg), at suitable concentration (typically 10–100 μg/ml), can be generated for the initial immobilisation. Additionally the use of affinity chromatographic procedures as part of the purification protocol would appear advantageous, providing that suitable elution conditions can be defined.

Optimisation of elution conditions for affinity chromatography

It is possible to consider the BIAcore as being analagous to an analytical affinity chromatography system, using step wise elution conditions with "on-column" detection. Additionally the NHS–EDC immobilisation chemistry used with the biosensor is similar to that offered with several currently available affinity chromatography supports [*e.g.* Affi-Gel 10 (Biorad), NHS–Superose (Pharmacia)], so that similar immobilised surfaces can be compared. By defining immobilisation and binding conditions for the sensor chip which can be directly translated to the corresponding affinity chromatography system, it is then possible to use the biosensor to rapidly investigate a series of elution/desorption conditions, and quantitatively check the surface (and the ligand treated under similar conditions) for denaturation following the analysis. The BIAcore can also be used to screen a range of antibodies to determine those which have suitable association/dissociation characteristics and stability for use as affinity matrices [14,55].

In the example presented herein we have investigated the use of the biosensor to define suitable conditions for the affinity purification of influenza virus N9 neuraminidase. A Fab fraction (NC41 Fab) of a monoclonal antibody raised against neuraminidase heads [43] was immobilised onto the sensor surface as described in Materials and Methods. Injection of tern neuraminidase (100 μg/ml, 50 μl injection, flow-rate 2 μl/min) over the NC41 Fab surface gave a positive response of 5213 RU (Fig. 8A), demonstrating the ability of the Fab fraction to bind the neuraminidase following immobilisation. Additionally, the shape of the sensorgram suggested rapid association and slow dissociation phases

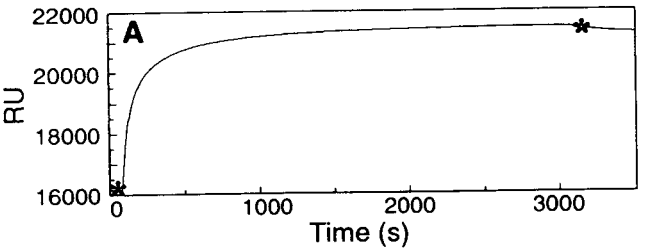

Time	AbsResp	Baseline	RelResp	Id
62.00	16140	YES	0	INJ_Neuraminidase
3162.00	21353	NO	5213	Neuraminidase

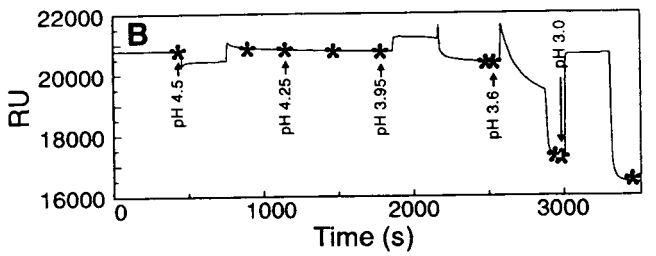

Time	AbsResp	Baseline	RelResp	Id
436.00	20795	YES	0	INJECT_AC-pH4.5
900.00	20900	NO	105	pH4.5
1140.00	20820	YES	0	INJECT_pH4.25
1480.00	20790	NO	-130	pH4.25
1800.00	20792	YES	0	INJECT_pH3.95
2488.00	20408	NO	-384	pH3.95
2536.00	20397	YES	0	INJECT_pH3.6
2948.00	17288	NO	-3109	pH3.6
2984.00	17222	YES	0	INJECT_pH3.0
3468.00	16397	NO	-825	pH3.0

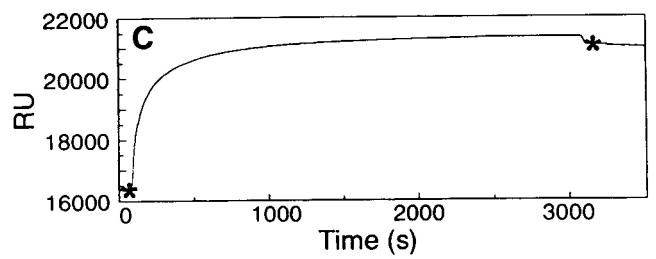

Time	AbsResp	Baseline	RelResp	Id
62.00	16363	YES	0	INJ_Neuraminidase
3162.00	21074	NO	4710	Neuraminidase

Fig. 8. The use of the biosensor to determine elution conditions for affinity chromatography. (A) Tern neuraminidase (100 μg/ml, 50-μl injection) was passed, at a flow-rate of 1 μl/min, over a sensor surface onto which NC41 Fab had been immobilised. (B) Following binding of the tern neuraminidase (Panel A), aliquots (25 μl) of buffers of decreasing pH were sequentially injected over the sensor surface. The flow was 5 μl/min. (C) Following desorption at pH 3.0 (Panel B) the NC41 Fab was rechallenged with tern neuraminidase using the conditions described in Panel A.

which are ideal characteristics for antibodies to be used in affinity supports, providing that suitable desorption conditions can be found. Following binding the flow-rate was increased to 5 μl/min and sequential 25-μl injections were performed using buffers of progressively reducing pH (Fig. 8B). Injection of pH 4.5 or pH 4.25 buffer caused no desorption. The use of pH 3.95 buffer caused desorption of 8.2% of the bound neuraminidase. Approximately 67% desorption was evident after lowering the pH to 3.6, with a further 18% eluted at pH 3.0.

When the sensor surface was rechallenged with tern neuraminidase (injection conditions as

for Fig. 8A), a response of 4710 RU was obtained (Fig. 8C), showing that the surface was at least 90% viable following the desorption at pH 3.0. The conditions derived using the BIAcore for the elution of tern neuraminidase from NC41 Fab can be used successfully for affinity purification (L.C. Gruen, personal communication).

CONCLUSIONS

We have presented a number of examples of the synergy between micropreparative HPLC and an optical biosensor (Pharmacia BIAcore). The eluent sample volumes and concentration achieved with the HPLC have been shown to be ideally suited for subsequent manipulation on the biosensor. We have also shown how the biosensor may be used as a detector to monitor the purification of fractions from the HPLC, and how it may be used to define elution conditions for affinity chromatography. Thus there is a "bidirectional" synergy between these two techniques which will facilitate the development of efficient purification schemes and permit quantitative kinetic analyses of the interactions.

ACKNOWLEDGEMENTS

This work was supported, in part, by grant no. 920525 from the National Health and Medical Research Council, Canberra, Australia and the Australian Government Cooperative Research Centres Scheme. The authors gratefully acknowledge Dr. L.C. Gruen and Dr. D. Jackson for the generous gift of some of the reagents used in these studies. We also would like to thank Dr. B. Persson of Pharmacia Biosensor for helpful advice and discussion and Professor R. Wettenhall, Department of Biochemistry, University of Melbourne for the use of the MALD-MS.

REFERENCES

1 U. Jonsson and M. Malmqvist, in A.P.F. Turner (Editor), *Advances in Biosensors*, Vol. 2, JAI Press, London, 1992, p. 291.
2 M. Malmqvist, *Nature*, 361 (1993) 186.
3 M. Brigham-Burke, J.R. Edwards and D.J. O'Shannessy, *Anal. Biochem.*, 205 (1992) 125.
4 K. Yasukawa, T. Futatsugi, T. Saito, H. Yawata, M. Narazaki, H. Suzuki, T. Taga and T. Kishimoto, *Immunol. Lett.*, 31 (1992) 123.
5 J.D. Marks, A.D. Griffiths, M. Malmqvist, T.P. Clackson, J. M Bye and G. Winter, *Biotechnology*, 10 (1992) 779.
6 D. Altschuh, M-C. Dubs, E. Weiss, G. Zeder Lutz and M.H.V. Van Regenmortel, *Biochemistry*, 31 (1992) 6298.
7 L.G. Fagerstam, A. Frostell, R. Karlsson, M. Kullman, A. Larsson, M. Malmqvist and H. Butt, *J. Mol. Recognit.*, 3 (1990) 208.
8 E. Nice, J. Layton, L. Fabri, U. Hellman, A. Engstrom, B. Persson and A.W. Burgess, *J. Chromatogr.*, 646 (1993) 159.
9 M-C. Dubs, D. Altschuh and M.H.V. Van Regenmortel, *Immunol. Lett.*, 31 (1992) 59.
10 P. End, G. Panayotou, A. Entwistle, M.D. Waterfield and M. Chiquet, *Eur. J. Biochem.*, 209 (1992) 1041.
11 T.C. VanCott, L.D. Loomis, R.R. Redfield and D.L. Birx, *J. Immunol. Methods*, 146 (1992) 163.
12 L.D. Ward, P.T. Shi and R.J. Simpson, *Biochem. Int.*, 26 (1992) 559.
13 G. Zeder-Lutz, D. Altschuh, H.M. Geysen, E. Trifilieff, G. Sommermeyer and M.H.V. Van Regenmortel, *Mol. Immunol.*, 30 (1993) 145.
14 R. Karlsson, A. Michaelsson and L. Mattsson, *J. Immunol. Methods*, 145 (1991) 229.
15 G. Panayotou, B. Bax, I. Gout, M. Federwisch, B. Wroblowski, R. Dhand, M.J. Fry, T.L. Blundell, A. Wollmer and M.D. Waterfield, *EMBO J.*, 11 (1992) 4261.
16 S. Felder, M. Zhou, P. Hu, J. Urena, A. Ullrich, M. Chaudhuri, M. White, S.E. Shoelson and J. Schlessinger, *Mol. Cell. Biol.*, 13 (1993) 1449.
17 S. Lofas and B. Johnsson, *J. Chem. Soc. Chem. Commun.*, 21 (1990) 1526.
18 B. Johnsson, S. Lofas and G. Lindquist, *Anal. Biochem.*, 198 (1991) 268.
19 B. Liedberg, C. Nylander and I. Lundstrom, *Sens. Actuators*, 4 (1983) 299.
20 M.T. Flanagan and R.H. Plantell, *Electron. Lett.*, 20 (1984) 968.
21 E.C. Nice, C.J. Lloyd and A.W. Burgess, *J. Chromatogr.*, 296 (1984) 153.
22 S. Cohen, G. Carpenter and L. King Jr, *J. Biol. Chem.*, 255 (1980) 4834.
23 E.C. Nice, B. Grego and R.J. Simpson, *Biochem. Int.*, 11 (1985) 187.
24 E.C. Nice and R.J. Simpson, *J. Pharmaceut. Biomed. Anal.*, 7 (1989) 1039.
25 R.J. Simpson, R.L. Moritz, G.S. Begg, M.R. Rubira and E.C. Nice, *Anal. Biochem.*, 177 (1989) 221.
26 E.C. Nice, *Nature*, 348 (1990) 462.
27 E.C. Nice, L. Fabri, A. Hammacher, K. Andersson and U. Hellman, *Biomed. Chromatogr.*, 7 (1993) 104.
28 R.J. Simpson and E.C. Nice, in A.R. Kerlavage (Editor), *The use of HPLC in receptor biochemistry*, A.R. Liss, New York, 1989, p. 201.

29 E.C. Nice, J.A. Smith, R.L. Moritz, M.J. O'Hare, P.S. Rudland, J.R. Morrison, C.J. Lloyd, B. Grego, A.W. Burgess and R.J. Simpson, in J.J. L'Italien (Editor), *Proteins*, Plenum, 1987, p. 37.
30 A.W. Burgess, D. Metcalf, I.J. Kozka, R.J. Simpson, G. Vairo, J.A. Hamilton and E.C. Nice, *J. Biol. Chem.*, 260 (1985) 16004.
31 E.C. Nice, R.J. Simpson and N.A. Nicola, *Chromatographia*, 24 (1987) 449.
32 R.J. Simpson, R.L. Moritz, C.J. Lloyd, L.J. Fabri, E.C. Nice, M.R. Rubira and A.W. Burgess, *FEBS Lett.*, 224 (1987) 128.
33 A.W. Burgess, C.J. Lloyd, S. Smith, E. Stanley, F. Walker, L. Fabri, R.J. Simpson and E.C. Nice, *Biochemistry*, 27 (1988) 4977.
34 R.J. Simpson, D.J. Hilton, E.C. Nice, M.R. Rubira, D. Metcalf, D.P. Gearing, N.M. Gough and N.A. Nicola, *Eur. J. Biochem.*, 175 (1988) 541.
35 E. Nice, P. Dempsey, J. Layton, G. Morstyn, D.F. Cui, R. Simpson, L. Fabri and A. Burgess, *Growth Factors*, 3 (1990) 159.
36 E.C. Nice, L. Fabri, R.H. Whitehead, R. James, R.J. Simpson and A.W. Burgess, *J. Biol. Chem.*, 266 (1991) 14425.
37 E.C. Nice, L. Fabri, A. Hammacher, J. Holden, R.J. Simpson and A.W. Burgess, *J. Biol. Chem.*, 267 (1992) 1546.
38 A.F. Wilks, *Proc. Natl. Acad. Sci. USA*, 86 (1989) 1603.
39 A.F. Wilks, *Methods. Enzymol.*, 200 (1991) 533.
40 W. Weber and G.N. Gill, *Science*, 224 (1984) 294.
41 L. Fabri, H. Maruta, H. Muramatsu, T. Muramatsu, R.J. Simpson, A.W. Burgess and E. C Nice, *J. Chromatogr.*, 646 (1993) 213.
42 R.C. Beavis, T. Chaudhary and B.T. Chait, *Org. Mass. Spectrom.*, 27 (1992) 156.
43 R.G. Webster, G.M. Air, D.W. Metzger, P.M. Colman, J.N. Varghese, A.T. Baker and W.G. Laver, *J. Virol*, 61 (1987) 2910.
44 D.C. Jackson and L.E. Brown, *Pept. Res.*, 4 (1991) 114.
45 A. Basu, M. Raghunath, S. Bishayee and M. Das, *Mol. Cell. Biol.*, 9 (1989) 671.
46 J.A. De Feijter, J. Benjamins and F.A. Veer, *Biopolymers*, 17 (1978) 1759.
47 L.G. Fagerstam, A. Frostell-Karlsson, R. Karlsson, B. Persson and I. Ronnberg, *J. Chromatogr.*, 597 (1992) 397.
48 P.M. Colman, W.R. Tulip, J.N. Varghese, P.A. Tulloch, A.T. Baker, W.G. Laver, G.M. Air and R.G. Webster, *Philos. Trans. R. Soc. London B.*, 323 (1989) 511.
49 E. Stenberg, B. Persson, H. Roos and C. Urbaniczky, *J. Colloid Interface Sci.*, 143 (1991) 513.
50 S. Cohen, H. Ushiro, C. Stoscheck and M. Chinkers, *J. Biol. Chem.*, 257 (1982) 1523.
51 D.R. Hurwitz, L. Stuart, M.H. Emanuel, N. Sarver, A. Ullrich, S. Felder, I. Lax and J. Schlessinger, *J. Biol. Chem.*, 266 (1991) 22035.
52 I. Lax, A.K. Mitra, C. Ravera, D.R. Hurwitz, M. Rubinstein, A. Ullrich, R.M. Stroud and J. Schlessinger, *J. Biol. Chem.*, 266 (1991) 13828.
53 C. Greenfield, I. Hiles, M.D. Waterfield, M. Federwisch, A. Wollmer, T.L. Blundell and N. McDonald, *EMBO J.*, 8 (1989) 4115.
54 M. Zhou, S. Felder, M. Rubinstein, D.R. Hurwitz, A. Ullrich, I. Lax and J. Schlessinger, *Biochemistry*, 32 (1993) 8193.
55 R. Karlsson, D. Altschuh and M.H.V. Van Regenmortel, in M.H.V. Van Regenmortel (Editor), *Structure of Antigens*, Vol. 1, CRC Press, Boca Raton, FL, 1992, p. 127.

Journal of Chromatography A, 660 (1994) 187–194
Elsevier Science B.V., Amsterdam

CHROMSYMP. 2909

Parallel-current open-tubular liquid chromatography with fluorimetric detection

Marie Horká, Vladislav Kahle and Karel Šlais*

Institute of Analytical Chemistry, Academy of Sciences of the Czech Republic, Veveří 97, 611 42 Brno (Czech Republic)

ABSTRACT

Some characteristics of the flowing retentive film in parallel-current open-tubular liquid chromatography with a cyclohexanol–water mobile phase and fluorimetric detection are considered. The internal surface of a fused-silica capillary was modified with octamethylcyclotetrasiloxane (D_4 reagent).

INTRODUCITON

Recently, a new mode of open-tubular liquid–liquid chromatography designed as parallel-current open-tubular liquid chromatography (PC-OTLC) was suggested [1–3]. In PC-OTLC, both the mobile phase and the retentive layer move in the same direction, the retentive layer at a lower velocity than the mobile phase. The internal surface of the capillary is modified so that it is wettable by the retentive phase and it is covered with a retentive film. A mathematical description of the retention of an analyte in an open-tubular column of circular cross-section has been derived [1].

In previous paper [2], we suggested criteria for solvent pair optimization on a glass capillary under the conditions of RP-PC-OTLC with electrochemical detection. When the surface layer is not spread uniformly around the inner capillary circumference, the average linear velocity of the film increases and the film cross-section decreases [2]. Consequently, both the solute retention and the phase ratio are lower then those calculated for a uniform film thickness. For maximizing the phase ratio (ϕ), the liquids with a maximum ratio of their viscosity to the interfacial tension (γ/η) between the two flowing liquids is to be preferred. Cyclohexanol represents the optimum choice amongst the liquids examined for RP-PC-OTLC [2].

For reversed-phase systems, the internal surface of the separation capillary should be hydrophobic. Therefore, the siliceous surface of the capillary should be suitably modified. The techniques for surface modification of capillaries for OTLC are based on methods known in gas chromatography [2–5]. Of the methods of glass modification examined, persilylation with octamethylcyclotetrasiloxane (D_4 reagent) is the optimum procedure giving a retention close to the theory [1]. Previously, we used glass capillaries for PC-OTLC [1–3]. Fused silica offers some advantages over with glass. However, the properties of the interface of these two materials with liquids are different [6,7]. On the basis of experience with the glass capillaries, we used persilylation with D_4 reagent in this study with fused-silica capillaries. Also, reversed-phase chromatography with the system water–cyclohexanol was adopted for model separations. In this work, we studied the basic characteristics of the production, rinsing and destruction of the retentive film under different PC-OTLC conditions.

* Corresponding author.

0021-9673/94/$07.00 © 1994 Elsevier Science B.V. All rights reserved
SSDI 0021-9673(93)E0875-U

In previous studies [1–3] we employed an electrochemical detector with a platinum microelectrode. Fluorescence detection offers the highest level of sensitivity obtainable in HPLC [8]. On-column fluorescence detection [9,10], in which the capillary column itself is used as a flow cell, is superior to postcolumn detection because of the negligible extra-column band broadening [11]. Also, on-column detection provides increased sensitivity compared with postcolumn detection [12] owing to the concentration of the solute in the retentive phase. The applicability of fluorimetric detection in PC-OTLC is demonstrated in this study.

EXPERIMENTAL

Capillary preparation

Fused-silica capillaries of 0.2 mm O.D. and 0.035 mm I.D. were purchased from the Institute of the Chemistry of Glass and Ceramic Materials, ČSAV (Prague, Czech Republic). The internal surface of the capillaries was modified with D_4 reagent [2]. The procedure was carried out once or twice. The length of the capillaries used in PC-OTLC experiments was 5–6 m. Measurements were carried out in a linear velocity range from 1.3 to 85 mm s^{-1}.

Chromatograph

The chromatographic system used has been described previously [13]. The pressure source was a VCM 300 micropump (Development Works, Czechoslovak Academy of Sciences, Prague, Czech Republic). The sample was injected using a six-port laboratory made valve with a 20-μl loop and a flow splitter. The splitting ratio was 1:500–7500. The capillary column was immersed in a water-bath connected with a U8 thermostat (MLW Prüfgeräte-Werk, Medingen/Sitz Freital, Germany). The column was maintained at 20.0–90.0°C; the mobile phase temperature was 20.0°C. For on-column fluorimetric detection we adapted [14] a Kratos FS 950 fluorimeter (Schoeffel Instruments) (see Fig. 1). To obtain a detection window, the polyimide coating was removed by burning from an 8-mm long section of the capillary. The radiation obtained from a low-pressure mercury lamp passed through a 254-nm interference excitation filter and fell on the cell. The emitted light passed through a 320-nm cut-off filter to a photomultiplier tube. The detector signal was monitored with a TZ 4100 line recorder (Laboratory Instruments, Prague, Czech Republic).

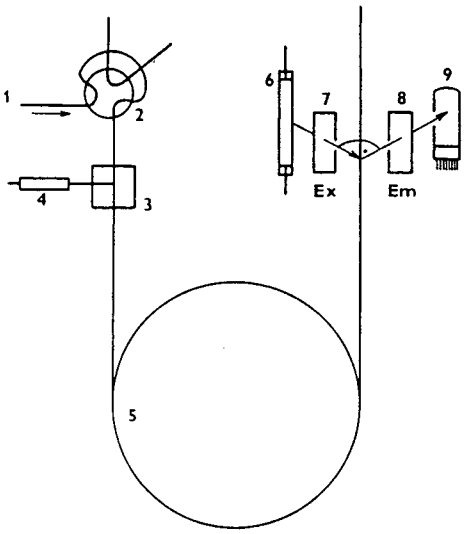

Fig. 1. Experimental arrangement of the chromatograph with fluorimetric detection. 1 = Mobile phase supply; 2 = six-port valve; 3 = splitter; 4 = restrictor; 5 = fused-silica capillary column (35 μm I.D.) immersed in a water-bath; 6 = mercury discharge lamp; 7 = 254-nm interference filter; 8 = 320-nm cut-off filter; 9 = photomultiplier tube.

Mobile phase

The pumped liquid was water saturated with cyclohexanol at 20.0°C. The differences in the solubilities of cyclohexanol in water between the pumped liquid temperature and the column temperature (20–90°C) used for the calculations are based on the interpolation of the reported data [15] and they were recalculated to volumetric units.

Chemicals and test solutes

The model analytes were salicylic acid (marker of the dead time, t_{ro}), DL-tryptophan, hydroquinone, catechol, resorcinol, indolylacetic acid, sulphanilamide, aniline sulphate, 2-methylaniline, 2,6-dimethylaniline and phenol. The test solutes and other chemicals used were purchased from Lachema (Brno, Czech Republic). D_4

reagent was obtained from VCHZ Synthezia (Kolín, Czech Republic).

Viscosity measurement

The viscosities of co-existing liquids in the cyclohexanol–water system at 20, 50 and 70°C were measured using a thermostated Ubbelohde viscosimeter. The liquid densities needed were determined pycnometrically. Using reference values for water [16], the densities of the aqueous and organic phases were determined. The date obtained are summarized in Table I.

Determination of the distribution constant, K_i

The solute K_i was determined by the method described previously [17]. A known amount of the analyte was dissolved in the aqueous phase and the absorbance at 278 nm for phenol was determined. The solution was then equilibrated for 2 days at 20 and 70°C with a known amount of cyclohexanol saturated with water and the absorbance of the aqueous phase was measured again. The K_i values for phenol at 50°C were taken from ref. 1. The data obtained are summarized in Table I.

Calculations

The experimental values of the reduced retention, k_i^*, were determined from the observed t_{ri} and t_{ro} values; the calculated – theoretical k_i^* value is related to the phase ratio ϕ, the flow ratio of the retentive and mobile phases q ($q = F_r/F_m$) and the liquid–liquid distribution coefficients of phenol, K_i, through the equation [1]

$$k_i^* = (\phi - q)/(1/K_i + q) \quad (1)$$

The theoretical value of ϕ was calculated from solubility and viscosity data using the equations [1]

$$q = \Delta s/(1 - \Delta s) \quad (2)$$

$$\phi = (1 - t + 1/\Delta s)/\{1/\Delta s - [1 + t(1/\Delta s - 1)]^{1/2}\} - 1 \quad (3)$$

where t is the viscosity ratio of the retentive and the mobile phases, $t = \eta_r/\eta_m$. In the suggested method, q is determined by the solubility difference of the retentive phase in the mobile phase at temperatures T_1 and T_2, $\Delta s = (s_{T_1} - s_{T_2})$. The linear velocity of the mobile phase was determined from the retention time of salicyclic acid (t_{ro}) and the capillary length.

RESULTS AND DISCUSSION

Long-term retention stability

This was tested by flushing the capillary with up to 1000 dead volumes of the mobile phase at 50°C (see Fig. 2). The linear flow velocity determined from the elution time of the unretained compound was 34.4 mm s^{-1}. The average k_i^* for phenol was 4.5 with fluctuations of up to 7.8%.

Time of retentive phase generation

This was tested by the measurement of the phenol k_i^* during column equilibration (see Fig. 3). The surface-modified capillary tempered at 20°C was flushed with distilled water until the retention of phenol vanished. The flow was then switched to mobile phase and the capillary temperature was increased to 50°C or 70°C (see

TABLE I

SOME EXPERIMENTAL AND CALCULATED CHARACTERISTICS OF THE PC-OTLC OF PHENOL IN THE CYCLOHEXANOL–WATER SYSTEM

T_2 (°C)	Δs (wt.%) [15]	q $\times 10^3$	η_{RP} (mN s m^{-1})	η_{MP} (mN s m^{-1})	t	ϕ	K_i	k_i^*	
								Exp.	Calc.
20	–	–	23.37	1.14	20.50	–	18.50	–	–
50	0.93	9.39	3.97	0.57	6.96	0.265	16.47	4.50	3.65
70	0.97	9.79	1.88	0.43	4.37	0.217	13.97	2.54	2.55

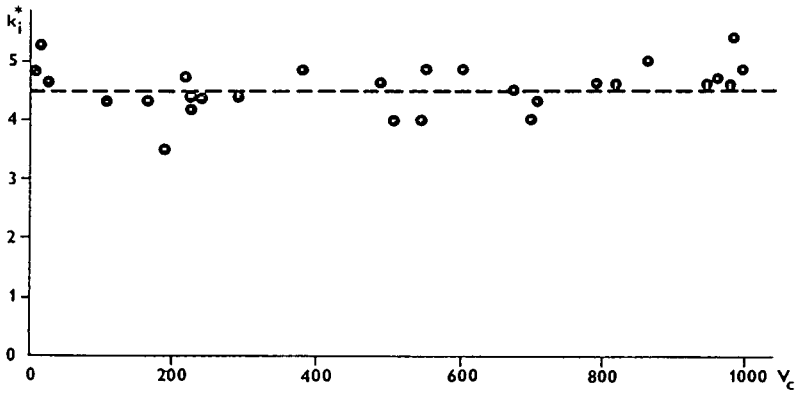

Fig. 2. Effect of the total volume of the mobile phase passed through the column on the reduced retention of phenol (k_i^*) under steady-state conditions. Column, fused-silica capillary (5 m × 35 μm I.D.) twice modified with D_4 reagent; column temperature, 50°C; mobile phase, water saturated with cyclohexanol at 20°C; solutes, salicylic acid (dead time marker) and phenol; splitting ratio, 1:7500; linear flow velocity, 34.4 mm s^{-1}; fluorimetric detection. Broken line = average k_i^* value of phenol; V_c = column volumes.

curves 1 and 2, respectively). Following curve 1 for 50°C, a nearly steady state was obtained after flushing with 17 V_c (column volumes); k_i^* for phenol was 3.7. Subsequently, the increase in k_i^* was slower until the steady state with $k_i^* = 4.4$ for phenol was obtained after 35 V_c. Similarly, following curve 2 for 70°C, a steady-state k_i^* for phenol of 2.35 was obtained after flushing with about 31 V_c. Curve 3 corresponds to the following experiment: the capillary was equilibrated with a flow of the mobile phase at 50°C, then it was left at 20°C without any flow for 16 h. The segmentation of the retentive film is expected within this time period [2,4]. The capillary was then tempered at 50°C and the flow of the mobile phase was renewed. The flushed volume needed for the regeneration of the retentive film was about four dead volumes, as follows from the retentions of the model analyte.

Time for retentive film elution

This was tested, similarly to the above, by the measurement of phenol retention (see Fig. 4). The capillary column was equilibrated at 50 and

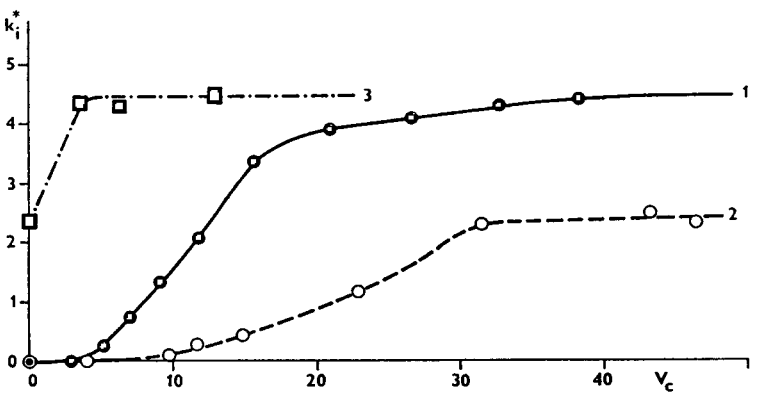

Fig. 3. Eluted volume necessary for generation of retentive layer by temperature rise. 1 = Temperature rise 20 to 50°C; 2 = temperature rise 20 to 70°C; 3 = column temperature 50°C, segmented film of retentive layer spread by flow only. V_c = column volumes; k_i^* = reduced retention of phenol. For other conditions, see Fig. 2.

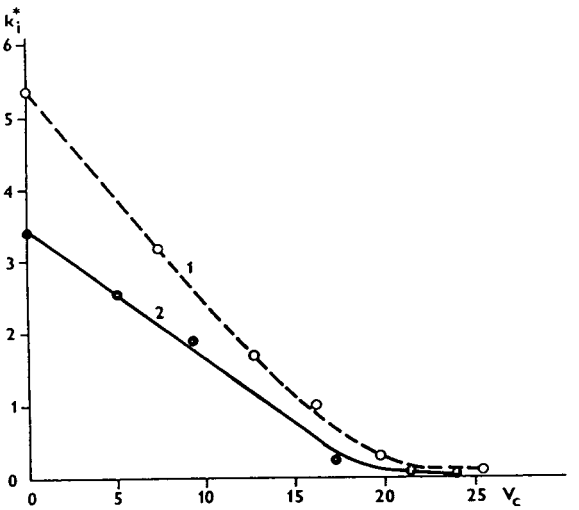

Fig. 4. Eluted volume necessary for removal of retentive layer by temperature drop. 1 = Temperature drop 50 to 20°C; 2 = temperature drop 70 to 20°C; V_c = column volumes; k_i^* = reduced retention of phenol. For other conditions, see Fig. 2.

70°C (see curves 1 and 2, respectively). After cooling the capillary to 20°C, the phenol retention continuously decreased and finally vanished when the capillary was flushed with about 25 V_c.

Dependence of retention on mobile phase velocity

As follows from the previous considerations [2], a decrease in u to below some critical value, u_c causes instability of the retentive film and the formation of segmented flow. Such conditions lead to decreases in the solute retention. In addition to this phenomenon, the presence of the segmented flow can also be reproducibly followed with the fluorimetric detector used, which displays increased noise under such conditions. Fig. 5, curves 1 and 2, represent the k_i^* *versus* u dependences in the capillary tempered at 50 and 70°C, respectively. In both instances, the pumped liquid was water saturated with cyclohexanol at 20°C. The calculated phase ratio in the capillary, ϕ, was 0.267 and 0.217, respectively. Curve 1a corresponds to the k_i^* *versus* u dependence at 50°C, when the capillary was flushed with water which contained cyclohexanol only in an amount corresponding to 97% saturation at 20°C. Then, the calculated ϕ was 0.244 and k_i^* for phenol was 3.0. With a decrease in u at 50°C, a marked increase in the phenol retention can be observed at around u_c. The probable explanation could be that ϕ increases under such conditions. As follows from Fig. 5, the critical velocity decreases with decrease in ϕ, as expected.

Temperature dependence of the solute retention

As supposed previously [1], the solute retention could be controlled by the temperature of

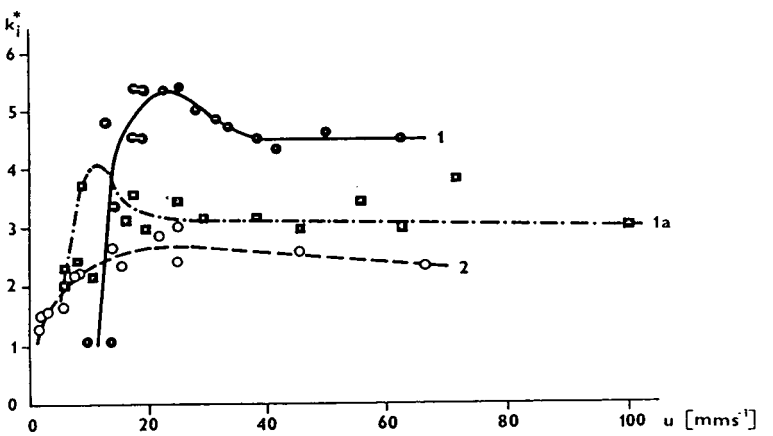

Fig. 5. Effect of flow velocity on reduced retention. 1 = Column temperature 50°C; 1a = column temperature 50°C, pumped liquid diluted with water (ϕ = 0.244); 2 = column temperature 70°C. u = Linear flow velocity (mm s^{-1}); k_i^* = reduced retention of phenol. For other conditions see Figs. 2 and 3.

the capillary column used in PC-OTLC. It follows from the nature of the method that k_i^* *versus* T_c dependence is a complex function of the solubilities and viscosities and their temperature dependences. To obtain an idea of the k_i^* *versus* T_c function, the amount of the data should be known. Nevertheless, some conclusions can be drawn from the above-mentioned measurements at 20, 50 and 70°C. In Fig. 6, the probable course of the k_i^* *versus* T_c function is shown as the broken curve. It was obtained from eqn. 1, where the viscosity and the solubility data needed were obtained by interpolation between the measured values (see Table I). The open points in Fig. 6 are the values calculated from the values in Table I and the closed points are the measured retentions of phenol at the respective temperatures. Although the calculated curve is only a rough approximation, it is in qualitative agreement with the experimental values. Further, the curve indicates that around ambient temperature, a steep dependence of retention on temperature occurs in the system used and, therefore, the strong demands are imposed on the instrument thermostating. In this way, the fluctuations of the analyte retentions can be explained.

Influence of acetonitrile concentration in the sample

To inject less water-soluble analytes, they should be dissolved in an organic or aqueous–organic solution. However, the injection of an organic solvent into the PC-OTLC column may disturb the steady-state conditions within the capillary. In order to obtain an idea about the possible disturbance, a model analyte (phenol) was injected in water–acetonitrile mixtures. A 24-nl volume of 5 m*M* solution was injected using a splitting ratio of 1:500. As follows from Fig. 7, concentrations of acetonitrile from 0 to 60% (v/v) have no influence on the solute retention. At higher concentrations, the phenol k_i^* value decreases from 4.4 to 3.4, which corresponds to a solution of phenol in pure acetonitrile. The decrease in retention can be caused by

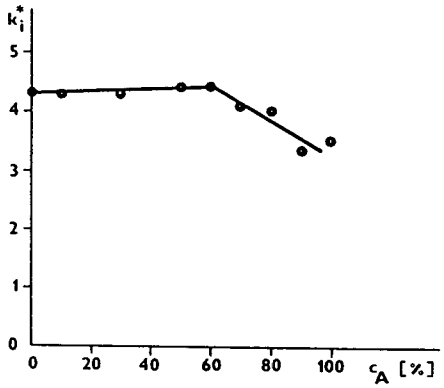

Fig. 7. Effect of sample acetonitrile concentration on reduced retention. c_A = Sample acetonitrile concentration (%, v/v); k_i^* = reduced retention of phenol; splitting ratio, 1:500. For other conditions, see Fig. 2.

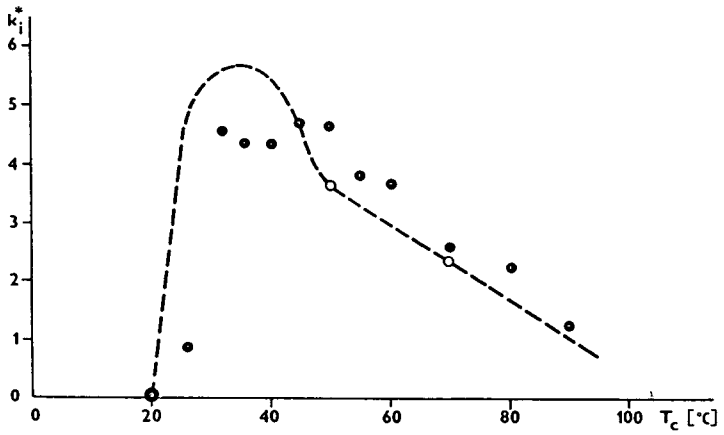

Fig. 6. Effect of column temperature on reduced retention. ● = Experimental points; ○ = calculated points; broken line = theoretical curve. T_c = column temperature (°C); k_i^* = reduced retention of phenol. For other conditions, see Fig. 2.

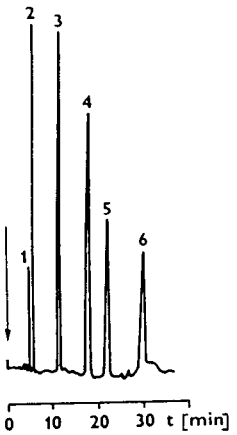

Fig. 8. PC-OTLC separation of a test mixture dissolved in acetonitrile–water (80:20%). Linear flow velocity, 17.9 mm s^{-1}. Peaks: 1 = salicylic acid (dead time marker); 2 = sulphanilamide; 3 = aniline sulphate; 4 = 2-methylaniline; 5 = phenol; 6 = 2,6-dimethylaniline. For other conditions, see Fig. 2.

a transient decrease in the film thickness and/or interfacial tension. An example of a chromatogram of the compounds dissolved in water–acetonitrile mixture (20:80, v/v) is shown in Fig. 8.

Influence of surface modification

In all the above experiments, a fused-silica capillary modified twice with D_4 reagent was used. As has been found previously, modification of the glass surface plays an important role in PC-OTLC [2]. To test the influence of modification of the fused silica on the performance of the capillary, the separation on a fused-silica capillary modified with only one persilylation step with D_4 reagent was carried out (see Fig. 9). It was found that the retentions are lower than those with the twice-modified capillary. Under otherwise identical conditions, a phenol k_i^* value of 3.0 was found at $u = 7.15$ mm s^{-1} and $T_c = 50°C$.

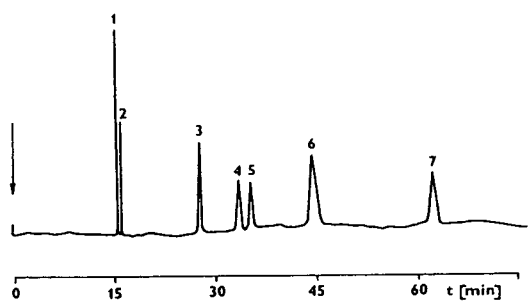

Fig. 9. PC-OTLC separation of a test mixture. Column, fused-silica capillary (6 m × 35 μm I.D.) modified once with D_4 reagent; linear flow velocity, 7.15 mm s^{-1}. Peaks: 1 = salicylic acid (dead time marker); 2 = DL-tryptophan; 3 = hydroquinone; 4 = catechol; 5 = resorcinol; 6 = indolylacetic acid; 7 = phenol. For other conditions, see Fig. 2.

CONCLUSION

The applicability of fluorimetric detection in RP-PC-OTLC was demonstrated. In comparison with electrochemical detection, it is less sensitive to the presence of the two phases in the detection cell, but the segmented flow causes the elevated noise. Simultaneously, the different selectivity also enables the number of detectable analytes to be increased.

Further, the applicability of the fused-silica capillaries in PC-OTLC was demonstrated. Unlike glass capillaries, the retentions found may differ considerably from the predicted values, either negatively or positively. The dynamic properties of the method seem to be advantageous for convenient changes of the separation system. Proper instrument thermostating and/or the use of a not fully saturated pumped liquid may improve the reproducibility of retention. Further studies are needed in order to elucidate all the observed phenomena and to make the method more generally applicable.

REFERENCES

1 K. Šlais, M. Horká and K. Klepárník, *J. Chromatogr.*, 605 (1992) 167.
2 K. Šlais and M. Horká, *J. Microcol. Sep.*, 5 (1993) 63.
3 K. Šlais and M. Horká, *J. High Resolut. Chromatogr.*, 16 (1993) 194.
4 K.D. Bartle, C.L. Wooley, K.E. Markides, R.S. Hansen and M.L. Lee, *J. High Resolut. Chromatogr. Chromatogr. Commun.*, 10 (1987) 128.
5 M. Novotny, *Anal. Chem.*, 60 (1988) 500A.
6 H.W. Fox, E.F. Hare and W.A. Zisman, *J. Phys. Chem.*, 59 (1955) 1097.
7 T. Wehr, *LC · GC Int.*, 6 (1993) 70.
8 H. Lingeman, W.J.M. Underberg, A. Takadate and A. Hulshoff, *J. Liq. Chromatogr.*, 8 (1985) 789.
9 F.J. Yang, *J. High Resolut. Chromatogr., Chromatogr. Commun.*, 3 (1980) 589.

10 F.J. Yang, *J. High Resolut. Chromatogr. Chromatogr. Commun.*, 4 (1981) 83.
11 T. Wang, R.A. Hartwick, P.B. Champlin, *J. Chromatogr.*, 462 (1989) 147–154.
12 E.J. Guthrie and J.W. Jorgenson, *Anal. Chem.*, 56 (1984) 483.
13 K. Janák, M. Horká and M. Krejčí, *J. Microcol. Sep.*, 3 (1991) 115.
14 V. Kahle and M. Janeček, *Chem. Listy*, 83 (1989) 867.
15 R. Stephenson and J. Stuart, *J. Chem. Eng. Data*, 31 (1986) 56.
16 R.C. Weast (Editor), *Handbook of Chemistry and Physics*, CRC Press, Boca Raton, FL, 68th ed., 1987–88, p. F4.
17 J.F.K. Huber, C.A.M. Meiers and J.A.R.J. Hulsman, *Anal. Chem.*, 44 (1972) 111.

Journal of Chromatography A, 660 (1994) 195–198
Elsevier Science B.V., Amsterdam

CHROMSYMP. 2912

Application of high-performance gel-permeation chromatography clean-up in the determination of hexaflumuron residues in soil

A. Khoshab* and R. Teasdale

DowElanco Europe, Letcombe Laboratories, Letcombe Regis, Wantage, Oxfordshire, OX12 9JT (UK)

ABSTRACT

A high-performance gel-permeation chromatography (HPGPC) column (7.5 mm I.D.), packed with a divinylbenzene cross-linked polystyrene gel (10 μm particles and 5 nm pore size) was used to produce a simple, one-stage clean-up procedure for determination of the insecticide hexaflumuron in three typical agricultural soils.

Conventionally, hexaflumuron extracts are purified by a series of time-consuming liquid–liquid partitions and solid-phase purification prior to high-performance liquid chromatography. HPGPC allows isolation of hexaflumuron from soil matrices with improved sensitivity in a shorter analysis time.

The use of HPGPC methodology has been validated over the range 0.01–1.0 mg/kg with recoveries in the range 73–119% (mean 98%). HPGPC gave excellent separation of hexaflumuron from other extracted materials with significant reduction in clean-up time and solvent consumption. This methodology has been successfully applied to samples derived from field trials.

INTRODUCTION

Hexaflumuron [1-(3,5-dichloro-4-(1,1,2,2-tetrafluoroethoxy)phenyl) - 3 - (2,6-difluorobenzoyl) urea] is the active ingredient of the insect growth regulator Consult (DowElanco), and is typically used on orchard fruits and vegetables.

Gel permeation chromatography (GPC) has been used to clean-up environmental samples for over 18 years. During this period the procedure has remained essentially unchanged, using preparative (25 mm I.D.) GPC columns based on 200–400 mesh Bio-Beads S-X resins (Bio-Beads S-X3 is the most commonly used), divinylbenzene cross-linked polystyrene gels. GPC is suitable for nearly all types of pesticides [1–5]. Tindle and Stalling [1] developed an automated clean-up apparatus which was evaluated by Griffitt and Craun [6] for use on a wide variety of fats and oils. Van Rhijn and Tuinstra [7], and Tuinstra *et al.* [8] described the use of a miniature (10 mm and 2 mm I.D.) GPC column, which effectively decreased solvent consumption and the collected fraction, but with limited sample loading.

Existing methods for the analysis of hexaflumuron use a number of liquid–liquid partitions which are time-consuming with high solvent consumption. In addition a silica solid-phase clean-up stage is sometimes required. This method still only achieves a lowest determination limit of 0.05 mg/kg.

This study investigates HPLC–UV quantitation of hexaflumuron residues in soil following the use of HPGPC as a clean-up procedure.

EXPERIMENTAL

Reagents and materials

Hexaflumuron analytical standard is from DowElanco Europe. Acetonitrile and water

* Corresponding author.

0021-9673/94/$07.00 © 1994 Elsevier Science B.V. All rights reserved
SSDI 0021-9673(93)E0878-X

were of HPLC grade; hexane and dichloromethane (DCM) were of Distol grade. 0.2 μm Minisart SRP 15 filters (PTFE membrane) were used.

Hexaflumuron standard stock solutions: 100 mg of analytical standard was dissolved in 60 ml of acetonitrile and diluted to 100 ml with water to give 1000 μg/ml stock solution. The solution was diluted to provide appropriate standard solutions.

GPC test solution: for testing the column performance, a mixture of corn oil (6.25 mg/ml), bis(2-ethylhexyl)phthalate (0.25 mg/ml), perylene (0.005 mg/ml) and sulphur (0.02 mg/ml) was prepared in DCM. A typical calibration chromatogram is shown in Fig. 1. GPC optimization solution: 1 μg/ml hexaflumuron standard in DCM.

HPGPC system and conditions

HPGPC was carried out using Spectra-physics SP8810 pump, Waters 486 UV detector, Waters Fraction collector, Waters autosampler, chart recorder, a PLgel 600 mm × 7.5 mm I.D. GPC column packed with polystyrene–divinylbenzene (10 μm particles and 5 nm pore size) and a PLgel 50 mm × 7.5 mm I.D. GPC guard column, packed with polystyrene–divinylbenzene (10 μm particle size) with DCM as the eluent at a flow-rate of 1.0 ml/min. The injection volume was 500 μl.

To establish the collect time (start and end time of the fraction peak) 1 μg/ml hexaflumuron optimization solution was injected onto the GPC column and monitored using UV detector at 254 nm (Fig. 2). A typical elution program for the fraction collector is: wait (dump) 14.3 min, collect 2.4 min.

HPLC system and conditions

Analyses were carried out using a Varian Star system consisting of 9050 UV detector, 9010 solvent delivery system, 9095 autosampler and a 250 mm × 2.1 mm I.D. Kromasil C18 (5 μm) column with following conditions: mobile phase: acetonitrile–water (gradient); solvent programme:

Time (min)	Acetonitrile (%)	Flow-rate (ml/min)
0.0	58	0.2
12.5	58	0.2
26.0	85	0.2
27.0	100	0.4
37.0	100	0.4
38.0	58	0.2

Equilibration time: 6 min; Injection volume: 50 μl; Wavelength: 254 nm; Range: 0.005 AUFS.

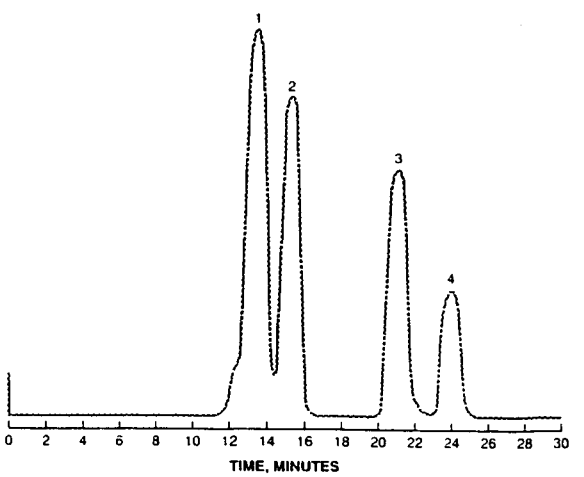

Fig. 1. Typical chromatogram of test solution. 1 = Corn oil (6.25 mg/ml), 2 = bis(2-ethylhexyl)phthalate (0.25 mg/ml), 3 = perylene (0.005 mg/ml), 4 = sulphur (0.02 mg/ml).

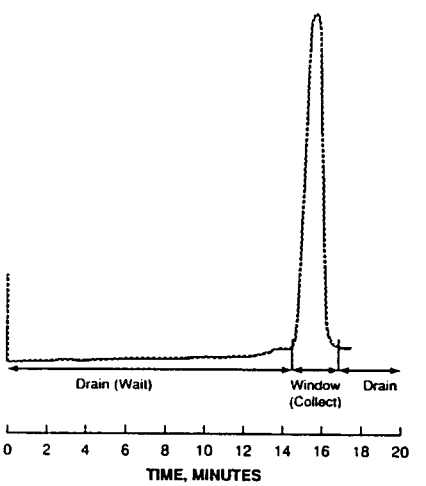

Fig. 2. Chromatogram of 1.0 μg/ml hexaflumuron optimization solution to establish the start and end time of the hexaflumuron fraction peak.

TABLE I

MEAN RECOVERY (%) DATA FOR HEXAFLUMURON

Soil type	Fortification rate (mg/kg)	No. of analysis	Mean recovery (%)
Sandy silt loam	0.01	2	100
Clay loam	0.01	4	91
Sandy loam	0.01	2	109
Sandy silt loam	0.10	2	102
Clay loam	0.10	5	105
Clay loam	1.00	2	88

Extraction and clean-up

Soil samples (10 g) were weighed into 50 ml vials and after addition of 20 ml acetonitrile–water (1:1) were shaken for 30 min. The extracts were centrifuged for 10 min at 1500 rpm (*ca.* 500 *g*) and the supernatants transferred to 240 ml jars. The extraction was repeated twice and the supernatants combined in 240 ml jars. After addition of 120 ml water, hexaflumuron was partitioned into 20 ml of hexane by shaking for 5 min. The extracts were centrifuged at 1500 rpm (*ca.* 500 *g*) and the hexane transferred into 50 ml vials. The partitioning was repeated once and the hexane extracts combined and evaporated to dryness in a gentle stream of nitrogen at 40°C. The residuum was reconstituted in 2.0 ml DCM.

The DCM solution was filtered using a 0.2-μm filter and 500 μl of this solution injected onto the GPC column. The hexaflumuron fraction was collected and evaporated to dryness in a gentle stream of nitrogen at 40°C. The residuum was reconstituted in 250 μl acetonitrile–water (60:40) using ultrasonication for 30 s. A 50 μl aliquot of this solution was chromatographed.

TABLE II

MEAN BACKGROUND VALUES FOR UNTREATED SOIL SAMPLES

Soil type	Mean concentration (mg/kg)
Sandy silt loam	0.0030
Clay loam	0.0000
Sandy loam	0.0018

RESULTS AND DISCUSSION

The analytical procedure was validated using three different untreated soil types fortified at various levels.

A summary of mean recovery data for three different soil types is given in Table I. All recoveries are corrected for the appropriate background values of the untreated samples.

A summary of mean background contribution from untreated soil is given in Table II. These values were used to calculate the lowest fortification and hence the determination limit of the method.

Typical chromatograms of hexaflumuron standard, untreated clay loam soil, untreated sandy silt loam and clay loam soil fortified at 0.1 mg/kg are shown in Figs. 3–6.

The use of HPGPC proved to be a very effective technique for the clean-up of agricultur-

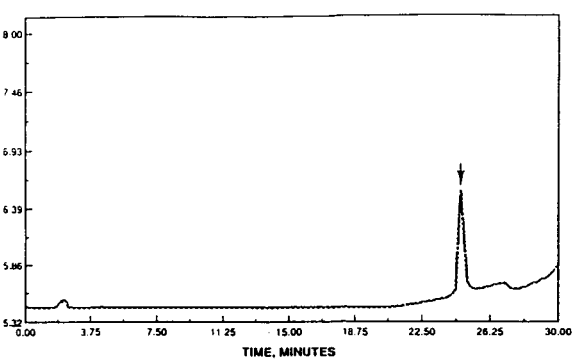

Fig. 3. Chromatogram of 0.5 μg/ml hexaflumuron standard. The *y*-axis represents UV absorbance (AU).

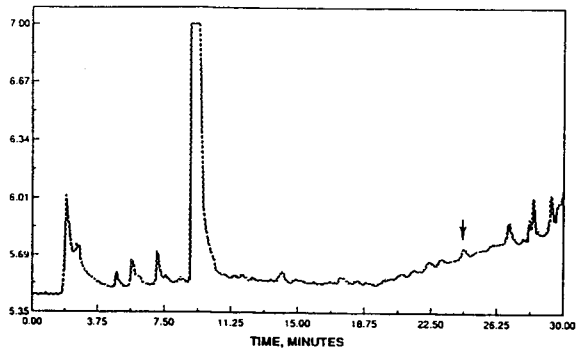

Fig. 4. Chromatogram of untreated soil sample (sandy silt loam). The *y*-axis represents UV absorbance (AU).

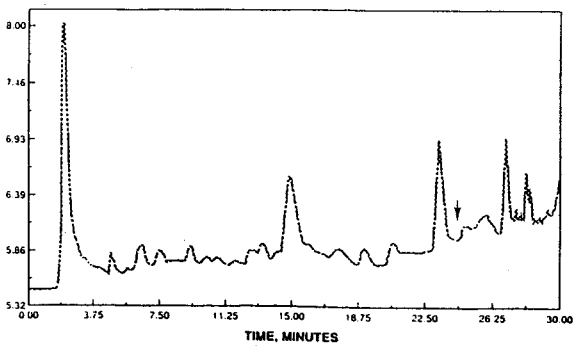

Fig. 5. Chromatogram of untreated soil sample (clay loam). The *y*-axis represents UV absorbance (AU)

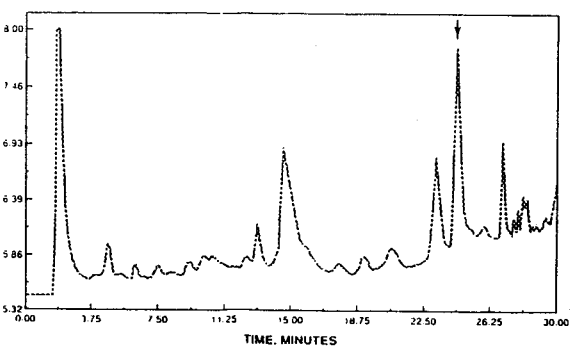

Fig. 6. Chromatogram of fortified soil sample (clay loam) at 0.1 mg/kg, 98% recovery. The *y*-axis represents UV absorbance (AU).

al soils. Using HPGPC, a determination limit of 0.01 mg/kg was achieved with excellent recovery data. This is an improvement by a factor of 5 on the standard method using conventional clean-up procedures. A different chromatographic profile was obtained for each soil type, clay loam being the "worst case"; however, the target determination limit was maintained with all soil types. The technique was successfully applied to the analysis of soil samples with improved sample throughput.

The use of analytical high-performance GPC column packed with 10 μm particle size and 5 nm pore size divinylbenzene cross-linked polystyrene provides a clean-up which results in increased speed of clean-up, sensitivity, and reduced solvent consumption.

ACKNOWLEDGEMENT

The authors thank members of Letcombe Residue Group for their support and contribution on this work.

REFERENCES

1 R.C. Tindle and D.L. Stalling, *Anal. Chem.*, 44 (1972) 1768–1773.
2 L.D. Johnson, R.H. Waltz, J.P. Ussary and F.E. Kaiser, *J. Assoc. Off. Anal. Chem.*, 59 (1976) 174.
3 W. Specht and M. Tillkes, *Fresenius' Z. Anal. Chem.*, 301 (1980) 300.
4 M.L. Hopper, *J. Agric. Food. Chem.*, 30 (1982) 1038.
5 S.J. Chamberlain, *Analyst*, 115 (1990) 1161–1165.
6 K.R. Griffitt and J.C. Craun, *J. Assoc. Off. Anal. Chem.*, 57 (1974) 168.
7 J.A. Van Rhijn and L.G.M.Th. Tuinstra, *J. Chromatogr.*, 552 (1991) 517–526.
8 L.G.M.Th. Tuinstra, F.R. Povel and A.H. Roos, *J. Chromatogr.*, 552 (1991) 259–264.

Journal of Chromatography A, 660 (1994) 199–204
Elsevier Science B.V., Amsterdam

CHROM. 2884

Analysis of sulphonated polyphenols, synthetic tanning agents in heavily polluted tannery wastewaters

Thorsten Reemtsma* and Martin Jekel

Technische Universität Berlin, FG Wasserreinhaltung, Sekr. KF 4, Strasse des 17. Juni 135, D-10623 Berlin (Germany)

ABSTRACT

A method is presented for the analysis of sulphonated polyphenols, acting as synthetic tanning agents, in heavily polluted tannery wastewater. It consists of ion-pair solid-phase extraction (RP-18) with tetrabutylammonium bromide followed by reversed-phase ion-pair liquid chromatography on a C_{18} stationary phase with UV detection. The detection limit is 15 μg/l. The influence of the wastewater matrix on extraction and the effects of pH and temperature on the HPLC separation are discussed. The procedure is not affected by the high contents of dissolved organic carbon and inorganic salts of tannery wastewater. The tannery effluents investigated contained around 40 mg/l of sulphonated polyphenols. These compounds appear to be refractory against both anaerobic and aerobic biological wastewater treatment. They might, thus, contribute to the dissolved organic sulphur content of surface waters.

INTRODUCTION

Sulphonated polyphenols (SPPs) are employed as synthetic tanning agents in leather production. Many of them contain naphthalenesulphonate-related structural components (Fig. 1), which are known to be hardly degradable by biological treatment [2]. Moreover, removal of less polar aromatic sulphonates such as linear alkylbenzenesulphonates (LASs) in municipal wastewater treatment plants was shown to be due to adsorption, rather than to biodegradation [3]. Hydroxylated aromatic sulphonates might form a substantial portion of dissolved organic sulphur (DOS) in surface waters, the nature of which is still poorly understood [4,5]. SPPs of tannery effluents, if refractory to a similar extent, would provide an additional source of DOS.

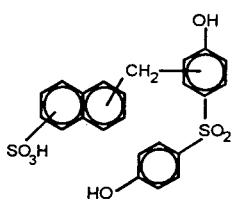

Fig. 1. Structure of a SPP syntane (according to ref. 1).

LASs, which are used as detergent products, are the most widely investigated group of aromatic sulphonates [6]. They were analyzed by anion-exchange chromatography [7], by RP-HPLC from river water [6,8], wastewater [9] and marine water [10]. Reversed-phase ion-pair liquid chromatography (RP-IPC) was invented for the analysis of biodegradation products of LASs [11].

However, other substances contributing to the pool of aromatic sulphonates are less thoroughly investigated. Amino- and hydroxynaphthalenesulphonates, which are employed in dye production and which do appear in effluents of textile industries, might also be analyzed by anion-exchange chromatography [7,12]. Nowadays, RP-IPC is more frequently employed [5,13,14] and was only recently investigated in detail [15].

In analogy to the colorimetric determination

* Corresponding author.

0021-9673/94/$07.00 © 1994 Elsevier Science B.V. All rights reserved
SSDI 0021-9673(93)E0805-5

of anionic surfactants as methylene-blue active substances (MBASs), liquid–liquid extraction with the methylene blue cation was first employed for the isolation of LASs from water [16]. It was superseded from solid-phase extraction [9] and ion-pair solid-phase extraction with tetraalkylammonium cations for the more polar compounds [5]. Enrichment on XAD resins [17] or freeze-drying was occasionally reported [12].

Commonly, the analysis of industrial wastewater constituents has to face a complex mixture of various organic substances, that hamper the extraction and analysis of the compounds under investigation. This is especially true for tannery wastewater, that might be loaded with natural and synthetic dissolved organics, comprising up to 3000 mg/l of dissolved organic carbon (DOC). Furthermore, it exhibits a high content of inorganic salts of up to 20 g/l.

We developed a method for the analysis of SPPs from tannery wastewater, in order to determine their amount, the *in plant* sources and to study their behaviour towards biological wastewater treatment. This publication presents an extension of ion-pair techniques towards other groups of aromatic sulphonates and to heavily contaminated waters.

EXPERIMENTAL

Extraction

Samples were stored frozen at −20°C until analyzed. They were filtered over 0.45-μm cellulose acetate membrane filters (Sartorius, Göttingen, Germany) before extraction and adjusted to pH 6.5 with phosphoric acid or sodium hydroxide. A 1-mmol amount of tetrabutylammonium bromide (TBABr) was added to the sample (10–50 ml), which was then applied to 500 mg Supelclean LC18 extraction cartridges (Supelco, Bellefonte, USA) and eluted from the wet column with 3 ml of methanol and 3 ml of acetonitrile. The extracts were dried in a Speed-Vac A 160 rotary evaporator (Savant, Farmingdale, USA) and dissolved in 1.0–1.5 ml of distilled water. Methanol or acetonitrile solutions obstruct the HPLC separation.

Analytical apparatus

The HPLC system consists of a Merck-Hitachi L 6200 gradient pump with low-pressure mixing, a Merck-Hitachi AS 2000-A autosampler and a Merck-Hitachi T 6300 column oven (all from Merck, Darmstadt, Germany). A 250 × 4 mm LiChrospher 100 RP-18 (5 μm) column (Merck) with a 4 × 4 mm precolumn of identical material was employed for the separation. Substances were detected at 260 nm by a Linear UVIS 204 (Linear, Reno, NV, USA) or a Shimadzu SPD-10A (Shimadzu, Kyoto, Japan) detector. UV spectra were obtained by a Waters 990 diode array detection (DAD) system (Millipore, Milford, MA, USA). Chromatographic data were stored and calculated with the Chromstar software (Bruker-Franzen, Bremen, Germany). A 20-μl volume of aqueous sample was injected.

Separation

Final chromatographic conditions were the following: solvent A: 40 μl H_3PO_4 (85%), 24 mmol NaH_2PO_4, 2 mmol TBABr, 1000 ml water; solvent B: 80 μl H_3PO_4 (85%), 12 mmol NaH_2PO_4, 2 mmol TBABr, 200 ml water, 800 ml MeOH; linear gradient from 45% B (0 min) to 69% B (40 min) at a flow of 1 ml/min, followed by 7 min equilibration. The column temperature was held at 40°C. t_0 was determined by the baseline signal obtained from the aqueous solutions.

Peak assignment and quantitation

The various components of the syntane mixtures are not separately available. Quantitation is, therefore, related to the peak areas of standard solutions of the technical mixtures with known total SPP content. Peak assignment in the wastewater extracts is based on retention times and UV spectra, gained by DAD analysis.

Chemicals

Chemicals for extraction were of analytical grade, and solvents for chromatography were of HPLC grade from various companies. TBABr of synthetical grade (Merck) was found to be less UV absorbing than analytical-grade TBABr of other companies (Fluka, Buchs, Switzerland;

Aldrich, Gillingham, UK). Further clean-up of TBABr, if necessary, can be easily performed by recrystallization from hot acetic acid ethyl ester. Technical SPP mixtures were manufactured by Ciba-Geigy (Basel, Switzerland) and Bayer (Leverkusen, Germany), while tannic acid was obtained from Fluka.

RESULTS AND DISCUSSION

Extraction

Although the amounts of SPPs in tannery effluent later detected (see below) would have allowed the direct HPLC analysis without prior enrichment, an extraction step appeared to be necessary, in order to free the SPPs from the complex organic mixture present in the tannery effluent and the high load of inorganic salts.

Freeze-drying and resolution of the compounds under investigation with methanol [12] did not yield reproducible results or sufficient recovery. Apparently, the complex sample matrix of tannery effluent hampered the dissolution of SPPs from the precipitate.

We expected ion-pair extraction of SPPs with TBABr on C_{18}-covered solid phases to be more satisfactory. This method has been employed for the extraction of naphthalenesulphonates and related compounds from water with a comparatively low DOC content [5]. The influence of pH, DOC and inorganic salts upon extraction was studied.

Variations of the pH of the samples between 4 and 6.5 did not substantially influence the overall recovery of two technical SPP mixtures (1–5 mg/l) from distilled water and wastewater (Table I). However, the relative standard deviation for individual components was lower at pH 6.5. Furthermore, extraction of SPPs at pH 6.5 from distilled water was less affected by the addition of salts (30 g/l), than at pH 4.

The recovery of SPPs from wastewater might be affected by the nature and the amount of the accompanying DOC. However, only little information is available on the nature of dissolved organics in tannery wastewater and, thus, studying its influence on SPP recovery by adding a synthetic DOC mixture to distilled water would have been rather speculative. Therefore, we determined the amount of DOC to be loaded on the extraction cartridges before SPP breakthrough. Untreated wastewater was applied to an extraction cartridge and 10-ml portions of the filtrate were subsequently reextracted for SPP analysis. Although 80 ml of wastewater (1200 mg/l DOC) were extracted, no SPPs became detectable in the filtrate. Accordingly, more than 100 mg DOC might be applied onto a 500-mg extraction cartridge, without breakthrough. A 10-ml volume of the sample would have been sufficient for SPP analysis. Solid-phase extraction with TBABr, hence, provides a reliable means for the extraction of SPPs, even from wastewater with a high organic and inorganic load.

TABLE I

RECOVERY (%) AND R.S.D. OF SPP EXTRACTION FROM WASTEWATER

Syntane	pH 4		pH 6.5	
	Recovery (%)	R.S.D. (%)	Recovery (%)	R.S.D. (%)
1	93	13.7	109	5.3
2	107	16.9	104	4.5

It was frequently observed that the extraction efficiencies of nominal identical solid-phase extraction cartridges of different manufacturers strongly differed. This is also true for the procedure presented here. For example, extractions with Adsorbex RP-18 (Merck) yielded only those components which elute comparatively late in RP-IPC analysis. The more polar, early-eluting components of the syntane mixtures, were not at all or not sufficiently extracted.

Chromatography

RP-IPC with cations such as cetyltrimethylammonium or tetrabutylammonium has formerly been employed for the separation of degradation products of LASs [11] and for other aromatic sulphonates [5,15]. Corresponding to the ion-pair extraction described above, we used TBABr for the separation of SPP mixtures, combined

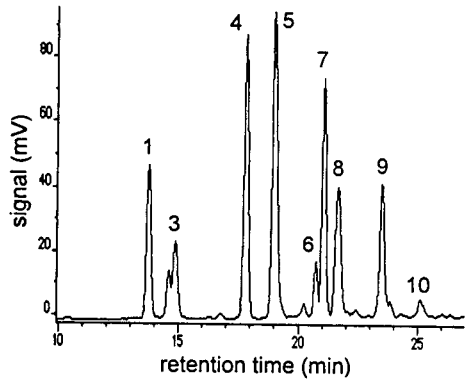

Fig. 2. Chromatogram of a SPP mixture (for chromatographic conditions see text). Peaks were not identified; peak numbers are given only to ease the peak assignment in the corresponding wastewater extract (Fig. 5).

with a phosphate buffer and a water–methanol gradient (Fig. 2).

The relation between the pK values of the acids under investigation and the appropriate pH value of the eluents for IPC is still a matter of debate [13,14]. We studied the influence of pH variation between 3 and 7 on the capacity factors of SPP components (Fig. 3). They all tend to increase above pH 4. These results are consistent with the data obtained for LASs [11], while, astonishingly, the adverse effect was reported for naphthalenesulphonates [13]. In order to obtain the most reproducible chromatographic conditions we employed a buffer system of pH 3.6 in the aqueous solvent.

Under these conditions, not necessarily all sulphonate groups within the molecules need to

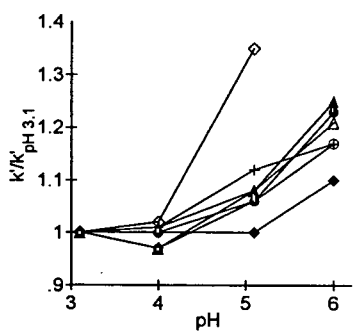

Fig. 3. Variation of capacity factors (k') in RP-IPC with the pH of eluents. Symbols refer to the peaks in Fig. 2: △ = peak 1; ○ = peak 2; ◆ = peak 3; ◇ = peak 4; ▲ = peak 5; ○ = peak 6; + = peak 7.

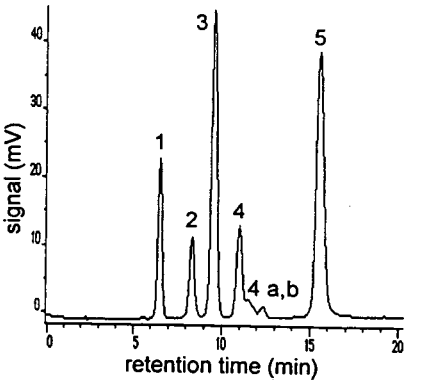

Fig. 4. Chromatogram of naphthalenesulphonates. Peaks: 1 = napththalene-1,5-disulphonate; 2 = 1-naphthol-4-sulphonate; 3 = 2-naphthol-3,6-disulphonate; 4 = naphthalene-1,3,6-trisulphonate; 4a, b = 1,3,5- and 1,3,7-isomers; 5 = naphthalene-2-sulphonate.

be ion-paired. This is illustrated by the elution order of naphthalenesulphonates under identical conditions (Fig. 4). If completely ion-paired, they should elute according to the degree of sulphonation. However, naphthalenedisulphonate elutes first, followed by naphthalenetrisulphonate and -monosulphonate.

The influence of column temperature is as strong as the effect of pH. Standard enthalpy changes of solute transfer from the mobile to the stationary phase (ΔH^0) might be calculated from plotting ln k' against $1/T$ (Van 't Hoff plot) [15]. We obtained fairly linear relationships in the investigated temperature range of 22 to 50°C ($r = 0.88$ to 0.98, $n = 4$) and ΔH^0 values of −0.4 to −0.98 kcal/mol (1 cal = 4.14 J) for the individual components. They are in the range of those reported for aminonaphthalenesulphonate separation on a Nucleosil C_{18} column (−2.5 to −5.5 kcal/mol) [15]. For stable chromatographic conditions we selected a column temperature of 40°C.

Fluorescence detection is frequently used for the determination of LASs and naphthalenesulphonates [6]. Unfortunately, SPPs do not exhibit fluorescence activity and must, therefore, be detected by UV measurement.

Evaluation of the whole procedure

The reproducibility of the whole procedure was evaluated by performing four analyses in

TABLE II

RELATIVE STANDARD DEVIATIONS OF SPP COMPONENTS AND TOTAL SPP CONTENTS ($n = 3$)

Total SPP content 5.1–29.6 mg/l.

	Sample No.			
	1	2	3	4
Single components (R.S.D., %)	1–12	3–6	2–8	1–8
Total (R.S.D., %)	4.8	4.2	3.1	3.5

TABLE III

TOTAL SPP CONTENT IN TANNERY WASTEWATER BEFORE AND AFTER BIOLOGICAL TREATMENT

Observation period three months, $n = 9$.

	Syntane (mg/l)	Syntane/DOC (mg/mg)
Untreated	41	0.03
After anaerobic treatment	45	0.11
After anaerobic and aerobic treatment	34	0.13

triplicate (spread over four weeks). Relative standard deviations (R.S.D.s) of individual SPP components vary between 0.5 and 12%, with an average of 3.5% ($n = 26$) (Table II). The R.S.D. of the total SPP content of the four samples was in the range 3.1–4.8%.

The detection limit ($S/N \geq 3$) is 40 ng of total SPP mixture injected onto the column. For quantitation ($S/N \geq 10$) around 130 ng have to be injected. If 500 ml are extracted and redissolved in 100 μl this results in a detection limit around 1.5 μg/l (for 20-μl injections). However, in the case of wastewater loaded with 2000 mg/l DOC, only 50 ml might be extracted in order not to saturate the extraction cartridge. The corresponding detection limit is around 15 μg/l.

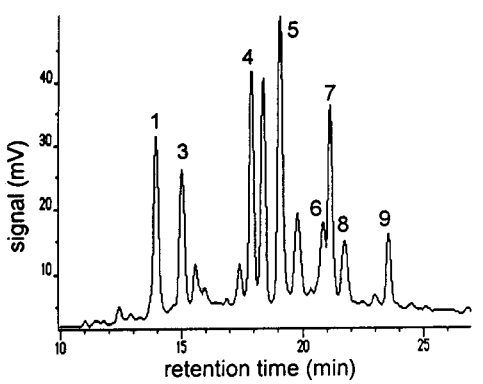

Fig. 5. Chromatogram of an extract from biologically treated tannery wastewater. Peaks as in Fig. 2.

Application

This analytical procedure was subsequently applied to the analysis of SPPs in tannery wastewater as well as in the effluents of a pilot plant, combining anaerobic and aerobic biological treatment [18] over a three-month period (Fig. 5). In fact, SPPs revealed to be highly refractory against both anaerobic and aerobic biodegradation (Table III). Neither their content, nor their composition was altered by the biological treatment. Slight diminution during aerobic treatment might be due to adsorption onto biomass. Consequently, SPPs become substantially enriched during the biological treatment and contribute to about 5% of the final DOC content. Hence, these compounds would pass a biological treatment plant and, finally, become part of the DOS pool of surface waters.

CONCLUSIONS

We developed a method for the analysis of synthetic tanning agents of the sulphonated polyphenol type from tannery wastewater. The method includes ion-pair extraction and RP-IPC with the TBABr. The high salt and DOC contents of the wastewater up to 20 mg/l and 2000 mg/l, respectively, do not affect the analysis. The detection limit is dependent on the DOC content of the wastewater and is in the order of 15 μg/l for 2000 mg/l DOC.

Application of this method to a combined anaerobic/aerobic biological treatment of tan-

nery wastewater revealed that SPPs are highly refractory and have a low adsorption tendency. These compounds will, therefore, contribute to the DOS content of surface waters.

The method described is suggested to be of value for the determination of (polyaromatic) sulphonates and carboxylates from various industrial wastewaters.

ACKNOWLEDGEMENTS

This work is being funded by the Deutsche Forschungsgemeinschaft (DFG, Bonn) through SFB 193: Biological treatment of industrial waste-water, project A3. We thank S. Södler for laboratory assistance.

REFERENCES

1 R. Schubert, K. Faber, H. Spahrkäs, K. Eitel, F. Schade, H. Träubel and G. Harmening, in E. Bartholomé (Editor), *Ullmanns Encyklopädie der technischen Chemie*, Verlag Chemie, Weinheim, 1978, Vol. 16, p. 109.
2 B. Nörtemann and H.-J. Knackmuss, *GWF: Gas-Wasserfach*, 129 (1988) 21.
3 W. Giger, P.H. Brunner, M. Ahel, J. McEvoy, A. Marcomini and C. Schaffner, *Gas, Wasser, Abwasser*, 67 (1987) 111.
4 K. Kümmerer and P. Krauss, *Gewässerschutz, Wasser, Abwasser*, 114 (1990) 109.
5 S. Schullerer, H.-J. Brauch and F.H. Frimmel, *Vom Wasser*, 75 (1990) 83.
6 M.A. Castles, B.L. Moore and S.R. Ward, *Anal. Chem.*, 61 (1989) 2534.
7 G.R. Bear, C.W. Lawley and R.M. Riddle, *J. Chromatogr.*, 302 (1984) 65.
8 A. Nakae, K. Tsuji and M. Yamanaka, *Anal. Chem.*, 53 (1981) 1818.
9 A. Marcomini, S. Capri and W. Giger, *J. Chromatogr.*, 403 (1987) 243.
10 A. Marcomini, S. Stelluto and B. Pavoni, *Intern. J. Environ. Anal. Chem.*, 35 (1989) 207.
11 P.W. Taylor and G. Nickless, *J. Chromatogr.*, 178 (1979) 259.
12 I.S. Kim, I. Sasinos, R.D. Stephens and M.A. Brown, *Environ. Sci. Technol.*, 24 (1990) 1832.
13 G.R. Bear, *J. Chromatogr.*, 371 (1986) 387.
14 H. Sirén, R. Dammert and L. Huhanantti, *Fresenius' Z. Anal. Chem.*, 332 (1988) 245.
15 H.F. Zou, Y.K. Zhang and P.C. Lu, *Chromatographia*, 34 (1992) 15.
16 J. McEvoy and W. Giger, *Environ. Sci. Technol.*, 20 (1986) 376.
17 Q.W. Osburn, *J. Am. Oil Chem. Soc.*, 63 (1986) 257.
18 E. Genschow and W. Hegemann, *GWF: Gas-Wasserfach, Wasser/Abwasser*, 134 (1993) 262.

Journal of Chromatography A, 660 (1994) 205–210
Elsevier Science B.V., Amsterdam

CHROMSYMP. 2937

Determination of traces of pyrethrins and piperonyl butoxide in biological material by high-performance liquid chromatography

R. Wintersteiger* and B. Ofner

Institute of Pharmaceutical Chemistry, Karl-Franzens-University Graz, Schubertstrasse 1, A-8010 Graz (Austria)

H. Juan

Institute of Experimental and Clinical Pharmacology, Karl-Franzens-University Graz, Universitätsplatz 4, A-8010 Graz (Austria)

M. Windisch

Department of Animal Biology, Karl-Franzens-University Graz, Roseggerweg 48, A-8036 Graz (Austria)

ABSTRACT

A liquid chromatographic method for the determination of pyrethrins and of the synergist piperonyl butoxide in human plasma after C_{18} solid-phase extraction is described. UV detection was found to be sensitive enough to determine concentrations far below the limit of toxicity. With respect to future investigations concerning studies in biological materials, a column-switching system for sample preparation was developed and compared with solid-phase extraction. Both methods show comparable limits of detection, but the column-switching technique has the advantage of fully automating the system.

INTRODUCTION

Pyrethrin extract is a biological product with low mammalian toxicity compared with synthetic pyrethroids. Pyrethrins are frequently used insecticides, especially in repellents. One of the disadvantages of pyrethrin extract is its rapid breakdown, which makes a combination with synergists necessary. A very important synergist that acts by delaying metabolic breakdown or by enhancing the penetrability of cell membranes is piperonyl butoxide (Pbo).

Recently, the possible absorption of pyrethrins by topical application and consequently its questionably harmless effect on humans, especially children, has been discussed. We tried to find a method to detect pyrethrins, particularly the main ingredients pyrethrin 1 and 2, and the synergist Pbo in plasma. Many methods for the determination of pyrethrins have been developed, including GC [1–5] and other techniques [6–11], but none of them is sensitive enough for quantification in biological material. The aim of this work was the development and optimization of an HPLC system that would permit the detection of trace concentrations of pyrethrins and Pbo in plasma.

* Corresponding author.

0021-9673/94/$07.00 © 1994 Elsevier Science B.V. All rights reserved
SSDI 0021-9673(93)E0944-P

EXPERIMENTAL

Chemicals and reagents

Methanol from Loba (Vienna, Austria) was distilled twice and water was purified with a Milli-Q reagent water system (Millipore). Pyrethrin extract (25% in isoparaffin) was obtained from Fettrelet (Delemont, Switzerland) and piperonyl butoxide (Pbo) (technical 90%, purification per distillation 99%), from Aldrich.

Standard solutions of pyrethrin extract (100 μl of pyrethrin extract, density 0.20774 g/ml, diluted with mobile phase to 100 ml) and Pbo (93.2 mg of 99% Pbo, diluted with mobile phase to 100 ml) were stored at 4°C. Flasks were wrapped in aluminium foil because of the sensitivity of pyrethrins to UV light [12].

For sample preparation, the following columns were tested: C_{18} (500 mg) and C_{18} (100 mg), Bond Elut, ICT; C_{18} (400 mg), Bakerbond, J.T. Baker; and C_{18} Adsorbex (400 mg), Merck. For ion exchange, samples were applied to Bond Elut SCX (500 mg), SAX (500 mg) and CN (100 mg) columns, ICT. For developing the HPLC method, human citrate–plasma (blood mixed 10:1 with sodium citrate) was centrifuged at 5500 *g* for 10 min. In order to carry out pharmacokinetic studies, citrate was added to 5 ml of blood from healthy persons, which was then centrifuged for 10 min at 5500 *g* and the supernatant plasma was finally stored at −20°C.

Two different pharmaceutical preparations, the repellent Tyrasan and the louse shampoo Aescalon forte, were applied to the skin of volunteers. One spray flask containing 110 ml of Tyrasan (Pharma Diffusion, Bienne Switzerland) contains 1% pyrethrins, 1% Pbo, some essential oils, 20% 2-propanol and water; 1 g of the louse shampoo (Aesca, Traiskirchen, Austria) contains 3.3 mg of pyrethrins 1 and 2, 33 mg of Pbo and shampoo base.

Instrumentation and chromatography

HPLC was performed using a Perkin-Elmer Binary 250 LC pump. For column switching a Milton Roy LC Constametric 3000 pump in combination with an LDC/Milton Roy Minimetric Tm II as an auxiliary pump was utilized. For the Aescalon study a Nucleosil RP-18 (10 μm) column (250 × 4.6 mm I.D.) was used and for the Tyrasan study a Nucleosil RP-18 (5 μm) column (250 × 4.6 mm I.D.) (Forschungszentrum Seibersdorf, Seibersdorf, Austria). Column switching was carried out using a LiChrosorb RP-18 (7 μm) column (250 × 4 mm I.D.) (Merck) and a precolumn (5 × 4 mm I.D.) packed in the laboratory with Perisorb RP-18, 30–40 μm (Merck). Samples were injected with a Rheodyne Model 7125 valve equipped with a 6-μl loop or alternatively with a Rheodyne Model 7125 valve in combination with a Rheodyne Model 7010 six-port valve and a 100-μl loop. Peaks were measured at a wavelength of 254 mm using a Perkin Elmer LC-15 UV detector (range 0.008) or a Perkin-Elmer LC-235 diode-array detector (210–260 nm) and printed by a LKB Model 2210 recorder or by an Epson PCAX2 personal computer in combination with an Epson printer. The mobile phase was methanol–water in different proportions (as described later) and the washing phase for column switching was methanol–water (10:90, v/v). All eluents were degassed with helium before use and the flow-rate was set at 0.5 ml/min.

Clean-up

Solid-phase extraction. A 1-ml volume of centrifuged human plasma (10 min, 5500 *g*) diluted with 3 ml of water, mixed on a vortex mixer for 10 s, was transferred to solid-phase extraction (SPE) columns preconditioned with 10 ml of methanol and 10 ml of water. The columns were washed with water (3 × 10 ml) and then with a wash solution of methanol–water (5:95, v/v) (1 × 12 ml). Finally, the pyrethrins were eluted with methanol (2 × 0.5 ml). After removing the solvent with a stream of nitrogen, the residue was dissolved in 100 μl of the mobile phase [methanol–water (75:25, v/v)] and 6 μl of this solution were injected into the HPLC system.

Column switching. A 1-ml volume of human plasma was diluted with 1 ml of water and spiked with pyrethrin extract and Pbo. A 100-μl volume of this solution were transferred to the precolumn by the auxiliary pump (pump 1) and cleaned from plasma substances by washing with

water; after 5 min, the analytes were transferred from the precolumn by switching over to the analytical column. The mobile phase was methanol–water (82:18, v/v).

RESULTS AND DISCUSSION

Pyrethrin extract contains pyrethrin 1 (35%), pyrethrin 2 (33%), jasmolin 1 (5%), jasmolin 2 (4%), cinerin 1 (10%) and cinerin 2 (14%). The detection is focused on the main ingredients pyrethrin 1 and 2 and on the synergist Pbo. As previously assumed and proved by several investigations, the structures of the compounds (Fig. 1) indicate that there is no intrinsic fluorescence or electrochemical activity and, further, no common functional groups for derivatization. Therefore, UV detection was applied. Pyrethrins show an absorption maximum at 210 nm. Additionally, the same concentration was measured at 220, 230, 240 and 254 nm. However, the best signal-to-noise ratio could be observed at 254 nm, which also permits the determination of Pbo.

The aim was a common determination of the main ingredients of the repellent Tyrasan and the shampoo Aescalon forte in plasma to detect possible absorption after topical application. Many different columns and mobile phases were tested in order to develop a simple isocratic HPLC technique. Utilizing a reversed-phase system, many by-products originating from plasma are to be expected during the first few minutes of the chromatographic run. Therefore, the analytes should be retained for at least 5 min.

In order to obtain sufficient sensitivity and selectivity necessary for the pharmacokinetic study, great attention was paid to the sample preparation. Consequently, we used the off-line technique of solid-phase extraction. As the analyte compounds have different polar and nonpolar groups, the best sorbent for SPE had to be found. After testing different columns from different producers, Bond Elut C_{18} was found to be the most appropriate sorbent. In addition to hydrophobic interactions, the formation of hydrogen bonds between the ester groups of the pyrethrins and the residual silanol groups of the sorbent can be assumed.

As human plasma contains many substances with acidic, basic and amphoteric groups, another way to clean plasma samples is ion-exchange SPE. Plasma ingredients are retained on the columns by interactions with the sorbent. The insecticides and the synergist are neutral and therefore are not retained by the sorbent material.

Strong ion-exchange columns, *e.g.*, SCX columns at pH 4, 6 and 8 and SAX columns at pH 6, 9 and 12, were used to decrease the amounts of plasma by-products as much as possible. Although ion-exchange columns showed good cleaning results, the Bond Elut C_{18} columns

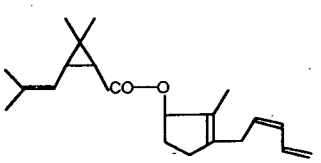

PYRETHRIN I

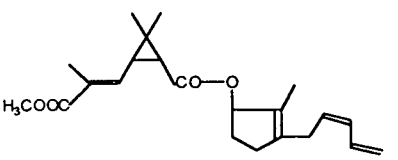

PYRETHRIN II

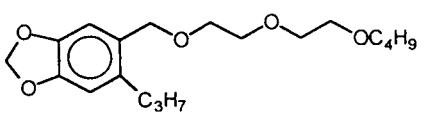

PIPERONYL BUTOXIDE

Fig. 1. Structures of the main ingredients of Tyrasan spray and Aescalon forte shampoo.

TABLE I

SCHEME FOR APPLICATION OF PHARMACEUTICAL PREPARATIONS TO HUMAN SUBJECTS

	No. of volunteers		Mass (kg)		Age (years)	Application	Sampling
	Male	Female	Male	Female			
Tyrasan repellent spray	3	3	61–85	49–60	22–31	Spraying an area of 25 × 25 cm on the back	Blank, 30, 60, 90, 150, 210, 330 min
Aescalon forte louse shampoo	4	3	68–81	47–60	23–33	On the head	Blank, 30, 60, 90, 120, 180, 240 min

proved to be even more efficient. Applying 60 ng of each substance, the recovery was 81.5% Pbo, 72% pyrethrin 1 and 70% pyrethrin 2. The reproducibility of this method was tested by spiking human plasma blanks with 60 ng per sample and relative standard deviations ($n = 8$) of 4.8%, 5.2% and 5.4% were obtained. Linearity was observed over a range of one order of magnitude starting at the detection limit. The correlation coefficients were between 0.998 and 0.999.

Two different pharmacokinetic studies were performed. The first was carried out with the repellent Tyrasan. Six healthy persons, non-smokers, were treated with nine sprayed strokes from a distance of 10 cm on the back over an area of 25 × 25 cm. After sampling (see Table I) the plasma was centrifuged (4°C, 10 min, 5500 *g*), the supernatant was transferred into test-tubes and stored at −20°C. All samples, injected twice, did not show absorption of either pyrethrins or Pbo. Fig. 2 shows the chromatogram

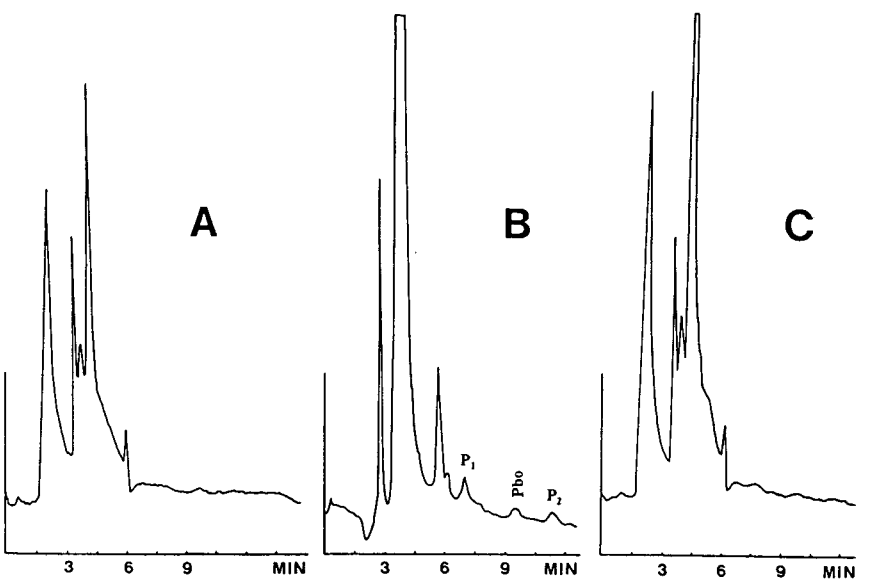

Fig. 2. Typical chromatogram of human plasma specimen after solid-phase extraction. (A) Plasma blank; (B) plasma spiked with 10 ng of pyrethrin 1, 10 ng of pyrethrin 2 and 10 ng of Pbo; (C) Human plasma 2 h after Tyrasan application. Detector, LC-15 UV detector; mobile phase, methanol–water (75:25, v/v); column, Seibersdorf RP-18, 10 μm; injection volume, 6 μl; flow-rate, 0.5 ml min^{-1}.

for a sample from a volunteer compared with spiked plasma.

The second study with the louse shampoo Aescalon forte gave similar results. Seven healthy volunteers, male and female, applied a large amount (*ca.* 30 g) of shampoo to their hair. The incubation time was 15 min, then the hair was washed. No reddening of the skin on the head became visible. Further, the chromatographic investigation of the plasma samples from all the volunteers showed that no absorption had occurred. As the detection limit of 10 ng in 6 μl corresponds to 167 ng pyrethrins/ml plasma (*ca.* 0.17 μg/kg), absorption of larger amounts would have been detected. As particularly the $LD_{50\ dermal}$ for pyrethrins is more than 2.0 mg/kg in the rat, there is a difference of the factor 10 000 between the detection limit and the $LD_{50\ dermal}$. No $LD_{50\ dermal}$ values for piperonyl butoxide could be found in literature, but the $LD_{50\ oral}$ is 6150–7500 mg/kg in the rat, indicating the low toxicity of this synergist. As a result, the application of insecticides containing pyrethrin extract seems to be allowable for children. Irritations and allergies did not appear, which can be traced back to the use of a purified extract [12].

As additional pharmacokinetic studies are planned, a column-switching method was developed with the aim of automating the system. As Fig. 3 shows, a switching valve including the injection valve with loop and precolumn and two pumps allows a parallel performance of the wash and analytical process. A schedule for a complete chromatographic cycle is given in Table II. In order to optimize the wash process, different wash solutions were tested. First pure water was used, and subsequently the methanol content was increased continuously from 5% up to 40%. Although no significant difference in the chromatographic behaviour could be observed, water–methanol (90:10, v/v) was used in further investigations. Higher contents of methanol may include the risk of protein precipitation, thereby producing enhanced pressure.

A critical point for attaining adequate recoveries is the duration of the wash process. Different wash intervals from 1 to 20 min were tested; a period of 5 min was found to be

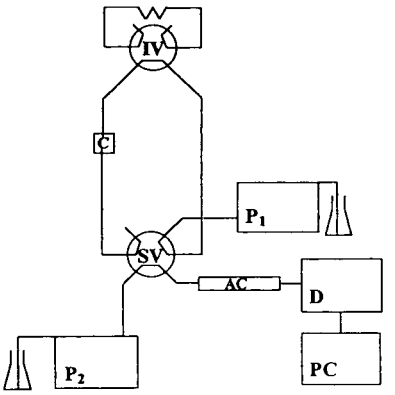

Fig. 3. Column-switching system. IV = injection valve; SV = switching valve; P_1 = Milton Roy LC Constametric 3000 pump; P_2 = LDC/Milton Roy pump; D = LC-15 UV detector; AC = analytical column, LiChrosorb RP-18, 7 μm; C = precolumn packed with Perisorb RP-18, 25–30 μm; PC = Epson PCA × 2.

optimum, providing recoveries of almost 100%. This period is also sufficient if the injection volume is increased from 6 to 20, 75 and 175 μl.

The investigations with different loops were performed in order to optimize the signal-to-noise ratio and thus to improve the detection limit. Fig. 4 shows a chromatogram obtained following an injection of 20 μl. On injecting 175 μl the peaks show some band broadening; however, the detection of 130 ng/ml of pyrethrins

TABLE II

SCHEDULE FOR COLUMN SWITCHING

Time (min)	Operation
0	Injection of the sample, washing the precolumn with water by fore flushing
1	Injection valve is switched from inject to load position
6	Switching valve is switched on; the eluent transfers the compounds to be analysed to the analytical column by back flushing
6.5	Switching valve is switched to the original position. Analytes are separated on the analytical column and at the same time conditioning of the wash system with wash solution occurs
17	End of chromatographic cycle

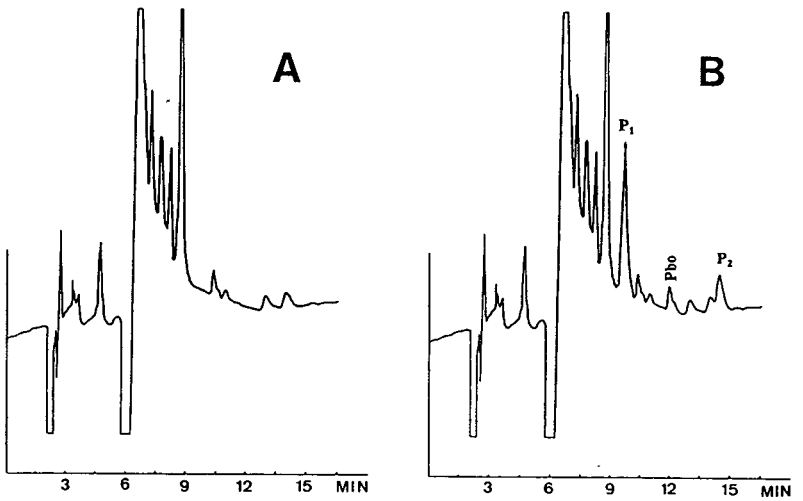

Fig. 4. Typical chromatogram obtained using column switching. (A) Plasma blank; (B) plasma spiked with 20 ng of pyrethrin 1, 20 ng of pyrethrin 2 and 20 ng of Pbo. Wash period, 8 min; wash phase, methanol–water (10:90, v/v); mobile phase, methanol–water (80:20, v/v); injection volume, 20 μl; other chromatographic conditions as in Fig. 3.

and Pbo in plasma is possible. Using this technique a slightly better detection limit is achieved compared with SPE.

CONCLUSIONS

This work has demonstrated the utility of a simple RP-HPLC system for the separation and identification of the main ingredients of natural insecticides in human plasma. Using solid-phase extraction interfering by-products of the biological material were removed, providing acceptable recoveries for pyrethrins 1 and 2 and the synergist piperonyl butoxide. Pharmacokinetic studies subsequent to the topical application of two different preparations, a repellent spray and a louse shampoo, indicate that absorption does not occur or, if it does occur, the amounts are below the detection limit. As the method developed is sensitive enough to detect amounts far below the toxicity levels of these compounds, the application of such preparations containing Pbo and pyrethrins from purified pyrethrin extract seem to be harmless, even for children. As an alternative to SPE, a column-switching system was developed for sample preparation in order to effect fully automated operation for further pharmacokinetic studies.

REFERENCES

1 W. Ebing, *Fresenius' Z. Anal. Chem.*, 327 (1987) 539.
2 C.R. Worthing and S.B. Walker, *The Pesticide Manual, a World Compendium*, British Crop Protection Council, Thornton Heath, 8th ed., 1987.
3 H.P. Thier and H. Zeumer, *Manual of Pesticide Residue Analysis*, Vol. 1, Deutsche Forschungsgemeinschaft, Kommission für Pflanzenschutz-, Pflanzenbehandlungs- und Vorratsschutzmittel and VCH, Weinheim, 1987.
4 J.J. Ryan, *J. Assoc. Off. Anal. Chem.*, 65 (1982) 904.
5 L. Sedea, *Riv. Ital. Sostanze Grasse*, 60 (1983) 133.
6 V.J. Meinen, *J. Assoc. Off. Anal. Chem.*, 65 (1982) 249.
7 S. Latif, *J. Chromatogr.*, 287 (1984) 77.
8 M. Wagner-Löffler, *GIT Fachz. Lab.*, 29 (1985) 982.
9 D.A. Otieno, I.J. Jondiko, P.G. McDowell and F.J. Kezdy, *J. Chromatogr. Sci.*, 20 (1982) 566.
10 L. Fishbein, *J. Chromatogr. Sci.*, 13 (1975) 238.
11 U. Nehmer and N. Dimov, *J. Chromatogr.*, 288 (1984) 227.
12 I. Jäger-Mischke and V. Wollny, *Pyrethrum und Pyrethroide, ein Beitrag zur Naturstoffdiskussion*, Institut für Angewandte Ökologie, Freiburg, 1988.

Journal of Chromatography A, 660 (1994) 211–217
Elsevier Science B.V., Amsterdam

CHROMSYMP. 2957

Determination of aluminium and its fluoro complexes in natural waters by ion chromatography

S. Motellier* and H. Pitsch

Commissariat à l'Énergie Atomique, Direction du Cycle du Combustible/Département Stockages Déchets/Service de Caractérisation et d'Études des Stockages/Laboratoire de Chimie Analytique en Solution et d'Hydrogéochimie, B.P. 6, 92265 Fontenay-aux-Roses Cedex (France)

ABSTRACT

Ion chromatography was applied to the determination of aluminium and its fluoro complexes in natural waters. The separation was carried out on a cation-exchange column. The aluminium species were detected by postcolumn reaction with Tiron followed by UV spectrophotometry. The method requires the adjustment of the pH and ionic strength of the sample to those of the mobile phase immediately prior to injection. Al^{3+}, AlF^{2+} and AlF_2^+ are eluted separately while all hydroxo complexes are readily dissociated and eluted along with Al^{3+} under these conditions. The sum of peak areas, which represents the total aluminium concentration, was conserved whatever the amount of fluoride in the sample. Linearity of calibration was observed over the range 20–2000 $\mu g\ l^{-1}$. Further, the speciation of fluoro–aluminium complexes as determined experimentally by ion chromatography is in good agreement with calculations based on complexation constants. The applications and limitations of the method are discussed.

INTRODUCTION

In its unique oxidized state, Al(III) is hydrolysed in aqueous media and forms hydroxo complexes. This phenomenon sometimes leads to dramatic decreases in pH and is therefore often involved in ecological concerns about acidic soils and hydrological systems. Recent studies have established the toxicity of aluminium to both fish [1–3] and plants [4]. However, this toxicity seems to be highly dependent on the chemical form of aluminium, the most dangerous form being assigned to the free cation, whereas fluoro and organic complexes tend to display only slight toxicity. It has been shown, for instance, that fish reproduction rates are enhanced in slightly acidic lake waters when complexing ligands (such as citrate or fluoride) are added [2]. To confirm such properties, a knowledge of total or free aluminium concentrations (as given by spectrofluorimetry [5–7] or ion-selective electrodes [8]) is no longer sufficient for an accurate description of the medium. Analytical methods that can account for the chemical speciation of this element are therefore necessary.

A controversial estimate of the distribution of inorganic, organic and polymeric species of aluminium in partially neutralized media is given by spectrophotometric methods that use the specific kinetic behaviour of each form [9–11]. In waters that contain little organic matter, OH^- and F^- are likely to form the major aluminium complexes. Some papers [12–18] have described the use of ion chromatography for the direct determination of Al(III) and the speciation of fluoride and organic complexes of aluminium in soils and aqueous solutions. The separation is based on slow kinetics of the decomplexation of the aluminium species. Most methods require a cation-

* Corresponding author.

0021-9673/94/$07.00 © 1994 Elsevier Science B.V. All rights reserved
SSDI 0021-9673(93)E1069-C

exchange column to separate the different species and postcolumn reaction for their detection. This paper describes a chromatographic method for the determination of AlF_2^+, AlF^{2+} and Al^{3+} in natural waters.

EXPERIMENTAL

Reagents

All reagents were of analytical-reagent grade. Ammonium chloride, ammonium acetate and hydrochloric acid were purchased from Merck and Tiron (disodium 1,2-dihydroxybenzene-3, 5-disulphonate) from Sigma.

Aluminium and fluoride standard solutions were prepared by dissolving $AlCl_3$ (Merck) and NaF (Merck) in dilute HCl adjusted to the desired pH.

The water used throughout was deionized with a Milli-Q system (Millipore) and all solutions were filtered through 0.45-μm filters (Millipore) and degassed.

Apparatus and chromatographic conditions

A Model 2000i ion chromatograph (Dionex), featuring a DQP-1 pump and a 50-μl loop injector was equipped with a reagent delivery module (RDM) (Waters) and an Opti-Ion UV–Vis detector set at 310 nm (Dionex). The separation was performed with a CS2 cation-exchange column (Dionex) protected by a CG2 guard column (Dionex).

The mobile phase consisted of 0.5 *M* NH_4Cl–0.01 *M* HCl unless stated otherwise, at a flow-rate of 1.1 ml min^{-1}. The postcolumn reagent, $3 \cdot 10^{-4}$ *M* Tiron in 3 *M* ammonium acetate, was introduced into the eluent stream via a T-piece located at the outlet of the column, at a rate of 0.75 ml min^{-1}. The final pH of the effluent was 6.70.

RESULTS AND DISCUSSION

The separation of the different fluoro–aluminium complexes was carried out on the cation-exchange column. Each eluted complex was detected via addition of a postcolumn reagent, Tiron, chosen for its ability to give stable complexes that can further be quantified spectrophotometrically.

Postcolumn reaction for spectrophotometric detection

The addition of a reagent to the eluent stream to complex the solute for on-line detection of the final product by UV spectrophotometry is a method that requires the following: (i) complete dissociation of the eluted complexes (*i.e.*, AlF_n^{3-n}) and quantitative complexation of Al^{3+} by Tiron; this condition is of major importance for quantitative speciation of a component; (ii) rapid kinetics to allow complete dissociation and recomplexation of the aluminium species within the connection between the RDM and the detector (a few seconds); and (iii) limited absorptivity of Tiron at 310 nm, which is the wavelength of maximum absorption of the Al–Tiron complex, to avoid baseline disturbances created by the injection.

The absorbance of a solution of $1 \cdot 10^{-4}$ *M* Tiron is plotted in Fig. 1. The titration curve of a solution ten times this concentration is also

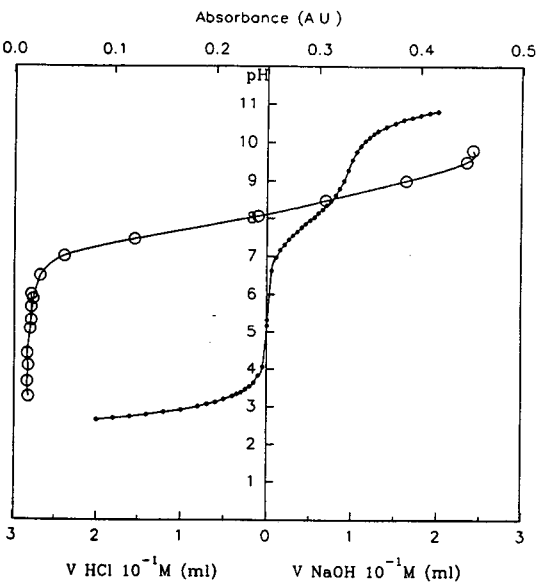

Fig. 1. Acid–base and spectrophotometric characteristics of Tiron. ● = Titration of $1 \cdot 10^{-3}$ *M* Tiron: pH *vs.* volume of reagent. ○ = pH *vs.* absorbance (310 nm) of $1 \cdot 10^{-4}$ *M* Tiron.

displayed for comparison ($pK_{a1} = 7.65$ and $pK_{a2} = 12.5$). Fig. 1 shows important alterations of the absorbance in the pH range 7.0–9.5. This range must be avoided to achieve both a steady baseline and a high signal-to-noise ratio. The best conditions are at pH 4–7, where the absorbance is low and independent of pH. The absorbance of the Al–Tiron complex is dependent on the pH: the more alkaline the medium, the higher is the absorbance of the complex. However, the signal-to-reference ratio is optimum around pH 6.7, which was chosen as a good compromise between no baseline offset but too low a signal and good sensitivity but too high a residual level. The molar absorptivity coefficients of Tiron and the Al–Tiron complex under such conditions were found to be 2000 and 18 000 l mol^{-1} cm^{-1}, respectively. The optimum pH value is in the range determined by Dean [17].

Chromatographic conditions

Although the postcolumn reaction conditions have previously been optimized to avoid perturbations of the baseline during the injection, a system peak occurs at the void volume when the injection solvent is water and interacts with the first-eluted peak. Changing the elution strength of the mobile phase had no perceptible effect on the capacity factor of this first peak as it is quasi-unretained on the CS2 column, whatever the conditions (see Fig. 2). The system peak disappears if the sample composition and pH are adjusted to those of the mobile phase. However, care should be taken to operate immediately prior to injections so that the equilibria be altered as little as possible, taking advantage of the slow kinetics of re-equilibration.

Fig. 3 shows some chromatograms of a solution containing $3.7 \cdot 10^{-5}$ *M* total aluminium and various amounts of fluoride in water. The relative evolution of the three peaks shows the following features. Fig. 3a displays a single peak that corresponds to Al^{3+} under the conditions of the injection; however, injections of alkaline samples containing aluminium in various $Al(OH)_m^{3-m}$ forms led to the same chromatogram, which suggests that $Al(OH)_m^{3-m}$ species are dissociated and eluted as Al^{3+}. Considering

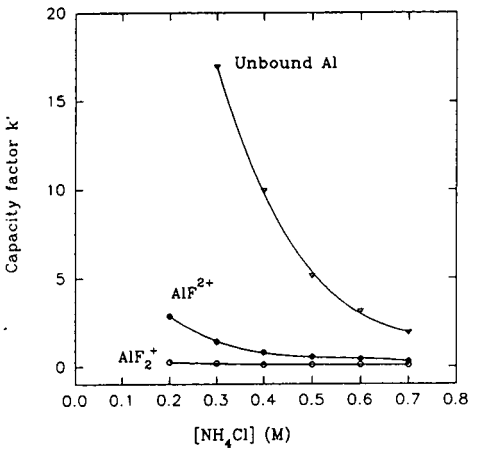

Fig. 2. Influence of the eluent strength of the mobile phase on the capacity factors (k') of the different fluoro–aluminium complexes. $[Al]_{Tot} = 3.7 \cdot 10^{-5}$ *M* and $[F]_{Tot} = 5.3 \cdot 10^{-5}$ *M*. Columns, CG2 + CS2; mobile phase, NH_4Cl–0.01 *M* HCl (flow-rate, 1.1 ml min^{-1}); postcolumn reagent, $3 \cdot 10^{-4}$ *M* Tiron in 3 *M* $CH_3CO_2NH_4$ (flow-rate, 0.75 ml min^{-1}); injection loop, 50 μl; detection wavelength, 310 nm.

the lability of hydroxo complexes, it is likely that they are decomplexed during pH adjustment of the sample. This phenomenon has been observed previously [15,16,19]. Peaks 1 and 2 were assigned to AlF_2^+ and AlF^{2+}, respectively, based

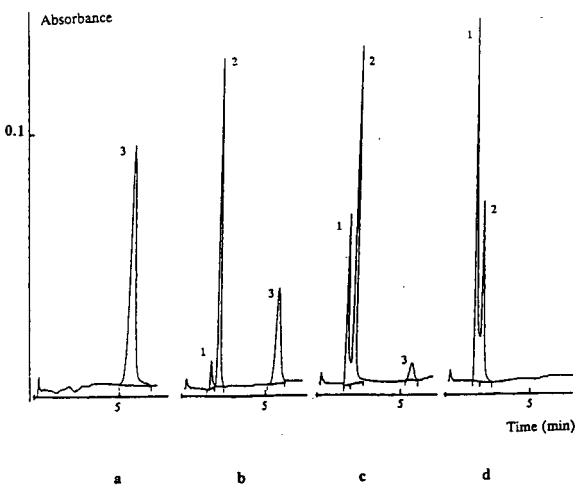

Fig. 3. Evolution of the distribution of fluoro–aluminium complexes as a function of total fluoride concentration. Chromatograms of standards containing $[Al]_{Tot} = 3.7 \cdot 10^{-5}$ *M* and (a) no fluoride, (b) $[F]_{Tot} = 2.6 \cdot 10^{-5}$ *M*, (c) $[F]_{Tot} = 5.3 \cdot 10^{-5}$ *M* and (d) $[F]_{Tot} = 10.5 \cdot 10^{-5}$ *M*. Mobile phase, 0.5 *M* NH_4Cl–0.01 *M* HCl; other conditions as in Fig. 2.

on their relative evolution in Fig. 3b, c and d and their charge. The calculations corresponding to the sample injected in Fig. 3d gave a share of 19% to the neutral species AlF_3. No peak can be observed for this species whereas peak 1 is increased by the corresponding amount to what is expected from the AlF_2^+ concentration; in this instance, the first peak accounts for both AlF_2^+ and AlF_3.

The quantitativity of the postcolumn reaction was also demonstrated: the sum of the areas of the three peaks representing the aluminium species is conserved whatever the amount of fluoride in the sample. This suggests that sufficiently rapid kinetics of AlF_n^{3-n} dissociation and Al–Tiron complex formation occur as these species successively react with Tiron before reaching the detector cell.

The influence of the concentration of NH_4Cl in the mobile phase on the capacity factors (Fig. 2), selectivity and resolution between the peaks of AlF_2^+ and AlF^{2+} was investigated. As expected, the higher the ionic strength, the lower were the capacity factors and the selectivity. The resolution presents a maximum value for NH_4Cl concentrations between 0.4 and 0.5 *M*. The latter was adopted throughout the study.

Calibration and performance

Linearity of the calibration for total aluminium was investigated over the range 20–2000 $\mu g\ l^{-1}$ ($7.4 \cdot 10^{-7}$–$7.4 \cdot 10^{-5}$ *M*). The calibration graph is shown in Fig. 4. For each aluminium concentration, distinction is made between standards containing only aluminium in water (injected in duplicate, open circles) and standards containing fluoride at various concentrations (namely, in mol l^{-1}, $[F]_{Tot} = 0.71[Al]_{Tot}$, $[F]_{Tot} = 1.42[Al]_{Tot}$ and $[F]_{Tot} = 2.84[Al]_{Tot}$) (closed circles). No statistical difference was observed between the

TABLE I

COMPARISON BETWEEN THE DISTRIBUTION OF THE FLUORO-ALUMINIUM COMPLEXES DETERMINED EXPERIMENTALLY BY ION CHROMATOGRAPHY AND CALCULATED BY MINEQL: INFLUENCE OF THE TOTAL ALUMINIUM CONCENTRATION OF THE SAMPLE

The standards were diluted in water; their final pH was between 4.5 and 5.1.

Sample		Al^{3+} (%)		AlF^{2+} (%)		AlF_2^+ (%)	
[F]/[Al]	$[Al]_{tot}$ (μM)	Exp.	Calc.	Exp.	Calc.	Exp.	Calc.
0.71	1.9	48.1	48.4	51.9	46.8	–	4.9
	3.7	34.0	42.8	59.0	51.4	7.0	5.8
	7.4	38.0	40.3	56.4	52.9	5.6	6.8
	18.5	35.3	38.0	59.5	54.5	5.2	7.4
	37.1	39.1	36.9	56.3	55.9	4.6	7.1
	74.1	33.5	36.9	61.3	55.7	5.2	7.4
1.42	1.9	16.5	19.8	67.0	61.1	16.5	19.0
	3.7	12.9	14.8	68.7	59.7	18.4	25.8
	7.4	12.4	10.2	68.3	57.5	19.3	31.8
	18.5	8.0	7.3	72.8	53.8	19.2	38.2
	37.1	7.1	7.3	61.7	50.0	31.2	41.9
	74.1	6.2	5.5	62.7	51.2	31.1	42.4
2.84	1.9	–	8.2	71.0	46.4	29.0	48.6
	3.7	5.3	1.5	52.6	34.5	42.1	63.1
	7.4	–	–	64.4	23.1	35.6	75.9
	18.5	–	–	40.6	12.1	59.4	87.3
	37.1	–	–	35.8	7.1	64.2	92.4
	74.1	–	–	32.7	4.1	67.3	94.9

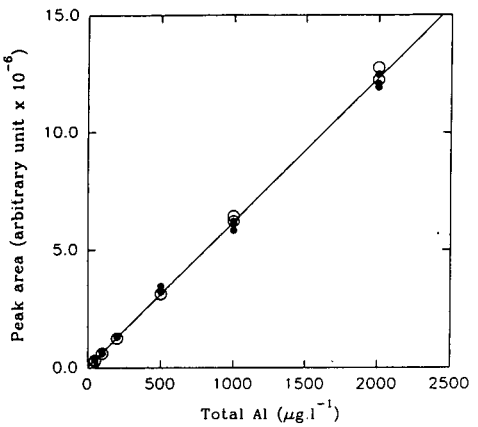

Fig. 4. Calibration graph and linear fit for total aluminium concentration in the range 20–2000 $\mu g\ l^{-1}$ ($7.4 \cdot 10^{-7}$–$7.4 \cdot 10^{-5}$ M). Conditions as in Fig. 3. ○ = $[F^-] = 0$; ● = $[F^-] \neq 0$.

two sets of data after linear regression. The final fit taking all the values into account yields $A = (6137 \pm 17)[Al] + (44\,860 \pm 15\,700)$.

The repeatability was tested by injecting the same standard containing $3.7 \cdot 10^{-5}$ M (1000 $\mu g\ l^{-1}$) aluminium seven times; the relative standard deviation was 5.3%.

The detection limit, determined as twice the average amplitude of the short-term noise, was 20 $\mu g\ l^{-1}$ for Al^{3+} and 9 $\mu g\ l^{-1}$ for both AlF^{2+} and AlF_2^+.

No interference was detected from Fe(III) at concentrations up to 10 mg l^{-1} but nitric acid induced baseline disturbances at the void volume.

Speciation

The influence of the composition of the samples ($[Al]_{Tot}$, $[F]_{Tot}$ and the sample matrix) was investigated in order to establish the feasibility and limitations of this method for accurate speciation determinations. Does the chromatographic process alter the relative concentrations of the aluminium species in the sample? In other words, is the chromatogram representative of the sample?

MINEQL software [20] was utilized in all theoretical calculations of solution equilibria. Thermodynamic constants were taken from ref. 21. Mixtures of aluminium and fluoride at different aluminium concentrations and [F]/[Al] ratios were prepared and analysed. Table I gives the result of speciation analysis; the experimental contribution of each species is deduced from the corresponding peak area and compared with the calculated value. Calculated values for Al^{3+} include labile hydroxo complexes which are dissociated into Al^{3+} prior to the chromatographic process.

Table I shows that the difference between the calculated and experimental values is not a function of total aluminium concentration but rather of that of total fluoride. The chromato-

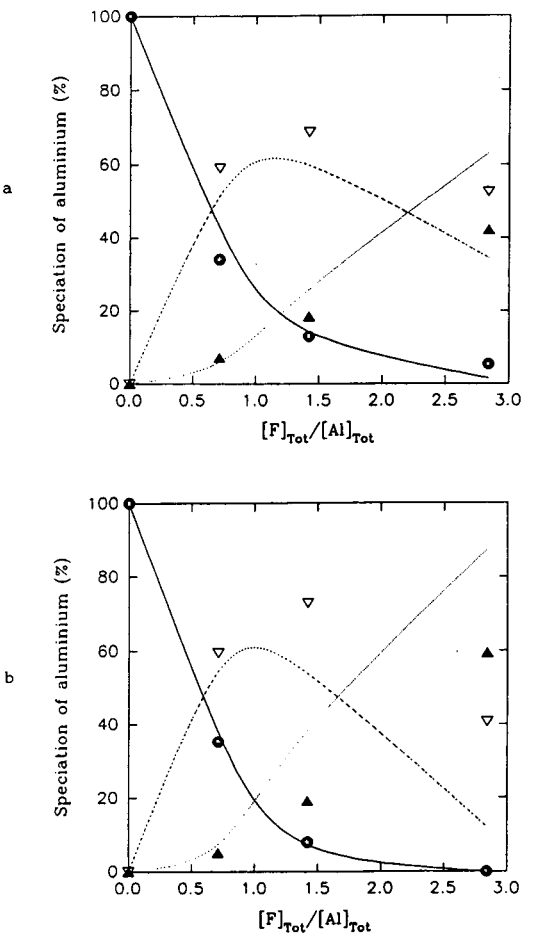

Fig. 5. Distribution of the fluoro–aluminium complexes in water as a function of the relative fluoride concentration. (a) $[Al]_{Tot} = 3.7 \cdot 10^{-6}$ M; (b) $[Al]_{Tot} = 18.5 \cdot 10^{-6}$ M. Conditions as in Fig. 3. Calculated: solid line = unbound Al; dashed line = AlF^{2+}; dotted line = AlF_2^+. Experimental: ● = unbound Al; ▽ = AlF^{2+}; ▲ = AlF_2^+.

graphic results for samples that contain little relative fluoride are in good agreement with the calculated values; at the highest fluoride concentrations, experimental speciation is no longer representative of the composition of the sample.

Further, peak 3 representing unbound aluminium seems to be less affected by the chromatographic conditions than peaks 1 and 2. Fig. 5 shows the experimental underestimation of AlF_2^+ simultaneously with the overestimation of AlF^{2+} and the correct estimation of unbound aluminium. This phenomenon is increased at high total fluoride concentrations and suggests a shift in the equilibrium $AlF_2^+ \rightleftharpoons AlF^{2+} + F^-$ in favour of AlF^{2+} during the chromatographic process: fluoride is not retained on the column and is eluted at the void volume whereas all cationic species are retained on the top of the column. This sudden lack of fluoride drives the complexes to react in order to provide for free fluoride. Further evidence for this exchange of fluoride between AlF_2^+ and AlF^{2+} is given by the shape of the chromatogram, where peaks 1 and 2 are separated by a plateau instead of displaying baseline resolution.

Table II shows the influence of the pH and the ionic strength of the sample on the accuracy of the speciation as determined by chromatography. Standards were prepared in dilute HCl or NaOH solution. Good agreement is obtained for acidic samples (pH ≈ 2), whatever the total fluoride concentration and the ionic strength. The agreement is still satisfactory at pH 4.7 for low fluoride contents.

In contrast, pH is a parameter of great influence at high values. In an alkaline medium, aluminium only exists as the species $Al(OH)_4^-$, whatever the total fluoride concentration. The chromatographic process with these standards should lead to a single peak 3. The existence of peaks 1 and 2 suggests a rapid alteration of the complexation equilibria to yield AlF_n^{3-n}, n depending on the relative fluoride concentration. This modification occurs during the adjustment of the sample matrix to the pH and ionic strength of the mobile phase prior to injection. It can be reasonably assumed that the higher the pH difference between the sample and the mobile phase and the ratio $[F]_{Tot}/[Al]_{Tot}$, the faster are the kinetics of the reactions

TABLE II

COMPARISON BETWEEN THE DISTRIBUTION OF THE FLUORO-ALUMINIUM COMPLEXES DETERMINED EXPERIMENTALLY BY ION CHROMATOGRAPHY AND CALCULATED BY MINEQL: INFLUENCE OF THE pH AND IONIC STRENGTH OF THE SAMPLE

$[Al]_{Tot} = 3.7 \cdot 10^{-5}$ *M*. MP = mobile phase.

Sample			Al^{3+} (%)		AlF^{2+} (%)		AlF_2^+ (%)	
[F]/[Al]	pH	Ionic strength	Exp.	Calc.	Exp.	Calc.	Exp.	Calc.
0.71	1.9	$1.3 \cdot 10^{-2}$	41.7	44.8	53.2	51.8	5.0	3.3
	4.7	$1.5 \cdot 10^{-4}$	37.4	36.9	59.2	55.9	3.3	7.1
	10.4	0.8	58.0	100.0	33.2	–	8.2	–
	2.0 (MP)	0.5	55.5	54.2	44.4	42.8	–	3.0
1.42	1.9	$1.3 \cdot 10^{-2}$	11.5	16.9	70.3	67.8	18.0	15.1
	4.7	$1.5 \cdot 10^{-4}$	5.0	7.3	66.6	50.0	28.3	41.9
	10.4	0.8	68.4	100.0	23.8	–	7.8	–
	2.0 (MP)	0.5	30.5	28.5	63.8	60.0	5.6	11.4
2.84	1.9	$1.3 \cdot 10^{-2}$	–	4.1	53.6	54.5	46.4	40.5
	4.7	$1.5 \cdot 10^{-4}$	–	–	33.5	7.1	66.4	92.4
	10.4	0.8	66.3	100.0	19.9	–	14.7	–
	2.0 (MP)	0.5	8.6	10.2	67.5	58.6	23.8	30.4

$$Al(OH)_4^- \rightarrow AlOH^{2+} \rightarrow Al^{3+}$$

$$Al^{3+} + F^- \rightarrow AlF^{2+}$$

$$AlF^{2+} + F^- \rightarrow AlF_2^+$$

On the column, rearrangement occurs between AlF_2^+ and AlF^{2+} during elution, as described previously. These modifications both in solution and on the column imply that, in contrast to what was observed for acidic samples, conservation of unbound aluminium is no longer verified.

The ionic strength of the sample, up to 0.5 *M*, did not seem to influence the accuracy of the experimental results.

CONCLUSIONS

The feasibility of ion chromatography for aluminium speciation in waters has been demonstrated. This method requires adjustment of the sample pH and ionic strength to match the mobile phase and limit interactions of system peaks with the first-eluted species. The total aluminium concentration can be measured by addition of the contributions of each aluminium complex; linearity of the calibration for total aluminium was observed over a wide range (20–2000 $\mu g\ l^{-1}$), whatever the fluoride content in the sample.

Provided that the sample pH is low (<4.5), ionic strength and total fluoride concentration have no significant influence on the accuracy of the experimental results; they are reliable estimates for aluminium speciation. With initial sample pH values higher than 5, acidification of the sample before injection favours rapid dehydroxylation followed by fluorination of Al^{3+}. The total aluminium concentration is still correctly deduced but the method is not suitable for speciation.

For natural samples, it is recommended that they be treated with HCl instead of HNO_3 in order to remove the system peaks on the chromatogram and to allow the quantification of AlF_2^+ and higher complexes.

REFERENCES

1 H. Leivestad and I.P. Muniz, *Nature*, 259 (1976) 391–392.
2 C.T. Driscoll, Jr., J.P. Baker, J.J. Bisogni and C.L. Schofield, *Nature*, 284 (1980) 161–164.
3 J.P. Baker and C.L. Schofield, *Water Air Soil Pollut.*, 18 (1982) 289–309.
4 D.R. Parker, L.W. Zelazny and T.B. Kinraide, in T.E. Lewis (Editor), *Environmental Chemistry and Toxicology of Aluminium*, Lewis, Chelsea, MI, 1989, pp. 117–145.
5 D.J. Hydes and P.S. Liss, *Analyst*, 101 (1976) 922–931.
6 F. Sanchez Rojas, A. Garcia de Torres, C. Bosch Ojeda and J.M. Cano Pavon, *Analyst*, 113 (1988) 1287–1290.
7 F. Carrillo, C. Pérez and C. Camara, *Anal. Chim. Acta*, 243 (1991) 121–125.
8 Nj. Radic, *Analyst*, 101 (1976) 657–660.
9 P.R. Bloom, R.M. Weaver and M.B. McBride, *Soil Sci. Soc. Am. J.*, 42 (1978) 713–716.
10 G.M. Morrison, *Analyst*, 115 (1990) 1371–1373.
11 B.R. James, C.J. Clarck and S.J. Riha, *Soil Sci. Soc. Am. J.*, 47 (1983) 893–897.
12 J. Kawase, A. Nakeae and K. Tsuji, *Anal. Chim. Acta*, 131 (1981) 213–222.
13 *Application Note 42*, Dionex, Sunnyvale, CA, 1983.
14 P.M. Bertsch and M.A. Anderson, *Soil Sci. Soc. Am. J.*, 52 (1988) 540–542.
15 P.M. Bertsch and M.A. Anderson, *Anal. Chem.*, 61 (1989) 535–539.
16 I.R. Willet, *Soil Sci. Soc. Am. J.*, 53 (1989) 1385–1391.
17 J.R. Dean, *Analyst*, 114 (1989) 165–168.
18 A. Tapparo and G.G. Bombi, *Anal. Chim. Acta*, 238 (1990) 279–284.
19 P. Jones, *Int. J. Environ. Anal. Chem.*, 44 (1991) 1–10.
20 J.C. Westall, Z.L. Zachary and F.M. Morel, *Technical Note No. 18*, Department of Civil Engineering, Massachusetts Institute of Technology, Boston, MA, 1976.
21 L.G. Sillén and A.E. Martell, *Stability Constants of Metal–Ion Complexes (Special Publication*, No. 17), Chemical Society, London, 1964, pp. 65, 66, 264 and 265.

Journal of Chromatography A, 660 (1994) 219–222
Elsevier Science B.V., Amsterdam

CHROMSYMP. 2950

Determination of triazines and dinitroanilines in waters by high-performance liquid chromatography after solid-phase extraction

Patrizia Vitali*, Emanuela Venturini, Cristina Bonora, Rino Calori and Raffaella Raffaelli

Settore Chimico Ambientale, Presidio Multizonale di Prevenzione, USL n.28, Via Triachini 17, 40138 Bologna (Italy)

ABSTRACT

A rapid and selective method for the simultaneous determination of triazines and dinitroanilines in real water matrices is suggested based on a preliminary adsorption on an RP-18 cartridge, an elution step using acetonitrile and HPLC separation with a Lichrosorb RP-Select B column and UV detection. The washing step cartridge is critical for triazines: terbutryn is eluted with quantitative recovery only after washing with an NH_3 solution. The degree of enrichment of the compounds studied has been determined: triazine recoveries are quantitative, while dinitroaniline recoveries are between 66% and 78% at the lowest fortification level. The detection limits for the ten herbicides are in the range 0.03–0.1 μg/l. The analysis time is 2 h.

INTRODUCTION

In the Polyspecialist Prevention Centre, we work to ensure that environmental laws are respected, to detect pollution and alterations of soil, water, food and air, and to survey quality trends and risk factors. Especially in emergency situations, it is not enough to prove analytically respect of the environmental law, it is necessary to have analytical results in real time. For this it is necessary to detect the origins, to define the consequences and to dictate the particular prevention steps.

In northern Italy environmental contamination from herbicides used in agriculture, particularly involving water matrices, is common.

The quantities reaching water by leaching will depend upon the herbicide, rainfall and soil type. Very important also is the question of accidental contamination of water supplies by a concentrate or a diluted spray. The Council of the European Community in 1980 adopted a directive [1] concerning standards for water intended for human consumption: the permitted level of any individual pesticide is 0.1 μg/l, and the total permitted concentration in water supplies is 0.5 μg/l.

Accordingly, the demands on analysis are very high, since relevant individual substances must be included, and the levels set by legislation necessitate an analytical method with high sensitivity. The traditional methods for determination of herbicides in water by HPLC or GC apply to compounds of the same structural class [2–10].

Therefore we developed an HPLC method that follows a preconcentration step, optimized for routine work and applied to ten herbicides in two different classes, triazines and dinitro-

* Corresponding author.

0021-9673/94/$07.00 © 1994 Elsevier Science B.V. All rights reserved
SSDI 0021-9673(93)E0997-9

TABLE I

HERBICIDES STUDIED AND TOXICITY LEVELS [12]

Common name	Toxicity LD_{50} for rats (mg technical grade/kg)
Triazines	
Atrazine	1869–3080
Metamitron	3343
Metribuzin	2200–2345
Propazine	>7700
Simazine	>5000
Terbuthylazine	2000
Terbutryn	2000
Dinitroanilines	
Ethalfluralin	>10 000
Pendimethalin	1050–1750
Trifluralin	>10 000

anilines. The ten herbicides studied and their toxicological data are reported in Table I. Although the use of atrazine in agriculture has been banned in Italy since 1991 [11], this compound is included in the list because its residues are still detected in the environment.

EXPERIMENTAL

Apparatus

A chromatograph equipped with a Model 501 solvent-delivery system and a Model 680 automated gradient controller was used, fitted with a Model 994 photodiode array detector (Waters, Division of Millipore, Milford, MA, USA) and a Rheodyne rotary injection valve (20-μl loop). The data-processing system was a Waters 746 Data Module. The column used was a LiChrosorb RP-Select B (5 μm), 250 × 4 mm I.D. (E. Merck, Darmstadt, Germany). Herbicides were extracted from water with a Vac-Elut vacuum system (Analitichem International, Harbor City, CA, USA).

Chemicals and materials

HPLC-grade acetonitrile (Carlo Erba, Milan, Italy), Milli-Q high-grade water (Millipore system) and 25% ammonia solution (E. Merck) were used. Herbicide standards were purchased from Labor Dr. Ehrenstorfer, Augsburg, Germany (metamitron, simazine, propazine, terbutryn, metribuzin, pendimethalin, terbuthylazine, ethalfluralin and trifluralin) and from Riedel De Haen Seelze, Hannover, Germany (atrazine). Bakerbond solid-phase extraction columns (3 ml size with sorbent octadecyl, weight of 500 mg; J.T. Baker, Phillipsburg, USA) were used in the preconcentration step. Sample filtration was obtained using a 0.45-μm HA filter (Millipore).

Fortification of the water

Stock standard solutions (*ca.* 100 mg/l each) were prepared in acetonitrile and stored at 4°C. Working standard solutions were obtained by dilution with acetonitrile, so that 0.5 ml of solution added to a 250-ml sample of water gave the required concentration of herbicides.

Extraction procedure

Extraction of triazines and dinitroanilines was carried out using the following procedure. An RP-18 cartridge was activated with two column volumes of acetonitrile followed by two column volumes of water. The sample (250 ml), after filtration through a 0.45-μm HA filter (Millipore), was added (using a reservoir) and allowed to percolate slowly, at 5 ml/min flow-rate (Vac-Elut system). The sorbent was washed using two column volumes of water to remove salt residues and 2 × 0.5 ml of 0.25% NH_3 solution. The cartridge was air dried under vacuum for 15 min and then herbicides were eluted with 2 × 1 ml of acetonitrile. The extract was completely evaporated with a gentle stream of nitrogen. The residue was recovered with 0.5 ml of acetonitrile.

Chromatographic determination

A LiChrosorb RP-Select B (5 μm) column (250 × 4 mm I.D.) was used for analysing the samples. The mobile phase was acetonitrile–water: 4 min at 40% acetonitrile, from 40% to 75% in 26 min, convex gradient curve, then 5 min in isocratic conditions, at 1 ml/min flow-rate.

The amount injected was 20 μl and the working wavelength 222 nm with a bandwidth of 3 nm.

Ten compounds were identified and quantified

by comparing their retention values, spectral data and integrated peak areas with those of known external standards.

RESULTS AND DISCUSSION

Triazine enrichment in the preconcentration procedure is critical. The pH conditions during the washing step, following the sample adsorption, dramatically affect the recovery of terbutryn. For instance, the recovery after washing with neutral water is *ca.* 5%, whereas it becomes approximately quantitative using an ammonia solution.

In contrast, the recovery was very low and poorly reproducible in the acidic region. Other studies [2] have shown that this low recovery can be ascribed to the conversion of triazines to other compounds under highly acidic conditions. Terbutryn is eluted only after a washing step with a NH_3 solution, probably owing to a secondary cation exchange of the reversed-phase column. Experiments at different pH values showed that the ideal washing pH is *ca.* 11. At pH >11 the recovery of metamitron decreases dramatically because of its instability in high alkaline conditions [12].

The percentage recoveries for the ten herbicides studied are reported in Table II. The average is based on five values.

Under the adopted experimental conditions the recovery of dinitroanilines is lower than that of triazines. Preliminary results [4] showed that

TABLE II

MEAN RECOVERIES (%) AND STANDARD DEVIATION OF HERBICIDES IN MILLI-Q WATER

Compound	Fortification level (μg/l)	Mean recovery (%)	±S.D. ($n = 5$)
Metamitron	3.0	89.7	10.0
	0.6	77.0	7.0
Simazine	0.84	95.1	5.7
	0.16	90.6	2.0
Metribuzin	2.6	97.6	4.9
	0.5	95.7	3.3
Atrazine	1.6	98.9	1.5
	0.3	95.6	5.7
Propazine	0.8	97.5	2.9
	0.16	94.0	5.4
Terbuthylazine	1.3	98.9	3.0
	0.26	98.5	1.6
Terbutryn	0.8	94.8	8.1
	0.16	98.4	4.6
Ethalfluralin	2.6	54.6	5.4
	0.5	77.5	6.5
Pendimethalin	2.9	54.7	3.4
	0.58	65.9	3.9
Trifluralin	4.16	50.7	4.6
	0.8	67.0	7.6

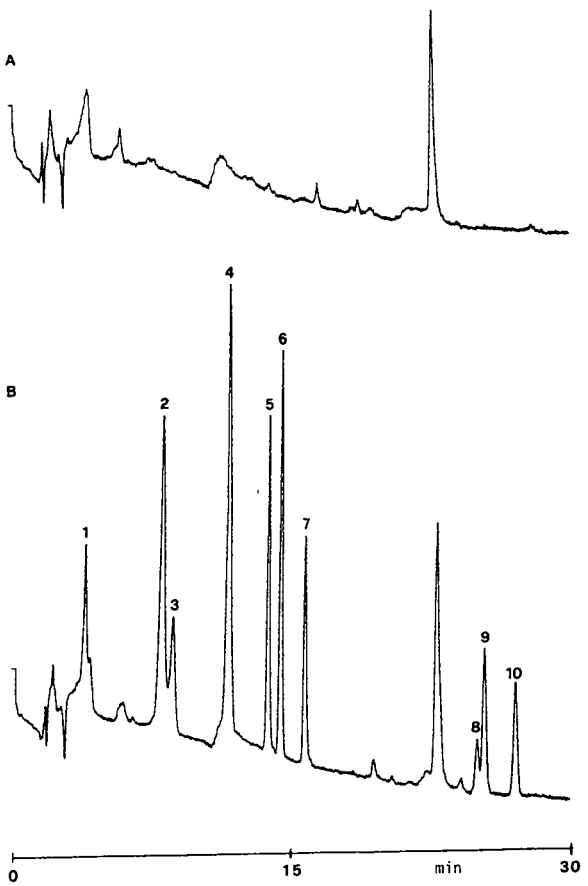

Fig. 1. Chromatography of triazine and dinitroaniline herbicides in surface water. Mobile phase: acetonitrile–water (convex gradient programme: 4 min, 40% acetonitrile; from 40% acetonitrile to 75% in 26 min). Flow-rate: 1 ml/min. Detection: UV at 222 nm. (A) Control, (B) sample fortified with: (1) metamitron 3.0 μg/l; (2) simazine 0.84 μg/l; (3) metribuzin 2.6 μg/l; (4) atrazine 1.6 μg/l; (5) propazine 0.8 μg/l; (6) terbuthylazine 1.3 μg/l; (7) terbutryn 0.8 μg/l; (8) ethalfluralin 2.6 μg/l; (9) pendimethalin 2.9 μg/l; (10) trifluralin 4.16 μg/l.

adoption of diethyl ether in the elution step improves dinitroaniline recovery, however the effect of this eluent on triazine recovery needs further verification.

The HPLC separation of herbicides in a surface water sample is shown in Fig. 1. There are no significant interferences due to the matrix. To optimize the separation between pendimethalin and ethalfluralin a gradient programme including a convex curve was used. A linear curve gradient does not allow satisfactory separation. Quantitative determinations were carried out using the external standard method.

The UV absorbances of solutions were measured at 222 nm as a compromise between the highest wavelength absorptions for triazines and dinitroanilines. The detector response is linear in the tested range (metamitron, 1.5–15.0 ng; terbutryn, 0.4–8.0 ng; pendimethalin, 1.5–15.0 ng; trifluralin 2.0–20.0 ng). The linear regression coefficients square root are between $r = 0.9947$ for pendimethalin and $r = 0.9989$ for terbutryn.

The detection limits for each compound are reported in Table III based on a signal-to-noise ratio of ≥ 2. After the preconcentration step, the herbicide enrichment factor is *ca.* 500. Consequently, under these conditions the detection limits are from 0.03 μg/l for propazine and terbutryn to 0.14 μg/l for trifluralin.

Work is in progress to improve the sensitivity of the analytical method: a larger volume of injected sample in HPLC analysis can be used. Other elution solvents can be tested to obtain a quantitative recovery for dinitroanilines, but it is necessary to evaluate the influence on triazine recoveries.

TABLE III

RETENTION TIME AND LIMITS OF DETECTION

UV detection at 222 nm.

Compound	Retention time (min)	Limit (μg/l)
Metamitron	3.9	0.1
Simazine	8.1	0.03
Metribuzin	8.7	0.1
Atrazine	11.7	0.05
Propazine	13.8	0.03
Terbuthylazine	14.5	0.05
Terbutryn	15.7	0.03
Ethalfluralin	24.9	0.09
Pendimethalin	25.3	0.1
Trifluralin	26.9	0.14

ACKNOWLEDGEMENT

We wish to thank Professor G. Longoni for his helpful comments.

REFERENCES

1 *80/778/EEC, Council directive of 15 July 1980 relating to the quality of water for human consumption*, European Commission, Official Journal L229, August 30th, 1980.
2 M. Popl, Z. Voznakova, V. Tatar and J. Strnadova, *J. Chromatogr. Sci.*, 21 (1983) 39.
3 Y. Xu, W. Lorenz, G. Pfister, M. Bahadir and F. Korte, *Fresenius' Z. Anal. Chem.*, 325 (1986) 377.
4 P. Cabras, M. Melis, L. Spanedda and C. Tuberoso, *J. Chromatogr.*, 585 (1991) 164.
5 L. Svoboda, P. Jandera and J. Churácek, *Collect. Czech. Chem. Commun.*, 54 (1989) 2120.
6 L.M. Davi, M. Baldi, L. Penazzi and M. Liboni, *Pestic. Sci.*, 35 (1992) 63.
7 H.J. Stan and A. Bockhorn, *Lebensmittelchemie*, 45 (1991) 40.
8 V. Coquart and M.C. Hennion, *J. Chromatogr.*, 585 (1991) 67.
9 P.C. Bardalaye and W.B. Wheeler, *Int. J. Environ. Anal. Chem.*, 25 (1986) 105.
10 H.B. Lee and Y.D. Stokker, *J. Assoc. Off. Anal. Chem.*, 69 (1986) 568.
11 *O.M. 705/475*, Italian Health Ministry, Rome, 1991.
12 C.R. Worthing (Editor), *The Pesticide Manual*, The British Crop Protection Council, Farnham 9th ed., 1991.

Journal of Chromatography A, 660 (1994) 223–229
Elsevier Science B.V., Amsterdam

CHROMSYMP. 2953

Clean-up by high-performance liquid chromatography of polychlorodibenzo-*p*-dioxins and polychlorodibenzofurans on a pyrenylethylsilica gel column

U. Pyell

Fachbereich Chemie der Philipps-Universität Marburg, Hans-Meerwein-Strasse, D-35032 Marburg (Germany)

P. Garrigues*

URA 348, CNRS, Laboratoire de Photophysique et Photochimie Moléculaire, Université de Bordeaux I, 351 Cours de la Libération, F-33405 Talence Cedex (France)

ABSTRACT

A clean-up step prior to the determination of polychlorodibenzo-*p*-dioxins (PCDDs) and polychlorodibenzofurans (PCDFs) based on normal-phase HPLC on a 2-(1-pyrenyl)ethyldimethyl silylated silica column is presented. With hexane as mobile phase, polychlorobiphenyls (including highly chlorinated non-*ortho* isomers) and organochlorine pesticides are eluted in the first fraction. The total fraction of PCDDs and PCDFs can be eluted by backflushing. By application of a gradient, all congeners are eluted within 75 min. The retention order of the PCDDs and PCDFs is predominantly governed by the degree of chlorination, but the substitution pattern also has a strong influence. Subfractions of the PCDD/PCDF fraction can be taken. The fraction containing 2,3,7,8-tetrachlorodibenzo-*p*-dioxin was isolated. The three tetrachlorodibenzo-*p*-dioxin isomers of this fraction were baseline separated on a non-polar capillary GC column.

INTRODUCTION

Clean-up by HPLC prior to the determination of polychlorodibenzo-*p*-dioxins (PCDDs) and polychlorodibenzofurans (PCDFs) has been already successfully utilized by several groups [1–17] and proved to be a valuable tool for isolating the PCDDs and PCDFs from very complex natural matrices. Most of the workers employed reversed-phase HPLC with alkylsilylsilica phases either for the improvement of isomer specifity [2,6,9] or for the removal of interfering matrix components [3,5,11,14] after matrix decomposition by chemical digestion with concentrated sulphuric acid or a silica column loaded with sulphuric acid.

Some groups utilized a two-step LC fractionation employing normal- and reversed-phase HPLC with silica and alkylsilica columns, respectively [4,7,14,15]. Swerev and Ballschmiter [10] reported the fractionation of PCDDs on cyanopropyl-, diphenyl- and phenylsilica gel. For clean-up HPLC with microparticulate alumina [1,16], aminopropylsilica [17] and nitro-bonded [8] stationary phases has also been reported.

Creaser and Al-Haddad [12] described the separation of polychlorobiphenyls (PCBs) and organochlorine pesticides from the PCDD/PCDF fraction on a porous graphitic carbon HPLC column. Owing to strong peak tailing and a high affinity of PCDDs and PCDFs for this

* Corresponding author.

0021-9673/94/$07.00 © 1994 Elsevier Science B.V. All rights reserved
SSDI 0021-9673(93)E1043-Y

phase, the method is solvent consuming and backflushing, which does not permit heart-cut techniques, is necessary.

A strong driving force behind the development of sophisticated clean-up steps by HPLC with various stationary phases was also the possibility of avoiding a final determination step for PCDDs and PCDFs by high-resolution GC–MS [7,13]. Expensive instrumentation impedes the general investigation of human food for PCDD/PCDF content. With the less selective but more sensitive electron-capture detection (ECD), the determination limit for PCDDs and PCDFs can be lowered with respect to the determination limit of a quadrupole MS detector.

In a previous paper [18], we reported the separation of thirteen tetrachlorodibenzo-*p*-dioxin (TCDD) isomers on a 2-(1-pyrenyl)ethyldimethylsilylated silica gel (PE-SG) column. PE-SG was designed as an electron-donor (ED) phase for donor–acceptor complex (DAC) LC. We were able to show that the formation of DACs can be assumed to be the predominant retention mechanism of PCDDs on PE-SG if the chromatographic separation is performed in the normal-phase mode. In a previous study by Barnhart *et al.* [19], the selectivity of PE-SG for TCDDs was only studied in the reversed-phase mode with methanol as mobile phase.

In this paper, we report PE-SG as a stationary phase in normal-phase HPLC as a clean-up step in PCDD/PCDF analysis. We studied not only the separation of PCDDs and PCDFs from interferring PCBs and organochlorine pesticides, but also the evaluation of PE-SG for the isolation of 2378-TCDD from its isomers and from TCDFs by fractionation of the sample extract.

EXPERIMENTAL

Chemicals

All solvents were of HPLC grade (Rathburn, Walkerburn, UK). Eleven TCDD isomers were purchased from Cambridge Isotope Labs. (Woburn, MA, USA) as solutions in nonane (50 ± 5 μg/ml); 1,2,3,6-, 1,2,3,9-, 1,2,6,7-, 1,2,8,9-, 1,3,7,8-, 1,4,7,8- and 2,3,7,8-TCDD were received as individual isomers and 1,2,3,7/1,2,3,8- and 1,3,6,8/1,3,7,9-TCDD as mixtures of two isomers. Peak assignment of the mixtures was described in previous papers [18,20]. The isomers 1,2,3,4- and 1,2,7,8-TCDD were received as crystals from Cambridge Isotope Labs. The pentachlorobiphenyls and organochlorine pesticides were provided by Promochem (Wesel, Germany).

A synthetic mixture of all PCDD congeners from mono- to octachlorodibenzo-*p*-dioxin (total concentration 10 μg/ml) and a purified fly-ash extract were provided by Dr. F.W. Karasek (Department of Chemistry, University of Waterloo, Ontario, Canada). A synthetic standard mixture of PCBs from mono- to decachlorobiphenyl was available as standard reference material (SRM 2262; NIST, Gaithersburg, MD, USA).

Apparatus

Fractionation was performed on an HP 1050 liquid chromatograph (Hewlett-Packard, Palo Alto, CA, USA) with a quaternary gradient pump and autoinjector in conjunction with an LDC Spectromonitor III UV detector. The PE-SG column (Cosmosil Pye, $d_p = 5$ μm, 250 mm $\times$ 4.6 mm I.D.) was supplied by Nacalai Tesque (Kyoto, Japan).

Fractions of the synthetic PCDD mixture were investigated using an HP 5890A gas chromatograph with ECD. Separations were performed on an apolar capillary column (50 m $\times$ 0.2 mm I.D. $\times$ 5.5 μm, PONA, Hewlett-Packard). Fractions of the purified fly-ash extract were further investigated using an HP 5890A gas chromatograph coupled with an HP 5971 mass-selective detector. The capillary column employed [CP-SIL 8 CB (0.2 μm) for pesticides, 50 m $\times$ 0.25 mm I.D.] was manufactured by Chrompack (Middelburg, Netherlands).

Separation studies

All retention data were obtained under isocratic and isothermal (25°C) conditions. The flow-rate was 1 ml/min in all instances. The UV detector was operated at 235 nm. Retention times were measured with solutions of the standards in 2-propanol or hexane, respectively. The solutions in nonane were diluted with appropriate solvents. In the case of mixtures, the

nonane was evaporated before dissolving the standard in 2-propanol in order to avoid peak broadening or distortion due to solvent effects of the sample solution.

The PCB-containing standard mixture (SRM 2262, NIST, Gaitherburg, MD, USA) and fractions were investigated using an HP 5890A gas chromatograph with ECD under the following conditions: injection mode, splitless; temperature programme, initially 50°C (0.3 min), increased at 1°C/min to 290°C; column, DB-5 (0.1 μm), 60 m × 0.20 mm I.D. (J & W, Folsom, CA, USA).

Fractionations

The PCDD mixture was fractionated either under isocratic conditions with hexane as mobile phase or by employing the following gradient: 0–24 min, 100% hexane, 0.8 ml/min; 24–60 min, linear gradient from 100% hexane to dichloromethane–hexane (90:10, v/v), linear gradient of flow-rate from 0.8 to 1.5 ml/min. The temperature of the column was not controlled. The UV detector was operated at 235 nm. The volume injected was 20–30 μl.

The fractions were collected in 10-ml glass vials, 20 μl of nonane were added and the solvent was concentrated in a gentle stream of nitrogen to the volume of the added nonane.

Gas chromatographic conditions and acquisition parameters

The GC–ECD operating parameters for the analysis of the concentrated fractions were the following: injection mode, splitless; injection port temperature, 300°C; injection volume, 1 μl; column, PONA (5.5 μm), 50 m × 0.20 mm I.D.; column head pressure, 280 kPa of helium; oven programme, initial temperature, 130°C; initial time, 0.5 min; ramp rate, 30°C/min to 230°C then 1°C/min to the final temperature, 290°C; detector temperature, 300°C; make-up gas (nitrogen) flow-rate, 60 ml/min.

The GC–MS operating parameters for the analysis of the concentrated fractions were as follows: injection port, on-column; inlet programme: initial temperature, 50°C; ramp rate, 20°C/min; final temperature, 300°C; injection volume, 1 μl; column, CP-SIL 8 CB (0.2 μm), 50 m × 0.25 mm I.D., column head pressure, 100 kPa of helium at 50°C, constant-flow mode (0.415 ml/min); oven programme, initial temperature, 50°C; ramp rate, 10°C/min to 230°C then 1°C/min to the final temperature, 280°C; transfer line temperature, 290°C; ionization mode, electron impact (70 eV); solvent delay, 20 min; detection mode, single-ion monitoring; dwell time, 300 ms. The ions monitored are listed in Table I.

TABLE I

IONS MONITORED IN MS DETECTION OF PCDD AND PCDF ISOMERS

Time (min)	*m/z*
20.0–28.5	303.9, 305.9, 319.9, 321.9
28.5–33.5	339.9, 341.9, 355.9, 357.9
33.5–41.0	373.8, 375.8, 389.8, 391.8
41.0–50.0	407.8, 409.8, 423.8, 425.8
50.0–65.0	441.7, 443.7, 457.7, 459.7

RESULTS AND DISCUSSION

Isolation of TCDDs from PCBs and organochlorine pesticides

The capacity factors, k', listed in Table II and the chromatograms presented in Fig. 1 show that the pyrene column tested is able to separate TCDD isomers from those classes of compounds which might interfere in TCDD determination, *i.e.*, organochlorine pesticides and pentachlorobiphenyls. Isolation of the TCDD fraction can be done much faster in the normal-phase mode. The best results were obtained with the solvent mixture hexane–methanol (95:5, v/v). In this instance, all possible interferents eluted within 8 min. The isolated fraction of TCDDs can be collected between 12 and 18 min. The conditions with hexane as mobile phase are similar. The retention times are longer, but working with hexane facilitates the evaporation of the solvent prior to GC analysis.

In order to study whether all PCB congeners elute before the TCDDs, we injected a synthetic standard mixture of PCBs containing 28 congeners of all degrees of chlorination, *ortho*-, 1-*ortho*-

TABLE II

CAPACITY FACTORS OF VARIOUS TCDD ISOMERS, PENTACHLOROBIPHENYLS (P5CBs) AND ORGANOCHLORINE PESTICIDES ON THE PE-SG COLUMN

Data for TCDD isomers were taken from ref. 18.

Solute	k' (methanol)	k' (hexane)
1,2,3,4-TCDD	17.32	3.19
1,2,3,6-TCDD	18.34	4.18
1,2,3,7-TCDD	15.01	3.90
1,2,3,8-TCDD	14.41	3.63
1,2,3,9-TCDD	15.94	4.22
1,2,6,7-TCDD	12.34	4.04
1,2,7,8-TCDD	13.28	4.01
1,2,8,9-TCDD	10.51	3.78
1,3,6,8-TCDD	19.26	3.42
1,3,7,8-TCDD	17.04	4.02
1,3,7,9-TCDD	16.47	3.63
1,4,7,8-TCDD	19.26	4.78
2,3,7,8-TCDD	15.59	4.74
2,2',4,5,5'-P5CB	1.34	0.48
3,3',4,4',5-P5CB	2.45	0.81
3,3',4,5,5'-P4CB	4.42	1.26
p,p'-DDT	1.15	0.87
o,p'-DDE	0.66	0.37
p,p'-DDE	0.94	0.45
o,p'-DDD	0.68	1.03
p,p'-DDD	0.95	2.03

and non-*ortho* substituted congeners. Haglund *et al.* [21] used fractionation on PE-SG for the isolation of the most toxic planar PCB congeners from the non-planar isomers. They observed that the non-*ortho* isomers elute in the last position within a group of PCBs of the same degree of chlorination. With hexane as mobile phase all congeners, contained in an industrial product, were eluted within 10 min at a flow-rate of 0.70 ml/min. The dimensions of the PE-SG column were 150 mm × 4.6 mm I.D.

In accordance with the results of Haglund *et al.*, we observed that all peaks of the synthetic PCB mixture eluted within 12 min with hexane as mobile phase. The eluate was collected. Comparison of the gas chromatogram of the concentrated eluate with that of the synthetic mixture proved that also highly chlorinated congeners and non-*ortho* congeners were eluted from PE-SG in the first 12 ml under the chosen chromatographic conditions.

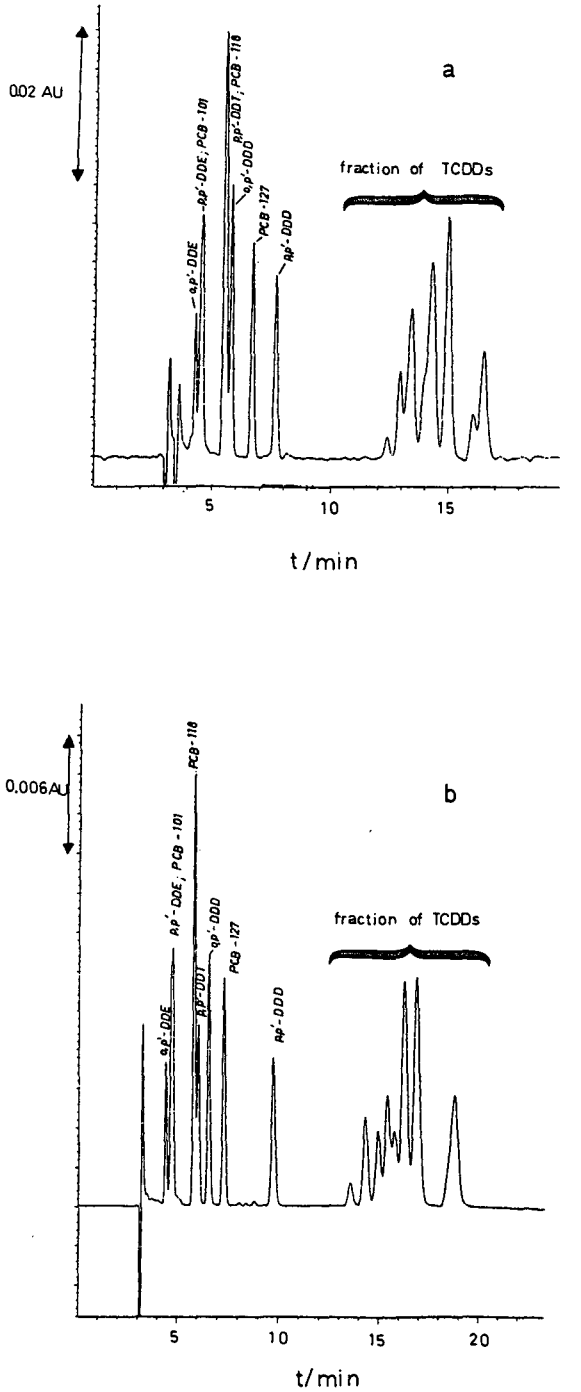

Fig. 1. Isolation of TCDD isomers from organochlorine pesticides and pentachlorobiphenyls. Column, PE-SG (250 mm × 4.6 mm I.D.); mobile phase, (a) hexane–methanol (95:5, v/v) and (b) hexane; temperature, 25°C; detection wavelength, 235 nm; flow-rate, 1 ml/min.

Fractionation of a synthetic PCDD mixture

Under isocratic conditions with hexane as mobile phase at a flow-rate of 0.8 ml/min only part of the injected congeners (mono- to pentachlorodibenzo-*p*-dioxins) eluted within 80 min. The monitored UV absorption peaks were identified by GC–ECD from the collected fractions. With TCDDs, identification was also possible by comparison of the HPLC trace of the synthetic PCDD mixture with that of thirteen TCDD isomers run under the same conditions on the PE-SG column [18] and comparison of the gas chromatograms of the fractions with a published gas chromatogram [22] of all TCDD isomers obtained with the same type of GC column as used in our studies.

Fig. 2 shows the HPLC results for the synthetic PCDD mixture. Only mono- to pentachlorodibenzo-*p*-dioxins were eluted within 80 min. The retention order is predominantly governed by the degree of chlorination. From the theory of DAC-LC [23], this retention order would be expected. The potential to form DACs as electron acceptors increases with increasing number of chlorine substituents. In Fig. 2 it can be seen that the substitution pattern of the PCDDs itself influences the retention to a great extent. A fraction of three TCDD isomers (t_R = 22–24 min), containing 2,3,7,8-, 1,2,6,9- and 1,4,7,8-TCDD, can easily be separated from higher chlorinated congeners and other TCDD isomers. In Fig. 3 a chromatogram of the isolated 2,3,7,8-TCDD-containing fraction is presented. On the apolar column employed, 2,3,7,8-TCDD is baseline separated from the other two isomers, which co-eluted on the PE-SG column.

In order to study the retention of the higher chlorinated congeners on PE-SG, a gradient from hexane to dichloromethane–hexane (90:10, v/v) was employed. With this gradient all congeners were eluted within 70 min. Also, the retention order of the higher chlorinated congeners is predominantly governed by the degree of chlorination. There is no overlapping of fractions containing isomers of the same degree of chlorination. The gradient causes an extreme drift of

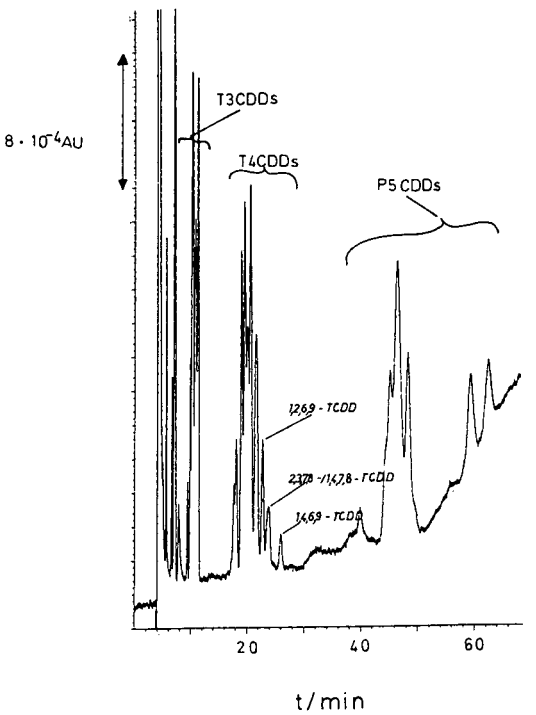

Fig. 2. Chromatogram of a synthetic PCDD mixture eluted from PE-SG. Column, 250 mm × 4.6 mm I.D.; mobile phase, hexane; temperature, ambient; detection wavelength, 235 nm; flow-rate, 0.8 ml/min. T3 = Tri; T4 = tetra; P5 = penta.

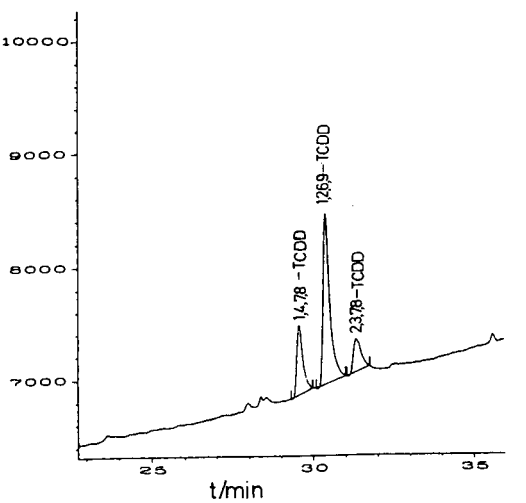

Fig. 3. Chromatogram of the isolated 2,3,7,8-TCDD-containing fraction analysed by GC–ECD. Injection mode, splitless; injection port temperature, 300°C; injection volume, 1 μl; column, PONA (5.5 μm), 50 m × 0.20 mm I.D.; column head pressure, 280 kPa of helium; initial oven temperature, 130°C; initial time, 0.5 min; ramp rate, 30°C/min to 230°C then 1°C/min to final temperature, 290°C.

the baseline at a detection wavelength of 235 nm.

Fractionation of a fly-ash extract

The same gradient as used for the fractionation of PCDDs was employed for the fractionation of a purified fly-ash extract containing PCDDs and PCDFs. A very high absorption, monitored during the elution of the first 10 ml of the mobile phase, indicates the elution of impurities. The elution of TCDDs could not be monitored directly by UV detection because of the presence of broad peaks, which are presumably partly due to impurities and partly to the large number of congeners that elute in this region.

Monitoring of the elution of higher chlorinated congeners was hampered by the baseline drift that resulted from the gradient of mobile phase, but was not impossible. Octachlorodibenzo-*p*-dioxin (OCDD) is separated from octachlorodibenzofuran (OCDF). OCDF elutes in the last position. Quantitative analysis of the octachlorinated and heptachlorinated congeners might be possible by HPLC on PE-SG with UV detection, as can be seen in Fig. 4. Fractions of the eluate were taken and analysed by GC–MS.

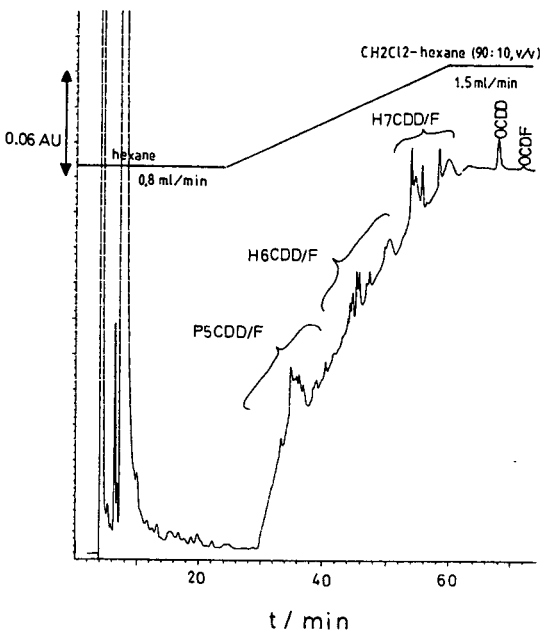

Fig. 4. Chromatogram of a fly-ash extract eluted from PE-SG. Column, 250 mm × 4.6 mm I.D.; gradient elution, 0–24 min, 100% hexane, 0.8 ml/min; 24–60 min, linear gradient of mobile phase composition from 100% hexane to dichloromethane–hexane (90:10, v/v); 24–60 min, linear gradient of flow-rate from 0.8 to 1.5 ml/min; temperature, ambient; detection wavelength, 235 nm. P5 = Penta; H6 = hexa; H7 = hepta.

Generally, the retention order of the PCDFs follows the retention order of the PCDDs. It is mainly governed by the degree of chlorination. The regions where PCDDs and PCDFs of the same degree of chlorination elute overlap. Also, slight overlapping of the TCDF and pentachlorodibenzofuran (P5CDF) fractions occurred.

The fraction containing 2,3,7,8-TCDD was isolated. Analysis by GC–MS proved that a TCDF isomer co-elutes from both the PE-SG and the non-polar GC columns employed, so that the separation sequence presented does not permit the determination of 2,3,7,8-TCDD by GC–ECD.

CONCLUSIONS

Normal-phase HPLC on PE-SG is a useful clean-up step in the analysis of PCDDs and PCDFs. It can be utilized as a rapid clean-up step separating possibly interferring PCBs and organochlorine pesticides from PCDDs and PCDFs. PCBs and organochlorine pesticides are eluted in the first 12 ml with hexane as mobile phase. The total fraction of PCDDs and PCDFs can be eluted by backflushing.

By application of a mobile phase with a stronger elution capacity, fractionation of the PCDDs and PCDFs is possible in the same chromatographic run in which clean-up is performed. This fractionation can be considered as a final "residue polishing" step. As could be demonstrated for 2,3,7,8-TCDD, the problem of peak overlap with isomers can be lowered to a large extent if small fractions are taken that contain only one of the seventeen congeners of the 2,3,7,8-TCDD class.

ACKNOWLEDGEMENTS

This work was supported by a grant from the Wissenschaftsausschuss der NATO via

Deutscher Akademischer Austauschdienst. We are indebted to M. Kobayashi (Nacalai Tesque, Kyoto, Japan), who provided a Cosmosil Pye column, and M. Breda (Atochem, Pierre Bénite, France) for the gift of some standards. The Ministère de la Santé et de l'Action Humaine (France) and Groupe BSN are also acknowledged for financial support of these studies.

REFERENCES

1 R.J. Dolphin and F.W. Willmott, *J. Chromatogr.*, 149 (1978) 161.
2 L.L. Lamparski, T.J. Nestrick and R.H. Stehl, *Anal. Chem.*, 51 (1979) 1453.
3 L.L. Lamparski and T.J. Nestrick, *Anal. Chem.*, 52 (1980) 2045.
4 M.L. Langhorst and L.A. Shadoff, *Anal. Chem.*, 52 (1980) 2037.
5 J.J. Ryan and J.C. Pilan, *J. Chromatogr.*, 197 (1980) 171.
6 P.W. O'Keefe, R. Smith, C. Meyer, D. Hilker, K. Aldous and B. Jelus-Tyror, *J. Chromatogr.*, 242 (1982) 305.
7 R.A. Niemann, W.C. Brumley, D. Firestone and J.A. Sphon, *Anal. Chem.*, 55 (1983) 1497.
8 M. Oehme and P. Kirschmer, *Anal. Chem.*, 56 (1984) 2754.
9 H.J. Tong, D.L. Shore and F.W. Karasek, *Anal. Chem.*, 56 (1984) 2442.
10 M. Swerev and K. Ballschmiter, *Chemosphere*, 15 (1986) 1123.
11 K. Junxing, R.E. Clement and L. Matchuk, *Acta Sci. Circumstant.*, 7 (1987) 212.
12 C.S. Creaser and A. Al-Haddad, *Anal. Chem.*, 61 (1989) 1300.
13 J.S. Jasinski, *J. Chromatogr.*, 478 (1989) 348.
14 L.L. Lamparski and T.J. Nestrick, *Chemosphere*, 19 (1989) 1165.
15 L.L. Lamparski and T.J. Nestrick, *Chemosphere*, 19 (1989) 1179.
16 T.S. Thompson, D.H. Schellenberg, K.P. Naikwadi and F.W. Karasek, *Chemosphere*, 19 (1989) 45.
17 Y. Zebühr, C. Naef, D. Broman, K. Lexen, A. Colmsjö and C. Östman, *Chemosphere*, 19 (1989) 39.
18 U. Pyell, P. Garrigues, G. Félix, A. Thienpont, P. Dentraygues and M.T. Rayez, *J. Chromatogr.*, 634 (1993) 169.
19 E.R. Barnhart, D.G. Patterson, N. Tanaka and M. Araki, *J. Chromatogr.*, 445 (1988) 145.
20 U. Pyell, P. Garrigues and M.T. Rayez, *J. Chromatogr.*, 628 (1993) 3.
21 P. Haglund, L. Asplund, U. Järnberg and B. Jansson, *J. Chromatogr.*, 507 (1990) 389.
22 R. Soniassy (Editor), *Environmental Analysis (Instrumental Teachniques)*, Hewlett-Packard, Palo Alto, CA, 1990, pp. 33–37.
23 L. Nondek, *J. Chromatogr.*, 373 (1986) 61.

Journal of Chromatography A, 660 (1994) 231–248
Elsevier Science B.V., Amsterdam

CHROMSYMP. 2932

Thermospray liquid chromatographic–mass spectrometric multi-residue determination of 128 polar pesticides in aqueous environmental samples

Dietrich Volmer and Karsten Levsen*

Department of Analytical Chemistry, Fraunhofer Institute of Toxicology and Aerosol Research, Nikolai-Fuchs-Strasse 1, D-30625 Hannover (Germany)

Gerold Wünsch

Institute of Inorganic and Analytical Chemistry, University of Hannover, Callinstrasse 3, D-30167 Hannover (Germany)

ABSTRACT

Thermospray (TSP) ionization was evaluated with respect to its suitability in the LC–MS determination of a broad range of pesticides. The sensitivity and the selectivity of this method for the determination of 128 pesticides having a wide range of structures and polarities were investigated. An LC separation in combination with postcolumn addition of a volatile salt solution was developed, which permits the analysis of 95 pesticides with a single LC–MS method using reversed-phase gradient elution. The retention data and TSP mass spectra of these compounds are presented. The advantages of TSP postcolumn techniques in comparison with conventional systems are discussed. The application of this method to the analysis of an environmental sample (river water) spiked with eight phenylureas is demonstrated. The method was evaluated with respect to detection limit, linearity and reproducibility. In addition, a simple method for enhancing the structural information from TSP spectra is reported, which makes use of specific instabilities found with many pesticides. As an example, possibilities for the confirmatory analysis of carbamates are described.

INTRODUCTION

The common European Community (EC) market and thus the anticipated large number of different pesticides used within the EC necessitate the development of rapid screening multi-purpose methods for as many as possible of the most relevant agents. Further, the EC drinking water guidelines demand analytical methods that allow the verification of the concentration limit of 100 ng l^{-1} for individual pesticide species [1]. Therefore, universal, specific, sensitive and reliable methods are required that with permit the determination of a broad variety of target and non-target compounds, preferable both volatile and non-volatile compounds.

Gas chromatography is still the most popular method for the determination of pesticides. GC–MS allows the identification and determination of a wide variety of pesticides in several matrices. However, owing to their thermal instability and polarity, many pesticides are not amenable to GC analysis. In many instances they can, however, be measured by column liquid chromatographic methods, which can be applied equally well to most typical "GC compounds". Conventional detection in HPLC is usually achieved with UV or diode-array detection (DAD). UV detection often provides adequate sensitivity. In combination with a diode-array detector, an unambiguous identification in en-

* Corresponding author.

0021-9673/94/$07.00 © 1994 Elsevier Science B.V. All rights reserved
SSDI 0021-9673(93)E0939-R

vironmental samples is sometimes possible for certain compound classes, *e.g.*, nitrophenols [2]. However, structural information is lacking for most pesticide compound classes, because the UV spectra of one compound class are often almost identical and differences between compound classes are frequently small. Further, several pesticides have a low UV absorbance as they lack a strong chromophore in the UV region for sensitive detection. Hence UV detection and DAD are not well suited for universal application.

The potential of combined LC–MS for the determination of both thermally labile and non-volatile compounds has been demonstrated [3]. Further, typical "GC pesticides" are also amenable to LC–MS, which makes LC–MS an ideal method for the determination of a broad range of pesticides. Different types of LC–MS interfaces have been applied to pesticide analysis such as a moving belt [4,5], direct liquid introduction [6,7], fast atom bombardment (FAB) [8], thermospray (TSP) [9,10] and particle beam [11]. The applicability of atmospheric pressure chemical ionization (APCI) and ionspray (ISP) compared with TSP and particle beam for trace-level determinations of pesticides has been demonstrated recently [12]. Among the different interfaces, TSP is the one most widely used today. As TSP mass spectra often show little fragmentation and thus lack structural information, several techniques are available to overcome these limitations, *e.g.*, the variation of the gas-phase and vaporizer temperature to induce controlled chemical reactions during TSP vaporization and ionization [13], the use of external ionization media and tandem MS techniques [14,15], repeller-induced fragmentation [16] and additional cluster ions with solvent or additive molecules and additional information gained from the complementary interpretation of positive- and negative-ion spectra [13,17,18]. By applying these techniques, LC–TSP-MS can be used as an ideal confirmatory method.

TSP has been employed in analyses for large variety of pesticides such as carbamates [12], organophosphorus [19,20] and quaternary ammonium compounds [21], phenylureas [22,23], phenoxy acids [22,24], triazines [25,26] and some other classes. However, so far applications of TSP only to special groups or compound classes of pesticides have been reported. Only a few workers, *e.g.*, Bellar and Budde [26] and Vreeken *et al.* [18], have reported methods applicable to a broad range of compounds with large differences in polarities and structures.

We have developed an LC–TSP-MS method for the extraction, separation and determination of *ca.* 130 pesticides from aqueous environmental samples including anilides, carbamates, phenylureas, phenoxy acids, oximes, organophosphorus and quaternary ammonium compounds, triazines and other N-heterocyclic compounds and some other classes. Special attention has been paid on the one hand to compounds with low UV absorbance and on the other to pesticides produced in the former German Democratic Republic ("GDR-specific" pesticides). Although the production of most "GDR-specific" pesticides was prohibited in Germany at the beginning of 1993, further application is still allowed for many of these compounds because the disposal of the large remainder as waste is too expensive. For many of these compounds, no methods for determination at trace levels are available. Trace enrichment from aqueous samples is achieved by means of a conventional off-line on an on-line preconcentration procedure using solid-phase extraction. A more detailed description of the extraction procedure will be presented in a subsequent paper.

The purpose of this work was to demonstrate the applicability of LC–TSP-MS as a rapid screening method for the identification and determination of pesticides. One objective was to develop a single method with a set of identical experimental parameters that allow the determination of a broad range of pesticides having widely differing structures and polarities. Moreover, a detection limit of 100 ng l^{-1} was sought. This required the ability to detect at least 2–5 ng of each compound after extraction and enrichment of the aqueous sample using both off-line or on-line preconcentration techniques. Further requirements were a precision of at least 15% (relative standard deviation) for determination and a linear dynamic range of $>10^3$ in order to allow external determination.

EXPERIMENTAL

Materials

Pesticide standards were purchased from Riedel-de Haën (Seelze-Hannover, Germany) and Promochem (Wesel, Germany). They were of purity >98% and were used as received. Buminafos and butonate were gifts from Dr. J. Efer (University of Leipzig, Leipzig, Germany). Methanol was purchased from Riedel-de Haën (Chromasolv HPLC grade) and reagent water was obtained from a Milli-Q water purification system (Millipore, Bedford, MA, USA). The solvents were passed through a 0.45-μm filter (Sartorius, Göttingen, Germany) before use. Ammonium acetate (Gold Label grade) was obtained from Aldrich (Steinheim, Germany). PEG-300, PEG-400 and caffeine were purchased from Fluka (Buchs, Switzerland).

Sample extraction

The pesticides were extracted from water (1 l, 10 ml min^{-1}) using solid-phase extraction cartridges filled with 2 g of C_{18} material (Amchro, Sulzbach-Taunus, Germany). Four 1-ml methanol washes carried the pesticides trapped on the cartridge to a sample vial. Thereafter, the volume was reduced to 1 ml using a gentle stream of nitrogen.

Liquid chromatography

Details of the experimental set-up have been described elsewhere [13]. Briefly, a postcolumn technique was employed in order to allow the separate optimization of the HPLC separation and the TSP ionization (see Results and Discussion).

The best results were obtained with narrow-bore (3 mm I.D.) columns, a column flow-rate of 0.6 ml min^{-1} and an additional buffer flow-rate of 0.4 ml min^{-1} (175 m*M* ammonium acetate). LiChrospher 60 RP-select B (5 μm) columns (125 × 3 mm I.D.) (Merck, Darmstadt, Germany) were used. Gradient elution was performed with methanol–water mixtures. The solvents were degassed in an ultrasonic bath and continuously purged with *ca.* 25 ml min^{-1} of helium to maintain very low levels of dissolved air. The methanol–water eluent composition was linearly programmed from 20 to 95% methanol in 45 min and then held for 15 min at 95% methanol. A Model 7125 injection valve equipped with a 20-μl loop from Rheodyne (Cotati, CA, USA) was used to introduce the samples. In order to avoid peak broadening of early-eluting compounds, it was necessary to inject sample solutions with a high water content ($\geq$80%).

For comparative studies, normal-bore LiChrospher 100 RP-18 columns (250 × 4 mm I.D.) (Merck) were used. A postcolumn addition of 0.2 ml min^{-1} of 450 m*M* aqueous ammonium acetate solution was employed. A slightly different methanol–water gradient programme was used within these experiments, from 10 to 90% methanol in 45 min, the latter composition being held for 15 min.

Thermospray mass spectrometry

The experiments described here were performed using a Finnigan MAT (San José, CA, USA) Model 4500 mass spectrometer equipped with a Vestec (Houston, TX, USA) thermospray source. Typical operating conditions of the TSP interface were as follows: vaporizer control temperature $T_1 \approx 135$–150°C; vaporizer temperature $T_v \approx 190$–220°C; tip heater temperature $T_3 = 270$°C; source jet temperature $T_g \approx 230$–240°C; source temperature $T_s = 250$°C and exit line pressure $p_g \approx 2$–4 Torr (1 Torr = 133.322 Pa). The mass spectrometer was operated in the positive-ion (PI) and negative-ion (NI) modes and was scanned at a rate of 1 s per scan over the range *m/z* 130–450 (PI) and *m/z* 185–500 (NI). The vaporizer temperature was optimized before each analysis to obtain a stable maximum ion intensity of the solvent cluster ions in the range *m/z* 18–139. In order to keep the vaporizer fraction of the carrier stream constant during gradient operation, the vaporizer temperature was adjusted by means of automatic gradient compensation control of the interface as the solvent composition changed. The mass scale was calibrated with an aqueous solution of caffeine, PEG-300 and PEG-400 containing 100 m*M* ammonium acetate where the solution was continuously pumped into the TSP ion source.

The polyethylene glycol–ammonium cluster ions were also used to tune the instrument.

In all experiments discharge-assisted buffer ionization (1000 V) was used, because the absolute signal intensities are approximately three times higher in this mode than with buffer ionization alone and at least 1.5 times higher than in the filament-assisted buffer ionization mode. The actual gain in sensitivity was lower, because a slight increase in noise was observed when using additional external ionization media.

Direct flow-injection experiments were performed using a carrier stream of methanol–water (50:50, v/v) with a salt concentration c_s (ammonium acetate) of 50 m*M* and a flow-rate of 1.0 ml min^{-1}. The samples were introduced via a sample loop of 50 μl.

LC–TSP-MS–MS was carried out on a Finnigan MAT TSQ 70 triple-stage quadrupole mass spectrometer (Q1, Q2, Q3). In these MS–MS experiments, the $[MH]^+$ or $[MHNH_3]^+$ ions were chosen as precursor ions and selectively transmitted by Q1 for further collisional dissociation to Q2. Argon was used as the collision gas with a collision chamber pressure of $1.3 \cdot 10^{-3}$ Torr. A collision offset (COFF) of 10 V was applied to Q2. The collision-activated dissociation (CAD) daughter ions thus obtained were then analysed by scanning with the third quadrupole (Q3) over the mass range 20–500. For the LC–MS–MS studies, direct flow injection was used to introduce the samples into the mass spectrometer. The TSP vaporizer control temperature was set to 90°C and the aerosol temperature was kept at 240°C.

RESULTS AND DISCUSSION

The 128 compounds listed in Table I were successfully determined by means of LC–TSP-MS, although not all of them are thermally labile, typical "HPLC compounds". Many typical "GC compounds" are also amenable to TSP and HPLC, hence the latter compounds were also included. Special compound classes such as quaternary ammonium compounds are not included here because their determination required specific HPLC or TSP conditions. The determination of these compounds will be described in a subsequent paper.

Improving selectivity and sensitivity via postcolumn techniques

Improvements in selectivity and sensitivity in the determination of pesticides by means of TSP can be achieved by postcolumn addition of aqueous buffer solution and the use of external ionization media as described under Experimental.

The TSP response is directly related to the water fraction, x_w, in the final TSP carrier stream and the dielectric constant of the mixed solvent, ε_{solv}. Fig. 1 shows a typical LC–MS trace obtained with a conventional 4 mm I.D. C_{18} column. Postcolumn addition of 0.2 ml min^{-1} of 450 m*M* aqueous ammonium acetate solution was employed in this instance. The sensitivity is much higher for early-eluting compounds than for compounds with longer retention times. This is probably due to changes in the fraction of water in the carrier stream during gradient elution. In Fig. 2a the dependence of the absolute ion intensities of two pesticides (carbofuran, m/z 222 and 239, and desmetryn, m/z 214) are plotted against ε_{solv}, which is approximately proportional to x_w (the salt concentration, c_s, was 50 m*M* in each instance). A factor of at least two in sensitivity can be gained if x_w is increased from 50% to 80% (ε_{solv} changes almost linearly with x_w when using methanol–water; ε_{solv} values were taken from ref. 27). However, one should note that the noise increases slightly with increasing x_w, so the actual increase in the signal-to-noise ratio for most pesticides is slightly lower.

It is interesting that this behaviour can be correlated with variations of the reagent gas ion intensities as x_w is changed. This is demonstrated in Fig. 2b, where the dependence of the integrated solvent ion current (m/z 18–139) on ε_{solv} and thus x_w is shown [$c_s = 50$ m*M* in all instances; carrier stream flow-rate 1.0 ml min^{-1}; T_v was adjusted to 3°C below the point of complete vaporization ("take-off" temperature) for each solvent composition]. A further correlation is possible with eqn. 4 in ref. 28. As shown there,

TABLE I

PESTICIDES INVESTIGATED IN THIS STUDY

No.	Compound	Chemical class	No.	Compound	Chemical class
1	Ametryn	Triazine	67	Aldicarb	Carbamate
2	Anilazine	Traizine	68	Aldicarb sulfone	Carbamate
3	Atraton	Triazine	69	Aldicarb sulfoxide	Carbamate
4	Atrazine	Triazine	70	Asulam	Carbamate
5	Atrazine-desethyl	Triazine	71	Barban	Carbamate
6	Atrazine-desisopropyl	Triazine	72	Benomyl	Carbamate
7	Cyanazine	Triazine	73	Cartap	Carbamate
8	Hexazinone	Triazine	74	Carbaryl	Carbamate
9	Desmetryn	Triazine	75	Carbendazim	Carbamate
10	Prometryn	Triazine	76	Carbetamide	Carbamate
11	Propazine	Triazine	77	Carbofuran	Carbamate
12	Secbumeton	Triazine	78	Chloropropham	Carbamate
13	Sebutylazine	Triazine	79	Desmedipham	Carbamate
14	Simazine	Triazine	80	Methiocarb	Carbamate
15	Terbutryn	Triazine	81	Methomyl	Carbamate
16	Terbutylazine	Triazine	82	Oxamyl	Carbamate
17	Bromacil	Pyrimidine	83	Phenmedipham	Carbamate
18	Chloridazon	Pyrimidine	84	Pirimicarb	Carbamate
19	Crimidine	Pyrimidine	85	Promecarb	Carbamate
20	Terbacil	Pyrimidine	86	Propham	Carbamate
21	Amitrole	Triazole	87	Propoxur	Carbamate
22	Terbuconazole	Triazole	88	Triallate	Carbamate
23	Triadimefon	Triazole	89	Prosulfocarb	Thiocarbamate
24	Metamitron	Pyridine	90	Thiodicarb	Thiocarbamate
25	Metribuzin	Pyridine	91	Chlorobromuron	Phenylurea
26	Aldimorph	Morpholine	92	Chloroxuron	Phenylurea
27	Fenpropimorph	Morpholine	93	Chlorotoluron	Phenylurea
28	Tridemorph	Morpholine	94	Difenoxuron	Phenylurea
29	Allidochlor	N-Substituted amide	95	Diuron	Phenylurea
30	Alachlor	Anilide	96	Fenuron	Phenylurea
31	Butachlor	Anilide	97	Fluometuron	Phenylurea
32	Dimethachlor	Anilide	98	Isoproturon	Phenylurea
33	Metalaxyl	Anilide	99	Linuron	Phenylurea
34	Metazachlor	Anilide	100	Methabenzthiazuron	Phenylurea
35	Methfuroxam	Anilide	101	Metobromuron	Phenylurea
36	Metolachlor	Anilide	102	Metoxuron	Phenylurea
37	Monalide	Anilide	103	Metsulfuron-methyl	Phenylurea
38	Pentanochlor	Anilide	104	Monolinuron	Phenylurea
39	Propachlor	Anilide	105	Monuron	Phenylurea
40	Propanil	Anilide	106	Isocarbamide	Thiourea
41	Prochloraz	Anilide	107	Benazolin	Carboxylic acid
42	Pendimetalin	Dinitroaniline	108	Chloramben	Carboxylic acid
43	Azinphos-ethyl	Organophosphorus	109	Dalapon	Carboxylic acid
44	Buminafos	Organophosphorus	110	Dicamba	Carboxylic acid
45	Butonate	Organophosphorus	111	TCA	Carboxylic acid
46	Chlorfenvinphos	Organophosphorus	112	2,4-D	Phenoxy acid
47	Demeton	Organophosphorus	113	2,4-DB	Phenoxy acid
48	Demeton-S-methyl	Organophosphorus	114	Dichlorprop	Phenoxy acid
49	Diazinone	Organophosphorus	115	MCPA	Phenoxy acid
50	Dichlorvos	Organophosphorus	116	MCPB	Phenoxy acid
51	Dimethoate	Organophosphorus	117	Mecoprop (MCPP)	Phenoxy acid
52	Disulfoton	Organophosphorus	118	Silvex (2,4,5-TP)	Phenoxy acid
53	Fenamiphos	Organophosphorus	119	2,4,5-T	Phenoxy acid
54	Fenithrotion	Organophosphorus	120	Bifenox	Carboxylic ester
55	Mecarbam	Organophosphorus	121	Chlorfenvinprop	Carboxylic ester
56	Merphos	Organophosphorus	122	Fluazifop-butyl	Carboxylic ester
57	Methamidophos	Organophosphorus	123	Haloxyfop-ethyl	Carboxylic ester
58	Monocrotophos	Organophosphorus	124	Naphthyl acetate	Carboxylic ester
59	Naled	Organophosphorus	125	Benzalkonium chloride	Quaternary ammonium
60	Oxydemeton-methyl	Organophosphorus	126	Chlormequat	Quaternary ammonium
61	Parathion-methyl	Organophosphorus	127	Diquat	Quaternary ammonium
62	Phosalone	Organophosphorus	128	Paraquat	Quaternary ammonium
63	Phosmet	Organophosphorus			
64	Prothiofos	Organophosphorus			
65	Triazinone	Organophosphorus			
66	Trichlorfon	Organophosphorus			

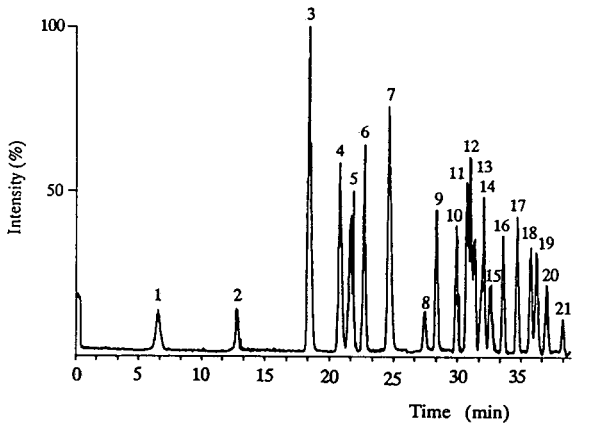

Fig. 1. LC–TSP-MS separation of 21 pesticides (180 ng each). Conditions: column, 250 × 4 mm I.D. LiChrospher 100 RP-18 (5 μm); mobile phase, methanol–water at a column flow-rate of 1.0 ml min^{-1}; gradient profile, from 10% methanol linearly to 90% methanol in 45 min and held for 10 min; postcolumn addition of 0.2 ml min^{-1} of 450 m*M* ammonium acetate. TSP: discharge ionization; $T_s = 250°C$; $T_g \approx 235°C$; $T_v = 210 \rightarrow 195°C$. Peak assignment: 1 = asulam; 2 = aldicarb sulfone; 3 = atrazine-desisopropyl; 4 = fenuron; 5 = dimethoate; 6 = chloridazone; 7 = atrazine-desethyl; 8 = aldicarb; 9 = metoxuron; 10 = cyanazine; 11 = terbacil; 12 = monuron; 13 = carbofuran; 14 = simazine; 15 = hexazinon; 16 = carbaryl; 17 = monolinuron; 18 = chlorotoluron; 19 = atrazine; 20 = isoproturon; 21 = diuron.

the dependence is directly related to the ammonium acetate ionic activity in the mixed solvent. Hence the Debye–Hückel theory can be used for the description of this dependence.

Fig. 2b demonstrates that the ion current of the solvent cluster ions directly reflects the dependence of the analyte signal intensities on the amount of water in the carrier stream. This is the expected behaviour as these solvent cluster ions act as ionizing reagents. However, the gain in sensitivity is higher for the solvent cluster ions compared with those obtained with both pesticides. As shown by Voyksner *et al.* [29], a postcolumn addition of a buffer salt can be used to enhance the sensitivity. In order to avoid dilution of the samples, one has to find an optimum ratio of the buffer flow-rate relative to the column flow-rate. A further parameter affects this ratio, namely the absolute flow-rate of the TSP carrier stream. For the varporization of high carrier stream flows, very high vaporizer temperatures are necessary and, as a consequence, chemical dissociations of the sample [13,30–32] and fragmentations of the quasi-molecular ions are enhanced [preliminary experiments with postcolumn addition of the buffer salt in combination with normal-bore 4 mm I.D. columns revealed that in the case of the Vestec source the vaporization of the resulting flow (*ca.* 1.5 ml min^{-1}) often requires vaporizer temperatures higher than 250°C]. In this study, in most instances 3 mm I.D. narrow-bore columns were

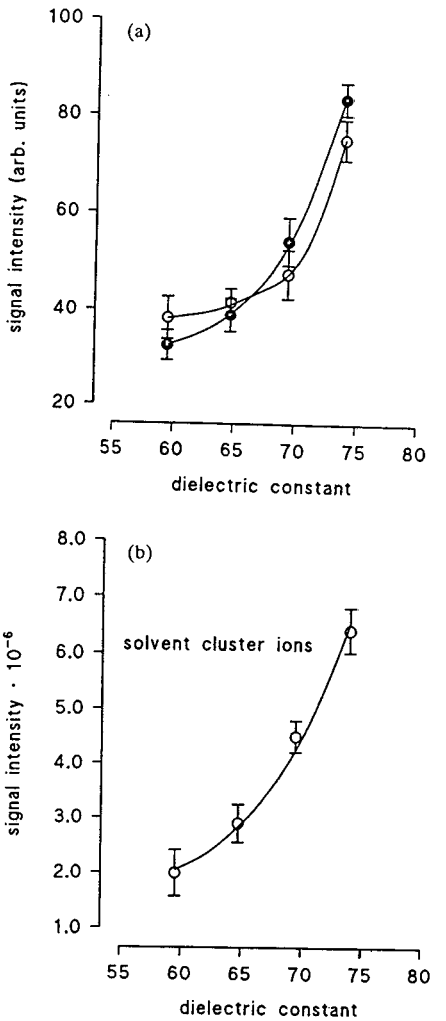

Fig. 2. Absolute ion intensities as a function of the bulk solvent dielectric constant ε_{solv} of the carrier stream (mixed solvent methanol–water; c_s = constant) for (a) ○ = carbofuran (*m/z* 222 and 239) and ● = desmetryn (*m/z* 214) and (b) the integrated solvent ion current (*m/z* 18–139).

TABLE II

LIQUID CHROMATOGRAPHIC RELATIVE RETENTION TIMES, MOLECULAR MASSES (M_r) AND IONS OBSERVED FOR THE INVESTIGATED PESTICIDES

Relative retention time, $\alpha_i = t_i/t_{caffeine}$. Experimental conditions: $T_v = 205 \rightarrow 195°C$; $T_g \approx 235°C$; discharge-assisted buffer ionization; $c_s = 70$ mM ammonium acetate (carrier stream).

α_i	Compound	M_r [a]	Main ions (PI): m/z (RA, %)[b]	No.[c]
0.107	Asulam	230	190 (100), 173 (5), 231 (5), 248 (10)	1d
0.259	Methamidophos	141	159 (100), 142 (15)	1f
0.548	Aldicarb sulfone	222	240 (100), 150 (42), 165 (70), 223 (14)	2d
0.638	Oxamyl	219	237 (100), 163 (33), 180 (13), 220 (4)	3d
0.744	Oxydemeton-methyl	246	247 (100), 264 (5)	2f
0.775	Methomyl	162	163 (100), 180 (12), 194 (10)	4d
0.832	Demeton-S-methyl sulfone	262	280 (100), 263 (52)	3f
0.993	Monocrotophos	223	241 (100), 224 (39)	4f
1.000	Caffeine	194	195 (100)	I.S.[e]
1.136	Atrazine-desisopropyl	174	175 (100)	2b
1.202	Trichlorfon	256	274 (100), 238 (12), 257 (23)	6f
1.243	Fenuron	164	165 (100), 182 (40)	2c
1.265	Metamitron	202	203 (100)	2a
1.392	Dimethoate	229	230 (100), 247 (38)	7f
1.544	Chloridazon	221	222 (100), 239 (20)	3a
1.697	Atrazine-desethyl	187	188 (100)	3b
1.746	Benomyl	290	192 (100), 134 (90), 149 (55)	6d
1.764	Isocarbamid[d]	185	186 (100), 146 (5)	
1.887	Aldicarb	190	208 (100), 148 (30), 191 (30), 222 (15)	7d
1.935	Allidochlor	173	174 (100), 191 (15)	2e
2.017	Metoxuron	228	229 (100), 201 (8)	3c
2.031	Crimidin	171	172 (100)	4a
2.241	Carbetamide	236	237 (100), 177 (28)	8d
2.294	Metribuzin	214	215 (100), 200 (10)	5a
2.315	Monuron	198	199 (100), 171 (5), 216 (5)	4c
2.362	Dichlorvos	220	238 (100), 221 (15)	8f
2.409	Propoxur	209	227 (100), 210 (20)	9d
2.444	Demeton-S-methyl	230	231 (100), 248 (15)	9f
2.468	Cyanazin	240	241 (100)	4b
2.476	Hexazinon	252	253 (100)	5b
2.502	Carbofuran	221	222 (100), 182 (15), 239 (35)	10d
2.521	Bromacil	260	261 (100), 183 (73)	6a
2.588	Simazin	201	202 (100), 168 (3)	6b
2.614	Terbacil	216	178 (100), 161 (23), 217 (1)	7a
2.751	Carbaryl	201	219 (100), 145 (7), 202 (18)	11d
2.754	Monolinuron	214	215 (100), 185 (10), 232 (10)	5c
2.762	Fluometuron	232	233 (100), 222 (10)	5c
2.852	Pirimicarb	238	239 (100)	12d
2.872	Metsulfuron-methyl	381	233 (100), 167 (13), 184 (89), 199 (78)	6c
2.877	Chlorotoluron	212	213 (100), 185 (5), 230 (5)	7c
2.900	Metobromuron	258	259 (100), 151 (15), 229 (5), 276 (10)	8c
2.949	Propham	179	197 (100), 180 (90)	13d
3.000	Methabenzthiazuron	221	222 (100), 165 (17)	9c
3.031	Naled	380	398 (100), 221 (2), 238 (3), 381 (7)	2g
3.035	Isoproturon	206	207 (100), 179 (12), 224 (8)	10c
3.065	Fensulfothion	308	309 (100), 326 (23)	3g
3.069	Atrazine	215	216 (100), 182 (5)	7b
3.127	Diuron	232	233 (100), 199 (4), 205 (5), 250 (10)	11c
3.162	Metazachlor	277	278 (100)	3e
3.185	Difenoxuron	286	287 (100), 216 (68), 259 (10)	12c
3.192	Propachlor	211	212 (100), 229 (10)	4e
3.222	Metalaxyl	279	280 (100), 256 (5)	5e
3.232	Phosmet	317	335 (100), 209 (30), 237 (40), 318 (35)	4g

(Continued on p. 238)

TABLE II (*continued*)

α_i	Compound	M_r [a]	Main ions (PI): m/z (RA, %)[b]	No.[c]
3.254	Dibutyl phosphite	194	212 (100), 195 (30)	10f
3.281	Desmetryn	213	214 (100)	8a
3.285	Dimethachlor	255	256 (100), 193 (5), 222 (25)	6e
3.293	Desmedipham	300	199 (100), 137 (60), 169 (45), 182 (50)	14d
3.326	Phenmedipham	300	185 (100), 151 (40), 168 (45), 210 (10)	15d
3.333	Thiodicarb	354	355 (5), 142 (10), 149 (10), 163 (100), 180 (25), 224 (85)	16d
3.355	Butonate	326	344 (100), 308 (70), 327 (30)	11f
3.386	Methfuroxam	229	230 (100)	7e
3.420	Linuron	248	249 (100), 219 (10), 266 (18)	13c
3.427	Parathion-methyl	263	281 (100), 264 (13)	5g
3.455	Secbumeton	225	226 (100)	9b
3.480	Chloropropham	213	231 (100), 214 (20)	17d
3.489	Anilazine	274	275 (100), 241 (15), 256 (10)	9a
3.508	Chlorobromuron	292	293 (100), 310 (5)	14c
3.549	Fenithrothion	277	295 (100), 278 (4)	6g
3.549	Ametryn	227	228 (100)	10a
3.582	Propazine	229	230 (100), 196 (3)	10b
3.632	Terbutylazine	229	230 (100), 196 (4)	11b
3.636	Propanil	217	218 (100), 184 (10), 235 (65), 250 (5)	8e
3.641	Methiocarb	225	243 (100), 226 (65)	18d
3.655	Mecarbam	329	330 (100), 347 (20)	7g
3.684	Azinphos-ethyl	345	160 (100), 346 (65), 363 (33)	8g
3.687	Barban	257	275 (100), 239 (10), 258 (10)	19d
3.716	Chloroxuron	290	291 (100), 220 (20)	15c
3.728	Triadimefon	293	294 (100), 168 (60)	11a
3.848	Fenamiphos	303	304 (100), 258 (10), 321 (5)	9g
3.875	Prometryn	241	242 (100)	12b
3.987	Terbutryn	241	242 (100)	13b
3.992	Alachlor	269	270 (100), 226 (65), 238 (20), 243 (36)	9e
3.999	Chlorfenvinphos	359	377 (100), 360 (55)	10g
4.048	Metolachlor	283	284 (100), 250 (22)	10e
4.073	Phosalone	367	385 (100), 368 (20)	11g
4.111	Disulfoton	274	275 (100), 292 (14)	12g
4.141	Monalide	239	240 (100)	11e
4.167	Prochloraz	375	376 (100), 342 (15), 180 (90)	12a
4.227	Tebuconazol	307	308 (100), 274 (5)	13a
4.319	Pentanochlor	239	240 (100), 257 (5)	12e
4.501	Prosulfocarb	251	252 (100)	20d
4.749	Triallate	303	304 (100), 162 (20)	21d
4.762	Prothiophos	344	345 (100), 362 (5)	13g
4.781	Merphos	298	315 (100), 299 (7)	14g
4.982	Butachlor	311	226 (100), 192 (10), 204 (38), 238 (78), 270 (60), 312 (30)	13e
5.092	Buminafos	347	212 (100), 154 (10), 195 (30)	12f

[a] Monoisotopic molecular mass calculated from the atomic masses of the isotopes with smallest masses.
[b] Relative abundance (in parentheses).
[c] Number of peak in Fig. 3a–g.
[d] Not shown in chromatogram in Fig. 3c.
[e] Internal standard.

used for the separation with typical flow-rates in the range *ca.* 0.5–0.6 ml min^{-1}. They are ideally suited for postcolumn addition, because the buffer flow can be varied over a wide range and the final carrier stream does not exceed critical values >1.5 ml min^{-1}. There are further advantages of this technique: the buffer salt concentration in the carrier stream is constant during gradient operation (c_s = 70 m*M* for all chromatographic experiments) and a negative influence of the buffer salt on the chromatographic separation is avoided [29,33].

The postcolumn techniques can also be used for the addition of reagent compounds to form

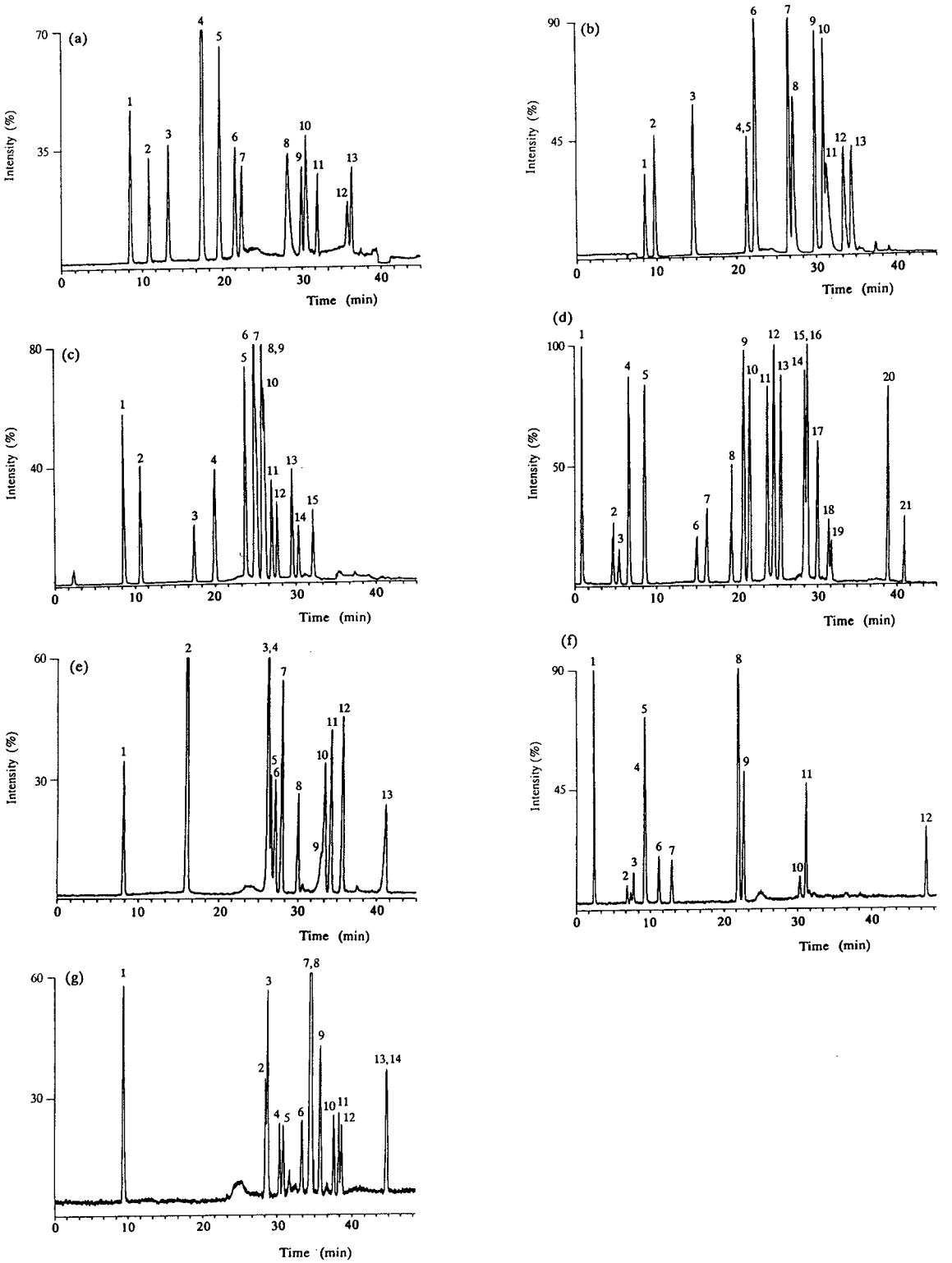

Fig. 3. LC–TSP-MS separation (full scan, m/z 130–450) of 95 pesticides. Conditions: column, narrow-bore 125 × 3 mm I.D. LiChrospher 60 RP-select B; column flow-rate, 0.6 ml min^{-1} methanol–water; postcolumn flow-rate 0.4 ml min^{-1} 175 m*M* ammonium acetate (for details, see Experimental). (a) N-Heterocyclic compounds; (b) N-heterocyclic compounds; (c) phenylureas and thioureas; (d) carbamates and thiocarbamates; (e) anilides and N-substituted amines; (f) "GDR-specific" organophosphorus compounds; (g) organophosphorus compounds. For peak assignments, see Table II.

cluster ions with the analytes or to induce derivatization reactions [14]. These additional ions are expected to be useful for an unambiguous identification of pesticides in real environmental samples.

Chromatography, detection limits, linear range and reproducibility

Of the 128 pesticides in Table I, 95 were chosen as target compounds for the development of a common method with identical experimental parameters for all compounds. These compounds were selected because they are priority pollutant pesticides. As mentioned in the Introduction, special attention was paid to compounds with low UV absorbance such as aldicarb, methomyl, oxamyl, triallate, allidochlor and several organophosphorus compounds. In this section all chromatographic and TSP mass spectrometric experiments were performed with the experimental set-up described under Experimental, *i.e.*, gradient elution with methanol–water on narrow-bore 3 mm I.D. columns in combination with postcolumn addition of buffer salt.

Table II shows the relative retention times, α_i, the molecular masses and the main ions and their abundances under typical operating conditions, *i.e.*, discharge-assisted buffer ionization with ammonium acetate ($c_s = 70$ mM). Most compounds produce only few fragment ions under the experimental conditions chosen, *i.e.*, the cationized molecular ions are observed, although some compound classes produce characteristic fragment ions owing to their chemical reactivity. In addition, in some instances "chemical dissociations" of the neutral precursors in the vaporizer probe or in the gas phase prior to ionization led to additional ions, *e.g.*, with organophosphorus compounds, carbamates and anilides. The usefulness of such reactions is explained in more detail later.

Liquid chromatography. A complete LC separation of 95 pesticides with only one set of identical experimental parameters is not possible and not necessarily required in combination with mass spectrometry. When two compounds do co-elute, LC–MS allows the identification and determination of both if each has different characteristic ions. Fig. 3 shows total ion current chromatograms of all pesticides obtained by injecting standard solutions of equal amounts (180 ng per compound). The arrangement of the pesticides in seven chromatograms according to their compound classes is arbitrary and has only practical reasons. Table II lists all the pesticides together with their relative retention times and their main TSP positive ions and abundances.

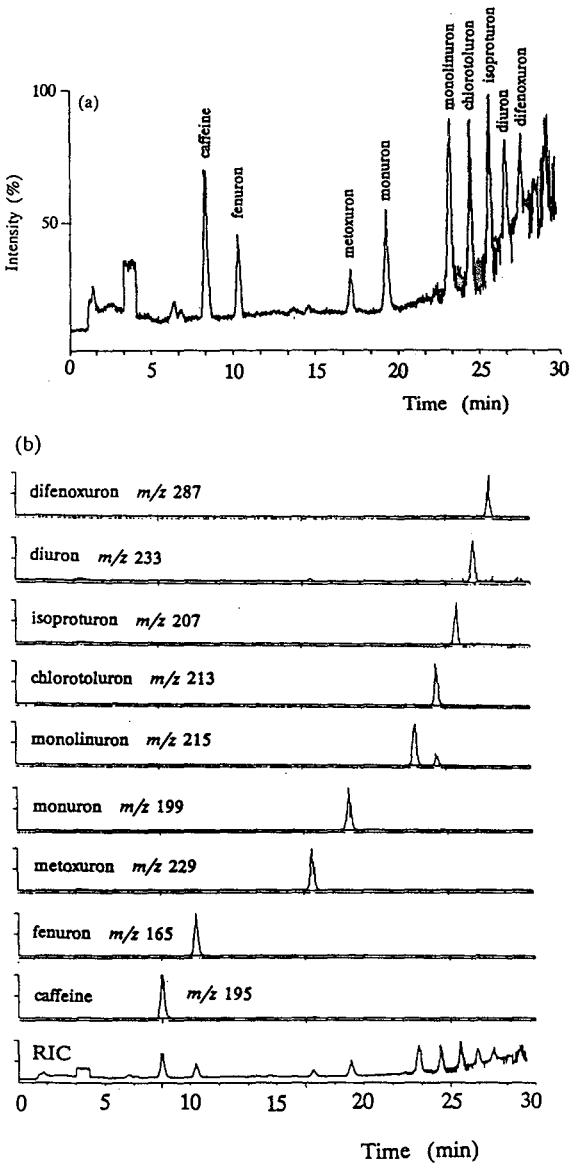

Fig. 4. Analysis of a water sample from the river Leine (Hannover) spiked with eight phenylureas at the 2 ppb level. (a) Full-scan TIC and (b) ion traces of the $[MH]^+$ ions.

This table also contains the peak assignments for Fig. 3. As can be seen, no co-elution of compounds with identical molecular masses occurs. In critical cases it is possible to distinguish between analytes by means of one of the confirmatory methods described later.

During all chromatographic experiments, caffeine was added to each standard and sample solution. This standard was used for several purposes. Caffeine was used as an internal standard for determinations in combination with off-line preconcentration. Further, slight changes of the retention times with temperature were compensated for by using relative retention times [relative to cafeine (Table II)]. With the exception of monocrotophos, caffeine does not co-elute with any of the compounds investigated (it was attempted to avoid co-elution of the chromatographic standard with one of the pesticides; this allows the comparison of the chromatogram with that obtained with a UV detector). Finally, we used caffeine as a standard for mass calibration and TSP performance tests and for the compensation of long-term reproducibility deviations (see explanations below).

To evaluate the performance of the LC–MS interface for the determination of these compounds in aqueous environmental samples, a water sample from the river Leine (Hannover) was spiked with eight phenylureas at the 2 ppb level. The spiked water sample was extracted (see Experimental) and the extract analysed by LC–TSP-MS (Fig. 4). At higher retention times a strong baseline drift and noise were observed, probably owing to matrix effects, which makes identification and quantification from the total ion chromatogram (TIC) difficult (Fig. 4a). However, as can be seen from the ion chromatograms of the $[MH]^+$ ions of all phenylureas, extracted from the full-scan TIC, the quality of these chromatograms is much better than that of the TIC and the identification, confirmation and determination of all compounds are readily possible (Fig. 4b).

Detection limits. The full-scan limits of detection (LOD) obtained for the different compound classes investigated are summarized in Table III. These LODs are very similar to those presented by other workers [17]. The LODs were calculated by either selecting a concentration of a standard solution that gave a signal-to-noise ratio of *ca.* 3:1 or by calculating the $S/N = 3$ values from the calibration data for at least three concentrations beginning near the detection limit. Exact full-scan and selected-ion monitoring (SIM) detection limits for typical pesticides and

TABLE III

INSTRUMENTAL DETECTION LIMITS FOR THE DIFFERENT PESTICIDE COMPOUND CLASSES INVESTIGATED

Experimental conditions: full-scan (*m/z* 130–450) detection limits (signal-to-noise ratio = 3); methanol–water gradient in combination with narrow-bore HPLC columns + postcolumn addition of aqueous volatile salt solution as described under Experimental; discharge-assisted buffer ionization (ammonium acetate).

Compound class	Positive ions (ng)	Negative ions (ng)
Triazines	0.5–5	n.d.[a]
Anilides	2–10	n.d.
Carbamates + thiocarbamates	0.1–5	5–20
Phenylureas + thioureas	2–10	20–50
Organophosphorus compounds, phosphates	1–5	50–100
Organophosphorus compounds, phosphorothioates and phosphorodithioates	10–100	>100
Organophosphorus compounds, phosphonates	2–10	>100
Carboxylic acids, phenoxy acids	>500	2–10
Carboxylic esters	5–15	>500
Quaternary ammonium compounds	5–20	n.d.

[a] Not determined.

the corresponding calibration data are presented in Table IV.

The EC drinking water guidelines demand a limit of 100 ng l^{-1} for pesticides. Assuming a 1000-fold concentration step (1 l to 1 ml) and an injection volume of 20 μl into the HPLC system, this requires the detection of at least 2 ng of the individual pesticides. However, by using higher injection volumes (50 μl) or higher concentration factors, this value can be increased to *ca.* 5–10 ng. Further, preliminary experiments with on-line preconcentration revealed higher preconcentration factors, while background signals were suppressed as compared with off-line solid-phase extraction. Unfortunately, Tables III and IV show that only some compound classes reach this criterion when performing full-scan experiments. However, for target analyte screening, time-scheduled SIM experiments may be used. This allows the detection limits to be lowered by a factor of 8–100 (Table IV). As an example, Fig. 5 shows SIM traces for repetitive injections

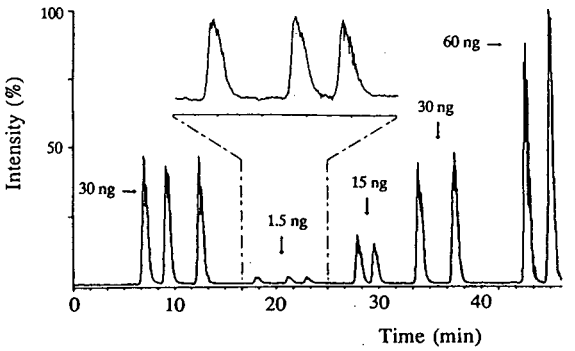

Fig. 5. SIM trace of the protonated molecule (*m/z* 222) for repetitive injections of different amounts of methabenzthiazuron under isocratic elution with methanol–water (50:50, v/v).

TABLE IV

LINEARITIES, FULL-SCAN AND SIM DETECTION LIMITS OBTAINED FOR SEVERAL PESTICIDES

Experimental conditions: full-scan (*m/z* 130–450) and SIM detection limits (signal-to-noise ratio = 3); linearity: log $s_i = a_i \log m + b_i$, s_i = ion current of the analyte ion i, m = amount injected; r = correlation coefficient.

Compound	Linearity[a]			Detection limit (ng)	
	a_i	b_i	r	Scan	SIM
Aldicarb	0.923	2.167	0.998	4.0	0.220
Ametryn	0.973	2.535	0.999	2.4	
Atrazine	0.971	2.830	0.999	1.2	
Carbaryl	0.955	2.490	0.999	5.0	0.080
Carbofuran	0.981	2.918	0.999	0.3	0.065
Chlorobromuron	0.897	2.273	0.999	8.2	
Chlorotoluron	1.133	2.358	0.999	3.6	0.035
Desmetryn	0.969	2.861	0.999	1.0	0.080
Difenoxuron	0.890	2.134	0.996	9.0	0.175
Diuron	0.991	2.389	0.999	5.0	0.140
Fenuron	0.915	2.792	0.999	3.2	0.380
Isoproturon	0.984	2.358	0.999	4.8	
Methabenzthiazuron	1.120	2.600	0.998	2.0	0.150
Methiocarb	1.042	2.057	0.999	2.7	
Metobromuron	1.001	2.499	0.999	3.9	0.190
Metoxuron	0.973	2.012	0.998	10.7	0.310
Monuron	1.052	2.543	0.999	2.3	0.100
Prometryn	0.863	2.782	0.999	4.9	
Propazine	1.032	2.467	0.992	1.9	
Simazine	0.971	2.773	0.999	1.2	
Trichlorfon	0.809	1.981	0.998	15.0	

[a] Data from three to five repetitive injections for at least three different amounts injected in the range 3–3000 ng.

of different amounts of methabenzthiazuron using isocratic elution with methanol–water (50:50, v/v). As expected, the detection limit observed is much lower than in the full-scan mode.

Linearity. The parameters derived from calibration graphs for several pesticides, obtained from three to five repetitive injections over a range of 3–3000 ng, are presented in Table IV. The quality of the linear relationships in the log–log diagrams was evaluated by calculating the slope of the regression lines and the correlation coefficients. As can be seen from these values, a linear range of at least 10^3 beginning from the detection limits was observed. This allows an external quantification in combination with on-line preconcentration.

Reproducibility. The inability of TSP to provide sufficiently stable and reproducible ion currents over extended periods is a serious problem. Whereas the reproducibility during one-day experiments is often excellent to satisfactory, it is often poorer if determined over longer periods. Typical reproducibilities for several pesticides from standard injections obtained during 8-h periods are presented in Table V. The R.S.D.s for different sample amounts range from 1.2 to 11.8%. The long-term reproducibility often exceeds 20%. To some extent, these reproducibilities can be improved if relative intensities or peak areas are used, *e.g.*, relative to caffeine as a TSP standard. However, the long-term variations of the sensitivity remain a major problem of TSP ionization.

Enhancing structural information from TSP mass spectra. Confirmation of pesticide residues in environmental samples

Ammonium acetate TSP mass spectra of pesticides usually show only quasi-molecular ions such as $[MH]^+$ and $[MHNH_3]^+$, which limits their specificity, while structural information is lacking. Several techniques are available to overcome these limitations: (1) the variation of interface temperatures, (2) the use of external ionization media (filament, discharge), (3) MS–MS techniques, (4) repeller-induced spectral changes [16], (5) additional cluster ions with solvent or additive molecules and (6) additional information gained from the complementary positive- and negative-ion spectra. As mentioned above, "chemical dissociations" of neutral precursors in the vaporizer probe or in the gas phase, *e.g.*, with asulam, carbendazim, alachlor, butachlor, metolachlor and several sul-

TABLE V

MEAN RESPONSES AND INTRA-DAY REPRODUCIBILITIES FOR SOME OF THE PESTICIDES

Data from three to five repetitive injections.

Compound	Amount injected (ng)					
	300		30		15	
	Area/ng[a]	R.S.D. (%)	Area/ng	R.S.D. (%)	Area/ng	R.S.D. (%)
Ametryn	11 623	7.4	13 001	5.2	13 583	1.2
Carbofuran	16 140	4.2	14 509	7.4	15 276	5.1
Chlortoluron	13 206	9.8	12 974	5.5	13 378	7.2
Desmetryn	15 650	5.0	13 545	8.2	17 613[b]	2.2
Methabenzthiazuron	16 889	3.5	17 007	8.3	19 040[b]	9.3
Metoxuron	10 376	6.3	11 199	4.2	10 912	7.7
Prometryn	12 641	2.4	12 910	5.0	11 488	8.2
Propazine	11 181	3.4	13 509	7.4	15 485[b]	7.2
Trichlorfon	3877	6.4	5136	5.2	6188	11.8

[a] Quantification ion abundances integrated over the LC peak.
[b] 3-ng injections.

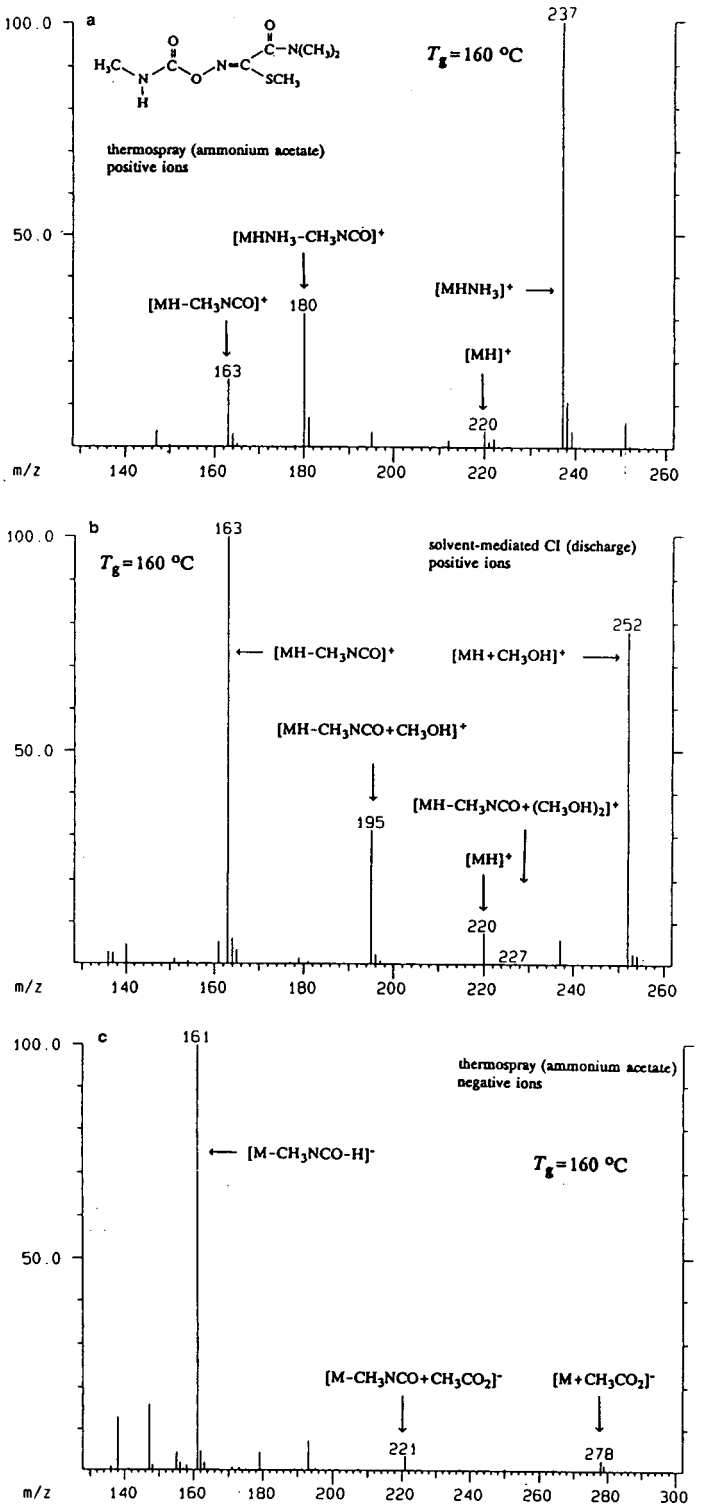

Fig. 6. TSP mass spectra of oxamyl under different ionization conditions (T_g, T_v = constant). (a) Discharge-assisted buffer ionization (ammonium acetate), positive ions; (b) solvent-mediated chemical ionization (discharge), positive ions; (c) discharge-assisted buffer ionization (ammonium acetate), negative ions.

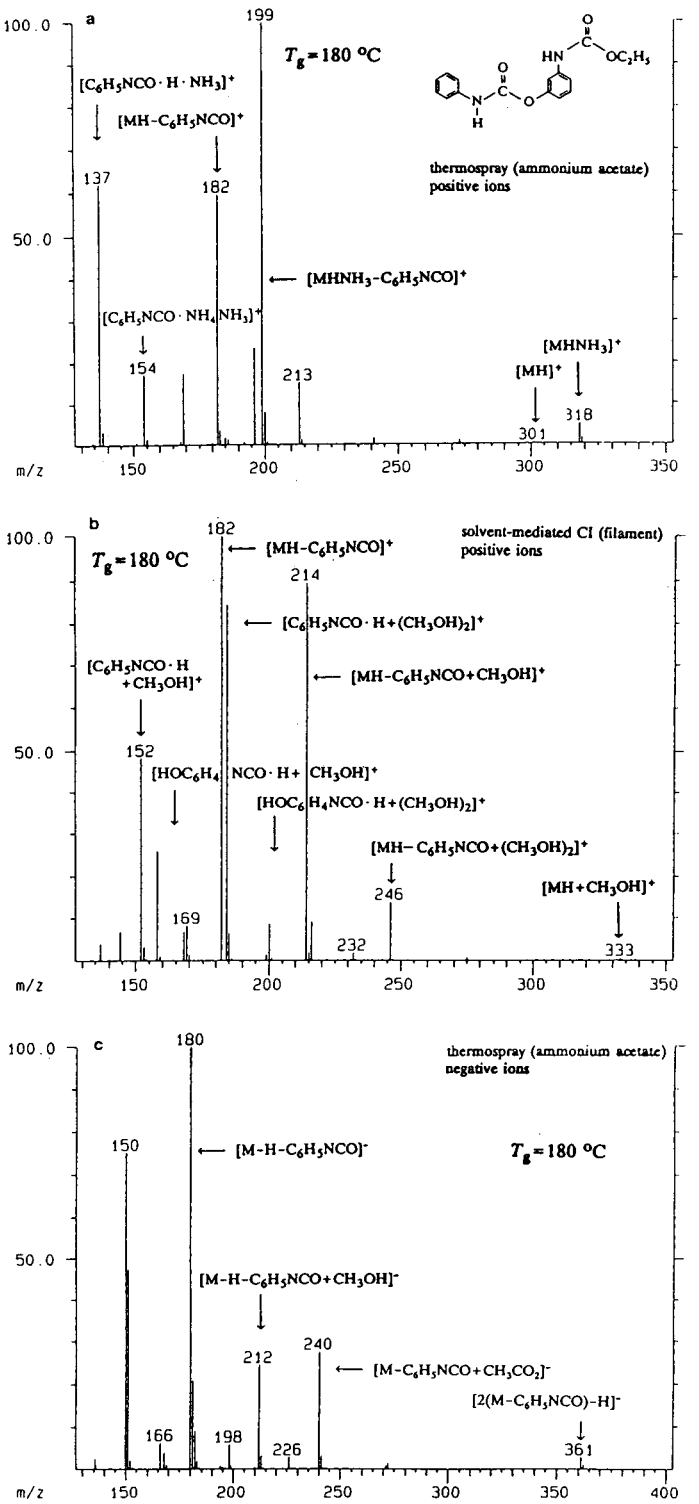

Fig. 7. TSP mass spectra of desmedipham under different ionization conditions (T_g, T_v = constant). (a) Filament-assisted buffer ionization (ammonium acetate), positive ions; (b) solvent-mediated chemical ionization (filament), positive ions; (c) filament-assisted buffer ionization (ammonium acetate), negative ions.

phonylurea and organophosphorus pesticides, were observed. This degradation is predominantly followed by ionization with, sometimes, successive fragmentation. These dissociations are strongly dependent on temperature, both T_g and T_v, and may be of value in the confirmation of pesticides in environmental samples. The usefulness of varying the interface temperatures is demonstrated in more detail elsewhere [13].

In this section, a simple example is shown which makes use of specific instabilities found in many pesticides and which can be used to enhance structural information. The confirmatory analysis can be done by using the postcolumn technique described above either with or without ammonium acetate and without changing the experimental set-up.

For example, with most carbamates and thiocarbamates no significant loss in sensitivity occurs when one switches from discharge-assisted buffer ionization with ammonium acetate to solvent-mediated chemical ionization (CI) with discharge or filament without ammonium acetate. Ionizing a compound with protonated methanol [proton affinity (PA) = 180 kcal mol^{-1} (1 kcal = 4.184 kJ)] is more exothermic than ionizing it with the ammonium ion (PA = 204 kcal mol^{-1}), that is, fragmentation is strongly enhanced. Further, in comparison with ammonia very intense solvent cluster ions $[MH(CH_3OH)_x]^+$ of the quasi-molecular and fragment ions are observed as the clustering depends strongly on the proton affinity of the solvent and the ionizing plasma [34]. For this reason, fewer water cluster ions than methanol cluster ions are observed with methanol–water mixtures. Further, carbamates, phenylureas, organophosphorus compounds and some other

TABLE VI

MAIN POSITIVE IONS AND THEIR RELATIVE ABUNDANCES OBTAINED FROM THE TSP, CI AND CAD MASS SPECTRA OF OXAMYL

Experimental conditions: flow-injection, amount injected = 300 ng; carrier stream, methanol–water (50:50, v/v); flow-rate 1.0 ml min^{-1}; CAD conditions, collision-offset 10 V, collision cell pressure = $1.3 \cdot 10^{-3}$ Torr (argon); T_g = 160°C, T_v = 190°C, p_g = 3.4 Torr. Ionization: TSP = discharge-assisted buffer ionization, c_s = 50 mM; CI = solvent-mediated CI with either discharge (D) or filament (F); discharge voltage = 1 kV; filament = 1 keV.

m/z	Tentative structure assignment	Relative abundance (%)[a]			
		TSP	CI(D)	CI(F)	CAD[b]
72	$[MH - CH_3NCO - CH_3SCH = NOH]^+$	+	+	+	100
90	$[MH - CH_3NCO - (CH_3)_2NC(O)H]^+$	+	+	+	58
104	$[MH - CH_3NCO - CH_3SCH = NOH + CH_3OH]^+$	+	+	+	
122	$[MH - CH_3NCO - (CH_3)_2NC(O)H + CH_3OH]^+$	+	+	+	
136	$[MH - CH_3NCO - CH_3SCH = NOH + (CH_3OH)_2]^+$		3	2	
154	$[MH - CH_3NCO - (CH_3)_2NC(O)H + (CH_3OH)_2]^+$		2	5	
163	$[MH - CH_3NCO]^+$	17	100	100	3
180	$[MHNH_3 - CH_3NCO]^+$	31			
194	$[MHNH_3 - CH_3NCO - H_2O + CH_3OH]^+$		3	3	
195	$[MH - CH_3NCO + CH_3OH]^+$	5	30	28	
220	$[MH]^+$	5	10	14	
227	$[MH - CH_3NCO + (CH_3OH)_2]^+$		1	3	
237	$[MHNH_3]^+$	100			
251	$[MHNH_3 - H_2O + CH_3OH]^+$	8			
252	$[MH + CH_3OH]^+$		79	85	
278	$[MHNH_3 + CH_3CO_2NH_4 - 2H_2O]^+$	19			
325	$[M_2H - 2CH_3NCO]^+$	<1	3	2	

[a] + = This ion was observed in SIM experiments.
[b] Precursor ion m/z 237 (=$[MHNH_3]^+$).

compound classes are detected very sensitively as negative ions, at least under solvent-mediated CI conditions. Therefore, the combination of discharge-assisted buffer ionization with either positive- or negative-ion discharge solvent-mediated CI offers valuable additional structural information for characterizing the pesticides.

This is demonstrated in Figs. 6 and 7, where the direct-flow injection TSP mass spectra of the carbamates oxamyl and desmedipham under different ionization conditions but with identical solvent composition and temperatures are presented. Both compounds show characteristic fragment ions especially under solvent-mediated CI conditions, which can be attributed to the alcohol and the isocyanate formed. In the case of aryl-N-alkyl carbamates such as desmedipham, the formation of the phenol is favoured and the $[MH\text{-}RNCO]^+$ ion often dominates the spectrum. In addition, very intense solvent clusters of both the quasi-molecular and the fragment ions were observed. Tables VI and VII summarize these ions and the CAD spectra of the compounds.

CONCLUSIONS

LC–TSP-MS is a sensitive, specific and versatile technique for the determination of pesticides in aqueous environmental samples. A reversed-phase gradient LC separation was developed which permits the determination of 95

TABLE VII

MAIN POSITIVE IONS AND THEIR RELATIVE ABUNDANCES OBTAINED FROM THE TSP, CI AND CAD MASS SPECTRA OF DESMEDIPHAM

Experimental conditions as in Table VI, expect $T_g = 180°C$.

m/z	Tentative structure assignment	Relative abundance (%)[a]			
		TSP	CI(D)	CI(F)	CAD[b]
94	$[C_6H_5NH_2 \cdot H]^+$	+	+	+	1
120	$[C_6H_5NCO \cdot H]^+$	10	15	13	<1
136	$[MH - C_6H_5NCO - C_2H_5OH]^+$	1	1		<1
137	$[C_6H_5NCO \cdot H \cdot NH_3]^+$	62			100
152	$[C_6H_5NCO \cdot H + CH_3OH]^+$		49	45	
154	$[C_6H_5NCO \cdot NH_4NH_3]^+$	17	<1	<1	<1
158	?		27	25	
168	$[MH - C_6H_5NCO - C_2H_5OH + CH_3OH]^+$	8			<1
169	?	10	24	20	<1
182	$[MH - C_6H_5NCO]^+$	60	100	100	5
184	$[C_6H_5NCO \cdot H + (CH_3OH)_2]^+$		84	89	
196	?	23			
199	$[MHNH_3 - C_6H_5NCO]^+$	100			
200	$[MH - C_6H_5NCO - C_2H_5OH + (CH_3OH)_2]^+$		10	10	
213	?	18			
214	$[MH - C_6H_5NCO + CH_3OH]^+$		90	85	
232	$[MH - C_6H_5NCO - C_2H_5OH + (CH_3OH)_3]^+$		5	5	
241	$[MH - C_6H_5NCO + CH_3CO_2NH_4 - H_2O]^+$	3			
246	$[MH - C_6H_5NCO + (CH_3OH)_2]^+$		16	20	
301	$[MH]^+$	<1			<1
318	$[MHNH_3]^+$	6			
332	$[M + CH_3NH_3]^+$	<1			
333	$[MH + CH_3OH]^+$		<1	<1	

[a] + = This ion was observed in SIM experiments.
[b] Precursor ion m/z 318 (=$[MHNH_3]^+$).

pesticides with one common LC–MS method. The TSP interface is operated under discharge-assisted buffer ionization conditions as the sensitivities obtained in this mode are much higher than those in the filament-on mode or with volatile salt ionization without external ionization media. The reproducibilities, linearities and instrumental detection limits obtained are adequate for environmental monitoring of a broad range of pesticides and will, in many instances, allow the verification of the EC drinking water guidelines even in the full-scan mode. In combination with time-scheduled SIM, the method should permit the detection of all pesticides down to the 10–100 ppt level in combination with conventional off-line solid-phase extraction or on-line preconcentration. By combining the retention data and TSP mass spectra of all the pesticides presented in this paper, LC–TSP-MS can be used as an ideal confirmatory method for the identification of almost all pesticides investigated in environmental samples. Further confirmation can readily be achieved by using either positive- or negative-ion solvent-mediated CI with discharge or filament operation.

ACKNOWLEDGEMENT

This study was carried out with funds provided by the Bundesministerium für Forschung und Technologie, Bonn.

REFERENCES

1 *EEC Drinking Water Guidelines, 80/779/EEC, EEC No. L229/11-29*, EEC, Brussels, 1980.
2 H.B. Böhm, J. Feltes, D. Volmer and K. Levsen, *J. Chromatogr.*, 478 (1989) 399.
3 K. Levsen, *Org. Mass Spectrom.*, 23 (1988) 406.
4 L.H. Wright, *J. Chromatogr. Sci.*, 20 (1982) 1.
5 T. Cairns, E.G. Siegmund and G.M. Dose, *Biomed. Mass Spectrom.*, 10 (1983) 24.
6 R.D. Voyksner and J.T. Bursey, *Anal. Chem.*, 56 (1984) 1582.
7 T.R. Covey and J.D. Henion, *Anal. Chem.*, 55 (1983) 2275.
8 M. Barber, R.S. Bordoli, G.J. Elliot, R.D. Sledgewick and A.N. Tyler, *Anal. Chem.*, 54 (1982) 645A.
9 C.R. Blakely and M.L. Vestal, *Anal. Chem.*, 55 (1983) 750.
10 M.L. Vestal, *J. Mass Spectrom. Ion Phys.*, 46 (1984) 193.
11 T.D. Behymer, T.A. Bellar and W.L. Budde, *Anal. Chem.*, 62 (1990) 1686.
12 S. Pleasance, J.F. Anacleto, M.R. Baily and D.H. North, *J. Am. Soc. Mass Spectrom.*, 3 (1992) 378.
13 D. Volmer, A. Preiss, K. Levsen and G. Wünsch, *J. Chromatogr.*, 647 (1993) 235.
14 D. Volmer and K. Levsen, *J. Am. Soc. Mass Spectrom.*, submitted for publication.
15 K.S. Chiu, A. Van Langenhove and C. Tanaka, *Biomed. Environ. Mass Spectrom.*, 18 (1989) 200.
16 W.M.A. Niessen, R.A.M. van der Hoeven, M.A.G. De Kraa, C.E.M. Herremans, U.R. Tjaden and J. van der Greef, *J. Chromatogr.*, 478 (1989) 325.
17 D. Barceló, G. Durand, R.J. Vreeken, G.J. De Jong, H. Lingeman and U.A.Th. Brinkman, *J. Chromatogr.*, 553 (1991) 311.
18 R.J. Vreeken, W.D. van Dongen, R.T. Ghijsen and U.A.Th. Brinkman, *Int. J. Environ. Anal. Chem.*, in press.
19 D. Barceló, *Biomed. Environ. Mass Spectrom.*, 17 (1988) 2076.
20 A. Farran, J. De Pablo and D. Barceló, *J. Chromatogr.*, 455 (1988) 163.
21 C.H. Vestal, *Vestec Thermospray Newsl.*, 3 (1987) 2.
22 D. Barceló, *Org. Mass Spectrom.*, 24 (1989) 219.
23 R.D. Voyksner, in J.D. Rosen (Editor), *Applications of New Mass Spectrometry Techniques in Pesticide Chemistry*, Wiley, New York, 1987, p. 146.
24 T.L. Jones, L.D. Betowsky and J. Yinon, in M.A. Brown (Editor), *Liquid Chromatography/Mass Spectrometry. Applications in Agricultural, Pharmaceutical, and Environmental Chemistry (ACS Symposium Series*, No. 420), Americal Chemistry Society, Washington, DC, 1990, p. 62.
25 R.D. Voyksner, in J.D. Rosen (Editor), *Applications of New Mass Spectrometry Techniques in Pesticide Chemistry*, Wiley, New York, 1987, p. 247.
26 T.A. Bellar and W.L. Budde, *Anal. Chem.*, 60 (1988) 2076.
27 P.S. Albright and L.J. Gosting, *J. Am. Chem. Soc.*, 68 (1946) 1061.
28 D.J. Liberato and A.L. Yergey, *Anal. Chem.*, 58 (1986) 6.
29 R.D. Voyksner, J.T. Bursey and E.D. Pellizari, *Anal. Chem.*, 56 (1984) 1507.
30 M.M. Siegel, R.K. Isensee and D.J. Beck, *Anal. Chem.*, 59 (1987) 989.
31 M.F. Bean, S.L. Pallante-Morell and C. Fenselau, *Biomed. Environ. Mass Spectrom.*, 19 (1989) 219.
32 W.M. Lagna and P.S. Callery, *Biomed. Environ. Mass Spectrom.*, 12 (1985) 699.
33 T.M. Chen, J.E. Coutant, A.D. Sill and R.R. Fike, *J. Chromatogr.*, 396 (1987) 382.
34 A.J. Alexander and P. Kebarle, *Anal. Chem.*, 58 (1986) 471.

Journal of Chromatography A, 660 (1994) 249–253
Elsevier Science B.V., Amsterdam

CHROMSYMP. 2928

Influence of the structure of the alcoholic modifier on the enantioselective separation of nadolol

A.M. Dyas and M.L. Robinson

Bristol-Myers Squibb Pharmaceutical Research Institute, Moreton, Merseyside L46 1QW (UK)

A.F. Fell*

Pharmaceutical Chemistry, School of Pharmacy, University of Bradford, Bradford BD7 1DP (UK)

ABSTRACT

The influence of the structure of the alcoholic modifier of the mobile phase on the liquid chromatographic separation of the optical isomers of nadolol on a Pirkle-type chiral stationary phase was investigated. The isomers were separated as their chiral 1-naphthylureides on a column consisting of 3,5-dinitrobenzoyl-L-leucine covalently bound to 3-μm aminopropylsilica, using an eluent consisting of *n*-hexane modified with an alcohol. A number of straight-chain, branched and unsaturated alcohols with carbon numbers ranging from 1 to 8 were evaluated. The choice of alcohol influenced both retention and selectivity, with optimum stereoselectivity being observed for C_3. The alcoholic modifiers selectively affected the retention and resolution of the two pairs of enantiomers that constitute nadolol. Thus chromatograms displaying two, three or four peaks could be obtained, depending on which modifier was employed. The best separation of all four isomers was achieved with ethanol as the modifier.

INTRODUCTION

The β-adrenoceptor-blocking drug nadolol is used as an antihypertensive agent in the treatment of high blood pressure. This molecule (Fig. 1) features three asymmetric carbon atoms in its structure although, as the two in the naphthalenediol ring are held in the *cis* configuration, there are only two chiral centres. Hence nadolol exists as four isomers, consisting of two pairs of enantiomers referred to as nadolol racemate A and nadolol racemate B, which are also diasteromeric pairs. Nadolol is produced by a non-stereoselective synthetic process and consequently the material contains all four isomers. A number of procedures have been reported for the analysis of nadolol [1], some of which are chirally discriminating.

During the investigation of stereoselective analytical methodology, we developed a procedure for the resolution of all four isomers on a Pirkle-type chiral stationary phase (CSP) [2]. The procedure required that the polar amino-function of nadolol was masked by derivatization prior to injection on to the column. The masking derivatization was based on reaction with isocyanates to form the corresponding ureide (Fig. 2). The isocyanate reagent used was achiral and the reaction proceeded rapidly under ambient conditions in unreactive solvents. The ureides produced were resolved on a Pirkle-type CSP comprising 3,5-dinitrobenzoyl-L-leucine (DNB-L-Leu) covalently bonded to 3-μm aminopropylsilica. The eluent employed was a mixture of *n*-hexane, ethanol and acetonitrile.

During the development of the procedure the effect of the hydrocarbons used in the eluent and of the substituent on the isocyanate reagent were investigated. These two "achiral" aspects had a

* Corresponding author.

0021-9673/94/$07.00 © 1994 Elsevier Science B.V. All rights reserved
SSDI 0021-9673(93)E0921-G

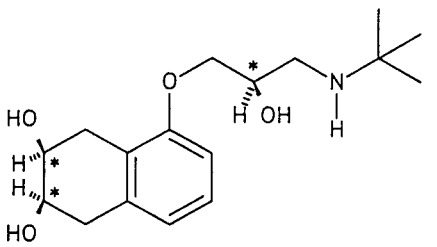

Compound Name		Sign of rotation Ring	Sign of rotation Side-chain	Compound Number
NADOLOL (SQ 11,725)	Racemate 'A' (SQ 12,181)	+	-	SQ 12,148
		-	+	SQ 12,150
	Racemate 'B' (SQ 12,182)	+	+	SQ 12,149
		-	-	SQ 12,151

Fig. 1. Structure of nadolol. Nadolol, (±)-2,3-*cis*-1,2,3,4-tetrahydro-5-(2-hydroxy-3-*tert.*-butylaminopropoxy)-2,3-naphthalenediol, features three asymmetric carbon atoms (marked with asterisks). However, the two within the tetrahydronaphthalene ring are held in a *cis* configuration, so there are only two chiral centres, one in the ring and one in the side-chain. This results in nadolol having four optical isomers, made up to two pairs of diastereomers.

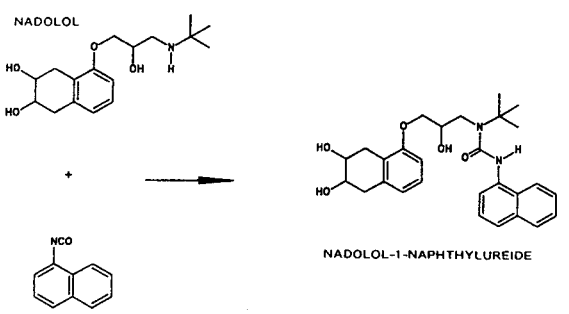

Fig. 2. Derivatization of nadolol with 1-naphthyl isocyanate to form the corresponding ureide. The amino group of nadolol reacts rapidly with 1-naphthyl isocyanate to yield the ureide derivative. The reaction goes almost to completion (>98% in 5 min) and does not require an excess of reagent. Although alcohols may also react with this reagent to form urethanes, under the reaction conditions employed (ambient temperature and no catalyst) reaction with the naphthalenediols does not occur.

profound influence on the chiral separation obtained [3,4]. This prompted an investigation of the alcoholic component of the eluent, itself also an achiral entity, and the results are presented herein.

EXPERIMENTAL

The chromatographic procedure for the separation of the four nadolol isomers has been reported previously [2]. In this system, acetonitrile is used as a modifier in the mobile phase, where it has some effect on the retention and separation of the isomers. However, it relies on the ethanol to remain in solution with the major component, *n*-hexane. Varying the nature of the alcohol used would vary the content of acetonitrile in the eluent, which would consequently influence the chromatographic result. To reduce the number of variables in the experiments and thus facilitate the evaluation of the resulting data, the eluents employed consisted only of a mixture of *n*-hexane and the alcohol under investigation.

The samples used were nadolol, a racemic mixture of all four isomers, racemate A and racemate B. Solutions of each were prepared at *ca.* 1 mg/ml in the test eluent. 1-Naphthyl isocyanate was added at 1 μl/ml and the samples were left to stand under ambient conditions for 15 min before being injected on to the column.

The column was prepared using a procedure that has been reported previously [2]. Briefly, 3,5-dinitrobenzoyl-L-leucine was covalently bound to 3-μm aminopropylsilica already packed into a 150 mm × 3.9 mm I.D. column, which was conditioned with the test eluent before use.

The test eluent was pumped at a rate of 2 ml/min and a detection wavelength of 239 nm was employed. Chromatograms were recorded using the PeakPro software feature of the Beckman CALS LIMS system and stored on an HP1000 computer. The test eluents consisted of mixtures of *n*-hexane and an alcohol at a ratio of 4:1; when the alcohol was a liquid under ambient conditions, it was added on a volume basis, but when it was a solid, it was added on a mass basis.

The eluents were degassed by sparging with

helium before use and 100-ml volumes were passed through the column to equilibrate it before any injections were made.

RESULTS

The chromatograms were each evaluated in terms of retention, selectivity and separation as follows.

For retention, the capacity factor quoted, k'_{med}, is the median capacity factor observed.

Three selectivity factors (α) were calculated. The factor $\alpha_{2/1}$ is the selectivity of separation of the first two peaks eluting. These are the least retained enantiomers of racemates B and A, compounds SQ 12151 and SQ 12150, respectively. This is therefore a diastereoselectivity factor. The factor $\alpha_{3/1}$ is the selectivity factor for the separation of the first- and third-eluting peaks. These are the enantiomers of racemate B, compounds SQ 12151 and SQ 12149, respectively. This is therefore an enantioselectivity factor. Likewise, $\alpha_{4/2}$ is the enantioselectivity factor for the separation of the second- and fourth-eluting peaks, which are the enantiomers of racemate A, compounds SQ 12150 and SQ 12148, respectively.

The quality of the separation attained is indicated by coding the peaks observed. Each peak observed is given a letter, *e.g.*, ABCD = four peaks, ABC = three peaks. The symbols between the peaks indicate the degree of separation: no symbol, *e.g.*, AB, = very poor separation (shoulder); solidus, *e.g.*, A/B, = poor separation (10–50%); comma, *e.g.*, A,B, = good separation (50–95%); point, *e.g.*, A.B, = baseline separation. The separation makes use of the Kaiser peak separation factor. This quantifies the separation as the depth of the valley as a percentage of the median peak height. Thus baseline separation yields a factor of 100%.

The resulting data for the test eluents are presented in Table I. An example chromatogram depicting the calculation of the chromatographic criteria is presented in Fig. 3.

TABLE I

RETENTION, SELECTIVITY AND SEPARATION DATA OBTAINED USING THE TEST ELUENTS

See text for experimental details.

Type of alcohol	Alcohol	Capacity factor, k'_{med}	Selectivity factor			Separation type
			$\alpha_{2/1}$	$\alpha_{3/1}$	$\alpha_{4/2}$	
Primary	Methanol[a]	45.52	1.064	1.118	1.154	A.B,C.D
	Ethanol	5.95	1.069	1.312	1.393	A,B.C.D
	1-Propanol	10.04	1.072	1.397	1.518	A/B.C,D
	2-Propen-1-ol	5.95	1.044	1.279	1.363	A/B.C,D
	1-Butanol	14.83	1.060	1.389	1.485	AB,C/D
	1-Pentanol	23.37	1.000	1.282	1.374	A,BC
	2,2-Dimethyl-1-propanol	101.39	1.000	1.463	1.463	A,B
	3-Methyl-1-butanol	30.98	1.000	1.262	1.362	A/BC
	1-Heptanol	41.70	1.000	1.242	1.242	A/B
	1-Octanol	43.99	1.000	1.013	1.209	AB/C
Secondary	2-Propan-2-ol	25.82	1.130	1.567	1.697	A,B.C,D
	(±)-2-Butanol	43.83	1.108	1.594	1.706	A/B.C,D
	(±)-2-Pentanol	68.74	1.056	1.448	1.573	AB,C,D
	(±)-3-Methyl-2-butanol	160.30	1.000	1.692	2.382	A.B.C
Tertiary	2-Methyl-2-propanol	199.25	1.164	1.715	1.910	A/B,C,D
	2-Methyl-2-butanol	239.63	1.193	1.655	1.789	A/B,C,D

[a] This eluent consisted of methanol-saturated *n*-hexane. A true 1:4 (v/v) solution could not be achieved at ambient temperature.

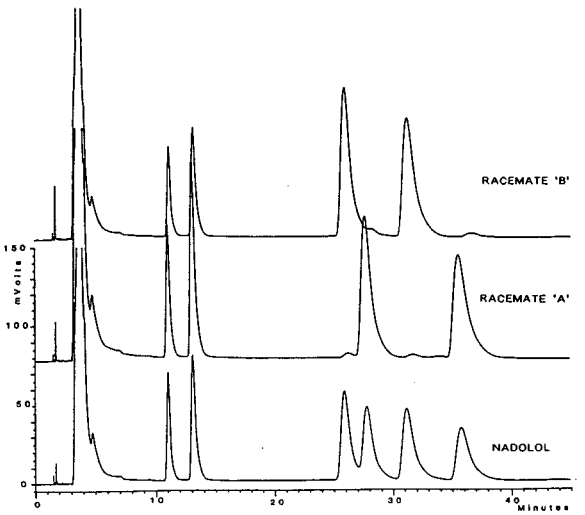

Fig. 3. Examples of chiral separations obtained for nadolol, racemate A and racemate B using the eluent containing 2-propanol as modifier. Conditions: eluent, *n*-hexane–2-propanol (4:1, v/v); flow-rate, 2 ml/min; column, DNB-L-Leu covalently bonded to 3-μm Hypersil APS (150 × 4.6 mm I.D.); injection volume, 20 μl; detection wavelength, 239 nm; sample, 1 mg of analyte dissolved in 1 ml of eluent and reacted with 1 μl of 1-naphthyl isocyanate under ambient conditions for 15 min before injection.

DISCUSSION

The data obtained indicate that the structure of the alcoholic modifier does influence the chromatographic performance. Increasing the length of the chain of primary alcohols consistently increases the retention, but the increased time on-column does not necessarily improve the resolution. For primary alcohols, the selectivity increases up to C_3 and thereafter it decreases. For secondary alcohols, where no C_1 or C_2 alcohol could be evaluated, the selectivity was a maximum at C_3 ($\alpha_{2/1}$) or C_4 ($\alpha_{3/1}$, $\alpha_{4/2}$). One case of unsaturation was studied, with 2-propen-1-ol (allyl alcohol). This alcohol exhibited decreased retention and separation in comparison with its saturated C_3 analogues. Few conclusions can be drawn from this isolated example, however.

Branching had a discernible effect, increasing both retention and selectivity (see 1-pentanol, 2-pentanol and 3-methyl-1-butanol). Hence it may be branching that is responsible for the observed differences in the performance of the primary and secondary alcohols. Use of the secondary alcohols consistently increased both retention and selectivity in comparison with their primary counterparts.

A peculiar complication arising out of the use of nadolol as a model system is that full separation requires both enantioselectivity and diastereoselectivity. The critical separation is of peaks 1 and 2, the first-eluting isomers of each racemate, *i.e.*, a diastereomer separation. Where loss of selectivity occurred it invariably led to a loss of resolution of those peaks. Further loss of separation lead to two-peak chromatograms where peaks 3 and 4 co-eluted. This also represents loss of diastereoselectivity with enantioselectivity being retained throughout.

Hence demonstration of good enantioselectivity is not necessarily followed by good separation. For example, 2,2-dimethyl-1-propanol showed good enantioselectivity for each racemate ($\alpha = 1.463$) but totally failed to resolve the diastereomers and yielded only two peaks. In contrast, methanol yield lower selectivities ($\alpha = 1.2$) but all four peaks were separated.

In assessing the data it is important to bear in mind that the eluents were prepared on a volumetric or gravimetric basis rather than on a molar basis. The densities of the alcohols were all similar and consequently a 1:5 (v/v) mixture of a higher alcohol, such as 1-octanol, contains significantly less modifier than a 1:5 (v/v) mixture of 1-propanol when the two are considered in terms of their molar concentrations. It is possible that it is the concentration of hydroxyl functions alone which critically influences chromatographic performance, in which case the eluents should be prepared on a molar basis for a true comparison to be made.

Notwithstanding these considerations, the data are useful from an empirical point of view. They indicate that there is no straightforward correlation between time on-column (retention) and separation or selectivity. The fact that there are optimum chain lengths (C_3 or C_4) giving rise to optimum separations implies that the size and/or structure of the alcohols are factors in the enantioselective mechanism occurring at the molecular level.

Also on an empirical basis, the investigation revealed that methanol and ethanol gave the best separations. Although that with methanol was marginally the better, ethanol is the preferred modifier as it is not a saturated solution (*i.e.*, is more controllable) and gives a shorter analysis time.

CONCLUSIONS

The choice of modifier alcohol, an achiral entity, has a significant influence on the resulting chiral separation of nadolol isomers. Retention may be related to the polarity of the alcohol but the separation of isomers is affected by a more complex relationship. The separation is optimum for C_3 or C_4 alcohols. This indicates that the structure of the alcohol, an achiral entity, is involved in the chiral recognition process, although the nature of the mechanism is not clear.

REFERENCES

1 L. Slusarek and K. Florey, in K. Florey (Editor), *Analytical Profiles of Drug Substances*, Vol. 9, Wiley, New York, 1980, p. 455.
2 A.M. Dyas, M.L. Robinson and A.F. Fell, *J. Chromatogr.*, 586 (1991) 351.
3 A.F. Fell, M.L. Robinson and A.M. Dyas, *Analyst*, 116 (1991) 1343.
4 A.M. Dyas, A.F. Fell and M.L. Robinson, *Chirality*, 2 (1990) 120.

Journal of Chromatography A, 660 (1994) 255–268
Elsevier Science B.V., Amsterdam

CHROMSYMP. 2887

Epimeric N-substituted L-proline derivatives as chiral selectors for ligand-exchange chromatography

E. Veigl and W. Lindner*

Institute of Pharmaceutical Chemistry, Karl-Franzens-University, A-8010 Graz (Austria)

ABSTRACT

Mainly N-alkyl derivatives of L-proline have proved useful as chiral selectors, particularly in the field of chiral ligand-exchange chromatography (CLEC). This paper describes the synthesis of new N-alkyl derivatives of L-proline, containing a second centre of chirality, and their immobilization on silica gel. The applicability of these chiral stationary phases in CLEC with either copper(II) or nickel(II) as complexing ion was investigated. Particular attention was paid to the effects of the organic modifier, buffer concentration and pH on stereoselectivity and retention. The aim of this study was also to elucidate the influence of the second centre of chirality, which contains a π-basic, space-filling phenyl group and a polar amide function, on enantioseparation and elution order. Based on simple molecular modelling studies, recognition mechanisms and the possibility of the amide oxygen coordinating with either copper(II) or nickel(II) are discussed. Both epimeric chiral selectors (either *R,S-* or *S,S*-configuration) resolved the enantiomers of various amino acids and derivatives thereof.

INTRODUCTION

Since the first attempts by Rogozhin and Davankov [1] to separate enantiomers via ligand-exchange chromatography, this technique has become increasingly popular. Davankov and co-workers made early systematic studies with chiral chelating resins containing immobilized amino acids (AAs) [2,3]. Subsequently, many ligand-exchange systems using different chemically bonded ligands and various kinds of transition metals have been studied. To overcome the limiting pressure resistance of polymeric soft resins, silica-bonded chiral stationary phases have been introduced in chiral ligand-exchange chromatography (CLEC), offering increased column efficiency, resolution and detection sensitivity [4–7]. Apart from the commonly separated enantiomers of amino acids and derivatives thereof, it is also possible to resolve enantiomers of carboxylic acids, hydroxy acids, amino alcohols and amino alcohols as their Schiff bases, barbiturates, hydantoins and succinimide derivatives. The various techniques of CLEC, including the use of chiral stationary phases (CSPs), chiral coated phases and chiral mobile phases, have been surveyed in several publications [8–12].

Mainly N-alkyl derivatives of L-proline have proved useful as chiral selectors (CSs) in CLEC. In this paper, two new chiral selectors (CSs) derived from L-proline are presented (see Fig. 1, CS-I and CS-II). These epimeric N-alkyl derivatives of L-proline, containing a second centre of chirality, were synthesized, fully characterized and immobilized on silica gel. The applicability of these CSPs in CLEC with either copper(II) or nickel(II) as complexing ion was investigated. Particular attention was paid to the effects of the organic modifier, buffer concentration, temperature and pH on resolution. The aim of this study was also to elucidate the influence of the second centre of chirality, containing a π-basic, space-

* Corresponding author.

0021-9673/94/$07.00 © 1994 Elsevier Science B.V. All rights reserved
SSDI 0021-9673(93)E0810-H

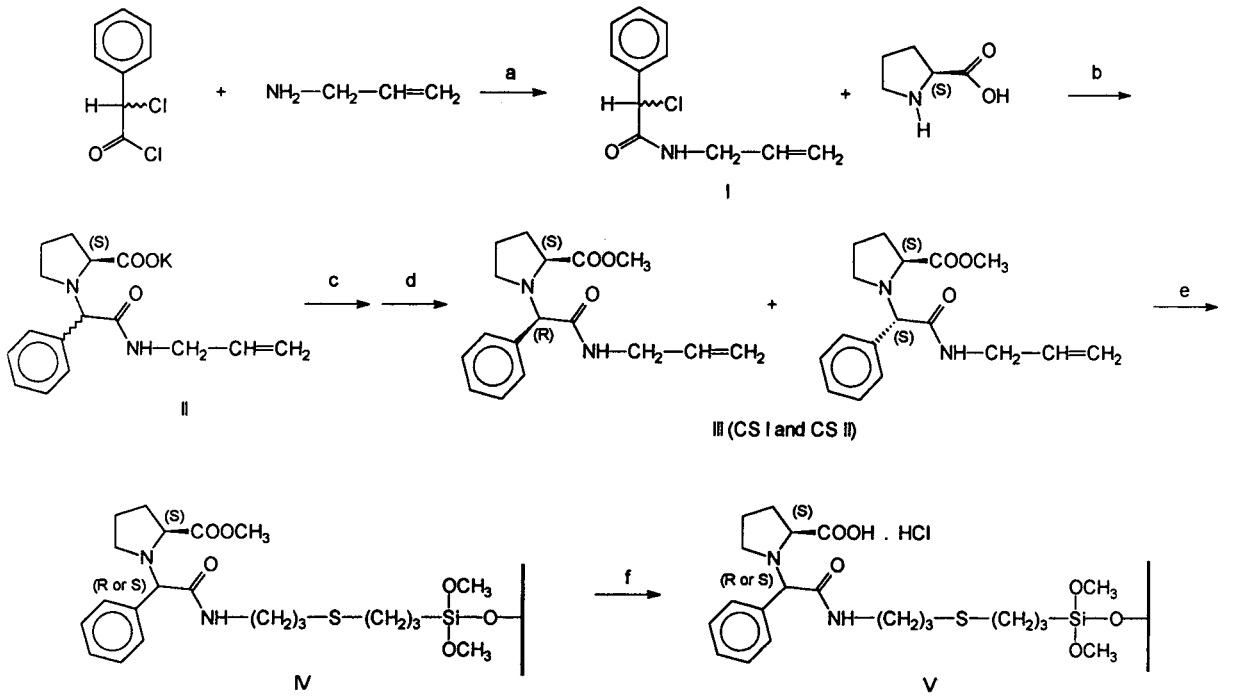

Fig. 1. Preparation of CSPs derived from L-proline. (a) Light petroleum, 25°C for 2 h; (b) potassium carbonate, ethanol, reflux for 20 h; (c) acetyl chloride, methanol, reflux for 5 days; (d) preparative resolution of diastereomers; (e) 3-mercaptosilane, AIBN, chloroform, reflux for 43 h; (f) Na_2CO_3–$NaHCO_3$ solution (pH 8.5), 25°C for 20 h, 50°C for 4 h.

filling phenyl group and a polar amide function, on chiral recognition and elution order. Models to explain the differing chromatographic properties of the epimeric CSPs based on the opposite configuration of the second centre of chirality are discussed.

EXPERIMENTAL

Apparatus

Liquid chromatography (LC) was performed with a modular liquid chromatograph (Merck–Hitachi, Darmstadt, Germany), equipped with a Model L-6200 intelligent pump, a Model AS-2000A autosampler with a 100-μl loop and a Model L-4250 UV–Vis detector, controlled via Model D-6000 chromatography data station software, HPLC Manager Vers. 2.09. Temperature control was provided with a column thermostat (B.O. Electronics, Lang-Enzersdorf, Austria). Standard operating conditions were a flow-rate of 1 ml/min and a column temperature of 30°C.

Preparative LC was performed with a modular liquid chromatograph (Merck–Hitachi), equipped with a Model L-6000 pump (preparative pump head) and a Model L-4000 UV detector (2-mm flow cell unit) with the wavelength set at 230 nm. Model D-6000 chromatography data station software, HPLC Manager Vers. 2.09, was used for data management. Solutes were injected via a Rheodyne Model 7125 injector (3-ml loop) and resolution was obtained on a Hibar column RT, 250 × 25 mm I.D., LiChrosorb Si 60 (7 μm) (Merck); the column temperature was maintained with a water-bath (Haake, Karlsruhe, Germany); a Model A-330 Semi-prep filter (Upchurch, Oak Harbor, WA, USA) was placed between injector and column to protect the latter from plugging.

Infrared spectra were recorded on a Perkin-Elmer (Beaconsfield, UK) Model 225 grating infrared spectrophotometer. Diffuse reflectance infrared spectra were recorded on a Perkin-Elmer Model 1720-x Fourier transform infrared spectrometer.

^{1}H NMR spectra were recorded at 60 MHz on a Hitachi–Perkin-Elmer R-248 High-resolution NMR spectrometer using tetramethylsilane as internal standard. Chemical shifts are given in parts per million.

Melting points were measured on a Büchi-Tottoli (Flawil, Switzerland) apparatus and are uncorrected.

Molecular modelling studies were undertaken with Hyperchem Release 2 for Windows software from Autodesk (Sausalito, CA, USA), using the MM+ force field for molecular mechanics calculations.

Chemicals

Heptane and methanol were of HPLC grade and methylene chloride and 2-propanol of analytical-reagent grade, all from Merck. Water obtained from a Milli-Q system (Millipore) was used. pH was adjusted with either glacial acetic acid or aqueous ammonia and buffer solutions were prepared with ammonium acetate, copper(II) acetate and nickel(II) acetate tetrahydrate, all of analytical-reagent grade from Merck. Mobile phases were filtered and degassed in an ultrasonic bath before use.

L-Proline was obtained from Bachem (Basle, Switzerland), (±)-2-chloro-2-phenylacetyl chloride and 3-mercaptopropyltrimethoxysilane from Aldrich (Steinheim, Germany) and LiChrospher Si 100 (5 μm) from Merck. Other reagents and solvents were purchased from Fluka (Buchs, Switzerland).

Racemic and optically pure 3,4-dehydroproline was obtained from Fluka and L, D- and DL-amino acids and derivatives therefore were purchased from Sigma or prepared from commercially available materials using conventional methods.

2-(R,S)-N-Allyl-(2-chloro-2-phenyl)acetylamide (I). N-Allylamine (6.32 ml, 84 mmol) in 40 ml of light petroleum was added dropwise to a cooled solution of 2-(*R,S*)-2-chloro-2-phenylacetyl chloride (6.43 ml, 40 mmol) in 200 ml of light petroleum. After stirring for 2 h, the yellow precipitate that formed was filtered and washed successively with water, dilute ammonia solution, water and dilute hydrochloric acid. The white solid showed impurities by thin-layer chromatography [mobile phase toluene–acetone (3:1, v/v)] and was recrystallized from cyclohexane. Chemical purity was monitored by HPLC on a C_{18} column with methanol–0.01 *M* ammonium acetate buffer (30:70, v/v) as the mobile phase. The final product was dried in air at 40°C to give 5.66 g (67%) of **I**, m.p. 79°C. ^{1}H NMR [C^2HCl_3, $(C^2H_3)_2SO$]: δ 3.70–4.01 (m, 2H, NCH_2CH), 4.90–5.35 (m, 2H, $CH_2=CH$), 5.49 (s, 1H, ClCHAr), 5.52–6.20 (m, 1H, $CH_2=CH$), 7.21–7.68 (m, 5H, Ar), 7.75–8.28 (s, 1H, $CONHCH_2$).

Potassium N-{(R,S)-[(2-propen-1-yl)aminocarbonyl]phenylmethyl}-L-prolinate (II). This was prepared in a similar manner to the procedure given by Lochead and Proctor [13] for N-benzylproline. L-Proline (1.15 g, 10 mmol), **I** (2.31 g, 11 mmol), potassium carbonate (1.38 g, 10 mmol) and ethanol (50 ml) were stirred at reflux for 20 h. To speed up the reaction a small portion of 18-crown-6 was added. After cooling, the solution was filtered and the solvent was removed under reduced pressure. The residue was dissolved in acetone (to remove potassium chloride and non-alkylated L-proline), filtered again and evaporated to dryness. The residue was dissolved in water and extracted several times with diethyl ether to recover unreacted amide **I**. After evaporating the aqueous phase, a yellow oil (3,7 g, 113%) was obtained, containing L-proline, amide, potassium chloride and other possible side-products, hence a theoretical yield above 100% was calculated.

N-{(R,S)-[(2-Propen-1-yl)aminocarbonyl]phenylmethyl}-L-proline methyl ester hydrochloride (III). The crude prolinate **II** (4.5 g, 0.014 mol) was dissolved in methanol (100 ml) and 25 ml of a mixture of acetyl chloride in methanol (10:90, v/v, forming a dry solution of hydrochloric acid in methanol) were added. After refluxing for 5 days, the white precipitate that formed was filtered off and the yellow solution was evaporated to dryness. The residue was dissolved in acetone, filtered and evaporated twice. The amount and speed of ester formation were determined during the reaction by RP-HPLC, using methanol–0.01 *M* ammonium acetate buffer (10:90, v/v) as the mobile phase. A yellow, non-crystalline product (3.86 g, 81%) was ob-

tained, obviously consisting of the desired diastereomeric methyl esters and unesterified N-alkyl-L-proline **II**.

Preparative resolution of the epimeric L-proline derivatives

Further purification and resolution of the diastereomers was carried out by preparative HPLC using a 250 × 25 mm I.D. RP-8 column with methanol–0.01 *M* ammonium acetate buffer (50:50, v/v) as the mobile phase at a flow-rate of 15 ml/min, a column temperature of 40°C and a detection wavelength of 230 nm. The amount of **III** injected per run was about 100 mg. The fractions collected from four runs containing the same diastereomer were combined, methanol was evaporated, then the solution was made alkaline with ammonia solution (pH ≈ 8) and extracted with diethyl ether. The organic layer was dried over magnesium sulphate, filtered and after evaporation under reduced pressure the pure diastereomeric bases were obtained as slightly yellow, viscous oils, with a yield of CS-I of *ca.* 20% (99.2% diastereomeric purity) and of CS-II of *ca.* 32% (99.3% diastereomeric purity). All attempts to crystallize the chromatographically pure product (following ion-exchange chromatography and freeze-drying of the free amines or of the hydrochloride, sulphate, tartrate and phosphate salts) failed. The physico-chemical characterization of the two diastereomers was realized on the basis of ^{1}H NMR and IR spectra and the results were in agreement with the proposed structures.

CS-I. ^{1}H NMR (C^2HCl_3): δ 1.65–2.03 (m, 4H, CH_2), 2.65–2.95 (m, 2H, CH_2CH_2N), 3.20–3.45 (m, 1H, $COCHCH_2$), 3.65 (s, 3H, OCH_3), 3.75–4.08 (d, 2H, NCH_2CH), 4.39 (s, 1H, NCHAr), 4.95–5.40 (m, 2H, $CH_2 = CH$), 5.60–5.95 (m, 1H, $CH_2 = CH$), 7.20–7.38 (m, 5H, Ar), 7.80 (s, 1H, NH).

CS-II. ^{1}H NMR (C^2HCl_3): δ 1.65–2.03 (m, 4H, CH_2), 2.65–2.95 (m, 2H, CH_2CH_2N), 3.40–3.55 (m, 1H, $COCHCH_2$), 3.63 (s, 3H, OCH_3), 3.75–4.08 (d, 2H, NCH_2CH), 4.39 (s, 1H, NCHAr), 4.95–5.35 (m, 2H, $CH_2 = CH$), 5.60–5.95 (m, 1H, CH_2–CH), 7.20–7.38 (m, 5H, Ar), 8.0 (s, 1H, NH).

3-Mercaptopropylsilica gel

A 10-g amount of LiChrospher Si 100 (5 μm) and 140 ml of distilled toluene (b.p. 109°C) were introduced into a 250-ml Quickfit flask equipped with a mechanical stirrer and a distilling apparatus. To remove traces of water, the toluene was azeotropically evaporated until the distillate had a boiling temperature of 108°C. After *ca.* 30 ml of toluene had been removed the distillation apparatus was replaced with a reflux condenser. Freshly distilled pyridine (16.7 ml) and 3-mercaptopropyltrimethoxysilane (16.7 ml, 87.5 mmol) were added dropwise under nitrogen. After refluxing for 40 h and sedimentation of the silica gel particles, the solvent was exhausted and the stationary phase was washed successively with toluene, diethyl ether and light petroleum. The modified silica (12.08 g) was dried in air at 40°C to give a 11.27 g yield. Elemental analysis indicated 970 μmol of bonded 3-mercaptopropyldimethoxysilyl residues per gram of modified silica gel (based on carbon elemental analysis). Analysis: found, 5.95% C; starting material, 0.12% C. DRIFT spectrum (KBr): 3649, 3346, 2946, 2848, 2582, 2362, 2340, 2000, 1881, 1633, 1457, 1412, 1345, 1094, 1082, 956, 808, 693. cm^{-1}.

CSP-I

CS-I (474.5 mg, 1.75 mmol), 3.3 g of 3-mercaptopropylsilica gel, 60 mg of AIBN [2,2′-azobis(2-methylpropionitrile), 0.4 mmole], and 100 ml of azeotropically dried chloroform were stirred and refluxed under nitrogen for 43 h. The derivatized silica was washed thoroughly with chloroform and methanol. To cleave the methyl ester, a solution of sodium carbonate and sodium hydrogencarbonate (pH 8.5) was added and the slurry was stirred for 20 h at room temperature and additionally for 4 h at 50°C. The reaction was stopped by adding 70 ml of water and adjusting the pH to 2.9 with dilute hydrochloric acid. The modified silica gel was washed with methanol–water (1:1) (twice), methanol (three times), acetone (twice) and light petroleum. After drying in air at 40°C, 2.92 g of white silica gel were obtained. Elemental analysis of CSP-I afforded 7.97% C, 1.57% H, 0.39% N. The calculated coverage was 139 μmol of chiral

selector bonded per gram (based on N analysis) and 105 μmol of chiral selector per gram g (based on C analysis). DRIFT spectrum (KBr): 3650, 3316, 2946, 2848, 2577, 2362, 2340, 2001, 1882, 1743, 1664, 1526, 1455, 1412, 1346, 1097, 1084, 957, 804, 705, 692 cm^{-1}.

CSP-II

CSP-II was similarly obtained from CS-II (426 mg, 1.41 mmol), 3 g of 3-mercaptopropylsilica gel, AIBN (50 mg, 0.3 mmol) and chloroform (100 ml), yield 2.64 g. Elemental analysis resulted in 7.24% C, 1.53% H, 0.31% N. From these data the coverage was calculated to be 110.6 μmol of chiral selector per gram (based on N analysis) and 67 μmol chiral selector per gram (based on C analysis). DRIFT spectrum (KBr): 3649, 3319, 2938, 2849, 2577, 2001, 1882, 1745, 1665, 1526, 1455, 1412, 1346, 1079, 957, 812, 694 cm^{-1}.

Both CSP-I and CSP-II were packed into 100 × 4.0 mm I.D. and 150 × 4.0 mm I.D. analytical columns by a conventional slurry technique and coupled in series for chromatography.

"End-capping" (reaction of accessible free thiol groups with 1-hexene)

Before end-capping, each column was flashed with heptane (30 ml) and chloroform (50 ml). End-capping of the remaining sulphydryl groups was performed by recycling a solution containing 1-hexene (1.17 ml, 10 m*M*) and AIBN (50 mg, 0.3 m*M*) in chloroform (150 ml) at a flow-rate of 0.3 ml/min and a water-bath temperature of 70°C for 24 h.

To calculate the coverage of "end-capping" judged by elemental analysis, small portions of CSP-I and CSP-II were treated with excess of 1-hexene and AIBN in glass tubes to give a loading of 369 μmol hexyl residues per gram for CSP-I (based on C analysis) and 422 μmol per gram for CSP-II (based on C analysis).

RESULTS AND DISCUSSION

Synthesis of chiral selectors, purification and immobilization

The preparation of CSP-I and CSP-II is outlined in Fig. 1. As mentioned under Experimental, the N-alkylation of sodium L-prolinate gave only impure compound **II**. Several attempts were made to optimize the alkylation reaction. To obtain better yields and a shorter reaction time, different carbonates were tested. Potassium carbonate seems to be superior to sodium carbonate because of forming better soluble prolinates and neutralizing the formed hydrochloric acid. A crown ether was additionally added to afford better phase-transfer catalysis. Tetrabutylammonium hydroxide did not speed up the alkylation via ion-pair formation resulting in enhanced solubility of L-proline. Further, applying ultrasound instead of refluxing resulted in poor yields. The reaction speed and amount of remaining amide **I** were measured via RP-HPLC, using methanol–10 m*M* ammonium acetate buffer (30:70, v/v) as the mobile phase. Formation of N-allyl-2-phenyl-2-ethoxyacetamide did not occur in the ethanolic solution, as was confirmed by a comparable test under identical conditions but without L-proline in the reaction mixture. A further possible by-product, O-[(allylaminocarbonyl)methylphenyl]-L-proline ester, was obviously not formed because of the lack of an ester band in the IR spectra. However, degradation of adduct **II**, forming a biscarboxylate by cleaving the amide bond, could not be excluded. As was also pointed out before, the epimeric L-proline derivatives in the form of their methyl esters were well resolvable by RP-HPLC. CS-I and CS-II exhibited satisfactory chemical purity.

In the literature several different possibilities have been described for the covalent binding of a chiral selector to a silica gel surface. However, based on our experience, it seems that the basic nitrogen of CS-I and CS-II may result in inactivation of the hexachloroplatinic acid or (cyclooctadiene)platinum chloride commonly used for the classical immobilization procedure via hydrosilylation of a vinyl group followed by immobilization of the siloxane to silica gel. To overcome this obvious limitation, the allylic residues of the CSs were reacted according to a radical anti-Markownikoff addition of a vinyl group with the thiol groups of 3-mercaptopropylsilica gel, as was described by Rosini *et al.* [14]. However, only 139 μmol of 970 μmol of mercapto groups available per gram of 3-mercap-

topropylsilica gel reacted with the CS-I to give CSP-I and 111 μmol with CS-II to give CSP-II. The remaining 831 μmol/g CSP-I and 859 μmol/g CSP-II, respectively, of mercapto groups represent polar residues being able to interact with polar solutes. Hence they may influence the overall selectivity of the chromatographic system, as was discussed recently by Pirkle and co-workers [15,16]. To reduce the number of remaining polar sulfhydride groups a new "end-capping" procedure was developed. 1-Hexene was reacted under the same conditions as the chiral selectors with the CSPs to produce a more lipophilic stationary phase, covering about 50% of the remaining free sulphydride groups. Despite the fact that the residual silanols are not alkylated under these reaction conditions, the accessibility of these groups to solute molecules should be decreased. Further, Feibush *et al.* [17] demonstrated the enhanced stereoselectivity of "diluted CSPs" compared with concentrated ones, owing to a decreased interference of neighbouring chelating ligands. Additional experiments dealing with the "end-capping" of mercapto residues are in progress and further studies with such "mixed" or "diluted phases" will be published elsewhere [18]. To summarize, there are at least three different covalently bound residues on the final CSPs, probably providing different retention and selectivity characteristics (Fig. 2). These CSPs, as almost all other CSPs described in the literature, represent randomly scattered surface structures and it is not clear how homogeneous the surface will be and/or how much "clustering" will take place.

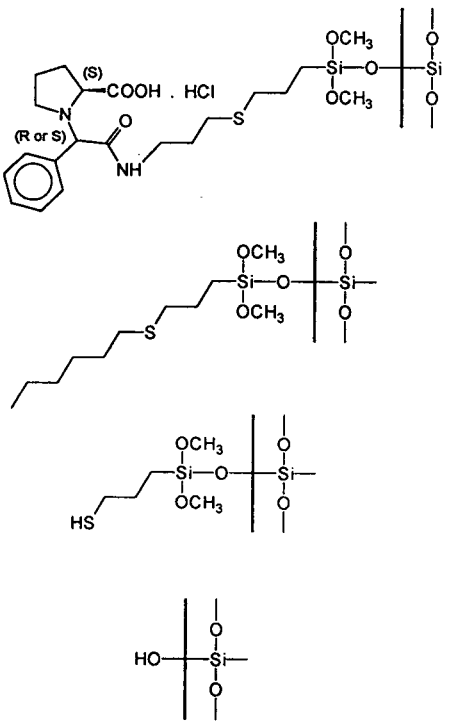

Fig. 2. Three different covalently bound residues on CSP-I and CSP-II.

Chromatographic properties

Tables I and II are giving a general view of the resolved solutes used in this study and the applicability of the epimeric selectors in CLEC with Cu(II) and Ni(II) as complexing metal ions. As can be seen, CSP-I and -II resolve a broad range of amino acids and amino acid derivatives. Representative chromatograms are shown in Figs. 3 and 4.

Underivatized AAs show similar capacity factors on both stationary phases with copper(II) as complexing ion. Simple molecular modelling studies were undertaken to elucidate the spatial arrangement of the chiral selectors. An outcome of such calculations is shown in Fig. 5. Formation of mixed-ligand sorption complexes with the silica-bonded chiral ligands is the most important retention mechanism for the amino acid solutes and seems to be the same for CSP-I and CSP-II. In contrast, the lipophilicity of the epimeric CSPs is different, as can be seen from the capacity factors of aromatic AAs and dansyl-AAs. These solutes are more strongly retained on the obviously more "lipophilic" stationary phase CSP-II. Although there is a slightly altered density of the CSs on CSP-I and CSP-II, the different retention characteristics are probably due to the different spatial arrangements of the chiral selectors and therefore altered Van der Waals and $\pi-\pi$ type interaction sites combined with chelation possibilities. This was also supported by the diastereoseparation of the two proline esters CS-I and CS-II (CS-I eluted before CS-II) on a reversed-phase column even on a preparative scale.

TABLE I

RESOLUTION OF AMINO ACIDS AND DERIVATIVES ON CSP-I AND CSP-II USING COPPER(II) AS COMPLEXING ION

Flow-rate, 1 ml/min; temperature, 30°C; detection at 240 nm. MP (mobile phases): 1 = 50 m*M* NH_4OAc–0.5 m*M* $Cu(OAc)_2$, (pH 4.5), 2 = 90% (v/v) 50 m*M* NH_4OAc–0.5 m*M* $Cu(OAc)_2$ + 10% (v/v) methanol (pH 5.5); 3 = 70% (v/v) 50 m*M* NH_4OAc–0.5 m*M* $Cu(OAc)_2$ + 30% (v/v) methanol (pH 5.5); 4 = 50 m*M* NH_4OAc–0.5 m*M* $Cu(OAc)_2$ (pH 6.5); 6 = 100 m*M* NH_4OAc–0.5 m*M* $Cu(OAc)_2$ (pH 6.5); 7 = 100 m*M* NH_4OAc–0.5 m*M* $Cu(OAc)_2$ (pH 5.5); 9 = 70% (v/v) 100 m*M* NH_4OAc–0.5 m*M* $Cu(OAc)_2$ + 30% (v/v) methanol (pH 7.5); 10 = 70% (v/v) 100 m*M* NH_4OAc–0.5 m*M* $Cu(OAc)_2$ + 30% (v/v) methanol (pH 4.5). Capacity factor $k_2' = (t_R - t_0)/t_0$; selectivity $\alpha = k_2'/k_1'$.

Solute[a]	CSP-I			CSP-II		
	MP	k_2'	α	MP	k_2'	α
Asn	2	0.79	1.00	7	0.57	1.09
Ile	2	2.09	1.08	6	3.94	1.15
Met	4	6.53	1.08	7	3.50	1.22
Nleu	2	2.62	1.12	6	4.73	1.21
Nval	2	1.58	1.09	7	1.19	1.21
Phe	2	6.77	1.00	7	6.82	1.28
p-Amino-Phe	2	6.82	1.00	7	4.94	1.10
Pro	2	1.52	1.39	8	3.42	1.19
Allo-4-OHPro	2	1.93	1.74	8	1.61	1.37
3,4-Dehydro-Pro	1	0.86	1.53	6	3.28	2.03
N-Hexyl-Pro	2	1.78	1.40	9	13.35	1.31
Ser	2	0.73	1.07	7	0.47	1.12
Thr	2	0.86	1.08	7	0.66	1.10
Trp	3	13.82	1.18	10	2.63	1.00
α-Methyl-Trp	3	18.94	1.44	10	2.62	1.00
5-OHTrp	3	8.90	1.19	10	1.49	1.00
Tyr	2	5.27	1.11	6	5.69	1.00
α-Methyl-m-Tyr	2	8.24	1.35	7	5.86	1.08
α-Methyl-Tyr	2	7.46	1.43	7	5.20	1.22
O-Methyl-Tyr	2	11.26	1.06	7	11.24	1.17
3-Methoxy-Tyr	2	7.22	1.21	6	9.27	1.00
Val	2	1.27	1.00	7	1.11	1.20
2-Aminolactic acid	4	1.63	1.00	7	0.65	1.12
DNS-Phe	3	12.21	1.12	10	9.31	1.00
DNS-Thr	2	10.10	1.06	10	2.06	1.00

[a] Commonly used abbreviations of amino acids.

Remarkably, using nickel(II) as complexing ion the two diastereomeric CSPs show opposite behaviour in terms of stereoselectivity and retention. Depending on the epimeric form of the chiral selector used, the capacity factors of AAs

TABLE II

RESOLUTION OF AMINO ACIDS AND DERIVATIVES ON CSP-I AND CSP-II USING NICKEL(II) AS COMPLEXING ION

Flow-rate, 1 ml/min; temperature, 30°C; detection at 254 nm. MP (mobile phases): 1 = 70% (v/v) 50 m*M* NH_4OAc–0.5 m*M* $Ni(OAc)_2 \cdot 4H_2O$ + 30% (v/v) methanol (pH 5.5); 2 = 70% (v/v) 50 m*M* NH_4OAc–0.5 m*M* $Ni(OAc)_2 \cdot 4H_2O$ + 30% (v/v) methanol (pH 6.5); 3 = 70% (v/v) 100 m*M* NH_4OAc–0.5 m*M* $Ni(OAc)_2 \cdot 4H_2O$ + 30% (v/v) methanol (pH 7.5); 4 = 70% (v/v) 100 m*M* NH_4OAc–0.5 m*M* $Ni(OAc)_2 \cdot 4H_2O$ + 30% (v/v) methanol (pH 6.5).

Solute	CSP-I			CSP-II		
	MP	k_2'	α	MP	k_2'	α
Tyr	1	4.67	1.25	3	3.16	1.76
α-Methyl-m-Tyr	1	5.24	1.73	3	1.99	1.70
α-Methyl-Tyr	1	5.41	1.87	3	1.50	1.73
3-Methoxy-Tyr	1	5.99	1.39	3	3.37	1.84
O-Methyl-Tyr	1	7.49	1.17	3	7.77	1.79
Trp	1	14.41	1.28	4	2.26	1.29
α-Methyl-Trp	1	20.67	1.70	3	5.62	1.35
5-Methyl-Trp	1	21.12	1.22			
6-Methyl-Trp	1	26.16	1.29	3	16.22	1.53
7-Methyl-Trp				3	14.77	1.47
5-OHTrp	1	9.77	1.30	3	5.15	1.52
DNS-Met	2	4.42	1.05	4	4.52	1.00
DNS-Phe	2	6.97	1.11	4	8.56	1.00
DNS-Thr	2	1.69	1.05	4	1.71	1.00
DNS-Trp	2	11.17	1.19			
p-Amino-Phe	1	4.44	1.11	3	2.75	1.63
Phenyl-Gly	1	2.05	1.28	3	1.62	1.00
β-Phenyllactic acid	1	0.74	1.00	4	0.31	1.44

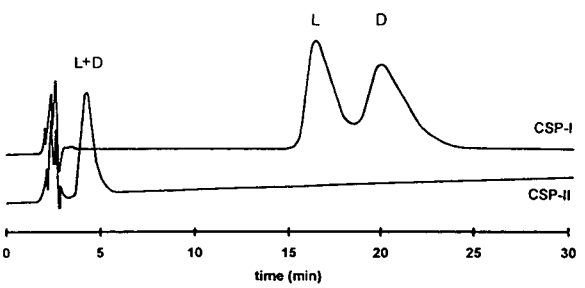

Fig. 3. Different capacity factors and enantioselectivity of CSP-I and CSP-II for D,L-phenylglycine. Mobile phase, 70% (v/v) 50 m*M* NH_4OAc–0.5 m*M* $Ni(OAc)_2 \cdot 4H_2O$ + 30% (v/v) methanol (pH 6.5).

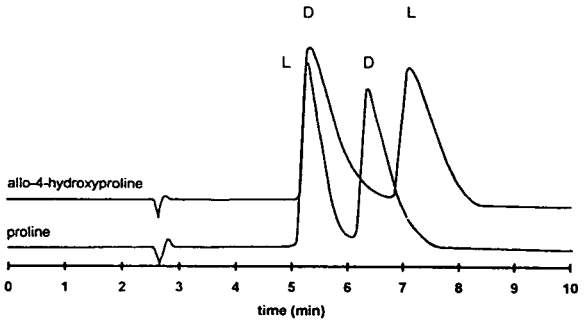

Fig. 4. Different capacity factors and enantioselectivity of CSP-I for D,L-proline and D,L-allo-4-hydroxyproline. Mobile phase, 90% (v/v) 50 m*M* NH_4OAc–0.5 m*M* $Cu(OAc)_2$ + 10% (v/v) methanol (pH 5.5).

and methylated derivatives thereof differ widely from one another (Fig. 3). The solutes are much more strongly retained on CSP-I, by a factor of 10–20. Despite the different amounts of chiral selector loaded on to CSP-I and CSP-II, there must be an additional reason for the altered capacity factors. As can be seen in Fig. 5, the phenyl residue occupies the lower axial position of the mixed-ligand complex of CSP-I and CSP-II. The chiral selector with an *S,S*-configuration may possibly form a hydrogen bond between its amide and carboxylate groups, causing hindered rotation of the prolyl residue and additional rigidity of the chelate complex. Subsequently, the CSs have different possibilities of coordinating with their carbonyl oxygen in the lower axial position of the octahedral nickel(II) complex. As a consequence, altered mixed ligand complexes will be formed. This assumption is supported by the similar retention behaviours of the solutes on CSP-I and CSP-II using copper(II) as complexing ion, because of its square-planar distribution of coordinate valences.

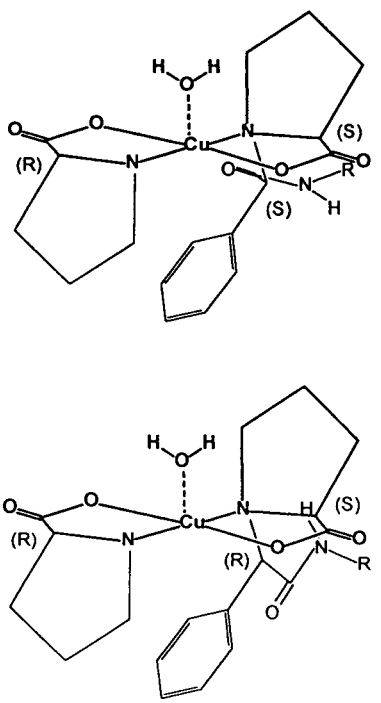

Fig. 5. Proposed mixed-ligand complexes of CS-I and CS-II using copper(II) as complexing ion and D-proline as guest molecule. The commonly used presentation of mixed-ligand planar copper(II) complexes of L-proline-derived CSPs (introduced by Davankov and co-workers) was used in combination with the outcome of the molecular modelling studies.

Particular attention was paid to the effects of the buffer concentration, temperature, organic modifier and pH on enantioselectivity and resolutions, as discussed below.

Influence of buffer concentration. As was demonstrated for CSP-II (Tables III and IV), the buffer concentration plays an important role on retention, enantioselectivity and resolution with either copper(II) or nickel(II) as complexing ion. Doubling the concentration of the ammonium acetate buffer resulted in decreased capacity factors (about 40% smaller) and enhanced α-values. Different buffer concentrations and type of buffer ions can be used to optimize resolution and retention.

Influence of temperature. Ligand-exchange chromatographic systems based on covalently bonded ligands are commonly used at elevated temperatures in order to improve mass transfer and column efficiency. As a rule, but with exceptions, the selectivity decreases with increasing temperature, *e.g.*, the resolution of N-benzylproline on an L-proline-containing polystyrene-type ligand exchanger described by Davankov *et al.* [19]. The temperature dependence of retention, enantioselectivity and resolution on CSP-I in the range of 30–60°C is shown in Figs. 6 and 7. As expected, the α-values decreased with increase in temperature, but there was also an exception, namely allo-4-hydroxyproline, where the highest enantioselec-

TABLE III

INFLUENCE OF BUFFER CONCENTRATION ON CAPACITY FACTOR, ENANTIOSELECTIVITY AND RESOLUTION ON CSP-II USING COPPER(II) AS COMPLEXING ION

Mobile phase, 0.5 m*M* copper(II) acetate–ammonium acetate buffer (pH 5.5); other conditions as in Table I.

Solute	50 m*M* ammonium acetate			100 m*M* ammonium acetate		
	k_2'	α	R_s [a]	k_2'	α	R_s
Asn	0.74	1.00	–	0.57	1.09	n.c.[b]
Ile	2.11	1.00	–	1.68	1.11	n.c.
Nval	1.80	1.14	0.72	1.19	1.21	0.89
Phe	9.75	1.25	1.22	6.82	1.28	1.50
Phenyl-Gly	3.81	1.20	1.19	2.07	1.12	–[c]
Pro	1.61	1.41	1.11	1.06	1.56	1.36
Ser	0.68	1.00	–	0.47	1.12	n.c.
Thr	0.87	1.00	–	0.66	1.10	n.c.
Val	1.63	1.14	0.65	1.11	1.20	n.c.
2-Aminobutyric acid	0.95	1.00	–	0.65	1.12	n.c.
3,4-Dehydro-Pro	2.09	1.37	–[c]	1.76	1.62	1.82
α-Methyl-m-Tyr	8.20	1.06	n.c.	5.86	1.08	n.c.
α-Methyl-Tyr	7.68	1.20	0.99	5.20	1.22	1.09
O-Methyl-Tyr	17.46	1.17	1.32	11.24	1.17	1.16
p-Amino-Phe	7.86	1.10	n.c.	4.94	1.10	n.c.

[a] $R_s = 1.18\ (t_{R_2} - t_{R_1}/w_{1/2_1} + w_{1/2_2})$.
[b] n.c. = Not calculated.
[c] Co-eluted with system peak.

TABLE IV

INFLUENCE OF BUFFER CONCENTRATION ON CAPACITY FACTOR AND ENANTIOSELECTIVITY ON CSP-II USING NICKEL(II) AS COMPLEXING ION

Mobile phase, 0.5 m*M* nickel(II) acetate–ammonium acetate buffer (pH 6.5); other conditions as in Table II.

Solute	50 m*M* ammonium acetate		100 m*M* ammonium acetate	
	k_2'	α	k_2'	α
Trp	2.52	1.00	2.26	1.29
Phe	1.51	1.00	1.26	1.32
6-Methyl-Trp	4.53	1.00	4.11	1.33
7-Methyl-Trp	4.29	1.00	3.82	1.27
O-Methyl-Tyr	1.96	1.20	1.90	1.58
β-Phenyllactic acid	0.22	1.46	0.31	1.44

tivity was obtained at 40°C. The resolution of the racemate of norvaline was, however, not influenced by temperature.

Influence of methanol content on the mobile phase. The effect of the organic component in the mobile phase was studied. Of various possible modifiers used in CLEC, *e.g.*, methanol, ethanol, acetonitrile and tetrahydrofuran, methanol was chosen in this study. The influence of the methanol content of the mobile was investigated between 0% and 30% (data not shown) and was found to be of minor importance with regard to retention and enantioselectivity.

Influence of mobile phase pH. In CLEC, retention and enantioselectivity are also optimized by varying the pH of the mobile phase. The common pH range examined with silica-bonded CSPs is between 4 (lower pH values result in dissociation of the copper–amino acid

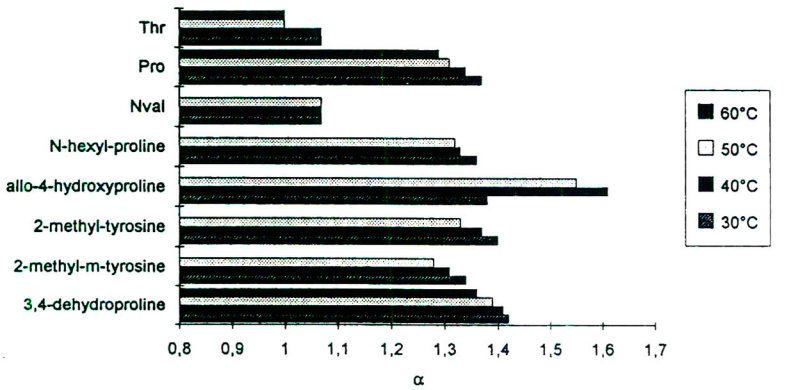

Fig. 6. Influence of temperature on enantioselectivity. Stationary phase, CSP-I; mobile phase, 50 m*M* NH_4OAc–0.5 m*M* $Cu(OAc)_2$ (pH 5.5); flow-rate, 1 ml/min; detection at 240 nm.

complexes) and 9 (higher pH values induce column degradation, especially in combination with elevated temperatures), assuming ammonium ions are present in the mobile phase. Raising the pH usually increases the capacity factors of the solutes as a consequence of the enhanced formation of mixed-ligand sorption complexes. CSP-I and -II were tested between pH 4.5 and 7.5 with regard to retention times of the solutes and enantioselectivity (see Tables V–VII). Employing copper(II) as the complexing ion, the highest enantioselectivity was observed on CSP-I at pH 5.5, except for 3,4-dehydroproline and 3-methoxytyrosine (pH 4.5). As an exception, allo-4-hydroxyproline showed a different behaviour, as can be seen in Fig. 8. The highest enantioselectivity with CSP-II was obtained between pH 5.5 and 6.5. No resolution was obtained at an eluent pH of 4.5 owing to the small capacity factors. A similar difference between CSP-I and CSP-II was observed when using nickel(II) as the complexing metal. CSP-I gave the best results at lower pH, except for dansylamino acids (see Table V), which are known to be better resolved at alkaline pH. In contrast, CSP-II displayed higher enantioselectivity at higher pH values.

Elution order and chiral recognition mechanism. When searching for simple recognition models, one must bear in mind the complex combination of hydrophobic, electrostatic and complexation interactions of the chiral analytes with the (inhomogenous) stationary phase. However, the elution order on a given stationary

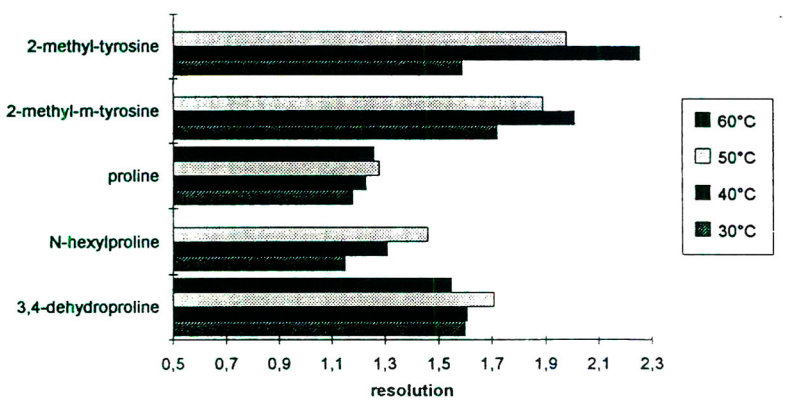

Fig. 7. Influence of temperature on resolution. Stationary phase, CSP-I; mobile phase, 50 m*M* NH_4OAc–0.5 m*M* $Cu(OAc)_2$ (pH 5.5); flow-rate, 1 ml/min; detection at 240 nm.

TABLE V

INFLUENCE OF pH ON RETENTION AND ENANTIOSELECTIVITY ON CSP-I USING NICKEL(II) AS COMPLEXING ION

Mobile phase, 70% (v/v) 50 m*M* ammonium acetate–0.5 m*M* nickel(II) acetate + 30% (v/v) methanol; flow-rate, 1 ml/min; temperature, 30°C; detection at 254 nm.

Solute	Mobile phase pH					
	5.5		6.5		7.5	
	k_2'	α	k_2'	α	k_2'	α
DNS-Thr	1.47	1.00	1.69	1.05	7.22	1.09
DNS-Trp	9.50	1.08	11.17	1.19	12.27	1.18
Phenyl-Gly	2.05	1.28	6.85	1.26		
Tyr	4.67	1.25	12.58	1.20		
3-Methoxy-Tyr	5.99	1.39	21.26	1.31		
O-Methyl-Tyr	7.49	1.17	22.64	1.11		
α-Methyl-m-Tyr	5.24	1.73	6.85	1.26		
α-Methyl-Tyr	5.41	1.87	17.82	1.62		

TABLE VI

INFLUENCE OF pH ON RETENTION AND ENANTIOSELECTIVITY ON CSP-II USING NICKEL(II) AS COMPLEXING ION

Mobile phase, 70% (v/v) 100 m*M* ammonium acetate–0.05 m*M* nickel(II) acetate + 30% (v/v) methanol; flow-rate, 1 ml/min; temperature, 30°C; detection at 254 nm.

Solute	Mobile phase pH			
	6.5		7.5	
	k_2'	α	k_2'	α
Phe	1.26	1.32	5.37	1.57
p-Amino-Phe	0.44	1.00	2.75	1.63
Tyr	0.45	1.00	3.16	1.76
3-Methoxy-Tyr	0.54	1.00	3.37	1.84
α-Methyl-m-Tyr	0.36	1.00	1.99	1.70
α-Methyl-Tyr	0.57	1.00	1.50	1.73
O-Methyl-Tyr	1.90	1.58	7.77	1.79
α-Methyl-Trp	1.20	1.00	6.62	1.35
6-Methyl-Trp	4.11	1.33	16.22	1.53
7-Methyl-Trp	3.82	1.27	14.77	1.47
5-OHTrp	1.06	1.00	5.15	1.52
β-Phenyllactic acid	0.31	1.44	0.41	1.42

TABLE VII

ELUTION ORDER ON CSP-I AND CSP-II WITH EITHER COPPER(II) OR NICKEL(II) AS COMPLEXING ION

First eluted enantiomer indicated.

Solute	Copper(II)		Nickel(II)	
	CSP-I	CSP-II	CSP-I	CSP-II
β-Phenyllactic acid	–	L = D	L = D	L
Met	L	L		
Phe	L = D	L	L = D	L
Phenyl-Gly	–	L	L	L = D
Pro	L	L		
Allo-4-OHPro	D	D		
3,4-Dehydro-Pro	L	L		
N-Hexyl-Pro	L	L		
Tyr	D	D = L	L	L
α-Methyl-Tyr	D	D	D	L
3-Methoxy-Tyr	L	L	L	L
Val	L = D	L		

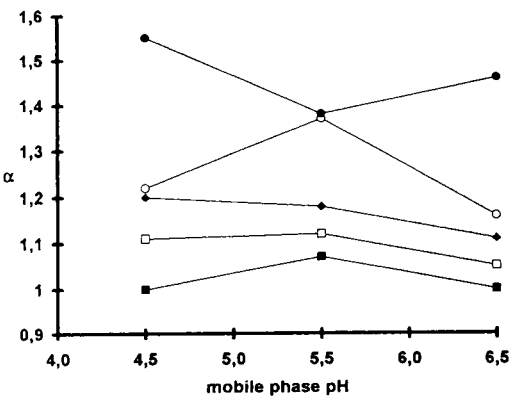

Fig. 8. Influence of pH on enantioselectivity. Stationary phase, CSP-I; mobile phase, 50 m*M* NH_4OAc–0.5 m*M* $Cu(OAc)_2$; flow-rate, 1 ml/min; temperature, 30°C, detection at 240 nm. ■ = Nval + Thr; ○ = Pro; □ = Tyr; ◆ = 3-methoxy-Tyr; ● = allo-4-OHPro.

phase is often the same for a series of amino acids or dansylated amino acids. L-Proline-containing polystyrene-type resins, for instance, show a stronger retention for the D-enantiomers of bidentate AAs and for the L-antipode of tridentate AAs. Polacrylamide-type and poly(2,3-epoxypropyl methacrylate)-type L-proline stationary phases display a higher affinity

towards the L-enantiomers, indicating that additional binding groups fixing the conformation of the chelate structure of the chiral selector together with space-filling barriers (including the surface of the described gel) may play an important role.

Davankov and Kurganov [20] and Boue *et al.* [21] proposed a chiral recognition model with donating OH and C=O groups of the immobilized selectors in the lower axial positions of the Cu(II) coordinating sphere. A similar behaviour has been observed on silica-based phases carrying N-alkyl-L-proline residues [4] or L-proline fixed via an amide bond [5]. Testing dansylated AAs on the latter CSP with copper(II) as complexing ion resulted in an elution order of L- before D-enantiomers, but the elution order was reversed on using cadmium(II) ions. This, however, clearly indicates that the different coordination and chelation characteristics of transition metal ions can become a dominant factor.

On CSP-I and -II the D-enantiomers of AAs are in general more retained than their antipodes (see Table VII), except for the D-antipodes of allo-4-hydroxyproline, tyrosine and α-methyltyrosine. The commonly used presentation of mixed-ligand planar copper(II) complexes of L-proline-derived CSPs (introduced by Davankov and co-workers) was used in the proposed chiral recognition models for proline, allo-4-hydroxyproline, α-methyltyrosine and 3-methoxytyrosine in Fig. 9. Reversal of the elution order from proline to allo-4-hydroxyproline seems to be due to the additional coordination of the hydroxy group of L-allo-4-hydroxyproline in the upper axial position of the planar copper(II) complex. The elution order of D- before L-enantiomer of α-methyltyrosine can be explained by the low stability of the D-α-methyltyrosine complex with the CSP due to steric hindrance. In contrast, the reversal of the elution order of the 3-methoxytyrosine antipodes compared with α-methyltyrosine cannot be fully explained by the stronger π-basic phenyl residue due to the additional methoxy group, and in this instance other influences must be dominating.

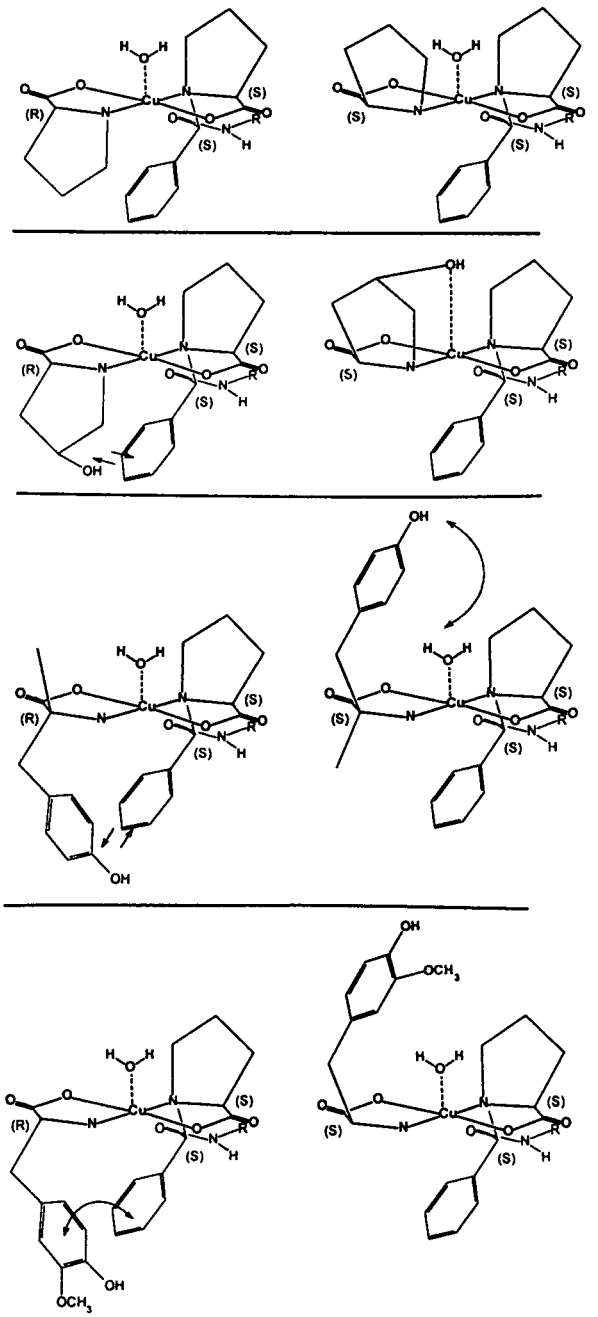

Fig. 9. Proposed chiral recognition mechanisms for Pro, allo-4-OHPro, α-methyl-Tyr and 3-methoxy-Tyr enantiomers using copper(II) as complexing ion.

As can be seen in Table I, the methylation of the chiral centre of tyrosine enhanced the observed enantioselectivity (the α-values increase at similar capacity factors from tyrosine to α-methyl-m-tyrosine and α-methyltyrosine). Reversal of the elution order on changing the metal ion from copper(II) to nickel(II) was observed for tyrosine (CSP-I) and α-methyltyrosine (CSP-

II). Varying the mobile phase pH did not cause a reversal of elution order.

To point out another interesting phenomenon, the resolutions of phenylglycine, phenylalanine and 2-phenyllactic acid using nickel(II) as complexing ion were compared. Phenylglycine is resolvable on CSP-I but the additional methylene group of phenylalanine induces a loss of stereoselectivity. In contrast, phenylalanine and its hydroxy homologue 2-phenyllactic acid are well resolvable on CSP-II but no resolution was obtained for phenylglycine. The chiral recognition mechanism on CSP-I seems to need the small and rigid structure of phenylglycine for discrimination between the two enantiomers, and CSP-II differentiates only the solutes with the mobile and more space-filling benzyl group.

At this point, and without having exact data from X-ray crystallographic measurements, it is speculative to define exactly the nature of the interactions between the solute molecules, chiral resolving agents and the non-chiral components of the chromatographic system. However, being aware of these shortcomings, and considering the unique elution order of the AAs studied, it seems evident that the influence of the second centre of chirality of the new chiral selectors derived from L-proline may be of minor importance for the enantioselectivity of the whole system and the general enantioselective recognition mechanism of the presented CSPs. The configuration of the epimeric phases affects the overall selectivity in a moderate manner and the two CSPs show approximately the same resolving power when using copper(II) as the complexing ion. Using nickel(II) as the central chelating ion the situation is, however, changed significantly.

CONCLUSION

Two novel chiral stationary phases based on epimeric N-alkyl derivatives of L-proline for chiral ligand-exchange chromatography were synthesized and the applicability of these CSPs to resolve chelating selectands was investigated. Because of the difficult synthesis of CSP-I and CSP-II, their practical applicability will be limited, but they offer excellent possibilities for investigating chiral recognition mechanisms in CLEC.

The CSPs showed good enantioselectivity for amino acids and derivatives thereof with either copper(II) or nickel(II) as the central transition metal ion. Buffer concentration, temperature and pH of the mobile phase influenced the chromatographic behaviour in a large scale. The epimeric stationary phases showed comparable enantioselectivity using copper(II) as complexing ion, the configuration of the second center of chirality had a moderate effect, due to the spacefilling, aromatic phenyl residue in vicinity of the five-membered ring of the metal complex. Using nickel(II) as chelating ion in the diastereomeric chiral selectors showed, however, different retentions for amino acids as a consequence of altered octahedral mixed-ligand sorption complexes.

The changes in chromatographic behaviour within a series of tyrosine analogues demonstrate effectively the great influence of slight variations of the solute structure on chiral discrimination mechanisms and it becomes complicated to explain the complex simultaneous interactions of matrix fragments, solvent molecules, solutes and immobilized selectors by simplified complex formation models.

ACKNOWLEDGEMENT

This project was supported by a grant from the Austrian Fonds zur Förderung der wissenschaftlichen Forschung (FWF), project number P-8898-CHE, which is gratefully acknowledged.

REFERENCES

1 S.V. Rogozhin and V.A. Davankov, *Chem. Commun.*, (1971) 490.
2 V.A. Davankov, *Adv. Chromatogr.*, 18 (1980) 139.
3 V.A. Davankov, A.A. Kurganov and A.S. Bochkov, *Adv. Chromatogr.*, 22 (1983) 71.
4 G. Gübitz, W. Jellenz, G. Löfler and W. Santi, *J. High Resolut. Chromatogr. Chromatogr. Commun.*, 2 (1979) 145.
5 W. Lindner, *Naturwissenschaften*, 67 (1980) 354.
6 H. Engelhardt and S. Kromidas, *Naturwissenschaften*, 67 (1980) 353.
7 P. Roumeliotis, K.K. Unger, A. Kurganov and V.A. Davankov, *J. Chromatogr.*, 255 (1983) 51.

8 W. Lindner and C. Pettersson, in J.W. Wainer (Editor), *LC in Pharmaceutical Development*, Aster, Springfield, VA, 1985, p. 63.
9 V.A. Davankov, *Ligand Exchange Chromatography*, CRC Press, Boca Raton, FL, 1988, p. 67.
10 V.A. Davankov, *Chromatographia*, 27 (1989) 475.
11 G. Gübitz, *GIT Fachz. Lab., Suppl. Chromatogr.*, 4/85 (1985) 6.
12 W. Lindner, *Chimia*, 35 (1981) 294.
13 A.W. Lochead and G.R. Proctor, *J. Chem. Soc., Perkin Trans. 1* (1984) 2477.
14 C. Rosini, C. Bertucci, D. Pini, P. Altemura and P. Salvadori, *Tetrahedron Lett.*, 26 (1985) 3361.
15 W.H. Pirkle and C.J. Welch, *J. Chromatogr.*, 589 (1992) 45.
16 W.H. Pirkle and R.S. Readnour, *Chromatographia*, 31 (1991) 129.
17 B. Feibush, M.J. Cohen and B.L. Karger, *J. Chromatogr.*, 282 (1983) 3.
18 E. Veigl, W. Lindner and B. Boehs, in preparation.
19 V.A. Davankov, Y.A. Zolotarev and A.A. Kurganov, *J. Liq. Chromatogr.*, 2 (1979) 1191.
20 V.A. Davankov and A.A. Kurganov, *Chromatographia*, 17 (1983) 686.
21 J. Boue, R. Audebert and C. Quivoron, *J. Chromatogr.*, 204 (1981) 185.

Journal of Chromatography A, 660 (1994) 269–273
Elsevier Science B.V., Amsterdam

CHROMSYMP. 2927

Stereoselective effects in the separation of enantiomers of omeprazole and other substituted benzimidazoles on different chiral stationary phases

Karin Balmér*, Bengt-Arne Persson and Per-Olof Lagerström

Bioanalytical Chemistry, Astra Hässle AB, S-431 83 Mölndal (Sweden)

ABSTRACT

The enantioselective separation of omeprazole on different chiral stationary phases was investigated. The two enantiomers could be resolved on three different phases with immobilized protein, Chiral-AGP, Ultron ES-OVM and BSA-DSC, employing aqueous mobile phases with 2-propanol as organic modifier. On Chiralpak AD, an amylose-based chiral stationary phase, the enantiomers of omeprazole and three analogues could be separated using a non-polar hexane–ethanol mobile phase. For omeprazole the retention order was reversed when 2-propanol was replaced with ethanol or methanol as the modifier of hexane in the mobile phase.

INTRODUCTION

The development of new chiral stationary phases for liquid chromatography has enormously enhanced the tools for the separation of stereoisomers in biomedical analysis. The interest in and the demand for studies on the pharmacokinetics of individual enantiomers after administration of drugs as racemates have rapidly increased. We have previously reported the enantioselective determination of metoprolol by liquid chromatography on Chiral-AGP [1] and Chiralcel OD [2] and also of almokalant [3], which in addition to an asymmetric carbon in the amino alcohol structure contains a sulphoxide group, giving a total of four isomers.

Omeprazole is an inhibitor of gastric acid secretion and is widely used as an antiulcer drug and against other acid-related diseases. Omeprazole is a substituted benzimidazole containing a sulphoxide group and is administered as a racemate. The two enantiomers of omeprazole and related benzimidazoles were separated by Allenmark *et al.* [4] using a stationary phase of bovine serum albumin (BSA) immobilized on silica. More recently, Erlandsson *et al.* [5] used trisphenylcarbamoylcellulose coated on 3-aminopropylsilica, Marle *et al.* [6] cellulase immobilized on diol silica and Vandenbosch *et al.* [7] three different protein-based phases in a comparative study. Gaffney *et al.* [8] resolved phenyl vinyl sulphoxide by liquid chromatography on a Chiralcel OB column and studied different alcohols as modifiers in the non-polar mobile phase.

In this study we examined the separation of the enantiomers of omeprazole on different chiral stationary phases and also of three structural analogues on one of the columns. We used three phases with immobilized protein: Chiral-AGP with α_1-acid glycoprotein, Ultron ES-OVM with ovomucoid and BSA-DSC with bovine serum albumin cross-linked into 3-aminopropylsilica using N-succinimidyl carbonate [9]. We could separate the enantiomers on all three columns and our studies were limited to the effect of pH and a comparison of two organic

* Corresponding author.

0021-9673/94/$07.00 © 1994 Elsevier Science B.V. All rights reserved
SSDI 0021-9673(93)E0922-H

modifiers in the aqueous mobile phase. On Chiralcel OD and Chiralpak AD, which contain cellulose and amylose tris(3,5-dimethylphenylcarbamate), respectively, coated on macroporous silica we also achieved the resolution of the enantiomers of omeprazole. The best enantioselectivity was achieved with Chiralpak AD, where interesting selectivity effects were observed by variation of the nature of the alcohol as modifier in the non-polar mobile phase. We also examined the enantioselectivity of this chiral stationary phase for a number of other benzimidazoles with different substitution patterns.

EXPERIMENTAL

Chemicals

Omeprazole, lansoprazole, pantoprazole and timoprazole (Fig. 1) were obtained from Medicinal Chemistry, Astra Hässle, acetonitrile, hexane, methanol and 2-propanol (HPLC grade) from Rathburn (Walkerburn, UK), ethanol from Kemetyl (Stockholm, Sweden) and 1-propanol and buffer substances of analytical-reagent grade from Merck (Darmstadt, Germany). A Milli-Q system (Millipore, Molsheim, France) was used to supply purified water.

Instrumentation

The liquid chromatograph was composed of a Gynkotek 480 pump (Germering, Munich, Germany), a Kontron 460 autosampler (Tegimenta, Rotkreuz, Switzerland) and a Kratos (Ramsey, NJ, USA) Spectroflow 783 UV detector operated at 302 mn. A thermostated bath (Lauda RMS, Königshofen, Germany) was used to control the water temperature in the column jacket to 35°C if not stated otherwise. The chromatograms were processed by an SP 4400 integrator (Spectra-Physics, San José, CA, USA).

The analytical columns were Chiral-AGP, 5 μm (100 × 4.0 mm I.D.) from ChromTech (Stockholm, Sweden), Ultron ES-OVM (150 × 4.6 mm I.D.) from Rockland Technologies (Newport, DE, USA), BSA-DSC (100 × 4.6 mm I.D.), kindly supplied by Professor S. Allenmark (Göteborg, Sweden) and Chiralpak AD and Chiralcel OD (250 × 4.6 mm I.D.) from Daicel Chemical Industries (Tokyo, Japan).

Test solutions

Standard solutions were prepared in the respective aqueous mobile phase for chromatography on the columns with a protein-bonded phase. With the Daicel columns and non-polar mobile phases the substituted benzimidazoles were dissolved in ethanol, which could be injected in small volumes (10–20 μl) without causing any peak distortion. Larger volumes, 50–100 μl, were injected after dilution with mobile phase.

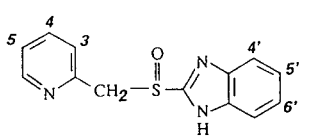

	3	4	5	4'	5'	6'
I	-	-	-	-	-	-
II	CH_3	OCH_3	CH_3	-	OCH_3	-
III	CH_3	OCH_2CF_3	-	-	-	-
IV	OCH_3	OCH_3	-	-	$OCHF_2$	-

Fig. 1. Structure of analytes. I = Timoprazole: II = omeprazole; III = lansoprazole; IV = pantoprazole.

RESULTS AND DISCUSSION

Most of the experiments were performed with omeprazole as the solute, as the two enantiomers of this substance were available and the elution order could be estimated. The other substituted benzimidazoles studied were included in the separation on the Chiralpak AD column in order to illustrate the resolution of compounds with different substituent patterns and to indicate the complexity but also the possibilities. The structures are shown in Fig. 1.

Protein stationary phases

The enantiomers of omeprazole could be separated on both the Chiral-AGP and the BSA-DSC column with the (+)-isomer eluting first. 2-Propanol was the organic modifier in phos-

phate buffer solution, pH 6.0–7.0 ($I = 0.1$), and the separation factor α was about 1.3 and 1.9, respectively. There was a decrease in α when the pH was increased from 6.0 to 7.0, in particular on the BSA-DSC phase. The Ultron ES-OVM column also resolved the two enantiomers, but they eluted in the reverse order, the (−)-enantiomer first, with a separation factor of about 1.2. With the Chiral-AGP stationary phase there was a major increase in α when 4% 2-propanol was replaced with 10% acetonitrile as the organic modifier in the aqueous mobile phase; α ranged from 2.0 to 2.4 and increased with increasing pH. For the analytical columns with a protein stationary phase the plate number was in the range 6000–10 000 per metre. The three stationary phases retained omeprazole to various extents, which was compensated for by the content of organic modifier as exemplified in the chromatograms in Fig. 2.

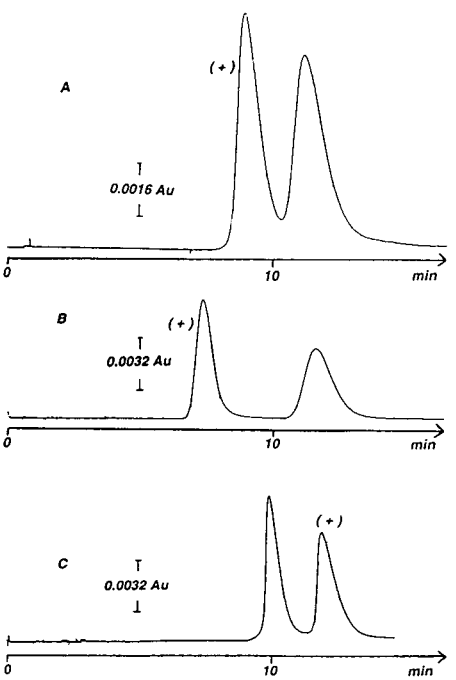

Fig. 2. Enantioselective separation of omeprazole on protein-based columns at pH 7.0 ($I = 0.1$), flow-rate 1.0 ml/min and ambient temperature. (A) Chiral-AGP, 3% 2-propanol, $\alpha = 1.26$; (B) BSA-DSC, 5% 2-propanol, $\alpha = 1.63$; (C) Ultron ES-OVM, 10% 2-propanol, $\alpha = 1.22$.

Amylose-based stationary phase

Previous attempts to achieve a baseline resolution of the enantiomers of omeprazole were not successful using cellulose-based chiral stationary phases, Chiralcel OD giving the best results of those tested and an α value of about 1.1. The corresponding amylose-based phase, Chiralpak AD, showed superior enantioselectivity for omeprazole, however, but also resolved racemates of the other sulphoxide-substituted benzimidazoles to different extents. The nonpolar mobile phase consisted of ethanol–hexane (20:80, v/v) and the capacity and separation factors are given in Table I. With this mobile phase omeprazole is resolved with an α value of 1.8 and the (−)-enantiomer is eluted first. The separation factor is even larger (3.6) for timoprazole, a compound without substituents (Fig. 1). The other two substances, drugs commercially available or in the clinical phase, with different kinds of substituents show much lower separation factors in this system.

When ethanol was replaced with 1- or 2-propanol as the modifier of hexane in the mobile phase, the retention order for omeprazole was changed and the (+)-isomer eluted first, as shown in Fig. 3. The separation factor was in the range 1.1–1.3. The chromatographic performance was lower than that with ethanol but was slightly improved by addition of water (1 g/l). An interesting effect was that the addition of water decreased the capacity factors, k', with 1-propanol as modifier but increased k' with 2-propanol as modifier. As the retention order

TABLE I

CAPACITY AND SEPARATION FACTORS FOR ENANTIOSELECTIVE SEPARATION OF SULPHOXIDE COMPOUNDS ON THE CHIRALPAK AD COLUMN

Mobile phase: ethanol–hexane (20:80, v/v).

Substance	k'_1	α
Timoprazole	3.98	3.63
Omeprazole	4.86	1.81
Lansoprazole	2.91	1.15
Pantoprazole	6.10	1.19

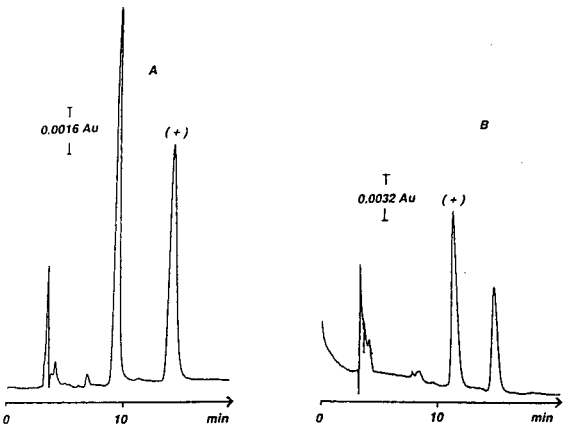

Fig. 3. Enantioselective separation of omeprazole on Chiralpak AD column, flow-rate 1.0 ml/min. (A) Mobile phase ethanol–hexane (35:65, v/v), $k'_1 = k'_{(-)} = 2.66$, $\alpha = 1.72$; (B) mobile phase 2-propanol–hexane, (14:86, v/v) $k'_1 = k'_{(+)} = 4.16$, $\alpha = 1.20$.

relative to the propanols is the opposite of that with ethanol, mixtures of these solvents in certain proportions will result into a single peak; $\alpha = 1.0$ was obtained with 4% of ethanol and 10% of one of the propanols. The addition of methanol gave the same retention order as ethanol but was only used together with 2-propanol owing to its poor solubility in hexane.

A chemometric approach was employed to study the influence of methanol on k' for the omeprazole enantiomers and to examine the retention mechanism. The design was a full factor system with the content of methanol and 2-propanol as factors and the quadratic terms were taken into consideration in the MODDE program version 2.0 from Umetri (Umeå, Sweden). The response factors were the logarithms of the k' values and the corresponding α value determined for the isomers of omeprazole. The influence of methanol and 2-propanol on $k'(+)$, $k'(-)$ and α is illustrated in Fig. 4. As can be seen, the addition of methanol reversed the retention order and α increased from 0.85 to 2.5. This enhancement of α was caused by the different influences on $k'(+)$ and $k'(-)$ by methanol; $k'(+)$ remains fairly constant with methanol addition whereas $k'(-)$ is influenced by both 2-propanol and methanol. A much more advanced study on the chiral resolution of benzimidazole sulphoxides using a multivariate statistical technique was presented recently [10].

The unsubstituted compound timoprazole showed the highest enantioselectivity in the ethanol–hexane phase (Table I). It was then of

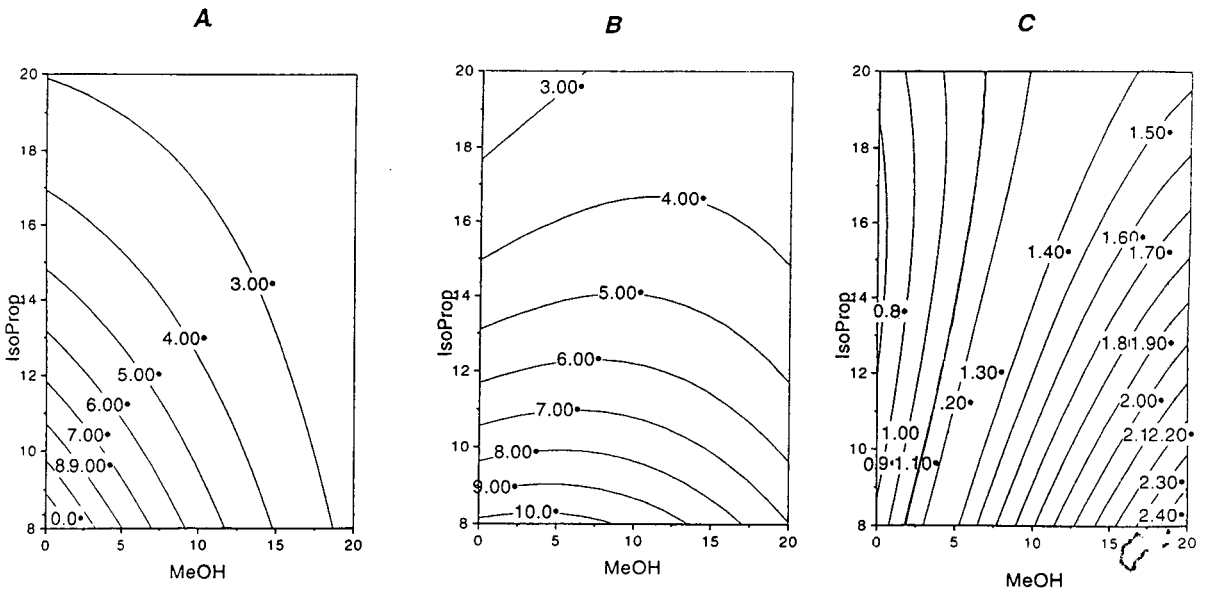

Fig. 4. Contour plots of (A) $k'_{(-)}$, (B) $k'_{(+)}$ and (C) α from the chemometric study of the isomers of omeprazole on Chiralpak AD.

interest to examine the influence of methanol addition to a mobile phase of hexane–2-propanol on the separation factor for this compound. One of the isomers of timoprazole had about the same capacity factor as the (−)-enantiomer of omeprazole and decreased in the same way when the methanol content increased. The other enantiomer of timoprazole, assumed to be the (+)-form, demonstrated a much more complex retention pattern. First it paralleled the (−)-enantiomer, giving a fairly constant α value of about 1.2, but with a further increase in methanol content the capacity factor of the (+)-isomer increased strongly. This is illustrated in Fig. 5, where the profiles of the capacity factors of timoprazole are plotted. The separation factor between the enantiomers reached a value of about 2.2 at 8% methanol in a mobile phase also containing 20% of 2-propanol in hexane. It seems that there is competition between the two alcohols as modifiers in the mobile phase. The drastic effect on the retention of one of the two enantiomers of timoprazole may be due to methanol at higher concentration displacing 2-propanol adsorbed on the chiral stationary phase. If conformational changes occurred, they were found to be completely reversible.

The different behaviours of the enantiomers of omeprazole and timoprazole show that the chiralselective stationary phase Chiralpak AD consists of different sites, as discussed in a previous paper on the separation of amino alcohols on Chiralcel OD [11]. For the (−)-antipodes of omeprazole and timoprazole there is almost no effect from methanol, which indicates that the (−)-enantiomer is not retained by the site influenced by this modifier. For the (+)-enantiomers there is a significantly different effect leading to a reversed retention order for the omeprazole isomers and a strange elution profile for timoprazole, despite the latter being an unsubstituted compound. This emphasizes the complexity of the chiral stationary phases and the difficulties of elucidating enantioselectivity effects, but also points to the possibilities of influencing the separation by components in the non-polar mobile phase. Conformational changes in the chiral stationary phase, which have been found to be reversible, mediated by low-molecular-mass alcohols, in this study and by water in previous work [11], can be considered to be responsible for the observed effects on the enantioselectivity.

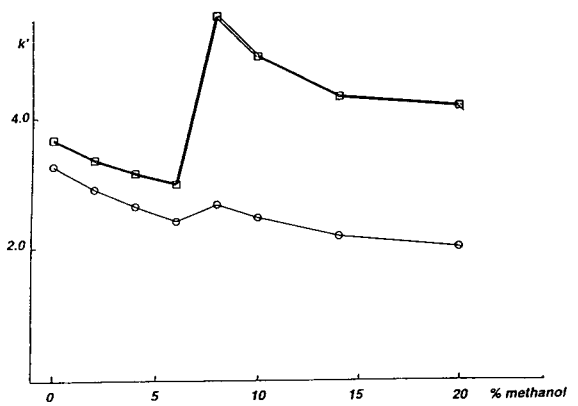

Fig. 5. Influence on the capacity factors, k', of the isomers of timoprazole of the addition of methanol to 2-propanol–hexane (20:80, v/v) mobile phase. Chiralpak AD column. □ = (+)-Isomer; ○ = (−)-isomer.

REFERENCES

1 B.A. Persson, K. Balmér, P.O. Lagerström and G. Schill, *J. Chromatogr.*, 500 (1990) 629.
2 K. Balmér, A. Persson, P.O. Lagerström, B.A. Persson and G. Schill, *J. Chromatogr.*, 553 (1991) 391.
3 K. Balmér, P.O. Lagerström, S. Larsson and B.A. Persson, *J. Chromatogr.*, 631 (1993) 191.
4 S. Allenmark, B. Bomgren, H. Borén and P.O. Lagerström, *Anal. Biochem.*, 136 (1984) 293.
5 P. Erlandsson, R. Isaksson, P. Lorentzon and P. Lindberg, *J. Chromatogr.*, 532 (1990) 305.
6 I. Marle, P. Erlandsson, L. Hansson, R. Isaksson, C. Pettersson and G. Pettersson, *J. Chromatogr.*, 586 (1991) 233.
7 C. Vandenbosch, D. Massart and W. Lindner, *J. Pharm. Biomed. Anal.*, 10 (1992) 895.
8 M.H. Gaffney, R.M. Stiffin and I.W. Wainer, *Chromatographia*, 27 (1989) 15.
9 S. Andersson, R.A. Thompson and S.G. Allenmark, *J. Chromatogr.*, 591 (1992) 65.
10 P. Camilleri, D.J. Livingstone, J.A. Murphy and D.T. Manallack, *J. Comput.-Aided Mol. Des.*, 7 (1993) 61.
11 K. Balmér, P.O. Lagerström, B.A. Persson and G. Schill, *J. Chromatogr.*, 592 (1992) 331.

Journal of Chromatography A, 660 (1994) 275–281
Elsevier Science B.V., Amsterdam

CHROMSYMP. 2879

Retention and enantioselective properties of ovomucoid-bonded silica columns

Influence of physical properties of base materials and spacer length

Jun Haginaka*, Chikako Seyama and Tokiko Murashima

Faculty of Pharmaceutical Sciences, Mukogawa Women's University, 11-68 Koshien Kyuban-cho, Nishinomiya 663 (Japan)

Hiroya Fujima and Hiroo Wada

Shinwa Chemical Industries Ltd., 50 Kagakatsu-cho, Fushimi-ku, Kyoto 612 (Japan)

ABSTRACT

The influence of the physical properties of base silica materials and spacer length on chiral separation of enantiomers on ovomucoid (OVM)-bonded materials was investigated. With regard to the pore size of the base silica materials, the 300-Å materials gave higher enantioselectivity than the 120-Å materials, despite the smaller amounts of bonded OVM proteins. However, higher resolution was obtained with the latter materials. With regard to the spacer length, aminopropyl (AP)-, aminobutyl-, N-(4-aminobutyl)-3-aminopropyl- and N-(6-aminohexyl)-3-aminopropyl-silica gels were activated by N,N'-disuccinimidyl carbonate (DSC) and the proteins were bound. The first two materials showed excellent chiral resolution properties for the solutes tested, and the AP materials gave higher enantioselectivity and resolution. On the other hand, only oxprenolol enantiomers were slightly resolved on the last two materials. Also, AP-silica gels activated by DSC were compared with glycerylpropyl (GP)-silica gels activated by 1,1'-carbonyldiimidazole. The former materials gave higher resolution for acidic and basic solutes despite the lower enantioselectivity, whereas for the uncharged hexobarbital the latter materials gave higher enantioselectivity and almost equal resolution. The above results reveal that the 120-Å base silica gels are more suitable than the 300-Å base silica gels for obtaining larger amounts of bonded OVM proteins and that a less hydrophobic spacer such as an AP group and a hydrophilic spacer such as a GP group are suitable.

INTRODUCTION

Protein-bonded stationary phases including albumins such as bovine serum albumin (BSA) [1] and human serum albumin [2] and mucoids such as α_1-acid glycoprotein [3] and ovomucoid [4] from egg white have been developed for the separation of enantiomeric forms. Among these, an ovomucoid-bonded silica column is of special interest because of its long-term stability and because it is suitable for separating a wide range of enantiomeric mixtures [5–7]. It is well known that many factors such as the physical properties of the base silica materials, spacer length and bonding method affect the resolution of enantiomeric pairs on protein-bonded stationary phases [8–10]. In this study, we investigated the in-

* Corresponding author.

0021-9673/94/$07.00 © 1994 Elsevier Science B.V. All rights reserved
SSDI 0021-9673(93)E0770-U

fluences of these factors on the retention, enantioselectivity and resolution of various solutes on ovomucoid-bonded silica columns.

EXPERIMENTAL

Reagents and materials

Ibuprofen, ketoprofen, chlorpheniramine maleate and hexobarbital were kindly donated by Kaken Pharmaceutical (Tokyo, Japan), Chugai Pharmaceutical (Tokyo, Japan), Essex Nippon (Osaka, Japan) and Teikoku Chemicals (Osaka, Japan). Tolperisone hydrochloride was purchased from Sigma (St. Louis, MO, USA). The structures of the racemic compounds used in this study are shown in Fig. 1. OVM proteins from egg white were purchased from Eisai (Tokyo, Japan). N,N′-Disuccinimidyl carbonate (DSC) and 1,1′-carbonyldiimidazole (CDI) were purchased from Sigma, 2-propanol, ethanol, methanol and acetonitrile of HPLC grade from Wako (Osaka, Japan) and 3-aminopropyl (AP)-triethoxysilane, 4-aminobutyl (AB)-triethoxysilane and 3-glycidoxypropyltrimethoxysilane from Chisso (Tokyo, Japan). N-(4-Aminobutyl)-3-aminopropyl (ABAP)-trimethoxysilane and N-(6-aminohexyl)-3-aminopropyl (AHAP)-trimethoxysilane were kindly donated by Shin-etsu Chemical Industries (Tokyo, Japan). Silica gels were obtained from Shinwa Chemical Industries (Ultron-120, particle diameter 5 μm, pore size 120 Å, specific surface area 300 m^2/g, and Ultron-300, particle diameter 5 μm, pore size 300 Å, specific surface area 100 m^2/g). Other solvents and reagents were used as received.

Water purified with a Nanopure II unit (Barnstead, Boston, MA, USA) was used for the preparation of the eluent and sample solutions.

Preparation of silica gels having different spacer lengths

Ultron silica gel (5 g) was dried *in vacuo* over P_2O_5 at 150°C for 6 h and added to 120 ml of dry toluene. The mixture was heated at reflux until all the water had been removed as an azeotrope into a Dean–Stark-type trap. Next, the silylating agents described above, corresponding to 10 μmol/m^2 of the specific surface area, were added and reacted for 8 h, except for 3-glycidoxypropyltrimethoxysilane (48 h). The reaction mixture was cooled to room temperature, filtered and washed with toluene and methanol. The isolated silica gels were dried *in vacuo* over P_2O_5 at 60°C for 2 h. To the silica gels reacted with 3-glycidoxypropyltrimethoxysilane, 80 ml of perchloric acid (pH 3.0) were added and the mixture was refluxed for 4 h. The reaction mixture was cooled to room temperature, filtered and washed with water and methanol. The isolated 3-glycerylpropyl (GP)-silica gel was dried *in vacuo* over P_2O_5 at 60°C for 2 h. The obtained silica gels having different spacers are abbreviated as shown in Fig. 2.

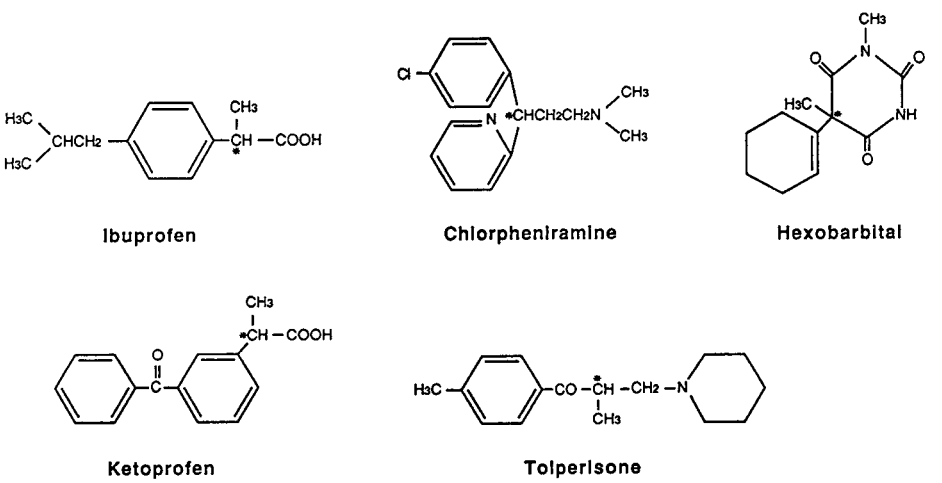

Fig. 1. Structures of the enantiomers studied.

AP: ≡Si–O–Si(–)–(CH2)3NH2

AB: ≡Si–O–Si(–)–(CH2)4NH2

ABAP: ≡Si–O–Si(–)–(CH2)3NH(CH2)4NH2

AHAP: ≡Si–O–Si(–)–(CH2)3NH(CH2)6NH2

GP: ≡Si–O–Si(–)–(CH2)3OCH2CH(OH)CH2OH

Fig. 2. Spacers used and their abbreviations.

Activation of silica gels having amino or hydroxyl groups

AP-, AB-, ABAP- and AHAP-silica gels were activated by DSC. Amounts of 5 g of the gels were slurried in 70 ml of acetonitrile and reacted with 5 g of DSC for 24 h at 30°C. The reaction mixture was filtered and washed with acetonitrile, water, methanol and dichloromethane. GP-silica gels were activated by CDI. Amounts of 5 g of the gels were slurried in 30 ml of dioxane. To the mixture, 4 g of CDI dissolved in 20 ml of dioxane were added and reacted for 4 h at 30°C. The reaction mixture was filtered and washed with dioxane and methanol. Both silica gels were dried *in vacuo* over P_2O_5 at 60°C for 2 h.

Preparation of OVM-bonded materials

OVM was bound to DSC-activated AP-, AB-, ABAP- and AHAP-silica gels as follows: 2 g of the DSC-activated silica gels were slurried in 20 m*M* phosphate buffer (pH 6.8). To the mixture, 2 g of OVM proteins dissolved in 20 ml of the same buffer were added slowly and stirred for 15 h at 30°C. Similarly, OVM was bonded to CDI-activated silica gels as follows: 2 g of the CDI-activated GP silica gels were slurried in 20 m*M* phosphate buffer (pH 7.8). To the mixture, 2 g of OVM proteins dissolved in 20 ml of the same buffer were added slowly and stirred for 15 h at 30°C. Both reaction mixtures were then filtered and washed with water and methanol. The isolated AP, AB, ABAP and AHAP materials were dried *in vacuo* over P_2O_5 at 40°C for 6 h.

These OVM-bonded materials were packed into a 150 or 100 × 4.6 mm I.D. stainless-steel column by the slurry packing method.

Chromatography

The HPLC system used was composed of an LC-9A pump, an SPD-6A spectrophotometer, a SIL-6B autoinjector, a C-R4A integrator and an SCL-6B system controller (all from Shimadzu, Kyoto, Japan). The flow-rate was maintained at 0.8 or 1.0 ml/min. Detection was performed at 220 or 254 nm.

Capacity factors were calculated from the equation $k' = (t_R - t_0)/t_0$, where t_R and t_0 are the elution times of retained and unretained solutes, respectively, and k'_1 and k'_2 correspond to the capacity factors of the first- and second-eluted peaks, respectively. The retention time of unretained solute, t_0, was measured by injecting a solution whose organic modifier content was slightly different from that of the eluent used. The enantioseparation factor was calculated from the equation $\alpha = k'_2/k'_1$. Resolution was calculated from the equation $R_s = 2(t_2 - t_1)/(t_{w1} + t_{w2})$, where t_{w1} and t_{w2} are the widths of the first- and second-eluted peaks, respectively. All separations were carried out at 25°C using a CO-1093C column oven (Uniflows, Tokyo, Japan).

The eluents, which are prepared by using phosphoric acid–sodium dihydrogenphosphate or sodium dihydrogenphosphate–disodium hydrogenphosphate and organic modifier, are specified in the tables.

Sample preparation

A known amount of racemic solute was dissolved in methanol or water and the solution was diluted with the eluent to the desired concentration. A 20-μl aliquot of the sample solution was loaded on to the column. The amount loaded was less than 0.5 μg.

RESULTS AND DISCUSSION

Amounts of bonded OVM proteins

Table I shows the amounts of bonded OVM proteins on the various materials. With regard to comparison of the base silica gels having pore sizes of 120 and 300 Å (AP-120 and AP-300,

TABLE I

AMOUNTS OF BONDED OVM PROTEINS ON VARIOUS MATERIALS

Spacer[a]	Pore size (Å)	Bonded protein (μmol/g)
AP-120[b]	120	4.1
AP-300[b]	300	1.3
AB	120	4.4
ABAP	120	3.9
AHAP	120	0.9
GP	120	2.0

[a] AP = 3-aminopropyl; AB = 4-aminobutyl; ABAP = N-(4-aminobutyl)-3-aminopropyl; AHAP = N-(6-aminohexyl)-3-aminopropyl; GP = glycerylpropyl.
[b] 120 and 300 refer to the average pore sizes of the base silica materials.

respectively), the former materials showed about three times larger amounts of the OVM proteins than the latter materials. As the coverages of AP phases of the AP-120 and AP-300 silica materials were about 1000 and 350 μmol/g, respectively, there are good correlations between the coverages of the AP phases and the amounts of bonded OVM proteins. Note that only 0.4% of the AP phases should be used for binding of the OVM proteins. For the preparation of BSA-bonded materials, Thompson *et al.* [8] compared 100- and 300-Å base silica materials, which resulted in amounts of the bonded proteins of 3.2 and 1.1 μmol/g, respectively. Taking into account the molecular masses of OVM (M_r 28 000) and BSA (M_r 68 000), our results agreed well with those of Thompson *et al.* [8]. The AP, AB and ABAP materials showed almost identical amounts of bonded OVM proteins, whereas the AHAP material showed smaller amounts, owing to the lower coverages of the AHAP than the AP, AB and ABAP phases. The GP materials showed about half the amounts of bonded proteins compared with the AP and AB materials. Taking into account the coverages of GP phases (*ca.* 500 μmol/g), the activation method does not affect the protein coverages. OVM proteins were bound to the AP, AB, ABAP and AHAP materials by a urea bond. On the other hand, the OVM proteins were bound to the GP materials by a carbamate bond. The results obtained above reveal that the amounts of bonded OVM proteins are mainly dependent on the coverages of the spacer phases.

Comparison of base silica materials

Table II shows the influence of pore size of base silica materials on the retention, enantioselectivity and resolution of ketoprofen, chlorpheniramine and hexobarbital. The eluent used was 20 m*M* phosphate buffer containing 10% and 5% of ethanol for the AP-120 and AP-300 materials, respectively. The retention properties of acidic, basic and uncharged solutes could be

TABLE II

COMPARISON OF BASE SILICA MATERIALS FOR RETENTION, ENANTIOSELECTIVITY AND RESOLUTION OF VARIOUS SOLUTES ON OVM-BONDED MATERIAL

HPLC conditions: column, OVM-bonded materials packed into a 100 mm × 4.6 mm I.D. stainless-steel column; eluent, 20 m*M* phosphate buffer–ethanol [90:10 (v/v) for the AP-120 materials and 95:5 (v/v) for the AP-300 materials]; flow-rate, 0.8 ml/min.

Column	Compound	pH 3.2[a]			pH 4.0[a]			pH 5.1[a]			pH 6.0[a]			pH 6.9[a]		
		k_1'	α	R_s	k_1'	α	R_s	k_1'	α	R_s	k_1'	α	R_s	k_1'	α	R_s
AP-120	Ketoprofen	23.6	1.34	3.00	32.3	1.24	2.58	13.0	1.11	1.15	3.54	1.00		1.16	1.00	
	Chlorpheniramine				0.19	1.77	0.59	2.05	1.88	2.51	11.2	2.09	5.80	41.3	2.12	7.28
	Hexobarbital	0.46	1.23	0.53	0.61	1.22	0.76	0.68	1.19	0.69	0.80	1.26	1.10	0.82	1.40	1.91
AP-300	Ketoprofen	8.26	1.49	1.92	15.3	1.45	2.24	6.28	1.32	1.88	1.44	1.17	0.80	0.47	1.00	
	Chlorpheniramine				0.30	1.00		1.72	1.95	2.46	6.67	2.33	3.92	25.3	2.49	4.05
	Hexobarbital	0.28	1.00		0.34	1.29	0.53	0.46	1.34	0.68	0.44	1.41	0.82	0.50	1.56	1.72

[a] Buffer pH.

elucidated by taking into account the isoelectric point of an ovomucoid protein (pI = 3.8–4.3) and the pK_a values of the solutes, as reported previously [11]. The capacity factors of all the solutes on the former materials are about double those on the latter materials, despite the higher organic modifier content. These results reveal that the retentions of solutes are dependent on the amounts of bonded OVM proteins. On the other hand, the AP-300 materials gave higher enantioselectivities than the AP-120 materials, despite the shorter retentions of the solutes on the former materials. This suggests that all the proteins bound to the AP-120 materials do not work effectively for chiral recognition of solutes. However, the resolution of basic and acidic solutes, except for ketoprofen at an eluent pH of 5.1, on the AP-300 materials was lower than that on the AP-120 materials. This might be because a solute might interact with the base silica materials, because of smaller amounts of the bonded proteins. We therefore prepared OVM-bonded materials by using base silica materials having an average pore size of 120 Å in the experiments described below.

Effect of spacer length for chiral recognition

Table III, IV and V show the influence of spacer length on the retention, enantioselectivity and resolution of acidic, basic and uncharged solutes, respectively, where ethanol is used as an organic modifier. It is well known [6,7,12] that organic modifiers affect the retention and enantioselectivity of solutes on an OVM-bonded column. We examined the influence of the type of organic modifier on the retentions and enantioselectivity of the solutes. Similar trends in retention and enantioselectivity were obtained with all five columns, and therefore only the data for ethanol are given in Tables III–V.

No enantioseparations of solutes on the ABAP and AHAP materials were observed except for a slight resolution of oxprenolol at an eluent pH of 6.9. Oda *et al.* [13] reported that a hydrophobic spacer with a C_6 carbon chain was suitable for obtaining higher enantioselectivity on avidin-bonded materials. We bound OVM to base silica materials by using the same spacer as Oda *et al.* [13]. However, the enantioselectivity obtained with the materials was poor, as with the ABAP and AHAP materials. Miwa *et al.* [14]

TABLE III

EFFECT OF SPACER LENGTH ON RETENTION, ENANTIOSELECTIVITY AND RESOLUTION OF ACIDIC SOLUTES ON OVM-BONDED MATERIAL

All materials were prepared by using the 120-Å base silica materials. HPLC conditions: column, OVM-bonded materials packed into a 150 mm × 4.6 mm I.D. stainless-steel column; eluent, 20 mM phosphate buffer–ethanol [90:10 (v/v) for the AP, AB, ABAP and AHAP materials and 95:5 (v/v) for the GP materials]; flow-rate, 1.0 ml/min.

Column	Compound	pH 3.2[a]			pH 4.0[a]			pH 5.1[a]			pH 6.0[a]			pH 6.9[a]		
		k_1'	α	R_s	k_1'	α	R_s	k_1'	α	R_s	k_1'	α	R_s	k_1'	α	R_s
AP	Ibuprofen	7.17	1.37	2.69	11.7	1.34	2.88	7.75	1.17	1.34	2.58	1.08	0.54	0.84	1.00	
	Ketoprofen	23.0	1.34	3.05	34.2	1.21	2.32	14.0	1.09	1.00	4.04	1.00		1.27	1.00	
AB	Ibuprofen	9.54	1.27	1.86	14.2	1.27	2.07	8.74	1.14	1.10	3.19	1.00		0.87	1.00	
	Ketoprofen	27.8	1.27	1.99	37.7	1.18	1.33	16.1	1.07	0.54	5.13	1.00		1.47	1.00	
ABAP	Ibuprofen	13.7	1.00		21.9	1.00		16.9	1.00		5.07	1.00		1.57	1.00	
	Ketoprofen	29.9	1.00		46.6	1.00		28.2	1.00		8.24	1.00		2.71	1.00	
AHAP	Ibuprofen	13.2	1.00		19.8	1.00		14.1	1.00		4.86	1.00		1.57	1.00	
	Ketoprofen	29.9	1.00		44.5	1.00		24.5	1.00		8.19	1.00		3.21	1.00	
GP	Ibuprofen	4.24	1.29	1.14	7.08	1.34	1.01	4.52	1.23	0.69	1.37	1.00		0.32	1.00	
	Ketoprofen	15.7	1.54	2.57	27.2	1.47	2.63	11.5	1.28	1.52	2.49	1.11	0.32	0.84	1.00	

[a] Buffer pH.

TABLE IV

EFFECT OF SPACER LENGTH ON RETENTION, ENANTIOSELECTIVITY AND RESOLUTION OF BASIC SOLUTES ON OVM-BONDED MATERIAL

All materials were prepared by using the 120-Å base silica materials. HPLC conditions: column, OVM-bonded materials packed into a 150 mm × 4.6 mm I.D. stainless-steel column; eluent, 20 m*M* phosphate buffer–ethanol [90:10 (v/v) for the AP, AB, ABAP and AHAP materials and 95:5 (v/v) for the GP materials]; flow-rate, 1.0 ml/min.

Column	Compound	pH 4.0[a]			pH 5.1[a]			pH 6.0[a]			pH 6.9[a]		
		k_1'	α	R_s	k_1'	α	R_s	k_1'	α	R_s	k_1'	α	R_s
AP	Chlorpheniramine	0.33	1.36	0.72	2.56	1.75	3.33	8.73	1.92	5.82	40.4	2.03	7.64
	Tolperisone				0.76	1.90	3.04	2.53	1.51	2.57	12.0	1.33	2.58
AB	Chlorpheniramine	0.44	1.41	1.04	3.40	1.74	3.77	13.2	1.89	4.84	56.5	1.97	4.60
	Tolperisone				0.96	1.75	2.60	3.74	1.41	1.74	16.4	1.27	1.54
ABAP	Chlorpheniramine	0.63	1.00		3.83	1.00		14.4	1.00		43.2	1.00	
	Tolperisone	0.13	1.00		1.32	1.00		4.88	1.00		12.1	1.00	
AHAP	Chlorpheniramine	0.62	1.00		5.55	1.00		23.7	1.00		48.7	1.00	
	Tolperisone	0.16	1.00		2.09	1.00		9.92	1.00		14.5	1.00	
GP	Chlorpheniramine	0.66	1.00		2.96	1.76	2.37	12.6	2.01	3.07	45.7	2.18	5.00
	Tolperisone	0.41	1.61	0.26	1.07	1.77	1.39	4.35	1.60	1.64	13.6	1.42	2.10

[a] Buffer pH.

reported that OVM-bonded polymer gels, which contain a polyamine (pentaethylenehexamine), had excellent chiral recognition properties for the basic chlorprenaline and chlorpheniramine. On the other hand, enhanced retention of acid ketoprofen was obtained with the polymer gels but no chiral resolution was achieved because of the strong achiral interaction with the polymer matrices. These results suggest that the superfluous achiral interaction of a solute with a hydro-

TABLE V

EFFECT OF SPACER LENGTH ON RETENTION, ENANTIOSELECTIVITY AND RESOLUTION OF HEXOBARBITAL ON AN OVM-BONDED MATERIAL

All materials were prepared by using the 120-Å base silica materials. HPLC conditions: column, OVM-bonded materials packed into a 150 mm × 4.6 mm I.D. stainless-steel column; eluent, 20 m*M* phosphate buffer–ethanol [90:10 (v/v) for the AP, AB, ABAP and AHAP materials and 95:5 (v/v) for the GP materials]; flow-rate, 1.0 ml/min.

Column	pH 3.2[a]			pH 4.0[a]			pH 5.1[a]			pH 6.0[a]			pH 7.0[a]		
	k_1'	α	R_s	k_1'	α	R_s	k_1'	α	R_s	k_1'	α	R_s	k_1'	α	R_s
AP	0.69	1.00		0.84	1.18	0.75	1.00	1.21	1.07	0.86	1.28	1.39	0.96	1.42	1.95
AB	0.68	1.15	0.34	0.86	1.18	0.54	1.06	1.20	0.75	1.03	1.25	0.70	1.09	1.40	1.18
ABAP	0.74	1.00		0.82	1.00		0.85	1.00		0.83	1.00		0.74	1.00	
AHAP	0.76	1.00		0.78	1.00		0.82	1.00		0.85	1.00		0.77	1.00	
GP	0.49	1.22	0.79	0.66	1.30	1.19	0.73	1.39	0.92	0.83	1.50	1.49	0.65	1.59	1.92

[a] Buffer pH.

phobic and/or positively charged spacer might diminish the chiral interaction of the solute with the OVM protein.

The capacity factors of acidic and basic solutes on the AP, AB, ABAP and AHAP materials were increased with an increase in the hydrophobicity of the spacer, except for those of basic solutes on the AB materials. With regard to enantioselectivity and resolution, the AP materials gave higher enantioselectivity and resolution for acidic solutes than the AB materials. For basic solutes, the AP materials gave almost the same enantioselectivity as the AB materials and higher resolution. The retentions of hexobarbital were almost the same with the four materials, whereas the AP materials gave better enantioselectivity and resolution than the AB materials except for an eluent pH of 3.2.

The enantioselectivity and resolution with the GP material were compared with those for the AP materials. For acidic ibuprofen, the GP materials gave lower enantioselectivity and resolution than the AP materials, whereas for ketoprofen, the GP materials gave higher enantioselectivity and resolution except for resolution at an eluent pH of 3.2. For hexobarbital, the GP materials gave higher enantioselectivity and almost equal resolution. The lower column efficiency of the GP materials for acidic and basic solutes might be due to the smaller amounts of bonded OVM proteins, that is, the solute might interact with the base silica material. However, the GP materials are suitable for the chiral resolution of the uncharged hexobarbital. It is interesting that the ABAP materials, whose spacer length is very similar to that of the GP materials, has no chiral recognition properties. The results obtained above reveal that a less hydrophobic spacer such as an AP group and a hydrophilic spacer such as a GP group are suitable for binding of OVM proteins to silica gels.

In conclusion, the AP materials of pore size 120 Å gave the highest chiral recognition properties among the OVM-bonded materials tested. However, by diminishing the superfluous achiral interaction, including interaction with the base silica material, much more efficient OVM-bonded materials might be obtainable.

REFERENCES

1 S. Allenmark, *J. Liq. Chromatogr.*, 9 (1986) 425.
2 E. Domenici, C. Bertucci, P. Salvadori, G. Felix, I. Cahagne, S. Montellier and I.W. Wainer, *Chromatographia*, 29 (1990) 170.
3 J. Hermansson, *J. Chromatogr.*, 269 (1983) 71.
4 T. Miwa, M. Ichikawa, M. Tsuno, T. Hattori, T. Miyakawa, M. Kayano and Y. Miyake, *Chem. Pharm. Bull.*, 35 (1987) 682.
5 J. Haginaka, J. Wakai, H. Yasuda, K. Takahashi and T. Katagi, *Chromatographia*, 29 (1990) 587.
6 J. Iredale, A.-F. Aubry and I.W. Wainer, *Chromatographia*, 31 (1991) 329.
7 K.M. Kirkland, K.L. Nelson and D.A. McCombs, *J. Chromatogr.*, 545 (1991) 43.
8 R.A. Thompson, S. Anderson and S. Allenmark, *J. Chromatogr.*, 465 (1989) 263.
9 S. Andersson, S. Allenmark, P. Erlandsson and S. Nilsson, *J. Chromatogr.*, 498 (1990) 81.
10 S. Andersson, R.A. Thompson and S.G. Allenmark, *J. Chromatogr.*, 591 (1992) 65.
11 J. Haginaka, T. Murashima, Ch. Seyama, H. Fujima and H. Wada, *J. Chromatogr.*, 631 (1992) 183.
12 J. Haginaka, Ch. Seyama, H. Yasuda, H. Fujima and H. Wada, *J. Chromatogr.*, 592 (1992) 301.
13 Y. Oda, H. Ohe, N. Asakawa, Y. Yoshida, T. Sato and T. Nakagawa, *J. Liq. Chromatogr.*, 15 (1922) 2997.
14 T. Miwa, S. Sakashita, H. Ozawa, J. Haginaka, N. Asakawa and Y. Miyake, *J. Chromatogr.*, 566 (1991) 163.

Journal of Chromatography A, 660 (1994) 283–291
Elsevier Science B.V., Amsterdam

CHROMSYMP. 2910

Monitoring of optical isomers of β-methylphenylalanine in opioid peptides

Antal Péter*

Department of Inorganic and Analytical Chemistry, Attila József University, P.O. Box 440, H-6701 Szeged (Hungary)

Géza Tóth and Erzsébet Cserpán

Hungarian Academy of Sciences, Biological Research Centre, Isotope Laboratory "B" Level, P.O. Box 521, H-6721 Szeged (Hungary)

Dirk Tourwé

Eenheid Organische Chemie, Vrije Universiteit Brussel, Pleinlaan 2, B-1050 Brussels (Belgium)

ABSTRACT

D,L-*erythro*- and D,L-*threo*-β-methylphenylalanines were synthesized and incorporated into the delta opioid receptor-selective deltorphin C peptide by solid-phase peptide synthesis. The enantiomeric composition of β-methylphenylalanine and the diastereomeric composition of the peptide were determined. To distinguish exactly between the two enantiomeric pairs of β-methylphenylalanine, different liquid, gas and thin-layer chromatographic methods are suggested, while the four diastereomers of [β-MePhe^3]deltorphin C can be identified and separated conveniently by high-performance liquid chromatography.

INTRODUCTION

Diastereomers of peptides with biological activity often exhibit antagonistic or agonistic properties which differ greatly from each other. Diastereomeric peptides, isomers in which one or more asymmetric centres have opposite configurations, may have similar or different physico-chemical or biological properties.

In the synthesis of receptor-selective peptides, unusual racemic amino acids are often used. It is therefore very important to develop effective chromatographic methods for the separation of the mixture of diastereomeric peptides and for the characterization and identification of the optical isomers of the amino acids in the pure peptide.

Several papers and reviews covering the development of enantioselective separations have been published. High-performance liquid chromatographic (HPLC) methods can be divided into three main groups: direct separation on chiral columns [1–3], separation on achiral columns with chiral mobile phase additives [3–5] and separation of the diastereoisomers formed by precolumn derivatization with chiral reagents [3,6–17].

The gas chromatographic (GC) separation of amino acid enantiomers is based on precolumn derivatization and analysis on a chiral capillary column [18–21]. The thin-layer chromatography (TLC) of enantiomeric compounds has been possible since Chiralplate (a plate containing a chiral selector) became available [22–27].

* Corresponding author.

0021-9673/94/$07.00 © 1994 Elsevier Science B.V. All rights reserved
SSDI 0021-9673(93)E0876-V

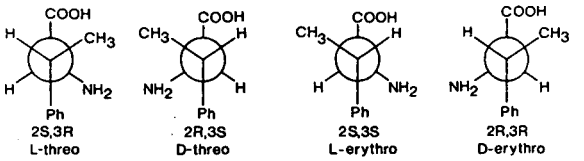

Fig. 1. Structures of four optical isomers of β-methylphenylalanine.

This paper describes the separation of the β-methylphenylalanine (β-MePhe) isomers by different chromatographic methods. β-MePhe has two chiral centres, and four stereoisomers are possible (Fig. 1). To separate these four isomers, different chromatographic methods were applied. HPLC was carried out with pre-column derivatization with acetic anhydride, *o*-phthaldialdehyde (OPA)–mercaptopropionic acid and 1-fluoro-2,4-dinitrophenyl-5-L-alaninamide (FDAA; Marfey reagent). GC was performed with the N-trifluoroacetylated isobutyl ester derivative and MS detection. For TLC analysis, the free amino acid was used.

The β-MePhe isomers were built into a peptide, [β-MePhe^3]deltorphin C (Tyr-D-Ala–β-MePhe–Asp–Val–Val–Gly–NH_2) and the diastereomers were separated by HPLC. Methods were developed to check the optical purity of the peptide by HPLC and TLC. The former is also suitable for preparative purification.

EXPERIMENTAL

Chemicals and reagents

β-MePhe was prepared by a slightly modified method of Kataoka *et al.* [28]. Pure *erythro*-(2*S*,3*S*)- and -(2*R*,3*R*)-β-MePhe · HCl were easily obtained from N-acetyl-β-MePhe by hydrolysis with 3 *M* HCl and crystallization from water. *threo*-(2*S*,3*R*)- and -(2*R*,3*S*)-β-MePhe · HCl were obtained from the mother liquor by repeated crystallization. Structures were confirmed by NMR spectroscopy; the chemical shifts and coupling constants are in agreement with the results of Tsuchihashi *et al.* [29] and Hruby *et al.* [30]. (2*S*,3*S*)-, (2*R*,3*R*)-, (2*S*,3*R*)- and (2*R*,3*S*)-β-MePhe · HCl were prepared by Kataoka *et al.*'s method [28] and used as standards.

Deltorphin C analogues were synthesized by solid-phase peptide synthesis by using Boc chemistry, starting from 4-methylbenzhydrylamine resin [30]. Two syntheses were carried out, using Boc-D,L-*erythro*-β-MePhe or Boc-D,L-*threo*-β-MePhe. Both syntheses gave crude diastereomeric peptides. The mixture of diastereomeric peptides were separated by HPLC using a Vydac semi-preparative column and an acetonitrile–aqueous trifluoroacetic acid (TFA) mobile phase system. Each crude peptide gave two main peaks, corresponding to the two diastereomeric peptides, and were isolated as white powders. The peptides containing optically pure β-MePhe were identified by an enzymatic method [31] using L-amino acid oxidase or other methods described below.

FDAA was purchased from Sigma (St. Louis, MO, USA), 4-methylbenzhydrylamine resin from Bachem Feinchemikalien (Bubendorf, Switzerland), trifluoroacetic anhydride (99+%) from Janssen Chimica (Beerse, Belgium) and HPLC-grade solvents (methanol and acetonitrile) and other reagents of analytical-reagent grade from Merck (Darmstadt, Germany).

Buffers were prepared with doubly distilled water and further purified by pumping through a 10-μm filter. The pH was adjusted with phosphoric acid (phosphate buffer), acetic acid (acetate buffer) or sodium hydroxide.

TLC was performed on commercially available precoated DC Fertigplatten Kieselgel F_{254} plates (Merck) and on a Chiralplate (Macherey–Nagel, Düren, Germany), which is coated with a reversed-phase silica gel and impregnated with a chiral selector (2*S*,4*R*,2′*RS*)-N-(2′-hydroxydodecyl)-4-hydroxyproline and copper(II) ions. Spots were revealed by spraying with 0.1% ninhydrin reagent.

Apparatus

The LC system consisted of a liquid chromatographic pump (Merck–Hitachi, Tokyo, Japan), a Model 308 variable-wavelength UV spectrophotometric detector (Labor MIM, Budapest, Hungary) and an HP 3395 integrator (Hewlett-Packard, Waldbronn, Germany). The columns used were Vydac 218TP104 C_{18} (250 × 4.6 mm I.D.), 10-μm particle size, a semi-preparative Vydac 218TP1010 C_{18} (250 × 10 mm I.D.), 10-

μm particle size (Separations Group, Hesperia, CA, USA), and Nucleosil $10C_{18}$ (250 × 4.6 mm I.D.), 10-μm particle size (Macherey–Nagel).

GC was performed on a Model 3200 GC–MS system (Finnigan, San Jose, CA, USA) connected to an on-line Finnigan Incos data system, which controlled repetitive data scanning of the mass spectrometer and acquired and processed all the data obtained. The samples were analysed on a Chirasil-L-Val III (Alltech, Deerfield, IL, USA) capillary column (50 m × 0.25 mm I.D.). The operating conditions were injection port temperature 250°C, carrier gas helium [0.5 atm inlet pressure (1 atm = 101 325 Pa)] and splitting ratio 1:30. The column temperature was varied in the range 65–220°C, depending on the nature of the amino acids.

Quantitative amino acid analysis was performed on an HP1090 Amino Quant amino acid analyser (Hewlett-Packard). The column used was Hypersil ODS C_{18} (200 × 2 mm I.D.), 5-μm particle size (Shandon Scientific, Runcorn, Cheshire, UK).

^{1}H NMR was performed on a Bruker (Zug, Switzerland) AM 400 spectrometer.

Peptide hydrolysis

The deltorphin C analogues containing different stereoisomers of β-MePhe in position 3 were hydrolysed in 6 *M* HCl at 110°C for 24 h in a Pierce Reacti-vial under argon pressure. The solvent was removed by flushing with argon. The dry sample was then derivatized for GC and LC or used for amino acid analysis.

Derivatization of the amino acid for HPLC

As D,L-*erythro*- and D,L-*threo*-β-MePhe are not separated on an RP-HPLC column, a suitable derivatization procedure is required. In the formation of N-acetyl-β-MePhe, conventional derivatization with acetic anhydride in acidic media leads to racemization. However, on derivatization in an alkaline medium racemization is not observed. The following procedure was used: 2 mg of β-MePhe were cooled in an ice-bath, 350 μl of 1 *M* NaOH were added, the mixture was stirred for a few seconds until the salt had dissolved, 20 μl of acetic anhydride were added and the solution was kept at 0°C for 40 min.

The OPA–mercaptopropionic acid derivatives of D,L-*erythro*- and D,L-*threo*-β-MePhe were formed in the automated Amino Quant system by method of Schuster [32].

FDAA was used for the formation of the four diastereomers with β-MePhe as described by Marfey [12].

Derivatization for GC–MS

The N-trifluoroacetylated isobutyl ester of the β-MePhe (TAB-β-MePhe) was prepared by the reaction with isobutanol in 3 *M* HCl following reaction with trifluoroacetic anhydride [33].

RESULTS AND DISCUSSION

Separation of β-MePhe isomers

In the course of the synthesis of the β-MePhe enantiomers, the first main stage is crystallization of the D,L-*erythro* and D,L-*threo* forms. Separation of the *erythro* and *threo* forms on an RP-HPLC column is not possible. To follow the crystallization, the N-acetyl form of β-MePhe was prepared and analysed. In some instances, resolution could be observed for the non-derivatized D,L-*threo*- and D,L-*erythro*-β-MePhe at higher pH (>6), but the separation was not reproducible. This separation was observed mostly during analysis with new columns, probably owing to the higher efficiency of such columns.

Fig. 2 shows the k' values for the N-acetyl-D,L-*threo* and N-acetyl-D,L-*erythro* forms of β-MePhe at different eluent compositions and pH values. The *threo* form elutes first. Separation of the two forms starts if the methanol concentration is below 20–40%, depending on the pH. The resolution (R_s) also increases with decreasing methanol concentration and with decreasing pH. Higher pH does not increase the separation of the N-acetyl forms, as was observed in some instances with non-derivatized β-MePhe. At low pH, the N-acetylamino acid is more protonated and has a more hydrophobic character and a higher k'. On changing the mobile phase composition, with acetonitrile being used instead of methanol and TFA or sodium acetate instead of

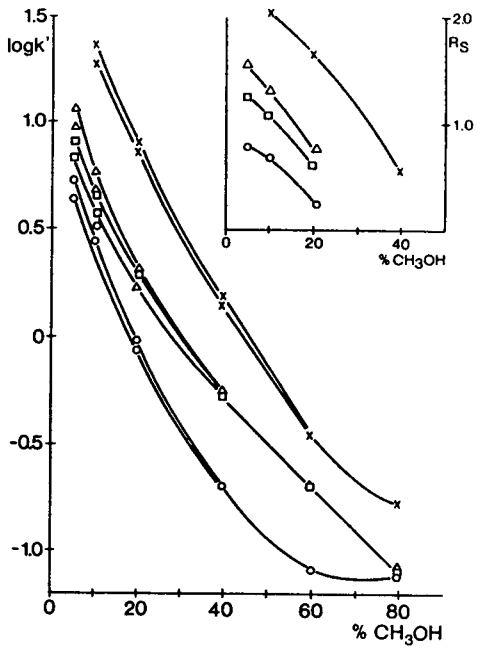

Fig. 2. Plots of capacity factor (k') and resolution (R_s) of D,L-*threo*- and D,L-*erythro*-N-acetyl-β-MePhe *vs.* percentage of methanol in eluent (*threo* elutes first). Column, Nucleosil $10C_{18}$ (250 × 4.6 mm I.D.); buffer, 0.01 *M* KH_2PO_4; detection, UV at 220 nm. pH: × = 2.2; △ = 4.2; □ = 6.5; ○ = 8.

phosphate buffer, the character of the curves was unchanged.

In amino acid analysis, after OPA derivatization, on a Hypersil ODS C_{18} column with acetonitrile–sodium acetate (pH 7.2) as the mobile phase [32], D,L-*erythro*-β-MePhe elutes first and D,L-*threo*-β-MePhe second. The k' value for the D,L-*erythro* form is 9.76 and that for the D,L-*threo* form is 10.55; $R_s = 1.70$.

With FDAA as derivatizing agent, four diastereomers were formed from the four stereoisomers of β-MePhe. The chromatographic behaviour of these diastereomers is not known; FDAA is generally used for the derivatization of amino acids containing one chiral centre. The results in Tables I and II reveal that predominantly the L-*erythro*,*threo*- and D-*erythro*,*threo*-β-MePhe derivatives are resolved. The effects of pH on the capacity factor (k'), selectivity factor (α) and resolution (R_s) were investigated (Table I). In a narrow range of pH around 2, the resolution is good for the L- and D-forms, but the high k' is disadvantageous. At pH 4, α and R_s have lower values. pH 3 seems suitable and in addition the *erythro* and *threo* forms are partially resolved.

The effect of the eluent composition is shown in Table II. A decrease of the organic content of the mobile phase increases the value of k' and improves the separation of the L- and D- forms. At a given mobile phase composition (organic content-to-buffer ratio = 30:70) the k' values depend on the nature of the buffer. The extremely high values of k' in the TFA system are disadvantageous and are probably connected with the pH being lower than 3. Of the three buffers, sodium acetate seems the most suitable

TABLE I

DEPENDENCE OF CAPACITY FACTOR (k'), SELECTIVITY FACTOR (α) AND RESOLUTION (R_s) OF β-METHYLPHENYLALANINE FDAA DERIVATIVES ON pH

Column, Nucleosil $10C_{18}$ (250 × 4.6 mm I.D.); eluent, CH_3CN–0.01 *M* KH_2PO_4 (30:70); detection, UV at 340 nm. α_{L-D} and $R_{s,L-D}$ represent separation of L- and D-forms.

pH of eluent	k'				α_{L-D}	$R_{s,L-D}$
	L-		D-			
	erythro	*threo*	*erythro*	*threo*		
2.0	11.66		18.66		1.60	5.52
3.0	4.32	4.65	8.38	8.98	1.80	5.60
4.0	3.95		5.00		1.27	1.91

TABLE II

DEPENDENCE OF CAPACITY FACTOR, SELECTIVITY FACTOR AND RESOLUTION OF β-METHYLPHENYLALANINE FDAA DERIVATIVES ON ELUENT COMPOSITION

Column, Nucleosil $10C_{18}$ (250 × 4.6 mm I.D.); detection, UV at 340 nm. Buffers: KH_2PO_4 = 0.01 *M* KH_2PO_4 (pH 3); TFA = 0.1% aqueous solution of trifluoroacetic acid; NaOAc = 0.01 *M* sodium acetate (pH 3). α_{L-L} and $R_{s,L-L}$ represent separation of L-*erythro*- and L-*threo*-β-MePhe derivatives; α_{L-D} and $R_{s,L-D}$ represent separtion of L-*threo*- and D-*erythro*-β-MePhe derivatives; α_{D-D} and $R_{s,D-D}$ represent separation of D-*erythro*- and D-*threo*-β-MePhe derivatives.

Composition of eluent	*k'*				α_{L-L}	α_{L-D}	α_{D-D}	$R_{s,L-L}$	$R_{s,L-D}$	$R_{s,D-D}$
	L-		D-							
	erythro	*threo*	*erythro*	*threo*						
CH_3OH–CH_3CN–KH_2PO_4										
30 : 70	4.32	4.65	8.38	8.97	1.08	1.80	1.07	0.63	5.60	0.63
40 : 7 : 53	5.25	5.95	13.33	14.00	1.13	2.24	1.05	1.09	10.54	0.65
CH_3OH–CH_3CN–TFA										
30 : 70	20.00	21.00	27.33	29.00	1.05	1.19	1.06	0.58	2.56	0.54
CH_3OH–CH_3CN–NaOAc										
30 : 70	5.41	5.91	10.80	11.22	1.09	1.82	1.04	0.98	6.38	0.44
10 : 20 : 70	8.83	9.83	24.33	24.33	1.11	2.47	1.00	1.11	9.45	–

as the chromatograms obtained have the best peak shape. The eluents containing two organic modifiers give better α and R_s values. For the separation of L-*erythro*,*threo* and D-*erythro*,*threo* derivatives, many systems are suitable. Separation of the *erythro* and *threo* forms is a more difficult problem. For the resolution of L-*erythro* and L-*threo* derivatives, we found some systems having an R_s greater than 1 (Table II and Fig. 3), but the D-*erythro* and D-*threo* derivatives overlapped.

In addition to HPLC, TLC and GC were also applied for resolution of the β-MePhe stereoisomers. The four stereoisomes of β-MePhe were analysed among the other amino acids originating from the hydrolysis of [β-MePhe^3]deltorphin C. The R_F values are given in Table III. On the plate, the elution sequence for the β-MePhe enantiomers was L-*threo*,*erythro*- and D-*threo*,*erythro*-β-MePhe. The L-*erythro* and L-*threo* forms gave one spot on the plate, whereas D-*threo*- and D-*erythro*-β-MePhe were resolved well.

For GC, the amino acid was derivatized into the N-trifluoroacetylated isobutyl ester form. With a GC–MS system for analysis, an electron impact (EI) ionization mass spectrum was obtained to confirm the expected structure of the derivative. Fig. 4 shows part of the chromatogram, registered at m/z 218.0 ± 0.5, for the separation of four TAB-β-MePhe derivatives. The elution sequence on a Chirasil-L-Val III column was D-*erythro*, L-*erythro*- D-*threo* and L-*threo* derivatives. The D-*threo* and L-*threo* derivatives could be resolved very well, whereas the D-*erythro* and L-*erythro* forms overlapped.

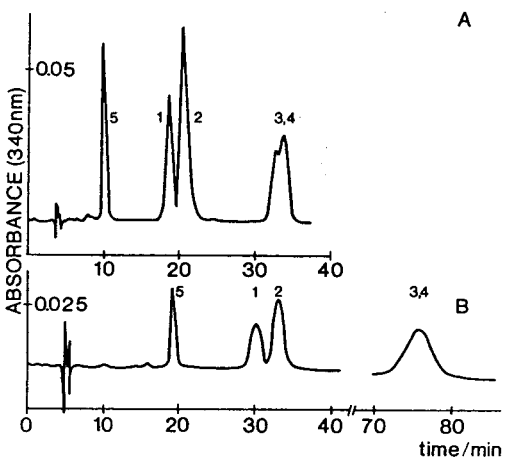

Fig. 3. Chromatograms of β-MePhe FDAA derivatives. Column, Nucleosil $10C_{18}$ (250 × 4.6 mm I.D.); eluent, (A) methanol–acetonitrile–0.01 *M* KH_2PO_4 (pH 3) (40:7:53) and (B) methanol–acetonitrile–0.01 *M* sodium acetate (pH 3) (10:20:70); detection, UV at 340 nm. Peaks: 1 = L-*erythro*; 2 = L-*threo*; 3 = D-*erythro*; 4 = D-*threo*; 5 = unreacted FDAA.

TABLE III

R_F VALUES OF FOUR ISOMERS OF β-METHYL PHENYLALANINE AND OTHER AMINO ACIDS FROM HYDROLYSED [β-MePhe^3]DELTORPHIN C, COMPARED WITH STANDARD AMINO ACIDS

Chiralplate with acetonitrile–methanol–water (4:1:1, v/v/v).

Amino acid	R_F	
	Hydrolysate	Standard
Tyr	0.63	0.62
L-*erythro*,L-*threo*-β-MePhe	0.58	0.58
Val	0.51	0.51
D-*threo*-β-MePhe	0.48	0.48
Asp	0.44	0.43
D-*erythro*-β-MePhe	0.39	0.40
D-Ala	0.37	0.38
Gly	0.32	0.32

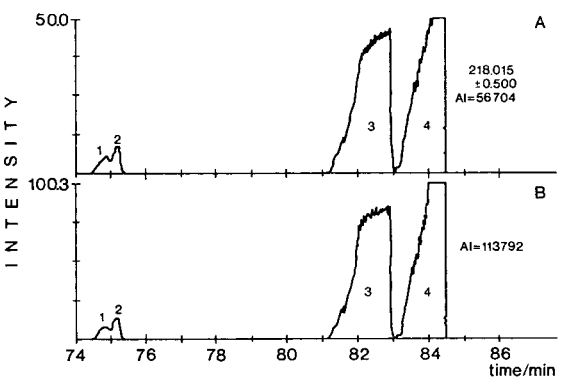

Fig. 4. GC–MS of TAB-β-MePhe derivatives. Column, Chirasil-L-Val III (50 × 0.25 mm I.D.); oven temperature, programmed from 65 to 220°C at 0.5°C/min. (A) Ion chromatogram of mass 218 $[M - CF_3 - CO - NH_2]^+$; (B) total ion chromatogram: 2.5% D,L-*erythro*-β-MePhe, 97.5% D,L-*threo*-β-MePhe. Peaks: 1 = D-*erythro*; 2 = L-*erythro*; 3 = D-*threo*; 4 = L-*threo*.

Separation of diastereomers of [β-MePhe]deltorphin C

The enantiomers of β-MePhe were incorporated into the peptide [β-MePhe^3]deltorphin C. Two separate syntheses were performed with D,L-*erythro*- and D,L-*threo*-β-MePhe. The crude peptide was purified by HPLC on a Vydac column with acetonitrile–0.1% TFA as the mobile phase. A suitable mobile phase system contained about 20% of organic modifier. Each chromatogram had two main peaks. These peaks were identified after separation of the peptide on a semi-preparative Vydac column following hydrolysis or enzymatic digestion. The hydrolysate containing the amino acids was analysed by one of the chromatographic methods mentioned above. In both instances, the first peak on the Vydac column corresponded to the D-*erythro* or D-*threo* isomers of deltorphin C and the second peak to the L-*erythro* or L-*threo* isomers.

HPLC of the [β-MePhe^3]deltorphin C diastereomers with the acetonitrile–TFA system led to the total separation of the four isomers (Fig. 5). On the Vydac column, the sequence of elution was D-*threo*, D-*erythro*, L-*threo* and L-*erythro*. With a 20% organic modifier content, the separation was very satisfactory and the α and R_s values were good. This result indicates that the four diastereomers can be separated and purified on the preparative column.

Analysis of the diastereomers of [β-MePhe^3]deltorphin C was also performed by TLC. The results are given in Table IV. With a convention Kieselgel F_{254} plate, the L-*threo* diastereomer can be separated partially from the other three (Table IV, column A). On the Chiralplate, three diastereomers can be resolved (column A'): L-*threo*, D,L-*erythro* (in one spot) and D-*threo*. With both plates these separations

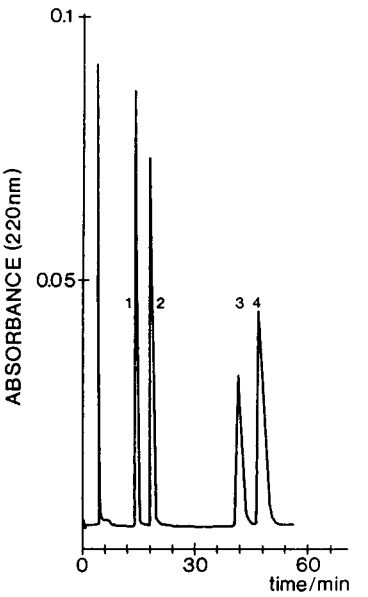

Fig. 5. Chromatogram of [β-MePhe^3]deltorphin C diastereomers Column, Vydac 218TP104 C_{18} (250 × 4.6 mm I.D.); eluent, acetonitrile–0.1% TFA (20:80); detection, UV at 220 nm. Peaks: 1 = D-*threo*; 2 = D-*erythro*; 3 = L-*threo*; 4 = L-*erythro*.

TABLE IV

R_F VALUES FOR THE FOUR ISOMERS OF [β-MePhe^3]DELTORPHIN C

A = Kieselgel with acetonitrile–methanol–water (4:1:1, v/v/v); A' = Chiralplate with acetonitrile–methanol–water (4:1:1, v/v/v); B = Kieselgel with *n*-butanol–acetic acid–water (4:1:1, v/v/v); C = Kieselgel with *n*-butanol–pyridine–acetic acid–water (13:12:3:10, v/v).

Peptide	R_F			
	A	A'	B	C
L-*threo*-[β-MePhe^3]deltorphin C	0.47	0.38	0.49	0.65
L-*erythro*-[β-MePhe^3]deltorphin C	0.43	0.33	0.48	0.64
D-*erythro*-[β-MePhe^3]deltorphin C	0.43	0.33	0.48	0.64
D-*threo*-[β-MePhe^3]deltorphin C	0.42	0.26	0.49	0.64

TABLE V

SEPARATION OF β-MePhe ISOMERS, DERIVATIVES AND ITS PEPTIDES BY DIFFERENT CHROMATOGRAPHIC METHODS

||| = $R_s > 2$ or difference between two R_F values $\Delta R_F > 0.1$. || = $2 > R_s > 1$ or difference between two R_F values $0.1 > \Delta R_F > 0.05$. | = $R_s < 1$ or difference between two R_F values $\Delta R_F < 0.05$.

Method	Analysed component	Elution sequence of β-MePhe isomers and derivatives			
		1	2	3	4
HPLC	N-Ac-β-MePhe	D,L-*threo*					D,L-*erythro*		
	OPA-β-MePhe	D,L-*erythro*					D,L-*threo*		
	β-MePhe + FDAA	L-*erythro*	||	L-*threo*	|||	D-*erythro*		D-*threo*
GC	TAB-β-MePhe	D-*erythro*	||	L-*erythro*	|||	D-*threo*	||	L-*threo*
Chiral TLC	β-MePhe	L-*erythro*,*threo*	|||	D-*threo*	||	D-*erythro*		
		Elution sequence of [β-MePhe^3]deltorphin C isomers			
		1	2	3	4
HPLC		D-*threo*	|||	D-*erythro*	|||	L-*threo*	|||	L-*erythro*
TLC	Kieselgel	L-*threo*		D-*threo*, D,L-*erythro*			
	Chiralplate	L-*threo*		D,L-*erythro*	||	D-*threo*		

can be achieved with the acetonitrile–methanol–water (4:1:1, v/v/v) system. With a more polar system (columns B and C), the R_F values are higher and no separation can be observed.

CONCLUSIONS

The described procedures can be applied for the separation and identification of the β-MePhe enantiomers and peptides containing them. A comparison of the different methods is given in Table V. The exact enantiomer content of β-MePhe can be determined with a combination of the procedures, and the four diastereomers of [β-MePhe^3]deltorphin C can be identified conveniently by HPLC.

ACKNOWLEDGEMENTS

This work was supported by grants from the Hungarian Research Foundation (OTKA 2993/91 and OTKA 71/91). We thank Dr. Georges Laus for discussions relating to the GC–MS analysis.

REFERENCES

1 W.H. Pirkle and J. Finn, in J. Morrison (Editor), *Asymmetric Synthesis, Vol. I, Analytical Methods*, Academic Press, New York, 1983, Ch. 6.
2 W.F. Lindner and C. Petterson, in I. Wainer (Editor), *Liquid Chromatography in Pharmaceutical Development: an Introduction*, Aster, Springfield, VA, 1985, Part 1.
3. D.W. Armstrong and S.M. Han, *CRC Crit. Rev. Anal. Chem.*, 19 (1988) 175.
4 V.A. Davankov, A.A. Kurganov and A.S. Bochkov, *Adv. Chromatogr.*, 22 (1983) 71.
5 C. Petterson, *Trends Anal. Chem.*, 7 (1988) 209.
6 W.F. Lindner, in L. Crane and B. Zief (Editors), *Chromatographic Chiral Separations*, Marcel Dekker, New York, 1987, p. 91.
7 W.F. Lindner, in J.F. Lawrence and R.W. Frei (Editors), *Chemical Derivatization in Analytical Chemistry*, Vol. 2, Plenum Press, New York, 1982, p. 145.
8 T. Nambara, in W.S. Hancock (Editor), *CRC Handbook of HPLC for the Separation of Amino Acids, Peptides and Proteins*, Vol. I, CRC Press, Boca Raton, FL, 1984, p. 383.
9 N. Nimura, H. Ogura and T. Kinoshita, *J. Chromatogr.*, 202 (1980) 375.
10 T. Kinoshita, Y. Kasahara and N. Nimura, *J. Chromatogr.*, 210 (1981) 77.
11 N. Nimura, A. Toyama and T. Kinoshita, *J. Chromatogr.*, 316 (1984) 547.

12 P. Marfey, *Carlsberg Res. Commun.*, 49 (1984) 591.
13 S. Einarsson, B. Josefsson, P. Möller and D. Sanchez, *Anal. Chem.*, 59 (1987) 1191.
14 H. Brückner and C. Gah, *J. Chromatogr.*, 555 (1991) 81.
15 H. Brückner, R. Wittner and H. Godel, *Chromatographia*, 32 (1991) 383.
16 H. Brückner and B. Strecker, *Chromatographia*, 33 (1992) 586.
17 S. Einarsson and G. Hansson, in C.T. Mant and R.S. Hodges (Editors), *High Performance Liquid Chromatography of Peptides and Proteins*, CRC Press, Boca Raton, FL, 1991, p. 369.
18 C.W. Gehrke, F.E. Kaiser, K.C.T. Kuo and R.W. Zumwalt, in R.W. Zumwalt, K.C.T. Kuo and C.W. Gehrke (Editors), *Amino Acid Analysis by Gas Chromatography*, Vol. I, CRC Press, Boca Raton, FL, 1987, Ch. 2.
19 E. Bayer, G. Nicholson and H. Frank, in R.W. Zumwalt, K.C.T. Kuo and C.W. Gehrke (Editors), *Amino Acid Analysis by Gas Chromatography*, Vol. II, CRC Press, Boca Raton, FL, 1987, Ch. 2.
20 H. Frank, in R.W. Zumwalt, K.C.T. Kuo and C.W. Gehrke (Editors), *Amino Acid Analysis by Gas Chromatography*, Vol. II, CRC Press, Boca Raton, Fl, 1987, Ch. 3.
21 I. Abe, S. Kuramoto, in R.W. Zumwalt, K.C.T. Kuo and C.W. Gehrke (Editors), *Amino Acid Analysis by Gas Chromatography*, Vol. III, CRC Press, Boca Raton, FL, 1987, Ch. 2.
22 K. Günther, J. Martens and M. Schickenadz, *Angew. Chem.*, 96 (1984) 514.
23 K. Günther, J. Martens and M. Schickenadz, *Naturwissenschaften*, 72 (1985) 149.
24 K. Günther, *J. Chromatogr.*, 448 (1988) 11.
25 *Chemolog Hi-Lites*, 13, No. 1 (1989) 10.
26 J. Martens and R. Bhushan, *Int. J. Pept. Protein Res.*, 34 (1989) 433.
27 G. Tóth, M. Lebl and V.J. Hruby, *J. Chromatogr.*, 504 (1990) 450.
28 YI. Kataoka, Y. Seto, M. Yamamoto, T. Yamada, S. Kuwata and H. Watanabe, *Bull. Chem. Soc. Jpn.*, 49 (1976) 1081.
29 G. Tsuchihashi, S. Mitamura and K. Ogura, *Bull. Chem. Soc. Jpn.*, 52 (1979) 2167.
30 V.J. Hruby, G. Tóth, C.A. Gehrig, L.-F. Kao, R. Knapp, G.K. Lui, H.I. Yamamura, T.H. Kramer, P. Davis and T.F. Burks, *J. Med. Chem.*, 34 (1991) 1823.
31 J.P. Greenstein and M. Winitz, *The Chemistry of Amino Acids*, Wiley, New York, 1961, p. 2065.
32 R. Schuster, *J. Chromatogr.*, 431 (1988) 271.
33 A. Péter, G. Laus, D. Tourwé, E. Gerlo and G. Van Binst, *Pept. Res.*, 6 (1993) 48.

Journal of Chromatography A, 660 (1994) 293–298
Elsevier Science B.V., Amsterdam

CHROMSYMP. 2947

High-performance liquid chromatographic determination of FCE 24928, a new aromatase inhibitor, in human plasma

E. Fontana*, E. Pianezzola, G. Basileo and M. Strolin Benedetti

Farmitalia Carlo Erba, Research and Development, Erbamont Group, Via per Pogliano, 20014 Nerviano, Milan (Italy)

ABSTRACT

A sensitive and selective high-performance liquid chromatographic method for the determination of FCE 24928 (4-aminoandrosta-1,4,6-triene-3,17-dione) in human plasma is reported. The drug was extracted from buffered (pH = 8) plasma samples with methylene chloride–isooctane, then analysed by reversed-phase liquid chromatography. Quantitation was achieved by ultraviolet detection of the eluate at 238 nm. Blank plasma samples from humans, dog and rat assayed as described showed no significant peak at the retention time of the compound of interest. The suitability of the method for *in vivo* samples was tested by measuring the plasma levels of FCE 24928 in rats that received oral doses of the test compound.

INTRODUCTION

Increasing attention is being focused upon the possibility of treating estrogen-dependent diseases [1], such as breast cancer, by inhibition of aromatase, the enzyme catalysing the conversion of androgen to estrogen [2].

Some promising irreversible aromatase inhibitors, including exemestane [3], a molecule synthesized and studied in the Laboratories of Farmitalia Carlo Erba, are at various stages of clinical development, and one of them, formestane [4], has been recently introduced onto the market for the treatment of post-menopausal breast cancer.

In a programme aimed at finding new irreversible aromatase inhibitors, a series of 4-aminoandrostenedione derivatives were synthesized and tested for their aromatase inhibitory properties [5,6]. Among them, FCE 24928 (Fig. 1) was found to be active both *in vitro* and *in vivo* [7]. The compound was orally active, showed no affinity for the rat androgen receptor and in immature castrated rats did not show androgenic activity [8].

In addition, FCE 24928 was effective against 7,12-dimethylbenzoanthracene-induced mammary tumours in ovariectomized rats treated with testosterone propionate, a post-menopausal mammary tumour model [9].

In the present paper a sensitive and selective HPLC assay for the determination of FCE 24928 in human plasma and its validation are described. The method has been developed for the quantitation of the compound in rat, dog and human plasma during toxicokinetic and pharmacokinetic studies.

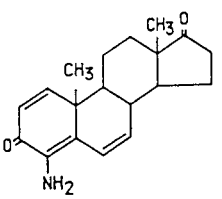

Fig. 1. Structural formula of FCE 24928 (4-aminoandrosta-1,4,6-triene-3,17-dione).

* Corresponding author.

0021-9673/94/$07.00 © 1994 Elsevier Science B.V. All rights reserved
SSDI 0021-9673(93)E0966-X

EXPERIMENTAL

Chemicals and solutions

FCE 24928 was supplied by the Chemical Development Department of Farmitalia Carlo Erba. All other chemicals and solvents were analytical grade from Farmitalia Carlo Erba (Milan, Italy). Buffer solutions were filtered before use through a Millipore 0.45-μm filter. The stock standard solution was prepared by dissolving a weighed amount of FCE 24928 in 0.1 *M* H_3PO_4. From this solution (stable for at least 2 weeks if stored at 0–4°C in the dark) working solutions were prepared daily by dilution with 0.1 *M* H_3PO_4.

Equipment

The chromatographic system consisted of a Milton Roy (Rochester, NY, USA) Model CM III pump equipped with a Rheodyne Model 7125 sampling valve with a 100-μl loop, a Fisons Instruments Model MICRO UVIS20 variable-wavelength detector (Milan, Italy) and a Spectra-Physics (San José, CA, USA) Model SP4100 integrator.

Chromatographic conditions

The chromatographic separation was performed on a Lichrocart, Superspher 100 RP-18 analytical column (25 cm × 4 mm I.D.; particle size 4 μm) purchased from Merck (Darmstadt, Germany), at ambient with a flow-rate of 0.4 ml/min. Isocratic elution with a mobile phase consisting of acetonitrile–0.05 *M* KH_2PO_4 adjusted to pH 4.3 with 1 *M* H_3PO_4 (1:1, v/v) was used. The detection wavelength chosen was 238 nm.

Sample extraction

Human plasma (1 ml) was placed into a 10-ml conical glass centrifuge tube, the working FCE 24928 solution (0.1 ml) added and mixed with 1 *M* pH 8 borate buffer (0.5 ml). The mixture was extracted with 3 ml of a methylene chloride–isooctane mixture (2:3, v/v) on a rotating tube holder (10 min) then centrifuged (10 min, 1200 *g*). The organic layer was collected and the extraction step was repeated as above. The organic phases were then combined and evaporated to dryness at room temperature in the dark under a stream of nitrogen. After reconstitution of the residue with the mobile phase (150 μl), an aliquot (100 μl) was injected onto the column.

Assay validation

Blank human plasma samples spiked with a known amount of the FCE 24928 working solution were processed as described above. All chromatograms obtained were evaluated by peak-height measurement. Three calibration curves were prepared and run on three different days in the concentration range 2.16–540 ng/ml in order to evaluate the linearity of the method. The precision was assessed by analysing three replicate samples of five concentrations (2.16, 10.8, 54, 108 and 540 ng/ml) prepared on three different days. The accuracy, expressed as mean percentage ratio of found to added amounts, was evaluated by repeated analyses carried out at three concentrations (13.5, 216 and 432 ng/ml).

The percentage of drug recovered was calculated by comparison of the peak height of the extracted plasma samples with the peak height obtained from direct injection of the unextracted standard solutions at four different concentrations.

Chromatographic system suitability test

The suitability [10] of the chromatographic system was checked daily before analysis by evaluating the following three parameters.

Column efficiency. This was evaluated as the number of theoretical plates of column calculated by the equation $N = 5.54(t_R/W)^2$, where t_R is the retention time (mm) of FCE 24928 and W (mm) is the peak width at half-height. N must be $\geq$9000.

Peak symmetry. This was evaluated as symmetry factor S_F calculated from the equation $S_F = W_{0.05}/2A$ where $W_{0.05}$ is the peak width (mm) measured at 1/20 of the peak height and A is the distance (mm) between the perpendicular dropped from the peak maximum and the leading edge of the peak at 1/20 of the peak height. S_F must be in the range 1–1.2.

System reproducibility. The detection response of four replicate injections of a standard

solution (50–100 ng/ml) must show a relative standard deviation (R.S.D.) not exceeding 2%.

RESULTS AND DISCUSSION

A range of pH values (4.5–8.8) was explored in order to define the best extraction yield of the product from plasma, and the maximum recovery was obtained at pH 8.

From several solvents (*e.g.* methylene chloride, ethyl acetate, diethyl ether, isooctane) tested as extractants, a mixture of methylene chloride–isooctane (2:3, v/v) provided the best compromise between high recovery of FCE 24928 and an acceptable degree of coextraction of interfering plasma components. The mean recovery of FCE 24928, using the liquid–liquid extraction conditions described above, was 72% with 6.9% R.S.D. (Table I).

A satisfactory and reliable separation of FCE 24928 from endogenous substances coextracted from human plasma samples was obtained with the Superspher C_{18} reversed-phase analytical column and the mobile phase system reported in the Experimental section (Fig. 2). Blank plasma samples from rat and dog assayed as described showed no significant peak at the retention time of the compound of interest (Fig. 3). The UV spectrum of FCE 24928 recorded in the mobile phase in the range 220–600 nm showed the highest absorption maximum at 238 nm; therefore this wavelength was chosen to quantify the product.

TABLE I

EXTRACTION RECOVERY OF FCE 24928 FROM HUMAN PLASMA ($n = 3$)

Concentration added (ng/ml)	Absolute recovery (%)	R.S.D. (%)
10.8	72.8	1.9
54.0	68.6	3.9
108.0	67.9	3.7
540.0	79.0	1.7
Overall average ($n = 12$)	72.1	6.9

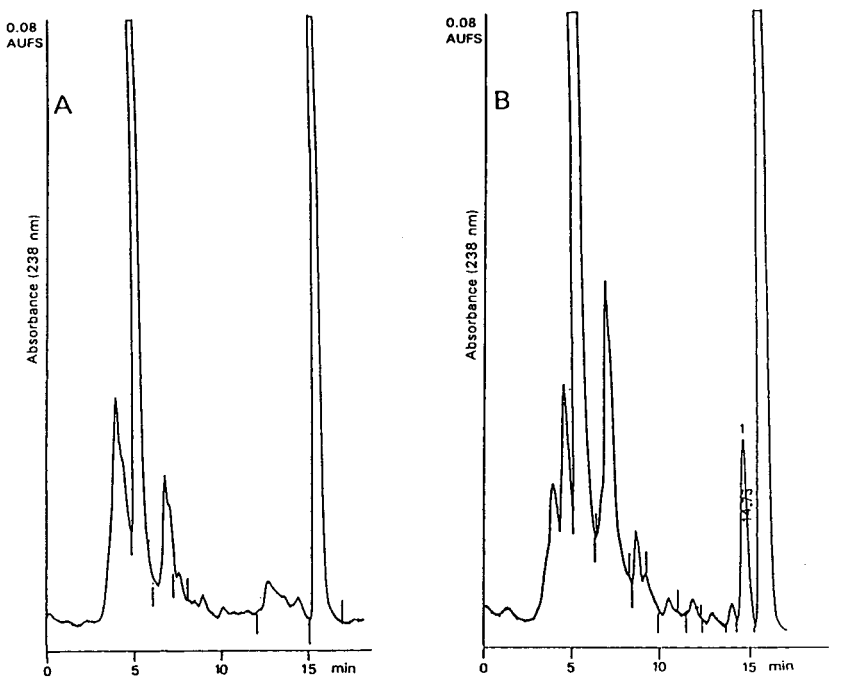

Fig. 2. Chromatograms obtained by assaying (A) 1 ml of human blank plasma and (B) 1 ml of human plasma spiked with 10.8 ng of FCE 24928 (1).

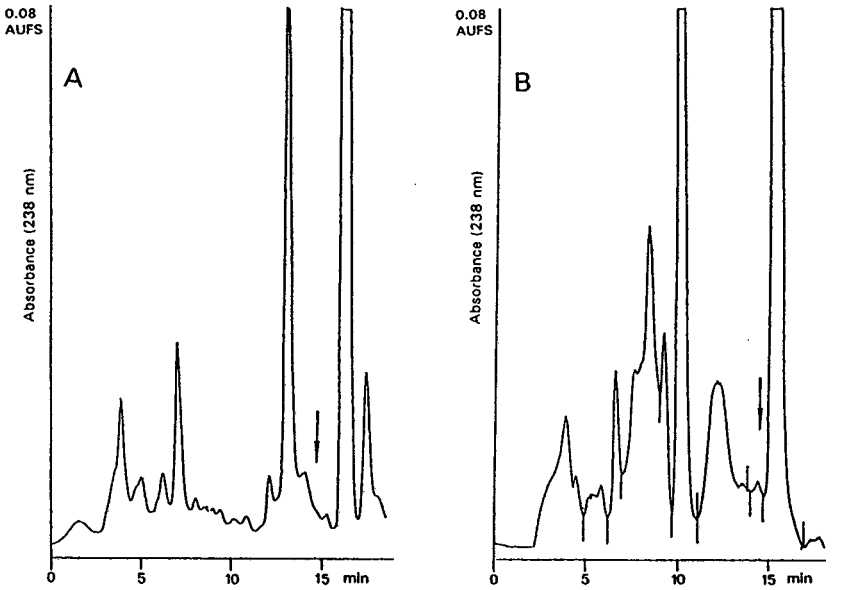

Fig. 3. Chromatograms obtained by assaying (A) 1 ml of blank dog plasma and (B) 1 ml of blank rat plasma. Arrows indicate the peak position of FCE 24928.

TABLE II

INTRA- AND INTER-DAY PRECISION OF THE METHOD FOR THE DETERMINATION OF FCE 24928 IN HUMAN PLASMA

Control sample (ng/ml)	Day	*n*	Mean found (ng/ml)	S.D.	R.S.D. (%)	
					Intra-day	Inter-day ($n = 9$)
2.16	1	3	2.15	0.17	7.90	
	2	3	2.40	0.17	7.08	
	3	3	2.23	0.04	1.79	7.38
10.8	1	3	11.25	0.23	2.04	
	2	3	11.25	0.77	6.84	
	3	3	11.18	0.74	6.62	4.87
54.0	1	3	52.49	2.30	4.38	
	2	3	50.01	3.67	7.34	
	3	3	48.61	2.22	4.57	5.89
108.0	1	3	100.6	1.65	1.64	
	2	3	98.0	3.61	3.68	
	3	3	102.5	5.76	5.62	3.98
540.0	1	3	577.0	35.18	6.09	
	2	3	549.0	26.49	4.82	
	3	3	582.6	2.77	0.48	4.74

TABLE III

ACCURACY OF THE METHOD FOR THE DETERMINATION OF FCE 24928 IN HUMAN PLASMA

Control sample (ng/ml)	*n*	Mean found (ng/ml)	Found/ added (%)	S.D. (%)	R.S.D. (%)
13.5	4	12.78	94.6	2.5	2.6
216.0	4	204.40	94.7	6.5	6.8
432.0	4	413.07	95.6	5.5	5.8
Overall average ($n = 12$)			95.0	4.7	4.9

Three separate calibration curves obtained on three different days by plotting the peak height *versus* concentration were found to be linear when evaluated by linear regression analysis in the concentration range 2.16–540 ng per ml of human plasma. The correlation coefficients were > 0.999 and the mean slope was 228 (R.S.D. = 3.8%). Intercept values, when submitted to Student's *t* test were not significantly different from zero ($p > 0.05$).

The inter-day precision ranged from 3.98 to 7.38% R.S.D. for concentrations between 2.16 and 540 ng/ml, and the intra-day precision was better than 7.9% R.S.D. (Table II).

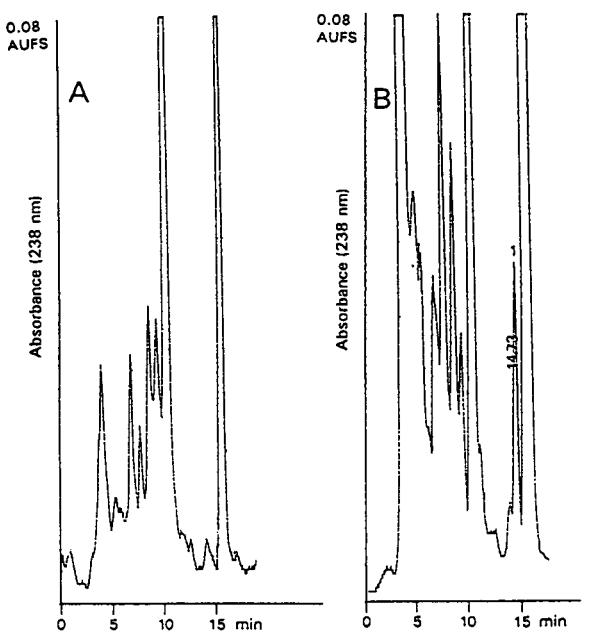

Fig. 4. Chromatograms obtained by assaying (A) 1 ml of rat plasma from a control animal and (B) 1 ml of rat plasma 4 h after oral administration of 40 mg/kg FCE 24928 (1).

The accuracy, expressed as mean percentage of the found to added amounts calculated at three concentrations (13.5, 216 and 432 ng/ml) with samples analysed on different days, was 95% with 4.9% R.S.D. (Table III).

The limit of quantitation, defined here as the lowest plasma concentration that can be measured routinely with acceptable precision (R.S.D. $< 10\%$) and accuracy (bias $\pm$ 10%), was 2.16 ng/ml (see Tables II and III).

The developed method has been used in a preliminary study to monitor the plasma levels of FCE 24928 after administration of a single oral dose of 40 mg/kg to three rats.

Blood samples were drawn from the animals kept under ether anaesthesia, from sublingual vein at 1 and 4 h and from abdominal aorta at 24 h after administration, and collected into heparinized tubes. Plasma was separated after centrifugation at 1200 *g* for 10 min at room temperature, then stored at −20°C until assayed. A typical chromatogram obtained from these *in vivo* samples is shown in Fig. 4B. Blank plasma samples of control animals showed no detectable peak with the same retention time as FCE 24928 (Fig. 4A). Mean plasma concentrations of 407 $\pm$ 85 ng/ml (mean $\pm$ standard error of the mean) occurred at 1 h after administration, then a relatively rapid disappearance of the compound was observed with mean levels of 75 $\pm$ 20 ng/ml and of 12 $\pm$ 4 ng/ml at 4 and 24 h, respectively. It may be interesting to express in molarity the

mean plasma concentrations obtained at 1, 4 and 24 h after administration of 40 mg/kg, a dose which is about three times the ED_{50} for reduction of ovarian aromatase activity in the rat [8]. These values (1368, 252 and 40 n*M*) are higher than or similar to the K_i value for inhibition of human placental aromatase [8].

CONCLUSIONS

The isocratic reversed-phase HPLC method described here is the first analytical method for the selective determination of FCE 24928 in plasma. It proved to be reproducible, linear, precise and accurate in the concentration range 2.16–540 ng/ml; therefore it is suitable for monitoring the unchanged drug plasma levels in animals and in humans.

ACKNOWLEDGEMENT

The authors thank Miss S. Cozzi for typing the manuscript.

REFERENCES

1 R.J. Santen, *J. Steroid Biochem. Molec. Biol.*, 37 (1990) 1029.
2 H. Taniguchi, H.R. Feldmann, M. Kaufmann and W. Pyerin, *Anal. Biochem.*, 181 (1989) 167.
3 D. Giudici, G. Ornati, G. Briatico, F. Buzzetti, P. Lombardi and E. Di Salle, *J. Steroid Biochem.*, 30 (1988) 391.
4 M. Dowsett, D.C. Cunningham, R.C. Stein, E. Evans, L. Dehenmin, A. Hedley and R.C. Coombes, *Cancer Res.*, 49 (1989) 1306.
5 R. D'Alessio, F. Faustini, V. Villa, E. Di Salle and P. Lombardi, *J. Steroid Biochem.*, 25 (1986) 46S.
6 F. Faustini, R. D'Alessio, V. Villa, E. Di Salle and P. Lombardi, *Br. Pat.*, GB-B-2171 100 (1985).
7 E. Di Salle, G. Ornati and D. Giudici, *J. Steroid Biochem.*, 36 (1990) 123S.
8 E. Di Salle, D. Giudici, G. Ornati, G. Briatico, R. D'Alessio, V. Villa and P. Lombardi, *J. Steroid Biochem. Molec. Biol.*, 37 (1990) 369.
9 T. Zaccheo and E. Di Salle, *Cancer Chemother. Pharmacol.*, 31 (1993) 308.
10 *US Pharmacopeia XXII*, US Pharmacopeial Convention, Rockville, MD, 1990, p. 1566.

Journal of Chromatography A, 660 (1994) 299–306
Elsevier Science B.V., Amsterdam

CHROMSYMP. 2899

Determination of paeoniflorin, ferulic acid and baicalin in the traditional Chinese medicinal preparation Dang-Guei-San by high-performance liquid chromatography

Yuh-Chuang Lee, Cheng-Yu Huang, Kuo-Ching Wen* and Tsi-Tee Suen

National Laboratories of Foods and Drugs, Department of Health, Executive Yuan, 161-2 Kuen-Yang Street, Nankang, Taipei (Taiwan)

ABSTRACT

A high-performance liquid chromatographic method for the determination of paeoniflorin, ferulic acid and baicalin in the traditional Chinese medicinal preparation Dang-Guei-San, which contains Paeoniae Radix, Swertiae Herba, Cnidii Rhizoma and Scutellariae Radix, was established. The samples were separated with a Cosmosil $5C_{18}$-AR column by gradient elution with 0.03% (v/v) phosphoric acid-acetonitrile (0 min 96:4, 5 min 84:16, 7 min 82:18, 14–30 min 78:22) as the mobile phase at a flow-rate of 1.0 ml/min, with detection at 245 nm. Methylparaben was used as the internal standard and three equations were derived showing linear relationships between the peak-area ratios of marker components (paeoniflorin, ferulic acid and baicalin) to methylparaben and concentration. The recoveries of paeoniflorin, ferulic acid and baicalin were 27.86, 33.89 and 49.31%, respectively. The repeatability (relative standard deviation) was generally less than 5% ($n = 5$). The effects of various processes such as concentration by reduced-pressure evaporation, freeze-drying and spray-drying were studied and commercial concentrated herbal preparations containing Paeoniae Radix, Swertiae Herba, Cnidii Rhizoma and Scutellariae Radix were also analysed.

INTRODUCTION

In analysing the constituents of Chinese medicinal preparations, studies on related topics generally started from the examination of a single herb component and then proceeded with the analysis of traditional prescriptions containing that specific component. As a result, most analytical work on Chinese medicines has been confined to single herbs. In order to promote the Good Manufacturing Practices (GMP) of Chinese medicinal preparations, our aim was to develop simple and expedient analytical methods for routine use in quality control.

In this study, we selected the Chinese medicinal preparation Dang-Guei-San and applied HPLC to develop suitable methods for determining the concentrations of its marker components. For determining paeoniflorin in Paeoniae Radix, we used the documented mobile phase [1] and obtained a satisfactory result. For determining baicalin in Scutellariae Radix, we also tried the documented mobile phase [2] with gradient elution. However, a poor peak shape was obtained and the whole process took much longer than expected. Ion-pair chromatography can also separate several flavonoids simultaneously in Scutellariae Radix [3,4], but this method damaged the column and pump. Therefore, we considered that a method using an aqueous acid–acetonitrile eluent would be a more feasible way to perform the analysis.

EXPERIMENTAL

Materials

According to ref. 5, the materials used to prepare Dang-Guei-San were Atractylodis Rhizoma (1.5 g) and Paeoniae Radix, Swertiae Herba, Cnidii Rhizoma, Scutellariae Radix (3 g

* Corresponding author.

0021-9673/94/$07.00 © 1994 Elsevier Science B.V. All rights reserved
SSDI 0021-9673(93)E0832-F

each). Each material was obtained from the market in Taipei and pulverized (8 mesh). For concentrated herbal preparations containing Paeoniae Radix, Swertiae Herba, Cnidii Rhizoma and Scutellariae Radix, three different commercial brands were obtained from the market.

Chemicals and reagents

Structures of the marker components are shown in Fig. 1. Paeoniflorin and baicalin were purchased from Nacalai Tesque (Kyoto, Japan). Ferulic acid and the internal standard methylparaben were obtained from Sigma (St. Louis, MO, USA). Acetonitrile and methanol (HPLC grade) were purchased from Labscan. Phosphoric acid was of analytical-reagent grade. Ultrapure distilled water with a resistivity greater than 18 MΩ was used.

Instruments

HPLC was conducted with a Waters Model 625 system equipped with a Waters Model 486 UV detector and a Rheodyne Model 9125-080 injector. Peak areas were calculated with a Shiunn Haw computing integrator. A Cosmosil $5C_{18}$-AR reverse-phase column (150 × 4.6 mm I.D.) and used. Concentrations by reduced-pressure evaporation, freeze-drying and spray-drying of a standard decoction were carried out with a Rotavapor (Buchi R110/RE120/EL-13), a freeze-drier (Virtis Freeze Mobile 3) and a mini spray dryer (Buchi Model 190), respectively.

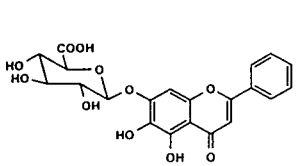

Baicalin

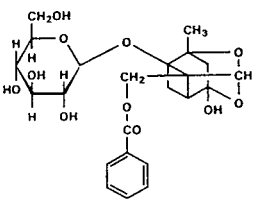

Paeoniflorin

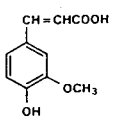

Ferulic acid

Fig. 1. Structures of marker components.

Liquid chromatography

The mobile phase was 0.03% (v/v) phosphoric acid–acetonitrile (0 min 96:4, 5 min 84:16, 7 min 82:18, 14–30 min 78:22), filtered through a 0.45-μm Millipore filter and degassed prior to used. The flow-rate was 1 ml/min. A constant operating temperature (room temperature) was maintained. The internal standard, methylparaben (3.4 mg), was dissolved in 35 ml of methanol and diluted to 50 ml with water to give the internal standard solution.

Preparation of standard solution

To prepare a standard solution containing paeoniforin, ferulic acid and baicalin, an appropriate amount of internal standard solution was added to an accurately weighed amount of paeoniflorin, ferulic acid and baicalin standards dissolved in 50% methanol to give various concentrations within the ranges 0.0107–0.0535, 0.00124–0.011088 and 0.0115–0.1495 mg/ml, respectively. Calibration graphs were plotted after linear regression analysis of the peak-area ratios with concentration.

Preparation of sample solutions

Standard decocation. Amounts of crude drugs equivalent to a daily dose of Dang-Guei-San were weighed and pulverized, a twentyfold weight of water was added and the mixture was boiled for more than 30 min to halve the original volume. After filtration while hot, the filtrate was diluted with methanol to give a 70% methanol solution and then a suitable amount of internal standard was added to the solution to give a concentration of 0.017 mg/ml of methylparaben.

Interference test. Amounts of crude drug equivalent to a daily dose of Dang-Guei-San without Paeoniae Radix, Swertiae Herba and Cnidii Rhizoma or Scutellariae Radix were weighed and pulverized, a twentyfold weight of water was added and the mixture was boiled for more than 30 min to halve the original volume. After filtration while hot, the filtrate was diluted with methanol to give a 70% methanol solution.

Content of paeoniflorin, ferulic acid and baicalin in raw herbs. Amounts of individual crude drug equivalent to a daily dose of Dang-Guei-San was weighed and pulverized, a twentyfold weight of water was added and the mixture was boiled for more than 30 min to halve the original volume. After filtration while hot, the filtrate was diluted with methanol to give a 70% methanol solution and then a suitable amount of internal standard was added to the solution to give a concentration of 0.017 mg/ml of methylparaben.

Various concentrated products of standard decoction. Concentrations by reduced-pressure evaporation, freeze-drying and spray-drying of a standard decoction were applied. After concentration, each residue was dissolved in a suitable amount of 70% methanol and internal standard was then added to give a concentration of 0.017 mg/ml of methylparaben.

Concentrated herbal preparations from market. An amount of the concentrated herbal preparation equivalent to a daily dose was weighed accurately and extracted with a tenfold weight of water for 30 min in an ultrasonic bath. After extraction, the samples were filtered and diluted with methanol to give a 70% methanol solution and internal standard was then added to give a concentration of 0.017 mg/ml of methylparaben.

Solutions for recovery study

Amounts of crude drugs equivalent to 50 daily doses of Dang-Guei-San without Paeoniae Radix were weighed and pulverized together. Then four doses of this powder, each of 10.5 g, were weighed precisely and separately. To these four doses were added 2, 3, 3.5 and 4 g of Paeoniae Radix with known paeoniflorin contents of 19.94, 29.91, 34.89 and 39.88 mg, respectively. A twentyfold weight of water was added and the mixture was boiled for more than 30 min to halve the original volume. A suitable amount of internal standard was added to the solution to give a concentration of 0.017 mg/ml of methylparaben.

For baicalin, as mentioned above, 2, 3, 3.5 and 4 g of Scutellariae Radix with known baicalin contents of 170.76, 256.14, 298.83 and 341.52 mg, respectively, were added for a recovery study. For ferulic acid in Swertiae Herba and Cnidii Rhizoma, 50 doses of Dang-Guei-San excluding both herbs were weighed and pulverized. Additionally, Swertiae Herba and Cnidii Rhizoma (50 g of each) were weighed and pulverized together. To these four doses of Dang-Guei-San were added 4, 6, 7 and 8 g of a mixture of Swertiae Herba and Cnidii Rhizoma with known ferulic acid contents of 1.44, 2.16, 2.52 and 2.88 mg, respectively. All samples were filtered through a Millipore filter and were injected for HPLC analysis to calculate the concentration of paeoniflorin, ferulic acid and baicalin from their calibration graphs.

RESULTS AND DISCUSSION

In order to elute the marker components within reasonable retention times, we adopted a method in which the pH was changed by gradient elution. In general, acidic compounds tend to be more hydrophilic when the mobile phase is adjusted to higher pH and more hydrophobic when the pH is lower. In other words, the retention time is lengthened for acidic compounds when the pH is lower than the pK_a value. The relationship between the retention time of a compound and pH was found to be sigmoid [6]. Methylparaben was used as the internal standard because its structure is similar to that of ferulic acid and there was no interference at the same retention time. The detection wavelength was chosen as 245 nm because the contents of paeoniflorin and ferulic acid in the prescription were low, whereas that of baicalin was high, and at 245 nm, baicalin absorbs weakly whereas paeoniflorin and ferulic acid absorb strongly.

A standard decoction was prepared by boiling raw herbs in water for more than 30 min. On one hand, this mimicked the traditional way of making a decoction. On the other hand, studies showed that paeoniflorin is best extractable with water at 60°C for 30 min [7]. The decoctions were eluted with 70% methanol solution in the final stage because the columns tended to become blocked when water was injected. In addition, the solubilities of the marker com-

TABLE I

INTER-DAY AND INTRA-DAY RELATIVE STANDARD DEVIATIONS ($n = 6$) FOR PAEONIFLORIN, FERULIC ACID AND BAICALIN

Marker component	Concentration (mg/ml)	Peak area of marker component/ peak area of methylparaben		R.S.D. (%)	
		Inter-day	Intra-day	Inter-day	Intra-day
Paeoniflorin	0.0321	0.188	0.185	1.01	1.13
Ferulic acid	0.0086	0.312	0.297	0.51	0.26
Baicalin	0.0575	0.739	0.714	1.23	0.42

ponents were satisfactory in 70% methanol solution. For ferulic acid assay, the standard solutions were prepared in 50% methanol solution in the final stage because ferulic acid split into two peaks in the HPLC profile when 70% methanol solution was used. The reason for this difference is that the solvent power of sample solutions should be lower than that of the mobile phase. Increasing the proportion of water can solve this problem.

To check the precision of this method, we injected standard solutions of paeoniflorin, ferulic acid and baicalin at the concentrations of 0.0321, 0.0086 and 0.0575 mg/ml, respectively, six times on the same day. The resulting relative standard deviations (R.S.D.s) were 1.13%, 0.26% and 0.42%, respectively. The R.S.D.s obtained from a 6-day period were 1.01%, 0.51% and 1.23%, respectively (Table I). All these values indicate satisfactory precision. When we measured the contents of marker components in a standard decoction and the preparations sold in the market, the R.S.D.s were about 5%. The reason for the higher R.S.D. values than for a standard solution is that they contain less ferulic acid. The contents of marker components in commercial preparations vary greatly from those in standard decoctions, as shown in Table II and Fig. 2. This is probably due to differences in the manufacturing process. The effects of different concentration devices on the manufacturing process were also explored using reduced-pressure evaporation, spray-drying and freeze-drying, and the results are given in Table III and Fig. 3.

To ensure the specificity and selectivity of the method, we prepared three blank decoctions for comparison: one with no Paeoniae Radix, one with no Swertiae Herba and no Cnidii Rhizoma and one with no Scutellariae Radix. The chromatograms are shown in Fig. 4. The retention times of the marker components, *i.e.*, paeoni-

TABLE II

CONTENTS OF PAEONIFLORIN, BAICALIN AND FERULIC ACID IN STANDARD DECOCTION AND COMMERCIAL CONCENTRATED HERBAL PREPARATION OF DANG-GUEI-SAN

Sample	Paeoniflorin		Baicalin		Ferulic acid	
	Mean ± S.D. (mg/g)[a]	R.S.D. (%)	Mean ± S.D. (mg/g)[a]	R.S.D. (%)	Mean ± S.D. (mg/g)[a]	R.S.D. (%)
Standard decoction	2.78 ± 0.05	1.97	27.26 ± 1.35	4.98	0.17 ± 0.01	4.05
Commercial preparation A	1.88 ± 0.06	3.06	4.72 ± 0.20	4.24	0.02 ± 0.001	6.25
Commercial preparation B	2.12 ± 0.11	5.64	0.02 ± 0.001	5.02	N.D.	–
Commercial preparation C	N.D.[b]	–	2.44 ± 0.07	2.89	N.D.	–

[a] $n = 5$ with 95% confidence limits.
[b] N.D. = Not determined.

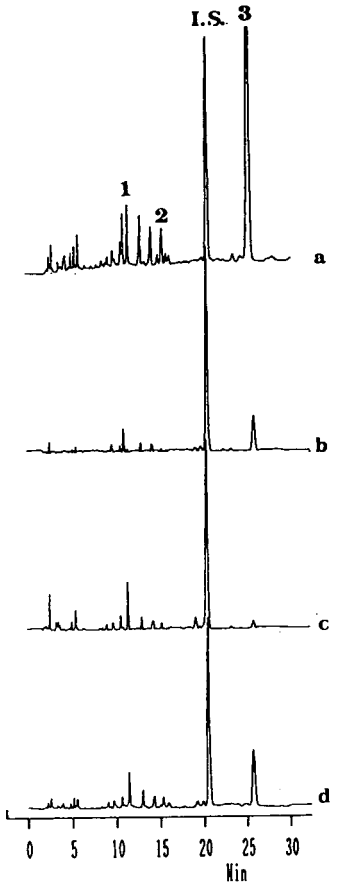

Fig. 2. Chromatograms of paeoniflorin, ferulic acid and baicalin in Dang-Guei-San: (a) standard decoction; (b) commercial preparation A; (c) commercial preparation B; (d) commercial preparation C. Peaks: 1 = paeoniflorin; 2 = ferulic acid; 3 = baicalin; I.S. = internal standard (methylparaben).

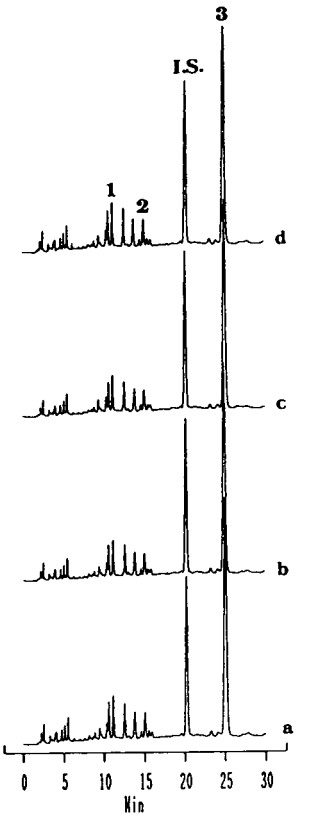

Fig. 3. Chromatograms of paeoniflorin, ferulic acid and baicalin in Dang-Guei-San: (a) standard decoction; (b) after concentration under reduced pressure; (c) after freeze-drying; (d) after spray-drying. Peaks as in Fig. 2.

TABLE III

CONTENTS OF PAEONIFLORIN, BAICALIN AND FERULIC ACID AFTER CONCENTRATION BY VARIOUS PROCESSES IN STANDARD DECOCTION AND IN PRODUCTS

Sample	Paeoniflorin		Baicalin		Ferulic acid	
	Mean ± S.D. (mg/g)[a]	R.S.D. (%)	Mean ± S.D. (mg/g)[a]	R.S.D. (%)	Mean ± S.D. (mg/g)[a]	R.S.D. (%)
Standard decoction	2.78 ± 0.05	1.97	27.26 ± 1.35	4.98	0.17 ± 0.01	4.05
Concentration under reduced pressure	2.24 ± 0.10	4.48	23.53 ± 0.31	1.31	0.16 ± 0.01	7.76
Freeze-drying	2.25 ± 0.09	4.04	23.15 ± 0.42	1.81	0.15 ± 0.01	5.88
Spray-drying	2.60 ± 0.12	4.58	26.27 ± 0.93	3.57	0.17 ± 0.01	7.56

[a] $n = 5$ with 95% confidence limits.

TABLE IV

RELATIONSHIPS BETWEEN CONCENTRATIONS OF PAEONIFLORIN, FERULIC ACID AND BAICALIN AND THE PEAK AREA RATIO

Paeoniflorin: $y = -3.934 \cdot 10^{-3}x + 0.15$ ($r = 0.9973$); baicalin: $y = -3.689 \cdot 10^{-3}x + 9.11 \cdot 10^{-2}$ ($r = 0.9943$); ferulic acid: $y = -6.645 \cdot 10^{-4}x + 2.47 \cdot 10^{-2}$ ($r = 0.9970$).

Marker component	Concentration (mg/ml)	Peak-area ratio[a]	R.S.D. (%)[b]
Paeoniflorin	0.0107	0.0879	1.25
	0.0214	0.1791	1.31
	0.0321	0.2400	1.13
	0.0535	0.3749	1.00
Baicalin	0.0115	0.1416	0.84
	0.0575	0.6926	0.42
	0.1150	1.3905	0.32
	0.1495	1.6047	0.37
Ferulic acid	0.001232	0.0649	0.52
	0.003696	0.1912	0.40
	0.008624	0.3856	0.26
	0.011088	0.4634	0.31

[a] Peak area of marker components/peak area of methyl paraben.
[b] $n = 5$.

TABLE V

CONTENTS OF MARKER COMPONENTS IN SINGLE HERB AND TURNOVER RATIO IN STANDARD DECOCTION OF DANG-GUEI-SAN

Single herb (daily dose)	Marker component	Content of marker component in single herb		Theoretical content of marker component in standard decoction (mg/g) (daily dose, A)	Content of marker component in standard decoction (mg/g) (daily dose, B)	Turnover ratio (B/A, %)
		Mean ± S.D. (mg/g)[a]	R.S.D. (%)			
Paeoniae Radix (3 g)	Paeoniflorin	9.97 ± 0.12	1.25	29.91	8.44	28.22
Scutellariae Radix (3 g)	Baicalin	85.38 ± 1.80	2.11	256.14	84.05	32.81
Swertiae Herba (3 g) and Cnidii Rhizoma (3 g)	Ferulic acid	0.35 ± 0.01	4.19	2.10	1.05	50.00

[a] $n = 5$ with 95% confidence limits.

florin, ferulic acid and baicalin, are 11, 15 and 25.5 min, respectively. On inspection of three-dimensional chromatograms, these three components all showed no interference. There was also no peak at their retention times in blank decoctions. The three commercial preparations also showed satisfactory separations.

The calibration graph for paeoniflorin and methylparaben was obtained over the range 0.0107–0.0535 mg/ml. The results, through linear regression analysis, showed a good linear relationship between peak-area ratio and concentration. Table IV gives the results and regression equation. Good linear relationships were also obtained from the calibration graphs for ferulic acid and baicalin.

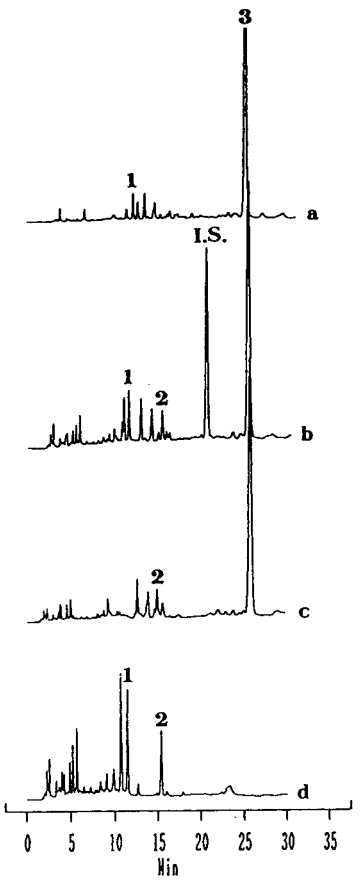

Fig. 4. Chromatograms of paeoniflorin, ferulic acid and baicalin in Dang-Guei-San and their blank solutions: (a) standard decoction without Swertiae Herba and Cnidii Rhizoma; (b) standard decoction; (c) standard decoction without Paeoniae Radix; (d) standard decoction without Scutellariae Radix. Peaks as in Fig. 2.

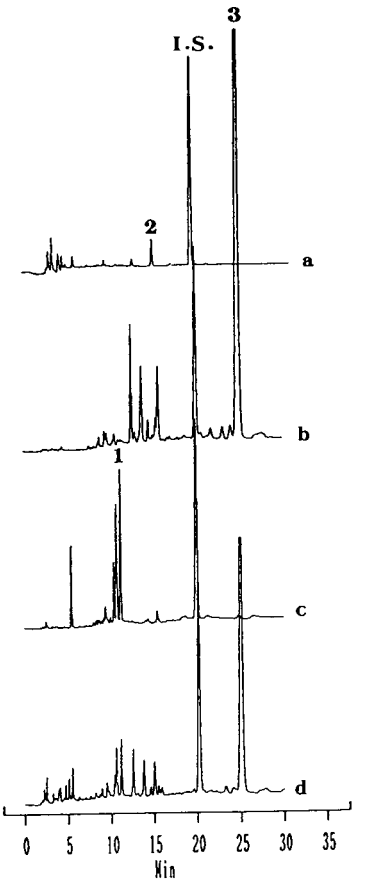

Fig. 5. Chromatograms of paeoniflorin, ferulic acid and baicalin in raw herbs and prescription: (a) Swertiae Herba and Cnidii Rhizoma; (b) Scutellariae Radix; (c) Paeoniae Radix (d) Dang-Guei-San. Peaks as in Fig. 2.

The turnover ratios of these constituents were defined as the percentage yields of these constituents in the Chinese medicinal preparations, calculated on the basis of their contents in the respective crude herbs. The turnover ratios for a certain marker component in different preparations vary greatly because each preparation has its own combination of raw herbs. The turnover ratios of the marker components of Dang-Guei-San prescription are shown in Table V and Fig. 5.

The recoveries of paeoniflorin, ferulic acid and baicalin were 27.86%, 33.89% and 49.31%, respectively, corresponding to turnover ratios of 28.22%, 32.81% and 50.00%, respectively. In fact, the turnover ratio was the same as the recovery when the added amount was a daily dose of Dang-Guei-San. When interaction is part of the procedure, the response measured from the matrix is generally compared with the response from the single raw herb, both subjected to the entire experimental procedure. In this case, the recovery is referred to as the relative recovery. When the amount of raw herb materials added was increased, the more the relative recovery decreased. It seems that a twentyfold weight of water was not enough when the amount of raw herb materials added was too great (Table VI).

TABLE VI

RECOVERY OF PAEONIFLORIN, BAICALIN AND FERULIC ACID FROM DANG-GUEI-SAN

Raw herb	Marker component	Raw herb material added (g)	Equal to marker component added (mg)	Found (mg)	Relative recovery (%)	Mean ± S.D. (%)[a]	R.S.D. (%)
Paeoniae Radix	Paeoniflorin	2.00	19.94	5.76	28.87	27.86 ± 0.86	3.08
		3.00	29.91	8.44	28.22		
		3.50	34.89	9.57	27.43		
		4.00	39.88	10.74	26.92		
Scutellariae Radix	Baicalin	2.00	170.76	60.82	35.62	33.89 ± 1.21	3.56
		3.00	256.14	84.02	32.81		
		3.50	298.83	100.71	33.70		
		4.00	341.52	114.24	33.45		
Swertiae Herba and Cnidii Rhizoma	Ferulic acid	4.00	1.44	0.77	53.74	49.31 ± 3.49	7.06
		6.00	2.16	1.08	50.00		
		7.00	2.52	1.21	48.04		
		8.00	2.88	1.31	45.47		

[a] $n = 5$ with 95% confidence limits.

ACKNOWLEDGEMENTS

This work was supported by the Department of Health, Executive Yuan, Taiwan (DOH81-TD-062a). The authors thank Miss Fang-Su Liu and Mr. Chi-Fang Lou for their assistance in the preparation of this manuscript. We thank Dr. Pei-Dawn Lee for critical review of the manuscript. We also thank Mr. Kuen-Sen Huang for technical assistance.

REFERENCES

1 N. Asakawa, T. Hottri, M. Ueyama, A. Shinoda and Y. Miyake, *Yakugaku Zasshi*, 99 (1979) 598–601.
2 Y. Takino, T. Miyahara, E. Arichi, S. Arichi, T. Hayashi and M. Karikura, *Chem. Pharm. Bull.*, 35 (1987) 3494–3497.
3 K. Sagara, Y. Ito, T. Oshima, T. Misaki and H. Murayama, *J. Chromatogr.*, 328 (1985) 289–297.
4 K. Sagara, Y. Ito, T. Oshima, H. Murayama and H. Itokawa, *Shoyakugaku Zasshi*, 40 (1986) 84–88.
5 H.-Y. Hsu and C.-S. Hsu, *Commonly Used Chinese Herb Formulas with Illustrations*, Oriental Healing Arts Institute, Taiwan, 1980.
6 B. Bourguignon, F. Marcenac, H.R. Keller, P.F. deAguiar and D.L. Massart, *J. Chromatogr.*, 628 (1993) 171–189.
7 K.-C. Wen, C.-Y. Huang and F.-S. Liu, *J. Chromatogr.*, 593 (1992) 191–199.

Journal of Chromatography A, 660 (1994) 307–312
Elsevier Science B.V., Amsterdam

CHROMSYMP. 2885

Simultaneous determination of L-693,612, a topical carbonic anhydrase inhibitor, and two potential metabolites in human whole blood by ion-pair high-performance liquid chromatography

E.J. Woolf*, T. Au, M. Kasper, M. Constanzer and B. Matuszewski

Merck Research Laboratories, Department of Drug Metabolism, West Point, PA 19486 (USA)

ABSTRACT

A method for the simultaneous determination of a topical carbonic anhydrase inhibitor, L-693,612, and two of its potential metabolites in human whole blood is described. The analytes are isolated from the matrix via liquid–liquid extraction with a mixture of toluene, ethyl acetate and isopropanol (49:50:1, v/v/v). The analytes are then back extracted into dilute phosphoric acid prior to injection into the HPLC system. A cyano column (Zorbax SB-CN, 150 × 4.6 mm) with a mobile phase of phosphoric acid(0.085%)–acetonitrile (73.5:26.5) containing 10 m*M* sodium decane sulfonate and adjusted to pH 3 is used for the analysis. Detection is based on UV absorbance at 252 nm. The assay was found to be linear in the concentration range of 5–500 ng/ml for each analyte when 1-ml aliquots of whole blood were extracted.

INTRODUCTION

Trans-(−)-5,6-dihydro-6-(3-methoxypropyl)-4-propylamino - 4H - thieno[2,3 - B]thiopyran - 2-sulfon-amide-7,7-dioxide (Compound **I**, L-693,612) is a member of a group of compounds that have been found to be potent inhibitors of the enzyme carbonic anhydrase. The ocular hypotensive activity that these compounds exhibit when applied topically has been demonstrated in various animal pharmacological models, as well as humans. During pre-clinical studies in rats, compounds **II** (O-desmethyl L-693612) and **III** (N-despropyl L-693612) were identified as active metabolites of **I** [1]. In order to support a clinical pharmacokinetic program, an assay of **I**, and its potential metabolites **II** and **III**, in human whole blood was required. An assay of **I**, **II**, and **III** in human whole blood using liquid–liquid extraction for analyte isolation followed by reversed-phase ion-pair high-performance liquid chromatography with UV detection is presented here.

MATERIALS AND METHODS

Materials

The hydrochloride salts of compounds **I**, **II**, and **III** (Fig. 1) were obtained from the Medicinal Chemistry Department of Merck Research Laboratories (West Point, PA, USA). Acetonitrile and hexane (Omnisolve grade) were from EM Science (Gibbstown, NJ, USA). Ethyl acetate and toluene were obtained from Burdick and Jackson (Muskegon, MI, USA). Isopropanol (Optima grade) was from Fisher Scientific (Springfield, NJ, USA). The sodium salts of C5–C8 alkane sulfonates were from Regis (Morton Grove, IL, USA). Sodium 1-nonane

* Corresponding author.

0021-9673/94/$07.00 © 1994 Elsevier Science B.V. All rights reserved
SSDI 0021-9673(93)E0784-R

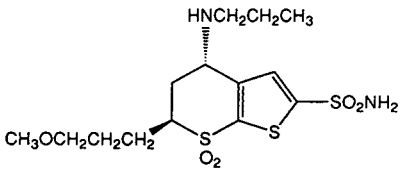

Compound I

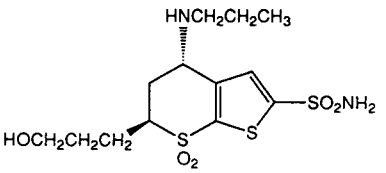

Compound II

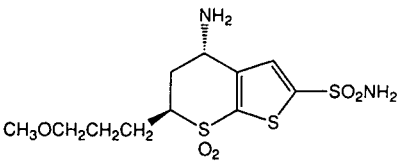

Compound III

Fig. 1. Structures of analytes

and sodium 1-decane sulfonates were purchased from Lancaster Synthesis (Windham, NH, USA). Drug-free heparinized human whole blood was supplied by Biological Specialties, Inc. (Lansdale, PA, USA). All other reagents were of ACS grade and were used as received.

Instrumentation

The HPLC system consisted of a Perkin-Elmer (Norwalk, CT, USA) Model 410 pump, a Waters (Milford, MA, USA) WISP 715 automatic injector and an Applied Biosystems (Foster City, CA, USA) Model 785 absorbance detector. The analog output from the detector (1 V/AU) was connected to a PE-Nelson (Cupertino, CA, USA) Access-Chrom data system via a PE-Nelson 941 analog-to-digital interface.

Chromatography conditions

The mobile phase consisted of 2.4 g of sodium 1-decane sulfonate dissolved in a mixture of 735 ml of 0.085% *o*-phosphoric acid and 265 ml of acetonitrile. The final pH of the mobile phase was adjusted to 3.0 with 10 *M* sodium hydroxide. Prior to use, the mobile phase was passed through a Rainin (Woburn, MA, USA) 0.20-μm nylon membrane filter.

A Zorbax SB-CN column (5-μm particles, 80 Å pore size, 150 × 4.6 mm, Mac-Mod Analytical, Chadds Ford, PA, USA) was used for the separation. The mobile phase flow rate was 1.2 ml/min. The sample injection volume was 200 μl. Ultraviolet absorbance at 252 nm was used for detection.

Preparation of standards

A methanolic stock solution containing 20 μg (free base)/ml of each analyte was prepared by weighing 1.09 mg of the hydrochloride salts of **I** and **II** and 1.10 mg of the hydrochloride salt of **III** into a 50-ml volumetric flask and filling the flask to volume with methanol. A 2.0 μg/ml stock solution was prepared by diluting 5 ml of the 20 μg/ml solution to 50 ml with methanol.

Working standards of 10, 8, 4, and 2 μg of each analyte/ml were prepared by dilution of the 20 μg/ml stock solution with methanol. Working standards of 1, 0.4, 0.2 and 0.1 μg of each analyte/ml were prepared by dilution of the 2.0 μg/ml stock with methanol. Working standard solutions were found to be stable for at least 2 weeks when stored at room temperature.

Whole blood standards were prepared by adding 50 μl of each working standard to 1 ml of drug free blood. The resulting standards ranged in concentration from 5 to 500 ng/ml of each analyte.

Sample preparation

A 1-ml aliquot of blood (sample or standard) was pipetted, using a large orifice polypropylene pipet tip (PGC Scientifics, Gaithersburg, MD, USA), into a 50-ml disposable screw cap glass conical centrifuge tube (Kimble, Vineland, NJ, USA). Following the addition of 1 ml of water, the tube was vortexed vigorously for 60 s to lyse any intact cells. 600 μl of a 10% (w/v) aqueous solution of trichloroacetic acid was added to the tube, after which it was vortexed for 60 s to denature proteins in the sample. Buffer (0.2 *M* phosphate, pH = 8.0, 3.0 ml) was added followed by 8.0 ml of extraction solvent mixture (ethyl acetate–toluene–isopropanol; 50:49:1, v/v/v). The tubes were capped with teflon lined

closures and shaken for 10 min. Following centrifugation (5 min, 1500 *g*), 7.0 ml of the upper organic layer was transferred to a clean 50-ml glass centrifuge tube. The aqueous layer was then re-extracted with an additional 8.0 ml of extraction solvent. The second 8.0 ml of extraction solvent was transferred to the tube containing the first portion of solvent, and the combined extracts were back-extracted into 0.5 ml of 0.085% *o*-phosphoric acid. The acid extract was washed with 2.0 ml of hexane in order to remove most of the residual toluene from the extraction solvent. Following aspiration of the hexane to waste, the acid extract was transferred to an autosampler vial prior to injection into the HPLC system.

RESULTS

Assay specificity

Fig. 2 shows chromatograms of extracted drug-free whole blood, a whole blood standard containing each analyte at a concentration of 200 ng/ml and a whole blood sample taken from a subject after receiving an ocular dose of a 2% solution of **I**. A comparison of Fig. 2A with Fig. 2B illustrates that no endogenous peaks co-elute with any of the analytes. The specificity of the method is further illustrated by the fact that all pre-dose blood samples from subjects involved in clinical trials were free of interfering peaks.

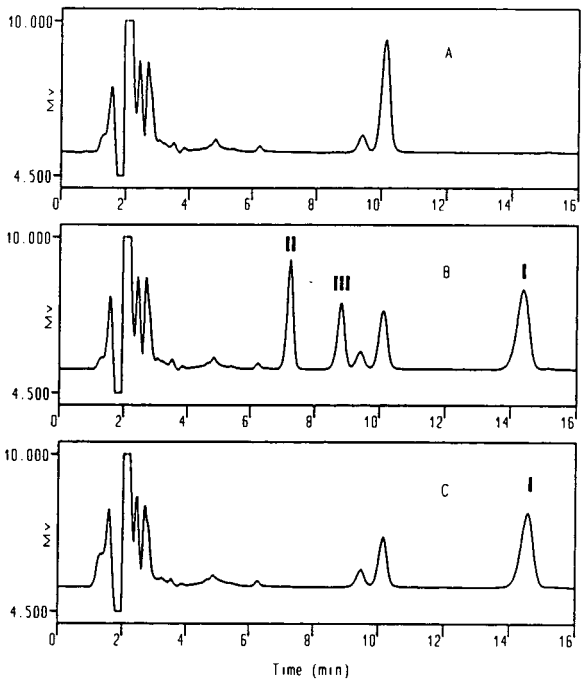

Fig. 2. Representative chromatograms of (A) control human whole blood, (B) whole blood spiked with 200 ng/ml of each analyte and (C) blood sample from human volunteer obtained after ocular administration of **I**; the concentration of **I** is equivalent to 184 ng/ml. Analytes **II** and **III** were not detectable. (*Y*-axis scale: 1 mV = 1 mAu).

Linearity

Weighted (weighting factor = $1/y$ where y = peak height) least-squares regression calibration curves, constructed by plotting the standard concentration of each analyte *vs.* peak height, yielded coefficients of regression typically greater than 0.999 over the concentration range, for each analyte, of 5–500 ng/ml of blood. The use of the weighted least-squares regression resulted in less than a 10% deviation between the nominal standard concentrations and the experimentally determined standard concentrations calculated from the regression equations.

Extraction recovery

The recovery of the extraction procedure was determined by comparing the responses of the working standards containing **I**, **II**, and **III**, with those of extracted whole blood standards. The results (Table I) indicate that the mean recoveries of **I**, **II**, and **III**, over the concentration range of 5–500 ng/ml blood, are 84.3, 62.1, and 41.5%, respectively. Although the extraction efficiency of **III** was under 50%, it was constant over the concentration range studied, and the precision of the extraction of **III** at each concentration, as measured by the relative standard deviation, was better than 6.0% (Table I).

Assay precision and accuracy

Replicate standards ($n = 5$) were analyzed to assess the within-day variability of the assay. The mean accuracy of the assayed concentration of each analyte as well as the relative standard deviation (R.S.D.) of the whole blood replicate standards are shown in Table I.

Standard curves over the assay range of 5–500

TABLE I

RECOVERY OF ANALYTES FROM HUMAN WHOLE BLOOD AND WITHIN-DAY VARIABILITY OF THE ASSAY

Nominal conc. of analyte (ng/ml)	Analyte I			Analyte II			Analyte III		
	Accuracy[a]	Precision[b]	Recovery (%)	Accuracy	Precision	Recovery (%)	Accuracy	Precision	Recovery (%)
5.0	98.6	5.9	72.9	97.0	3.9	65.2	98.0	5.7	41.3
10.0	97.3	2.0	84.3	97.6	2.4	62.7	99.5	1.7	41.1
20.0	103.9	1.9	85.8	99.0	1.9	60.8	100.4	3.1	40.9
50.0	96.1	6.5	87.8	98.4	3.7	64.5	98.1	3.9	43.5
100.0	98.8	5.8	85.5	100.3	2.0	58.7	99.9	1.8	39.6
200.0	102.9	2.8	88.0	103.9	2.1	63.6	104.8	2.0	43.1
400.0	99.7	2.4	84.9	98.1	1.5	60.4	98.5	1.5	41.0
500.0	95.4	6.5	85.6	98.6	2.6	62.1	98.2	4.3	41.3
Mean	99.1	4.2	84.3	99.1	2.6	62.1	99.7	3.0	41.5

[a] Calculated as [mean ($n = 5$) observed concentration/nominal concentration] × 100.
[b] Expressed as relative standard deviation.

ng/ml of each analyte per ml of blood were analyzed on each of 3 days to determine the inter-day variability of the assay. The inter-day mean accuracy and precision data is presented in Table II. The R.S.D.s of the slopes of the regression lines over the 3 runs were 4.5, 1.7, and 2.6% for analytes **I**, **II**, and **III**, respectively.

Analyte stability

Whole blood quality control samples were prepared at concentrations of 15.0 and 350 ng of each analyte per ml and stored frozen at −20°C. Analysis of these samples over a one-month period showed no degradation of any of the analytes.

Limit of quantification

The limit of quantification of the assay, defined as the lowest concentration that yielded an within-day R.S.D. of less than 10% and an within-day accuracy between 90 and 110% of nominal concentration, was 5 ng/ml for each analyte.

DISCUSSION

The red blood cell (RBC) to plasma ratio of **I** in rats has been found to be concentration-dependent, presumably due to saturable binding of **I** to carbonic anhydrase in RBCs [2]. To eliminate the contribution of this effect, an assay of **I**,

TABLE II

INTER-DAY VARIABILITY OF THE ASSAY AS ASSESSED BY THE PRECISION AND ACCURACY OF THE CALCULATED STANDARD CONCENTRATIONS FROM THE REGRESSION LINES ON EACH OF 3 DAYS

Nominal conc. of analyte (ng/ml)	Analyte I		Analyte II		Analyte III	
	Accuracy[a]	Precision[b]	Accuracy	Precision	Accuracy	Precision
5.0	101.7	5.4	98.9	6.7	101.1	9.4
10.0	97.9	1.0	98.7	3.8	99.0	1.1
20.0	100.9	2.2	101.1	3.6	101.2	2.9
50.0	101.1	2.9	102.1	3.3	100.9	3.2
100.0	99.6	4.3	101.3	6.4	99.4	5.8
200.0	98.8	3.0	98.4	2.4	98.5	1.8
400.0	99.0	1.9	99.1	1.8	99.1	1.5
500.0	101.3	0.2	101.0	0.4	101.5	0.6

[a] Calculated as [mean ($n = 3$) observed concentration/nominal concentration] × 100.
[b] Expressed as relative standard deviation.

II, and **III** in whole blood rather than plasma was required.

In order to develop a simultaneous assay for **I**, **II**, and **III**, two problems had to be addressed. First, a method to simultaneously extract the analytes from the blood matrix was required. Second, a chromatographic system capable of not only separating the analytes from each other, but also, resolving them from co-extracted endogenous substances had to be developed.

We have previously reported that another carbonic anhydrase inhibitor, possessing structural similarities to **I**, was effectively extracted from buffered, deproteinized whole blood with a mixture of toluene, ethyl acetate and isopropanol [3]. Such an approach proved to be successful for the isolation of **I**, **II**, and **III**. Although the extraction recoveries of **II** and **III** were significantly less than that of **I**, the recovery of all analytes appeared to be constant and reproducible over the concentration range studied (Table I).

Development of a chromatographic system that could be used to analyze whole blood extracts proved to be more difficult. Initial attempts to chromatograph the extracts under isocratic reverse phase conditions using a base deactivated C-18 column (Zorbax Rx-C18) with mobile phases at pH = 3 and pH = 6.5 resulted in wide capacity factor differences between the possible metabolites (**II** and **III**) and the parent compound, **I**. Such chromatography led to poor assay sensitivity and long run times. The use of gradient conditions was not thought to be a viable option, as it was felt that the time saved by running a gradient would be lost in column re-equilibration time.

The use of a "stable bond" cyano column (Zorbax SB-CN) with a mobile phase at pH = 3 containing 9% acetonitrile allowed all analytes to be chromatographed with capacity factors ranging from 2 to 6. Unfortunately, interferences were present in whole blood extracts. The majority of the interferences could be moved to the solvent front by increasing the strength of the mobile phase to 27% acetonitrile; however, as expected, the retention of the analytes was also decreased. Adding alkane sulfonate ion-pairing agents to a mobile phase containing 27% acetonitrile was found to dramatically affect the retention of the analytes; retention was found to increase as the length of the carbon chain of the ion-pairing agent increased (Fig. 3). The behavior of the endogeneous species was unaffected by the ion-pairing agents; the majority continued to elute near the solvent front. Apparently,the endogenous material did not interact with any of the ion-pair reagents, whereas the retention of the analytes was found to be highly dependent on the ion-pair reagent used in the mobile phase. The retention of two remaining endogenous peaks, eluting between 9 and 11 min, was also found to be unaffected by any of the ion-pair reagents. These peaks could, how-

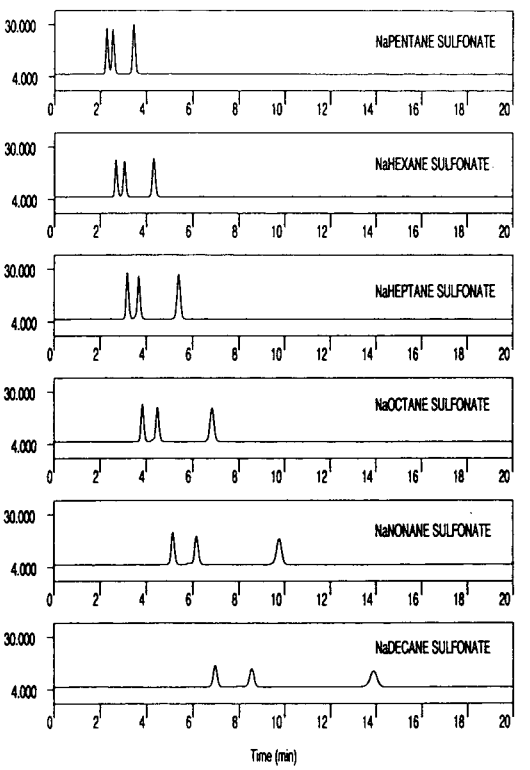

Fig. 3. Chromatography of analytes **I**, **II**, and **III** with mobile phases containing different ion-pairing reagents. The mobile phase in each case consists of acetonitrile–water (27:73, v/v) containing 1.4 ml/l *o*-phosphoric acid and 10 m*M* of the indicated ion-pair reagent. The final pH of the mobile phase was adjusted to 3.0 with 10 *M* NaOH. Column, Zorbax SB-CN (150 × 4.6 mm); flow rate, 1.2 ml/min; detection, UV absorbance at 252 nm, 1 mV = 1 mAu. Elution order: **II**, **III**, **I**. Each peak corresponds to approximately 200 ng of analyte injected on column.

ever, be resolved from the analytes by slightly adjusting the percentage of acetonitrile in the mobile phase. The optimum ion-pair mobile phase consisted of approximately 10 m*M* sodium decane sulfonate dissolved in a 26.5:73.5 (v/v) mixture of acetonitrile and phosphate buffer at pH = 3. Using this mobile phase, all analytes were resolved from endogenous substances in under 16 min (Fig. 2).

The described assay has been used to analyze clinical samples obtained after ocular administration of **I**. Twice a day, study subjects received 1 drop of a 2% solution of **I** in each eye. This dose was administered for seven days. Blood samples were collected pre-dose, and on days 2 and 7. Additional samples were collected at one week, three weeks, and 3 months post administration of the last dose. The resulting levels of **I** for two subjects are presented in Table III. As is the case with other members of this class of compounds [3], **I** has an extremely long terminal half-life; significant levels are still observed 3 months after drug administration. Metabolites **II** and **III**, previously identified in rat blood [1], were not detectable in any of the clinical samples.

TABLE III

WHOLE BLOOD LEVELS OF **I** AFTER OCULAR ADMINISTRATION OF A 2% SOLUTION

Time	Concentration (ng/ml)	
	Subject 1	Subject 2
Pre-dose	0.0	0.0
Day 2	32.1	36.9
Day 7	254.6	222.4
1 Week p.a.[a]	214.6	206.2
3 Weeks p.a.	188.1	170.5
3 Months p.a.	123.4	139.1

[a] Post administration.

CONCLUSIONS

An ion-pair HPLC assay for the simultaneous determination of **I** and its potential metabolites, **II** and **III**, in human whole blood has been developed. The method has been found to be precise, accurate, and suitable for the analysis of whole blood samples collected during clinical pharmacokinetic studies. Analytes **II** and **III** were not detected in human whole blood samples obtained after 7 days of ocular dosing of **I**.

ACKNOWLEDGEMENTS

The human blood samples were obtained from a clinical study directed by Dr. E. Strahlman, Department of Clinical Research, Merck Research Laboratories. The authors would like to thank J. Baldwin, G. Ponticello, and O. Woltersdorf of the Medicinal Chemistry Department of Merck Research Laboratories for synthesizing analytes **II** and **III**.

REFERENCES

1 B.K. Wong, P.J. Bruhin, J.D. Gilbert and J.H. Lin, *Pharm. Res.*, 9 (1992) S-292.
2 B.K. Wong, J.H. Lin and P.J. Bruhin, *Pharm. Res.*, 8 (1991) S-292.
3 B.K. Matuszewski, M.L. Constanzer, G.A. Hessey and W.F. Bayne, *J. Chromatogr.*, 526 (1990) 461.

Journal of Chromatography A, 660 (1994) 313–318
Elsevier Science B.V., Amsterdam

CHROMSYMP. 2882

Retention of some monoamine oxidase inhibitory drugs on a β-cyclodextrin polymer-coated silica column

Tibor Cserháti* and Esther Forgács

Central Research Institute for Chemistry, Hungarian Academy of Sciences, P.O. Box 17, H-1525, Budapest (Hungary)

ABSTRACT

The retention of seventeen monoamine oxidase inhibitory drugs (mono- and disubstituted derivatives of propargylamine) was determined on a β-cyclodextrin polymer (β-CDP)-coated silica column using methanol–0.05 *M* K_2HPO_4 (6:4, v/v) as the eluent. The inclusion complex formation between the drugs and a water-soluble β-cyclodextrin polymer was studied by charge-transfer chromatography carried out on reversed-phase TLC layers. The capacity factors were correlated with the various physico-chemical parameters and with the inclusion complex-forming capacity of the monoamine oxidase inhibitory drugs. Calculations indicated that the inclusion complex-forming capacity of the drugs does not influence their retention on a β-CDP column, that is, the water-soluble and water-insoluble β-CDPs show different retention characteristics. The specific hydrophilic adsorption surface of the solutes significantly influences the retention in HPLC. The results suggest that the selectivity of the β-CDP-coated silica support may be different from that of the traditional alkyl-bonded reversed-phase columns.

INTRODUCTION

Cyclodextrins (CDs) and various CD derivatives have found growing acceptance and application in many fields of chromatography [1]. They have been used in reversed-phase thin-layer chromatography (TLC) to study their interaction with various bioactive compounds such as barbiturates [2,3] and chlorophenol derivatives [4,5]. CDs modify the effective mobilities of various inorganic ions in isotachophoresis [6], improve the separation of peptides in capillary electrophoresis [7] and enhance the efficiency of enantiomeric separation in gas chromatography [8–11]. In high-performance liquid chromatography (HPLC), CDs are used in two different manners, either by adding CDs to the eluent [12–15] or by covalently bonding CDs to the silica surface [16–19]. CDs are used either to improve the separation of non-chiral compounds [20] or to separate enantiomers in both normal- [10] and reversed-phase systems [21]. So far as we are aware, CD polymers have not been applied frequently in HPLC [22].

Propargylamine derivatives are selective inhibitors of B-type monoamine oxidase [23,24] and the determination of their lipophilicity [25] and their TLC behaviour [26] have been recently reported.

The objectives of this work were to explore the separation characteristics of a β-cyclodextrin polymer (β-CDP)-coated HPLC column [27] using propargylamine derivatives as model compounds and to find the relationships between their retention behaviour and molecular structure.

EXPERIMENTAL

The structures of the steroid drugs studied are given in Table I.

Determination of the retention behaviour of drugs by high-performance liquid chromatography

The β-CDP-coated support (patent pending) was prepared at the Cyclolab Research and

* Corresponding author.

0021-9673/94/$07.00 © 1994 Elsevier Science B.V. All rights reserved
SSDI 0021-9673(93)E0811-8

TABLE I

STRUCTURES OF MONOAMINE OXIDASE INHIBITORS

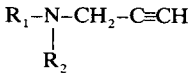

No.	R_1	R_2	No.	R_1	R_2
1 (+)	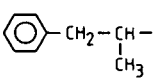	CH_3	10		CH_3
2 (−)		CH_3	11	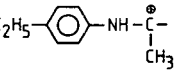	H
3	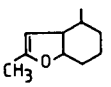	CH_3	12	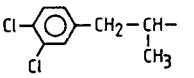	CH_3
4	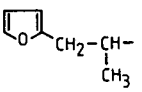	H	13		CH_3
5	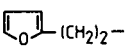	CH_3	14	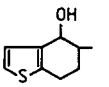	CH_3
6	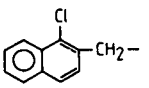	CH_3	15	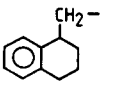	CH_3
7	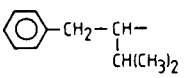	CH_3	16	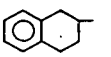	CH_3
8	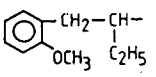	CH_3	17	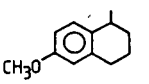	CH_3
9	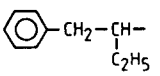	C_4H_7			

Development Laboratory (Budapest, Hungary). A 25 cm × 4 mm I.D. column was filled in our laboratory with a Shandon (Pittsburgh, PA, USA) analytical HPLC packing pump by the procedure proposed for the filling of reversed-phase columns. The HPLC equipment consisted of a Liquopump Type 312 (Labor MIM, Budapest, Hungary), a Cecil (Cambridge, UK) CE-212 spectrophotometer used as the detector, a Valco (Houston, TX, USA) 20-μl injector and a Waters (Milford, MA, USA) Model 740 integrator. The flow-rate was 0.6 ml/min and the detection wavelength was 225 nm. The eluent was methanol–50 m*M* K_2HPO_4 (6:4, v/v). Methanol was used in both the HPLC and TLC experiments because it forms only weak inclusion complexes with CDs [28,29]. The drugs were dissolved in the eluent at a concentration of 0.05 mg/ml. The retention time of each compound was determined by three consecutive determinations. The capacity factor and the relative standard deviation (R.S.D.) of the capacity factor were calculated for each compound.

Determination of the interaction between drugs and water-soluble β-cyclodextrin polymer by reversed-phase thin-layer chromatography

Silcoplat UV_{254} plates (Kavalier, Brno, Czech Republic) were impregnated with *n*-hexane–paraffin oil (95:5, v/v) by overnight predevelopment. The eluents were methanol–water mixtures, the methanol concentration varying between 45 and 60% (v/v) in steps of 5% (v/v). To determine the strength of the interaction between the drugs and β-CD, a water-soluble β-CDP (SCDP) was added to the eluent. Its concentration in the eluent was varied between 0 and 20 mg/ml. SCDP was prepared by cross-linking β-CD with butylene glycol bis(epoxypropyl ether) in aqueous alkaline solution. The product contained 66.04% β-CD. It should be emphasized that β-CDP and SCDP were prepared with different processes of polymerization, and therefore their inclusion forming capacities may also differ. After development the plates were dried at 105°C and the spots were detected under UV radiation and with iodine vapour. Each determination was run in quadruplicate.

The R_M values were calculated from the equation

$$R_M = \log(1/R_F - 1) \quad (1)$$

The dependence of the R_M value on the eluent composition was calculated from

$$R_M = R_{M0} + b_1C_1 + b_2C_2 \quad (2)$$

where R_M is the actual R_M value of a compound determined at given methanol and SCDP concentrations, R_{M0} is the R_M value of a compound extrapolated to zero methanol and SCDP concentrations, b_1 is the decrease in the R_M value caused by a 1% increase in the methanol concentration in the eluent (related to the specific hydrophobic surface area [30], b_2 is the decrease in the R_M value caused by 1 mg/ml change in the concentration of SCDP in the eluent (related to the relative strength of interaction) [31,32] and C_1 and C_2 are the methanol and SCDP concentration, respectively.

Calculation of relationships between retention behaviour and physico-chemical parameters of propargylamine derivatives

To elucidate the role of the physico-chemical parameters of drugs on their retention behaviour on a β-CDP column, stepwise regression analysis was applied [33]. The capacity factors of drugs determined on the β-CDP column were the dependent variables. The independent variables were the various hydrophobic and hydrophilic physico-chemical parameters of drugs taken from ref. 26 and the relative strength of inclusion formation with SCDP (b_2 value in eqn. 2). When the b_2 value was not significant, $b_2 = 0$ was included in the data matrix. The number of accepted independent variables was not limited and the acceptance limit was set to a 95% significance level.

RESULTS AND DISCUSSION

The retention order of propargylamine derivatives does not follow the lipophilicity order (Fig. 1); the less lipophilic compound **17** elutes after the more lipophilic compound **15**. This suggests that the retention characteristics of the β-CDP column differ from those of alkyl-bonded silica columns, where the retention order is determined by the lipophilicity order of the solutes.

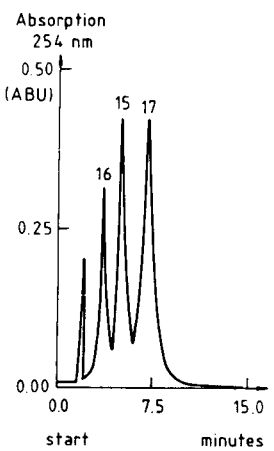

Fig. 1. Separation of monoamine oxidase inhibitory drugs on a β-cyclodextrin polymer-coated column. Numbers refer to drugs in Table I.

The log k' values and the R.S.D.s are given in Table II. The log k' values show wide variations, supporting our previous qualitative conclusions that the drugs can be separated on this column. The R.S.D.s are fairly low (in most instances less than 0.5%), indicating good reproducibility of retention times on the β-CD column.

The R_M values of some drugs decrease linearly with increasing concentration of water-soluble β-CDP in the eluent (Fig. 2). This can be explained by the assumption that the hydrophilic β-CDP interacts with the more lipophilic drugs and the complexes (probably inclusion complexes) exhibit lower lipophilicity.

The parameters of eqn. 2 are given in Table III. Eqn. 2 fits the experimental data well, the significance level always being over 95%. The ratio of variance explained by the independent variables varied between 45 and 95% (see r^2 values). Both the lipophilicity value extrapolated to zero methanol and SCDP concentration (R_{M0})

TABLE II

RETENTION OF MONOAMINE OXIDASE INHIBITORY DRUGS ON A β-CYCLODEXTRIN POLYMER-COATED COLUMN

Eluent; methanol–50 m*M* K_2HPO_4 (6:4, v/v).

Compound	Log k'	
	Mean[a]	R.S.D. (%)[a]
1	0.167	0.13
2	0.207	0.24
3	0.110	0.41
4	−0.178	0.19
5	0.166	0.25
6	0.748	0.61
7	0.463	>0.10
8	0.174	0.12
9	0.705	0.61
10	0.186	0.49
11	−0.132	0.18
12	0.524	0.14
13	0.526	0.36
14	−0.029	0.16
15	−0.033	0.16
16	0.289	0.11
17	0.525	0.29

[a] $n = 3$

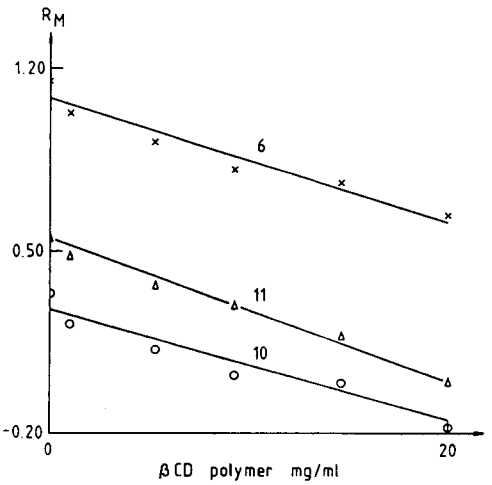

Fig. 2. Relationship between the R_M value of monoamine oxidase inhibitory drugs and the concentration of water-soluble β-cyclodextrin polymer in the eluent [water–methanol (45:55, v/v)]. Numbers refer to drugs in Table I.

and the specific hydrophobic surface area (b_1) differ considerably. This indicates that these parameters can be applied in quantitative structure–activity relationship (QSAR) calculations, and the drugs can easily be separated under reversed-phase chromatographic conditions. The interaction of SCDP with drugs **3–5**, **8**, **9** and **14** was not proved by the experiments. This result indicates that either the interaction does not take place or it is so weak that it is below the detection limit of the method.

According to the results of stepwise regression analysis, only the hydrophilic parameters of drugs influence their retention on the β-CDP column:

$$\log k' = 0.36 - (0.50 \pm 0.12)X_1 - (0.59 \pm 0.11)X_2 \quad (3)$$

$$n = 17;\ F_{calc.} = 43.41;\ r^2 = 0.8611$$

where X_1 = adsorption capacity of the drugs on a silica surface determined with acetonitrile–acetone eluents and X_2 = adsorption capacity of the drugs on an alumina surface determined with *n*-hexane–2-propanol eluents.

Eqn. 3 fits the experimental data well, the significance level being over 99.9% (compare $F_{calc.}$ values with the corresponding tabulated F

TABLE III

RELATIONSHIP BETWEEN THE LIPOPHILICITY (R_{M0}) OF MONOAMINE OXIDASE INHIBITORY DRUGS AND THE CONCENTRATIONS OF METHANOL (C_1) AND OF WATER-SOLUBLE β-CYCLODEXTRIN POLYMER (C_2) IN THE ELUENT

$R_M = R_{M0} + b_1C_1 + b_2C_2$. Compounds **1** and **2** were omitted from the calculations as they showed irregular spot shapes.

Parameter	3	4	5	6	7	8	9	10	11	12	13	14	15	16	17
n	13	13	13	13	13	13	11	13	13	13	13	12	13	13	13
R_{M0}	3.41	2.36	2.58	4.29	3.45	3.45	3.09	3.49	4.11	4.42	3.29	2.57	3.61	3.70	3.25
$-b_1$	5.58	4.70	4.79	5.92	4.59	5.29	2.92	5.98	6.71	6.27	4.64	5.43	5.77	5.18	4.75
s_{b1}	1.11	1.31	1.57	0.77	0.56	1.23	0.97	0.79	1.06	0.75	0.50	1.06	1.83	0.54	0.32
b'_1 (%)	–	–	–	65.85	65.72	–	–	71.85	71.08	60.91	71.78	–	66.17	72.79	66.61
$-b_2$	n.s.[a]	n.s.	n.s.	1.90	1.48	n.s.	n.s.	1.45	1.69	2.50	1.13	n.s.	1.83	1.20	1.48
s_{b2}	–	–	–	0.48	0.35	–	–	0.49	0.66	0.46	0.31	–	0.45	0.34	0.20
b'_2 (%)	–	–	–	34.15	34.28	–	–	28.15	28.92	39.09	28.22	–	33.83	27.21	33.39
r^2	0.6958	0.5408	0.4595	0.8582	0.8725	0.6277	0.5025	0.8523	0.8007	0.8852	0.8975	0.7235	0.8658	0.9011	0.9585
$F_{calc.}$	–	–	–	30.25	34.22	–	–	28.85	20.08	38.54	43.79	26.17	32.25	45.53	115.40

[a] n.s. = Not significant.

values). Two physico-chemical parameters explain about 86% of the retention behaviour of drugs on the β-CDP column (see r^2 value). Neither the lipophilicity parameters nor the strength of inclusion complex formation between the drugs and SCDP have a significant impact on the retention behaviour of drugs on the β-CDP column. This finding suggests that the retention characteristics of the β-CDP column differ from those of traditional reversed-phase columns, the impact of lipophilicity being insignificant, and the inclusion complex-forming capacities of water-soluble and water-insoluble β-CD polymers differ considerably, the complex stability values determined with the water-soluble β-CD polymer having no predictive value for the retention behaviour of the water-insoluble β-CD polymer.

The fact that only adsorption parameters influence the retention of drugs on the β-CDP column makes it probable that the hydrophilic surface of cyclodextrin and/or the cross-linking agent turns towards the eluent and the cyclodextrin cavities are not available or hardly available for the solutes in the eluent. The path coefficient values are comparable to each other (X_1 = 45.42% and X_2 = 54.58%), that is, the acidity (silica) or alkalinity (alumina) of the support surface has a commensurable effect on the retention. This suggests that silica is fairly well covered by the β-CD polymer.

It can be concluded that the β-CDP-coated silica is a promising reversed-phase support with a different selectivity to ODS silica. However, its capacity as a chiral stationary phase needs further investigation.

ACKNOWLEDGEMENT

This study was supported in part by a grant (OTKA 2670) from the Hungarian Academy of Sciences.

REFERENCES

1 W.L. Hinze and D.W. Armstrong, *Ordered Media in Chemical Separations* (*ACS Symposium Series*, No. 342), American Chemical Society, Washington, DC, 1987.
2 T. Cserháti, J. Bojarski, É. Fenyvesi and J. Szejtli, *J. Chromatogr.*, 351 (1986) 356.
3 T. Cserháti, J. Szejtli and J. Bojarski, *Chromatographia*, 28 (1989) 455.
4 T. Cserháti, J. Szejtli and É. Fenyvesi, *J. Chromatogr.*, 439 (1988) 393.
5 T. Cserháti, J. Szejtli and M. Szögyi, *J. Chromatogr.*, 509 (1990) 255.
6 K. Fukushi and K. Hiiro, *J. Chromatogr.*, 518 (1990) 189.
7 J.P. Liu, K.A. Cobb and M. Novotny, *J. Chromatogr.*, 519 (1990) 189.
8 D.W. Armstrong, W. Li and J. Pitha, *Anal. Chem.*, 62 (1990) 914.
9 D.W. Armstrong, W. Li, C.-D. Chang and J. Pitha, *Anal. Chem.*, 62 (1990) 914.

10 D.W. Armstrong, A.M. Stalcup, M.L. Hilton, J. Duncan, J.R. Faulkner and S.-C. Chang, *Anal. Chem.*, 62 (1990) 1610.
11 M. Jung, D. Schmalzing and V. Schurig, *J. Chromatogr.*, 552 (1992) 43.
12 K. Shimada, T. Oe and M. Suzuki, *J. Chromatogr.*, 558 (1991) 1306.
13 M. Gosselet and B. Sebille, *J. Chromatogr.*, 552 (1991) 563.
14 B. Agnus, B. Sebille and M. Gosselet, *J. Chromatogr.*, 552 (1991) 583.
15 M. Seno, M. Lin and K. Iwamoto, *J. Chromatogr.*, 523 (1990) 293.
16 D.W. Armstrong, C.-D. Chang and S.H. Lee, *J. Chromatogr.*, 539 (1991) 83.
17 R.R. West and J.H. Cardellina, II, *J. Chromatogr.*, 539 (1991) 15.
18 C.A. Chang, H. Ji and G. Lin, *J. Chromatogr.*, 522 (1990) 143.
19 K. Fujimura, S. Suzuki, K. Hayashi and S. Masuda, *Anal. Chem.*, 62 (1990) 2198.
20 J.W. Ho, *J. Chromatogr.*, 508 (1990) 375.
21 J. Haginaka and J. Wakai, *Anal. Chem.*, 62 (1990) 997.
22 B. Sebille, N. Thuaud, J. Piquion and N. Behar, *J. Chromatogr.*, 409 (1987) 61.
23 J. Knoll, Z. Ecsery, K. Kelemen, J.G. Nievel and B. Knoll, *Arch. Int. Pharmacodyn. Ther.*, 155 (1965) 154.
24 J. Knoll, E.S. Vizy and G. Somogyi, *Arzneim.-Forsch.*, 18 (1968) 109.
25 T. Cserháti and K. Magyar, *J. Chromatogr.*, 575 (1992) 57.
26 T. Cserháti and K. Magyar, *J. Biochem. Biophys. Methods*, 24 (1992) 249.
27 T. Cserháti and E. Forgács, *Anal. Chim. Acta*, 279 (1993) 107.
28 A. Buvári, J. Szejtli and L. Barcza, *J. Inclus. Phenom.*, 1 (1983/84) 151.
29 A. Harada and S. Takahashi, *Chem. Lett.*, (1984) 2089.
30 C. Horváth, W. Melander and I. Molnár, *J. Chromatogr.*, 125 (1976) 129.
31 K. Csabai, T. Cserháti and J. Szejtli, *Int. J. Pharm.*, 91 (1993) 15.
32 T. Cserháti, E. Fenyvesi and J. Szejtli, *J. Inclus. Phenom.*, 14 (1992) 181.
33 H. Mager, *Moderne Regressionsanalyse*, Salle, Sauerlander, Frankfurt/Main, 1982, p. 135.

Journal of Chromatography A, 660 (1994) 319–325
Elsevier Science B.V., Amsterdam

CHROMSYMP. 2944

Automated assay for GV104326, a novel tribactam antibiotic, in human plasma by high-performance liquid chromatography and solid-phase extraction

R.J. Barnaby* and L. Iavarone

Research Laboratories, Glaxo S.p.A., Via Fleming 4, Verona 37100 (Italy)

ABSTRACT

A highly automated, rapid, robust and specific plasma assay for GV104326, a novel tribactam antibiotic, has been developed to monitor human volunteer trials. The method involves automated solid-phase extraction with a strong anion-exchange phase and HPLC on a reversed-phase column with ultraviolet detection. The calibration range for the assay is 0.05–2 μg/ml. The assay is linear over this range and is specific with respect to endogenous interference and likely metabolites of GV104326. Both intra- and inter-assay variability were <8% and intra- and inter-day bias <10%.

INTRODUCTION

GV104326 (Fig. 1) is the first member of a new class of tricyclic β-lactam (tribactam) antibiotics, possessing a potent and particularly broad spectrum of activity against Gram-positive, Gram-negative, and anaerobic bacteria [1]. In addition, it has a remarkably good resistance to hydrolysis by either β-lactamases or renal dehydropeptidases [2].

Beta-lactam antibiotics have traditionally been assayed by microbiological methods [3,4], and by HPLC [5–14]. HPLC is the generally preferred technique because of its sensitivity, speed, robustness and above all specificity. The determination of GV104326 in biological fluids during preliminary animal studies was performed by an HPLC method utilizing protein precipitation with acetonitrile, evaporation of the supernatant and direct injection of the redissolved residue. Although sufficiently sensitive (100 ng/ml) and specific, the method was rather labour-intensive and was also highly dependent on the selectivity of the HPLC column because of the critical separation of co-extracted endogenous components. This separation could vary between batches of columns and also during ageing of the column.

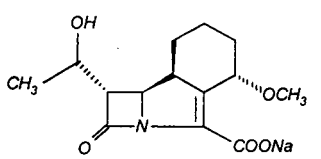

GV104326B

Fig. 1. Structure of GV104326B.

An improved assay method was required to monitor GV104326 plasma levels in volunteers after intravenous administration. Of importance was a more robust, rapid and automated method to efficiently assay the large number of samples generated. Another important issue with GV104326, as with most β-lactam antibiotics, is the limited stability in plasma, hence the speed of the assay is of prime importance. Techniques considered were direct injection onto restricted access stationary phases, column-switching HPLC and solid-phase extraction (SPE). The first two techniques were considered to pose

* Corresponding author.

0021-9673/94/$07.00 © 1994 Elsevier Science B.V. All rights reserved
SSDI 0021-9673(93)E0968-Z

more problems because of the high polarity of the molecule. Very little retention was obtained on a Pinkerton column at pH 6. In order to obtain more retention by hydrophobic mechanisms it would be necessary to use pH values <4 to protonate the carboxylic acid, however the stability of GV104326 is very poor at these pH values. Column switching using reversed-phase enrichment precolumns would suffer from the same problem of low retention, and alternative anion-exchange precolumns tend to have low capacity, restricting the number of samples that can be injected before repacking is necessary. SPE was attempted initially with C_{18} packing, but recovery was very low, again because of poor retention. Attention was switched to a strong anion-exchange (SAX) phase (trimethyl quaternary ammonium) and we here describe the assay developed using this SPE phase. The assay is highly automated, as a result of the use of a Gilson Aspec (automated sample preparation with extraction columns) and the direct injection of the SPE eluate onto the column. We also present the results from the assay validation and compare them with those obtained using the acetonitrile deproteinization assay in human plasma.

To our knowledge, this approach to the HPLC assay of β-lactam antibiotics has not been published in the literature.

EXPERIMENTAL

Materials and reagents

GV104326B (sodium salt) was synthesized by Chemical Development, Glaxo. The structure is shown in Fig. 1. Acetonitrile (HPLC grade) and glacial acetic acid (analytical grade) were obtained from Carlo Erba (Milan, Italy). Sodium hydroxide (1 *M*), ammonium acetate and trisodium citrate 2-hydrate (all analytical grade) were obtained from Merck-Bracco (Milan, Italy). Water was purified through a Milli RO/Milli-Q (Millipore, Milan, Italy) system.

Chromatography

The HPLC system consisted of a Waters 590 (Milan) isocratic pump, an Aspec (Gilson/Biolabo, Milan, Italy) containing a Rheodyne 7010 injection valve with a 100-μl loop, a SM4000 (Milton Roy, Milan) UV detector and data acquisition by an Access-Chrom (PE-Nelson, Milan, Italy) VAX-based system.

The chromatography column was stainless steel and packed with 5-μm Hypersil ODS (Hewlett-Packard, Milan, Italy). Internal dimensions were 100 × 4.6 mm. A precolumn packed with the same phase and of dimensions 20 × 4.6 mm was used. Mobile phase consisted of 7% acetonitrile in 0.1 *M* ammonium acetate at pH 5.7 with glacial acetic acid (15.42 g in 2 l of Milli-Q water and 1 ml of glacial acetic acid added and filtered through a 0.45-μm filter). The flow-rate was 1 ml/min and the column temperature ambient. Retention time of GV104326 was approximately 7 min. The UV detector was set at 268 nm.

Standard preparation

Plasma calibration standards in the range 0.05–2 μg/ml were prepared by spiking heparinized control human plasma (700 μl) with standard solutions of GV104326B (sodium salt) dissolved in 50 m*M* 2-(N-morpholine)ethanesulphonate (MES) buffer at pH 6.5, and diluting to 1.4 ml with the same buffer. The standards were vortex mixed and immediately placed in the aluminium Aspec rack at 4°C.

Sample extraction

Plasma samples, previously stored at −80°C, were thawed at 4°C and centrifuged at the same temperature to remove fibrin. A 700-μl aliquot was transferred to a 3-ml glass vial, 700 μl of 50 m*M* MES buffer added and the mixture vortexed and placed immediately in an aluminium Aspec rack maintained at 4°C. Completely automated SPE and injection were performed by the Aspec. The Aspec programme, which was performed in sequence mode so that the HPLC separation of the extracted sample was carried out during the preparation of the next sample, is shown in Table I.

Assay validation

Both intra- and inter-day validations were performed, the former by assaying six replicates of spiked samples at the same concentration

TABLE I

ASPEC PROGRAM FOR FULLY AUTOMATED SOLID-PHASE EXTRACTION AND HPLC INJECTION

SPE cartridges	500 mg Bond-Elut SAX
Conditioning	1 × 3 ml 100 m*M* ammonium acetate (pH 6.5)
	1 × 6 ml water
Sample	1 ml (+2 ml air flush)
Wash	1 ml water (+2 ml air flush)
Elution	2 × 0.5 ml trisodium citrate (0.5 *M*) pH 7.9 (+2 ml air flush)
Mixing	Two cycles of aspiration and dispensing of the sample
Injection	0.5 ml onto the 0.1-ml loop (full-loop injection)

levels as the calibration standards, and the latter by assaying, on four different days, duplicate spiked samples at four different concentration levels in the calibration range. On each occasion, the calibration curve was constructed from single standards at each of six concentrations, using independent standard solutions.

In addition, linearity, specificity, recovery and total analysis time were determined. The data were compared with those obtained by the preliminary acetonitrile deproteinization method. The accuracy was expressed by the bias (difference from the theoretical) and the precision expressed by the relative standard deviation (R.S.D.). Both bias and precisions are presented as percentages.

Stability

The stability of GV104326 under four different storage conditions was studied as follows:

(a) Stability in plasma diluted either in MES buffer (1:1) or in water (1:1) at 4°C (in the Aspec rack) at a concentration of 1 μg/ml over 24 h after preparation.

(b) Stability in a pooled plasma spiked sample, after extraction, at ambient temperature (in the Aspec collection rack) at a concentration of 1 μg/ml up to 24 h after preparation.

(c) Stability, in frozen plasma, at −25°C, at a concentration of 0.5 μg/ml, for up to 1 month after preparation.

(d) Stability, in frozen plasma, at −80°C, at a concentration of 0.5 μg/ml, for up to 7 months after preparation.

Spiked samples were prepared by addition of aqueous solutions, except study (a), of GV104326, minimizing the dilution of the sample to 5%.

RESULTS AND DISCUSSION

Solid-phase extraction

A strong anion-exchange phase was selected in order to ensure complete retention of GV104326, through interaction with the relatively weak carboxylic anion. It was thought essential to dilute the plasma to some extent, to ensure disruption of protein binding and also to stabilize GV104326. The use of pH 6.5 was optimum for stability and also was high enough to ensure good retention on the packing ($pK_a \approx 4$). Also, the use of a zwitterionic buffer (MES) should minimize the competition for retention with GV104326. The SPE packing was washed with a concentrated acetate buffer initially to ensure that the phase was in the acetate form and then washed with water to remove excess competing anions. Initial studies using 100-mg packing and 100-μl plasma loadings gave reasonable recoveries, but washing, even with a small volume of water, could not be performed without loss of recovery. A wash of some kind was considered essential to eliminate as much as possible of the plasma remaining on the packing. Therefore attention was switched to 500-mg packings and 500 μl of loaded plasma. Again retention was good and up to 1 ml of water could be used as a wash. Use of a wash with low-concentration buffers at pH 6–8 always caused loss of recovery. Possibly the low capacity of the phase, the presence of retention mechanisms

other than ion exchange or the presence of competing anions in plasma could explain the loss of GV104326 on washing. In order to obtain complete recovery, elution with high salt-containing buffers or acids could be used but, considering the instability of GV104326 in acid, salts were studied for elution. The highest recovery was obtained with two 0.5-ml elutions with 0.5 *M* citrate at pH 7.9. The direct injection of 100 μl of this is fully compatible with the reversed-phase conditions, but unfortunately the stability in this solvent is somewhat limited (3 h at ambient temperature), making reinjection of the eluted sample, the morning after an overnight run, impossible.

Chromatography and specificity

Typical chromatograms of blank and spiked plasma standards are shown in Fig. 2. Control human plasma from six different volunteers did not reveal any measurable interference in GV104326 peak-area measurement. The chromatograms are exceptionally clean, owing to the use of two different mechanisms of retention for SPE (anion exchange) and chromatography (reversed phase) and the reasonably long UV wavelength monitored. The use of anion exchange as the SPE clean-up enables removal of lipophilic and/or basic endogenous components from plasma, improving the selectivity of the clean-up compared with using a reversed-phase mechanism and, importantly, eliminates the need to wash the analytical column after every injection to remove late-eluting components.

The retention time of GV104326 is approximately 7 min. This could probably be shortened; however, the rate-limiting step is the Aspec clean-up, which takes approximately 14 min. At present, no information is available on possible metabolism of GV104326 in man, but studies of pure solution degradation and metabolism in rat urine suggest that the major metabolite would be the open lactam form of GV104326, as observed elsewhere for β-lactam antibiotics [15,16]. This product is well separated from GV104326 on reversed-phase columns. Furthermore, intact GV104326 is excreted extensively in rat urine and the urine GV104326 peak has been shown, by particle beam mass spectrometry, to be pure.

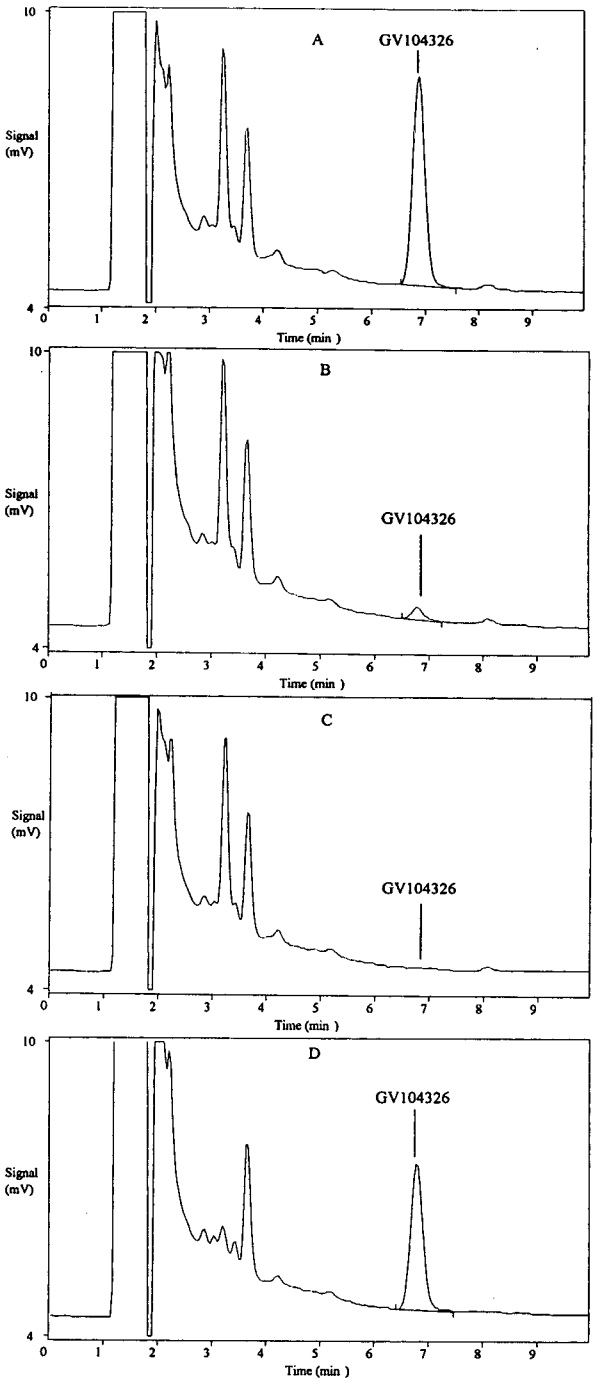

Fig. 2. Typical chromatograms obtained with the assay: (A) 1 μg/ml GV104326 plasma calibration standard; (B) 0.05 μg/ml GV104326 plasma calibration standard; (C) human plasma blank standard; (D) human plasma sample obtained 2 h after a single intravenous administration of 250 mg/kg GV104326B (concentration = 0.67 μg/ml).

Putting all this information together suggests that it is very unlikely that possible metabolites of GV104326 would interfere in the human plasma assay.

Lifetime of the HPLC column

As reported elsewhere [17,18] in assays in which neat plasma is added directly to SPE cartridges without prior protein precipitation, column efficiency has a tendency to decrease steadily with the number of injections of extracted plasma, to a point where integration of the lowest concentration standard becomes problematical. The lifetime of the column is extended by using a precolumn containing the same phase as the analytical column, and when changed approximately every 100 injections the lifetime of the column is approximately 300 injections. Alternatively, if a sensitivity of 100 ng/ml is sufficient, 50 μl of the final extract can be injected and the column life is doubled. As an exercise, an intra-day validation was performed with a column containing, 15,000 theoretical plates/m (as measured from the peak height/area ratio), and acceptable results were obtained (*i.e.* accuracy and precision $< 10\%$). The column was discarded when the number of plates dropped below 15,000/m. Some extended column life could be obtained by reversing the direction of flow. The column was not washed with strong solvents but washed with about 100 column volumes of mobile phase at the end of every analytical batch.

Validation

The results of the intra- and inter-day variability are shown in Tables II and III. Intra-day and inter-day bias ranged from 4 to 9% and from 1 to 5%, respectively. Intra-day and inter-day variability ranged from 1 to 5% and from 4 to 7%, respectively. The validation results are compared with those obtained with the preliminary acetonitrile deproteinization method in Table IV. With both intra-day and inter-day studies, the precision of the Aspec method was superior to the preliminary method. In addition, the manual labour time and total analysis time were considerably shorter using the Aspec method, liberating the analyst to perform other tasks.

Standard lines were all calculated using linear regression, weighted by the reciprocal of the concentration and not forcing through zero. Also, the blank standard was not included in the regression and only served as an interference

TABLE II

INTRA-DAY VARIABILITY

Calibration concentration (μg/ml)	Observed concentrations (μg/ml)	Mean concentration (μg/ml)	S.D.	R.S.D. (%)	Bias (%)
0.05	0.052, 0.054, 0.054 0.053, 0.056, 0.053	0.054	0.014	2.6	8.0
0.1	0.111, 0.109, 0.110, 0.106, 0.100, 0.105	0.107	0.004	3.7	6.7
0.2	0.214, 0.210, 0.218, 0.213, 0.190, 0.210	0.209	0.010	4.6	4.6
0.5	0.570, 0.544, 0.541, 0.547, 0.540, 0.536	0.546	0.012	2.3	9.2
1	1.08, 1.04, 1.06, 1.05, 1.05, 1.06	1.06	0.014	1.3	5.7
2	2.18, 2.18, 2.16, 2.18, 2.13, 2.15	2.17	0.020	0.9	8.3

TABLE III

INTER-DAY VARIABILITY

Calibration concentration (μg/ml)	Observed concentrations (μg/ml)	Mean concentration (μg/ml)	S.D.	R.S.D. (%)	Bias (%)
0.05	0.049, 0.051, 0.049, 0.050 0.052, 0.055, 0.055, 0.048	0.051	0.003	5.5	2.0
0.1	0.091, 0.099, 0.110, 0.093, 0.092, 0.097, 0.109, 0.091	0.098	0.076	7.7	−2.0
0.5	0.467, 0.481, 0.492, 0.491, 0.419, 0.469, 0.509, 0.473	0.475	0.027	5	−5.0
2	1.90, 1.91, 1.98, 2.07, 1.82, 1.90, 2.04, 2.01	1.96	0.086	4.4	−2.0

check. All lines were linear with intercepts always <10% of the peak area of the lowest standard. Regression coefficients were always >0.995 and typically >0.998.

Recovery was determined at three concentration levels, in the calibration range, by comparing mean calculated plasma concentrations of two standards spiked before extraction with the mean of two control human plasma standards spiked after extraction, at each concentration level. The mean recovery was 87%, 84% and 86% at 0.05, 0.5 and 2 μg/ml, respectively.

The limit of reliable quantification is defined as the lowest concentration of GV104326 determined with acceptable accuracy and precision and hence is 0.05 μg/ml (100-μl injection) or 0.1 μg/ml (50-μl injection).

Stability, in the short-term studies at 4°C, was defined as the time after which the GV104326 peak area decreased by 5% of its initial area, at the time of spiking. Data were fitted to a log peak area/time regression and the stability determined from the regression line. GV104326 was stable in water-diluted plasma for 7 h and MES-diluted plasma for 11 h, at a concentration of 1 μg/ml. After SPE extraction, GV104326, at a concentration of 1 μg/ml, was stable for 3 h at room temperature. The use of a zwitterionic

TABLE IV

COMPARISON OF VALIDATION PARAMETERS BETWEEN ASPEC METHOD AND MANUAL DEPROTEINIZATION METHOD

Validation test	Aspec method	Deproteinization method
Intra-day precision	1–5%	2–8%
Intra-day bias	4–9%	1–8%
Inter-day precision	4–8%	4–16%
Inter-day bias	2–5%	−5–1%
Linearity of calibration	>0.995	>0.995
Recovery	84–87%	90–91%
Limit of quantification	0.05 μg/ml	0.1 μg/ml
Speed (total time 50 samples including standards and quality controls)	13 h	22 h
Manual labour time (50 samples)	1.5 h	4 h

buffer (MES) has been shown to stabilize β-lactam antibiotics compared with anionic buffers such as phosphate and acetate [7,19,20]. Previous studies have shown that the optimum pH for GV104326 stability in plasma is pH 6.5. Also, studies showed that the use of a more concentrated buffer solution (0.5 *M*) improved GV104326 plasma stability from 11 h to 4.5 days at 4°C, but unfortunately this concentration of MES drastically affected the SPE recovery, hence a compromise concentration of 50 m*M* was used. The limited stability of GV104326 in diluted plasma restricted the batch size to around 45 samples, including standards and quality controls, although a batch size of 50 in the validation studies always gave good results.

For the studies at −25 and −80°C, the data were fitted to an unweighted linear regression of log plasma concentration with time. The 95% lower confidence limit of the regression line was calculated using a one-sided test. GV104326 was considered to be stable in plasma up to a time when the concentration was greater than or equal to 90% of the initial concentration. This was shown by the time at which the lower 95% confidence limit intersected 90% of the initial concentration.

GV104326 was stable in human plasma for 10 days at −25°C and at least 7 months at −80°C.

REFERENCES

1 A. Perboni, D. Donati, T. Rossi, B. Tamburini, G. Tarzia and G. Gaviraghi, presented at the *32nd Interscience Conference on Antimicrobial Agents and Chemotherapy, Anaheim, CA*, 1992, abstract No. 127.

2 L. Lowther, E. di Modugno, S.M. Hammond, E. Ratti and G. Gaviraghi, presented at the *32nd Interscience Conference on Antimicrobial Agents and Chemotherapy, Anaheim, CA*, 1992, abstract No. 129.

3 R.S. Griffith, H.R. Black, G.L. Brier and J.D. Wolny, *Antimicrob. Agents Chemother.*, 10 (1976) 814.

4 R.D. Foord, *Antimicrob. Agents Chemother.*, 9 (1976) 74.

5 P.M. Kovach, *J. Chromatogr.*, 567 (1991) 129.

6 A. Matsuura, T. Nagayama and T. Kitagawa, *J. Chromatogr.*, 494 (1989) 231.

7 W.J. Ebey, B.A. Boucher and J.A. Pieper, *J. Liq. Chromatogr.*, 11 (1988) 3471.

8 J. Knoeller, W. Koenig, W. Schoenfeld and K.D. Bremm, *J. Chromatogr.*, 427 (1988) 257.

9 J. Godbillon, M. Duval, S. Gauron and J.P. Dupois, *J. Chromatogr.*, 427 (1988) 269.

10 G.W. Whitaker and T.D. Lindstrom, *J. Liq. Chromatogr.*, 11 (1988) 901.

11 S.T. Forgue, K.A. Pittman and R.H. Barbhaiga, *J. Chrom. Biomed. Appl.*, 58 (1987) 343.

12 J.O. Miners, *J. Liq. Chromatogr.*, 8 (15) (1985) 2827.

13 S.A. Signs, T.M. File and J.S. Tan, *Antimicrob. Agents Chemother.*, 26 (1984) 652.

14 D.G. Gravallese, D.G. Musson, L.T. Pauliukonis and W.F. Bayne, *J. Chromatogr.*, 310 (1984) 71.

15 M.P. Harrison, S.R. Moss, A. Featherstone, A.G. Fowkes, A.M. Sanders and D.E. Case, *J. Antimicrob. Chemother.*, 24 (Suppl. A) (1989) 265.

16 H. Kropp, J.G. Sundelof, R. Hajdu and F. Kahan, *Antimicrob. Agents Chemother.*, 22 (1982) 62.

17 Ph. Hubert and J. Crommen, *J. Liq. Chromatogr.*, 13 (1990) 3891.

18 Ph. Hubert, P. Chiap and J. Crommen, *J. Pharm. Biomed. Anal.*, 9 (1991) 877.

19 G.S. Smith and E.F. Schoenewaldt, *J. Pharm. Sci.*, 70 (1980) 272.

20 J.S. Kahan, F.M. Kahan, R. Goegelman, S.A. Currie, M. Jackson, E.O. Stapley, T.W. Miller, A.K. Miller, D. Hendlin, S. Mochales, S. Hernandez, H.B. Woodruff and J. Birnbaum, *J. Antibiot.*, 32 (1979) 1.

Journal of Chromatography A, 660 (1994) 327–337
Elsevier Science B.V., Amsterdam

CHROMSYMP. 2960

Rapid, high-resolution high-performance liquid chromatographic analysis of antibiotics

K.M. Kirkland* and D.A. McCombs

ZENECA Pharmaceuticals Group, A Business Unit of ZENECA Inc., Wilmington, DE 19897 (USA)

J.J. Kirkland

Rockland Technologies, Inc., 538 First State Boulevard, Newport, DE 19804 (USA)

ABSTRACT

A HPLC column devised for high separation speed combined with highly practical operating features has been found useful for separating antibiotics. Important characteristics involve compromises in packing particle size, column configuration and support–stationary phase combinations. We determined that these columns are useful for rapid, high-resolution separations with unmodified state-of-the-art HPLC equipment without the extra-column band-broadening effects typical of so-called "fast" HPLC columns. The proposed columns feature efficient sterically-protected monofunctional silane stationary phases that provide good separation reproducibility and high column stability. The combination of these unique bonded silanes and a highly purified, less-acidic silica support give superior peak shapes for antibiotic compounds. The proposed column configuration can halve separation times and double peak heights without loss in resolution, compared to widely used analytical columns. Increased mobile phase flow-rates permit even faster separations of antibiotics with only modest loss in resolution and peak heights for trace analyses in biological systems.

INTRODUCTION

HPLC is effective and convenient for analyzing antibiotic compounds in many types of samples. This method also is often preferred for determining trace quantities of antibiotics and their metabolites in a variety of animal tissues and fluids [1,2]. Typically, silica-based reversed-phase columns with bonded alkyl ligands are used for these applications. These columns generally are preferred because of their high plate numbers for superior separating efficiency, and their convenient availability from many reliable sources.

Current needs in HPLC method development for antibiotics and other drugs stress easily reproduced, rugged methods that are developed rapidly. Often required are fast separations that permit the analysis of large numbers of samples at minimum cost. But these fast separations also must provide needed separation resolution, especially in trace analyses where potentially interfering sample components are a special problem. Further, the methods need to be conducted on existing instrumentation to minimize capital investment cost. Finally, decreased solvent consumption is becoming increasingly important, to minimize cost and waste disposal problems. This study evaluates a column configuration that has the potential to meet these goals.

It has been known for some time that the separation goals stated above could be attained by using columns with particles smaller than the widely used 5-μm materials [3–5]. Smaller particles permit higher column bed efficiency for better separations. Also, higher mobile phase

* Corresponding author.

0021-9673/94/$07.00 © 1994 Elsevier Science B.V. All rights reserved
SSDI 0021-9673(93)E1112-D

flow-rates are allowed without sacrificing improved column efficiency. Although commercial columns of high-efficiency 3-μm silica particles have been available for many years, this particle size accounts for only about 10% of columns in use [6]. Users typically complain that columns of 3-μm particles have a tendency to "plug", greatly shortening their lifetime compared to columns of larger particles. Also, 3-μm columns often exhibit plate numbers that are lower than predicted. The stability of columns with 3-μm particles also is often faulted, as well as different selectivity, relative to columns of larger particles. Another complaint against columns of 3-μm particles is the unusually high back pressure. Finally, extra-column effects from some HPLC apparatus broadens the sharp, low-volume peaks from columns of 3-μm particles, decreasing their potential advantage [7].

We evaluated a small-particle column designed to minimize the disadvantages of conventional columns with 3-μm particles. Small-particle columns certainly are not new in HPLC. However, the unique feature of the proposed column is a combination of desirable and practical characteristics that have not previously been available. A general goal of this study was to increase the speed and detectability of analyzing antibiotics without sacrificing separation resolution. Of special interest was the effect of mobile phase flow-rate and temperature on column efficiency and separation speed. Also, a study of the effect of sample injection, guard columns/filters on the observed performance of these small-particle columns was required. Finally, comparison of the new column type with conventional columns was desired for analyzing trace antibiotics in biological matrices.

The experimental difficulties often associated with using small-particle (≤ 3 μm) columns apparently can be minimized by appropriate design compromises, as described in ref. 8. Briefly, a very narrow particle-size distribution of 3.5-μm porous silica microspheres without "fines" permits the use of 2-μm porosity column inlet frits. These replace the easily plugged 0.5-μm frits commonly used in columns of 3-μm particles. This combination provides a column that exhibits high efficiency without the usual tendency to "plug". The use of 3.5-μm particles allows a short (7.5 or 8 cm) column to develop the plate number required for difficult separations, often halving separation time with the same resolution as conventional 15 cm columns of 5-μm particles. The proposed column also was prepared with a high-purity, low-acidity silica support and efficient monomeric sterically protecting stationary phases whose stability and reproducibility have been documented [9–12].

Of particular interest was the potential increase in peak height and solute detectability that might be available from the small-particle column, because of the small peak volumes and predicted sharper peaks that should occur. However, because of the low-volume peaks expected from these columns, a practical question arose: Can existing HPLC equipment be used without the undue extra-column band broadening and resultant loss of column efficiency that often is associated with conventional short, small-particle columns? To answer these questions about the proposed column configuration, studies were designed to determine the effect of important separation parameters on separation performance: flow-rate, temperature, sample injection procedures, and detector response time [13].

EXPERIMENTAL

Columns

Prototype 8.0×0.46 cm columns were prepared by slurry packing within Rockland Technologies (Newport, DE, USA). The high-purity ($>99.995\%$) [14], low-acidity type B porous silica microspheres (Zorbax Rx-SIL) used for these columns had a pore diameter of 8 nm and a nitrogen surface area of 152 m^2/g. These particles were prepared by the coacervation of silica sols using methods previously described [15–17]. The number-average particle size of these particles was 3.65 μm as measured with a Coulter Multisizer (Coulter, Hialeah, FL, USA). These silica microspheres were densely bonded with sterically-protecting diisopropyl-*n*-octylsilane ligands [9,10]. Carbon value for this packing was 4.94%, resulting in a ligand surface coverage of 2.10 $\mu mol/m^2$. Similar 7.5×0.46 cm and $15 \times$

0.46 cm columns of both 3.5- and 5-μm particles are available from Mac-Mod Analytical (Chadds Ford, PA, USA) as Zorbax SB-C_8. Additional characteristics of columns with this and other highly stable sterically protecting silane stationary phases have been described recently [11,12]. The C-270 guard column cartridge holder, C-280 1.0×0.20 cm ODS cartridge, and A-318 pre-column filter were from Upchurch Scientific (Oak Harbor, WA, USA).

Apparatus

HPLC separations were performed either with a Hewlett-Packard Model 1050 instrument (Avondale, PA, USA), or with a modular instrument consisting of a Hewlett-Packard Model 1050 pump, an ABI Model 783 variable-wavelength detector (ABI, Foster City, CA, USA), a Model 7125 valve injector with 20-μl sample loop (Rheodyne, Cotati, CA, USA), and a DuPont column heater compartment (DuPont Instruments, Wilmington, DE, USA). The detector cell on the Hewlett-Packard Model 1050 was 1 μl, and 12 μl for the ABI detector. Mobile phase flow-rates were 1.0 ml/min, except as noted. Detector wavelength usually was set at maximum absorption for each antibiotic compound. Detector rise (response) time was 0.2 s, except as given. Sample sizes typically were 50–100 ng, except as noted. Chromatographic data were monitored and processed with a Multichrom Version 2.0 data system (VG Laboratory Systems, Manchester, UK) or a ChromPerfect Version 5.0 (Justice Innovations, Palo Alto, CA, USA) data station. Data collection with these units was 2 and 10 points/s, respectively.

Reagents and chemicals

HPLC-grade solvents were from J.T. Baker (Phillipsburg, NJ, USA). Trifluoroacetic acid and triethylamine were obtained from Pierce (Rockford, IL, USA). Antibiotic compounds were procured from Sigma (St. Louis, MO, USA). Ciprofloxacin and imipenem were from Glaxo Pharmaceuticals (Research Triangle Park, NC, USA) and Merck, Sharp and Dohme (West Point, PA, USA), respectively.

Extraction procedure and HPLC analysis of chloramphenicol from dog plasma and rat urine

Aliquots (0.2 ml) of control dog plasma and rat urine were spiked with 10 μl of a 10 μg/ml aqueous solution of chloramphenicol. Non-spiked samples were processed in parallel. The rat urine samples were made basic with 50 μl of a reagent-grade ammonium hydroxide–water (1:1) mixture. All samples were extracted with 1.0 ml of methyl *tert.*-butyl ether and centrifuged to separate the phases. The organic layer was taken to dryness under nitrogen and reconstituted in 100 μl of mobile phase for injection into the column using a 20-μl sample loop. Mobile phase for both separations was 0.1% trifluoroacetic acid adjusted to pH 3 with ammonium hydroxide and acetonitrile in the ratio of 75:25 (v/v). Mobile phase flow-rate was 1.0 ml/min and UV detection was at 278 nm.

RESULTS AND DISCUSSION

The prototype column type was tested with different classes of antibiotics and a range of mobile phase types, as summarized in Table I. Different concentrations of acetonitrile modifier were required to maintain the solute capacity factor at $k' \approx 3$. Plate numbers for these antibiotics varied from a low of about 3000 (imipenem) to more than 8000 (chloramphenicol) under the conditions used with this 8.0-cm column. Asymmetry factors, A_s, ranged from 1.02 to 1.27, indicating good peak shapes for these compounds.

A simple acetonitrile/0.1% trifluoroacetic acid (pH $\approx$ 1.8) mobile phase produced good results with the first five compounds listed in Table I. These compounds and the silanol groups remaining on the silica support are fully protonated under these conditions. Low-pH operation often produces the best results for basic compounds in terms of column plate number, peak shape, and recovery [19]. However, under these low-pH conditions, the highly water-soluble imipenem, which is zwitterionic at pH 4–9.5, is unstable. A pH 7 acetic acid–triethylamine mobile phase produced satisfactory retention for imipenen, although a very low concentration of acetonitrile was required. Under these conditions, imipenem

TABLE I

SUMMARY OF ANTIBIOTICS TESTED

Column, 8 × 0.46 cm Zorbax SB-C_8 with 3.5-μm particles. Samples, 50–100 ng in 20 μl; flow-rate, 1.0 ml/min; ambient temperature. k' = Capacity factor; N = column plate number; A_s = peak asymmetry factor; ACN = acetonitrile; TFA = trifluoroacetic acid.

Class	Antibiotic	Mobile phase	UV (nm)	k'	N	A_s
Penicillin	Nafcillin	ACN–0.1% aqueous TFA (44:56)	235	2.7	4425	1.02
Cephalosporin	Cefazolin	ACN–0.1% aqueous TFA (20:80)	272	2.9	6767	1.12
	Cefotaxime	ACN–0.1% aqueous TFA (18:82)	254	2.6	6320	1.22
	Ceftazidime	ACN–0.1% aqueous TFA (12:88)	254	2.4	5172	1.26
Quinolone	Ciprofloxacin	ACN–0.1% aqueous TFA (20:80)	277	3.1	7063	1.27
Carbapenem	Imipenem	ACN–0.1% aqueous acetic acid pH 7 with triethylamine (0.5:99.5)	296	3.5	3001	1.20
Sulfonamide	Sulfamethoxazole	ACN–0.1% aqueous TFA pH 3 with triethylamine (27:73)	267	2.8	7883	1.13
Chloramphenicol	Chloramphenicol	ACN–0.1% aqueous TFA pH 3 with triethylamine (25:75)	278	3.8	8431	1.06
Trimethorprim	Trimethorprim	ACN–0.1% aqueous TFA pH 3 with triethylamine (16:84)	220	3.0	7120	1.12

apparently is unionized or only partially protonated. (Note that this particular acetic acid mobile phase at pH 7 has poor buffering capacity, so sample size must be kept very small —a phosphate buffer probably would have been a better choice).

The last three compounds in Table I produced excellent results with a mobile phase prepared by titrating 0.1% trifluoroacetic acid to pH 3.0 with triethylamine. Plate numbers were especially favorable for these compounds with this mobile phase.

The plate height *vs.* mobile phase velocity plots for ciprofloxacin in Fig. 1 illustrate the effect of particle size on column performance. Theory predicts that smaller particles should produce higher column efficiency for well packed columns [4,5]. Although plate heights (column efficiencies) are significantly enhanced with the column of 3.5-μm particles, the improvement was somewhat less than predicted. The reduced plate height (in particle diameters) for the column of 5-μm particles was 2.1, compared to 2.5 for the column of 3.5-μm particles. The lower performance of the smaller particles could be due to a non-optimized procedure of packing the prototype columns. An equally likely reason could be secondary band broadening that is known to occur especially in packed beds. This secondary band broadening caused by temperature gradations across the column bed with increased flow is especially a factor with columns of very small particles [20,21].

The data in Fig. 1 show another known characteristic of operating with columns of smaller particles: the plate height minimum is shifted to higher mobile phase velocities, as predicted by

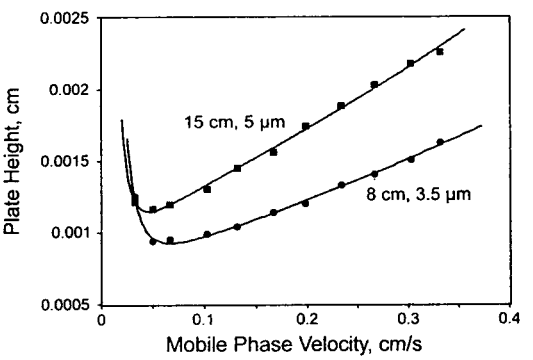

Fig. 1. Effect of column configuration on plate height. Columns: Zorbax SB-C_8, 0.46 cm I.D.; solute: ciprofloxacin; mobile phase: acetonitrile–water with 0.1% trifluoroacetic acid (80:20); 22°C; each data point represents the average of duplicate measurements.

theory [3–5]. A result of this effect is that columns of these smaller particles can be operated at higher mobile phase velocities (or flow-rates) without sacrificing column efficiency. Therefore, faster separations can be achieved at higher flow-rates without degrading separation resolution because of the superior kinetics associated with smaller particles. Fig. 2 gives an illustration of a rapid separation of an antibiotic mixture with the column of 3.5-μm particles by operating at 60°C and a flow-rate of 3.0 ml/min. Even at this high mobile phase velocity (≈ 0.3 cm/s), the plate number for this 8.0-cm column was still about 6000. The homogeneity of the packed bed and the rapid kinetics of the system is verified by the near-Gaussian peaks that were formed at this high flow-rate. Peak asymmetry factors approximated unity for all antibiotic peaks with $k' > 1$.

The chromatogram in Fig. 2 was obtained with standard state-of-the-art HPLC equipment (Hewlett-Packard Model 1050). No special modifications were required. The configuration of this column is such that extra-column effects apparently are minimal when this column is used with well designed, modern equipment. Significant extra-column effects would have caused tailing peaks rather than the near-Gaussian peaks actually observed. Note also that the pressure required for this high-flow-rate separation was well within the practical operating range for routine analyses (111 bar).

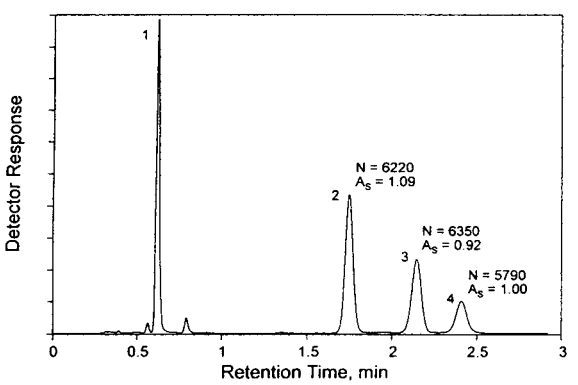

Fig. 2. High-speed separation of antibiotics mixture. Column: 8.0 × 0.46 cm Zorbax SB-C_8 (3.5 μm); mobile phase: acetonitrile–0.1% aqueous trifluoroacetic acid (8:92); flow-rate: 3.0 ml/min; sample: 1 μl containing 0.40, 0.36, 0.10 and 0.35 μg each of ceftazidime (1), cefotaxime (2), ciprofloxacin (3) and cefazolin (4); 60°C; UV detector: 260 nm.

The effect of temperature on the plate height of the column of 3.5-μm particles is shown in Fig. 3. One might predict that operation at higher temperatures should improve solute diffusion, decrease mobile phase viscosity, and, therefore, decrease plate height with increase in column efficiency. The data for ciprofloxacin in Fig. 3 actually shows a slight increase in plate height (decreased column efficiency) as the column temperature was increased from 20 to 60°C. This effect suggests that the secondary band broadening effects discussed above [20,21] negate the expected improvement in solute diffusion. These and other results not given here indicate that higher temperature operation with very-small-particle columns may not be desirable for separating small molecules, unless special operating procedures are adopted [21]. On the other hand, high-temperature separations of macromolecules with such columns often are both advantageous and practical [11]. Apparently, the significant improvement in diffusion with macromolecules more than overcomes any secondary band broadening effects that occur.

A study was made on the effect of sample injection volume on the efficiency of the new column type. Because of the low-volume, sharp peaks generated, it was important to determine the sample volume limit. This information is particularly useful for trace analysis applications where large sample volumes often are required

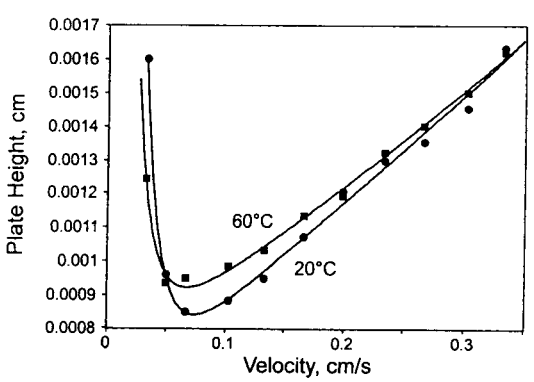

Fig. 3. Effect of column temperature on plate height. Conditions as in Fig. 2, except: 0.10 μg ciprofloxacin; mobile phase velocity and temperatures as shown.

to obtain adequate measurement sensitivity. Table II shows the results of various sample volumes of ciprofloxacin solution injected into the 3.5-μm column with different loop sizes (volumes). Plate numbers and plate heights were essentially constant, within experimental error, with volumes up to 20 μl with the solute at $k' = 2.1$. Partially filling the 10- and 20-μl loops maintained observed column efficiency. Increases in peak heights were commensurate with sample volumes injected with completely or partially filled loops up to 20 μl. However, increasing the sample volume to 50 and 100 μl increasingly degraded observed column efficiency. Also, expected increases in peak heights were not obtained with the larger sample sizes, because of band broadening.

The Table II data indicate that, for components with $k' \approx 2$, highest column efficiency and peak heights are obtained with sample volumes of no more 20 μl. Note, however, that sample volumes can be increased for solutes with larger k' values, since peak volumes increase with k' increase. As peak volume increases, the potential for band broadening is reduced. Other studies not reported here used 100-μl injections

TABLE II

EFFECT OF SAMPLE VOLUME ON COLUMN EFFICIENCY

Column, 8 × 0.46 cm Zorbax SB-C_8 (3.5 μm); sample, 100 ng ciprofloxacin $k' = 2.1$; mobile phase, acetonitrile–0.1% aqueous trifluoroacetic acid (20:80); 22°C. HETP = Height equivalent to a theoretical plate. Peak height in Multichrom counts.

Sample loop volume (μl)	Peak height	Injection volume (μl)	Plate number	HETP $\times 10^3$ (cm)
5	4803	5	8574	0.933
	4929		8555	0.935
10	9313	10	8719	0.918
	9303		8613	0.929
	5161	5	8810	0.908
	5135		8455	0.946
20	17 739	20	8228	0.972
	18 156		8431	0.949
	10 188	10	8441	0.948
	10 137		8450	0.947
	5103	5	8560	0.935
	5122		8603	0.930
50	46 434	50	7589	1.05
	47 037		7593	1.05
	21 063	20	8237	0.971
	21 029		8265	0.968
	10 652	10	8361	0.957
	10 677		8384	0.954
100	83 756	100	6501	1.23
	86 931		6578	1.22
	50 818	50	7661	1.04
	50 705		7580	1.06
	21 238	20	8333	0.960
	21 179		8219	0.973
	10 763	10	8589	0.931
	10 801		8370	0.956

with this column for a solute of $k' \approx 4$ with no noticeable change in column efficiency.

Decreasing particle size and column length has an important effect on increasing the peak height of solutes [22,23]. This increased peak height increases the detectability of components of interest, particularly in trace analyses. Fig. 4 shows relative peak heights obtained for ciprofloxacin at varying flow-rates on a 15×0.46 column of 5-μm particles. These values are compared to those for a 8×0.46 cm column of 3.5-μm particles, both with the same stationary phase. Peak heights for the column of 3.5-μm particles were about twice that for the 5-μm particle column, resulting in a significant potential increase in solute detectability. Also, the peak height optimum for the column of 3.5-μm particles is about 0.6 ml/min, compared to about 0.4 ml/min for the 5-μm particle column. With the column of 3.5-μm particles, flow-rates apparently can be increased for faster analyses, without a large sacrifice in peak heights or detectability.

In the routine application of HPLC columns for "real" samples, guard columns and column filters are often recommended to protect the analytical column from strongly retained endogenous contaminants and particulates [24]. A question arose as to the contribution of the mixing volumes associated with these devices to the efficiency of the 3.5-μm column. Therefore, a study was undertaken to determine possible extra-column band-broadening effects of appropriate guard columns and in-line column filters. Table III shows the results of this study using chloramphenicol as the test solute at a $k' \approx 4$. These results indicate that there is no detrimental influence of this column filter on peak height, plate number or column pressure. The guard column also had no significant effect on observed column performance, with only a slight increase in pressure. Combining the column filter and the guard column still produced no problems, with essentially the same column performance. The data suggest that appropriate column filters and guard columns often can be used without sacrificing column performance. Of course, observed column efficiency could increasingly degrade for components eluting with sharper peaks at lower k' values.

The narrow, sharp peaks generated by the short column of 3.5-μm particles requires that the response time of the detector is sufficiently fast to follow the true shape of the peak. Accordingly, we studied the effect of the Model 783 variable-wavelength detector response (rise) time on peak height and plate number measurements for chloramphenicol. This detector was equipped with a "standard" 12-μl flow cell. Measurements were made with three different concentrations of acetonitrile mobile phase modifier, to generate peaks with varying k' values and resulting differ-

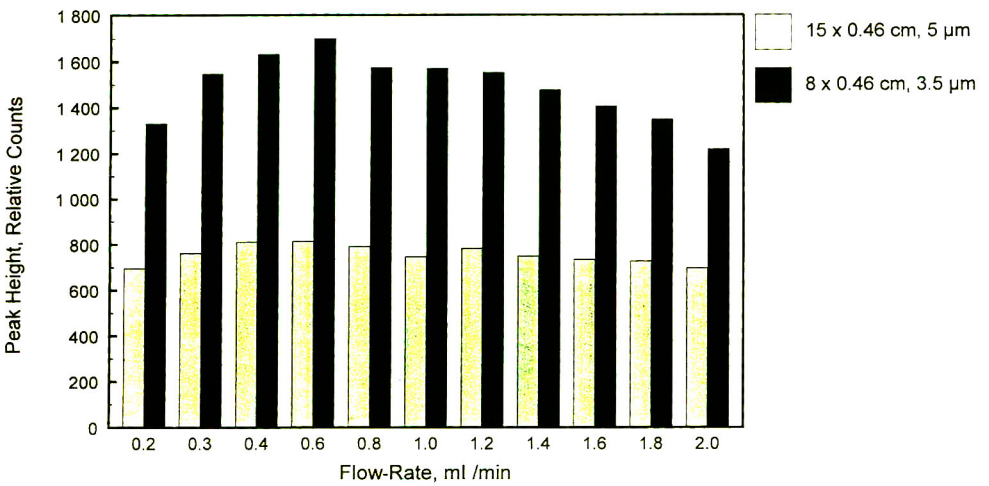

Fig. 4. Effect of column configuration on peak height. Conditions as in Fig. 1 except: 0.10 μg ciprofloxacin; $k' = 2.1$.

TABLE III

EFFECT OF COLUMN FILTER AND GUARD COLUMN ON EFFICIENCY AND BACK PRESSURE

Column, 8 × 0.46 cm Zorbax SB-C_8 (3.5 μm); 20 μl sample, 100 ng chloramphenicol; mobile phase, acetonitrile–0.1% aqueous trifluoroacetic acid pH 3 with triethylamine (75:25); flow-rate 1.0 ml/min; 22°C. Peak height in Multichrom counts.

Status	Peak height	k'	Pressure (bar)	Plate number
No guard	18 865	3.99	81	8251
With filter	18 892	4.01	82	8185
With guard	18 412	4.09	92	8083
With filter and guard	17 947	4.18	96	8013

TABLE IV

EFFECT OF DETECTOR RESPONSE RISE TIME ON PEAK-HEIGHT MEASUREMENTS

Column, 8.0 × 0.46 cm Zorbax SB-C_8 (3.5 μm); sample, 100 ng chloramphenicol in 20 μl. Mobile phase: acetonitrile–0.1% aqueous trifluoroacetic acid, pH 3 with triethylamine: I = 45:35, II = 35:65, III = 25:75; flow-rate, 1.0 ml/min; ambient temperature. Peak height in Multichrom counts.

Detector rise time (s)	I		II		III	
	Peak height, $k' = 0.6$	Plate number	Peak height, $k' = 1.4$	Plate number	Peak height, $k' = 3.9$	Plate number
0.02	38 036		31 595		18 390	
	37 451	3964	31 392	5733	18 559	8280
0.05	37 968		31 974		18 451	
	37 768	3958	32 063	5845	18 299	8336
0.10	38 383		31 563		18 639	
	37 711	3694	31 803	5935	18 077	8289
0.20	37 632		31 537		18 390	
	38 035	3707	31 112	5666	18 279	8379
0.50	37 453		32 133		18 181	
	37 269	3593	30 816	5767	17 870	8351
1.00	35 940		29 561		18 234	
	36 125	3433	30 096	5581	18 272	8240
2.00	31 551		27 785		17 881	
	31 545	2614	27 846	4643	17 635	7906
5.00	20 833					
	20 837	1136				

ent peak widths. Table IV summarizes the data obtained in this study. For the narrowest peak at $k' = 0.6$, rise times of > 0.2 s increasingly degraded plate numbers and peak heights. The peak at $k' = 1.4$ showed no degradation as long as the rise time did not exceed 0.5 s. For the widest and most retained peak at $k' = 3.9$, rise times up to 1.0 s could be used without degrading column performance. These results confirmed that the prototype column can be used without band-broadening difficulties with state-of-the-art detection systems having modest response characteristics.

The studies described so far suggested that the new column configuration should be useful for measuring trace antibiotics in matrices of interest in drug metabolism investigations. Accordingly, trace separations were conducted with chloramphenicol in two matrices using a 8.0×0.46 cm column of 3.5-μm particles and a 15×0.46 cm of 5-μm particles with the same type silica support and the same stationary phase. Recovery of chloramphenicol under the described experimental conditions was 85% for dog plasma and 70% for rat urine, relative to a calibration curve determined with standard solutions. Fig. 5 gives results obtained with extracts of dog plasma. Fig. 5A shows chromatograms with the longer column of 5-μm particles obtained with control extract and an extract containing chloramphenicol. Fig. 5B shows results on the same samples obtained of the shorter column of 3.5-μm particles. As anticipated, using the same flow-rate, separation time was nearly halved. Component k' values were essentially identical for the two columns with the same silica–stationary phase combination. But the height of the cleanly separated chloramphenicol peak for the column of 3.5-μm particles was about twice that of the longer column of 5-μm particles. This enhanced peak height effectively doubles the detectability of the trace component.

Results with a more complex sample are shown in Fig. 6 with extracts of rat urine. Fig. 6A gives chromatograms with the 5-μm column obtained with a control extract and an extract containing chloramphenicol. Fig. 5B shows results obtained on the same extracts with the 3.5-μm column. Again, k' values are comparable while separation time was about halved with the shorter column; peak height for chloramphenicol was about doubled. As before, a faster separation was performed with the potential for higher sensitivity. This new column type has been used in our laboratories for hundreds of sample injections without significant change in separation and efficiency characteristics. Based

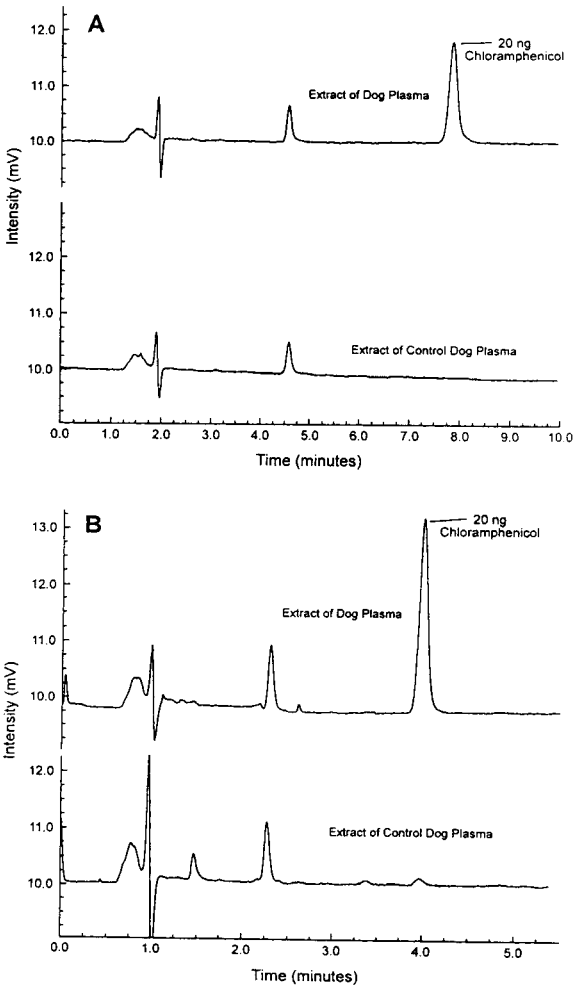

Fig. 5. Effect of column configuration on separation of chloramphenicol in extract of dog plasma. Sample: 20 μl of extract; mobile phase: acetonitrile–0.1% aqueous trifluoroacetic acid (25:75), pH 3 with NH_4OH; 22°C; UV detector: 278 nm; flow-rate: 1.0 ml/min. (A) Column: 15×0.46 cm Zorbax SB-C_8 (5 μm); upper, extract with 100 ng of chloramphenicol; lower, control extract. (B) Column: 8×0.46 cm Zorbax SB-C_8 (3.5 μm); upper, extract with 100 ng of chloramphenicol; lower, control extract.

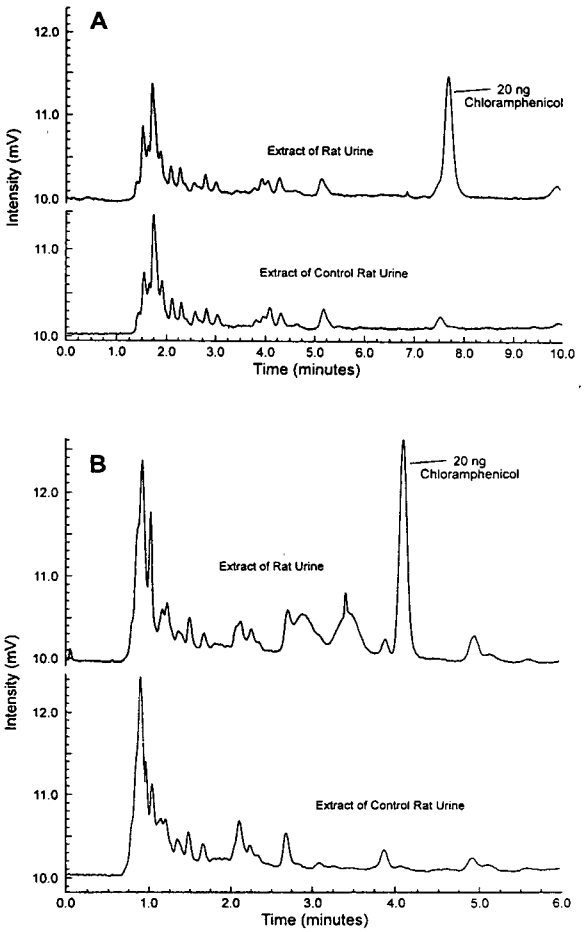

Fig. 6. Effect of column configuration on separation of chloramphenicol in extract of rat urine. Conditions as in Fig. 5.

on experience to date, the long-term stability of this column type appears comparable to equivalent columns of 5-μm particles in routine applications.

CONCLUSIONS

A new 8.0 × 0.46 cm column type with 3.5-μm particles and monomeric sterically protected silane stationary phase has been found effective for the rapid analysis of antibiotic drugs. Compared to conventional 15 × 0.46 cm columns of 5-μm particles, separations were performed in one-half the time, with no significant loss in separation resolution. The faster separations means that solvent consumption per analysis is significantly reduced. Peaks heights also were increased about two-fold for higher component detectability. Higher operating temperatures lowers mobile phase viscosity so that higher flow-rates can be used at modest back pressures for still faster separations. The new column configuration was utilized with state-of the-art HPLC equipment without special modifications. No significant extra-column band broadening was observed for component peaks with $k' \geq 1$. Appropriate guard columns and inlet filters also were used with the new column configuration without extra-column band-broadening problems. Sample volumes of at least 20 μl were permitted.

ACKNOWLEDGEMENT

We thank C.H. Dilks, Jr. for his assistance with some of the experiments.

REFERENCES

1 C.Y. Chan, K. Chan and G.L. French, *J. Antimicrob. Chemother.*, 18 (1986) 537.
2 K. Borner, E. Borner, H. Hartwig and H. Lode, in E. Reid and I. Wilson (Editors), *Analysis for Drugs and Metabolites Including Anti-Infective Agents*, Royal Society of Chemistry, Cambridge, 1990, p. 131.
3 J.C. Giddings, *Dynamics of Chromatography*, Marcel Dekker, New York, 1965.
4 J.H. Knox, *J. Chromatogr. Sci.*, 15 (1977) 352.
5 Cs. Horváth and H.-J. Lin, *J. Chromatogr.*, 149 (1977) 43.
6 R.E. Majors, *LC·GC*, 9 (1991) 686.
7 L.R. Snyder and J.J. Kirkland, *Introduction to Modern Liquid Chromatography*, Wiley, New York, 1979, Ch. 2.
8 J.J. Kirkland, *J. Chromatogr. Sci.*, in press.
9 J.L. Glajch and J.J. Kirkland, *US Pat.*, 4 705 725 (Nov. 10, 1987).
10 J.J. Kirkland, J.L. Glajch and R.D. Farlee, *Anal. Chem.*, 61 (1988) 2.
11 J.J. Kirkland, C.H. Dilks. Jr. and J.E. Henderson, *LC·GC*, 11 (1993) 290.
12 J.J. Kirkland and B.E. Boyes, *Peptide Res.*, 6 (1993) 249.
13 K.M. Kirkland, D.A. McCombs and J.J. Kirkland, presented at the *17th International Symposium on Column Liquid Chromatography, Hamburg, May 9–14, 1993*, poster 1-219.
14 J.J. Kirkland, C.H. Dilks, Jr. and J.J. DeStefano, *J. Chromatogr.*, 635 (1993) 19.
15 J.J. Kirkland, *US Pat.*, 3 782 075 (Jan. 1, 1974).

16 J.J. Kirkland and J. Köhler, *US Pat.*, 4 874 518 (Oct. 17, 1989).
17 J.J. Kirkland and J. Köhler, *US Pat.*, 5 032 266 (July 16, 1991).
18 L.R. Snyder and J.J. Kirkland, *Introduction to Modern Liquid Chromatography*, Wiley, New York, 1979, p. 222.
19 M.A. Stadalius, J.S. Berus and L.R. Snyder, *LC·GC*, 9 (1991) 686.
20 N.H.C. Cooke, B.G. Archer. K. Olsen and A. Berick, *Anal. Chem.*, 54 (1982) 2277.
21 H. Poppe and J.C. Kraak, *J. Chromatogr.*, 282 (1983) 399.
22 J.J. Kirkland, *Analyst*, 99 (1974) 859.
23 B.L. Karger, M. Martin and G. Guiochon, *Anal. Chem.*, 46 (1974) 1640.
24 L.R. Snyder, J.L. Glajch and J.J. Kirkland, *Practical HPLC Method Development*, Wiley, New York, 1988, p. 80.

Journal of Chromatography A, 660 (1994) 339–350
Elsevier Science B.V., Amsterdam

CHROMSYMP. 2924

Liquid chromatographic retention behaviour and separation of promethazine and isopromethazine on a β-cyclodextrin bonded-phase column

Stavroula Piperaki

Division of Pharmaceutical Chemistry, Department of Pharmacy, University of Athens, Zografou 15771, Athens (Greece)

Anastasios Perakis

Department of Biology, University of Athens, Zografou 15771, Athens (Greece)

Maria Parissi-Poulou*

Division of Pharmaceutical Chemistry, Department of Pharmacy, University of Athens, Zografou 15771, Athens (Greece)

ABSTRACT

A liquid chromatographic method for the separation of promethazine (PR) and its positional isomer isopromethazine (IPR) is described. PR is an N-substituted phenothiazine with the actions and the uses of the antihistamines (H1-receptor antagonists). IPR is an impurity in the pharmaceutical preparations of PR and must be controlled at a level below 1%. The liquid chromatographic behaviour of PR and IPR on a hydrolytically stable β-cyclodextrin (β-CD) column with respect to mobile phase composition, pH, ionic strength and the nature of the organic modifier was also investigated. Based on the results, conditions were chosen for the isocratic separation of the two isomers. The proposed separation method is simple and rapid and permits the simultaneous determination of PR and IPR. The separation selectivity of a cyclodextrin bonded-phase column was examined. Special attention was devoted to modelling the inclusion complexes of PR and IPR with β-CD in order to predict their optimum orientation within the β-CD cavity.

INTRODUCTION

Even though much progress has been achieved in the separation of structural [1] and positional isomers [2] of a number of compounds, most of the effort has been directed at developing complex mobile phases that can provide the required selectivity. In the last few years, however, some attention has been directed towards the development of tailor-made column packing materials specifically designed to provide multi-point or specific chemical interactions with analytes in order to achieve more selective separations. Among such column packings are a number of stable cyclodextrin (CD)-bonded phases, which were first described in 1984 [3]. This allows cyclodextrin columns to effect numerous chemical separations by selectively including, in solution, a wide variety of organic and inorganic guest molecules in the cyclodextrin cavity [4].

Cyclodextrins are toroidally shaped oligosaccharides formed by the action of *Bacillus macerans* amylase on starch. These supramolecules contain 6–12 D-glycopyranose units bonded through α-(1,4)-glycosidic linkages. The physical shape of the molecule is that of a truncated cone, with an internal hydrophobic

* Corresponding author.

0021-9673/94/$07.00 © 1994 Elsevier Science B.V. All rights reserved
SSDI 0021-9673(93)E0889-3

cavity whose dimensions are determined by the number of glycose units and hydrophylic exterior faces [5,6].

The ease with which CD packings discriminate between molecules of different chemistry, size, shape and spatial geometry is obviously due to its ability to form intimate inclusion complexes of different strength. In the mechanism of separation a variety of interactions are involved, including hydrophobic interactions with the interior of the cavity, hydrogen bonding with the hydroxyl groups at the periphery of the cavity, the release of high-energy water or modifier during complex formation or a combination of these factors [7,8].

Promethazine (PR) hydrochloride is an N-substituted phenothiazine (Fig. 1) with the actions and uses of the antihistamines (H1-receptor antagonists). It also has some antimuscarinic, antiseretoninergic and marked local anaesthetic properties [9]. It is commonly used in pharmaceutical preparations such as tablets, injections and elixirs. Thus it is a molecule of great analytical interest and it has been determined by colorimetric [10], spectrophotometric [11], spectrofluorimetric [12], flow injection [13], GC [14], GC–MS [15] and LC [16–26] methods.

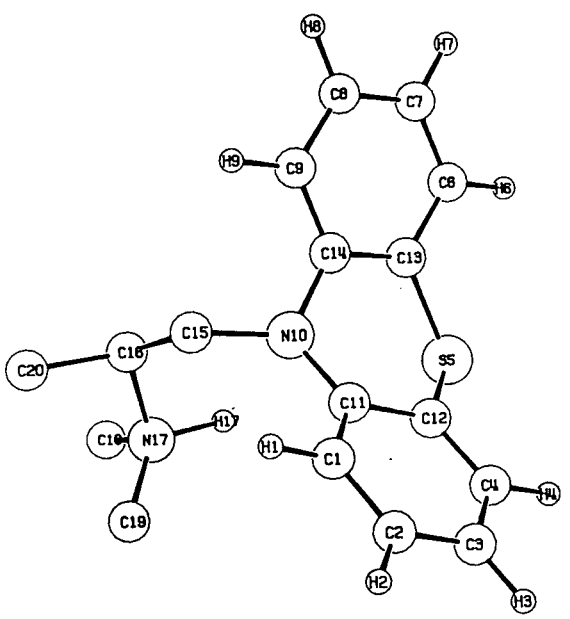

Fig. 1. Crystallographic structure of promethazine. In isopromethazine the methyl group at C-20 is attached to C-15.

On the other hand, isopromethazine (IPR) is an impurity in PR pharmaceutical preparations and its level must be controlled below 1%. Their simultaneous determination has been performed by high-speed LC [27].

Our initial motivation in undertaking this work was the direct LC separation of PR and its positional isomer IPR. To the best of our knowledge, this is the only separation of these two isomers by HPLC using a β-CD column. Further, we investigated the LC behaviour of PR and IPR on a hydrolytically stable β-CD column with respect to mobile phase composition, pH, ionic strength and the nature of the organic modifier. Based on the results, chromatographic conditions for the isocratic separation of the two isomers were chosen. Special attention was devoted to modelling the inclusion complexes of PR and IPR with β-CD, in order to predict their optimum orientation within the β-CD cavity.

EXPERIMENTAL

Apparatus

The LC system consisted of a Waters Model 501 pump, a Rheodyne Model 7125 injector with a 20-μl loop and a Waters Model 486 spectrophotometer with an 8-μl flow cell. The chromatograms were obtained by using an HP-3394A integrator (Hewlett-Packard).

A Cyclobond I column (250 × 4.6 mm I.D.) was obtained from Advanced Separation Technologies. It has β-CD molecules chemically bonded to a spherical silica support through a five-atom, non-nitrogen bonded-containing spacer arm [1]. When not in use the column was stored in 100% methanol.

pH readings were obtained using a Metrohm Model 654 pH meter.

Chromatographic conditions

The effect of pH on the retention of PR and IPR was investigated by changing the pH of the aqueous phase of mobile phase from 3.5 to 7.0 with triethylamine acetate buffer (2.0%, w/v). The effect of ionic strength on retention was examined by varying the concentration of tri-

ethylamine buffer (pH 4.5) from 0.1 to 2.5 (w/v).

The effect of the organic modifier on the resolution of two isomers was examined by preparing binary aqueous–organic mobile phases with the same polarity index (*ca.* 8.64). The polarity of each mobile phase was calculated according to Snyder based on the following equation:

$$P_m = \varphi_1 P_1 + \varphi_2 P_2$$

where P_m is the polarity of the mixture, P_1 and P_2 are the polarities of the pure solvents and φ_1 and φ_2 are the volume fractions of the two solvents. The organic modifiers used were methanol (MeOH), ethanol (EtOH), 2-propanol (i-PrOH), *tert.*-butanol (t-BuOH), acetonitrile (ACN) and tetrahydrofuran (THF).

All experiments were performed at room temperature (about 25°C). The compounds were detected at a wavelength of 254 nm. The mobile phases, consisting of triethylammonium acetate buffer and the appropriate amount of the organic modifier, were freshly prepared, filtered and degassed under vacuum using a Millipore system.

Solutions

Stock standard solutions of all drugs (1.00 mg/ml) were accurately prepared by dissolving an appropriate amount of the compound in HPLC-grade water and were kept in an amber-coloured bottle in a refrigerator and renewed every week. Working standard solutions (for promethazine and isopromethazine) were prepared every day in the mobile phase. Typically a volume of 20 μl of each solution was injected.

To obtain comparable results, experiments were performed under identical chromatographic conditions, *i.e.*, a flow-rate of 0.8 ml/min and an integrator attenuation of 3. The void volume of the column was determined by injecting 20 μl of pure methanol each time.

To evaluate the reproducibility of the retention times, each run was performed three times.

Materials

Methanol, acetonitrile, ethanol, 2-propanol, *tert.*-butanol and tetrahydrofuran were of HPLC-grade and purchased from Tech-Line. Triethylamine and glacial acetic acid were of analytical-reagent grade and purchased from Aldrich. Pure promethazine and isopromethazine, in form of hydrochloride salts, were kindly provided by Rhone-Poulenc Rorer and used as received.

RESULTS AND DISCUSSION

Effect of mobile phase composition

The effect of the mobile phase composition on the retention times and the resolution of the two positional isomers was investigated by changing the methanol-to-buffer ratio in the mobile phase from 10:90 to 60:40. It was observed that the dependence of log k' of each compound on the methanol content in mobile phase was mostly linear, suggesting a reversed-phase mechanism for the interaction between the solute and stationary phase [28].

After these preliminary studies, buffer–methanol (85:15) was chosen as the mobile phase composition providing the optimum chromatographic conditions for the studies described below. The flow-rate was 0.8 ml/min.

Effect of ionic strength

The effect of ionic strength on the separation of PR and IPR was investigated in the concentration range 0.1–2.5% (w/v) triethylamine acetate (TEAA) at pH 4.5, where both PR and IPR are expected to be mostly in their ionic forms (pK_a of PR = 9.1 [29]).

As shown in Table I, the retention times of PR and IPR decrease as the electrolyte concentration increases. This type of behaviour can be rationalized in terms of the TEAA molecules included in the β-CD cavity, thus competing with the solute molecules. This mechanism may be possible through the formation of a TEAA ion pair within the hydrophobic environment of the cavity. The binding constant for such a complex is likely to be enhanced by the hydrophobic interactions between the cavity and the hydrophobic shell provided by the ethyl moieties of the triethylamine cation, which surround and shield its central, positively charged nitrogen atom. Owing to the comparable sizes of the

TABLE I

EFFECT OF TEAA CONCENTRATION ON RETENTION, RESOLUTION AND SELECTIVITY OF PROMETHAZINE AND ISOPROMETHAZINE USING A β-CYCLODEXTRIN-BONDED COLUMN

TEAA concentration (%, w/v)	t_1 (min)	t_2 (min)	R	α	Log α
0.10	19.61	19.61	0.000	1.000	0.000
0.50	19.45	21.15	0.324	1.087	0.036
0.75	18.54	21.02	0.558	1.135	0.055
1.00	17.94	20.64	0.675	1.150	0.061
1.25	17.47	20.23	0.736	1.158	0.064
1.50	16.95	19.87	0.973	1.172	0.069
1.75	16.30	19.21	1.058	1.179	0.072
2.00	16.19	19.05	1.185	1.201	0.080
2.25	14.86	18.00	1.256	1.211	0.083
2.50	14.44	17.51	1.505	1.213	0.084

β-CD cavity and the triethylamine cation, these interactions are likely to be of considerable magnitude [28].

An alternative mechanism may be that the TEAA molecules interact with the hydrophilic secondary hydroxyls at the opening of the β-CD cavity, thus blocking the entry of the analytes [28].

This decrease in the retention time of the analytes as the concentration of TEAA increases was described by eqns. 1 and 2 for IPR and PR, respectively, which express the linear relationship between the retention time (t) of the solute and the TEAA concentration (% w/v).

$$t = 20.57\ (\pm 0.22) - 2.47\ (\pm 0.13)\ [\text{TEAA}] \qquad n = 9,\ r = 0.990 \quad (1)$$

$$t = 22.41\ (\pm 0.21) - 1.85\ (\pm 0.13)\ [\text{TEAA}] \qquad n = 9,\ r = 0.983 \quad (2)$$

The negative slope values are in agreement with the above theoretical concept. It is important to note that the slope in eqn. 1 is much greater than that in eqn. 2. Hence the influence of the variation of electrolyte concentration on the retention time of IPR (first-eluted component) is much greater than that on the retention of PR.

Resolution is also affected by ionic strength. It has been reported [30] that peak shapes become sharper with increasing buffer concentration and the resolution is slightly affected. However, the separation of PR and IPR is greatly affected by ionic strength. As is shown in Fig. 2, an increase in salt concentration in the range 0.1–2.5% (w/v) results in a variation of the resolution (R) between 0 and 1.5, *i.e.*, complete resolution.

There is a linear relationship between R and TEAA concentration (%, w/v) and eqn. 3 describes the fit of all the experimental data:

$$R = 0.038\ (\pm 0.042) + 0.580\ (\pm 0.027)\ [\text{TEAA}] \qquad n = 10,\ r = 0.991 \quad (3)$$

The selectivity of the separation is affected very slightly by the ionic strength, as evidenced by the absence of any changes in the elution order of the solutes; in all instances IPR is eluted before PR. In the molecule of PR, one of the three methyl groups is in an α-position with respect to the nitrogen of the ethanamine group. In contrast, in the molecule of IPR this methyl group is in a β-position and gives rise to steric effects in the formation of the inclusion complex with β-CD. As the ionic strength of the mobile phase increases, the above selectivity is expressed more by the following possible mechanism.

Chromatographic separations using CD-bonded phases are mainly the result of variations in the stability of the inclusion complexes of the analytes with the CD [7], which reflects the respective variations in the stability constants of the complexes (K_f). The molecule of PR and also that of IPR have a hydrophobic three-ring system (phenothiazine structure) and a hydrophilic chain carrying an ionizable nitrogen group which at pH 4.5 is mostly positively charged. It has been assumed that the hydrophobic part is buried inside the hydrophobic CD cavity and the hydrophilic part can participate in hydrogen-bonding interactions with the hydroxyl groups located outside the cavity.

On the other hand, as the ionic strength increases, the polarity of the mobile phase also increases. Consequently, the hydrophobic part of the PR molecule is forced to be "hidden" in the

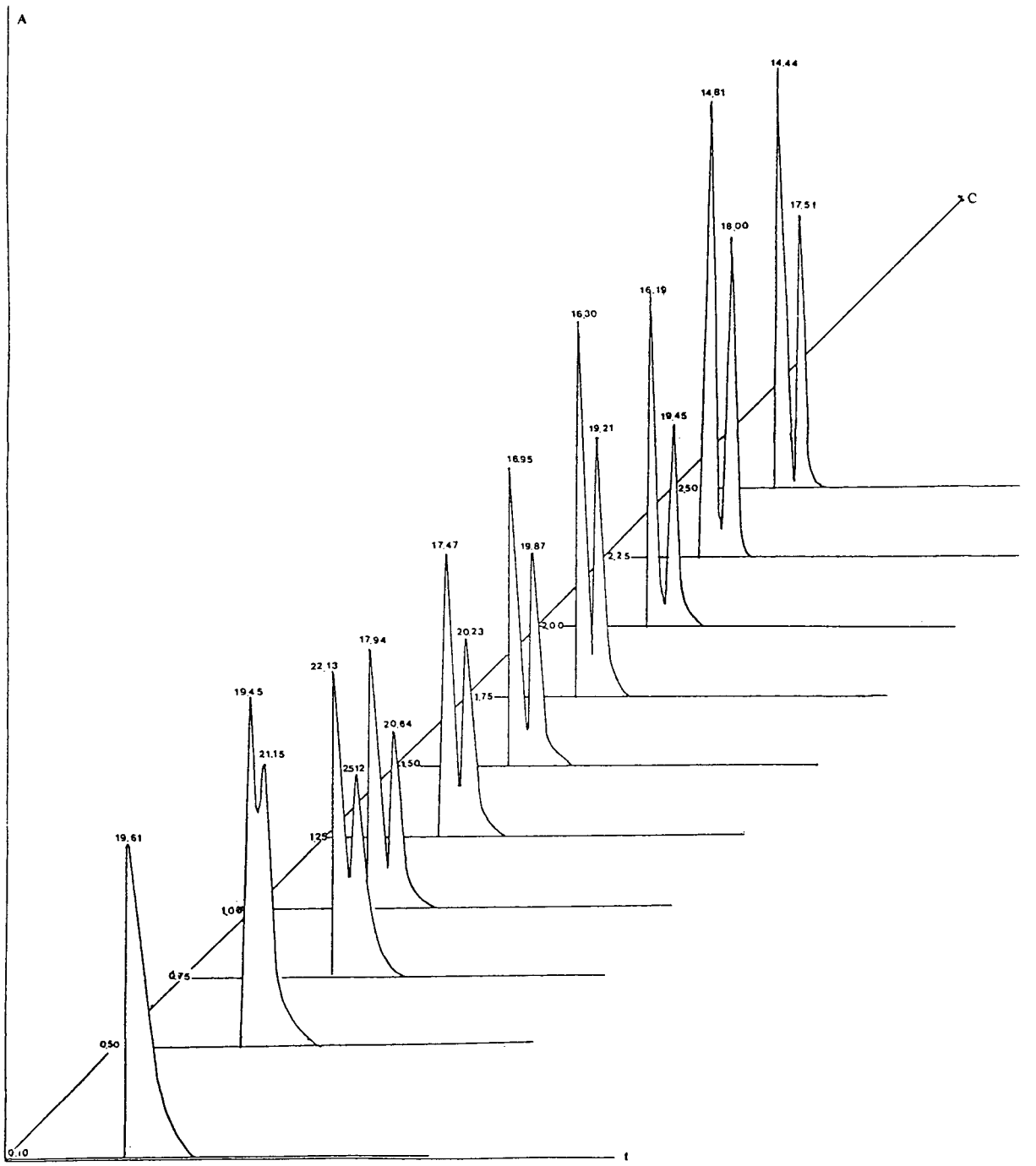

Fig. 2. Effect of ionic strength on the chromatographic separation of IPR and PR. C = Salt concentration in %C (w/v) and t = retention time in min.

CD cavity in order to avoid contact with the hydrophillic mobile phase environment. Hence the stability constant of the inclusion complex which is formed between PR and β-CD increases as the ionic strength of the mobile phase increases. In contrast, the inclusion complex formation between IPR and β-CD is characterized, as mentioned above, by a steric effect. Thus, as the TEAA concentration increases the above variation in the stability constants of the two complexes increases.

The chromatographic selectivity factor (α) is an important experimental probe in studies of the solute retention process. It reflects the difference between two solutes in the Gibbs free energy of transfer from the mobile phase to the stationary phase:

$$\alpha = k_2'/k_1' \quad (4)$$

$$\ln \alpha = -\Delta(\Delta G)/RT \text{ or } \log \alpha = -\Delta(\Delta G)/2.303RT \quad (5)$$

where k_1' and k_2' are the capacity factors of the two solutes, ΔG is the Gibbs free energy, R is the gas constant and T is the absolute temperature [31].

As shown, the regression analysis plot represent a multiplicative model described by the equation

$$\alpha = a\,[\text{TEAA}]^b \quad n = 10,\ r = 0.995 \quad (6)$$

where $a = 0.1368(\pm 0.0020)$ (the intercept is equal to log a) and $b = 0.0609(\pm 0.0021)$ represent the intercept and the slope, respectively. Eqn. 6 can be rearranged to eqn. 7, which express a linear relationship between log a and TEAA concentration (%, w/v):

$$\log \alpha = \log a + b(\log [\text{TEAA}]) \quad n = 10,\ r = 0.995 \quad (7)$$

where $a = 0.05954(\pm 0.00085)$ and $b = 0.0611(\pm 0.0022)$. From eqns. 5 and 7, it is evident that the effect of the ionic strength on the selectivity factor (α) reflects an effect on the difference between the two solutes in the Gibbs free energy of transfer from the mobile phase to the stationary phase.

Effect of pH

The effect of pH on the retention of PR and IPR was investigated by changing the Ph of the aqueous component of the mobile phase from 4.00 to 7.00 (respecting the column limitations) using triethylamine buffer (2.5%, w/v). In order to obtain comparable results, experiments were performed under chromatographic conditions identical with those mentioned under Experimental.

Table II shows the effect of pH on retention, resolution and selectivity of PR and IPR using a β-CD-bonded stationary phase.

As discussed earlier, inclusion has been suggested as the predominant mode for their retention. The existence of a well defined hydrophobic part in the molecules of PR and IPR provides opportunities for hydrophobic interactions with the interior of the β-CD cavity. On the other hand, the charged hydrophilic nitrogen group provides opportunities for hydrogen bonding interactions with the OH groups on the circumference of β-CD molecule. These two kinds of interactions are slightly affected by pH, owing to the higher pK_a values of PR and IPR than the maximum pH value examined.

However, an increase in retention time with increasing pH is observed (Fig. 3). A plausible explanation may be that the charged hydrophilic nitrogen group in the molecules of PR and IPR and the acetate anion form an ion pair within the CD cavity.

TABLE II

EFFECT OF pH OF THE AQUEOUS COMPONENT OF THE MOBILE PHASE ON RETENTION, RESOLUTION AND SELECTIVITY OF PROMETHAZINE AND ISOPROMETHAZINE USING A β-CYCLODEXTRIN-BONDED COLUMN

pH	t_1 (min)	t_2 (min)	R	α
4.00	13.63	16.12	1.072	1.182
4.50	14.32	17.02	1.160	1.188
5.00	15.62	18.81	1.245	1.204
5.50	17.61	21.57	1.320	1.225
6.00	20.74	25.93	1.260	1.250
6.50	25.02	31.95	1.153	1.277
7.00	36.30	47.26	1.089	1.288

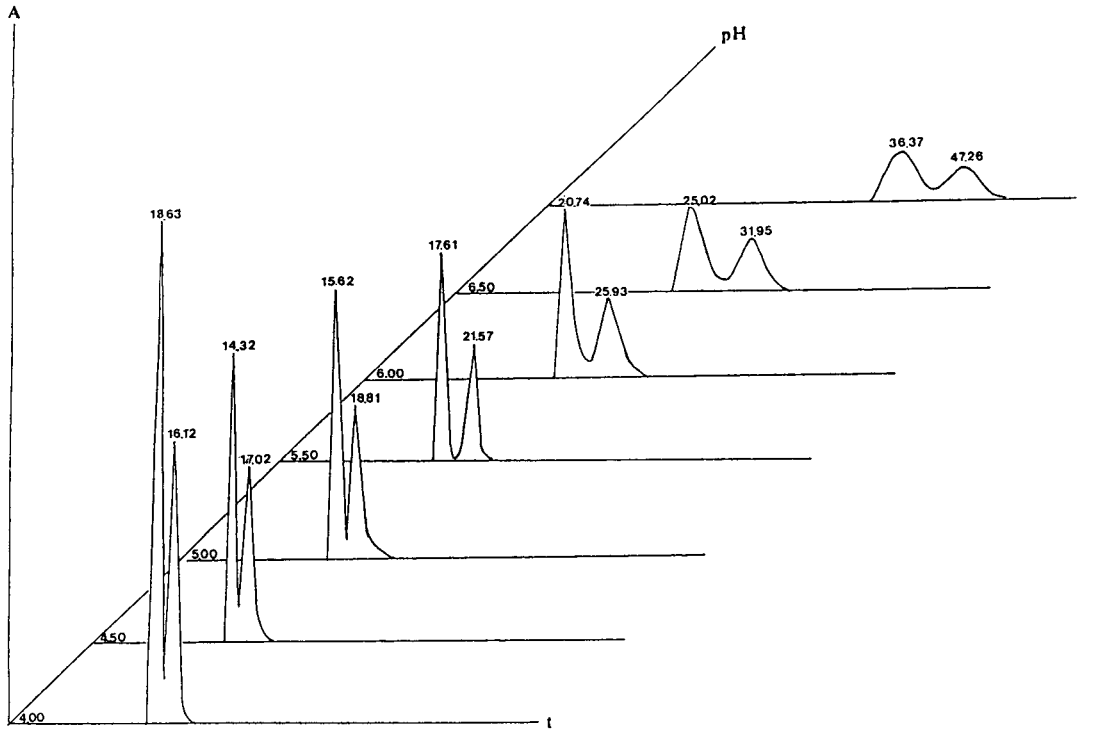

Fig. 3. Effect of pH on the separation of IPR and PR.

The dependence of the retention time of IPR and PR on the pH of the aqueous component of the mobile phase is described by a reciprocal model (eqns. 8 and 9, respectively):

$$1/t = 0.1380(\pm 0.0062) - 0.0152(\pm 0.0011)\ \text{pH} \qquad n = 7,\ r = 0.987 \quad (8)$$

$$1/t = 0.1200(\pm 0.0047) - 0.01372(\pm 0.00084)\ \text{pH} \qquad n = 7,\ r = 0.991 \quad (9)$$

By increasing the pH the solutes become more retained and hence the column's inclusion selectivity also increases. The dependence of the selectivity factor (α) on pH is described by the equation

$$\alpha = 1.018(\pm 0.015) + 0.0388(\pm 0.0026)\ \text{pH} \qquad n = 7,\ r = 0.990 \quad (10)$$

It could be expected that the resolution R would also increase with increase in pH owing to the increase in column selectivity. However, in the pH range 4.0–5.5 the resolution increases whereas it decreases at pH >5.5. This dependence follows a linear model described by eqns. 11 and 12, respectively:

$$R = 0.412(\pm 0.020) + 0.1658(\pm 0.0042)\ (\text{pH})_{aq} \qquad n = 4,\ r = 0.9994 \quad (11)$$

$$R = 2.206(\pm 0.080) - 0.160(\pm 0.013)\ (\text{pH})_{aq} \qquad n = 4,\ r = 0.994 \quad (12)$$

This behaviour can be rationalized by considering that as the pH increases both retention and selectivity increase, whereas concurrently at pH >5.5 the peaks become broader in such a way that the resolution decreases.

Effect of solvent selectivity

"Selectivity" primarily refers to the ability of a solvent to exhibit specific solute interactions which another solvent of approximately similar strength or polarity do not undergo. Polarity describes the gross solvent strength. Selectivity

describes the fine structure of strength, the profile of polarity sub-parameters [32].

Selectivity describes the degree to which a solvent is chromatographically stronger for a particular solute by virtue of its ability to enter into specific intermolecular interactions to a greater extent than for other solutes.

With CD-bonded phases, retention is predominantly due to inclusion complex formation. Because molecules of different chemistry, size, shape and spatial geometry form inclusion complexes of different strengths with CDs, separation is readily achieved. The organic mobile phase modifier tends to compete with all solutes. There are a definite number of adsorption sites on the stationary phase on which the solute and the mobile phase components can bind. It is assumed that the organic modifier has a greater affinity for the adsorption site than water but lower than solutes [3].

It was of interest to estimate the solvent selectivity using different organic modifiers in the mobile phase which had the same polarity index (*ca.* 8.64). Thus, all the differences observed in separation and resolution reflect differences in the inclusion process.

As shown in Fig. 4, when methanol, ethanol or acetonitrile was used, a very good resolution between IPR and PR was achieved. The use of 2-propanol provided partial resolution of the two isomers but using THF or *tert.*-butanol no resolution was obtained.

It may be useful to investigate the relationship between resolution and the logarithm of the partition coefficient (octanol–water) of each solvent (log P) (Table III). There is a linear relationship between R and log P, described by the equation

$$R = 0.82(\pm 0.15) - 2.2(\pm 0.33) \log P$$
$$n = 6,\ r = 0.956 \quad (13)$$

This good relationship ($r > 0.94$) suggests that the hydrophobicity of the organic modifier is one of the dominant factors with respect to solvent selectivity in inclusion process phenomena. The competition between solutes and the organic modifier for the same retention site (β-CD cavity) controls the retention, which in this instance depends on the relative hydrophobicity of the solvent and solute. Obviously, as the hydrophobicity of the organic modifier increases its affinity for the adsorption site (β-CD cavity) also increases.

For log P values greater than 0.35 no resolution was observed for the two isomers. It is important to note that other workers have suggested the use of log P as a solvent "strength" parameter in RPLC [33]. According to the present observations, this concept can be extended to inclusion complex chromatography.

It should be noted that the relationship between R and log P shows excellent linearity ($r > 0.999$) when the point for acetonitrile is omitted:

$$R = 0.9060(\pm 0.0029) - 2.428(\pm 0.061) \log P$$
$$n = 5,\ r = 0.9994 \quad (14)$$

The interaction potential of acetonitrile is different to those of the other solvents used [34]. Using acetonitrile as the organic modifier, selective dipole–dipole interactions between solutes and the solvent may occur owing to the high dipole moment of acetonitrile. These dipole–dipole interactions usually occur between individual polar functional groups of solvent and solute molecules. Both PR, and IPR possess a polar amine group which can participate in such interactions. On the other hand, it has been reported that acetonitrile will bind more strongly to CD than other solvents [3]. For these two reasons, solutes are less retained and consequently would tend to elute more quickly using acetonitrile as organic modifier.

The selectivity factor (α) in the chromatographic separation of PR and IPR is also affected by solvent selectivity. A reciprocal model relationship exists between α and log P, described by the equation

$$1/\alpha = 0.9014(\pm 0.0080) + 0.222(\pm 0.018) \log P$$
$$n = 6,\ r = 0.990 \quad (15)$$

Isocratic separation of PR and IPR

After studying the LC retention behaviour of PR and IPR on a β-CD column with respect to

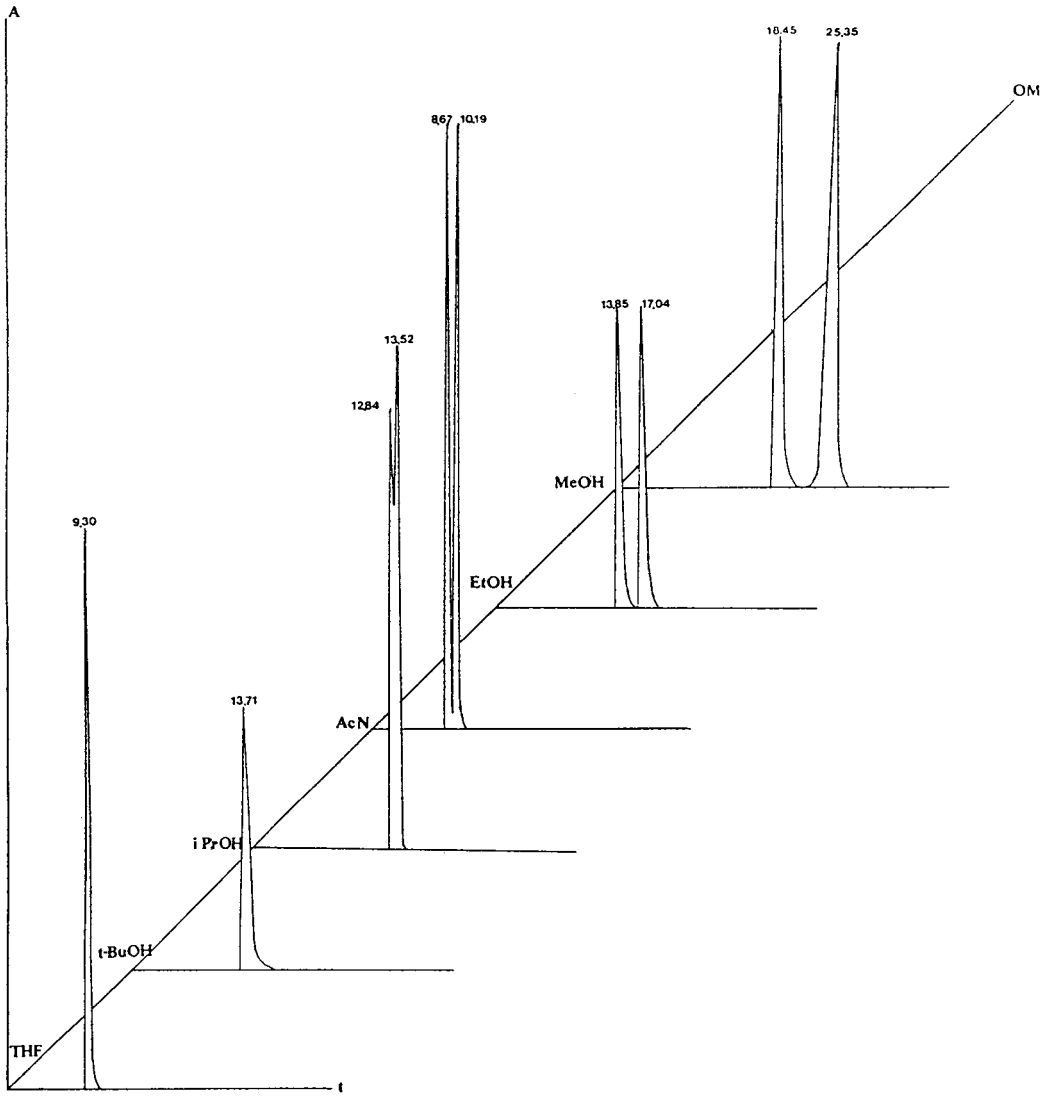

Fig. 4. Effect of solvent selectivity on the separation of IPR and PR.

mobile phase composition, pH, ionic strength and solvent selectivity, a set of chromatographic conditions were chosen for the simultaneous separation of the two positional isomers. These conditions are as follows: methanol–buffer (83:17); buffer, 2.5% (w/v) TEAA; pH, 5.50; and flow-rate, 0.8 ml/min. These conditions permit the determination of 1% of IPR in PR solution using a UV–Vis detector at 254 nm (Fig. 5).

Molecular modelling for the PR– and IPR–β-CD complexes

In order to understand the basis of the separation of these positional isomers using a β-CD column, the interactions of the crystal structures of PR and IPR [35,36] with β-CD were examined using computer graphic modelling. Computer modelling using the program CHEM-X revealed interesting docking arrangements. The computer program positioned the two posi-

TABLE III

EFFECT OF SOLVENT TYPE AND HYDROPHOBICITY ON RETENTION, RESOLUTION AND SELECTIVITY OF PROMETHAZINE AND ISOPROMETHAZINE USING A β-CYCLODEXTRIN-BONDED COLUMN

Solvent	t_1 (min)	t_2 (min)	R	α	Log P
MeOH	18.45	25.35	2.760	1.374	−0.77
EtOH	13.85	17.04	1.707	1.230	−0.32
ACN	8.67	10.19	0.933	1.181	−0.34
i-PrOH	12.84	13.52	0.227	1.053	0.30
t-BuOH	13.71	13.71	0.000	1.000	0.35
THF	9.30	9.30	0.000	1.000	0.46

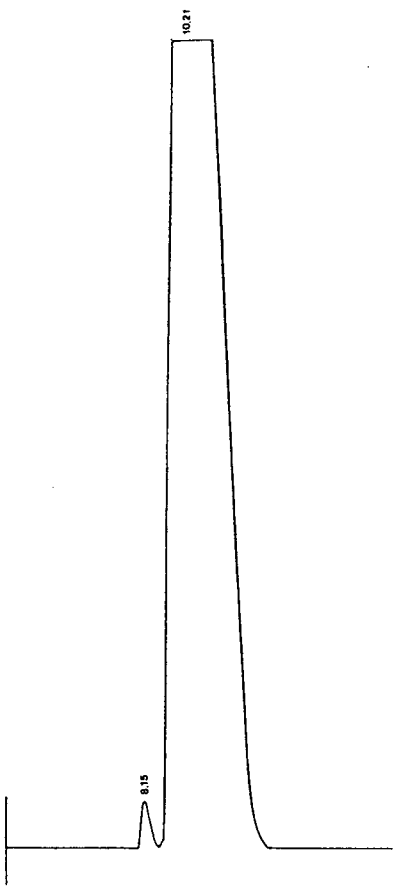

Fig. 5. Chromatographic separation of IPR and PR (1% IPR in PR solution).

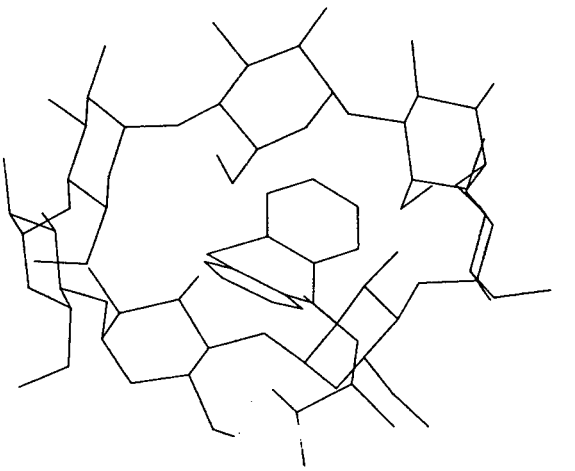

Fig. 6. Stick model of the inclusion complex of PR with β-CD.

tional isomers minimizing steric and electronic hindrances.

A model of the binding of the two isomers to β-CD is proposed. In both instances it is assumed that the hydrophobic part (three-ring system) of the two molecules is buried inside the cavity while the other part is pointing towards the outside. It is apparent that PR is able to form a better inclusion complex than IPR. The three-ring system of PR was found to penetrate deeper in the β-CD cavity compared with IPR, as can be seen in Figs. 6 and 7. Further, Fig. 8 shows

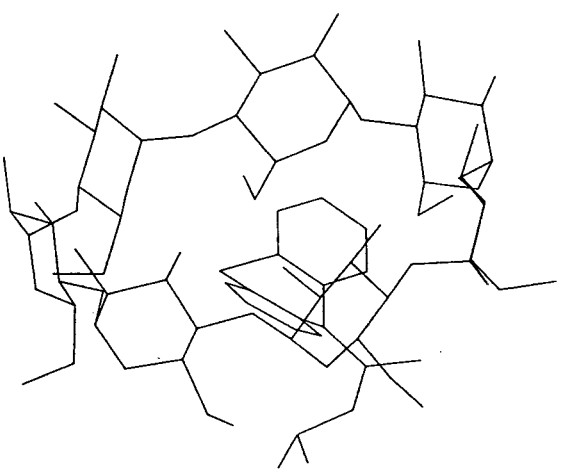

Fig. 7. Stick model of the inclusion complex of IPR with β-CD.

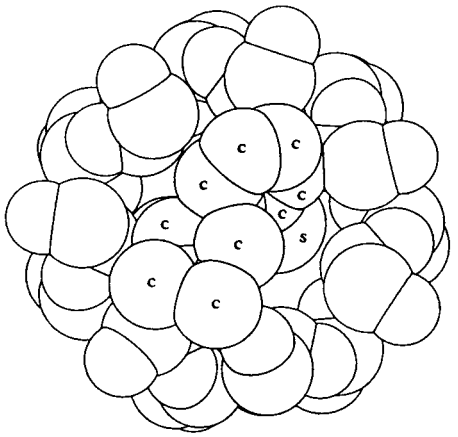

Fig. 8. Space-filling model of the inclusion complex of PR with β-CD.

the space-filling model of the PR inclusion complex with the β-CD cavity.

This difference was qualified by measuring the distance from the mouth of the β-CD cavity. For the molecule of PR (crystallographic numbering system, Fig. 1) the rings are modelled to enter as deeply as possible inside the β-CD cavity without having any bad contacts, in such a way that a possible hydrogen bond is formed between N-17 and one OH group located at the ring of β-CD cavity (N–O distance 2.71 Å). Supposing that the orientation of the rings remains the same for IPR when bonded to β-CD, the three-ring system cannot enter as deeply as in the first case because the methyl group at C-20, now in a β-position, closer to the rings, has bad contacts with the hydrophobic cavity. In order to remove these contacts, IPR must be dragged towards the outside. This procedure also weakens the hydrogen bond mentioned above (N–O distance 2.93 Å) and minimizes the hydrophobic interaction between the β-CD cavity and the three-ring system of the molecule of IPR.

The difference in penetration allows PR to be more tightly complexed in the hydrophobic cavity of β-CD. This result corresponds with the chromatographic data.

REFERENCES

1 R.D. Armstrong, T.J. Ward, N. Pattabiraman, C. Benz and D.W. Armstrong, *J. Chromatogr.*, 414 (1987) 192–196.
2 F.C. Marziani and W.R. Sisco, *J. Chromatogr.*, 465 (1989) 422–428.
3 D.W. Armstrong and W. DeMond, *J. Chromatogr. Sci.*, 22 (1984) 411–415.
4 T.J. Ward and D.W. Armstarong, *Cyclodextrin Stationary Phase in Chromatographic Chiral Separations (Chromatographic Science Series*, Vol. 40), Marcel Dekker, New York, 1988, pp. 131–163.
5 D.W. Armstrong, W. DeMond, A. Alak, N.L. Hinze, T.E. Riehl and K.H. Bui, *Anal. Chem.*, 57 (1985) 224–237.
6 W.L. Hinze, T.E. Riehl, D.W. Armstrong, W. DeMond, A. Alak and T. Ward, *Anal. Chem.*, 57 (1985) 237–242.
7 S.L. Abidi, *J. Chromatogr.*, 362 (1986) 33–46.
8 D.W. Armstrong, G.L. Bertrand, K.D. Ward, T.J. Ward, H.V. Secor and J.I. Seeman, *Anal. Chem.*, 62 (1990) 332–338.
9 *Martindale, the Extra Pharmacopoeia*, Pharmaceutical Press, London, 29th ed., 1989, pp. 393–394.
10 M. Tarasiewicz, *Anal. Pol. Pharm.*, 29 (1972) 578.
11 M. Gayarama, M.V. D'Souza, H.S. Yathirajan and Y. Rangaswam, *Talanta*, 33 (1986) 352.
12 C. Danhua, A. Rios, M.D. Luque de Castro and M. Valcarcel, *Analyst*, 116 (1991) 171–176.
13 S.M. Sultan, *Analyst*, 116 (1991) 177–181.
14 J. Quinn and R. Calvet, *J. Pharm. Pharmacol.*, 28 (1976) 59P.
15 H. Maurer and K. Pfleger, *J. Chromatogr.*, 306 (1984) 125–145.
16 G. Taylor, R.T. Calvert and J.B. Houston, *Anal. Lett.*, 12(B14) (1979) 1435–1442.
17 U.Th. Brinkman, P.W. Welling, G. De Vries, A.T. Scholten and R.W. Frei, *J. Chromatogr.*, 217 (1981) 463–471.
18 G.J. Gresgorio and F. Ruch, *J. Pharm. Sci.*, 69 (1980) 1457–1459.
19 J.E. Wallance, E.L. Shimek, Jr., S.C. Harris and S. Stavchansky, *Clin. Chem.*, 27 (1981) 253–255.
20 J.E. Wallace, E.L. Shimek, Jr., S. Stavchasky and S.C. Harris, *Anal. Chem.*, 53 (1981) 960–962.
21 S.H. Curry, E.A. Brown, O.P. Hu and J.H. Perrin, *J. Chromatogr.*, 231 (1982) 361–376.
22 G. Taylor and J.B. Houston, *J. Chromatogr.*, 230 (1982) 194–198.
23 S. Melethil, A. Dutta, V. Chungi and L. Dittert, *Anal. Lett.*, 16(B9) (1983) 701–709.
24 W.Th. Kok, W.H. Voogt, U.A.Th. Brinkman and R.W. Frei, *J. Chromatogr.*, 354 (1986) 249–259.
25 B. Gawdzik, *J. Chromatogr.*, 600 (1992) 115–121.
26 A. Fox and D.A. McLoughlin, *J. Chromatogr.*, 631 (1993) 255–259.
27 N.J. Pound and R.W. Sears, *Can. J. Pharm. Sci.*, 8, No. 3 (1973) 84–88.
28 M. Paleologou, S. Li and W.C. Purdy, *J. Chromatogr. Sci.*, 28 (1990) 311–318.
29 D.W. Newton and R.B. Kluza, *Drug Intell. Clin. Pharm.*, 12 (1978) 546.
30 *Cyclobond Handbook*, Astec, Whippany, NJ, 1992, p. 17.
31 K.B. Sentell and J.G. Porsey, *J. Chromatogr.*, 461 (1989) 193–207.

32 S.R. Bakalyar, R. McIlwrick and E. Roggendorf, *J. Chromatogr.*, 142 (1977) 353–365.
33 H.B. Patel and T.M. Jefferies, *J. Chromatogr.*, 389 (1987) 21–32.
34 T. Braumann, *J. Chromatogr.*, 373 (1986) 191–225.
35 W.J. Geary, N.J. Mason, L.A. Nixon and I.W. Nowell, *J. Chem. Soc., Chem. Commun.*, (1980) 1064–1065.
36 W.J. Geary, N.J. Mason, I.W. Nowell and L.A. Nixon, *J. Chem. Soc., Dalton Trans.*, (1982) 1103–1107.

Journal of Chromatography A, 660 (1994) 351–358
Elsevier Science B.V., Amsterdam

CHROMSYMP. 2974

Sensitive procedure for the determination of reboxetine enantiomers in human plasma by reversed-phase high-performance liquid chromatography with fluorimetric detection after chiral derivatization with (+)-1-(9-fluorenyl)ethyl chloroformate

E. Frigerio*, E. Pianezzola and M. Strolin Benedetti

Farmitalia Carlo Erba, Research and Development, Pharmacokinetics and Metabolism Department, Via per Pogliano, 20014 Nerviano, Milan (Italy)

ABSTRACT

A sensitive and selective high-performance liquid chromatographic method for the determination of reboxetine enantiomers in human plasma was developed. Although two chiral centres are present in reboxetine, its stereospecific synthesis leads to two rather than four possible enantiomers. After extraction from plasma and reaction with (+)-1-(9-fluorenyl)ethyl chloroformate, reboxetine enantiomers were separated as diastereoisomeric derivatives by reversed-phase high-performance liquid chromatography (HPLC) and determined by fluorimetric detection. The HPLC analysis time was about 90 min. The linearity, precision, accuracy and limit of quantification of the method were evaluated. No interference from blank plasma sample was observed. The suitability of the method for *in vivo* samples was assessed by the analysis of plasma samples obtained from a healthy male volunteer who had received a single oral dose of 4 mg of reboxetine in tablet form.

INTRODUCTION

Reboxetine, (*RS*)-2-[(*RS*)-α-(2-ethoxyphenoxy)benzyl]morpholine methanesulphonate [laboratory code FCE 20124, (**I**)] is a compound developed by Farmitalia Carlo Erba (Milan, Italy) which has shown high potency in classical pharmacological models predictive of antidepressant efficacy in humans: reserpine antagonism and norepinephrine reuptake inhibition [1]. In addition, **I** has been found to prevent clonidine-induced hypothermia in rodents after a single oral dose [1]. When the effects of **I** on the resting pupil diameter and the pupillary responses to light stimuli were studied in healthy volunteers, the results obtained probably reflected blockage of norepinephrine uptake and of muscarinic receptors by **I** [2]. The compound is extensively metabolized in rodents, where no unchanged drug is recovered in the urine, whereas some unchanged **I** is detected in the urine of dog and monkey, although less than in humans [3]. **I** shows important structural similarities with viloxazine, nisoxetine and fluoxetine. With viloxazine and nisoxetine it also shares the property of being a selective norepinephrine uptake inhibitor, whereas it shows only structural similarities with fluoxetine, which is a selective serotonin uptake inhibitor. Two chiral centres are present in 2-[α-(2-ethoxyphenoxy)benzyl]morpholine (Fig. 1A). However, as **I** is prepared by stereospecific synthesis [4], only two enantiomers are present: the *R,R*-(−) enantiomer (**II**) (laboratory code FCE 22071) and the *S,S*-(+)-enantiomer (**III**) (laboratory code FCE 21684). In the tests considered as predictive of antidepressant activi-

* Corresponding author.

0021-9673/94/$07.00 © 1994 Elsevier Science B.V. All rights reserved
SSDI 0021-9673(93)E1140-U

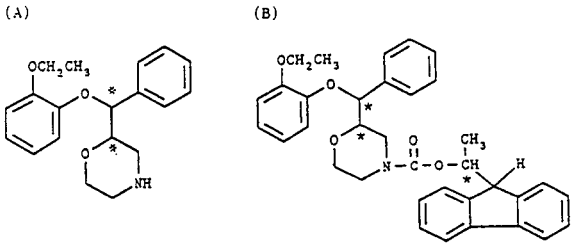

Fig. 1. Structures of (A) reboxetine and (B) its resulting diastereoisomers after derivatization with FLEC.

ty, **III** was found to be more potent than **II** [5]. In the development of a racemic drug it is required that the pharmacokinetic behaviour of each enantiomer be adequately studied [6], as any attempt to establish a plasma concentration–response relationship should be made using only the values of the more active enantiomer or possibly those of both enantiomers, but analysed separately, in order to establish the contribution of each to the therapeutic response and/or to the side-effects. This involves the availability of an analytical method able to determine the two enantiomers in biological fluids [7]. The HPLC method with UV detection available for the determination of **I** in human plasma [8] is characterized by a good limit of quantification (10 ng/ml) but it does not permit the separation of the two enantiomeric forms of the drug.

Different methodologies can be used for enantiomer separation: the precolumn derivatization of the two enantiomers with a chiral reagent to obtain a pair of diastereoisomers, which can then be separated by a conventional achiral column and suitably determined, has wide applications [9]. The applicability of (*R*)-1-(1-naphthyl)ethyl isocyanate (10), (*S*)-1-(1-naphthyl)ethyl isothiocyanate [11,12] and N-trifluoroacetyl-L-prolyl chloride [13] as chiral reagents for the derivatization of **I** enantiomers has been investigated. All these compounds reacted with **I** under suitable conditions to give a pair of diastereoisomers. However, although several different columns and several combinations of different mobile phases were tested, no satisfactory separation of the diastereoisomers formed with these reagents was achieved. A different approach for the chromatographic separation of **I** enantiomers involving the use of chiral stationary phases has been investigated. Several chiral columns have been evaluated so far without success [14].

In this study, optimum conditions were developed for the determination of enantiomers of **I** by reversed-phase HPLC with fluorimetric detection after a derivatization reaction with (+)-1-(9-fluorenyl)ethyl chloroformate (FLEC) which occurs in less than 5 min (Fig. 1B). FLEC shows several advantages over other chiral reagents: it forms stable diastereoisomers that can be assayed by automated procedures with high detection sensitivity and generally with good resolution [15].

The HPLC method developed was fully validated down to concentrations of 1 ng/ml in plasma for each enantiomer and used in a preliminary determination of the two enantiomers in plasma samples obtained from a healthy male volunteer who had received a single oral dose of 4 mg of **I** in tablet form.

EXPERIMENTAL

Chemicals and solutions

Compounds **I**, **II** and **III**, and the racemic mixture of the two other *RS*- and *SR*-enantiomers (all as methanesulphonate salts) were supplied by the Chemical Development Department of Farmitalia Carlo Erba. All other chemicals and solvents were of analytical-reagent grade from Farmitalia Carlo Erba. Tris buffer, 0.05 *M* (pH 9.1), was prepared by mixing 25 ml of 0.2 *M* Tris solution and 5 ml of 0.1 *M* HCl and diluting to 100 ml with water. Dibasic ammonium phosphate buffer, 0.1 *M* (pH 7.5), was prepared by dissolving 13.2 g of $(NH_4)_2$ HPO_4 in about 900 ml of distilled water and adding 85% H_3PO_4 to pH 7.5 and then water to 1000 ml. Borate buffer, 1 *M* (pH 8.0), was prepared by dissolving 61.8 g of H_3BO_3 in about 900 ml of distilled water and adding 20% NaOH to pH 8.0 then water to 1000 ml. FLEC reagent was prepared by diluting 1 ml of 18 m*M* FLEC in acetone solution to 50 ml with acetonitrile. A stock standard solution of **I** was prepared by dissolving a weighed amount of the compound in distilled water. From this solution, which is stable for at least 3 months if stored at 4°C, working standard solutions were

prepared weekly by dilution with 5 m*M* H_3PO_4. Stock and working standard solutions were stored at 4°C until use.

Instrumentation

The HPLC system used in this study consisted of a pump (Model P1000), an autosampler (Model AS 3000) with a 200-μl loop, a fluorescence detector (Model FP 820) and a data acquisition system (Winner 386) with LABNET software. Real-time chromatograms were obtained on an integrator (Datajet). All these instruments were supplied by Spectra-Physics (Santa Clara, CA, USA), except the detector, which was purchased from Jasco (Hachioji, Japan). The excitation and emission wavelengths were set at 260 and 315 nm, respectively. The detector was wired to send a 1-V signal to the data system.

Direct probe mass spectra were obtained on a Finnigan Mat (San Jose, CA, USA) Model 4600 instrument operating in the chemical ionization mode, with ammonia as the reagent gas.

Chromatographic conditions

The chromatographic separation was carried out on a 250 × 4.6 mm I.D. LiChroCART Supersphere 60 RP-8 (end-capped) reversed-phase column (particle size 4 μm) (Merck, Darmstadt, Germany) with a Survival precolumn packed with pellicular ODS (particle size 30–38 μm) (Whatman, Clifton, NJ, USA). The mobile phase was 0.1 *M* dibasic ammonium phosphate buffer (pH 7.5)–tetrahydrofuran (53.5:46.5, v/v). The mobile phase was prepared daily and degassed under vacuum. The separation of the analytes was performed at a flow-rate of 0.5 ml/min. A typical back-pressure was 220 bar.

Sample preparation

Blood samples were drawn from a healthy male volunteer participating in a clinical trial of reboxetine, through an intravenous cannula in the forearm and collected in heparinized plastic tubes before and 1, 2, 3, 4, 6, 8, 12, 24, 36, 48 and 72 h after administration. The tubes were immediately centrifuged (1200 *g* for 10 min) and the plasma stored at −20°C until analysed.

A 1.0-ml aliquot of the plasma sample was placed in a glass-stoppered test-tube and 1 ml of Tris buffer (0.05 *M*, pH 9.1) was added. The buffered plasma was extracted with 7 ml of diethyl ether by vortex mixing for 1 min then centrifuged at 1200 *g* for 5 min. The organic phase was carefully separated and transferred into another glass tube where the compounds were back-extracted from the diethyl ether with 0.2 ml of 0.01 *M* H_3PO_4 by vortex mixing for 1 min. After centrifugation (5 min at 1200 *g*), the upper organic phase was separated and discarded. The aqueous phase was mixed with 0.2 ml of 1 *M* borate buffer (pH 8) and 0.2 ml of the FLEC reagent (0.36 m*M* in acetonitrile), shaken and left to react for 5 min at room temperature. Then 0.1 ml of a 100 m*M* aqueous solution of L-proline was added and left to react for 2 min with excess reagent (L-proline gives a water-soluble derivative). The diastereoisomers formed were extracted from the reaction mixture with 3 ml of *n*-hexane (vortex mixer, 1 min) and the organic phase was carefully separated from the aqueous phase. After extraction with 1 ml of acetonitrile, the upper phase (*n*-hexane) was discarded. After further washing with 1 ml of *n*-hexane, the acetonitrile solution was evaporated to dryness on a water-bath (40°C) under a stream of nitrogen. Finally, the residue was dissolved in 0.5 ml of the mobile phase and 200 μl of the resulting solution were analysed by HPLC.

Determination of quality control and calibration samples

Blank human plasma samples spiked with known amounts of **I** were analysed by the above procedure. The linearity was evaluated from six calibration graphs with six calibration points prepared and run on six different days in the concentration range 1–270 ng/ml for both enantiomers. The precision and accuracy were evaluated by repeated analyses of the two enantiomers at five concentrations (3.2, 16.0, 40.0, 80.0 and 160.0 ng/ml) in three replicate samples analysed on four different days. All chromatograms obtained were evaluated by peak-area measurement.

Chromatographic performance

The suitability of the chromatographic system for the analysis of the two diastereoisomers was checked during the validation assay by calculating the column efficiency, the peak symmetry and the resolution factor of the peaks of the two analytes. This evaluation was carried out according to the USP [16] using the System Suitability Test software supplied by Spectra-Physics. The column efficiency was expressed as the number of theoretical plates (N). This value must be higher than 10 000 for both enantiomers. The tailing factor (T) must be less than 1.35 for **III** and within the range 0.9–1.1 for **II**. The resolution factor (R_s) between the diastereoisomer peaks must be ≥ 1.

RESULTS AND DISCUSSION

The chromatogram obtained from a standard solution of the analytes shows that enantiomers of **I** are sufficiently resolved. The resolution factor between the diastereoisomer peaks was 1.15 and the peak symmetry factors were 1.01 for **II** and 1.12 for **III**. These parameters are characteristic of the day-to-day performance of the separation and can be used to evaluate column ageing or condition and proper mobile phase preparation. If the percentage of tetrahydrofuran is reduced even slightly, the resolution factor improves but the retention times increase drastically. However, the day-to-day reproducibility of the analytical conditions is quite good. The two diastereoisomers of reboxetine elute at about 57 and 59 min. The assignment of the peaks was unambiguous for the two derivatives, since the pure (−)- and (+)-isomers were available. The derivative of **II** eluted first, followed by the derivative of **III**. The enantiomeric purity of FLEC and its chiral integrity under derivatization reaction conditions were determined by derivatizing the reagent with optically pure **II** or **III**. The presence of only one detectable peak under the chromatographic conditions revealed that the racemization of FLEC, if any, was negligible and the reagent used was of very high optical purity.

In order to establish the specificity of the assay for the *RR*- and *SS*-enantiomers, the separation of the two other enantiomers, *RS* and *SR*, from each other and from *RR* and *SS* was investigated. Under the assay conditions, *RS* and *SR* (the second enantiomeric pair) were separated from each other after derivatization with chiral FLEC (resolution factor = 1.1). The first-eluted peak of the *RS* and *SR* mixture was not separated from the *SS*-enantiomer. However, considering the structure of **I**, the possibility of *in vivo* inversion of configuration at the benzylic position is highly unlikely to occur. Indeed, the formation of the corresponding carbocation would give rise to rearrangement with loss of O-ethoxyphenol, and formation of the corresponding carbanion would not cause racemization owing to the absence of the possibility of resonance of the negative charge to form an intermediate species, in which the absolute configuration of the carbanion would be lost, *e.g.*, the formation of a double bond involving the chiral centre, as is the case for profen derivatives. In addition, administration of the *RR*- or *SS*-enantiomers to humans [17] has been shown to result in the absence of detectable peaks at the retention times of the other isomers.

A representative chromatogram for blank human plasma sample is presented in Fig. 2A. The chromatogram exhibits a clean chromatographic window in the region of the two diastereoisomer peaks, although several additional peaks co-eluted until about 90 min after the injection, which prevented us from using an internal standard during the analysis. A significant advantage of using FLEC as derivatizing reagent lies in the remarkable stability of the derivatives formed. The diastereoisomers **II** and **III** can be kept at room temperature dissolved in the mobile phase without apparent degradation. This allowed us to use an autosampler for automatic injection of the samples with an evident increase in the productivity of the system. Considering the HPLC analysis time (90 min) and the total analysis time (including sample preparation), about fifteen samples can be processed in 24 h.

The linearity of this HPLC assay was evaluated from six separate calibration graphs with six calibration points carried out on differ-

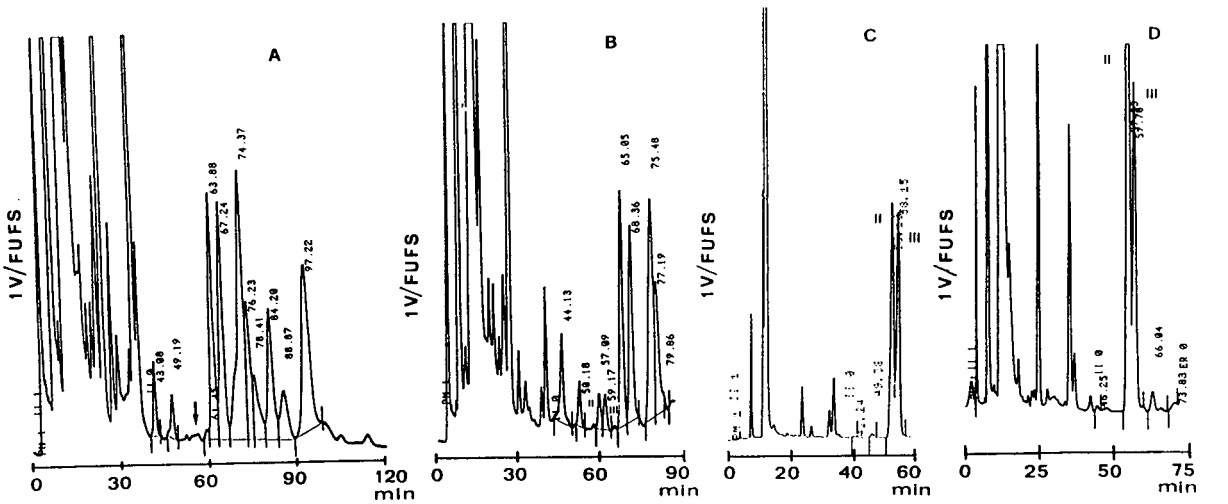

Fig. 2. Chromatograms of (A) blank human plasma (the arrow shows where the two reboxetine diastereoisomers are eluted), (B) human plasma spiked with the lowest concentration of reboxetine (2 ng/ml) used for the calibration graph, (C) human plasma spiked with the highest concentration of reboxetine (540 ng/ml) used for the calibration graph and (D) plasma from a subject dosed with 4 mg of reboxetine (3 h after administration). Peaks: II = (−)-enantiomer; III = (+)-enantiomer.

ent days in the range 2–540 ng/ml of **I** (1–270 ng/ml for each enantiomer). Calibration graphs were obtained by plotting the measured peak areas (counts) *versus* the enantiomer concentrations in plasma (ng/ml). Weighted linear regression (weighting factor $1/x^2$) was used to determine the back-calculated standard values or the enantiomer concentration in unknown samples.

Correlation coefficients (r) for the regression ranged from 0.9843 to 0.9925 for **II** and from 0.9785 to 0.9952 for **III**. The mean calibration graphs obtained were described by the equation $y = 1222 \cdot 10^3 x - 163 \cdot 10^3$ (slope R.S.D. = 10.3%, $n = 6$) for **II** and $y = 1230 \cdot 10^3 x - 71 \cdot 10^3$ (slope R.S.D. = 10.8%, $n = 6$) for **III**, where y = peak area (counts) and x = amount of enantiomer (ng) added to 1 ml of plasma. The back-calculated standard values exhibited an R.S.D. <10.3% for **II** and <11.6% for **III**.

The precision of replicate determinations of enantiomers of **I** evaluated at five concentrations on four different days is presented in Tables I and II. The inter-day precision (expressed as R.S.D.) ranged from 5.1 to 15.1% for **II** and from 6.7 to 15.0% for **III** for concentrations ranging from 3.2 to 160.0 ng/ml. At the same concentrations, the intra-day precision was better than 16.9 and 16.8% for **II** and **III**, respectively.

The accuracy of replicate determinations of enantiomers of **I** evaluated at five concentrations on four different days is summarized in Tables I and II. Accuracy, expressed as the ratio of found to added amount of each enantiomer, ranged from 81.2 to 117.5% for **II** and from 81.2 to 113.3% for **III**. The pooled accuracy (inter-day) over the 4-day validation period ranged from 93.7 to 105.0% for **II** and from 91.0 to 106.7% for **III**.

The limit of quantification (LOQ), defined as the lowest concentration of an analyte that can be measured with a given level of confidence [18], and chosen as the lowest point on the calibration graph having a back-calculated concentration within 20% of the nominal value, for both enantiomers was 1 ng/ml plasma. For this level the inter-day precision (expressed as R.S.D.) of replicate determinations ($n = 6$) was less than 4% and the mean ± S.D. inter-day accuracy (expressed as the ratio of found to added amount) was 101.5 ± 3.7% for **II** and 98.5 ± 3.7% for **III** with a signal-to-noise ratio higher than 10 for both enantiomers (Fig. 2B).

TABLE I

ACCURACY AND PRECISION OF THE METHOD FOR THE DETERMINATION OF THE (−)-ENANTIOMER IN HUMAN PLASMA

Control sample (ng/ml)	Day	n	Accuracy			Precision		
			Mean found (ng/ml)	Mean recovery (%) (intra-day)	Pooled recovery (%) (inter-day)	S.D. (ng/ml)	R.S.D. (%) (intra-day)	Pooled R.S.D. (%) (inter-day)
3.2	1	3	3.4	106.2	103.1	0.23	6.8	15.1
	2	3	3.7	115.6		0.35	9.4	
	3	3	2.6	81.2		0.10	3.8	
	4	3	3.6	112.5		0.26	7.2	
16.0	1	3	16.3	101.9	105.0	1.81	11.1	14.3
	2	3	18.8	117.5		3.12	16.6	
	3	3	16.9	105.6		1.65	9.8	
	4	3	15.4	96.2		2.61	16.9	
40.0	1	3	37.7	94.2	93.7	1.17	3.1	5.1
	2	3	37.9	94.7		3.35	8.8	
	3	3	38.3	95.7		1.94	5.1	
	4	3	36.3	90.7		0.25	0.7	
80.0	1	3	79.3	99.1	98.0	8.76	11.0	9.6
	2	3	81.7	102.1		2.70	3.3	
	3	3	82.2	102.7		8.75	10.6	
	4	3	70.3	87.9		4.01	5.7	
160.0	1	3	154.0	96.2	100.6	15.27	9.9	7.6
	2	3	160.5	100.3		15.85	9.9	
	3	3	169.3	105.8		10.34	6.1	
	4	3	160.4	100.2		7.23	4.5	

Validation data presented in Tables I and II are for the 1:1 mixture only. Quality control data at the more unfavourable ratios of the two enantiomers, a common case in the post-dose plasma samples, were also evaluated. The precision (expressed as R.S.D.) of replicate determinations ($n = 3$) for reconstituted control mixtures of the derivatives **II** and **III**, at enantiomeric ratios (**II**:**III**) of 50:50, 66.7:33.3, 84.2:15.8 and 96.2:3.8, was <0.32% for **II** and <5.26% for **III**. The accuracy evaluated on the same samples and expressed as percentage recovery ranged from 99.2 to 99.9% for **II** and from 100.8 to 105.1% for **III**.

The ammonia ionization mass spectrum confirmed the structure of the reboxetine FLEC derivative. The pseudomolecular ion $[M + H]^+$ appeared as expected at m/z 550, and it was accompanied by an $[M + NH_4]^+$ ion at m/z 567.

This method was applied to the determination of the two enantiomers of **I** in a healthy male volunteer (39 years, 79 kg, 175 cm) who had received a single oral dose of 4 mg of **I** in tablet form. A typical chromatogram obtained from this subject is shown in Fig. 2D. The peak plasma level (C_{max}), the corresponding peak time (t_{max}) and the area under the plasma concentration–time curve up to 72 h ($AUC_{0-72\,h}$) were evaluated for both **I** enantiomers. C_{max} and t_{max} were read directly from the raw plasma data and AUC values were calculated by the linear trapezoidal rule. Peak plasma concentrations of 108 ng/ml (**II**) and 52 ng/ml (**III**) were found 1 h after dosing. The experimental areas

TABLE II

ACCURACY AND PRECISION OF THE METHOD FOR THE DETERMINATION OF THE (+)-ENANTIOMER IN HUMAN PLASMA

Control sample (ng/ml)	Day	*n*	Accuracy			Precision		
			Mean found (ng/ml)	Mean recovery (%) (intra-day)	Pooled recovery (%) (inter-day)	S.D. (ng/ml)	R.S.D. (%) (intra-day)	Pooled R.S.D. (%) (inter-day)
3.2	1	3	3.2	100.0	100.0	0.23	7.2	15.0
	2	3	3.5	109.4		0.50	14.3	
	3	3	2.6	81.2		0.10	3.8	
	4	3	3.6	112.5		0.35	9.7	
16.0	1	3	15.9	99.4	103.7	1.66	10.4	12.6
	2	3	18.1	113.1		2.18	12.0	
	3	3	16.1	100.6		2.08	12.9	
	4	3	16.5	103.1		2.78	16.8	
40.0	1	3	36.3	90.7	91.0	0.92	2.5	6.7
	2	3	34.6	96.5		4.12	11.9	
	3	3	38.0	95.0		2.29	6.0	
	4	3	36.9	92.2		0.68	1.8	
80.0	1	3	76.0	95.0	94.6	8.82	11.6	8.1
	2	3	75.6	94.5		1.79	2.4	
	3	3	79.5	99.4		8.09	10.2	
	4	3	71.6	89.5		3.75	5.2	
160.0	1	3	162.4	101.5	106.7	15.82	9.7	7.2
	2	3	165.2	103.2		13.21	8.0	
	3	3	181.3	113.3		5.99	3.3	
	4	3	174.1	108.8		6.42	3.7	

($AUC_{0-72\,h}$) were 2123 ng h/ml (**II**) and 847 ng h/ml (**III**).

CONCLUSIONS

The method described is sensitive and selective for the determination of enantiomers of **I** in human plasma. It proved to be precise and capable of accurately determining the two enantiomers in the 1–270 ng/ml concentration range. This method is the first enantiospecific analytical methodology developed for the determination of enantiomers of **I** in biological fluids and can be very useful in further clinical pharmacological studies attempting to correlate the individual enantiomer plasma concentrations with the clinical response or the side-effects observed. Trials to establish such correlations with viloxazine were not successful [19], which is not surprising as no pharmacokinetic studies of the individual enantiomers of viloxazine were carried out, despite the fact that the *S*-isomer is apparently solely responsible for the drug activity, whereas the *R*-isomer is essentially devoid of activity [20].

ACKNOWLEDGEMENTS

The authors thank Dr. S. Stegnjaich for his contribution to this study, Dr. C. Allievi for recording the mass spectrum, Dr. P. Dostert for helpful discussions on stereochemistry and Mrs. S. Cozzi for typing the manuscript.

REFERENCES

1 P. Melloni, G. Carniel, A. Della Torre, A. Bonsignori, M. Buonamici, O. Pozzi, S. Ricciardi and A.C. Rossi, *Eur. J. Med. Chem.*, 19 (1984) 235–242.
2 N. Theophilopoulos, G. McDade, E. Szabadi and C.M. Bradshaw, *Br. J. Clin. Pharmacol.*, 33 (1992) 545P.
3 G. Cocchiara, R. Battaglia, P. Pevarello and M. Strolin Benedetti, *Eur. J. Drug Metab. Pharmacokinet.*, 16 (1991) 231–239.
4 P. Melloni, A. Della Torre, E. Lazzari, G. Mazzini and M. Meroni, *Tetrahedron*, 41 (1985) 1393–1399.
5 P. Dostert, personal communication.
6 F. Jamali, R. Mehvar and F.M. Pasutto, *J. Pharm. Sci.*, 78 (1989) 695–711.
7 B. Testa, *Xenobiotica*, 16 (1986) 265–279.
8 E. Frigerio, unpublished work.
9 C. Lochmuller and R. Souter, *J. Chromatogr.*, 113 (1975) 283–302.
10 G. Gubitz and S. Mihellyes, *J. Chromatogr.*, 314 (1984) 462–466.
11 J. Gal, D.M. Desai and D.C. Bloedow, *Abstracts of the 10th International Symposium on Column Liquid Chromatography, San Francisco, CA, May 18–23, 1986*, p. 406.
12 E. Pianezzola, V. Bellotti, E. Fontana, E. Moro, J. Gal and D.M. Desai, *J. Chromatogr.*, 495 (1989) 205–214.
13 M. Strolin Benedetti, V. Bellotti, E. Pianezzola, E. Moro, P. Carminati and P. Dostert, *J. Neural Transm.*, 77 (1989) 47–53.
14 S.R. Perrin, personal communication.
15 S. Einarsson, B. Josefsson, P. Möller and D. Sanchez, *Anal. Chem.*, 59 (1987) 1191–1195.
16 *US Pharmacopoeia XXII*, Pharmacopoeial Convention, Rockville, MD, 1990, pp. 1566–1567.
17 P. Dostert, personal communication.
18 Conference Report, *J. Pharm. Sci.*, 81 (1992) 309–312.
19 T.R. Norman, G.D. Burrows, B.M. Davies, K.P. Maguire and J.M.E. Wurm, *J. Affect. Disorders*, 2 (1980) 157–164.
20 T.P. Blackburn, G.A. Foster, D.T. Greenwood and R. Howe, *Eur. J. Pharmacol.*, 52 (1978) 367–374.

Intelligent Software for Chemical Analysis

Edited by **L.M.C. Buydens** and **P.J. Schoenmakers**

Data Handling in Science and Technology Volume 13

Various emerging techniques for automating intelligent functions in the laboratory are described in this book. Explanations on how systems work are given and possible application areas are suggested. The main part of the book is devoted to providing data which will enable the reader to develop and test his own systems. The emphasis is on expert systems; however, promising developments such as self-adaptive systems, neural networks and genetic algorithms are also described.

Contents:

1. Introduction. Automation and intelligent software. Expert systems. Neural networks and genetic algorithms. Reader's guide. Concepts. Conclusions.

2. Knowledge-based Systems in Chemical Analysis (P. Schoenmakers). Computers in analytical chemistry. Sample preparation. Method selection. Method development. Instrument control and error diagnosis. Data handling and calibration. Data interpretation. Validation. Laboratory management. Concluding remarks. Concepts. Conclusions. Bibliography.

3. Developing Expert Systems (H. van Leeuwen). Introduction. Prerequisites. Knowledge acquisition. Knowledge engineering. Inferencing. Explanation facilities. The integration of separate systems. Expert-system testing validation and evaluation. Concepts. Conclusions. Bibliography.

4. Expert-System-Development Tools (L. Buydens, H. van Leeuwen, R. Wehrens). Tools for implementing expert systems. Tool selection. Knowledge-acquisition tools. Concepts. Conclusions. Bibliography. **5. Validation and Evaluation of Expert Systems for HPLC Method Development - Case Studies** (F. Maris, R. Hindriks). Introduction. Case study I: Expert systems for method selection and selectivity optimization. Case study II: System-optimization expert system. Case study III: Expert system for repeatability testing, applied for trouble-shooting in HPLC. Case study IV: Ruggedness-testing expert system. General comments on the evaluations. Concepts. Conclusions. Bibliography.

6. Self-adaptive Expert Systems (R. Wehrens). Introduction - maintaining expert systems. Self-adaptive expert systems: Methods and approaches. The refinement approach of SEEK. Examples from analytical chemistry. Concluding remarks. Concepts. Conclusions. Bibliography.

7. Inductive Expert Systems (R. Wehrens, L. Buydens). Introduction. Inductive classification by ID3. Applications of ID3 in analytical chemistry. Concluding remarks. Concepts. Conclusions. Bibliography. **8. Genetic Algorithms and Neural Networks** (G. Kateman). Introduction. Genetic algorithms. Artificial neural networks. Concepts. Conclusions. Bibliography. **9. Perspectives.** Limitations of Intelligent Software. Dealing with intelligent software. Potential of intelligent software. **Index.**

© 1993 366 pages Hardbound
Price: Dfl. 350.00 (US $ 200.00)
ISBN 0-444-89207-9

ORDER INFORMATION

For USA and Canada
ELSEVIER SCIENCE INC.
P.O. Box 945
Madison Square Station
New York, NY 10160-0757
Fax: (212) 633 3880

In all other countries
ELSEVIER SCIENCE B.V.
P.O. Box 330
1000 AH Amsterdam
The Netherlands
Fax: (+31-20) 5862 845

US$ prices are valid only for the USA & Canada and are subject to exchange rate fluctuations; in all other countries the Dutch guilder price (Dfl.) is definitive. Customers in the European Community should add the appropriate VAT rate applicable in their country to the price(s). Books are sent postfree if prepaid.

ELSEVIER SCIENCE B.V.

Environmental Analysis

Techniques, Applications and Quality Assurance

Edited by **D. Barceló**

Techniques and Instrumentation in Analytical Chemistry Volume 13

Three aspects of environmental analysis are treated in this book:

- the use of various analytical techniques
- their applications to trace analysis of pollutants, mainly organic compounds
- quality assurance aspects, including the use of certified reference materials for quality control of the entire analytical process.

The book will serve as a general reference for post-graduate students as well as a practical reference for environmental chemists who need to use the analytical techniques for environmental studies. Analytical chemists needing information on the complexity of environmental sample matrices and interferences will also find this an invaluable reference.

Contents: Part 1. Field Sampling Techniques and Sample Preparation. 1. Sampling techniques for air pollutants (R. Niessner). 2. Sample handling strategies for the analysis of organic contaminants from environmental samples (M.-C. Hennion, P. Scribe). 3. Extraction, clean-up and recoveries of persistent trace organic contaminants from sediment and biota samples (D.E. Wells).
Part 2. Application Areas. 4. Current developments in the analysis of polychlorinated biphenyls (PCBs) including planar and other toxic metabolites in environmental matrices (D.E. Wells). 5. Official methods of analysis of priority pesticides in water using gas chromatographic techniques (D. Barceló). 6. Coupled-column reversed phase liquid chromatography as a versatile technique for the determination of polar pesticides (E.A. Hogendoorn, P. van Zoonen). 7. Liquid chromatographic determination of phenols and substituted derivatives in water samples (G. Marko-Varga). 8. HPLC methods for the determination of mycotoxins and phycotoxins (J.F. Lawrence, P.M. Scott). 9. Determination of radionuclides in environmental samples (V. Valkovic).
Part 3. Quality Assurance and Reference Materials. 10. Quality assurance in environmental analysis (W.P. Cofino). 11. Certified reference materials for the quality control of measurements in environmental monitoring (E.A. Maier). 12. Standard reference materials for the determination of trace organic constituents in environmental samples (S.A. Wise).
Part 4. Emerging Techniques. 13. Application of fluorescence spectroscopic techniques in the determination of PAHs and PAH metabolites (F. Ariese, C. Gooijer, N.H. Velthorst). 14. Characterization of surfactants in water by desorption ionization methods (F. Ventura). 15. Utilization of various LC-MS interfacing systems in environmental analysis; application to polar pesticides (M.H. Lamoree, R.T. Ghijsen, U.A.Th. Brinkman). 16. Hyphenated techniques applied to the speciation of organometallic compounds in the environment (O.F.X. Donard, R. Ritsema). 17. The potential of capillary electrophoresis in environmental analysis (M.W.F. Nielen).
Subject index.

© 1993 660 pages Hardbound
Price: Dfl. 465.00 (US $ 265.75)
ISBN 0-444-89648-1

ELSEVIER SCIENCE B.V.

ORDER INFORMATION

For USA and Canada
ELSEVIER SCIENCE INC.
P.O. Box 945
Madison Square Station
New York, NY 10160-0757
Fax: (212) 633 3880

In all other countries
ELSEVIER SCIENCE B.V.
P.O. Box 330
1000 AH Amsterdam
The Netherlands
Fax: (+31-20) 5862 845

US$ prices are valid only for the USA & Canada and are subject to exchange rate fluctuations; in all other countries the Dutch guilder price (Dfl.) is definitive. Customers in the European Community should add the appropriate VAT rate applicable in their country to the price(s). Books are sent postfree if prepaid.

PUBLICATION SCHEDULE FOR THE 1994 SUBSCRIPTION

Journal of Chromatography A and *Journal of Chromatography B: Biomedical Applications*

MONTH	O 1993	N 1993	D 1993	J	F	
Journal of Chromatography A	652/1 652/2 653/1	653/2 654/1 654/2 655/1	655/2 656/1 + 2 657/1 657/2	658/1 658/2 659/1 659/2	660/1 + 2 661/1 + 2 662/1 662/2	The publication schedule for further issues will be published later.
Bibliography Section						
Journal of Chromatography B: Biomedical Applications				652/1	652/2 653/1	

INFORMATION FOR AUTHORS

(Detailed *Instructions to Authors* were published in *J. Chromatogr. A.*, Vol. 657, pp. 463–469. A free reprint can be obtained by application to the publisher, Elsevier Science B.V., P.O. Box 330, 1000 AH Amsterdam, Netherlands.)

Types of Contributions. The following types of papers are published: Regular research papers (full-length papers), Review articles, Short Communications and Discussions. Short Communications are usually descriptions of short investigations, or they can report minor technical improvements of previously published procedures; they reflect the same quality of research as full-length papers, but should preferably not exceed five printed pages. Discussions (one or two pages) should explain, amplify, correct or otherwise comment substantively upon an article recently published in the journal. For Review articles, see inside front cover under Submission of Papers.

Submission. Every paper must be accompanied by a letter from the senior author, stating that he/she is submitting the paper for publication in the *Journal of Chromatography A* or *B*.

Manuscripts. Manuscripts should be typed in **double spacing** on consecutively numbered pages of uniform size. The manuscript should be preceded by a sheet of manuscript paper carrying the title of the paper and the name and full postal address of the person to whom the proofs are to be sent. As a rule, papers should be divided into sections, headed by a caption (*e.g.*, Abstract, Introduction, Experimental, Results, Discussion, etc.) All illustrations, photographs, tables, etc., should be on separate sheets.

Abstract. All articles should have an abstract of 50–100 words which clearly and briefly indicates what is new, different and significant. No references should be given.

Introduction. Every paper must have a concise introduction mentioning what has been done before on the topic described, and stating clearly what is new in the paper now submitted.

Experimental conditions should preferably be given on a *separate* sheet, headed "Conditions". These conditions will, if appropriate, be printed in a block, directly following the heading "Experimental".

Illustrations. The figures should be submitted in a form suitable for reproduction, drawn in Indian ink on drawing or tracing paper. Each illustration should have a caption, all the *captions* being typed (with double spacing) together on a *separate sheet*. If structures are given in the text, the original drawings should be provided. Coloured illustrations are reproduced at the author's expense, the cost being determined by the number of pages and by the number of colours needed. The written permission of the author and publisher must be obtained for the use of any figure already published. Its source must be indicated in the legend.

References. References should be numbered in the order in which they are cited in the text, and listed in numerical sequence on a separate sheet at the end of the article. Please check a recent issue for the layout of the reference list. Abbreviations for the titles of journals should follow the system used by *Chemical Abstracts*. Articles not yet published should be given as "in press" (journal should be specified), "submitted for publication" (journal should be specified), "in preparation" or "personal communication".

Vols. 1–651 of the *Journal of Chromatography*; *Journal of Chromatography, Biomedical Applications* and *Journal of Chromatography, Symposium Volumes* should be cited as *J. Chromatogr.* From Vol. 652 on, *Journal of Chromatography A* (incl. Symposium Volumes) should be cited as *J. Chromatogr. A* and *Journal of Chromatography B: Biomedical Applications* as *J. Chromatogr. B.*

Dispatch. Before sending the manuscript to the Editor please check that the envelope contains four copies of the paper complete with references, captions and figures. One of the sets of figures must be the originals suitable for direct reproduction. Please also ensure that permission to publish has been obtained from your institute.

Proofs. One set of proofs will be sent to the author to be carefully checked for printer's errors. Corrections must be restricted to instances in which the proof is at variance with the manuscript.

Reprints. Fifty reprints will be supplied free of charge. Additional reprints can be ordered by the authors. An order form containing price quotations will be sent to the authors together with the proofs of their article.

Advertisements. The Editors of the journal accept no responsibility for the contents of the advertisements. Advertisement rates are available on request. Advertising orders and enquiries can be sent to the Advertising Manager, Elsevier Science B.V., Advertising Department, P.O. Box 211, 1000 AE Amsterdam, Netherlands; courier shipments to: Van de Sande Bakhuyzenstraat 4, 1061 AG Amsterdam, Netherlands; Tel. (+31-20) 515 3220/515 3222, Telefax (+31-20) 6833 041, Telex 16479 els vi nl. *UK*: T.G. Scott & Son Ltd., Tim Blake, Portland House, 21 Narborough Road, Cosby, Leics. LE9 5TA, UK; Tel. (+44-533) 753 333, Telefax (+44-533) 750 522. *USA and Canada*: Weston Media Associates, Daniel S. Lipner, P.O. Box 1110, Greens Farms, CT 06436-1110, USA; Tel. (+1-203) 261 2500, Telefax (+1-203) 261 0101.

Ovomucoid Bonded Column for Direct Chiral Separation

ULTRON ES-OVM

Narrow-Bore Column (2.0 I.D. x 150 mm) for Trace Analyses
Analytical Column (4.6 I.D. , 6.0 I.D. x 150 mm) for Regular Analyses
Semi-Preparative Column (20.0 I.D. x 250 mm) for Preparative Separation

Analysis of Trace FLURBIPROFEN in Metabolite with NARROW-BORE COLUMN

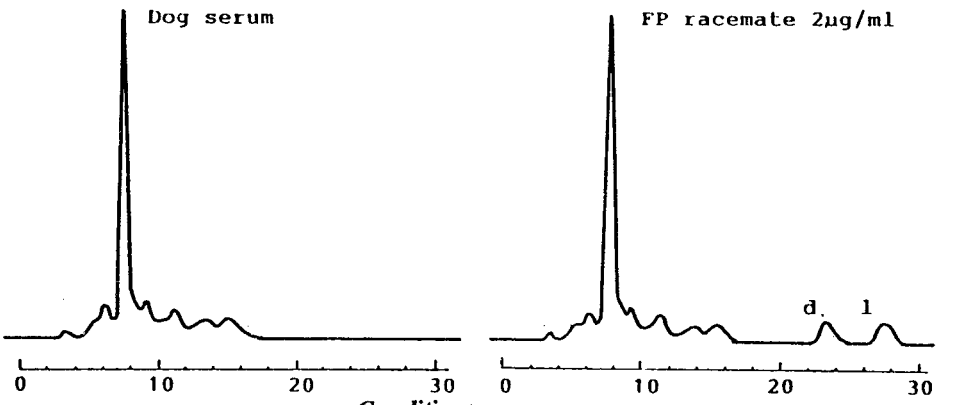

Conditions

Column: ULTRON ES-OVM(2.0I.D. x 150mm)
Mobile Phase: 20mMPhosphate Buffer(pH=3.0)/CH3CN =100/15
Flow Rate: 0.1ml/min
Temperature: 25°C
Injection: 5µl
Detection: UV- 247nm(0.05AUFS)

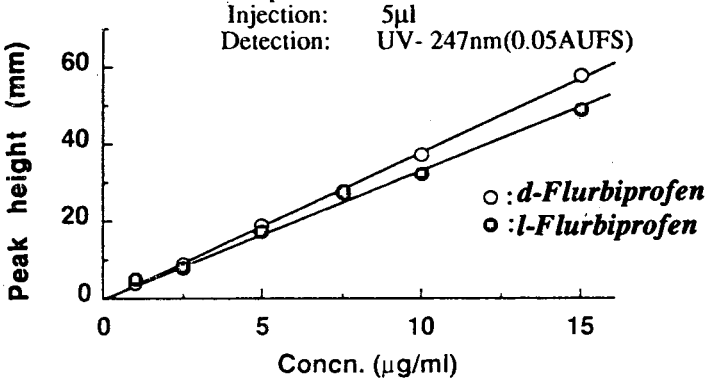

Calibration Curve for Each Enantiomer of Flurbiprofen

SHINWA CHEMICAL INDUSTRIES, LTD.

50 Kagekatsu-cho, Fushimi-ku, Kyoto 612, JAPAN
Phone:+81-75-621-2360 Fax:+81-75-602-2660

In the United States and Europe, please contact:

Rockland Technologies, Inc.

538 First State Boulevard, Newport, DE 19804, U.S.A.
Phone: 302-633-5880 Fax: 302-633-5893

This product is licenced by Eisai Co., Ltd.